HYDRAULIC AND BIOLOGICAL ASPECTS OF FISH PASSES FOR DAMS

VOLUME I OF II (MAIN TEXT)

VOL. II BOUND INSIDE THIS VOLUME

Eliane M. Guiny
(Eng. ESTP Paris, M.Sc.)

Thesis submitted for the degree of
Doctor of Philosophy
In the Department of Civil Engineering,
The University of Glasgow

Department of Civil Engineering
University of Glasgow
Rankine building
Oakfield Avenue
Glasgow G12 8LT

September 2001

SUMMARY:

The primary purpose of the dissertation is to quantify the efficiency and operation of various types of fish passes for dams. This is achieved through a novel experiment of testing juvenile salmon in a scale model fish-passes with a range of small structures including vertical slots, orifices, weirs and combinations of all three. Direct comparisons of the efficiency of each type of fish pass in terms of upstream migration.

Two identical physical models were constructed, one at the Fisheries Research Services Freshwater Laboratory at Almondbank, Perth, Scotland where observations were made of fish behaviour. The other model at the University of Glasgow, Glasgow tested only hydraulic conditions. The physical models were simplified representations of a reach of a river downstream of a dam, weir or any other obstruction to fish migration. A removable cross wall incorporating one of the types of pass tested divided the flume into two pools.

A significantly higher proportion of fish moved through submerged orifices or vertical slots than through weirs for a given flow rate and velocity. The orifice and vertical slot passing efficiencies are directly correlated to the velocities existing in their vicinity. To reach the weir/slot/orifice devices, salmon parr tended also to stay near the bottom of the flume and followed a path along the sides of the arena, which provided them with low velocities and cover.

In the vicinity of the weir/orifice/slot devices, the movements of salmon parr were consistent with energy-conserving strategies.

Clearly, the extrapolations of results from the behaviour of small to large salmon remains cautious, the intention of this research being to characterise the behaviour of small salmon and to develop clear testable hypotheses about how large salmon may respond to water flow.

Preliminary field tests were then conducted at Tongland Dam fish pass to test the main recommendation extrapolated from the parr behavioural study. The particular situation of this fish pass, which contains both weirs and orifices, allows a comparison between the two. Passive Integrated Transponder (PIT) tags together with antennae installed at a weir and an orifice were used to individually monitor the movement of wild spawning salmon passing through the fish pass. The results of the field test are as yet, inconclusive.

ACKNOWLEDGEMENTS:

I am most grateful to my parents, my family and William for their support and patience during the course of my studies.

Special thanks to my supervisors, Professor Alan Ervine, Department of Civil Engineering, University of Glasgow and Dr John Armstrong, Freshwater Fisheries Laboratory, Pitlochry, for their excellent support and advice throughout this study.

I would like also to express my gratitude to Tim Montgomery, hydraulic technician, who built the experimental set up at Glasgow University. I am also grateful to Laura Buchanan, who helped me to carry out the hydraulic experiments.

My thanks also to thank Mike Miles and Steve Keays, Salmon Rearing Station, Almondbank for the construction of the experimental set up at Almondbank. I am also grateful to the personnel of the Freshwater Fisheries Laboratory who contributed to the tagging of the wild spawning salmon during the field tests at Tongland Dam.

Many thanks to Mr G. Ross, Scottish Power for allowing field experiments to be carried out at Tongland Dam fish pass.

TABLE OF CONTENT:

CHAPTER 3:

BIOLOGY OF ATLANTIC SALMON 48

CHAPTER 4:

EXPERIMENTAL FACILITIES 64

vol. II bound together with vol I

NOTATION

A	surface
a	acceleration
b, b_0, B	width
b_y, b_z	length scales in the Y and Z directions
B	buoyant forces
c	dimensionless coefficient
c_F	skin friction coefficient
C_a	air concentration
C_c	coefficient of contraction
C_d	drag coefficient
C_F	coefficient of fish condition
C_v	coefficient of velocity
C_1, C_2, C_3	constants
d, D	distance, depth
E	energy spend by the fish
E_p	potential energy
F_{vm}	virtual mass force experimented by the fish
g	gravitational acceleration (=9.81 m/s^2);
h_1	upstream head, head measured above the weir crest
h_2	downstream head
k	energy dissipation
l	nixing length

L	length
L_f	fish length
M	mass of the fish ($N/m/s^2$)
M_a	virtual mass of the fish ($N/m/s^2$)
M_0	Momentum flux of a plane jet
p	pressure
P	propulsive force
P_c	potential chemical power
P_d	power dissipation factor
P_r	power from oxygen uptake
Ps	height of crest above the approach invert
q, Q	discharge
Q_{ideal}	ideal discharge
Q_o	discharge through an orifice
Q_w	discharge over a weir
Q+, Q*	dimensionless discharge
S_0	slope
t	time
t_m	endurance time
T	temperature
T_u	turbulence intensity
U	fish speed with respect to the water
u, v, w	longitudinal velocity components in horizontal measurements planes

u_m	maximum velocity (centre line)
V	volume
V_f	fish speed with respect to the ground
V_{FB}	burst speed of the fish
V_w	average mean water velocity
W	weight of a fish
X,Y,Z	Cartesian coordinates
x_0	length of potential core
y_0	characteristic depth of the flow
y_{cr}	critical flow depth
Z	submergence, height of the jump

Dimensionless numbers:

Fr	Froude Number
Re	Reynolds number

Greek symbol:

α, β	dimensionless coefficient;
α_1, α_2	angles of the shear layer;
ε	coefficient of kinematic eddy viscosity;
θ	angle;
μ	viscosity
ν	kinematic viscosity
ρ	density

ρ_f	average density of the fish
ρ_w	water density
τ_0	wall shear stress
τ_l	laminar shear stress
τ_t	turbulent shear stress
Φ_1, Φ_2	lines
Δh	head difference from one pool to the next
ΔU	difference of velocity between two points

Subscript

a	air
i	denotes pool impact
f	fish
o	orifice
vc	vena contracta
w	weir or water

Superscript

-	Mean component of quantity
'	R.M.S. of fluctuating component

CHAPTER 1:

INTRODUCTION TO THE PROBLEM OF FISH PASSES

CHAPTER 1:

INTRODUCTION TO THE PROBLEM OF FISH PASSES

1-1 General Introduction

Atlantic salmon or Atlantic trout have a key role in the economy of many countries such as Scotland, United States, Canada or Scandinavia as they support commercial and recreational fisheries. Fisheries, especially anadromous, contribute for example over US$ 25 billion annually to the economy of the United States.

The two main keys for maintenance of important stocks of anadromous fish are the health of anadromous fisheries habitat and their accessibility. The latter might be prevented either by large-scale dams or by small-scale weirs and blockages. In the river, the installation of hydroelectric dams has the potential to affect seriously populations of salmon by blocking their spawning migrations (Katopodis & Rajaratnam, 1983;Webb, 1990; Struthers, 1993).

Fish passes may allow fish to move past dams. An example of fish pass is shown in figure 1-1. Clay (1961,1995) defines a fishway as "a water passage around or through an obstruction, designed to dissipate the energy in the water in

such a manner as to enable fish to ascend without undue stress". However, these structures create challenging flow conditions for the migratory fish such as high flow velocities, large-scale turbulence, shear stress or high concentrations of air bubbles.

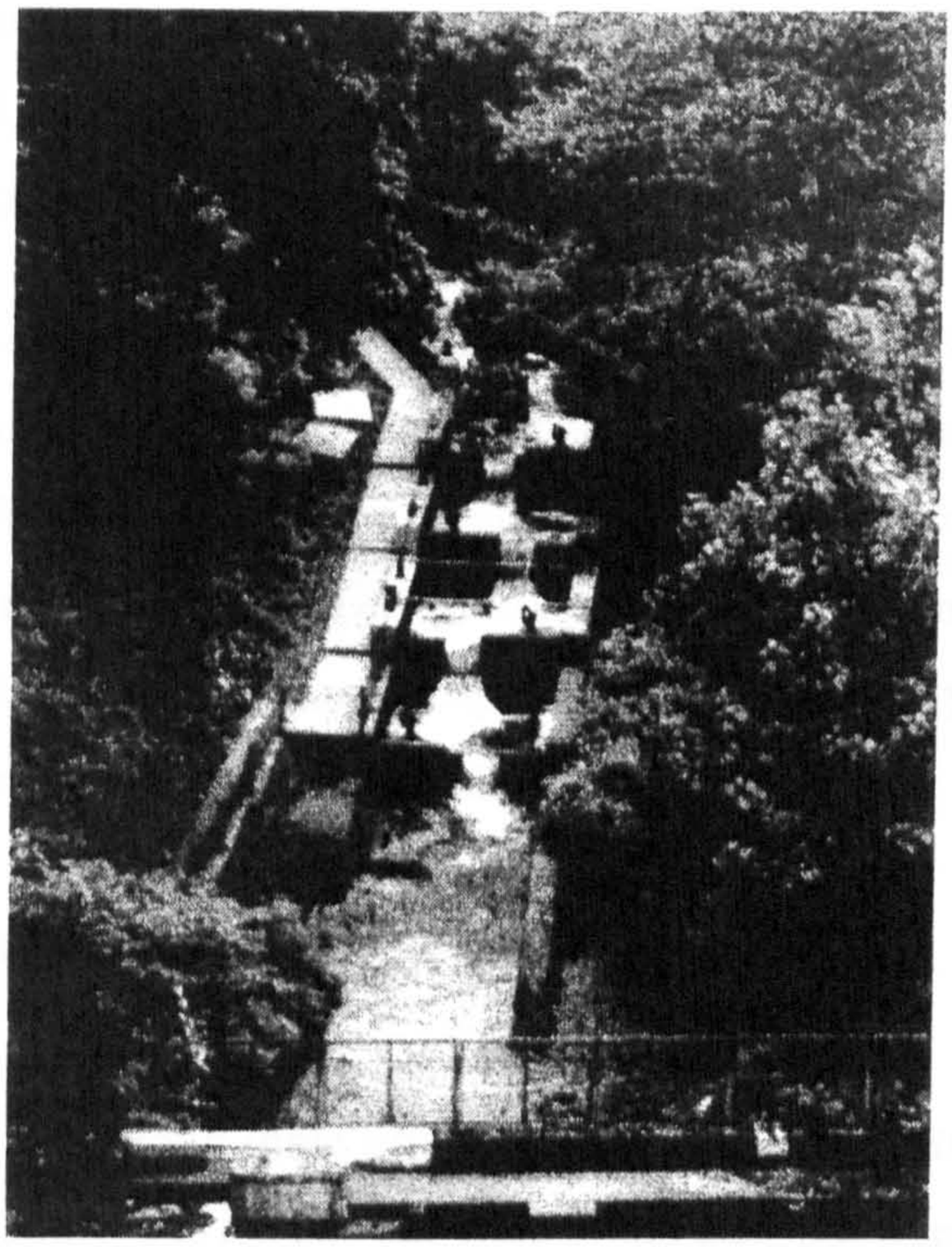

Figure 1-1: View of Tongland dam fish pass facility from the dam

Fish passage facilities are complicated structures creating complex hydraulic phenomena. To enhance the efficiency of these bioengineering systems, engineers and biologists need to work in collaboration. On one side, engineers need to understand fish biology to design better systems based on basic biological criteria such as swimming abilities or fish energetics. On the other side, biologists need to understand hydrodynamic phenomena occurring in the system including velocity, turbulence and shear stress. Both hydraulic and biological aspects of fish passage have therefore to be considered together to ensure that flows and designs of fish pass readily attract and pass fish.

A valuable approach to studying movements of salmon through fish passes is to track the behaviour of large numbers of wild fish remotely in natural situations (Gowans & al, 1999). This approach may allow assessments of the efficiencies of

fishways and may provide insights into the proportions of the migrating populations that actually move upstream and the proportions that find the entrances of fishways. However, the behaviour of salmon in the wild is influenced by so many factors that research based only on field surveys may not establish clearly the behavioural mechanisms that enable approaching fish to locate passes efficiently. Furthermore, field studies generally do not permit an experimental analysis of how modifying aspects of fish pass designs influences the behaviour of fish.

To determine fish pass design criteria, it is necessary to measure precisely fish behaviour response to individual hydraulic phenomena. This kind of experimental set up where field hydraulics are simulated and carefully controlled can be done most easily in a laboratory. To identify, the effect of a single parameter on the behaviour of fish, the experimental apparatus has to amplify it and to ensure that other phenomena do not affect the fish.

1-2 Fish pass entrance design

Fish passes can be divided in three primary subsystems: the entrance, centre ladder and the exit (Rainey, 1991). The entrance of the pass has been recognised as a particularly important part of the system (Bonnyman, 1953; Clay, 1961; Rainey, 1991; Struthers, 1993; Uedda, 1990). The location of the entrance is critical. Ideally, upstream migrating salmon should be attracted directly to the entrance and should not be distracted by other flows, for example, the tailrace from the turbines in generating stations or a spillway.

Fish passage facilities are commonly divided in four main groups: the pool and traverse, the Denil, the vertical slot and the fish lift and fish lock (Clay, 1995; Bell, 1973). Diagrams of the different fish passes will be given in Chapter 2. Each design has particular hydraulic characteristics but the success of a particular fish pass at a particular location depends on its attractiveness for the targeted species, its ease of maintenance ant the range of flow for which it is operational.

While a considerable number of projects are conducted worldwide on the appropriate hydraulic characteristics of passes, less has been done on investigating the way salmon find the upstream or downstream entrances to a pass. More research is therefore required to investigate the detailed movements of fish close to passes such as weir-and-pools, orifice-and-pools or vertical slots.

1-3 Aims and objectives

Following a study of the Tongland dam fish pass in 1997 and reported by Ervine et al (1999), the impetus was gained to investigate systematically the major fish pass design principles by combining studies of real fish with detailed hydraulics.

The research, described in this thesis, focuses therefore on the effectiveness of different type of fish pass designs to attract fish. The work combined biological and hydraulic expertise as the Civil Engineering Department of Glasgow University collaborated with the Freshwater Fisheries Laboratory, Pitlochry.

1-4 Structure of thesis

Chapter 2 briefly explores the history of fish passage technology development, and presents the principal upstream fish passage facilities currently. This chapter also points out the importance of fish pass entrance design in the overall efficiency of the system.

The life cycle of the Atlantic salmon, its abilities, as well as its habitat requirements for the different parts of its life cycle are briefly discussed in Chapter 3.

Chapter 4 describes the experimental apparatus used in the research. Two identical flumes have been built: one at the Almondbank laboratory of the FFL and the other at Glasgow University. The flume at Almondbank was used to observe behaviour of the fish and the flume at Glasgow was used to make detailed

measurements of the hydraulics such as flow patterns, velocity and turbulence of the approach area over a range of water flows.

The success of fish at passing through the various devices tested is described and analysed in chapter 5. This chapter reports on the number of fish successful at negotiating the entrance to the fish pass and the length of time needed to negotiate the tested design.

Chapter 6 presents detailed hydraulic flow measurements in the flume for the tested designs. Hydraulic measurements include three-dimensional velocity patterns and contours of turbulence.

In chapter 7, hypotheses are made on the effect of hydraulic phenomena on the behaviour of fish by integrating the parr behaviour (Chapter 5) with the hydraulic models (chapters 6) (Guiny et al, 2000(a), 2000(b), 2001(a), 2001(b)). Chapter 7 reports also on the paths chosen by the parr in relation to the hydraulic conditions. These hypotheses will be refined and tested later using adult fish in the field.

Chapter 8 reports on the comparison of passage through weirs and orifices for fish undergoing spawning migration. The purpose of this chapter is to assess the hypothesis (made in chapter 5 and 7) that spawning salmonids prefer orifices to weirs. Chapter 8 reports, in a first part, on the behaviour of mature male parr and adult male brown trout confronted with the alternative of passing through a weir or a submerged orifice in the model flume (Guiny et al, 2001(c)). The second part reports on the preliminary field test conducted with wild adult salmon at Tongland dam.

In chapter 9, the main conclusions are finally drawn and some suggestions are made for future research to be done in the field of fish pass design.

CHAPTER 2:

LITERATURE REVIEW OF FISH PASS DESIGN

CHAPTER 2:

LITERATURE REVIEW OF FISH PASS DESIGN

2-1 Introduction

Fish passes or fish passage facilities are man-made structures to facilitate migration of fish past natural obstructions such as waterfalls or rapids and artificial obstructions such as dams or weirs. An example of a fish pass at a dam is shown in figure 2-1.

The construction of fish passes is not a new idea in river engineering (Pasche & al, 1995). In Europe, rivers have been regulated through the construction of weirs for the purpose of navigation or power generation since the Middle Ages. The first fish passes were designed to allow the migration of fish such as salmon past weirs. However most were poorly designed due to a lack of understanding of fish behaviour and capabilities. Efficient design is required to ensure salmon and trout, as well as other species, return to spawning areas.

Northcote (1998) identified 67 threatened species out of the 200 European freshwater fish species. Problems in movement around dams or fish passes accounted for more than 55% of the cases whose cause of endangerment was known. For example, Deedler (1958) reported the extinction of the salmon popu-

lation in the 1930s in the river Meuse because the salmon were unable to pass the Denil and pool-type passes constructed. The optimisation and design of fish passage facilities is therefore an important factor in preserving and increasing the populations of many migratory species of fish still living in freshwater.

The purpose of this chapter is to introduce the reader to the various concepts developed for the design of fish passes since the 1900s and, as the chapter proceeds, to review the hydraulic characteristics and limitations of the different passes. The design needs of the entrance to the fish pass will be also discussed.

9-2 Fish Pass Design

As already noted in the introduction of this chapter, attempts to build fish passes have been conducted since the Middle Ages. The earliest recorded constructions were made in the 17^{th} century. However the first attempt to design fish passes using a scientific approach started only at the beginning of the 20^{th} century with the publication by Denil (Clay, 1995) in 1909 concerning a new type of fishway. For the first time, fish passes were considered as hydraulic structures built to dissipate energy. Thirty years later, McLeod and Nemenyi (Clay, 1995) in 1939-1940 undertook research comparing fish capabilities and fish pass design.

In the last fifty years, the advances in design of modern fish passes and fish locks, or elevators, have occurred, but better designs are still required based on understanding of the biological requirements of the fish and how that matches with hydraulic phenomena.

Clay (1995) defined passes as "a water passage around or through an obstruction, designed to dissipate the energy in the water in such a manner as to enable fish to ascend without undue stress". Their function is to control the water flow. They dissipate the energy of the water and maintain velocities within the biokinetic capabilities of targeted species.

Fish passage facilities are generally divided in four main groups [cf Fig 2.4 – 2-18]: (1) the pool and traverse, (2) the Denil, (3) the vertical slot fish pass and (4) the fish lift and fish lock (Bonnyman, 1958; Clay, 1995; Bell, 1973; Katopo-

dis & Rajaratnam, 1983). Their design depends on biology, life cycle, the capabilities especially swimming and leaping ability of targeted species, and on space and hydraulic conditions on the site.

The success of a particular fish pass at a particular location depends on three key- factors: (1) the range of flow through which it operates successfully, (2) its attractiveness for the targeted species and (3) its ease of maintenance.

A critical point is to design fish pass so that they attract and pass fish during periods of high stream flow. Designs that minimise operation and maintenance needs are also highly desirable (Bates, 1991) as they represent a reduction in operating costs.

From the three first main types of fish passages, hybrid fishways have been developed through the years. They attempt to combine the advantages of several fish ladder designs.

The pool and chute fishway (Bates, 1991) is one of these hybrid designs. It combines "weir and pools" and "roughened chutes". Natural looking fish passes have been built in Germany or Canada. For example, an earthen bypass channel has been successfully built at Walkerton in Canada (Crook, 1991). It is effective for dams lower than 5 m and has a low cost. A fish pass can also be designed to act, at the same time, as a passage for one species and as a barrier for another species (Holloway, 1991).

2-3 Hydraulic Characteristics and Limitations of different Fish Passes

Up until 1908, there was only one type of fishway, the pool and traverse pass with the traverse either weir or orifice. It was usually a simple construction designed with little consideration of the needs and abilities of fish. Since 1908, many studies have established design criteria of the pool sizes and head difference between pools to satisfy fisheries requirements (Anon., 1942).

2-3.1 *Pool type*

A pool and traverse fish pass consists of a rectangular channel sloping typically between 5 and 18%. The channel is partitioned into pools by walls and water passes via weirs or/and orifices. Weirs and orifices may take various shapes in order to provide gradual hydraulic head drops and water velocities that targeted fish can easily negotiate.

There are three main types of pool and traverse pass: the pool and weir as shown in figure 2-2, the pool and orifice as shown in figure 2-3 and the pool – orifice – weir.

The principal characteristics of a pool type fish pass are governed by the hydraulic conditions in the pass (e.g.: flow, difference of water level between each pool, turbulence, aeration) as a function of the water levels upstream and downstream of the structure. These characteristics are the dimensions of the successive pools and the geometry of the weirs or/and the orifices (shape of notch, size and elevation of the orifices or slots).

The drop between each pool is chosen as a function of the swimming abilities of the targeted species Typically, it varies between 0.30 m and 0.45 m for salmon and trout. It can, however, for shorter passes, rise up to 0.60 m for salmon.

The volume of the pool is determined by the power dissipation factor P_d expressed in equation 2-1. It provides an average measure of turbulence in the pool. This criterion has been fixed at a maximum value of 200 watts per m^3 for salmonids (Larinier, 1992).

$$P_d = \rho g Q \frac{\Delta h}{V} \qquad (2\text{-}1)$$

where ρ is the mass density of water (1000 kg/m^3), g is the acceleration caused by gravity (9.81m/s^2), Q is the discharge in the fish pass (m^3/s), Δh is the head loss between two pools (m) and V is the volume of water in the pool (m^3). Equation 2-1 will determine the minimum pool volume. In general the length of the pools is between 2.5 m and 3.5 m in passes designed for salmonids and the minimum

depth of the pool is around 1.0 m. Ideally the volume of the pool should be large in comparison with flow, so it absorbs turbulence and energy before water flows to the next pool.

The pool-type fish pass is the one most frequently used in France. Over the last 15 years, more than 150 such fish passes have been installed with discharges varying between 0.1 m^3/s and 2 m^3/s (Larinier, 1998). Kumar et al (1995) also estimates that almost 95% of the 10,000 fish passes installed in the Japanese rivers are of the pool type.

a. Pool and weir

The actual flow over a weir is a complex phenomenon. Using the Bernoulli equation, it is possible to develop a simple numerical model of a weir as shown in equation 2-2. This is based on the assumption of no energy loss to a point upstream when the head h_1 is above crest level.

$$Q = C_d Q_{ideal}$$

$$Q_{ideal} = \frac{2}{3} b \sqrt{2g} h_1^{3/2} \qquad (2\text{-}2)$$

where Q is the discharge, (m^3/s), Q_{ideal} is the ideal discharge (m^3/s), C_d is the discharge coefficient ($m^{1/2}/s$), b is the width of the weir crest (m), and h_1 is the head measured above the weir crest (m).

Ideal discharge derivates from the assumptions that (1) the pressure distribution in the flow passing over the weir is atmospheric, (2) the flow approaching the weir is not subject to viscous forces and (3) the cross-sectional area of the jet just downstream of the weir is equal to the cross-section of the flow at the weir itself.

The discharge coefficient is a function of the Reynolds number, the Weber number and the ratio h_1/Ps. The coefficient of discharge C_d for a fully contracted weir is given in equation 2-3 where h_1 is the head measured above the weir crest (m) and Ps is the height of crest above the approach invert (m).

$$C_d = 0.602 - 0.083h_1 / Ps \quad \textbf{(2-3)}$$

The flow over the weir may be plunging or streaming with a transition state depending on the depth of flow over the weir. The flow is in the plunging mode when the water level in the downstream pool is below the crest of the weir while it is in the streaming mode when a surface stream flows over the crest of the weirs and skims over the water surface in the pools in between as shown in figure 2-5.

If the flow is in the plunging mode, fish will have to enter the jet to jump over the weir whereas if it is in the streaming mode, fish will have to swim over the weir. The maximum velocity of the water at the jet is derived from the head loss Δh and the acceleration caused by gravity g (m^2/s) as shown in equation 2-4:

$$V = 2g\sqrt{\Delta h} \quad \textbf{(2-4)}$$

The swimming abilities of the targeted species will therefore limit the maximum drop between each pool. For the plunging mode, the rise between each pool is around 0.30 m but can be up to 0.60 m for shorter passes. For the streaming mode, this drop varies between 0.30 and 0.40 m.

Clay (1995) reported that studies on plunging and/or streaming flow were carried out both by the U.S. Army Corps of Engineers and the University of British Columbia but none of the results were published. However, a further study conducted by Rajaratnam et al (1988) delimits the conditions in which these two types of flow occurred. The plunging flow occurs when Q_+ (Eq 2-5) varies over a very narrow range with the average value 0.61. b_0 is the width of the weir, h is the upstream hydraulic head and Q_w is the discharge. The flow range through which the plunging flow condition is present in the pools can be extended with the right shape for the crest and by adding orifices within the weir.

$$Q_+ = \frac{Q_w}{b_0 h^{1.5}\sqrt{g}} = 0.61 \quad \textbf{(2-5)}$$

The streaming regime exists when the dimensionless discharge Q_* is equal to $1.5\sqrt{(L/d)}$ where L is the length of the pool and d is the depth of the surface stream as shown in equation 2-6.

$$Q_* = \frac{Q_w}{b_0 y_0^{1.5}\sqrt{gS_0}} = 1.5\sqrt{L/d} \qquad (2\text{-}6)$$

where b_0 is the width of the crest, g is the gravitational acceleration, Q_w is the discharge over the weir, S_0 is the slope of the fishpass bed and y_0 is the characteristic depth of the flow.

A criterion Q_t predicting the transition from plunging to streaming flow was also established and is given in equation 2-7.

$$Q_t = \frac{Q_w}{b_0 S_0 L^{1.5}\sqrt{g}} = 0.25 \qquad (2\text{-}7)$$

Wu & Rajaratnam (1996) carried out complementary work on submerged flow regimes of rectangular sharp-crested weirs. They described the four different possible regimes: impinging jet, breaking wave, surface and surface jet shown in figure 2-6. They also developed a diagram to predict the occurrence and connect the boundaries of these regimes to the direction of change of the tail water.

Pool/weir fishways are limited at their upper flow design by flow instability, including excess turbulence and aeration of water, as well as oscillating water surface. Turbulence can eliminate the steady circulation patterns, which guide the motion of the fish upstream, as well as the area where fish can rest (Bates, 1991).

In the past ten years, a new type of pool-weir fish pass with V-shaped over falls (Boiten, 1990) has been increasingly constructed in small steep rivers, either in the river itself, or as a bypass. The maximum discharge passing through this design ranges from 0.35 m^3/s to 5.5 m^3/s.

b. Pool and orifice

Pool and orifice passes consist of a series of pools. In this case, the water flows through submerged orifices, often near the fish pass bed as shown in figure 2-7. The head rise between should be no more than 0.45 m (Aitken & al, 1966).

The discharge through an orifice is given in equation 2-8 using Bernoulli equation. The discharge is a function of the area of the orifice A_0, the head loss Δh and a coefficient of discharge C_d.

$$Qo = C_d A_0 \sqrt{2g\Delta h} \tag{2-8}$$

The theoretical velocity through the orifice shown in equation 2-9 is obtained using Bernoulli equation.

$$V_{th} = \sqrt{2g\Delta h} \tag{2-9}$$

According to Torricelli theorem, the actual velocity at the orifice given in equation 2-10 is a function of the theoretical velocity by a coefficient of velocity C_v.

$$V_{Vc} = C_v V_{th} \tag{2-10}$$

where C_v = velocity at vena contracta/ theoretical velocity.

Due to a contraction phenomenon, the area of the jet at the orifice is smaller than the effective area of the orifice. C_c the coefficient of contraction, given in equation 2-11 characterises this phenomenon.

C_c = area of jet/area of orifice (2-11)

At a section just downstream the orifice shown in figure 2-8, the velocities are normal to the cross-section of the jet. This section is called the vena contracta. The discharge equation 2-8 is in fact calculated at this location with C_d a function of the coefficient of velocity and contraction:

$$C_d = C_c C_v \tag{2-12}$$

C_d is uniquely related with the parameter (a/h_1) by a linear relation described in equation 2-13 where a is the height of the orifice and h_1 is the water surface elevation upstream (Kumar et al, 1995).

$$C_d = \alpha\left(a/h_1\right) + \beta \qquad (2\text{-}13)$$

An orifice-pool fish pass has the advantage of being more flexible than a weir-pool or even a weir-orifice-pool type when the headwater level fluctuates a lot and rapidly (Clay, 1995). Bonnyman (1958) demonstrated that the flow can stay almost constant in such designs during small head pond fluctuations if all the orifices are similar. The main drawback for this type of pass is their need for maintenance, as orifices are easily blocked with debris.

A particular type of orifice-pool fish pass is used in Scotland and at the Pitlochry dam (Gowans, 1998) as seen in figure 2-9. Successive pools are connected by inclined cylindrical pipes of diameter around 0.70 m. The axis of the orifice is inclined at 20^0. In order to obtain good energy dissipation and avoid turbulence in the pool, the length and width are 6 and 4 times the diameter of the orifice. Bonnyman (1958) suggests that 5.185 m in length and 3.05 m in width are optimal.

c. Pool-orifice-weir

Bottom orifices were initially added to pool and weir fish passes to stabilise the flow in the pool. This combination of weir and orifice type has then been developed over the years.

It has been experimentally demonstrated by Rajaratnam et al (1989) that for this type of pool-orifice-weir fish pass, the flow over the weirs and through the orifices may be cumulated to obtain the total flow over the fish pass. For this type of design, the flow over the weir can still either be plunging or streaming. The total flow rate can therefore be written as:

$$Q = Q_w + Q_o \qquad (2\text{-}14)$$

For the plunging mode, the computed total flow is generally higher by 0 to 20 % than the measured total flow, whereas for the streaming mode, the calculated total flow is lower by 0 to 25% than the measured total flow.

The Ice Harbour, shown in figure 2-10, is one such fish pass. The first Ice Harbour fish pass was designed in the 1960s for the river Columbia by the fisheries Engineering Research Laboratory at Bonneville dam. It has become increasingly popular in Canada, America and Japan. Kumar et al (1995) carried out various model studies of this design using the work previously done by Rajaratnam et al (1989).

2-3.2 *Denil*

In 1908, Denil designed a fish pass thought to be the first one whose design was based on a combination of scientific principles, laboratory measurements and fish behaviour observation.

Denil passes consist of a rectangular chute with closely spaced baffles along the side and bottom, pointing upstream at an angle of 30 - 45 degrees to the fishway floor as shown in figure 2-11.

It is usually used for dams less than 2 m high and operates at gradients between 5 and 31.5%. It offers a straight route and some choice of swimming depth to the fish.

Its good energy dissipation allows a large flow, which in turn improves the attraction at the entrance (Clay, 1961) but its efficiency is limited to a small range of flows. It has the disadvantage of not being easily adaptable to water surface variations upstream and downstream. This pass is also very selective and only suitable for species which possess strong endurance and high swimming speed.

Variants, including the Larinier pass and the Alaskan steep pass have tried to improve the initial Denil design.

Denil passes were widely used on European rivers during the first half of the 20th century. Recently, around a hundred passes have been installed in small coastal streams or in small hydroelectric developments for salmonids. The Alaskan steep has also been extensively used in Alaska (Rajaratnam and Katopodis, 1991) and the Larinier passes have been installed at some diversion weirs in Japanese rivers (Nakamura et al, 2000)

a. Plain Denil fishpass

The characteristic parameters of a typical plain Denil are shown in figure 2-11. It has a total width B of 0.56 m and a clear central width b_0 of 0.36 m. The longitudinal spacing between the baffles is equal to 0.25 m and the baffles are inclined at 45^0.

Hydraulic modelling studies of Denil fish passes with various geometries have been conducted and their results have been analysed and generalised. Katopodis and Rajaratnam (1983) conducted a review of the hydraulics of Denil Fishways through a laboratory study of three simple designs. The three designs were tested with full-scale models. The first one was the steep pass using the dimensions given by Ziemer (1961) and two others were simple and quite similar to the original Denil design. Further variations of the Denil fish pass were studied by scale models (Rajaratnam et al, 1987,1991 1997; Katopodis et al, 1997).

Based on theoretical considerations and using the various experimental results of the previous experiments, Rajaratnam and Katopodis developed a relation (Eq 2-15) between the dimensionless discharge Q_* and the relative depth d/b where d is the depth of the flow and b_0 is the clear width of the Denil. α and β are coefficients that depend on the geometry of the pass.

$$Q_* = \alpha\left(\frac{d}{b_0}\right)^{\beta} \qquad (2\text{-}15)$$

Table 2-1: Values of α and β for four different configurations of Plain Denil (from Katopodis, 1990)

B/b_0	L/b_0	Limits of validity	α	β
1.58	0.715	$0.5<y_0/b_0<5.8$	0.94	2.0
2	1.37	$1.12< y_0/b_0<1.2$	1.12	1.16

2	0.91	$1< y_0/b_0<5$	1.01	1.92
2	1.82	$0.8< y_0/b_0<4.3$	1.35	1.57

For the plain Denil passes, velocities increase from the bottom of the channel toward the water surface. Recirculation flows form between the side baffles. These secondary flows are in the form of vortices. Katopodis and Rajaratnam (1983) observed that the water enters these vortices near the water surface, flows down following a helical path and leaves near the bed of the channel. These re-circulation flows provoke large momentum exchange and therefore strong energy dissipation (Katopodis, 1990; Larinier, 1992).

b. Alaska steep pass

Ziemer (1961) developed this design from a prototype tested by McLeod and Nemenyi (1940). This design has been successfully used in Alaska at natural waterfalls in remote areas. The characteristic parameters of the steep pass are shown in figure 2-12.

The dimensions of the pass are relatively small: the total width B is around 0.56 m and the total height of the structure is around 0.70 m. These small dimensions allow a steep slope varying between 25 and 35%. This pass has efficient energy dissipation but has a small flow range and low tolerance to upstream water level variations.

Ziemer (1961) and Katopodis & Rajaratnam (1983, 1991) have performed hydraulic model studies on the Alaska steep pass. They have developed a general flow equation using theoretical considerations and experimental observations.

$$Q_* = \frac{Q}{\sqrt{g S_0 b^5}} = 0.97\left(y_0/b\right)^{1.55} \qquad (2\text{-}16)$$

Equation 2-16 has been validated for a range of relative depth (y_0/b) between 0.1 and 4 and for the configurations $B/b_0 = 1.58$ and $L/b_0 = 0.715$.

Combining the results from the experimental observations obtained in 1983 and 1991, Rajaratnam and Katopodis conclude that if the relative depth is less

than 1.2, the maximum velocities occur at the bottom of the channel while if the relative depth is greater than 1.2, the maximum velocities drift toward the water surface and the velocity profiles become roughly symmetrical.

It was also found that for large values of Q_*, the depth of water in the side pockets was similar to the depth of water in the passage between the baffles whereas for small values of Q_*, the depth of water in the side pockets was greater than the depth of water in the passage. They also observed that for the last conditions, the water entered the side pockets near the bed of the channel, flowed up following a helical path and left near the water surface.

c. Larinier passes: pass with superactive-type bottom baffles and thick chevron shaped baffles

Larinier (1984) developed two new Denil passes: a pass with superactive-type bottom baffles shown in figure 2-14 and a pass with thick chevron-shaped baffles, shown in figure 2-13.

According to Larinier (1992), the superactive-type bottom baffle was developed as a modified form of a model tested by Denil in 1936-1938. In this model, the baffles are at the bottom only. Their height is between 0.08 and 0.20 m. The pass with thick chevron shaped baffles was developed in 1984 using scaled models. This pass is less efficient than earlier versions but may be used also by canoe-kayaks.

The main advantages of these passes are the small flow resistance even in swollen streams, their high attraction and their low maintenance cost (Nakamura & al, 2000). Their disadvantages are the need for long and deep resting pools, as they are quite selective and the fact that the slope needs to be relatively low, in the range of 15-16%.

2-3.3 *Vertical slot*

Vertical slot fish passes consist of a rectangular channel with a sloping floor that is divided into a number of pools as shown in figure 2-15. The slope of the chan-

nel usually varies between 5 and 15%. Vertical slots are at one or both sides of each cross wall and each slot extends from top to bottom of the cross wall, which has an upstream projection to generate more lateral mixing and reduce the water velocity. The width of slot b_0 is typically of the order 0.3 m, but may vary up to 0.6 m. Pool lengths of $10b_0$ and a width of 8 b_0 are common in the United States and Canada.

The first vertical slot pass was built on the Fraser River in British Colombia at Hell's Gate in 1943 (Clay, 1995; Andrew, 1990). The pass is a rectangular channel divided into 7 pools, each 6.1 m wide by 5.49 m long. Each pool is partitioned from the others by vertical baffles. Two vertical slots 0.61 m wide extend the full height of each baffle.

Vertical slot fishways have the ability to cope with fluctuations in water level in the upstream forebay and the downstream tailrace if these fluctuations are in the same direction. Velocities and turbulence remain also fairly stable regardless of the water level in the pass (Larinier, 1998; Clay, 1995). The vertical slot pass enables the fish to swim through the slots at any desired depth, offers a clear and simple path to the fish and the zones of recirculation within the pools offer good resting areas.

The maximum velocity at the slot is approximately equal to $\sqrt{(2g\Delta h)}$. The vertical slot is therefore designed to ensure a certain value of head loss Δh, which suits the targeted fish species.

The water runs downstream through the channel as shown in figure 2-16, by passing through the vertical slot and forms a jet. The energy of the flow is dissipated by jet mixing in the pool where k indicates the efficiency of energy dissipation for any design.

Rajaratnam et al (1986, 1992) have conducted hydraulic modelling studies on 18 vertical slots passes with various geometries for both uniform and non-uniform flows. Wu et al (1999) carried out a complementary study on the structure of flow for the best design of the previous 18.

Rajaratnam et al (1986, 1992) found a linear relation between the dimensionless discharge Q_* and the relative flow depth y_0/b_0:

$$Q_* = \frac{Q}{\sqrt{gS_0 b_0^5}} = \alpha\left(y_0/b_0\right) + \beta \qquad \textbf{(2-17)}$$

where y_0 is the average depth of flow in the pool occurring at the centre of the pool, Q is the discharge, g is the acceleration due to gravity, S_0 is the slope of the pass and b_0 is the width of the slot. The coefficients α and β depend on the geometry of the pass.

The energy dissipation in the pools, k, is defined by the equation 2-18 where g is the acceleration due to gravity, ρ is the mass density of water, B is the width and L the length of the pool with a mean depth of y_0. Bell (1973) suggests a maximum value of 0.191 kW/m^3.

$$k = \frac{Q\Delta h g \rho}{BLy_0} \qquad \textbf{(2-18)}$$

Wu et al (1999) showed that for a given geometry (the width of the flume and the width of the slot are fixed), k varies with the slope of the flume but is independent of the flow.

Clay (1995) defined a discharge coefficient C_d for the slots as shown in the equation 2-19 where y is the depth of the flow at the slot up to the water surface on the upstream side

$$Q = C_d(b_0 y)\sqrt{2g\Delta h} \qquad \textbf{(2-19)}$$

According to Rajaratnam et al (1986), the discharge coefficient is dependent on the relative flow depth, the geometry of the slot, and the shape of edges. C_d usually varies between 0.65 and 0.85 (Rajaratnam et al, 1986). In France, it varies between 0.65 and 0.70 (Larinier, 1992). For the Hell's Gate-type pass an average value of 0.76 has been found.

Tsujimoto et al (1995) described the flow in a standard vertical slot by two-dimensional numerical analysis employing a k-ε model and compared successfully their numerical results with the experimental data of Rajaratnam et al (1986). Tsujimoto et al (1995) described the flow in one simplified pool (between two vertical slots) of the pass using the equation of continuity, the equation of momentum, the equation of turbulent energy and the equation of dissipation rate of turbulent energy. They made the assumption that the flow in every pool of a vertical slot pass is two-dimensional and that the slot strictly controls the flow through the pass: the energy losses due to skin friction and boundary effects were neglected in comparison with the energy losses due to the slot's contraction.

2-3.4 *Fish locks and Fish elevators*

The Borland fish lock, shown in figure 2-18, is another type of pass used in Scotland and other countries. The Borland lift pass was especially designed to overcome the large difference in river height between both sides of hydro dams (Payne, 1988; Travade et al, 1992). Nowadays, around 40 of these passes are in operation in Scotland (Smith et al, 1997). Salmon are raised hydraulically from a lower chamber at the downstream level to an upper chamber at reservoir level (Bonnyman, 1953). This type of fish passage facility has been in use since 1948 (Clay, 1995). At this time, this structure was so popular that Deelder (1958) even recommended that all the inefficient fish passes in the Dutch river, in particular in the Meuse be converted to fish lock.

When the downstream gate is open, fish are attracted into the lock by water flowing through the pass. This is the fishing phase. The downstream gate then closes, trapping fish into the lock, and an upstream gate opens. Water then slowly fills the lock until it reaches the forebay elevation. This is the lifting phase. The fish can then exit the device. In general, the fishing period last 3 hours compared to 1 hour for the lifting period but the length and frequency of these phase may vary from one Borland lift to another (Anon., 1995).

According to Bonnyman (1953), the Borland lift pass has many advantages over the typical traverse and pool pass: it is less expensive to build, it needs less

water to operate and the effort required by salmon is low. However the Borland lift pass has the weakness that not all the fish may exit from the upper pool of the system in the limited time permitted (Clay, 1995). Smith et al (1997) observed salmon behaviour at the Borland fish pass at the Kilmorack Power station dam on the river Beauly, Invernesshire, Scotland. Only 20.5% of the fish entering the lower chamber during the fishing period were still present during the lifting period and only 40 % of the salmon in the system during the lifting period successfully exited the upper chamber.

Crook (1991) presents the fish lock of Thornbury as a successful alternative construction for the passage of salmonids or no-salmonids. It has the enormous advantage of being low cost and is easily used on dams higher than 10 m. It also has the advantage of requiring little space.

2-3.5 *Other fish passes*

Pool and chute fishways (Bates, 1991) combine "weir and pools" and "roughened chutes". Their main advantage is the relatively wide range of flows through which they operate successfully. At low flows it acts like a pool and weir and resembles at a baffled chute at moderate to high flow.

Bates (1991) developed preliminary analysis and design standards. This concept offers an excellent attraction for fish, a good passage of debris due to a streaming flow in the centre of the fishway and a good efficiency of fish passage near the fall by the plunging flow. However it can be only used in a straight configuration as it is sensitive to bed-load deposition, which decreases the volume of the pools.

Fishways can act as well, in the same time, as a passage for some species and a barrier for other. Holloway (1991) described a combination of fish ladder and sea lamprey barrier at a low head dam in north-western Wisconsin. This facility was designed to allow the free passage of salmonids but block sea lampreys, which cannot leap clear of the water. During the sea lamprey spawning run, the fish ladder consists of a weir and pool ladder with a "lamprey" barrier at mid-

point. After the spawning run of this species, the facility is converted to a standard vertical slot ladder.

2-4 Fish passes Entrance

2-4.1 *General*

A fish pass can be divided in three primary subsystems: the entrance, units or centre ladder and the exit (Powers and Orsborn, 1985; Rainey, 1991).

The entrance of the pass has been recognised as probably the most important part of the system (Bonnyman, 1953; Clay, 1961; Rainey, 1991; Struthers, 1993; Uedda, 1990). Attracting the target fish to the fish pass entrance is critical as any excessive delay can result for the fish in the failure to reach the spawning area. The rate of sexual maturity may not be able to adjust to delay (Powers et al, 1985). Moreover, fish constrained below obstruction maybe particularly vulnerable to predators and disease.

The obvious purpose of the entrance is to provide an access to the fish pass. The entrance is also a transition area between a natural environment, the river, and, an artificial environment, the pass. Entrance designs (geometry, elevation) also control the hydraulic conditions that attract the fish. The hydraulic characteristics of the entrance jet are its shape, its orientation, its stability, and its nature: plunging or streaming.

According to Larinier (1990) most of the failures at fish passes in France are due to a lack of attraction: badly located entrances and too low discharge through the pass. It has also been shown during the improvement of fish ladders on tributaries of the Colombia River (Rainey 1991), that most delays in rivers, enhanced with hydraulic power schemes, occur in the tailrace. There, the turbulence of the flow, coming from the spillway or the turbines, obscures the low-energy flow coming from the entrance of the fish passage.

Attraction criteria are the velocities and the flow at the entrance as well as its location and design. They depend on the behaviour of the target species and its motivation and are best obtained through biological experiments (Katopodis, 1990).

Most of the information available has been obtained through observation during field survey but there has been little thorough testing by controlled experiments.

2-4.2 *Hydraulic conditions at the entrance*

As previously explained, the entrance has a major role in fish attraction as the entrance jet penetrating the tailwater serves to guide fish to the fish pass. The entrance shape, its alignment and its jet momentum are the key factors to carry the path created by the entrance jet deep into the tailwater.

According to Rainey (1991), the jet flow at the entrance should have an adequate combination of flow velocity and hydraulic drop (e.g. the flow must be more shooting than plunging to be perceived by fish at the greatest distance from the entrance). Bates (2000) also suggested that a streaming jet flow reaches further into the tailrace than does a plunging flow. The downstream effect of a plunging flow ceases just downstream the entrance in the area of the roll it created while a streaming flow skims along the water surface (for weirs design) or at the elevation of an orifice entrance and reaches deeply into the tailwater.

Thompson (1970) found that Chinook salmon can equally ascend pool and weir passes under plunging or streaming regimes and were delayed only at the transition regime.

2-4.3 *Location of the entrance:*

Salmon are shoreline oriented (Hinch & Rand, 1998). It means that they follow the riverbanks for guidance as well as taking advantage of the lower velocities during high flow periods. Salmon also tend not to swim back downstream to find a passage route if they are blocked by a hydraulic barrier which can cause serious

delays. Spilling water or jets coming from a powerhouse may also distract salmon. Following these behavioural observations, various recommendations on the location of the fish pass were extracted from review of literature.

- The entrance has to be as close as possible to the point or line to which the fish penetrate farthest upstream at the obstruction to minimise delay (Andrew, 1990; Rainey, 1991; Clay, 1995).

- The location of the entrance should take into account the locations where fish hold before going through the pass as well as the paths by which they approach the pass entrance (Bates, 2000).

- The main entrance to the fish pass has to be located either along the shore or between the powerhouse and the spillway (Powers, 1985; Clay, 1995).

- The entrance of the pass has to be designed so that the attraction water forms a right angle with the main direction of the river's flow (Deedler, 1958).

These recommendations may have to be altered as a function of the particular characteristic of the considered site as well as through the flow range. Field observation may therefore be valuable or even necessary.

For example, through the monitoring of four fish passes on two rivers in the south–west of France, various observations were made on the best location for the entrance of the pass. Travade et al (1998) concluded that the location of the pass at the powerhouse with its entrances in the vicinity of the turbine outlet is a good solution. They also find that in order to create attractive velocities, it is important to maintain a certain head, therefore a certain velocity, using a submerged gate at the entrance.

2-4.4 *Hydraulic conditions at the entrance*

a. Entrance flow:

There are no specific criteria for the entrance flow. However, the momentum of the jet should be as great as possible to reach as far as possible into the tail water

(Bates, 2000). The attraction flow should range up to 10% of the total stream flow (Rainey, 1991). Larinier (1992) recommends between 1 and 5 %. Bell (1973) advises that the velocities at fishway entrances should be between 1.22 m/s and 2.44 m/s for Pacific salmon. Clay (1995) also recommends that (1) the depth of water at the entrance should be greater than 1.22 m and that (2) the flow coming through the low flow entrance should have the same orientation as the flow coming through the spillway in order to maximise the penetration of the entrance jet into the channel at low flow regime. For high flow regime, it is beneficial to angle the high flow entrances at around 30° to the high flow streamline in order to penetrate into the highly turbulent tailwater.

b. Entrance head

Fish capabilities and the type of flow wanted (plunging or streaming) determine the head difference between the pool entrance and the tail water. Bates (2000) recommends an entrance head range of 0.30 to 0.45 m for Pacific salmon, which is similar to the head difference recommended between two pools of a fish pass for Atlantic salmon.

In order to avoid backwater and submergence phenomena at weir or vertical slot entrances when the stream flow increases, the entrance can be mechanically raised using entrance gates. Another possibility is to increase the entrance flow.

c. Shape and dimension

The entrance to a fish pass can take the shape of a weir, a contracted weir, a vertical slot or a submerged orifice. For weir entrance designs, Clay (1995) recommends that the width of the entrance should be equal to the width of the fish ladder. However a narrow weir with end contractions can enhance the jet (Bates, 2000).

The attraction of the entrance jet is determined by its momentum. As the shear forces at its boundaries dissipate its momentum, the best shape for the entrance is circular and the worst is a narrow vertical slot. The behaviour of the fish has also an influence on the design requirements. For example, Thompson et al (1967)

discovered that chinook, coho and steelhead prefer submerged rectangular orifices oriented vertical to those oriented horizontally.

In practice, the entrance to a fish pass usually takes the shape of a rectangular orifice and the ratio between the width and the height varies between 0.6 and 1.25 m. The minimum width for an orifice is around 0.8 m and only around 0.45 m for a weir.

2-4.5 *Optimisation of the attractiveness:*

To enhance the attractiveness of the flow coming from fish passes at dams, where the flow coming through the turbine or the spillway is important, two major modifications have been elaborated: (a) the auxiliary water supply system and (b) the powerhouse collection system.

a. The auxiliary water supply system

When the flow coming from a fish pass is small in comparison with the flow in the river, an auxiliary water supply is used to increase the velocity of the flow out of the pass entrance. This additional water provided through the auxiliary water supply system extends the area of intensity of velocity of outflow, and strengthens the entrance attraction jet to encourage the fish to keep moving upstream.

The auxiliary water is supplied to the fish pass either by gravity from the forebay or pumped from the tailrace. It can also be a combination of both methods. The water should always come from the primary water supply. Any other water may confuse the homing instinct of the fish, which use water scent to find its way.

Auxiliary water introduction should also create as little aeration and turbulence as possible as these phenomena discourage fish to move upstream (Stuart, 1962, Bell, 1973). Therefore a low-pressure system without air supplies the attraction water. An example of auxiliary water injection at fish passes is shown in figure 2-19. The auxiliary water is introduced to the fish pass through wall or floor diffusers, constructed from bar grating, perfored plate or wood racks.

Clay recommends an auxiliary flow within the range of 0.08 m/s to 0.23 m/s when it enters the entrance pool, whereas Larinier (1992) recommends it to be around 0.30 to 0.40 m/s.

b. The powerhouse collection system

The powerhouse collection system is "an arrangement of fish pass entrances above the power house draft tubes, so placed as to enable fish attracted to the out-flow from the draft tubes to find an entrance as readily as possible" (Clay, 1995). An example of powerhouse collection system is shown in figure 2-20.

The powerhouse collection system was first designed for the Bonneville dam. It consisted of a flume attached to the downstream face of the powerhouse with multiple entrances across the breath of the tailrace. Clay (1995) and Larinier (1992) describe it extensively. The interest of this system is to use the water coming from the powerhouse as attraction water. Thompson (1967) recommends the entrances to the powerhouse collection systems to be vertical adjustable orifices, 0.60 m wide by 1.52 m high and located at a depth of 2.7 m.

2-5 A brief note on hydraulics of turbulent jets

The purpose of this section is to introduce the reader to the fundamental concepts of turbulence and jet behaviour both in submerged pools at orifices or vertical slots and at overfall weirs. In fact, this section proceeds to introduce the theory behind the design of fish pass structures whose function is to dissipate energy.

In general, energy dissipation occurs at (1) sudden expansion, (2) abrupt deflection, (3) counter flow, (4) rough walls and even at (5) vortex devices and spray inducing devices (Vischer & Hager, 1995). Inflow to an energy dissipation system behaves like a turbulent jet whose momentum is reduced or annihilated through a mixing process .The energy dissipators of interest in this thesis are the dissipators either using hydraulic structures such as drop structures and plunge pools or using jet diffusion. The free nappe jet of an overflow on a plunge pool is

effectively subject to an expansion and a deceleration like a submerged jet passing through an orifice.

This section will therefore briefly report on the theoretical and experimental aspects of submerged jet behaviour in an infinite medium and then on the behaviour of plunging jet.

2-5.1 *Submerged jet behaviour in an infinite medium*

Turbulent submerged jets diffusing in a stagnant finite or semi-finite medium with similar properties or/and impinging on a solid plunge pool have been extensively investigated. Only the following three particular cases of submerged jets will be considered in this section because of their interest to describe and understand the flow behaviour downstream orifices or vertical slots devices:

a) The plane turbulent free jet

b) The plane turbulent wall jet

c) The three dimensional jet

2-5.1.1 *The plane turbulent free jet*

The following paragraph will concentrate on the submerged diffusion of a plane jet of water through a stagnant body of water. A schematic representation of the plane turbulent free jet is shown in figure 2-21 as proposed by Rajaratnam (1976).

The jet, with uniform velocity profiles, diffuses in the initially quiescent fluid creating turbulence. According to Albertson et al. (1948), because of the important discontinuity between the discharging jet and the surrounding fluid, a shear layer is set up producing a lateral mixing process of the two mediums: the jet and the surrounding fluid. As a result, the jet is gradually decelerated or retarded and the surrounding fluid is gradually accelerated or entrained which means that the width of the jet gradually increases in magnitude while the lateral extent of the potential core gradually decreases. The potential core is the region around the

axis of the jet and near the nozzle where the velocity is constant and equal to the velocity at the nozzle exit.

It is clear from figure 2-21 that the diffusion pattern can be divided in two distinct zones: (1) the region of flow establishment and (2) the region of established flow. The area of flow establishment stretches from the nozzle to the end of the potential core. The zone of established flow is beyond the end of potential core and is characterised by the decay of the central velocity at a steadily rate and the propagation of the jet in the transverse direction. However this representation of jet diffusion pattern is a simplification of the reality as the zone of transition between these two regions has been neglected. It is also important to note that the boundaries of the diffusion region are only nominal designation as it is impossible to locate the lateral limit of the mixing process because of its statistical nature.

a. Equation of motion:

The Reynolds equations are a fundamental expression of the conservation of momentum in fluid flow. They were developed by Reynolds (1894) who substituted to the instantaneous velocity a turbulent mean velocity u and fluctuating velocity u' in the Navier-Stokes equations. The result is given below for the three-dimensional coordinate system:

$$\frac{\partial u}{\partial t}+u\frac{\partial u}{\partial x}+v\frac{\partial u}{\partial y}+w\frac{\partial u}{\partial z}=-\frac{1}{\rho}\frac{\partial p}{\partial x}+\nu\left(\frac{\partial^2 u}{\partial x^2}+\frac{\partial^2 u}{\partial y^2}+\frac{\partial^2 u}{\partial z^2}\right)-\left(\frac{\partial \overline{u'^2}}{\partial x}+\frac{\partial \overline{u'v'}}{\partial y}+\frac{\partial \overline{u'w'}}{\partial z}\right) \qquad \textbf{(2-20)}$$

$$\frac{\partial v}{\partial t}+u\frac{\partial v}{\partial x}+v\frac{\partial v}{\partial y}+w\frac{\partial v}{\partial z}=-\frac{1}{\rho}\frac{\partial p}{\partial y}+\nu\left(\frac{\partial^2 v}{\partial x^2}+\frac{\partial^2 v}{\partial y^2}+\frac{\partial^2 v}{\partial z^2}\right)-\left(\frac{\partial \overline{v'^2}}{\partial y}+\frac{\partial \overline{u'v'}}{\partial x}+\frac{\partial \overline{v'w'}}{\partial z}\right) \qquad \textbf{(2-21)}$$

$$\frac{\partial w}{\partial t}+u\frac{\partial w}{\partial x}+v\frac{\partial w}{\partial y}+w\frac{\partial w}{\partial z}=-\frac{1}{\rho}\frac{\partial p}{\partial z}+\nu\left(\frac{\partial^2 w}{\partial x^2}+\frac{\partial^2 w}{\partial y^2}+\frac{\partial^2 w}{\partial z^2}\right)-\left(\frac{\partial \overline{w'^2}}{\partial z}+\frac{\partial \overline{u'w'}}{\partial x}+\frac{\partial \overline{v'w'}}{\partial y}\right) \qquad \textbf{(2-22)}$$

For a plane turbulent jet, the mean flow is two-dimensional and steady. Therefore, the Reynolds equations can be written (Rajaratnam, 1976) as:

$$u\frac{\partial u}{\partial x}+v\frac{\partial u}{\partial y}=-\frac{1}{\rho}\frac{dp}{dx}+\nu\frac{\partial^2 u}{\partial y^2}-\frac{\partial(\overline{u'^2}-\overline{v'^2})}{\partial x} \quad \textbf{(2-23)}$$

The laminar and turbulent shear stresses are defined as:

$$\tau_l=\mu\frac{\partial u}{\partial y} \text{ and } \tau_t=-\rho u'v' \quad \textbf{(2-24)}$$

where μ is the coefficient of dynamic viscosity and ρ is the mass density of the fluid.

As the turbulence shear stress is much larger than the laminar shear stress in a free turbulent jet and as in equation 2-23 the last term is much smaller than the other terms, it is reasonable to neglect the laminar shear stress and the last term of equation 2-23. According to Forthmann (1936), the variation of the pressure gradient in the axial direction of a horizontal diffusing jet is negligible; the Reynolds equation for the plane turbulent free jet is then:

$$u\frac{\partial u}{\partial x}+v\frac{\partial u}{\partial y}=\frac{1}{\rho}\frac{\partial \tau_t}{\partial y} \quad \textbf{(2-25)}$$

The continuity equation for a two-dimensional turbulent jet is also written as:

$$\frac{\partial u}{\partial x}+\frac{\partial v}{\partial y}=0 \quad \textbf{(2-26)}$$

Equations 2-25 and 2-26 are the equations of motion for a turbulent plane jet. These equations are valid both in the zone of flow establishment and in the zone of established flow. For a more complete derivation of theses equations see Schlichting (1968) and Rajaratnam (1976).

b. In the zone of established flow

It is clear that since there is no external force acting on the plane turbulent jet discharging into an initially quiescent environment that the momentum of the jet

must be constant for all normal sections of a given flow pattern. The integral of the momentum equation 2-25 from y = 0 to y = ∞ can be written as:

$$\frac{d}{dx}\int_0^{\infty} \rho u^2 dy = 0 \qquad \textbf{(2-27)}$$

which means exactly that the rate of change of the momentum flux is zero in the axial direction X and the momentum flux M_o of a plane jet issuing from an orifice of height $2b_o$ with a uniform velocity is therefore obtained by integrating 2-27:

$$M_0 = \int_0^{\infty} \rho u^2 dy \qquad \textbf{(2-28)}$$

The earliest experimental results on plane turbulent jets appear to be those of Forthmann (1934). Further experiments were also conducted by Albertson et al (1948) and Zijnen et al (1958). The experimental results of Forthmann regarding mean velocity distributions at various cross–sections in the region of established flow are reproduced in figure 2-22.

Forthmann found that if the ordinates in figure 2-22 are made dimensionless by dividing them by the appropriate velocity and length scale then the velocity distribution at different cross sections has the same geometrical shape as shown in figure 2-23. U_m is the maximum velocity and b is the value of y where u is equal to half the maximum velocity at every cross-section.

In accordance with the findings by Forthmann that the velocity distribution in the zone of established zone is similar and using equation 2-28, a relationship can be developed for the jet diffusion velocity and length scales as follows:

$$u/u_m = f(y/b) \qquad \textbf{(2-29)}$$
$$where \;\; y/b = \eta$$

$$u_m \propto X^p \; and \; b \propto X^q \qquad \textbf{(2-30)}$$

By substituting 2-29 and 2-30 in 2-28, we obtained:

$$\frac{d}{dx}\rho b u_m^2 \int_0^{\infty} f^2(\eta) = 0 \qquad \textbf{(2-31)}$$

As the definite integral in 2-31 is a constant then it can be conclude that bu_m^2 is independent of X, which means that:

$$2p + q = 0 \qquad \textbf{(2-32)}$$

To evaluate these two unknown exponents, a second equation is needed. According to Rajaratnam (1976), there are four possible methods to develop a solution. These methods consist of (1) the similarity analysis of equations of motions, (2) the integral energy equation, (3) the entrainment hypothesis and (4) the integral moment of momentum equation. Only the shortest method will be detailed below, namely the entrainment hypothesis introduced by Morton et al (1956) in connection with the analysis of plumes. For further details refers to Rajaratnam (1976).

At any section of the jet, the rate of flow per unit length can be written as:

$$Q = 2\int_0^{\infty} u dy \qquad \textbf{(2- 33)}$$

As the jet entrains surrounding fluid, at any cross-section I, the ratio Q/Q_i is greater than unity and increases quickly with X. Therefore, the variation of the forward flow rate per unit length in the axial direction can be expressed as a function of v_e the velocity of entrainment as seen in equation 2-34:

$$\frac{dQ}{dx} = 2\frac{d}{dx}\int_0^{\infty} u dy = 2v_e \qquad \textbf{(2-34)}$$

From dimensional considerations, the entrainment velocity can be seen as a linear function of the maximum velocity by α_e the entrainment coefficient:

$$\frac{d}{dx}\int_0^{\infty} u dy = v_e = \alpha_e u_m \qquad \textbf{(2-35)}$$

$$\frac{\frac{d}{dx}(u_m b)\int_0^{\infty} f(\eta)d\eta}{u_m} = \alpha_e \text{ or } \frac{\frac{d}{dx}(u_m b)}{u_m} \propto X^o \text{ or } p+q-1-p=0 \qquad \textbf{(2-36)}$$

Therefore q = 1 and p = -1/2 and for the plane turbulent jet the velocity distribution can be described by the two following expressions:

$$u_m \propto \frac{1}{\sqrt{x}} \qquad \textbf{(2-37)}$$

$$b \propto x \qquad \textbf{(2-38)}$$

Using the principles of dimensional analysis, useful expressions for the velocity and the length scale can be obtained. It has previously been shown that the maximum velocity at a cross-section can be expressed as a function of the momentum flux , the fluid density and its axial location:

$$u_m = g(M_0, \rho, x) \qquad \textbf{(2-39)}$$

Using the Buckingham π-theorem neglecting the molecular viscosity (as the Reynolds number is large for free jet), and since $M_o = 2b_o\rho U_o^2$ the equation 2-39 can be reduced to:

$$u_m / U_0 = C_1 / \sqrt{x / b_o} \qquad \textbf{(2-40)}$$

where C_1 is a constant. Similarly the length scale can be expressed as a function of the flux momentum, the fluid density and the axial location X and therefore be reduced to the following equation:

$$b / x = C_2 \qquad \textbf{(2-41)}$$

where C_2 is also a constant. Furthermore, it can be demonstrated that the forward flow at any cross-section can be expressed as:

$$Q / Q_0 = C_3 \sqrt{x / b_0} \qquad \textbf{(2-42)}$$

where C_3 is a constant. The unknown constants C_1, C_2 and C_3 have been determined from experimental measurements done by Forthmann (1934), Reichart (1942)and Albertson et al (1948). Summarising all the experimental results, Rajaratnam produced the following convenient results for plane free jets:

$$C_1 = 3.50$$
$$C_2 = 0.10 \qquad \textbf{(2-43)}$$
$$C_3 = 0.44$$

So far the equations of motion provide two equations: the Reynolds equation (2-25) and the continuity equation (2-26) and three unknowns (u, v, and τ). It is therefore necessary to provide a third equation to solve the equations of motion and obtain the velocity distribution.

There are two major possible approaches to the problem, respectively known as the Tollmien (1926) solution and the Goertler (1942) solution. Both solutions are based on the expressions of the turbulent shear stress by Prandtl. Tollmien used the Prandtl mixing length formula (2-44) while Goertler used the second equation of Prandtl (2-45).

$$\tau = \rho l^2 \left(\frac{\partial u}{\partial y}\right)^2 \qquad \textbf{(2- 44)}$$

$$\tau = \rho \varepsilon \frac{\partial u}{\partial y} \qquad \textbf{(2- 45)}$$

where l is the mixing length and ε is the coefficient of kinematic eddy viscosity. Other models of turbulence can be used to predict the velocity distribution for turbulent jets. For more information on the various models used, the reader is referred to Launder and Spalding (1972).

The solution produced by Tollmien is shown in figure 2-24 while the solution found by Goertler is shown in figure 2-25. It was found that near the axis of the jet, Goertler solution is superior to Tollmien solution whereas in the outer regions Tollmien curves fit much better with the experimental data available.

c. In the zone of flow establishment

In the zone of flow establishment between the nozzle to the end of the potential core, an exchange of momentum takes place between a portion of the jet and the stagnant fluid: the stagnant fluid is accelerated while the jet is decelerated. The mixing layer or free shear layer represents the layer of fluid affected by this exchange of momentum. The velocity distribution within this layer has been studied by Liepman and Laufer (1947). They showed the similarity of velocity distribution in plane shear layers. Using the correct shear-stress model, it also possible to develop a relation for the mixing region growth and to predict the mean velocity distribution (Rajaratnam, 1976).

The equations of motion in the zone of flow establishment are the same than in the zone of established flow [Eq 2-25 and 2-26]. If we assume:

$$u/U_0 = f(\eta) \qquad \textbf{(2-46)}$$

$$\tau/\rho U_0^2 = g(\eta) \qquad \textbf{(2-47)}$$

By substituting 2-46 and 2-47 in 2-25 and 2-26, this leads to:

$$b = C_2 x \quad \text{and} \quad y_* = C_{2*} x \qquad \textbf{(2-48) and (2-49)}$$

where C_2 and C_{2*} are two constants and y_* is the value of y where v = 0. For more details, the reader is referred to Rajaratnam (1976).

As for the zone of established flow, there are two solutions to solve the equations of motions in the free shear layer: Tollmien solution and Goertler solution based on the two different expressions of the turbulent shear stress [Eq 2-44 & 2-45].

Liepmann and Laufer (1947) found that Tollmien and Goertler solutions are in good accordance with their experimental observations. The shear layer is included between the lines $\Phi_1 = 0.981$ and $\Phi_2 = -2.040$, therefore the thickness of the shear layer is:

$$\bar{b} = ax(\phi_1 - \phi_2) = 0.263x \qquad \textbf{(2-50)}$$

It can be also note that as the shear layer is included between the lines Φ_1 = 0.981 and Φ_2 = -2.040, then the angles of the shear layer according to the axial direction of the jet are α_1=4.8° and α_2=9.5°.

The length of the potential core x_o is defined as the distance from the nozzle to the point where the mixing layer cross the axe of the jet. Therefore, if $2b_o$ is the height of the jet at the nozzle:

$$x_0 = \frac{b_0}{\tan \alpha_1} = 11.91 b_0 \qquad \textbf{(2-51)}$$

2-5.1.2 *The plane turbulent wall jets*

In the case of plane turbulent wall jet two different layers develop on each side of the turbulent jet when it diffuses in a semi finite medium with similar properties. On the side of the fluid as seen in figure 2-27, a shear layer develops in a similar way than for a plane turbulent free jet but on the side of the flume bed (or wall), a boundary layer develops.

The diffusion pattern is still divided in two regions: the region of flow establishment located between the nozzle and the end of the potential core and the zone of established flow beyond the end of the potential core. The potential core region ends when the boundary layer and the shear layer meet.

Forthmann (1934) found that in the zone of established flow the velocity distributions are similar at all the cross sections.

a. Equations of motion

Proceeding in the same way than in section 2-5.1.1 for the plane turbulent free jet, the equation of motion for a plane turbulent jet can be obtained from the Reynolds Equations [2-20, 2-21 & 2-22] and the continuity equation [2-26] and be written as follow:

$$u\frac{\partial u}{\partial x} + v\frac{\partial v}{\partial y} = -\frac{1}{p}\frac{dp}{dx} + \nu\frac{\partial^2 u}{\partial y^2} + \frac{1}{\rho}\frac{\partial \tau_t}{\partial y} \qquad \textbf{(2-52)}$$

$$\frac{\partial u}{\partial x}+\frac{\partial v}{\partial y}=0 \qquad \textbf{(2-53)}$$

b. Established flow region

In accordance with the findings of Forthmann and in the same optic than for the precedent situation, a relationship can be developed for the jet diffusion velocity and the length scale as follow:

$$u/u_m = f(y/b) \qquad \textbf{(2-54)}$$

where b is the value of y where $u = 0.5u_m$ and $\partial u/\partial y$ is negative.

$$\tau/\rho u_m^2 = g(\eta) \qquad \textbf{(2-55)}$$

By substituting 2-55 and 2-54 in 2-53, the equation of motion can first be reduce. Then by using similarity laws and the integral momentum equation it can be found that for a plane turbulent wall jet:

$$u_m \propto 1/\sqrt{x}, \quad b \propto x \quad \text{and} \quad \tau_0 \propto 1/x$$

where τ_o is the wall shear stress, u_m is the maximum velocity at each cross-section and b is the value of y where $u = 0.5u_m$. If we consider that u_m, b and τ_o can be expressed as function of the flux momentum from the nozzle, M_o, the fluid density, ρ and the axial location, X, by following dimensional consideration, it is possible to show that:

$$u_m/\sqrt{M_0/\rho x} = C_1 \quad \text{or} \quad u_m/U_0 = C_1\frac{1}{\sqrt{x/b_0}} \qquad \textbf{(2-56)}$$

$$b/x = C_2 \quad \text{or} \quad b = C_2\ x \qquad \textbf{(2-57)}$$

$$\tau_0/(M_0/x) = C_3 \quad \text{or} \quad c_F = \frac{\tau_0}{\rho U_0^2/2} = C_3\frac{b_0}{x} \qquad \textbf{(2-58)}$$

where C_1, C_2 and C_3 are constants and c_F is the skin-friction coefficient. According to Rajaratnam (1976), these coefficients can be obtained from experiments conducted for example by Forthmann (1934). Taking into account all the data available, Rajaratnam and Subramanya (1967) came up with the following results for the plane wall jet:

$$C_1 = 3.50$$
$$C_2 = 0.068 \qquad \text{(2-59)}$$
$$C_3 = \frac{0.20}{(U_0 b_0 / \nu)^{1/12}}$$

By comparing the results obtained for a turbulent free jet or a turbulent wall jet, it can be found that the decay of the velocity scale are similar for both situations but the growth of the wall jet in comparison with the free jet is 0.68 time smaller.

c. Flow establishment zone

To determine the length of the potential core, it is important to consider the inward growth of the mixing region as well as the inward growth of the boundary layer. It has been seen that on the fluid side, the shear stress layer spreads inwards at an angle of 4.8°. For the boundary layer, the assumption will be made that the distance from the wall to the maximum velocity level follows the 1/7 power law. The length of the potential core is therefore given by the following equation:

$$0.0875\frac{x_0}{b_0} + 0.37\left(\frac{x_0}{b_0}\right)^{4/5} \frac{1}{(U_0 b_0 / \nu)^{1/5}} = 1 \qquad \text{(2-60)}$$

2-5.1.3 *Three dimensional jet*

In the two precedent paragraphs, the behaviour of plane turbulent free or wall jets has been discussed. However the situations met in this research correspond more to three-dimensional jets as the aspect ratio B/h for the orifices tested is equal to 2 (for the 20 x 10 cm orifice) and 1 (for the 10 x 10 cm orifice).

There are two types of three-dimensional jets: the slender jets and the bluff jets. The distinction between the two is based on the nature of the decay of the centre line velocity. A sketch of the variation of u_{mo}/U_o with x/h is shown in figure 2-29.

For slender jets, the decay of the centre line velocity can be divided in three regions. The first region correspond to the potential core area, thus the velocity is constant. In the second region, the centre line velocity decays at a rate similar as that of plane jet and in the third region, it decays at a rate similar to axisymmetric jets. For bluff jets, the decay of the centre line velocity is only divided into two regions, which correspond to the first and third region of a slender jet. If the aspect ratio B/h is greater than 5, the jet is called a slender jet and if the aspect ratio is smaller than 5, the jet is a bluff jet.

a. Bluff jets

Bluff jets and in particular jets with an aspect ratio equal to 1 have been studied by Yevdjevich (1966), Trentacoste and Sforza (1966,1967) and Pani (1972). Pani (1972) found that the velocity distribution in the Y and Z directions is the same for square orifices. Therefore, if u_{mo} is the centre line velocity, u_m is the turbulent mean velocity in the X direction on the central plane (z = 0) and u is the velocity in the x- direction on any non central plane, then

$$u_m/u_{mo} = f(y/b_y) \quad \text{and} \quad u/u_m = g(z/b_z) \qquad \textbf{(2-61) and (2-62)}$$

And the growth of the length scales b_y and b_z are linear and similar for square nozzle:

$$b_y/h = 0.097x/h \quad \text{and } b_z/h = 0.097x/h \qquad \textbf{(2- 63) and (2-64)}$$

Equation 2-67 is valid for an aspect ratio up to 10 but equation 2-68 is valid only if the nozzle is square (Rajaratnam and Subramanya, 1967), for rectangular nozzle, it is difficult to predict the variation of the length scale b_z.

Using the motion equations, it is possible to demonstrate that for the three-dimensional bluff jet:

$$u_{m0} \propto 1/x \qquad b_y \propto x \qquad \text{and} \qquad b_z \propto x \tag{2-65}$$

Through the use of dimensional considerations and the pi-theorem, it can be shown that:

$$u_{m0}/U_0 = \frac{C\sqrt{A}}{x} \tag{2-66}$$

where A is the cross-sectional area of the nozzle and C is a constant.

b. Bluff wall jets

Bluff wall jets have been studied by Sforza and Herbst (1967) and Rajaratnam and Pani (1974). Like for the bluff free jets, the behaviour of the velocity distribution can be divided into two regions: the potential core region and the radial wall –type decay region.

Rajaratnam and Pani (1974) found that the velocity distribution in the xy and xz planes could be expressed as:

$$u_m/u_{mo} = f(y/b_y) \quad \text{and} \quad u/u_m = g(z/b_z) \tag{2-67) and (2-68}$$

By proceeding in the same way than previously, it is possible to show that:

$$u_{m0} \propto 1/x \qquad b_y \propto x \qquad \text{and} \qquad b_z \propto x \tag{2-69}$$

And finally dimensional considerations will also show that:

$$\tau_{0m} \propto 1/x^2 \tag{2-70}$$

Using their experimental results, Rajaratnam and Pani (1974) were able to demonstrate that the growth of the length scales b_y and b_z is linear but b_z growths faster than b_y:

$$\frac{b_y}{h} = 0.90 + 0.045\frac{x}{h} \quad \textbf{(2-71)}$$

$$\frac{b_z}{B} = 0.20\frac{x}{B} - 1.25 \quad \textbf{(2-72)}$$

where B is the width of the nozzle and h is the height of the nozzle. They were also able to show that in the centre plane of a bluff wall jets, for $x/\sqrt{A}>50$, the skin friction factor is equal to 0.0065.

For more information on the turbulent jets, the reader is referred to Rajaratnam (1976) as well as to the authors cited in the text. The purpose of this last section was simply to demonstrate that the behaviour of a jet passing through an orifice/vertical slot and discharging in a quiescent pool could be simply described.

1. In all the cases of interest for this research, the diffusion pattern can be divided into two regions known as the flow establishment region and the established flow region.

2. Along the jet centreline, the velocity stays constant and equal to the initial velocity at the orifice up to the end of the potential core region and then decays following a simple equation.

3. The growth of the length scale(s) is (are) a linear function of the longitudinal location x.

4. The angles of the shear layer and the length of the potential core can be simply calculated.

2-5.2 *Behaviour of a free falling jet in the atmosphere*

In this section, only the particular case of drop and impact [plunge pool] structures will be considered. In a first part, the hydraulic characteristics of a free falling jet will be simply described and in a second part, the impact phenomenon of the jet in the plunge pool will be explained.

a. Hydraulic characteristics of a free-falling jet

The physical mechanisms describing water jets plunging through the atmosphere are complex. They are also important to understand the hydraulic characteristics of a jet as it impacts with the free water surface of a plunge pool. In this section only the case of a jet passing over a sharp-crested weir with submerged tailwater flow will be considered.

It has already been shown that the conventional equation that quantifies the discharge of an overflow is:

$$Q = C_d Q_{ideal}$$
$$Q_{ideal} = \frac{2}{3} b \sqrt{2g} h_1^{3/2} \qquad \textbf{(2-73)}$$

An attempt was made by Scimeni (1930) and Lencastre (1961) to describe the shape of the free falling free jet. Lencastre (1961) studied using models the spill of overflows for different profiles but he found that the differences between model and prototype generated non-depreciable errors. Scimeni studied with great detail the shape of a free falling jet without lateral contraction and came up with the solution shown in figure 2-31.

In a more simple way, it is possible to determine the nappe trajectory of an aerated nappe by means of the equations of motion if the following assumptions are made: (1) the flow direction at the brink of the weir is horizontal, (2) the horizontal acceleration is zero and (3) the vertical acceleration is opposite to the gravity acceleration. The trajectory equations of the nappe centreline is therefore:

$$x = V_0 t$$
$$y = Ps + \frac{d_0}{2} - \frac{1}{2} g t \qquad \textbf{(2-74) \& (2-75)}$$

where V_o and y_o are the flow velocity and the flow depth at the notch and Ps is the height of the crest. From these equations of motion, it is then possible to determine the length of the drop L, the nappe thickness d_i and the velocity of the jet at impact of the jet with the pool as well as the angle of the falling nappe (Chan-

son, 1994) as function of y_o, the flow depth at the notch, y_{cr}, the critical flow depth, Ps, the height of the crest and h_2 the water surface elevation behind the over falling water:

$$\frac{L}{Ps} = \left(\frac{y_{cr}}{Ps}\right)^{3/2} * \sqrt{\frac{Ps}{y_0}} * \sqrt{1+2\frac{Ps}{y_0}} \qquad \textbf{(2-76)}$$

$$\frac{d_i}{d_c} = \left(\left(\frac{y_{cr}}{y_0}\right)^2 + 2\frac{Ps+\frac{y_0}{2}-h_2}{y_{cr}}\right)^{-1/2} \qquad \textbf{(2-77)}$$

$$\frac{V_i}{V_c} = \sqrt{\left(\frac{y_{cr}}{y_0}\right)^2 + 2\frac{Ps+\frac{y_0}{2}-h_2}{y_{cr}}} \qquad \textbf{(2-78)}$$

$$\tan\theta = \sqrt{2 * \frac{y_0}{y_{cr}} * \frac{Ps+\frac{y_0}{2}-h_2}{y_{cr}}} \qquad \textbf{(2-79)}$$

Assuming that the flow depth at the notch is a linear function of the critical flow such as $y_0 = 0.715\ y_{cr}$, (Rouse, 1936), then the length of the drop L, the nappe thickness d_i and the velocity of the jet at impact of the jet with the pool V_i and the angle of the falling nappe with the horizontal can be expressed as function of the flow Q_w, the height of the crest Ps and the water surface elevation h_2.

b. Impact mechanisms

Xu Duo-Ming et al (1983) and Beltaos & Rajaratnam (1973) have distinguished three zones of impact flow as shown in figure 2-32: (1) the free turbulence zone in the approaching jet or diffusion zone, (2) the zone of impact or zone de deflection and (3) the wall jet zone.

1. Zone 1: free jet

In this zone, the flow has analogue characteristics than the one of a free jet in the atmosphere, although the fluid, in this case, spreads in a medium with the same properties. The pyramid of diffusion displays a kind of widening line, with an angle greater than the one than obtained in the air. In this zone, due to the action of suction of the vortices undulations form on each sides of the jet.

2. Zone 2: zone of impact with the bottom of the flume

The streamlines of the flow are deflected due to the influence of the bottom, the speed decreases and relatively elevated gradients of pressure next to the bottom occur. The deflection of the jet constituted by a mixture of water and air dragged of the atmosphere, when hitting on the bed, produces a high level of turbulence, creating important pressure fluctuations next to the bottom.

3. Zone 3: the wall jet zone

In this zone a submerged rebound usually takes place and the velocity distribution in the main part of the jet has characteristics similar to those of a wall jet.

The turbulence free zone (1) can be treated independently of the influence of the bottom. In the specialised literature, the jet when impacting with the quiescent water of the pool can be analysed from two points of view: as a turbulent jet or as an aired turbulent jet. In the particular case that concerns us, the aeration is not negligible; nevertheless, it is difficult to be modelled, since it depends on the Weber and Reynolds numbers.

Aeration in hydraulic structures is effectively a very complex process and not yet amenable to numeral solution. Ervine (1976) produces an equation for rectangular jets becoming circular, as it is the case in this study. A simplified expression of air/water ratio β is given in equation 2-80 where k is equal to 0.2 for smooth turbulent jets, and k equal 0.3-0.4 for very rough turbulent jets. L is the jet fall through the atmosphere and d the jet diameter.

$$\beta = k\sqrt{L/d}\left(1-\frac{1}{V_i}\right) \qquad \textbf{(2-80)}$$

A further study by Ervine (1998) produced a generalised equation, which fit several physical model studies. q_a is the rate of air entrainment per unit jet width at the plunge point (m^3/sm), and V_i is the jet velocity at plunges point (m^2/s). Equation 2-81 needs to be multiplied by the perimeter of the jet in contact with air to obtain the total flow rate.

$$q_a = 0.00002(V_i - 1)^3 + 0.0003(V_i - 1)^2 + 0.0074(V_i - 1) - 0.0058 \qquad \textbf{(2-81)}$$

The rate of air entrainment is a function of the velocity of the jet at impact with the downstream water surface, and consequently is a function of the head above the crest of the weir, h_1. This equation is valid up to 15 m/s for the jet velocity and for a jet thickness greater than 20-30 mm. The air concentration or void ration can be fixed from the ratio β of air/flow to water/flow ($= q_a/q_w$):

$$C_a = \frac{\beta}{\beta + 1} \qquad \textbf{(2-82)}$$

2-6 Conclusion

Fish passage facilities are devices used to facilitate the migration of fish past dams or any other obstructions along the river corridor. They have a long history and have been used in most areas of the world: Europe, North America, Australia and Asia. Various types of fish pass have been developed over the years to answer different needs correlated to the nature or location of the obstruction as well as to the targeted species. The main designs have been described in this review as well as their advantages and their weaknesses. Further hydraulic modelling studies of more complex designs still need to be conducted, but there is a particular need to conduct controlled experiments with fish. These experiments will provide information to quantify preferences for appropriate hydraulic conditions in the pass and at the entrance to the pass. An understanding of the capabilities and behaviour of targeted species for this kind of research, and therefore collaboration with biological scientists is necessary, as highlighted in this chapter.

Research conducted in this project focused in particular on the optimisation of fish pass for Atlantic salmon (*Salmo salar L.*). Therefore, the next chapter gives some insight into the life cycle, the habitat requirements, the swimming capabilities and the behaviour of Atlantic salmon.

CHAPTER 3:

BIOLOGY OF ATLANTIC SALMON (*SALMO SALAR L.*)

CHAPTER 3:

BIOLOGY OF ATLANTIC SALMON (*SALMO SALAR L.*)

3-1 Introduction

This chapter introduces aspects of the biology that influence the design of fish passage facilities. It is evident from the previous chapter that fish passes are complex hydraulic structures, the designs of which intrinsically depend on the behaviour and the swimming and leaping abilities of the targeted species. Thus some knowledge of biology is required to promote the efficiency of these bioengineering systems. This chapter will briefly describe the life cycle of Atlantic salmon as well as their habitat requirements, swimming abilities and energetics.

Atlantic salmon occur on the eastern and western coasts of the Atlantic Ocean in Europe (UK, Scandinavia, Ireland, France, Portugal, Spain and even Arctic Russia) and in North America (Canada and USA). There is only one species of Atlantic salmon (*Salmo salar*) and it should not be confused with the Pacific salmon (*Oncorhynchus*) which refers to 6 different species: pink, chum, chinook, coho, sockeye and masou. Atlantic salmon are anadromous fishes, which migrate from the sea into fresh waters to spawn. When returning from sea, they range between circa 1 kg and 29 kg. Though fished commercially in certain areas, they

are now exploited chiefly as sport fish. In 1995 salmon caught by rod fishing in Scotland had a net economic value of £350 million.

Since the 1960s, the number of salmon has declined (Parrish et al, 1998). This decline might be in part due to the development of hydroelectric plant along spawning and nursing rivers, over-fishing (Struthers, 1996) or acidification of the water in the spawning rivers (Laine et al, 1993). The upstream movement of spawning salmon can effectively be delayed or blocked by chemical or physical obstructions. In this thesis, chemical obstructions are disregarded and only the physical obstructions will be considered.

Physical obstructions are associated most of the time with waterfalls, rapids, weirs and dams. These obstructions can be classified as total: impassable to all fish at any time, partial: impassable to some fish at all time or temporary: impassable to all fish some of time. Fish passes are devices built to over come these obstructions. However, if the passes are badly adapted to the site, the flow conditions in the river or the targeted species, they can also become obstructions.

3-2 Life Cycle

Atlantic salmon is one of the groups of species that migrates between fresh water and sea at various periods of time in its life cycle and may be classified as an amphibiotic potamotoque migratory. It lives in general in fresh water as a juvenile, migrates to sea where they grow rapidly and returns to fresh water to spawn. However some "land-locked" salmon spend their complete life history in freshwater. They may be geographically isolated and are genetically distinct from anadromous stocks (Berg, 1998).

The life cycle of anadromous Atlantic salmon as described by Youngson and Hay (1996) can also be divided into eight different periods corresponding to eight different morphologic and physiologic changes of the animal. These are, eggs, alevins, fry, parr, smolt, salmon at sea, returning adult and breeding pair as shown in figure 3-1.

Many fish spawn in upland areas and therefore have to move through long stretches of rivers during their migrations.

After hatching (Egglishaw and Shackley, 1977; Mills, 1991), dispersing and taking up station in the river, the salmon (now called "parr") feed on invertebrates from the water column (Egglishaw, 1967) and for much of the time occupy localised areas of substrate (Gibson, 1978; Saunders and Gee, 1964). Salmon may also forage in the substrate (Stradmayer and Thorpe, 1987). The larger parr may also eat fry and ova (Egglishaw, 1967).

Salmon parr are also poikilotherm animals. Their vital activities and growth rate are triggered and controlled by temperature (Crisp, 1996, Elliot, 1981).

Parr are able to hold station in relatively high flow by "adopting a hydrodynamically correct position" (Kalleberg, 1958) and tend to stay close to the streambed. This habit of holding station in contact with the substrate in fast water can be explained by the fact that water velocities decrease logarithmically towards the stream bottom (Hynes, 1970; Smith, 1975). In general parr select their feeding station for a positive ratio: energy gained over energy expended although sheltering from predators is also important (Fausch, 1984; Gibson, 1993).

Even at this stage, the fish have a strong homing urge, and many of them will return to their local area when displaced downstream. During spring, older juvenile parr make upstream movements or downstream (Huntsman, 1945) movements in search of new territories to colonise (Armstrong et al, 1997). A second peak of activity also takes place in autumn. At this time, a large movement of parr occurs (Calderwood, 1906), the majority being precocious males in search of adult females (Buck and Youngson, 1982).

Small stream-dwelling salmon or parr move upstream when displaced downstream (Huntingford et al, 1999) with those individual most strongly attached to a site being more likely to return home. For example, Saunders and Gee (1964) observed that parr displaced up or down stream were observed at their original sites within 14 to 39 days. This capacity to return home has also been demonstrated for

brown trout (*Salmo trutta L*) (Halvorsen and Stabell, 1990; Armstrong and Herbert, 1997).

When the salmon have grown to around more than 9cm (Elson, 1975a and b), which may take from one to as many as eight years (Metcalfe and Thorpe, 1990; Mills, 1991; Gibson, 1993) depending on the food availability and the water temperature, those of them that are destined to migrate change into the marine form (Hoar, 1976) and are called smolts. In Scotland (Youngson and Hay, 1996), the fresh water growth lasts at least one year and in general two or three years.

Smolts leave rivers in the spring.

Salmon remain and feed at sea for a variable number of years before returning to their native river (Mills, 1991). Salmon stay at least one winter at sea (in this case, they are called grilse). They can stay up to four winters before leaving for home water (Hutchings and Jones, 1998). Their return is prompted by the first stages of sexual development.

The returning adults may enter rivers at any time of year, but the run timing varies among rivers. The timing is also likely to depend on the temperature (Webb and McLay, 1996; Heggberget, 1988). Early running salmon or spring salmon start their journey in fresh water in May while some salmon will return to fresh water only in late autumn/early winter (Mills, 1991;Shearer, 1992). Most of the fish have a strong homing urge and return to their natal area of river to spawn.

Because of the migratory habit of the fish, access through rivers is very important. Of key importance are the swimming abilities of fish, and in particular, how these relate to size and temperature.

3-3 Atlantic Salmon abilities

The objectives of this section is to provide information on the swimming speeds, swimming distances and leaping capabilities of juvenile and adult Atlantic

salmon in order to evaluate the passability of fish passage facilities and the different degrees of difficulties salmon encounter to go through them.

3-3.1 *Three levels of swimming speed*

The design of fish passage facility mainly depends on the swimming abilities of the fish. Fish have three levels of speed (Beach, 1984; Bell, 1973; Webb, 1975; Beamish, 1978), which depend on the type of muscles used:(1) the cruising speed or sustained activity level, (2) the sprint speed or burst activity level and (3) the sustained speed or prolonged activity level as shown in Table 3-1.

Table 3-1: Nominal upper limits of swimming speeds for adult Atlantic salmon (in Powers and Orsborn, 1985)

	Cruising speed	Darting speed	Burst speed
Salmo salar L	1.22 m/s	3.7 m/s	7.00 m/s

a. The cruising speed

The cruising speed corresponds to a speed that the fish will be able to maintain for a long period of time. At this speed, the fish exhibit aerobic activity and uses mostly red muscle. The nominal upper limit of cruising speed of adult Atlantic salmon has been estimated to be typically around 2-3m/s (Blaxter, 1969).

b. The darting speed

The darting speed corresponds to a single and intense effort. The fish will not be able to maintain it for more than 15-20 seconds. The fish is using its white muscles with energy derived from anaerobic processes, which results in fatigue. The nominal upper limit of burst speed of Atlantic salmon has been estimated from leap height of 3.5 m and is around 6-8 m/s (Bell, 1973).

c. The sustained speed

The sustained speed corresponds to a speed the fish will be able to maintain for only few minutes before feeling tiredness. The nominal upper limit of sustained speed of adult Atlantic salmon is typically around 4-5 m/s.

salmon in order to evaluate the passability of fish passage facilities and the different degrees of difficulties salmon encounter to go through them.

3-3.1 *Three levels of swimming speed*

The design of fish passage facility mainly depends on the swimming abilities of the fish. Fish have three levels of speed (Beach, 1984; Bell, 1973; Webb, 1975; Beamish, 1978), which depend on the type of muscles used:(1) the cruising speed or sustained activity level, (2) the sprint speed or burst activity level and (3) the sustained speed or prolonged activity level as shown in Table 3-1.

Table 3-1: Nominal upper limits of swimming speeds for adult Atlantic salmon (in Powers and Orsborn, 1985)

	Cruising speed	Sustained speed	Burst speed
Salmo salar L	1.22 m/s	3.7 m/s	7.00 m/s

a. The cruising speed

The cruising speed corresponds to a speed that the fish will be able to maintain for a long period of time. At this speed, the fish exhibit aerobic activity and uses mostly red muscle. The nominal upper limit of cruising speed of adult Atlantic salmon has been estimated to be typically around 2-3m/s (Blaxter, 1969).

b. The burst or spring speed

The darting speed corresponds to a single and intense effort. The fish will not be able to maintain it for more than 15-20 seconds. The fish is using its white muscles with energy derived from anaerobic processes, which results in fatigue. The nominal upper limit of burst speed of Atlantic salmon has been estimated from leap height of 3.5 m and is around 6-8 m/s (Bell, 1973).

c. The sustained speed

The sustained speed corresponds to a speed the fish will be able to maintain for only few minutes before feeling tiredness. The nominal upper limit of sustained speed of adult Atlantic salmon is typically around 4-5 m/s.

According to Bell (1973), the speed, at which a fish swims, depends on the context. It employs cruising speed for routine activities, foraging, holding or schooling. It uses sustained speed to go through difficult areas such as high velocities zones and it uses burst speed only for escape purpose, feeding or to negotiate high water velocities.

The speed at which a fish swims depends also on its condition. The fish does not effectively have the same capabilities if it is just fresh out of salt water or if it is very close to the spawning ground and has used most of its energy reserves. Powers and Orsborn (1985) identified three coefficients (C_F) of fish condition to take into account the different conditions of the fish during its spawning journey. These coefficients are shown in table 3-2. For example at a waterfall, the speed of a fish will be:

$$V_F = C_F V_{FB} \tag{3-1}$$

where V_{FB} is the burst speed of the fish and V_F is the actual speed of the fish.

Table 3-2: Coefficient of fish condition (from Powers and Osborn, 1985)

Fish condition	Coefficient, C_F
Bright: fresh out of salt water	1.00
Good: in the river for a short time	0.75
Poor; in the river for a long time	0.50

The swimming abilities of a fish depend mainly on its length and on the temperature of the water. The swimming speed is actually closely related to the tail beat frequency of the fish and the distance done during each body wave corresponds approximately to 0.7 (between 0.6 and 0.8) of the fish length (Wardle, 1975).

Through a series of experimental studies, Wardle (1975) found an empirical formula relating the maximum swimming speed to the muscle twitch contraction time and Zhou (1982) obtained the empirical formula relating the muscle twitch contraction time to the length of the fish and the temperature of the water.

$$U = 0.7 L/2t$$
$$t = 0.1700 L^{0.4288} + 0.0028 \log_e T - 0.0425 L^{0.4288} \log_e T - 0.0077 \tag{3-2}$$

where U is the maximum swimming speed, L is the length of the fish and T is the muscle temperature. 0.7 is a coefficient defining the distance moved through the water for each body wave. Figure 3-2 represents the maximum speed against fish length over a temperature range of 2 to 25^{0}C for salmonids (Beach, 1984).

3-3.2 *Swimming speed and Endurance*

For each swimming speed is associated an endurance. It corresponds to the period of time a fish will be able to face a fixed water velocity. Endurance depends on the stock of glycogen in the muscles. The fish starts to use this stock as soon as it swims at a speed higher than the cruising speed. The rate of diminution of this store depends on the length of the fish, its morphology and the water temperature. If the store of glycogen is completely depleted, the fish will need a relatively long period of rest and oxygen to rebuild it (Wardle, 1978). Zhou (1982) derivated also the endurance time versus the fish length and the temperature as shown in equation 3-4.

$$t_m = E/(P_c - P_r)$$

where

$$E = 1790 * 10.836 L^{2.964} \qquad \textbf{(3-3)}$$

$$P_c = 0.9751 * e^{-0.00522T} * U^{2.8} * L^{-1.15}$$

$$P_r = 4.44 * 10.836 L^{2.964}$$

The endurance time t_m (s) is a function of the total energy store E (J) divided by the difference between the potential chemical power P_c (W) and the power from oxygen uptake P_r (W). The endurance time depends finally on the length of the fish (L), its swimming speed (U) and the temperature of the water (T).(Figure 3-3)

3-3.3 *Maximal distance covered by fish*

Knowing the mean endurance time and swimming speed of a fish (using empirical or experimental data) at a given water velocity and temperature, it is possible

to determine the mean swimming distance, the fish will be able to cover. This distance can simply be given by the formula:

$$D = (V_f - V_w)t \tag{3-4}$$

where D (m) is the swimming distance completed by fish swimming at the speed V_f (m/s) against a flow of mean velocity V_w (m/s).

Ziemer (1961) and Evans & Johnston (1980) provided a semi –empirical equation to express the relation between the water velocity and the maximal swimming distance for salmon and trout. However this semi-empirical formula used by Ziemer ignores the influence of the water temperature on the swimming capacity of the fish.

Using only empirical relations, Larinier (1992) proposed the maximum swimming distance versus water velocity and temperature for salmonids of length 0.20 m or 0.35 m.

Colavecchia et al (1998) did also experiments in an Ichthyo-hydraulics flume to measure the swimming ability of 78 adult Atlantic salmon. For mean water temperatures of 9.3^{0}C to 19.2^{0}C, mean water velocities ranged from 1.6 to 3.2 m/s, the average burst speeds ranged between 2.1 and 4.5 m/s with mean swimming distances between 11.7 and 17.6 m, while the mean endurance time ranged between 9.0 and 33.5 s.

3-3.4 *Leaping abilities*

Atlantic salmon and other salmonid species are able to jump in order to clear obstacles such as waterfalls. The success of the leap depends on several factors including geographical and hydraulic conditions at the bottom of the obstacle. These factors are the height of the fall, the presence of a standing wave, and the depth of the pool at the base of the fall. According to Stuart (1964), the force of impact of the falling water is the stimulus that will cause a move forward to leap over the weir. The standing wave or hydraulic jump created by the falling water is also closely related to the success of the leap. Stuart observed that the initiation

of the leap commences very near the water surface just downstream of the standing wave. In fact, the motion of a salmon leaping over a waterfall can be associated with a projectile trajectory. Neglecting the resistance of the air, equations for projectile motion are as follow:

$$x = (V_0 \cos\phi)t$$
$$y = (V_0 \sin\phi)t - \tfrac{1}{2} g t^2 \qquad \textbf{(3-5)}$$

where V_o is the initial velocity of the fish, ϕ is the angle of leap from the water surface for the fish, x and y are the longitudinal and vertical distances travelled by the fish and t is the time of travel. The trajectory of the leaping fish is then a parabolic. If we make the assumption that at the highest point of the fish's leap, its vertical velocity is zero, then:

$$t = \frac{1}{g} V_0 \sin\phi$$

hence

$$\text{Xmax} = \frac{1}{g} V_0^2 \cos\phi \sin\phi \qquad \textbf{(3-6)}$$

and

$$\text{Ymax} = \frac{1}{2g} V_0^2 \sin\phi \sin\phi$$

X_{max} and Y_{max} are the maximal horizontal and vertical distances traveled by the fish with an initial velocity V_o. The maximum height of the fish's leap depends therefore on the water temperature and its length.

However these equations (3-7) provide only conservative values as the additive effects of the fish length or the standing wave are neglected. Aaserude (1984) effectively noted that the effective leaping height above the water surface is Ymax plus the fish's length L as the fish uses its propulsive power until its tail leaves the water. Stuart (1962) noted also that fish use the upward velocity component or standing wave present at the foot of a waterfall to leap.

3-4 Interaction between water and Atlantic salmon

In this section, the physical property of water and the hydrostatic and hydrodynamic interactions between salmon and water are introduced. Emphasis is put on density and viscosity. Density has an important role in the static and dynamic interaction between the fish and the water it swims through. Viscosity is the main source of drag during swimming and therefore determines the flow pattern in the boundary layer close to the fish.

There is an interaction between salmon and the water it lives in. The morphology, physiology or even behaviour of salmon are governed by the physical laws of (1) conservation of mass, (2) energy and (3) momentum. It will be shown further in this section that Archimedes' law; Newton principles and Bernoulli equation describe the main forces and momentum acting on a fish swimming through a body of water.

3-4.1 *Property of water*

Fresh water is considered as almost incompressible with a density of 1000 kgm^{-3} and a viscosity of 0.0011 Nsm^{-2} for a water temperature of 15°C and an atmospheric pressure of 1 Atm. Viscosity and density of water decrease while the temperature increases and increase with the salinity of the water. The ratio of dynamic viscosity over density is called the kinematic viscosity. It decreases as temperature increases.

3-4.2 *Reynolds and Froude numbers*

Two dimensionless parameters: the Reynolds number (Re) and the Froude Number (Fr) are important in the hydrodynamics of swimming fish. The Reynolds number is the ratio of inertial forces over viscous forces: it expresses the relative importance of inertial forces over viscous forces in a dimensionless way. The Froude number is the ratio of inertial forces over gravity force.

$$\mathrm{Re} = UL\rho_w \,/\, \mu = UL/\nu$$
$$Fr = U \,/\, (gL)^{0.5} \qquad (3\text{-}7)$$

where U is the fish speed (m/s), L is the fish length (m), ρ_w is the water density (kg/m^3), μ is the viscosity (kg/ms), ν is the kinematic viscosity (m^2/s) and g is the gravitational acceleration (=9.81 m/s^2).

All swimmers (fish, dolphin, whales...) with a Reynolds number greater than 10^4 are called nekton (Videler, 1993): they travel independently of the water motion and the main forces acting on them are the horizontal thrust and drag forces. The majority of fish swimming in fresh or saline water have a Reynolds number between 10^5 (herring) and 10^7 (tuna). It is important to notice that for a fish swimming at the same speed, the Reynolds ratio decreases, and hence the viscous forces increase as the temperature decreases.

The Froude number is particularly useful when fish swim near the water surface as they might create additional drag by generating waves (Katopodis, 1998).

3-4.3 *Forces acting on the fish*

The forces, which might act on a swimming salmon, are: gravity forces, pressure forces, viscosity, virtual mass forces, surface tension or even water elasticity (Videler, 1993; Webb, P.W. and D. Weihs, 1983). Most of the time, the two last components are negligible in comparison with the four first components. Inertia forces are caused by acceleration of a mass of fluid and the resistance of the fluid to shearing motion causes viscosity. Viscosity is the main drag force. For salmon swimming in a river, the gravity forces are balanced by buoyancy.

Figure 3-5 depicts the various fundamental forces acting on a swimming fish. W is the fish's weight, B is the buoyant force, D is the drag force and P is the propulsive force generated by the fish.

a. Archimedes law:

According to Archimedes law, the buoyancy B equals the weight of the displaced mass of water. This is shown in equation 3-9 where B is the buoyant force acting on the fish, V is the volume of the fish, g is the acceleration and ρ_w is the water density. The position of the centre of buoyancy is determined by the volume distribution along the body.

$$B = V\rho_w g \tag{3-8}$$

Equation 3-9 is a particular case of the fundamental law of fluid mechanics shown in equation 3-10. This law states "at any point in the fluid the buoyant force per unit volume of fluid displaced is equal but opposite in direction to the vector gradient of the pressure, Vp". Equation 3-9 applies only if the streamlines are straight, parallel and horizontal and if the water surface is horizontal.

$$\vec{B} = (-\overline{\forall} p)(V) \tag{3-9}$$

The weight of the fish is a function of the average density of the fish ρ_f, its volume and the acceleration g due to gravity as shown in equation 3-11. The centre of mass is relative to the densities of the different part of the fish.

$$W = V\rho_f g \tag{3-10}$$

For the situation shown in figure 3-5, if the density of the fish is equal to the density of the water, the buoyant force and the weight of the fish are equal and opposite, and hence cancel each other. Therefore the only forces acting on the fish, in this particular case, are the drag force and the thrust or propulsive force.

b. Bernoulli equation:

For incompressible fluid, the principle of energy conservation can be written as:

$$p + 0.5\rho U^2 + 2\rho g z = Cst \tag{3-11}$$

where U is the velocity, ρ_w is the water density and *Cst* is a constant. If the potential or elevation head is constant, then the Bernoulli equation can be rewritten as:

$$p + 0.5\rho_w U^2 = Cst \qquad \textbf{(3-12)}$$

The drag force described in the semi-empirical equation 3-14 is a function of the surface area A, a drag coefficient C_d as well as the dynamic pressure $0.5\rho wU^2$ expressed in equation 3-13. Behlke (1991) assumed A to be equal to bL^2 where L is the fish length and b a dimensionless coefficient.

$$D = (0.5\rho_w U^2)AC_d \qquad \textbf{3-13}$$

Based on the work done by Rosen (1959) and Aleyev (1977), Videler (1993) extrapolated the impact of a swimming fish on the water around it .The effects of the fish on the water are depicted in figure 3-6.

The layer of water very close to the fish travels at the same speed as the fish because of the viscosity. This layer of water is called the boundary layer and its thickness corresponds to the distance between the fish and the last particles affected by the viscosity. Water beyond this layer is not dragged. The gradient of velocity created in this way by the difference of particle speeds causes a skin friction drag between the particles of water. This drag is proportional to the surface area of the fish A. A difference of pressure also occurs along the body of the fish. This is the result of the congestion created by the water in front of the upper part of the fish when this water has to give way to the moving fish. This pressure drag is proportional to the dynamic pressure given in equation 3-14.

The drag coefficient C_d depends on the geometry of the fish body and on its Reynolds number (Eq 3-8). Using the work done by Brett (1964) on young sockeye salmon, Ziemer and Behlke (1966) developed an empirical relationship given in equation 3-15 below.

$$C_d = 3.3 / R_e^{0.417} \qquad \textbf{(3-14)}$$

Webb (1975) recommended another empirical equation for the drag coefficient. In the following equation, k is a dimensionless coefficient varying from 3 to 5.

$$C_d = 0.072k / R_e^{0.2} \quad \textbf{(3-15)}$$

If equations 3-8, 3-15 and 3-16 are combined, the profile drag is expressed as:

$$D = 0.036bk\rho v^{0.2} L^{1.8} U^{1.8} \quad \textbf{(3-16)}$$

where L is the fish length, U is the velocity of the fish with respect to the water, ρ_w is water density, ν is the kinematic viscosity of the water and b and k are two dimensionless coefficients depending on the fish.

c. Newtons law:

The second law of Newton, in the absence of any external forces can be expressed as "The rate at which the velocity of a fish changes is equal to the resultant of all forces on the fish divided by its body mass"(Webb, 1975) and is given in equation 3-17. M is the mass of the fish and a(t) is the acceleration of the fish.

$$\sum \overrightarrow{F(t)} = m\overrightarrow{a(t)} \quad \textbf{(3-17)}$$

However when a fish accelerates, it carries some of the surrounding fluid with it. This surrounding fluid with a mass M_a is accelerated with the fish. Therefore equation 3-17 becomes:

$$\vec{F}_{vm} = (M + M_a)\vec{a} \quad \textbf{(3-18)}$$

where $M+M_a$ is the virtual mass of the fish, a is the acceleration of the fish and F_{vm} is the virtual mass force experimented by a fish when it accelerates. Webb (1975) assumed M_a to be equal to 0.2M. For a steady flow, and if considering a 1-dimensional motion, the acceleration a can be expressed in the following finite element form:

$$a = U\frac{\Delta U}{d} \quad \textbf{(3-19)}$$

where U is the mean velocity of the fish with respect to the water between two points, d is the distance apart this two points and ΔU is the difference of velocity between the two points.

At waterfalls during the leaping of the fish or at vertical slots where water accelerates, this virtual mass force acts in fact against the forward progress of the fish and should not therefore be neglected.

d. Propulsive force or Thrust

In accordance with the second law of Newton, the propulsive force P is equal and opposite to the resultant of the forces previously described: Weight, Buoyancy, Drag and Virtual Mass.

$$\vec{P} = \vec{B} + \vec{D} + \vec{W} + \vec{F_{vm}} \qquad \textbf{(3-20)}$$

The propulsive force P is therefore a function of L, the length, U the speed and a the acceleration of the fish, ρ the density, ν the kinematic viscosity of the water, and g the gravitational acceleration.

The power delivered by the fish to its surrounding while it swims is function of its speeds with respect to the water and the propulsive force (Eq 3-22) and the energy spent by the fish to pass a structure is expressed in equation 3-23.

$$Pwr = PU \qquad \textbf{(3-21)}$$

$$E = \int_0^t Pwr\,dt \qquad \textbf{(3-22)}$$

To use as little energy as possible, a fish should move as fast as possible. To reduce also their consumption of energy fish have to try to reduce their propulsive force by reducing their speed (Videler, 1993).

Behlke (1987, 1988, 1991) and Behkle et al (1993) gave detailed explanations of energy and power requirements for a fish swimming through a lake, a steep channel (or chute) and a culvert. It demonstrated the importance of non-Archimedean forces as well as the virtual mass forces at a fish passage structure.

The principles and forces described in this section will be further discussed and used in Chapter 7.

3-5 Conclusion

In the previous sections of this chapter, the life cycle of Atlantic salmon has been briefly described; the habitat requirements of the juveniles (parr) and of the spawning adults (salmon) have also been briefly introduced. It has been demonstrated that swimming and leaping abilities of salmon depend mainly on the water temperature and their size.

The physical laws of mass, energy and momentum conservation govern the motion of salmon through water. Therefore, in this chapter, the difference forces acting on a fish moving have been identified and described. They are the weight, the drag, the buoyancy, the virtual mass and the propulsive forces.

CHAPTER 4:

EXPERIMENTAL FACILITIES

CHAPTER 4:

EXPERIMENTAL FACILITIES

4-1 Introduction

This chapter describes the experimental set-up for two physical model tests conducted, one at Almondbank, Perth, testing parr, and the other one at Glasgow University measuring hydraulic phenomena. Both models test a range of flow conditions and a range of devices including weirs, vertical slots, orifices and combinations of the three precedent devices.

At an early stage of the project, the possibility of obtaining both field scale hydraulic measurements and data on the behaviour of spawning salmon at the fish pass of a hydroelectric dam was considered. A valuable approach to studying movements of salmon through fish passes is effectively to track remotely the behaviour of large numbers of wild fish in natural situations (Smith & al, 1994; Gowans & al, 1999).

However, the behaviour of salmon in the wild is influenced by so many factors that research based only on field surveys alone may not establish clearly the behavioural mechanisms that enable approaching fish to locate passes efficiently.

Furthermore, field studies generally do not permit an experimental analysis of how modifying aspects of fish pass designs influences the behaviour of fish.

In this work it was been decided to use model studies at least initially, completed by field studies in the later stages. A complementary method to field studies is the use of scaled-down model passes coupled with observations of juvenile salmon (Stuart, 1962). We used such a system to compare the hydraulic characteristics of a number of types of fish pass including weirs, vertical slots, submerged orifices and other combinations.

The work described in this chapter concerns the design, construction, calibration, instrumentation and running of two scale down models of a portion of a river downstream of a dam, weir or any other obstruction to fish migration as shown below in figure 4-1.

Two identical flumes were built, one at Almondbank, the rearing station unit of the Freshwater Fisheries Laboratory and the other in the hydraulic laboratory of Glasgow University. The flume at Almondbank was used to observe behaviour of the fish and the flume at Glasgow was used to make detailed measurement of the hydraulics such as flow patterns, velocity and turbulence of the approach area over a range of water flow.

4-2 General consideration of the models

Four basic types of openings were tested: weirs, orifices, vertical slots and combinations of the three over four biological series of tests. Over the two summers periods of 1999 and 2000, a total of 33 hydraulic cases have been tested. These 33 situations are linked to 12 structures as seen in figure 4-2 and table 4-1.

Two types of weirs were tested: a contracted rectangular weir and a partially contracted weir. Both designs had a 0.20 m wide and 0.30 m height crest. Two different water surface elevations downstream the weir were tested: 0.20 m and 0.30 m.

Orifices investigations were restricted to three rectangular designs as shown in figure 4-2. The first design had an opening of 0.10 m high by 0.20 m wide. The second design had a smaller opening with a width of 0.10 m and a height of 0.10 m. Each may take on two different locations either in the middle or at the side of the flume. The orifices may also take three different elevations in the water column: at the bottom of the flume, at 0.05 m and 0.10 m from the bottom of the flume.

Two additional particular designs were also tested. The 0.10 by 0.10 m orifice located at the bottom of the flume on the side was associated (1) with a weir or (2) with another 0.05 by 0.50 m orifice blocked by a grid as shown in figure 4-2.

Two vertical slot designs were tested. Both were located on the side of the flume. The width of the slot was 0.05 or 0.10 m wide as shown in figure 4-2. All designs were generally tested for two typical discharges: 0.012 and 0.02 m^3s^{-1}.

For brevity, each test run was coded as follow: $WS_{12\text{-}\ 0.2}$ where W denotes weir, S the side of the flume, 12 the flow in litres per seconds and 0.2, the water depth in metres downstream of the weir. For other cases, Ob denotes orifice at the bottom, O denotes orifice and V denotes the vertical slots. 5 and 10 denote the width of the vertical slot 0.05 and 0.10 m, F and T denote the location of the orifice at 5 and 10 centimetres from the bottom respectively, 0.3 denotes the water depth downstream of the weir and 20 the flow in litres per second. For the orifices, 0.01 and 0.02 denote the area of the orifice.

Table 4-1: Designs tested

Code	Details	Nber of hydraulic situations tested
WS	Weir on the side	2
WM	Weir in the middle	3
$ObS_{0.02}$	Orifice on the side: 0.20 x 0.10 m	2
$ObS_{0.01}$	Orifice on the side :0.10 x 0.10 m	2
$ObM_{0.02}$	Orifice in the middle:0.20 x 0.10 m	2
$ObM_{0.01}$	Orifice in the middle :0. 10 x 0.10 m	1
$OFM_{0.02}$	Orifice at 0.05m from the bottom in the middle:0.20 x 0.10 m	2
$OTM_{0\ 02}$	Orifice at 0.10 m from the bottom in the middle:0.20 x 0.10 m	2
V5	Vertical slot 0.05 m wide	2
V10	Vertical slot 0.10 m wide	2
$WOb_{0\ 02}$	Orifice at the bottom :0.20 x 0.10 m associated with a weir	2

A special codification was adopted for the last series with the double orifices shown in figure 4-2. That it to say, each test run was coded as follow: AR_{12} where A denotes the flow ratio between the two orifices, e.g. 1:1, R denotes the introduction of the parr on the right side and 12 the flow in litre per seconds. For other cases, B denotes the flow ratio 1:5, L the introduction of the parr on the left side and 20 the flow in litre per seconds.

Table 4-2: Designs tested

Code	Details	Number of hydraulic situations tested
AR	Double orifices with ratio 1:1, parr introduced on the right side	2
AL	Double orifices with ratio 1:1, parr introduced on the left side	2
BR	Double orifices with ratio 1:5, parr introduced on the right side	2
BL	Double orifices with ratio 1:5, parr introduced on the left side	2

4-3 Experimental apparatus at Almondbank

4-3.1 *Physical Model*

The physical model at Almondbank designed by the author consisted of a flume 1,22 m wide, 6 m long and 0.8 m high provided with a continuous through-flow of water from the River Almond at a maximum discharge of 0.045 m^3s^{-1}. The flume was constructed of plywood and steel. A tilting gate at the end of the flume enabled control of the water level downstream of the dam. A slot gate upstream of the weir enabled regulation and control of the flow going through the weir/ orifice/ vertical slot/ combination opening. This is shown in figure 4-3.

The physical model is a simplified representation of a portion of a river downstream of a dam, weir or any other obstruction to fish migration. A removable/vertical crosswall 1.22 m wide with an opening 0.20 m by 0.10 m divides the flume into two pools.

A general view of the physical model at Almondbank is shown in figure 4-4 and two photos taken during the reconstruction of the flume in spring 2000 are shown in figures 4-5 and 4-6.

4-3.2 *Test series*

The biological experiments were divided in five series over spring/summer 1999 and spring/summer 2000. Table 4-3 shows the division of the 5 series over the years 1999 and 200.

In series 1, a weir, an orifice at the bottom of the flume; orifices at higher elevations (0.05 m or 0.10 m from bottom of the flume) were compared. Each opening was tested both in the middle and at the side. There were thus six different designs and each was tested at two different discharges 0.012 and 0.020 m^3s^{-1}. This experimental set up gave 12 different situations as shown in table 4-3.

In series 2, a weir and two orifices at the bottom of the flume were considered. The openings were tested only in the middle and for a sole discharge of 0.012 m^3s^{-1}. These three scenarios completed the previous group of 12 as shown in table 4-3.

In series 3, a weir, an orifice at the bottom of the flume, an orifice associated with a weir, and two vertical slots were compared. The openings were tested only at the side for two discharges 0.012 $m^3s^{-1}$and 0.020 m^3s^{-1}. Thus in this series, there were 10 different situations as shown in table 4-3.

In the last series of experiments, only one design was considered. It integrated two orifices: one representing the entrance to the fish pass and the other one, blocked by a grid, representing the water coming from the powerhouse or the spillway. It was tested at two different discharges: 0.012 m^3s^{-1} and 0.020 m^3s^{-1}, for two different flow ratios noted A (1:1) and B (1:5) between the orifices and for two locations of introduction of the parr, right or left side of the flume. For the flow ratio 1:1, the flows are the same through the two orifices. For the ratio 1:5, the flow from the 0.10 x 0.10 m orifice is 5 times smaller than the flow from the 0.10 x 0.50 m orifice. In the previous series, the parr had only been introduced on the right side of the flume, looking upstream. It gave 8 different scenarios as shown in table 4-3.

Table 4-3: Division of situations in series

Code	Details	Nber of parr
	Series I: July - September 1999	**240**
$WS_{12\text{-}0.2}$	Weir on the side at low flow – wsel = 20cm	20
$WS_{20\text{-}0.2}$	Weir on the side at high flow - wsel = 20cm	20
$WM_{12\text{-}0.2}$	Weir in the middle at low flow - wsel = 20cm -	20
$WM_{20\text{-}0.2}$	Weir in the middle at high flow - wsel = 20cm	20
$ObS_{12\text{-}0.02}$	Orifice at the bottom on the side at low flow – area orifice = 0.02 m^2	20
$ObS_{20\text{-}0.02}$	Orifice at the bottom on the side at high flow – area orifice = 0.02 m^2	20
$ObM_{12\text{-}0.02}$	Orifice at the bottom in the middle at low flow– area orifice = 0.02 m^2	20
$ObM_{20\text{-}0.02}$	Orifice at the bottom in he middle at high flow– area orifice = 0.02 m^2	20
$OFM_{12\text{-}0.02}$	Orifice at 5 cm from the bottom at low flow – area orifice = 0.02 m^2	20
$OFM_{20\text{-}0.02}$	Orifice at 5 cm from the bottom at high flow– area orifice = 0.02 m^2	20
$OTM_{12\text{-}0.02}$	Orifice at 10 cm from the bottom at low flow – area orifice = 0.02 m^2	20
$OTM_{20\text{-}0.02}$	Orifice at 10 cm from the bottom at high flow – area orifice = 0.02 m^2	20
	Series II: June 2000	**60**
$WM_{12\text{-}0.3}$	Weir in the middle at low flow - wsel = 30cm -	20
$ObM_{12\text{-}0.02}$	Orifice at the bottom in the middle at low flow– area orifice = 0.02 m^2	20
$ObM_{12\text{-}0\,01}$	Orifice at the bottom in the middle at low flow– area orifice = 0.01 m^2	20
	Series III: August 2000	**320**
$WS_{12\text{-}0.2}$	Weir on the side at low flow – wsel = 20cm	20
$WS_{20\text{-}0.2}$	Weir on the side at high flow - wsel = 20cm	20
$ObS_{12\text{-}0.01}$	Orifice at the bottom on the side at low flow – area orifice = 0.01 m^2	40
$ObS_{20\text{-}0.01}$	Orifice at the bottom on the side at high flow – area orifice = 0.01 m^2	40
$WOb_{12\text{-}0.01}$	Orifice at the bottom associated with a weir at low flow – a = 0.01 m^2	40
$WOb_{20\text{-}0.01}$	Orifice at the bottom associated with a weir at high flow – a = 0.01 m^2	40
$V5S_{12}$	Vertical slot 5 cm wide on the side at low flow	40
$V5S_{20}$	Vertical slot 5 cm wide on the side at high flow	40
$V10S_{12}$	Vertical slot 10 cm wide on the side at low flow	20
$V10S_{20}$	Vertical slot 10 cm wide on the side at high flow	20
	Series IV: September 2000	**160**
AR_{12}	Double orifices with ratio 1:1, parr introduced on the right side at low flow	20
AR_{20}	Double orifices with ratio 1:1, parr introduced on the right side at high flow	20
AL_{12}	Double orifices with ratio 1:1, parr introduced on the left side at low flow	20
AL_{20}	Double orifices with ratio 1:1, parr introduced on the left side at high flow	20
BR_{12}	Double orifices with ratio 1:5, parr introduced on the right side at low flow	20
BR_{20}	Double orifices with ratio 1:5, parr introduced on the right side at high flow	20
BL_{12}	Double orifices with ratio 1:5, parr introduced on the left side at low flow	20
BL_{20}	Double orifices with ratio 1:5, parr introduced on the left side at high flow	20

4-3.3 *Protocol of tests*

Seven hundred and eighty hatchery-reared salmon parr (length range: 8–14 cm) were used during the investigation (240 between July 1999 – September 1999 and 540 between June 2000 - September 2000). The fish were held in a large tank (2m diameter) supplied with a constant flow of aerated water from the river. Water from the holding tank was pumped into the flow entering the flume to provide a possible olfactory stimulus to facilitate homing behaviour. Each fish was han-

dled only once and placed in another tank subsequently. Fish were fed to satiation, once daily.

For each design of fish pass entrance, 20 or 40 fish were tested individually. Each fish was left in the flume at least 40 minutes before being removed if it did not go through the device (weir, vertical slot, orifice,...). The protocol was to assemble the type of pass entrance to be tested. Then a fish was captured and released as quickly as possible at the downstream end of the flume adjacent to the viewing window. The location of parr introduction is shown in figure 4-7.

For each series, the different types of fish pass tested were alternated sequentially as the trials progressed to avoid any seasonal variations influencing the results.

4-3.4 *Direct observation and video recording*

The fish were observed continually from time of introduction to the flume and records were made of changes in position with time. Video recordings using a network of cameras in the upstream half of the flume supplemented the direct observations. These cameras focused particularly on the behaviour of the fish near the pass entrance.

Eight small waterproof cameras were placed in the upstream zone of observation, inside or outside the flume as shown in figure 4-8. These cameras were connected to an eight channels duplex multiplexer, itself connected to a videocassette recorder and a monitor. This is shown in figure 4-9. A digital camera, placed above the flume, was also occasionally used to record precisely the position of the fish as a function of the time.

4-3.5 *Influence of temperature on tests*

The first series of experiments were done between July and September 1999. During this period, the temperature of the water in the flume varied between 11.3^{0}C and 19.2^{0}C, the mean temperature being 14.9^{0}C as shown in figure Fig 4-10.

The second series was run over two weeks in June 2000 [12/6 to 24/06]. The temperature of the water varied between 12.8^{0}C and 17.5^{0}C [mean = 15.34°C] as shown in figure 4-11. The third series was conducted in August 2000 [01/08 to 31/08]. The temperature of the water over the month varied between 12.6^{0}C and 18^{0}C [mean = 15.47°C]. The last series of experiments was done in September 2000 [01/09 to 22/09]. The temperature of the river during this month was lower. It varied only between 9.3^{0}C and 13.5^{0}C [mean = 11.57°C]. The averaged temperature of the water over the three months between June and September 2000 is 14.6^{0}C.

Temperature of water affects swimming performance of salmon (Beach, 1984). Typically, the maximum swimming speed increases with the temperature (Fig 4-12) whereas the time of endurance at the maximum speed decreases with increasing water temperature. An eight cm parr has a maximum swimming speed between 1.2 and 1.8 m/s for the range of water temperature at which the tests had been conducted. The maximum speed of a fourteen centimetre long parr varies between 1.5 m/s and 2.5 m/s. Comparison of the different designs is therefore complicated by the fact that the maximum speed of a parr might increase or decrease by 1.0 m/s with the water temperature.

4-4 Experimental Apparatus at Glasgow

The experimental apparatus for hydraulic measurements was constructed at the University of Glasgow and is shown in figure 4-13. Manometers used in flow measurement are omitted for clarity. Photographs of the general layout are also shown in figures 4-14 and 4-15.

The physical model consists basically of a recirculating flow system with a main flume. Connected to the channel flume are two connected tanks, which supply flow back to the pump for recirculation. The physical model has been build from an existing system, which provided the two steel galvanized tanks, the pump and a part of the pipe network

4-4.1 *Design and construction*

4-4.1.1 *The flume*

The dimensions of the main flume were chosen in order to represent a scaled down river downstream of a dam, weir or any other obstruction proportionally to the swimming abilities and size of small stream dwelling salmon (parr) in comparison with those of adult spawning salmon. The model was designed to be a replica of the flume at Almondbank.

The total length and width of the flume were 4.78 m and 1.22 m respectively. The height of the flume was chosen in order to provide sufficient head loss between the main flume and the sump tank at high discharge. The chosen height was 1.1 m.

The flume was constructed from plywood, including steel reinforcing bars encased on the side of the flume. Extra strength was afforded to the channel by adding four steel bars across the channel. A removable/vertical cross wall 1.22 m wide with an opening 0.20 m by 0.10 m divides the flume into two pools.

4-4.1.2 *Galvanised steel Tank:*

The two galvanised steel tanks were 1.86 m long, 1.22 m wide and 1.0 m high. The tanks were connected to the pump through a pipe 1.00 m long. A 150 mm butterfly valve was incorporated on the other end to isolate the main flume from the pump during period of maintenance as shown in figure 4-13. Two others 150 mm butterfly valves were incorporated between the galvanised tanks and the downstream end of the main flume as shown on figure 4-16.

4-4.1.3 *Pump:*

The pump had the ability to discharge up to 0.060 m^3s^{-1} through the system but its use will be restricted to a maximum discharge of 0.025 m^3s^{-1}. The pump is a MYSON MSK 150-4210 centrifugal pump (Fig 4-17).

4-4.1.4 *Tailgate weir:*

A tailgate was placed at the end of the flume to act as a control section for the channel flow. A brass plate 1.22 m x 0.40 m x 0.005 m thick was hinged to the inside of the downstream end of the flume. Rubber seals prevented any significant leakage between the brass plate and the flume sidewalls. A screwed rod arrangement was attached to the brass plate and by this mechanism, the gate could be raised or lowered and the water level controlled. Water depths downstream of weir/orifice/slot device were maintained at the same level as the Almondbank flume.

4-4.2 *Instrumentation and Calibration*

4-4.2.1 *Introduction*

Each of the 25 test runs involved accurate measurement and recording of the following parameters:(1) water discharge rate, (2) head loss between the two pools through the weir/orifice/slot device and (3) velocity and turbulence measurement. The instrumentation used to record the above parameters and their calibrations are described below.

4-4.2.2 *Flow rate measurement*

The apparatus was a recirculating flow system. The flow rate measurement was achieved using a calibrated orifice plate with pressure tappings at a distance of D and D/2 upstream and downstream from the orifice plate, with D the internal diameter of the pipe. The orifice plate was inserted into the pipeline between the main flume and the tank acting as a contraction to the flow and producing an energy loss as the flow passes through the throat of the orifice plate. This energy loss could be measured on a manometer by measuring the pressure between the pressure tappings upstream and dòwnstream of the orifice plate. The discharge through the orifice was given by:

$$Q = 1.238\sqrt{h} \qquad \textbf{(4-1)}$$

where Q is the discharge in (l/s) and h is the head difference at the manometer in mm.

4-4.2.3 *Head loss and water surface measurements*

The water surface elevation downstream of the weir was controlled by the position of a tailgate. Lines at elevations 200, 300 and 400 mm (the elevation zero is at the bottom of the flume) were drawn on the sidewall of the flume. All water surface measurements were done using a digital pointer gauge. The head loss from upstream pool to downstream pool was measured by comparing the losses at the centre of each pool.

4-4.2.4 *Velocity and turbulence readings*

Velocity and turbulence measurements were measured over an area of 1.22 m wide by 1.50 m long located immediately downstream the weir/orifice/slot device at the plane of the jet centre line for the orifice designs, and at 1/3 and 2/3 of the water depth for weir notch and vertical slot designs. Supplementary measurements were also done for some situations in a horizontal plane at 0.01 m from the bottom.

The instrument used for this purpose was a Sontek Acoustic Doppler Velocimeter as shown in figure 4-18. The ADV uses remote sensing techniques to simultaneously measure three velocity components (x, y, z) of flowing water using a single sampling volume positioned approximately 0.06 m below the transit transducer located at the centre of the probe. The operation of the ADV is based on the Doppler principle.

A short acoustic pulse of 25 Hz is transmitted along the vertical axis through an acoustic transmitter and three acoustic receivers receive an echo from the water. This echo is amplified and analysed in the conditioning module and the processing board. The difference of frequency between the transmitted pulse and the received echo is proportional to the velocity in the water.

The scattering strength of the echo is function of the concentration and size of the particles present and in suspension in the water. A low concentration of suspended particles in the water causes low "signal to noise ratio" (SNR). A possibility to improve too low SNR, is to seed the flume with almost neutrally buoyant particles. In this study, hollow sphere with a size around 10 μm were used.

The data recorded through the ADV are a number of internal configuration parameter as well as velocity data, SNR data, correlation data, time and standard deviation data of the three velocity components. Using software called WindAdv, specific data are extracted from ADV data binary files to generate tabular files.

Two different measurement grids were used, one for the weir/orifice/vertical slot/combination opening on the side and other for the weir/orifice in the middle. The measurement grids are shown in figure 4-19 and 4-20. They were chosen to be closely spaced near to the orifice, vertical slot or weir with larger spacing further away from this region.

4-4.3 *Experimental procedure*

A total of 25 test runs were carried out during the present investigation and the experimental procedure outlined below was adopted for each run.

1. The removable wood board was inserted into the flume corresponding to the chosen design (weir/orifice/slot/combination).

2. The two connected tanks were filled with water as well as the main flume.

3. The three-gate valves were opened and the pump was switched on and a discharge was selected by adjusting the gate valve accordingly. The discharge was evaluated from the orifice plate and the manometer and generally set at a lower flow rate of 0.012 m^3s^{-1} or a higher one of 0.020 m^3s^{-1}.

4. The water surface elevation downstream the removable weir was selected using the tailgate.

5. The head loss differences between the upstream and downstream pool was measured using the pointer gauge.

6. The Acoustic Doppler Velocimeter on the instrument carriage was used to measure velocity and turbulence over a grid, described in paragraph (4.5). At each chosen point on the grid, instantaneous measurements of velocity and turbulence were taken over time period between 1 and 3 minutes. This was function of the degree of correlation. If the correlation was around 90% the measurements were taken for 1 minute. For a lower correlation, the recording lasted 3 minutes.

7. After completion of the test run, the pump was switched off, the valves gates were closed and the main flume was emptied to allow a change of orifice/weir/ slot device.

8. The velocity and turbulence data were then processed using software called WinAdv to obtain the time average of three components of velocity (longitudinal, lateral and vertical) and the three components of turbulence corresponding, at each point of the chosen measurement grid.

9. At the end of each test run the recorded data would include the following parameters:

    a) The chosen design (weir/ orifice/ slot/ combination).

    b) Total discharge Q.

    c) Head loss between higher and lower pools, Δh.

    d) The water surface elevation in the main flume.

    e) Three-velocity components at each chosen point in the flume, Vx, Vy and Vz.

    f) Three turbulence components at each chosen point in the flume, RMS (vx), RMS (vy) and RMS (vz).

The overall testing programme is summarised with a flow chart shown in figure 4-21.

4-5 Conclusion

Two almost identically flumes were designed to represent a scaled down portion of a river downstream a dam or a weir. The flume at Almondbank was used to observe behaviour of parr (juvenile salmon) and the flume at Glasgow was used to make detailed measurements of the hydraulics. In this chapter, the different apparatus and measuring techniques developed for the present study were described in detail. Chapter 5 presents the experimental results of the behaviour of parr at weir/orifice/vertical slot devices and chapter 6 presents the hydraulic measurements at Glasgow flume.

CHAPTER 5:

EXPERIMENTAL RESULTS OF THE BEHAVIOUR OF PARR AT WEIR/ORIFICE/SLOT DEVICES

CHAPTER 5:

EXPERIMENTAL RESULTS OF THE BEHAVIOUR OF PARR AT WEIR /ORIFICE/ VERTICAL SLOT DEVICES

5-1 Introduction

This chapter describes the experimental results of the behaviour of parr (juvenile salmon) at various devices including weirs, orifices and slots over a range of flow conditions. The tests were conducted at the FRS laboratory in Almondbank, Perth.

When artificially displaced, stream-dwelling salmonid fishes can return to the point where they were captured (Garcia de Leanniz, 1988; Halvorsen & Stabell, 1990; Armstrong & Herbert, 1997; Huntingford et al, 1999). This ability to home probably influences the structures of fish populations in space and time, perhaps tending to reduce the disruption of factors such as spates and predators.

The ability of fish to home will also be influenced by the physical structure of their habitat. Waterfalls and fast-flowing water may constitute complete barriers to upstream movement. Homing of fish may also be impeded by slower flows, which may result in high-energy costs of locomotion, a delay in homing and in-

creased vulnerability to predation. It seems reasonable to suppose that the decision of whether or not to home may be influenced by the costs and benefits of the behaviour, which can be expected to depend on the habitat. A further consideration is the availability of requisite stimuli to release homing behaviour. Odours play a role in homing by salmonid fishes (Mills, 1989). Also, local water flow characteristics may be important.

Small stream-dwelling salmon (commonly termed "parr") move upstream when displaced downstream (Huntingford & al. 1999) Like anadromous adults, salmon parr move upstream, both spontaneously and following downstream displacement, and have been used already as models to explore the response of salmon to water flows in scaled-down fish passes (Stuart, 1962).

In the present study, this behaviour was used to encourage salmon parr to attempt to locate and move through fish pass entrances. The intention of this research is to characterise the behaviour of small salmon to develop clear testable hypotheses about how large salmon may respond to water flow. Stuart (1962) commented that after detailed observations he believed the migrations of his small salmon to be "similar in most respects to those of mature fish, except for the ultimate spawning behaviour".

Stuart (1962) reported that juvenile Atlantic salmon (commonly termed "parr") moved upstream in response to water falling over a weir. Stuart noted, they did not move readily through submerged water jets because when the flow was sufficient to attract them, they could not swim fast enough to surmount it. These observations have implications for understanding variation in the homing behaviour of salmon parr and have prompted this research to look again, but in a more structured experimental fashion, at the issue of whether displaced Atlantic salmon parr move most readily through submerged orifice jets or falling water weirs flows or slots flow or combinations of all three.

Delay of the normal migration schedule might have disastrous effects on the spawning success of salmon. It can effectively prevent them from reaching their spawning grounds in time. Hence, efficiency of fish pass entrance covers not

only the percentage of fish to clearing but also the delay of migration induced by the obstacle. Therefore the failure or success of each tested fish was recorded as well as its time of passage through the device.

5-2 Experimental Results

The experiments were conducted over a two year period during the spring and summer seasons of 1999 and 2000. Five series of tests were conducted over this period. The first series of tests was conducted between July and September 1999 and concentrated on the difference between the behaviour of parr approaching weirs and orifices as well as on the influence of the location of the orifice on the parr's behaviour. The second series, conducted in June 2000, completed the research done both on the comparison between weirs and orifices and between various orifices. In the third series, conducted in August 2000, orifices were then compared with vertical slots. In the 4th series of tests, the parr were confronted with two orifices on each side of the flume; one of them being blocked by a coarse grid representing the outflow from a power station.

These experiments permit the observation and comparison of displaced parr confronted with various designs such as weirs, orifices and verticals slots. They also supply valuable information on the influence of small design alterations on the behaviour of parr.

The comparison of the proportion of success and path taken by parr between situations were done with a statistical chi-square or Fisher's exact test analysis. The influence of factors such as the type of passage, the location of the passage, the flow rate, the opening area for the orifices, the water surface elevation for the weir, the location of introduction were correlated to the time of passage. Statistical analyses were performed in MINITAB and tests were considered significant at an alpha level of 0.05. A reminder of the tests conducted is given in table 5-1 and figure 5-1 overleaf.

Table 5-1: details of experiments done over the two summers period

Code	Details	Nber of parr
Series I: done between July and September 1999		**240**
$WS_{12\text{-}0.2}$	Weir on the side at low flow – wsel = 20cm	20
$WS_{20\text{-}0.2}$	Weir on the side at high flow - wsel = 20cm	20
$WM_{12\text{-}0.2}$	Weir in the middle at low flow - wsel = 20cm -	20
$WM_{20\text{-}0.2}$	Weir in the middle at high flow - wsel = 20cm	20
$ObS_{12\text{-}0.02}$	Orifice at the bottom on the side at low flow – area orifice = 0.02 m^2	20
$ObS_{20\text{-}0.02}$	Orifice at the bottom on the side at high flow – area orifice = 0.02 m^2	20
$ObM_{12\text{-}0.02}$	Orifice at the bottom in the middle at low flow– area orifice = 0.02 m^2	20
$ObM_{20\text{-}0.02}$	Orifice at the bottom in he middle at high flow– area orifice = 0.02 m^2	20
$OFM_{12\text{-}0.02}$	Orifice at 5 cm from the bottom at low flow – area orifice = 0.02 m^2	20
$OFM_{20\text{-}0.02}$	Orifice at 5 cm from the bottom at high flow– area orifice = 0.02 m^2	20
$OTM_{12\text{-}0.02}$	Orifice at 10 cm from the bottom at low flow – area orifice = 0.02 m^2	20
$OTM_{20\text{-}0.02}$	Orifice at 10 cm from the bottom at high flow – area orifice = 0.02 m^2	20
Series II: done in June 2000		**60**
$WM_{12\text{-}0.3}$	Weir in the middle at low flow - wsel = 30cm -	20
$ObM_{12\text{-}0.02}$	Orifice at the bottom in the middle at low flow– area orifice = 0.02 m^2	20
$ObM_{12\text{-}0.01}$	Orifice at the bottom in the middle at low flow– area orifice = 0.01 m^2	20
Series III: done in August 2000		**320**
$WS_{12\text{-}0.2}$	Weir on the side at low flow – wsel = 20cm	20
$WS_{20\text{-}0.2}$	Weir on the side at high flow - wsel = 20cm	20
$ObS_{12\text{-}0.01}$	Orifice at the bottom on the side at low flow – area orifice = 0.01 m^2	40
$ObS_{20\text{-}0.01}$	Orifice at the bottom on the side at high flow – area orifice = 0.01 m^2	40
$WOb_{12\text{-}0.01}$	Orifice at the bottom associated with a weir at low flow – a = 0.01 m^2	40
$WOb_{20\text{-}0.01}$	Orifice at the bottom associated with a weir at high flow – a = 0.01 m^2	40
$V5S_{12}$	Vertical slot 5 cm wide on the side at low flow	40
$V5S_{20}$	Vertical slot 5 cm wide on the side at high flow	40
$V10S_{12}$	Vertical slot 10 cm wide on the side at low flow	20
$V10S_{20}$	Vertical slot 10 cm wide on the side at high flow	20
Series IV: done in September 2000		**160**
AR_{12}	Double orifices with ratio 1:1, parr introduced on the right side at low flow	20
AR_{20}	Double orifices with ratio 1:1, parr introduced on the right side at high flow	20
AL_{12}	Double orifices with ratio 1:1, parr introduced on the left side at low flow	20
AL_{20}	Double orifices with ratio 1:1, parr introduced on the left side at high flow	20
BR_{12}	Double orifices with ratio 1:5, parr introduced on the right side at low flow	20
BR_{20}	Double orifices with ratio 1:5, parr introduced on the right side at high flow	20
BL_{12}	Double orifices with ratio 1:5, parr introduced on the left side at low flow	20
BL_{20}	Double orifices with ratio 1:5, parr introduced on the left side at high flow	20

5-3 Comparison of the different type of designs

5-3.1 *Comparison of the behaviour of fish passage at orifices and weirs*

The comparison of the behaviour of fish at falling water and submerged orifices was conducted in two stages. A first series of experiments was conducted in July 1999 to compare one bottom orifice with one rectangular weir. The two designs types were located at the side or in the middle of the flume (Figure 5-2) and were tested for two discharges, namely 0.012 and 0.020 m^3/s.

The second comparison of the behaviour of parr approaching weirs and orifices was done in June 2000. The intention of the second series of test was to confirm the observations obtained during the previous series. The passage through the orifice was made more difficult by decreasing the size of the opening and the passage over the weir was eased by increasing the water surface elevation from 0.20 m to 0.30 m. The three designs (figure 5-3) were tested for a sole discharge of 0.012 m^3/s and 20 parr were individually tested for each situation.

A - Series I:

The success in fish passage between the orifices and weirs are shown in table 5-2a if the devices are in the middle and in table 5-2b if the devices are at the side. The difference of success between orifices and weirs is significant (Fisher's exact test, in all the cases $p < 0.001$). Orifices at the bottom passed most fish (between 70 - 95% success) at both discharges tested. Weirs were totally unsuccessful at a discharge of 0.012 m^3/s and passed only a single fish at the discharge of 0.020 m^3/s.

Table 5-2a: Successful parr in function of situation (the device in the middle)

Code	Success	Success rate
$WM_{12\text{-}0.2}$	0	0%
$WM_{20\text{-}0.2}$	1	5%
$ObM_{12\text{-}0.02}$	19	95%
$ObM_{20\text{-}0\ 02}$	17	85%

Table 5-2b: Successful parr in function of situation (the device in the middle

Code	Success	Success rate
$WS_{12\text{-}0.2}$	0	0%
$WS_{20\text{-}0.2}$	1	5%
$ObS_{12\text{-}0.02}$	14	70%
$ObS_{20\text{-}0\ 02}$	17	85%

B - Series II

The weir design was again unsuccessful. No fish managed to swim through the weir even though there was no drop in level from the weir crest to the water surface level downstream as shown in figure 5-3. The 0.20 x 0.10 m orifice passed 16 out of 20 parr and the 0.10 x 0.10 m orifice passed 8 parr.

The weir design was less efficient than the orifice designs for the tested conditions. This result is in accordance with the results of the previous series: fish moved more readily through orifices even when the velocities downstream of the opening reached up to 1.60 m/s (Fisher's exact test: $WM_{12\text{-}0.3}$ versus $ObM_{12\text{-}0.02}$, $p < 0.001$; $WM_{12\text{-}0.3}$ versus $ObM_{12\text{-}0.01}$, $p=0.0033$).

Table 5- 3: Numbers of success and failure per situation

	Success	% Success
$WM_{12\text{-}0.3}$	0	0 %
$ObM_{12\text{-}0\,02}$	16	80%
$ObM_{12\text{-}0\,01}$	8	40%

For the two series, parr moved readily through the orifices located at the middle or at the side with an opening of 0.01 or 0.02 m^2 but they were reluctant to jump or swim over the weir.

5-3.2 *Comparison of the behaviour of parr approaching orifices and vertical slots*

The comparison of parr behaviour approaching a vertical slot and an orifice was done in August 2000. The 0.10 by 0.10 m orifice located at 0.05 m from the right side of the flume was compared with a 0.05 m wide vertical slot located at 0.10 m from the right side of the flume as shown in figure 5-4. These two designs were also tested under two different flows, namely 0.012 and 0.020 m^3/s.

Forty parr were individually tested for each situation. The orifice passed 72.5% of the parr at 0.012 m^3/s but only 7.5% at 0.020 m^3/s ($p<0.001$). The vertical slot passed 50 % of the parr at 0.012 m^3/s and 22.5 % at 0.020m^3/s ($p = 0.0072$). The results are shown in table 5-4.

Table 5-4: Number of successful parr for each situation

Code	Success	% Success
$ObS_{12\text{-}0.01}$	29	72.5 %
$ObS_{20\text{-}0.01}$	3	7.5%
$V5_{12}$	20	50 %
$V5_{20}$	9	22.5 %

There were significantly differences between the 0.10 by 0.10 m orifice and the 0.05 m wide vertical slot at 0.012 m^3/s (Fisher, $p = 0.033$) but not at 0.020

m^3/s (Fisher, $p = 0.115$). The efficiency of this orifice and this vertical slot changed significantly within the flow rate (ObS: $p < 0.001$; V5: $p = 0.0072$).

Due to an insufficient number of successful parr for the bottom orifice at 0.020 m^3/s, this situation has been disregarded in the analysis of the length of time for the fish to negotiate the orifice/vertical slot. For the observed situations, half of the successful parr passed through the orifice or the vertical slot in less than ninety seconds. The time of passage through the slot can be seen as a function of the flow rate (0.012 or 0.020 m^3/s) and the design (Bottom orifice or 0.05 m wide vertical slot).

A proportion of the successful parr introduced in the flume have some time resting before going through the opening. These resting times might be divided in two categories: (1) the delay between the introduction of the parr in the flume and its first movements and (2) the time spent at rest after their first or second exploration of the flume.

Some parr did not start to move as soon as introduced in the flume but spent some time in the corner where they were introduced. For the orifice at the side, 4 out of the 29 successful parr spent between 1 and 17 in the right corner of the flume before moving. For the vertical slot design, 5 out of 20 successful parr did not move at the beginning for a period of 2 to 5 minutes at low flow. At high flow, all the successful parr moved as soon as introduced.

The fish might also have some time resting after their first exploration of the flume. These periods of rest might allow the parr to recover from intense swimming activities. A simple regression analysis shows that the time spent at rest increase with the time spent in the flume (Fig 5-6).

Table 5-5: Results of regression analysis: influence of the time spent in the flume on the resting time ($p < 0.001$)

Situation	F	R^2	Regression equation
$ObS_{12\text{-}0.01}$	388.72	0.935	Rest = - 13.9 + 0.867 time
$V5_{12}$	88.17	0.830	Rest = - 16.7 + 0.643 time
$V5_{20}$	24.46	0.777	Rest = - 17.1 + 0.755 time

The parr went through the 0.10 by 0.10 m orifice more readily than through the vertical slot at 0.012 m^3/s but there were no significant differences on the time of success. For a higher flow, such as 0.020 m^3/s, the vertical slot is more efficient than the 0.10 by 0.10 m orifice. Both designs have their efficiency reduced with increasing flow.

5-3.3 *Comparison of the behaviour of salmon approaching orifices alone and orifices combined with a weir*

In this section, an orifice alone and an orifice combined with a weir as shown in figure 5-7 are investigated. For both designs, parr have to pass through a 0.10 by 0.10 m wide orifice located on the right side of the flume. Parr were introduced in the jet centre line of the orifice. The objectives of the "orifice associated with a weir" design are first to offer a second way to pass the obstacle by jumping over the weir and secondly to have lower velocities downstream the 0.10 by 0.10 opening than the "orifice" design as a part of the flow passes over the weir.

At 0.012 m^3/s, the bottom orifice alone had the highest percentage of success with 72.5 % of success against 62.5 % for the orifice combined with a weir. On the other hand, for a discharge of 0.020 m^3/s, the orifice's efficiency was as low as 7.5% while the efficiency of the orifice with the weir was still as high as 52.5% as shown in table 5-6.

The efficiency of the bottom orifice alone (ObS) changes with the flow rate (Fisher test, $p < 0.001$) while the flow, for the range tested, had no impact on the efficiency of the orifice combined with the weir (Fisher test, $p = 0.50$). There was therefore a particular difference in success for the two designs for a discharge of 0.020 m^3/s (Fisher test, $p<0.001$) but not for the lower flow (Fisher test, $p = 0.47$).

Table 5- 6 Proportion of successful parr for each situation

Code	Success	% Success
$ObS_{12\text{-}0.01}$	29	72.5 %
$ObS_{20\text{-}0.01}$	3	7.5%
$WOb_{12\text{-}0\,01}$	25	62.5 %
$WOb_{20\text{-}0.01}$	21	52.5 %

Due to an insufficient number of successful parr for the bottom orifice design at 0.020 m^3/s, this situation has been disregarded in the analysis of the length of time for a fish to negotiate orifices

The orifice and the weir/orifice combination create very attractive hydraulic conditions for the parr. The first parr swam through the orifice in five seconds or less, and half the successful parr succeeded within the first minute of introduction. The weir/orifice combination at 0.020 m^3/s passed more fish in the first twenty seconds than the 2 other set ups, presently 17 parr against 10 for the orifice alone at 0.012 m^3/s and 12 for the weir/orifice combination at 0.012 m^3/s.

The introduction of a weir combined with the 0.10 by 0.10 m orifice improved the overall efficiency of the orifice over the range of flow tested by reducing the velocities downstream the opening just enough to keep it attractive. The influence of velocity on the efficiency of dish at passing through devices will be further discussed in Chapter 7.

5-4 Influence of orifice elevation

During the first series of test conducted between July and September 1999, the influence of the orifice elevation in the water column was investigated. Three locations were tested. The orifice was placed (1) at the bottom of the flume, (2) at 0.05 m and (3) 0.10 m from the bottom of the flume as shown in figure 5-9.

The bottom orifice passed most fish at both discharges tested while the raised orifices passed only between 25 and 65%. The efficiency of the orifice did not change with the flow range tested (Fisher test, $p > 0.05$), but the orifice efficiency varied with its elevation for a discharge of 0.012 m^3/s (chi square test, chisq = 20.870, df = 2, p=0.000), as well as for a discharge of 0.020 m^3/s (chi square test, chisq = 8.750, df = 2, p=0.013). These results are shown in table 5-7.

The bottom orifice passed 75% of successful parr within the three first minutes. To reach the same success rate, in the case of the orifices at 0.05 and 0.10 m

from bottom, 23 and 21 minutes were needed respectively. This is shown in figure 5-10.

Table 5- 7: Successful parr in function of situation

Code	Success	% Success
$ObM_{12\text{-}0.02}$	19	95%
$ObM_{20\text{-}0\,02}$	17	85%
$OFM_{12\text{-}0.02}$	13	65%
$OFM_{20\text{-}0.02}$	8	40%
$OTM_{12\text{-}0.02}$	5	25%
$OTM_{20\text{-}0\,02}$	11	55%

The time needed to succeed does not appear to be correlated to the flow for the three different designs for the range of flow tested. However parr need less time to go through an orifice at the bottom of the flume than an orifice raised at 0.05 or 0.10 m, but the time taken by the parr does not increase significantly when comparing 0.05 m and 0.10 m elevations.

5-5 Influence of orifice size

The size of the orifice had an important effect on the hydraulic conditions created downstream the obstacle. In this section, the effect of the size of the opening, which in turn affected the velocity on parr behaviour, is analysed. Two sizes were tested: 0.10 x 0.10 m and 0.20 x 0.10 m as shown in figure 5-11. The results are shown in table 5-8.

The efficiency of the two orifices was significantly different (Fisher test, $p = 0.022$). Orifice efficiency is directly correlated to the velocities existing in their vicinity. For an orifice of 0.02 m^2, the velocities at the vena contracta have been measured to be around 0.80 m/s while for an orifice of 0.01 m^2, the velocities reached 1.60 m/s. The number of parr passing through the orifice decreased as the velocities in the vicinity of the orifice increased.

Table 5-8: Numbers of success and failure per situation

	Success	% Success
$ObM_{12\text{-}0\,02}$	16	80%
$ObM_{12\text{-}0\,01}$	8	40%

For the orifice with an area of 0.02 m^2 ($ObM_{12\,-\,0.02}$), 25 % of the successful parr went through the opening in less than 18 second, 50% in less than 34 sec-

onds but it took around 19 minutes to pass 75% of the successful fish as shown in figure 5-12. For the orifice with an area of 0.01 m^2 ($ObM_{12-0.01}$), the successful fish needed much more time to go through the opening: only 2 passed in the five first minutes, 4 in the 10 first minutes and 6 in the 18 first minutes as shown in figure 5-12.

5-6 Influence of orifice location

The location of a fish pass in relation to the obstruction is critical. The comparison of the parr behaviour in relation to the location of a 0.20 x 0.10m orifice therefore was conducted during the first series of experiments in July-September 1999. Two locations were tested. The orifice was placed at the bottom at the side and in the middle of the flume as shown in figure 5-13.

The success rate varied between 70 and 85% when the orifice was located on the side and between 85 and 95% when the orifice was the middle (Table 5-9).

Table 5- 9: Successful parr in function of situation

Code		Success	Success rate
$ObS_{12-0.02}$	SIDE	14	70%
$ObS_{20-0.02}$	SIDE	17	85%
$ObM_{12-0.02}$	MIDDLE	19	95%
$ObM_{20-0\ 02}$	MIDDLE	17	85%

Orifices efficiency did not change significantly with the flow range tested (Fisher tests, $p > 0.05$). The effects of the location did not also varied with the flow. For a discharge of 0.012 m^3/s, the difference of success between the bottom orifice at the middle and the bottom orifice at the side was not significant (Fisher test, $p = 0.092$) and at 0.020 m^3/s (Fisher test, $p = 1$).

The bottom orifice in the middle passed three quarter of successful parr within the three first minutes. This is shown in figure 5-14. To reach the same success rate, in the case of the bottom orifice on the side, 17 minutes were needed respectively. The location of the orifice at the bottom of the flume in the middle offered better results in the time taken for passage compared with the orifice at the side. This was in consistent with the higher rate of success for the bottom orifice in the middle. The time needed to succeed does not appear to be cor-

in the middle. The time needed to succeed does not appear to be correlated to the flow for the orifices for the range of flow tested.

5-7 Influence of vertical slot width

In this section, two vertical slots are compared. Both designs were located at 0.10 m from the right side of the flume, but their widths differed. The first one was 0.05 m wide and the second one 0.10 m. The two vertical slots are shown in figure 5-15.

Vertical slot efficiency changes significantly with the width of the opening [5 or 10 cm] at high flow but not at low flow (Fisher, $p = 0.04$ and 0.58 respectively) (Table 5-10). At 0.020 m^3/s, the wide vertical slot V_{10} had a higher success rate than the narrow vertical slot V_5. There was also a significant difference between the low and high flow situations for the narrow slot V_5 (Fisher test, $p = 0.02$) that did not occur for the wide slot V_{10} ($p = 0.53$). For the narrow vertical slot, the success rate dropped from 50% to 22.5 % while the flow increases from 0.012 to 0.020 m^3/s.

Table 5- 10: successful parr in function of situation

	Success	% Success
$V5_{12}$	20	50%
$V5_{20}$	9	22.5%
$V10_{12}$	12	60%
$V10_{20}$	9	45%

Figure 5-16 shows the time needed to pass each vertical slot. Parr need in general more time to go through the wider slot. More than 9 and 23 minutes are needed to allow respectively the passage of 50 and 75 % of the successful parr for the wide vertical slot V_{10} design against 90 seconds and 12 minutes for the narrow vertical slot V_5.

$V5_{12}$ appears to offer the best situation by passing the greatest proportion of parr (50 %) in the shortest period of time (75 % in 12 min) while the fish only went through the wider slot ($V10_{12}$) after spending at least 100 seconds in the flume.

5-8 Double orifice design

In this series only one type of design was tested. The removable vertical board, which divided the flume into two pools, incorporated two openings. The first opening was an orifice 0.10 wide by 0.10 m high, on the right side and at the bottom of the flume. The second opening was also an orifice, but it was 0.50 m wide by 0.05 m deep and located on the left side at 0.05 m from the bottom. The second opening was blocked by a coarse grid, which allowed flow but not fish passage. To succeed, the parr had to find the small orifice in spite of the diversion created by the flow coming through the 0.5 x 0.05 orifice. The 0.5 m x 0.05 m orifice was designed to simulate flow from a power station.

The purpose of this series of experiments was to compare the influence of (1) the flow ratio at the openings and (2) the location of introduction of the parr on the percentage of parr going through the 0.10 m by 0.10 m orifice.

5-8.1 *Proportion of fish finding the small orifice*

For each situation, 20 parr were individually introduced in the flume. Between 35 and 95% of the fish found and went through the small orifice representing the entrance to a fish pass.

Table 5-11: Number of successful parr for each situation

Code	Success	Success rate
AR_{12}	19	95%
AR_{20}	12	60%
AL_{12}	8	40%
AL_{20}	7	35%
BR_{12}	11	55%
BR_{20}	12	60%
BL_{12}	14	70%
BL_{20}	16	80%

At low flow, the situation "equal orifice flows and right side introduction" AR_{12}, offered significantly the best situation for parr to find and go through the orifice with 95% success. On the other hand, there were no significant differences between AL_{12}, BR_{12} and BL_{12}, the success rate varying between 40 and 70% as shown in table 5-11 and 5-12

At high flow, the success of the parr depended significantly on the flow ratio between the two orifices if the parr were not introduced in the jet centreline of the 0.10 by 0.10 m orifice. For situation BL_{20}, the success rate was indeed as high as 80% against only 40% for AL_{20}. However there were no significant differences between situations where parr were introduced along the axis of the jet centreline or/and the velocities were highest at the small orifice. Situations AR_{20} and BR_{20} had the same success rate and situations AL_{20} and AR_{20} had a non-significant difference of success, as shown in table 5-12.

The flow rate seemed to have no influence on the efficiency of the different situations AL, BR and BL with the exception of the case AR where parr were introduced along the axis of the jet coming from the small orifice and the highest velocities come from the small orifice.

Table 5-12: p-value for Fisher tests on situations having at least two elements in common in the following three: ratio, location & flow rate

	AR_{12}	AR_{20}	AL_{12}	AL_{20}	BR_{12}	BR_{20}	BL_{12}	BL_{20}
AR_{12}	X							
AR_{20}	0.02	X						
AL_{12}	0.0004	X	X					
AL_{20}	X	0.2	1	X				
BR_{12}	0.008	X	X	X	X			
BR_{20}	X	1	X	X	1	X		
BL_{12}	X	X	0.11	X	0.51	X	X	
BL_{20}	X	X	X	0.0044	X	0.30	0.72	X

5-8.2 *Length of time for fish to find and go through the orifice*

For all double orifice situations, the minimum time taken by parr to succeed was between 3 and 5 seconds if parr were introduced in the right side of the flume and between 5 and 15 seconds if parr were introduced in the left side. Similarly, for every situation with the exception of case BL_{20}, 25% of the success fish passed through the orifice in less than 20 seconds. For the 50% of successful parr through the orifice (median),, however, the differences between each situation was much more important and spread over a range of 6 seconds to 10 minutes. For 75 % of the successful parr through the opening, the time varies between 90 seconds and 27 minutes.

The time taken by the parr to find and go through the opening was correlated to three factors: flow ratio between the two orifices, (A or B), the location of introduction of parr in the flume (on the right or left corner) and the total flow rate (12 or 20l/s). Thus there were 8 possible combinations. The effect of these factors on the time of passage were analysed as well as their interaction. The situations were compared two by two with the compared situations having at least two common variables as shown in table 5-13.

Table 5-13:One-way analysis of variance for the logarithm of the time taken by parr to succeed.

Compared situations	Difference	F	p-value
$AR_{12} - AR_{20}$	Flow	4.59	0.041
$AL_{12} - AL_{20}$	Flow	0.08	0.778
$BR_{12} - BR_{20}$	Flow	0.07	0.796
$BL_{12} - BL_{20}$	Flow	1.38	0.249
$AR_{12} - AL_{12}$	Location	6.35	0.019
$BR_{12} - BL_{12}$	Location	0.35	0.567
$AR_{20} - AL_{20}$	Location	0.48	0.500
$BR_{20} - BL_{20}$	Location	0.36	0.553
$AR_{12} - BR_{12}$	Ratio	5.47	0.027
$AL_{12} - BL_{12}$	Ratio	0.15	0.704
$AR_{20} - BR_{20}$	Ratio	0.05	0.824
$AL_{20} - BL_{20}$	Ratio	0.46	0.503

At 0.012 m^3/s, AR_{12} offered significantly the best situation for the parr to go through the opening in the shortest period of time in comparison with AL_{12} and BR_{12}. Parr had therefore a better chance of going through the opening quickly if they were introduced in the right side of the flume and also if the velocities at the entrance of the 10 x 10 cm orifice were higher than at the 5 x 50 cm orifice. If these two conditions were not met, there were no significant differences in the time taken by the parr to succeed. There were indeed no differences between AL_{12}, BR_{12} and BL_{12}. At high flow, there were no differences between AR_{20} & AL_{20}, AR_{20} & BR_{20}, BR_{20} & BL_{20} and AL_{20} & BL_{20} (One way analysis of variance on the log (time): $p > 0.05$).

Like for the success rate, there was no significant influence of the two flows 0.012 and 0.020 m^3/s on the time taken by the parr to succeed with the exception of situation AR (One way analysis of variance, on log (time): $f = 4.59$, $p = 0.041$). For this situation, parr were introduced on the right side of the flume, and

the velocity at the orifice increased from 0.815 m/s at a discharge of 0.012 m^3/s to 1.08 m/s at a discharge of 0.020 m^3/s.

5-8.3 *Influence of the 5 x 50 cm orifice on the success of the parr passing through the 10x10 cm orifice.*

The fish that travelled upstream along the window (right) side ignored the 5 x 50 cm orifice, with the exception of one fish for situation AR_{20}. (Introduced on the right side of the flume, this fish started to move up along the window but at 40 cm of the small orifice, it diverted toward the left side of the flume and tried to go through the blocked orifice.) Most of the parr, which tried to go through this orifice, originated from the left side of the flume. However all the parr, coming from the left side of the flume, did not try to pass through the 0.5 by 0.05 m orifice as shown in table 5-14. Between 25 and 100 % of the parr coming from the left side of the flume tried to pass through the blocked orifice.

When parr arrived in the vicinity of the 0.5 x 0.005 m orifice, the decision to attempt or not to go through the orifice was influenced by the flow rate (0.012 or 0.020 m^3/s), by the flow ratio between the two openings as well as their previous experience in the flume (e.g.: what they know of the flow conditions in the flume in function of where they have been introduced).

Table 5-14: Comparison of the number of parr trying to pass through the blocked orifice with the number of parr coming from the left side of the flume.

Situation	Nber of parr approaching from the left side of the flume	Nber of parr trying to go through blocked orifice
AR_{12}	5	5 (100%)
AL_{12}	8	5 (62.5%)
BR_{12}	12	12 (100%)
BL_{12}	12	10 (83.3%)
AR_{20}	8	2 (25%)
AL_{20}	15	8 (66.7%)
BR_{20}	12	7 (58.3%)
BL_{20}	10	7 (70%)

The success of a parr to find the 0.10 by 0.10 m orifice in spite of the diversion created by the flow coming through another orifice highly depended on the relative position of the parr in relation with the opening as well on the flow ratio between the two orifices.

5-9 Discussion

Salmon parr readily moved upstream through submerged orifices and vertical slot but were reluctant to jump over the weir.

The results of this study are totally at odds with the observation of Stuart (1962). Stuart observed parr moving readily over waterfalls but not through submerged jets. One difference in the two experimental designs is that in the present study a supply of water from the stock tank was provided, which may have given the requisite cues to release normal homing behaviour. Fish were observed soon after they were released whereas it appears from Stuart's report that his fish were held in the apparatus for many days. The rapid upstream movement observed is similar to that seen in a field study of brown trout displaced downstream (Armstrong & Herbert, 1997). It is possible that Stuart was observing a response exhibited by fish stranded for long periods in small pools, rather than less inhibited homing behaviour.

By comparison with movement through jets, jumping at falling water (at weirs) is likely to be risky, due to the possibilities of damage and of attracting predators and is likely to be expensive in energy terms. In section 7-4 of the following chapter, an attempt will be made to evaluate the energy cost associated with the different devices tested (orifice/slot/weir) and to check if the behaviour of salmon parr in the flume was consistent with the general observation that fish exhibit energy-saving strategies during migration (Weihs, 1973,1974).

The size of the orifice has an important effect on the efficiency of the device. Stuart (1962) noted that the attraction of the fish to underwater increased proportionally with the velocity. The opening needs therefore to be calculated to create attractive velocities within the abilities of the targeted fish but not too high so the fish have difficulty passing. The window of suitable velocity is therefore the most important parameter in any design. Like for the orifice design, the efficiency of the vertical slot depends on the width of the opening and on the flow range at which it will be operated. Further discussion on the correlation existing

between the velocity in the vicinity of the orifices and vertical slots tested and their efficiency will be carried out in section 7-2.

The behaviour of the parr in the flume was consistent with the observation that parr tend to stay near the bottom of the flume (cf section 3-2.3) (Kallerberg, 1958;). This may have decreased their abilities to detect jets above the bottom and may account for the fact that the distance of the orifices from the base of the flume influenced the success rate and the time it took the fish to move through them. This observation will also be discussed further in section 7-2.

5-10 Conclusion

Salmon parr prefer swimming through orifices or vertical slots rather than jumping or swimming over weirs. With the exception of the weir designs, the great proportion of the successful parr went through the orifice/vertical slot within the first few minutes of introduction.

Area, elevation in the water column above the flume bed, and location across the flume laterally influence the efficiency of orifices. The area of an opening should be designed to create velocities, for the range of flow it will be operated at, high enough to attract and low enough not to discourage the parr (Series II & III).

Combining an orifice with a weir seems to be an efficient idea to reduce the velocity at the orifice's entrance (Series III). However this weir will need to be designed to operate only for the higher flow. It is also preferable to position orifices near the bottom of the flume (Series I), as parr tend to stay near the bottom. The location of the orifice across the flume seems also to influence the success of parr especially if there are others jets in the flume (series IV).

Vertical slots appear to be an acceptable solution to helping fish pass over an obstacle. Vertical slots need to be designed wide enough to provide velocities within the right range (Series III). However the time it takes the parr to swim through the vertical slot increases with the width of the slots (Series III).

CHAPTER 6:

HYDRAULIC MEASUREMENTS AT GLASGOW FLUME

CHAPTER 6

HYDRAULIC MEASUREMENTS AT GLASGOW FLUME

6-1 Introduction

As discussed in chapter 4, an identical flume was constructed at the University of Glasgow and used purely for detailed hydraulic measurements of head loss, water level, velocity and turbulence data.

A total of 25 tests runs were carried out for the different designs and the experimental procedure adopted for each test run has been described in Chapter 4. An Acoustic Doppler Velocimeter (ADV) was used to measure three components of velocity and turbulence at various elevations in an area 1.22 m wide by 1.50 m long located immediately downstream of the tested design. Typical grids are shown in figures 6-1 and 6-2.

For each test, all of the relevant data was stored on computer and each test run had an associated Excel data file store on computer disk. Three computer programs were written in Matlab, which would present horizontal velocity profiles at various depths in the water column and also vertical velocity profiles

at various distances from the tested design as well as contours of mean velocity and turbulence intensity.

The turbulence data obtained with the ADV was the root-mean square (RMS) values of the turbulent velocity fluctuations u' in the (x) direction, v' in the lateral (y) direction and w' in the vertical direction. The turbulence intensity is the ratio of the mean value of all three components u', v' and w' to the mean flow velocity U_0 at the weir/orifice /slot device. Thus the three-dimensional relative turbulence intensity is:

$$T_u = \frac{\sqrt{[(u^2 + v^2 + w^2)/3]}}{\overline{U_0}} \qquad (6\text{-}1)$$

6-2 Flow conditions for the Weirs

6-2.1 General considerations for the Weirs

A weir is an overflow structure built perpendicular to an open channel axis. It has a unique depth of water in the upstream pool (or upstream head) for a given shape and a given discharge. There are a great variety of weirs. However, only two different types of weirs were tested: the fully contracted rectangular weir and the partially contracted weir. For both designs, the width of the crest b was 0.20 m and the crest height above flume base Ps was 0.30 m.

The discharge over a weir shown in equation 6-2 has been explained in chapter 2. Q is the discharge, (m^3/s), Q_{ideal} is the ideal discharge (m^3/s), C_d is the discharge coefficient, b is the width of the weir crest (m), and h_1 is the head measured above the weir crest (m).

$$Q = C_d Q_{ideal}$$
$$Q_{ideal} = \frac{2}{3} b \sqrt{2g} h_1^{3/2} \qquad (6\text{-}2)$$

The coefficient of discharge C_d for a fully contracted weir given in equation 6-3 is a function of h_1, the head measured above the weir crest (m) and Ps, the height of crest above approach invert (m).

$$C_d = 0.602 - 0.083(h_1 / Ps) \qquad \textbf{(6-3)}$$

For the designs tested, b and Ps are constant values. b is equal to 0.20 m and Ps to 0.30 m. Thus, the discharge over the weirs can be expressed as a function of only the head over the weir crest as shown in equation 6-4:

$$Q = 0.5906\left(0.602 - 0.083\frac{h_1}{0.3}\right)h_1^{3/2} \qquad \textbf{(6-4)}$$

The hydraulic characteristics of flow over a weir dictate flow conditions in the downstream pool. These are the velocity of the jet at impact with the water V_i, the diameter of the jet and the angle of the jet θ, the air concentration β and the turbulence. Using the Bernoulli equation along one streamline and assuming (1) no energy losses at the weir and (2) a small velocity of approach, equation 6-5 is obtained. h_1 is the head measured above the weir crest (m), V_0 is the velocity of approach (m^2/s), Z is the distance between the bottom crest of the weir and the water surface downstream of impact (m), V_i is the velocity of jet at impact (m^2/s). Z is a constant for all the experiments, and was equal to zero or 0.10 m.

$$\begin{aligned} H_1 &= H_i \\ h_1 + \frac{V_0^2}{2g} + 0 &= 0 + \frac{V_i^2}{2g} - Z \\ V_i &= \sqrt{2g(Z + h_1)} \end{aligned} \qquad \textbf{(6-5)}$$

The velocities at impact for the different situations tested are shown in table 6-1 below:

Table 6-1: Head above the crest of the weir for a given discharge for the situation tested

Flow (m^3/s)	h_1 calculated (m)	Vi (m/s) for Z = 0.1 m	Vi (m/s) for Z = 0 m
0.012	0.1071	2.01	1.45
0.020	0.1522	2.22	1.72

For a rectangular notch weir, solid jets either converge to a circular cross section or diverge to a flat rectangular shape. Novak (1980) gives the criterion

below for a jet to diverge: if h_1/b is greater than 1.288, the jet is divergent and if h_1/b is lower than 1.288, the jet is convergent. Thus for a width equal to 0.20 m, the jet will diverge if h_1 is greater than or equal to 0.2576 m. h_1 is only a function of the Q_w the water discharge (m^3/s) and the width of the weir b (equation 6-6). In addition the author suggests that at the height h at which it is convergent, the jet should be circular

$$h = 431 b^{0.36} Q_w^{0.8} \qquad \textbf{(6-6)}$$

In the previous experiments, the head measured above the crest of the weir is always less than 0.25 m, so the jet becomes circular. The depth of the jet at impact is then directly obtained from the fundamental equations of the flow with q the discharge per unit width, D_i the depth of the jet and V_i the velocity at the point of impact as shown in the following equation:

$$D_i = \frac{q}{V_i} \qquad \textbf{(6-7)}$$

To determine, the angle at which the plunging jet of water penetrates the downstream water surface, the water discharging over the weir is considered to be a body falling freely with an initial horizontal velocity $V_x = V_{cr}$ and a vertical velocity $V_{y\,equal}$ to 0. The equations of motion then give:

$$\begin{array}{lll} \ddot{x} = 0 & & \ddot{y} = -g \\ \dot{x} = v_{cr} & \textbf{and} & \dot{y} = -gt + 0 \\ x = v_{cr} t + x_0 & & y = -1/2 g t^2 + 0 + y_0 \end{array} \qquad \textbf{(6-8)}$$

From these equations of motion, it is then possible to determine the length of the drop L, the angle of the falling nappe (Chanson, 1994) as a function of y_o, the flow depth at the notch, y_{cr}, the critical flow depth, Ps, the height of the crest and h_2, the water surface elevation behind the over falling water:

$$\frac{L}{Ps} = \left(\frac{y_{cr}}{Ps}\right)^{3/2} * \sqrt{\frac{Ps}{y_0}} * \sqrt{1 + 2\frac{Ps}{y_0}} \qquad \textbf{(6-9)}$$

$$\tan\theta = \sqrt{2 * \frac{y_0}{y_{cr}} * \frac{Ps + \frac{y_0}{2} - h_2}{y_{cr}}} \qquad \textbf{(6- 10)}$$

Assuming that the flow depth at the notch is a linear function of the critical flow such as $y_0 = 0.715\ y_{cr}$, (Rouse, 1936) and considering Ps and h_2 as constant and equal to 0.30 m and 0.20 m [or 0.30 m] respectively, then the length of the drop and the angle of the jet at impact can be expressed as function of the critical velocity V_{cr} and the critical depth y_{cr} and therefore as a function of the sole discharge Q_w. V_{cr} and y_{cr} are given in equations 6-11 and 6-12.

$$y_{cr} = \left(\frac{q^2}{g}\right)^{1/3} \qquad \textbf{(6-11)}$$

$$V_{cr} = \frac{q}{y_{cr} b} \qquad \textbf{(6-12)}$$

The hydraulic conditions existing at the impact of the falling free jet with the water surface level downstream for the various situations tested are shown in the following table [6-2].

Table 6-2: Impact flow conditions for the different situations tested

Flow (m^3/s)	h_2 (m)	L (m)	Vi (m/s)	Di (m)	θ in degree
0.012	0.20	1.01	2.01	0.03	68
	0.30	1.01	1.45	0.04	27
0.020	0.20	1.21	2.22	0.05	62
	0.30	1.21	1.72	0.06	27

The rate of air entrainment per unit width at the plunge point for the situation where the distance between the bottom crest of the weir and the water surface downstream of impact is equal to 0.10 m has been calculated using a generalised equation produced by Ervine (1998) [Eq 2-85]. The air concentration can then be determined as a function of the ratio β [Eq 2-86]. The air concentration for 0.012 and 0.020 m^3/s has been calculated to be around 5-6%.

6-2.2 Results

6-2.2.1 Flow conditions for the weir at the side of the flume

a. Weir at the side, flow 12l/s, z = 0.1 m ($WS_{12-0.2}$)

Velocity profiles for the weir at the side for a discharge of 0.012 m^3/s and a downstream water depth of 0.20 m are shown in figure 6-6 for elevation of 0.067 and 0.12 m above the flume bed.

In the zone of impact, a very low degree of correlation was obtained while using the ADV to measure the velocities and turbulence. At this location, the degree of correlation was lower than 10 % despite the use of buoyancy free particles. Information obtained in the zone of impact of the falling water with the downstream pool might therefore be incorrect.

The submerged jet spreads radially but not symmetrically at the plunge pool stagnation point. The plunging jet mainly follows a longitudinal path along the left hand side of the flume. A strong recirculation occurs on the right hand side of the flume toward the upstream right corner of the flume. Highest velocities are 0.30 m downstream the weir and are around 0.40 m/s. Contours of mean velocity are shown in figure 6-7. There are two zones of high velocity measured to be around 0.35 m/s in the axis of the weir. The first zone, 0.30 m downstream the weir corresponds to the jet plunging into the pool and the second zone, starting 0.90 m downstream the weir corresponds to the jet reflecting off the bottom of the pool.

Contours of turbulence intensity are shown in figure 6-8 for z = 0.067 m and z = 0.125 m. Turbulence intensity contours reveal a circular spread of turbulence from the zone of impact. Turbulence decreases rapidly radially and goes from 50% to 10% in less than 0.10 m.

Figure 6-9 shows the velocity vectors over two vertical slides [x = 0.05 and 0.1 m]. It clearly shows that the flow pattern is three-dimensional as the plunging jet strikes the flume bed and is deflected back up.

b. Weir at the side, flow 20l/s, z = 0.1 m ($WS_{20-0.2}$)

Velocity profiles for the weir at the side for a discharge of 0.020 m^3/s and a downstream water depth of 0.20 m are shown in figure 6-10 for elevation of 0.067 m and 0.125 m above the bed.

Contours of mean velocity for the side weir at 0.020 m^3/s are shown in figure 6-11. Maximum mean velocities reach 0.50 m/s in the axis of the jet.

Contours of turbulence intensity are shown in figure 6-12. Turbulence in most parts of the flume was lower than 5%. High turbulence concentrates in the zone of missing data and is presumed to be as high as 50 % (Ervine et al, 1999).

Similarly to the case $WS_{12\text{-}0.2\text{-}0.2}$, a strong clockwise recirculation occurs. In figure 6-13, it appears clearly that over vertical slices at 0.05, 0.10 and 0.20 m downstream, velocities are meanly lateral and not vertical.

c. Weir at the side, flow 12l/s, z = 0 m ($WS_{12-0.3}$)

For this situation, measurements have been taken at two elevations corresponding to 1/3 and 2/3 of the water depth downstream the weir, thus 0.10 and 0.20 m above the flume bed.

Mean velocity profiles are given in figure 6-14. Like most of the previous profiles for the weir on the side, a strong clockwise recirculation phenomenon occurs. The comparison of the velocity profiles at 0.10 and 0.20 m also shows that the velocity in most parts of the flume is higher at 1/3 than at 2/3 depth above the bottom of the bed.

Contours of mean velocities at these elevations are shown in figure 6-15. Mean velocities vary between 0.40 m/s and 0.05 m/s at elevation 0.10 m from the bottom of the flume and between 1.40 and 0.20 m/s at elevation 0.20 m from the bottom of the flume. High velocities concentrate 0.20 m downstream in the jet centre line. The concentration of high velocities is higher at 0.20 m from the bottom of the flume. This concentration decreases in inverse proportion with the elevation at which measurements have been taken.

Contours of turbulence intensity are shown in figure 6-16. At 0.10 m from the bottom of the flume, the maximum turbulence intensity reaches 37%, which corresponds to a longitudinal RMS value of 0.50 m/s for a mean longitudinal velocity at this point of 0.24 m/s. At 0.20 m from the bottom of the flume, the maximum turbulence intensity is 41%. In most of the flume, intensity of turbulence is lower than 5%. Turbulence concentrates inside a circle of center (x= 0.15, y= 0.3) with a diameter of 0.10 m in the horizontal plane at 0.10 m from the bottom. In the horizontal plan at 0.20 m from the bottom, turbulence concentrates also in a circle of diameter 0.10 m but its center is only 0.20 m downstream the weir.

Velocity profiles over vertical slides 0.05 m and 0.10 m downstream the weir are shown in figure 6-17. On this figure, the lateral diversion of the jet toward the left side of the flume is obvious.

d. Weir at the side, flow 20 l/s, z = 0 m (WS $_{20-0.3}$)

The mean velocity pattern in the horizontal plans at 0.10 and 0.20 m from the bottom are shown in figure 6-18. These mean velocity patterns are similar to those of the 0.012 m^3/s case at the same elevations. Maximum velocities reach 0.50 m/s and spread along the jet centre line at an elevation of 0.10 m from the bottom. The high velocities are higher (they reach 1.40 m/s, 0.30 m downstream the weir) at an elevation of 0.20 m from the bottom of the flume and concentrate inside a circle of centre (x = 0.30, y = 0.15) and of diameter of 0.15 m.

Velocity profiles at 0.10 and 0.20 m from the bottom are shown in figure 6-18. The comparison of figures 6-14 and 6-18 shows a slight difference in the orientation of the main jet. At 0.020 m^3/s, the main jet is slightly orientated towards the left. This phenomenon increases the clockwise recirculation.

Turbulence intensity contours are shown in figure 6-20. Turbulence occurs more particularly near the surface of the water. At 0.20 m from the bottom, turbulence intensity reaches 45%, which corresponds to a RMS (Vx) of 0.86 m/s for a longitudinal velocity of 0.34 m/s.

Turbulence is concentrated in a small part of the flume at 0.20 m from the bottom. The turbulence decreases and spreads radially as the elevation in the flume decreases. Hence the highest turbulence at 0.10 m from the bottom is as low as 8%.

Velocity vector profiles over vertical slides at 0.05 m and 0.10 m from the bottom in figure 6.21 reveal the same phenomenon than in figure 6-21. Vertical velocities are positive for any point of longitudinal location lower than 0.25 m and negative for any point of longitudinal location x greater than 0.25 m. This figure also shows a lateral motion of the water near to the barrier.

6-2.2.2 Flow conditions for the weir in the middle

a. Weir in the middle, flow 12l/s, z = 0.1 m ($WM_{12-0.2}$)

The mean velocity flow pattern at elevation z = 0.067 m is given in figure 6-22a. The main jet goes in the longitudinal direction. The jet diffuses radially and gives birth to two lateral recirculations on the right and left sides of the flume. Highest velocities at elevation z = 0.067 m occur at a distance of 0.30 m downstream the weir similarly to situation $WS_{12-0.2}$.

The mean velocity contour is given in figure 6-22b. As for $WS_{12-0.2}$, there are two main zones of high velocities. The first one is due to the entrance of the impinging jet in the pool. The second one is due to the rebound of the jet from the bottom of the pool. Maximum longitudinal, lateral and vertical velocities are around 0.35 m/s, 020 m/s and 0.20 m/s respectively.

Contours of turbulence intensity are given in figure 6-22c. High turbulence is concentrated within a circle of diameter 0.30 m and centred at a distance of 0.30 m downstream the weir. The intensity reaches 50% and decreases to 20% in less than 0.20 m. This corresponds to RMS longitudinal, lateral and vertical velocities of 1.50 m/s, 1.45 m/s and 0.30 m/s.

b. Weir in the middle, flow 20l/s, z = 0.1 m ($WM_{20-0.2}$)

The velocity profile for the weir in the middle for a discharge of 0.020 m^3/s, a water surface elevation of 0.20 m, at an elevation of 0.067 m above the flume bed is given in figure 6-23a.

This profile is similar to the one of situation $WM_{12\text{-}0.2}$, but the velocities are higher. The flow in the 0.20 m wide central band is in the same direction as the total overflow. On both sides of the pool, there are recirculation patterns towards the upstream corners. Recirculation velocities are particularly high on the left hand side of the flume and reach 0.20-0.25 m/s. Contours of mean velocity are shown in figure 6-23b.

Contours of turbulence intensity are shown in figure 6-23c. There are three zones of high turbulence (intensity around 45%). Two are within the zone of the impact of the falling water with the water surface of the pool. The other one corresponds to the rebound of the impinging jet with the bottom of the pool.

6-3 Flow conditions for Orifices

6-3.1 General considerations for Orifices

Eight different designs of submerged rectangular orifices were tested as shown in table 6-3. The orifices were either 0.10 m wide by 0.10 m high or 0.20 m wide by 0.10 m high. They were positioned at three different vertical positions at 0.00 m, 0.05 m or 0.10 m from the bottom of the flume and at two lateral positions on the side or in the middle of the flume. An orifice 0.10 m wide by 0.10 m high was also successively associated with a 0.60 m wide weir and with another orifice 0.50 m wide by 0.05 m high.

Table 6-3: orifices designs tested

Code	Details	Nber of hydraulic situations
$ObS_{0.02}$	Orifice on the side: 0.20 x 0.10 m	2
$ObS_{0\,01}$	Orifice on the side :0.10 x 0.10 m	2
$ObM_{0.02}$	Orifice in the middle:0.20 x 0.10 m	2
$ObM_{0\,01}$	Orifice in the middle :0. 10 x 0.10 m	1
$OFM_{0.02}$	Orifice at 0.05m from the bottom in the middle:0.20 x 0.10 m	2
$OTM_{0\,02}$	Orifice at 0.10 m from the bottom in the middle:0.20 x 0.10 m	2
$WOb_{0\,02}$	Orifice at the bottom :0.20 x 0.10 m associated with a weir	2
DO	Doubles orifices with ratio 1:1 or 1:5	4

The discharge of a standard submerged rectangular orifice is expressed in equation 6-13 with Q the discharge (m^3/s), C_d the coefficient of discharge, A the area of the orifice (m^2/s), g the acceleration caused by gravity (m^2/s), h_1 the upstream head (m) and h_2 the downstream head (m).

$$Q = C_d A\sqrt{2g(h_1 - h_2)} \qquad \textbf{(6-13)}$$

The coefficient of discharge, C_d is the product of a coefficient of contraction, a coefficient of velocity caused by friction loss and a coefficient to account for exclusion of approach velocity head from equation 6-13. In practice, the shape of the edge of the orifice also affects the coefficient C_d. The head loss equation is given as a function of the velocity at the orifice and a coefficient K as shown in equation 6-14 or alternatively as a function of the velocity at the vena contracta as shown in equation 6-15.

$$h_1 - h_2 = K\frac{V_0^2}{2g} \qquad \textbf{(6- 14)}$$

$$h_1 - h_2 = \frac{V_{vc}^2}{2g} \qquad \textbf{(6- 15)}$$

V_0 is the velocity at orifice (m^2/s), V_{vc} is the velocity at the vena contracta (m^2/s), g is the acceleration caused by gravity (m^2/s), h_1 is the upstream head (m) and h_2 is the downstream head (m).

The coefficient C_d has been determined experimentally for the bottom orifices with a cross section of 0.01 m^2 and 0.02 m^2 as shown in figure 6-3. C_d is equal to 0.69 and 0.71 respectively for the 0.01 and 0.02 m^2 orifices. It is also possible to determine the velocity at the vena contracta and the coefficient K for the different situations if the difference (h_1- h_2) is measured as shown in table 6-4.

Table 6-4: coefficients for the orifice design

Design	h_1-h_2	C_d	K	V_0	V_{vc}
Bottom orifice 0.01m2 – 12l/s	0.1528	0.69	2.08	1.20	1.73
Bottom orifice 0.01m2 – 20l/s	0.4244	0.69	2.08	2.00	2.88
Bottom orifice 0.02m2 – 12l/s	0.0360	0.71	1.962	0.60	0.84
Bottom orifice 0.02m2 – 20l/s	0.1001	0.71	1.964	1.00	1.40

It has been explained in Chapter 2, that for pool-orifice-weir passes, the flow over the weirs and through the orifice can be cumulated to obtain the total flow over the fish pass. Therefore using equation 2-14, 6-2, 6-3 and 6-13, it possible to predict the discharge at a pool-weir-orifice pass in relation to h_1 the upstream head and h_2 the downstream head:

$$Q = 0.69\sqrt{(2g(h_1 - h_2)} + C_d \frac{2}{3} 0.62\sqrt{2g}(h_1 - 0.3)^{3/2} \quad \textbf{(6-16)}$$

$$C_d = 0.602 - 0.083(\frac{h_1 - 0.3}{0.3}) \quad \textbf{(6-17)}$$

Figure 6-4 is a plot of the flow through the device "0.10 by a.10 m orifice associated with a 0.62 m wide weir" against the head loss between the upstream and downstream part of the flume. From this figure, it is clear that if the upstream head is lower than 0.30 m, the device behaves like a sole orifice. Figure 6-4 shows also that for a given discharge greater than 0.010 m^3/s, the head difference between the upstream and downstream part of the pool is higher for the bottom orifice alone than for the bottom orifice associated with a weir.

6-3.2 Results

6-3.2.1 Flow conditions for the bottom orifice at the side

a. Orifice at the side, with an area of 0.01 m^2, flow of 12 l/s ($ObS_{12-0.01}$)

Mean velocity patterns, velocity contours and turbulence intensity contours were obtained in the horizontal plane at 0.05 m from the bottom (Fig 6-24a). The maximum velocity at the vena contracta was measured to be around 1.60 m/s. The maximum velocity at the cross section has been calculated to be around 1.20 m/s.

The incoming jet goes towards the end of the flume (Fig 6-24b). Velocities higher than 0.60 m/s concentrate inside a band 0.10 m wide between y = 0.05 and 0.10 m. A large recirculation pattern is also revealed in the flume with mean velocity in the recirculation around between 0.20 and 0.40 m/s.

Contours of turbulence intensity are shown in figure 6-24c. The turbulence intensity reaches 20%, 0.10 m and 0.50 m downstream of the square orifice. This corresponds to longitudinal RMS turbulence velocities of the order of 0.3 to 0.4 m/s. High turbulence intensities are in the same zone as high velocities. In the remaining part of the flume, turbulence intensity is around 4 to 6%.

b. Orifice at the side, with an area of 0.02 m^2, flow of 12 l/s ($ObS_{12-0.02}$)

For this situation, hydraulic conditions were measured at four different elevations: 0.01 m, 0.05 m, 0.10 m and 0.14 m from the flume bed in order to get a 3-D representation of the flow.

The mean velocity patterns for these different elevations are shown in figure 6-25. The maximum velocity at the vena contracta (x = 0.20 m, y = 0.15 m and z = 0.05m) is around 0.97 m/s. At the four different elevations, high velocities concentrate in a longitudinal band 0.2 m wide at the side of the flume and a clockwise recirculation occurs on the opposite side. In the vicinity of the opening, the area of high horizontal velocities decreases as the elevation increases.

Contours of turbulence intensity for the design $OS_{12-0.2-0.02}$ are shown in figure 6-27. Turbulence is more radially spread than for the design $ObS_{12-0.01}$ and its intensity is higher. Maximum intensity is around 25 to 30%, which corresponds to RMS longitudinal velocities of 0.30 m/s. Lateral and vertical RMS velocities reach only 0.15 m/s.

Velocity vectors over two vertical slides (at x = 0.05 and 0.10 m) are shown in figure 6-28. It is clear from these two vertical slides that the jet issuing from the orifice can be considered as two-dimensional.

c. Orifice at the side, with an area of 0.02 m^2, flow of 20 l/s ($ObS_{20-0.02}$)

The mean velocity pattern in the plane of the jet centre line for $ObS_{20-0.02}$ is shown in figure 6-29a. It reveals a similar pattern to $ObS_{12-0.02}$ at an elevation of 0.05 m. The velocity at the vena contracta has been measured to be around 1.37 m/s, 0.20 m downstream the orifice. Contours of mean velocity are shown in

figure 6-29b. Velocities higher than 0.80 m/s concentrate in a zone near to the opening that is 0.50 m long by 0.25 m wide.

Contours of turbulence intensity are shown in figure 6-29c. Turbulence intensity reaches values as high as 50% in the jet centre line, 0.05 m downstream the orifice. In the zone of high velocity, RMS longitudinal velocities vary between 0.20 and 0.4 m/s. Lateral and vertical velocities are quite low in this area (less than 0.20 m/s) but turbulence fluctuations laterally and vertically are of similar value to the longitudinal velocities.

6-3.2.2 Flow conditions for the bottom orifice in the middle

a. Orifice in the middle, area 0.01 m^2, flow 12 l/s ($ObM_{12-0.01}$)

For this situation the orifice is in the middle and has a cross-sectional area of 0.01m^2. The water depth downstream of the cross wall is 0.20 m.

The velocity profile for the case $ObM_{12-0.01}$ is shown in figure 6-30a. It has the same characteristics as the velocity profile obtained for the orifice at the middle for a cross section of 0.02 m^2. There is a longitudinal band 0.10 m wide of high velocity in the axis of the jet centre line and a large anticlockwise recirculation pattern occurs. Maximum velocities are much higher than for $ObM_{12-0.02}$ and reach 1.57 m/s, 0.05 m downstream the opening as shown in figure 6-30b. A second small recirculation in the right hand corner of the flume has been identified.

Contours of turbulence intensity are shown in figure 6-30c. Maximum turbulence occurs 0.30 m downstream the orifice. The maximum turbulence intensity is around 30% and concentrates in a very small area, which corresponds to a turbulent longitudinal velocity of 0.30 m/s.

b. Orifice in the middle, area 0.02 m^2, flow 12l/s ($ObM_{12-0.02}$)

For this situation the orifice is in the middle and has a cross-sectional area of 0.02 m^2. The water surface elevation downstream is 0.20 m.

The velocity profile for the case $ObM_{12-0.02}$ is shown in figure 6-31a. It has similar characteristics to the velocity profile for the orifice on the side. There is a longitudinal band 0.20 m wide of high velocity in the axis of the jet centre line and a large recirculation pattern occurs. The flow pattern is asymmetric. An anticlockwise recirculation pattern occurs with the inflow jet moving slowly toward the right hand side of the flume. Maximum velocities are slightly lower for the orifice in the middle than for the orifice on the side [fig 6-31b]. The velocity at the vena contracta has been measured to be around 0.80 m/s rather than 0.98 m/s.

Contours of turbulence intensity are shown in figure 6-31c. Maximum turbulence occurs 0.10 m downstream the orifice. The maximum turbulence intensity is around 30%, which corresponds to a turbulent longitudinal velocity of 0.30 m/s. Turbulence spreads slightly toward the right. It also spreads more radially for the orifice on the middle than for the orifice on the side.

c. Orifice in the middle, area 0.02 m^2, flow 20 l/s ($ObM_{20-0.02}$)

The mean velocity profile for the orifice at the middle for a discharge of 0.020 m^3/s and for a water depth downstream of 0.20 m is shown in figure 6-32a.

The maximum velocity at the orifice was calculated to be around 1.00 m/s. At the vena contracta, the velocity is around 1.30 m/s. This is 0.40 m/s lower than for the orifice at the side for the same discharge and water surface elevation. The mean velocity profile for a discharge of 0.020 m^3/s is similar to mean velocity profiles for a discharge of 0.012 m^3/s.

Inside the band of high velocities, the velocities vary between 1.40 and 0.8 m/s (0.50 m downstream the opening). Velocities in the zone of recirculation (left hand side of the flume) increase in the longitudinal direction. The mean velocity at a distance x = 1.50 m, y = 0.10 m, z = 0.05 m is around 0.43 m/s while the mean velocity at a location [x = 0.30 m, y = 0.10 m, z = 0.05 m] is around 0.03 m/s (Fig 6-32b).

Contours of turbulence intensity are shown in figure 6-32c. There is a zone of high turbulence in the vicinity of the opening. The maximum turbulence intensity is around 35%. This is lower than for the orifice on the side for the same discharge and elevation.

6-3.2.3 Orifice in the middle at 5 cm off the flume bottom

a. Orifice at 5 cm off the bottom of the flume, flow 12 l/s ($OF_{12-0.02}$)

The flow pattern for the orifice at 0.05 m from the bottom of the flume for a discharge of 0.012 m^3/s and a water surface elevation of 0.20 m is shown in figure 6-33a.

The velocity pattern at 0.10 m from the bottom for the orifice at 0.05 m above the flume bed is similar to the velocity pattern at 0.05 m from the bottom for the bottom orifice in the middle. The maximum velocity at the vena contracta is 0.80 m/s and quickly reduces to 0.20 m/s at a distance of 0.50 m downstream the opening. The jet rapidly diverges towards the left hand side of the flume. Contours of mean velocity are shown in figure 6-33b.

Contours of turbulence intensity are shown in figure 6-33c. The maximum turbulence intensity occurs 0.20 to 0.30 m downstream the orifice in the axis of the jet and reaches 25%. This is 5% higher than for the orifice at the bottom for the same conditions. Turbulence intensity is otherwise less than 10% in most of the flume.

b. Orifice at 5 cm off the flume bottom, flow 20 l/s ($OF_{20-0.02}$)

The flow pattern for the orifice at 0.05 m from the bottom for a discharge of 0.020 m^3/s and a water surface elevation of 0.20 m is shown in figure 6-34a. The maximum velocity at the vena contracta is around 1.35 m/s. It decreases rapidly to 0.05 m/s at a distance of 0.50 m downstream the flume in the axis of the jet. Contrary to all the other situations for the orifice in the middle, the main recirculation is clockwise. A small recirculation on the left side of the flume has also been identified.

Mean velocity contours are shown in figure 6-34b. The mean velocity decreases radialy from 1.35 m/s to 0.20 m/s. Mean velocities for a discharge of 0.020 m^3/s are higher than for a discharge of 0.012 m^3/s but decrease more quickly.

Contours of turbulence intensity are shown in figure 6-34c. The maximum turbulence intensity is around 25%. It is not higher than for a discharge of 0.012 m^3/s, but the zone of high turbulence is slightly wider.

6-3.2.4 Orifice in the middle at 10 cm off the flume bottom

a. Orifice 10 cm off the flume bottom, flow 12 l/s ($OT_{12-0.02}$)

The flow pattern for the orifice at 0.10 m from the bottom for a discharge of 0.012 m^3/s and a water depth of 0.20 m is shown in figure 6-35a. The 0.20 m wide jet goes straight in the direction of the end of the flume. Recirculation occurs along the left hand side of the flume. Recirculation patterns are different from those with for the orifice at the bottom. The maximum velocity at the vena contracta has been measured to be 0.80 m/s. It decreases quickly to 0.20 m/s at a distance of 1.50 m downstream as shown in figure 6-35b. Mean velocities shown in figure 6-35b decrease more quickly laterally than longitudinally. The vertical velocities are very small in comparison with the longitudinal mean velocities. They are around 0.02 m/s at the orifice.

Contours of turbulence intensity are shown in figure 6-35c. Turbulence is low near the orifice. It varies between 15 and 20%. The RMS longitudinal velocities are around 0.30 m/s. The RMS lateral and vertical velocities never exceed 0.15m/s.

b. Orifice 10 cm off the bottom flume, flow 20 l/s ($OT_{20-0.02}$)

Flow patterns for the orifice at 0.10 m from the bottom for a discharge of 0.020 m^3/s for a surface elevation of 0.20 m are shown in figure 6-36a. These are similar to all the other flow patterns for orifices and in particular to the orifice at 0.010 m off the flume bottom for a discharge of 0.012 m^3/s. Maximum velocity at

the vena contracta was 1.20 m/s, which is lower than for the orifice at 0.05 m from the bottom [Fig 6-36b].

Contours of turbulence intensity are shown in figure 6-36c. Maximum turbulence occurs in the vicinity of the orifice. The intensity reaches 45%, 0.05 m downstream the flume in the axis of the jet.

6-3.2.5 Orifice at the side associated with a weir

a. Orifice at the side associated with a weir, flow 12 l/s ($WobS_{12\text{-}0.01}$)

Mean velocity patterns, velocity contours and turbulence intensity contours were obtained in two horizontal planes at 0.01 and 0.05 m from the bottom. The flow patterns at 0.01 and 0.05 m from the bottom of the flume for the orifice at the side associated with a weir and a water surface elevation of 0.20 m are shown in figure 6-37. The velocity is around 1.20 m/s at the cross section and has been measured as around 1.50 m/s at the vena contracta.

Contours of velocity are shown in figure 6-38. Velocities higher than 0.40 m/s concentrate inside a band 0.20 m wide and a large but weak recirculation occurs in the mean part of the flume. The recirculation velocities are lower than 0.20 m/s.

Contours of turbulence intensity are shown in figures 6-39. The turbulence intensity reaches up to 20-25% in the axis of the orifice at both elevations [0.01 and 0.05 m] between 0.10 and 0.40 m downstream the orifice.

Velocity vectors over two vertical slides are also shown in figure 6-40. This figure shows clearly that in the vicinity of the orifice the flow is mainly two-dimensional.

For a discharge of 0.012 m^3/s, the flow conditions existing in the flume and in particular near the bed for a 0.10 x 0.10 m side orifice associated with a 0.60 m wide weir are similar to the flow conditions created by a similar orifice on its own at a discharge of 0.012 m^3/s even if the velocity at the vena contracta is 0.10

m/s smaller when the orifice is associated with a weir. This is mainly due to the fact that the head of water above the weir crest is only around 0.01 m; therefore most of the flow still passed through the orifice and the small proportion of flow passing over the weir has only a weak impact on the water surface.

b. Orifice at the side associated with a weir, flow 20 l/s ($WObS_{20\text{-}0.01}$)

As for the previous situation, flow patterns, velocity contours and turbulence intensity contours were obtained in two horizontal planes at 0.01 and 0.05 m from the flume bed and the water surface elevation downstream the orifice is 0.20 m but the discharge was increased to 0.020 m^3/s.

The velocity patterns at 0.01 and 0.05 m are shown in figure 6-41. They reveal a very similar pattern to the previous situation and to the situation "$ObS_{12\text{-}0.01}$". The velocity at the vena contracta has been measured to be around 1.60 m/s. Velocity vectors over two vertical slides in figure 6-44 show also a two-dimensional flow pattern in the vicinity of the orifice.

Contours of mean velocity are shown in figure 6-42. High velocities concentrate within a 0.20 m wide band either side of the orifice centerline. A recirculation patterns occurs in most parts of the flume but the recirculation velocities are lower than 0.10-0.20 m/s.

Contours of turbulence intensity are shown in figure 6-43. They are again very similar to the contours of turbulence intensity for the previous situation but the turbulence intensity is slightly higher at 0.05 m above the bed of the flume than at 0.01 m.

As in the previous situation, the hydraulic conditions in the pool, and in particular in the vicinity of the orifice, created by a 0.10 m by 0.10 m orifice at the side associated with a weir for a flow of 0.020 m^3/s are similar to those created by a similar orifice on its own for a discharge of 0.012 m^3/s. For both situations, the velocity at the vena contracta is around 1.60 m/s. This means that in the case of the orifice associated with a weir, a flow of 0.012 m^3/s passes through the orifice while a flow of 0.008 m^3/s passes over the 0.60 m wide weir.

The head above the weir crest is then equal to 0.04 m. However the flow passing over the weir do not seem to have a significant influence on the main flow pattern, at least near the bed of the flume.

6-3.2.6 Double orifice

Like for the previous "orifice" situations, flow patterns, velocity contours and turbulence intensity contours are obtained in two horizontal planes at 0.01 and 0.05 m from the bottom. The water surface elevation downstream of the orifice is maintained constant and equal to 0.20 m at the two discharges tested: 0.012 and 0.020 m^3/s and the two flow ratios tested: 1:1 and 1:5.

a. Double orifice for ratio 1:1 at 12 l/s ($DO_{12\text{-}1:1}$)

For this situation, the flow passes both through the 0.10 m by 0.10 m orifice and the 0.05 m by 0.5 m orifice. The velocity ratio between the two orifices is 1/1, which means that the flow passing through the two orifices are both around 0.06 m^3/s.

Figure 6-45, which represents the velocity vectors at 0.01 and 0.05 m from the bed of the flume clearly shows that the discharge of the two side jets into the pool created a recirculation area in the center of the pool. In fact the jet issuing from the 0.10 by 0.10 m orifice generates a clockwise recirculation while the jet issuing from the 0.05 by 0.5m orifice generates an anticlockwise recirculation.

The mean velocity contours in the planes z = 0.01 m and z = 0.05 m are shown in figure 6-46. This figure clearly shows that there are two zones of relatively high velocities separated by a zone of low velocities (v< 0.10 m/s). The zones of high velocity are located in the jet centerlines of both orifices. The velocity reaches up to 0.80 m/s at the square orifice and 0.65 m/s at the rectangular orifice.

Figure 6-47 shows the contours of turbulence intensity recreated by the two orifices in the planes z = 0.01 m and z = 0.05 m. It can be noted that the turbulence intensity does not vary at the two elevations tested and that it reaches

14%, 0.10 m downstream the square orifice while it reaches up to 20 %, just downstream the rectangular orifice. High turbulence intensities concentrate in the same zone as high velocities and remain around 8% in the remaining part of the flume.

Figure 6-48 represents the velocity vectors over three vertical slides (y = 0.10, 0.15 or 0.70 m). This figure clearly shows that the energy of the jet issuing from the 0.5 by 0.05 m orifice dissipates more quickly than the energy of the jet issuing from the 0.10 by 0.10 m orifice.

b. Double orifice for ratio 1:1 at 20 l/s ($DO_{20\text{-}1:1}$)

The mean velocity profiles for the double orifice for a velocity ratio 1/1 a discharge of 0.020 m^3/s and a water depth of 0.20 m are shown in figure 6-49. They are similar to the velocity profiles obtained at 0.012 m^3/s but the overall velocities are higher. At the vena contracta of the square orifice and at the rectangular orifice, the velocity has been measured around 1.00 m/s [Fig 6-50]. As for the preceding situation, there are two side regions of relatively high velocity separated by a relatively low velocity region (v <0.10/0.20 m/s).

Figure 6-49 also clearly shows that this region of relatively low velocity corresponds to a recirculation zone generated by both high velocities regions.

The contours of turbulence intensity are shown in figures 6-51. They are almost identical to the contours of turbulence intensity obtained for a 0.012 m^3/s discharge. Maximum turbulence occurs again downstream both orifices and the maximum turbulence intensity reaches up to 12 % at the square orifice and 18 % at the rectangular orifice, which correspond to turbulent longitudinal velocity of 0.20 m/s and 0.30 m/s respectively.

Figure 6-52 represents the velocity vectors over three vertical slides [y = 0.10, 0.15 and 0.70 m] and is very similar to figure 6-48.

c. Double orifice for ratio 1:5 at 12 l/s ($DO_{12\text{-}1:5}$)

For this situation, the flow passes both through the 0.10 m by 0.10 m orifice and the 0.05 m by 0.5 m orifice as for the two preceding situations but in this case the flow ratio between the two orifices is 1: 5 which means that the flows passing through the small and large orifices are around 0.002 m^3/s and 0.01 m^3/s as the total discharge is 0.012 m^3/s.

Velocity vector profiles at 0.01 and 0.05 m from the flume bed are shown in figure 6-53. These velocity vector profiles are similar to those obtained for the flow ratio 1:1 between the two orifices [Fig 6-45]. It is however obvious that the jet issuing from the 0.05 by 0.5 m orifice has much higher velocities that the jet issuing from the 0.10 by 0.10 m orifice.

The mean velocity contours in the planes z = 0.01 m and 0.05 m are shown in figure 6-54. These velocity contours also show that the velocity of the flow passing through the large orifice is much higher than the velocity of the flow passing through the 0.10 m by 0.10 m orifice. The maximum velocity of the flow in the vicinity of the 0.10 by 0.10 m orifice is around 0.20 m/s while it reaches 0.75 m/s downstream the 0.05 by 0.5 m orifice.

Figure 6-55 shows the contours of turbulence intensity. The turbulence intensity in most parts of the flume varies between 10 and 20 % at both elevations [z = 0.01 or 0.05 m]. High turbulence intensity concentrates in the vicinity of the large orifice. It reaches 60%, 0.10 m downstream the 0.05 by 0.5 m orifice while it reaches only 30% in the vicinity of the small rectangular orifice.

Figure 6-56 represents the velocity vectors profiles over three vertical slides [y = 0.10, 0.15 and 0.70 m]. This figure clearly shows that, the jet passing through the 0.10 by 0.10 m orifice is confronted with the recirculating flow generated by the large orifice, 0.7/0.8 m downstream the orifice. These conflicting flows conceal each other.

d. <u>Double orifice for ratio 1:5 at 20 l/s</u> ($DO_{12\ 1:5}$)

For this situation, the flow passes both through the 0.10 m by 0.10 m orifice and the 0.05 m by 0.5 m as for the three preceding situations but in this case the flow

ratio between the two orifices is 1:5 which means that the flows passing through the small and large orifices are around 0.0035 m^3/s and 0.0165 m^3/s as the total discharge is 0.020 m^3/s.

Figure 6-57 clearly shows that at 0.01 and 0.05 m from the bed of the flume, the discharge of the two side jets into the pool created a recirculation in the center of the pool as for the same design with the ratio 1:1. However as the flow passing through the large orifice is 5 times stronger than the flow passing through the 0.10 m by 0.10 m orifice, the recirculating flow generated by the large orifice seems to meet the jet issuing from the rectangular orifice and cancel its effect. The maximum velocity for the square orifice is around 0.35 m/s and 1.1 m/s for the rectangular orifice.

The mean velocity contours in the planes z = 0.01 m and 0.05 m are shown in figure 6-58. These velocity contours clearly show that the velocity of the flow passing through the large orifice is much higher than the velocity of the flow passing through the 0.10 m by 0.10 m orifice.

Figure 6-59 shows the contours of turbulence intensity. The turbulence intensity varies between 10 and 20 % at both elevations [z = 0.01 or 0.05 m]. High turbulence intensities concentrate in the vicinity of the large orifice. The turbulence intensity reaches 50%, 0.10 m downstream the 0.05 by 0.5 m orifice while it reaches only 20% in the vicinity of the small rectangular orifice.

Figure 6-60 represents the velocity vectors over three vertical slides [y = 0.10, 0.15 or 0.20 m]. This figure is very similar to figure 6-56. The recirculating flow generated by the large orifice meets with the jet issuing from the 0.10 m by 0.10 m orifice and these conflicting flows conceal each other.

6-4 Flow conditions for Vertical slots

6-4.1 General considerations for vertical slots

Two different designs of vertical slot were tested. The vertical slots were either 0.05 m or 0.10 m wide. They were positioned at 0.10 m from the side of the flume.

The discharge of a standard vertical slot is expressed in equation 6-18 . Q is the discharge (m^3/s), Cd is the coefficient of discharge, b_0 is the width of the slot (m), y is the depth of the flow between the slot and the water surface on the upstream side (m), g is the acceleration caused by gravity (m^2/s), h_1 is the upstream head (m) and h_2 is the downstream head (m).

$$Q = C_d(b_0 y)\sqrt{2g(h_1 - h_2)} \qquad \textbf{(6-18)}$$

The coefficient of discharge C_d has been determined experimental for the two vertical slots as shown in figure 6-5. C_d is equal to 0.59 for the 0.05 m wide vertical slot and 0.63 for the 0.10 m wide vertical slot.

The maximum velocity at the slot is approximately equal to $\sqrt{}$ ($2g\Delta h$). The maximum velocities for the two designs for the two discharges 0.012 and 0.020 m^3/s are shown in table 6-5. The maximum velocity varies between 0.80 m/s for the 0.10 wide vertical slot for a discharge of 0.012 m^3/s and 1.82 m/s for the 0.05 m/s wide vertical slot for a discharge of 0.020 m^3/s. The maximum velocity at the 0.10 m wide slot is 40% smaller than the maximum velocity at the 0.05 m wide slot.

Table 6- 5: Maximum velocity at the slot for the 4 different situations

Situation	Δh (m)	Maximum velocity (m/s)
0.05 m wide vertical slot, 12l/s	0.0904	1.335
0.05 m wide vertical slot, 20l/s	0.1690	1.8209
0.10 m wide vertical slot, 12l/s	0.0334	0.810
0.10 m wide vertical slot, 20l/s	0.0712	1.182

6-4.2 Results

6-4.2.1 Flow conditions for the 0.05 m wide vertical slot

a. Vertical slot, 0.05 m wide, flow of 12l/s ($V5_{12}$)

Mean velocity patterns, velocity contours and turbulence intensity contours were obtained in three horizontal planes at 0.01 m, 0.067 m and 0.125 m above the flume bed for the 0.05 m wide vertical slot for a discharge of 0.012 m^3/s and a downstream water depth of 0.20 m. The maximum velocity at the slot has been calculated to be around 1.35 m/s.

Velocity profiles are shown in figure 6-61 and mean velocity contours are shown in figure 6-62. The incoming jet goes towards the end the flume. For the three different elevations, high velocity concentrates inside a band 0.20 m wide included between y = 0.05 and 0.25 m. However the highest velocity occurs at 0.067 m above the flume bed. A large and weak recirculation pattern is also revealed in the flume. Mean velocities in the recirculation are below 0.10 m/s.

Contours of turbulence intensity are shown in figure 6-63. The turbulence intensity reaches 50% in the vicinity of the slot, in particular at 0.125 m above the flume bed, but decreases very quickly longitudinally and laterally. Turbulence intensity is below 5% for most of the flume in the whole water column.

Velocity vectors over three vertical slides [at y = 0.10, 0.125 and 0.15 m] are shown in figure 6-64. Along the jet centreline [y = 0.125m], the vertical component of the velocity seems to be negligible.

b. Vertical slot, 0.05 m wide, flow of 20l/s ($V5_{20}$)

For this situation, the vertical slot is 0.05 m wide, the discharge is equal to 0.020 m^3/s, and the water surface elevation downstream is 0.20 m.

The velocity profiles for the 0.020 m^3/s are shown in figure 6-65. They have the same characteristics as the velocity profiles for the previous situation for a 0.012 m^3/s discharge but the recirculation pattern is more important. There is also a longitudinal band 0.20 m wide of velocities greater than 0.40 m/s.

The mean velocity contours are shown in figure 6-66. These contours are again similar to those obtained for the lower discharge of 0.012 m^3/s but the maximum velocities are higher.

Contours of turbulence intensity are shown in figure 6-67. Turbulence in most parts of the flume is lower than 10%. High turbulence concentrates in the vicinity of the slot and reach up to 75%. The greatest difference between the 0.012 and 0.020 m^3/s situations is the fact that turbulence intensity in the vicinity of the slots is more marked at 0.020 m^3/s.

The velocity vectors over three vertical slides [y = 0.10, 0.125 and 0.15m] are shown in figure 6-68. The comparison of this figure with figure 6-64 clearly shows that for a discharge of 0.020 m^3/s, the vertical component [Vz] is more important than for a discharge of 0.012 m^3/s.

6-4.2.2 Flow conditions for the 0.10 m wide vertical slot

c. Vertical slot, 0.10 m wide, flow of 12l/s ($V5_{12}$)

Velocity profiles at 0.01, 0.067 and 0.125 m above the flume bed are shown in figure 6-69. These velocity profiles are similar to those obtained for the 0.05 m wide slot. However in the vicinity of the vertical slot, the velocity vectors are not parallel but at angle around 30-45° with the axis of the slot.

The mean velocity patterns in the horizontal planes, at 0.01, 0.067 and 0.125 m above the flume bed, are shown in figure 6-70. These mean velocity patterns are similar to those of the 0.05 m wide slot. Maximum longitudinal velocities reach 0.80 m/s in the vicinity of the slot for the three elevations.

Turbulence intensity contours are shown in figure 6-71. Turbulence occurs mainly in the vicinity of the slot, near the bottom of the flume. Turbulence intensity reaches up to 30%.

Velocity profiles over the vertical slides at y = 0.10, 0.15 and 0.20 from the side of the flume shown in figure 6-72 reveal the same pattern than in figure 6-64. The vertical component [Vz] of velocity is negligible. The jet issuing from the 0.10 m wide vertical slot for a discharge of 0.012 m^3/s can therefore be considered as two-dimensional.

d. Vertical slot, 0.10 m wide, flow of 20l/s ($V5_{20}$)

The flow patterns for the 0.10 m wide vertical slot for a discharge of 0.020 m^3/s and a water surface elevation of 0.20 m are shown in figure 6-73 at 0.01, 0.067 and 0.133 m above the flume bed.

The velocity patterns for this situation are similar to the velocity patterns for the 0.10 m wide vertical slot for a discharge of 0.012 m^3/s but at 0.01 m above the flume bed, high velocities occur further downstream along the jet centre line. The lateral velocities are also more important in the vicinity of the slot and recirculation velocities are also slightly higher.

Mean velocity contours are given in figure 6-74 and contours of turbulence intensity are given in figure 6-75. High turbulence is concentrated within a column of diameter 0.10 m and centred at a distance of 0.10 m downstream the slot. The intensity reaches 47% and decreases to less than 20% in less than 0.10 m. RMS longitudinal and lateral velocities are more important than the RMS vertical velocities.

Velocity profiles over the vertical slides at y = 0.10, 0.15 and 0.20 m from the side of the flume shown in figure 6-76 reveal the same pattern as in figure 6-72. On the contrary to the 0.05 m wide slot, the jet stays two-dimensional even if the flow is increased from 0.012 to 0.020 m^3/s.

6-5 Summary

This chapter presented the hydraulic conditions existing within an area 1.5 m long by 1.22 m wide located just downstream of various energy dissipation devices. These devices are the overflow weir, the submerged orifice, the vertical slot and combinations of the three.

I. It has been shown that in most situations, the velocities in most parts of the flume are less than 0.20 m/s. High velocities concentrate in the vicinity of the device tested and/or along the longitudinal axis of the device.

II. For the orifice and vertical slot devices, it has been shown that the flow can be considered in a first approach as two-dimensional. However in the case of the vertical slot if the slot is very narrow and if the discharge is high, the flow becomes three-dimensional. On the contrary, the hydraulic conditions created by a flow passing over a weir are three-dimensional in all circumstances.

III. It has also been noticed that a recirculation phenomenon occurred in almost all situations. If the device [weir, orifice or slot] was located at the side, the recirculation always occurred on the right hand side of the flume toward the upstream right corner of the flume. If the device was located in the middle, the jet issuing from the device gave birth to two lateral recirculations on the right and left side of the flume. However in the case of the orifice in the middle, the flow pattern was asymmetric, the anticlockwise recirculation being more important.

IV. The association of a 0.60 m wide weir with a bottom side orifice decreased the range of velocities at the vena contracta for the given range of flows (0.012-0.020 m^3/s) in comparison with a bottom side orifice on this own.

V. For the weir devices, the calculated velocity at impact varies between 1.46 and 2.23 m/s while the measured velocity at 1/3 of the water depth varies between 0.35 and 0.45 m/s. The maximum turbulence intensity is around 50%.

VI. For the orifice devices, the velocity at the vena contracta varies between 0.80 m/s and 1.73 m/s. The maximum turbulence intensity is around 20-30%.

VII. For the vertical slot devices, the velocity near the bed (at 1 cm from the flume bed) varies between 0.30 and 0.78 m/s. The calculated maximum velocity at the slot varies between 0.80 and 1.82 m/s. The maximum turbulence intensity is between 25 and 35%.

In the following chapter, these results will be associated with the experimental results described in chapter 5 on the behaviour of parr and analysed in more details in order to elaborate a biomechanical model connecting hydrodynamics and fish energetics.

CHAPTER 7

INTEGRATION OF FISH BEHAVIOUR DATA AND HYDRAULIC MEASUREMENTS

CHAPTER 7

INTEGRATION OF FISH BEHAVIOUR DATA AND HYDRAULIC MEASUREMENTS

7-1 Introduction

Chapter 7 sets out to integrate fish behaviour studies reported in chapter 5 with the hydraulic measurements in the vicinity of the tested devices presented in chapter 6.

The purpose of this chapter is to build a bridge between two approaches to fish pass design: one followed by biologists and the other by engineers. This chapter is therefore divided into three principal sections. The first introduces an elementary comparison between the efficiency of a device, the hydraulic conditions in its vicinity and the capabilities of the parr. The second part reviews the travel paths selected by parr in relation to the hydraulic conditions existing in the flume. In the last part, an attempt has been made to quantify the energy used by parr to pass through the selected devices for a given flow and a given path.

7-2 Device efficiency and hydraulic conditions

7-2.1 *Introduction*

It was been statistically shown in chapter 5 that for the four series of tests conducted and at the two discharges studied (0.012 and 0.020 m^3/s), salmon parr moved most readily through orifices and vertical slots than through weirs. A summary of the tests conducted between 1999 and 2001, as well as the success rate of each situation are given in table 7-1. The designs tested have already been schematically represented in figure 4-2.

The conclusions drawn from series 1 tests revealed that orifices with an average efficiency of 65% were much more effective than the weirs. A Fisher's exact test confirmed that the degree of success between the orifice and the weir designs were significant (Fisher test, $p< 0.00$). It was also found that the elevation of the orifice in the water column had an influence on the success rate.

The purpose of series 2 was to confirm the findings of series 1 over a wider range of velocity. The weir was again unsuccessful even though the drop in level from the weir crest to the water surface downstream had been reduced from 0.10 m to 0 m. It was also significantly less efficient than the two orifices even when the opening of the orifice was reduced from 0.02 m^2 to 0.01 m^2 thereby doubling the velocity range from 0.6-1.0 m/s to 1.2-2.0 m/s (Fisher test, $p= 0.0033$).

With series 3, two new designs were investigated: the vertical slot and a weir-orifice combination. The better efficiency of the vertical slot (with an average efficiency of 45%) over the weir for the two discharges tested was significantly demonstrated (Fisher test, $p = 0.003$ at 12 m^3s^{-1}, and $p = 0.022$ at 20 m^3s^{-1}). It was found that if the velocity downstream an orifice is greater than the swimming capabilities of the targeted fish, the orifice could also become an impassable barrier. However it was also discovered that the association of a weir with an orifice increased the efficiency of the orifice in comparison with an orifice on its own.

Table 7- 1: Situations tested and their success rate

Code	Details	Success
	Series I: July - September 1999	
$WS_{12\text{-}0.2}$	Weir on the side at low flow – wsel = 20cm	0%
$WS_{20\text{-}0.2}$	Weir on the side at high flow - wsel = 20cm	5%
$WM_{12\text{-}0.2}$	Weir in the middle at low flow - wsel = 20cm -	0%
$WM_{20\text{-}0.2}$	Weir in the middle at high flow - wsel = 20cm	5%
$ObS_{12\text{-}0.02}$	Orifice at the bottom on the side at low flow – area orifice = 0.02 m^2	70%
$ObS_{20\text{-}0.02}$	Orifice at the bottom on the side at high flow – area orifice = 0.02 m^2	85%
$ObM_{12\text{-}0.02}$	Orifice at the bottom in the middle at low flow– area orifice = 0.02 m^2	95%
$ObM_{20\text{-}0.02}$	Orifice at the bottom in he middle at high flow– area orifice = 0.02 m^2	85%
$OFM_{12\text{-}0.02}$	Orifice at 5 cm from the bottom at low flow – area orifice = 0.02 m^2	65%
$OFM_{20\text{-}0.02}$	Orifice at 5 cm from the bottom at high flow– area orifice = 0.02 m^2	40%
$OTM_{12\text{-}0.02}$	Orifice at 10 cm from the bottom at low flow – area orifice = 0.02 m^2	25%
$OTM_{20\text{-}0\ 02}$	Orifice at 10 cm from the bottom at high flow – area orifice = 0.02 m^2	55%
	Series II: June 2000	
$WM_{12\text{-}0.3}$	Weir in the middle at low flow - wsel = 30cm -	0%
$ObM_{12\text{-}0.02}$	Orifice at the bottom in the middle at low flow– area orifice = 0.02 m^2	80%
$ObM_{12\text{-}0.01}$	Orifice at the bottom in the middle at low flow– area orifice = 0.01 m^2	40%
	Series III: August 2000	
$WS_{12\text{-}0.2}$	Weir on the side at low flow – wsel = 20cm	0%
$WS_{20\text{-}0.2}$	Weir on the side at high flow - wsel = 20cm	0%
$ObS_{12\text{-}0.01}$	Orifice at the bottom on the side at low flow – area orifice = 0.01 m^2	72.5%
$ObS_{20\text{-}0.01}$	Orifice at the bottom on the side at high flow – area orifice = 0.01 m^2	7.5%
$WOb_{12\text{-}0.01}$	Orifice at the bottom associated with a weir at low flow – a = 0.01 m^2	62.5%
$WOb_{20\text{-}0.01}$	Orifice at the bottom associated with a weir at high flow – a = 0.01 m^2	52.5%
$V5S_{12}$	Vertical slot 5 cm wide on the side at low flow	50%
$V5S_{20}$	Vertical slot 5 cm wide on the side at high flow	22.5%
$V10S_{12}$	Vertical slot 10 cm wide on the side at low flow	60%
$V10S_{20}$	Vertical slot 10 cm wide on the side at high flow	45%
	Series IV: September 2000	
AR_{12}	Double orifices with ratio 1:1, parr introduced on the right side at low flow	95%
AR_{20}	Double orifices with ratio 1:1, parr introduced on the right side at high flow	60%
AL_{12}	Double orifices with ratio 1:1, parr introduced on the left side at low flow	40%
AL_{20}	Double orifices with ratio 1:1, parr introduced on the left side at high flow	35%
BR_{12}	Double orifices with ratio 1:5, parr introduced on the right side at low flow	55%
BR_{20}	Double orifices with ratio 1:5, parr introduced on the right side at high flow	60%
BL_{12}	Double orifices with ratio 1:5, parr introduced on the left side at low flow	70%
BL_{20}	Double orifices with ratio 1:5, parr introduced on the left side at high flow	80%

7-2.2 *Comparison Weir-Orifice-Vertical Slot*

An important design parameter recognised by both engineers and biologists and certainly used in the design of fish passage structures is the velocity. In effect, engineers have to design fish passes so that the velocity existing in the structures are within the swimming abilities of the targeted species defined by the biologists.

In the following section, an attempt will be made to explain the difference in efficiency of the various designs as a function of the hydraulic conditions existing in the flume and in particular the velocities.

(a) Velocity at weirs

Pilot experiments, in which groups of fish were allowed up to 24h to pass, confirmed that weirs did not constitute a physical barrier to passage for the size of fish used. However within the 40 minutes allowed for the experiments, either no fish or only one passed through the different weir situations as shown in table 7-2.

Table 7-2: Efficiency of the different weirs designs in relation to velocities at impact and at 1/3 of the water surface elevation

Design	Success	Velocity at 1/3 of d/s water depth	Velocity at impact
Weir on the side at 12 l/s – wsel = 20cm	0%	0.35 m/s	2.02 m/s
Weir on the side at 20l/s - wsel = 20cm	5%	0.45 m/s	2.23 m/s
Weir in the middle at 12l/s - wsel = 20cm	0%	0.45 m/s	2.02 m/s
Weir in the middle at 20l/s - wsel = 20cm	5%	0.45 m/s	2.23 m/s
Weir in the middle at 12l/s - wsel = 30cm	0%	0.40 m/s	1.46 m/s

Sections 2-3.1 and 6-2.1 have already dealt with the complex nature of a falling jet at a drop structure. It was explained that the characteristics of the flow downstream a weir are dictated to a large extend by the discharge, the shape of the crest and the pool depth. For this work, the notch had been chosen rectangular with a width of 0.20 m and the pool depth had been fixed at 0.20 m for series 1 & 3 and at 0.30 m for series 2. The flow varied between 0.012 and 0.020 m^3/s.

The optimum conditions for leaping (as defined by Powers and Orsborn (1985)) were met: the depth of the plunge pool [wsel = 0.20 m or 0.30 m] was greater than the depth of penetration of the falling water [d = 0.15m] and of the same order or greater than the length of the fish [0.08 to 0.14 m].

Stuart (1962) defined also another criterion to obtain the optimum leaping conditions, based on the location of the standing wave. According to Stuart, the optimum leaping conditions depend on the presence and location of the standing wave formed downstream a weir or an overfall and are obtained when the stand-

ing wave is submerged exactly at the toe of the fall, which corresponds to a ratio of height of fall to depth of pool equal to 1:1.25.

For series 1 & 3 this ratio was equal to 1:2, the flow being in the plunging mode at the two discharges tested [figure 2-5]. Series 2 corresponds to the particular case, where there is no drop in level from the weir crest to the water surface downstream. In this case, the flow regime is oscillating between the surface wave and the surface jet regime shown in figure 2-6.

A schematic representation of the flow at an overflow weir in plunging mode is shown in figure 7-1. The flow is three-dimensional: the jet passes over the notch, plunges downward and becomes fully submerged as it sweeps the flume bed. The submerged jet spreads radially but not symmetrically at the plunge pool floor stagnation point forming two submerged rollers. The jet generates coherent and random turbulent structures. Turbulence intensity contours reveal indeed a wide circular spread of turbulence from the zone of impact. In addition, the impinging jet entrains air around the circumference of the jet intersection with the free water surface creating a phenomenon of aerated white water.

The two submerged rollers are part of the stimulus to the fish preceding the leap. Furthermore, turbulence and noise caused by the falling water are thought to be factors that enable parr to find its way (Stuart, 1962). In his report on the leaping behaviour of salmon and trout at falls and obstructions based both on observation of adults in the wild and parr in laboratory experiments, Stuart describes the behaviour of parr very precisely as they approach the weir and when they leap over the obstacle. He observes that the leap is always initiated at the surface of the pool on the neutral point of the standing wave and describes the approach to this point as slow, the fish swimming in mid water with their head pointing downward at an angle of 20 to 30°. The fish then rise with the current to break the surface as they meet the upward current (submerged roller) in front of the nappe. Leaving the water, the fish speed then through the air and stroke the water near the crest of the weir.

The maximum velocities occur at the water surface in the zone of impact. They reached values as high as 2 m/s and 2.2 m/s at discharges of 0.012 and 0.020 m^3/s for a water surface elevation of 0.20 m. For a water surface elevation of 0.30 m, the maximum velocities decrease respectively to 1.50 m/s and 1.75 m/s.

It is important to notice at this point that according to Beach (1984) water velocities of 2 m/s or more exceed the swimming capabilities of 0.08 to 0.14 m long parr [Figure 4-12; the average water temperature being around 15°C]. However parr did not have to swim against such high velocities to pass over the weir because they tended to move near the bed where the velocities are low while swimming toward the upstream part of the flume and secondly because in the vicinity of the jump they used the upward current of the roller to reach the water surface and initiate their leap. It has effectively been shown in chapter 6, that the water velocity in the flume near the zone of impact decreases as it gets nearer the flume bed and that high velocities and high turbulence concentrate exclusively around the zone of impact.

Stuart also concluded that the white water phenomenon observed at the weir overflow could block the stimulus to jump if the concentration of air was too important but without providing any quantitative value (Fig 7-2). Using an empirical relationship to predict aeration rate, the air concentration for the two discharges of 0.012 and 0.020 m^3/s has been calculated in chapter 6 and has been found to be around 5-6 % (Ervine, 1998).

The slow response of parr at an overflow weir in this research in comparison with the work done by Stuart may be due to the fact that this study observed fish within 40 minutes of their release whereas the parr in Stuart's work were held in the apparatus for many days. And the great difference between the success rate of orifices and weirs might be explained by the fact that jumping at falling water is likely to be risky due to the possibilities of damage and attracting predators and is also likely to be expensive in energy expended.

We have seen in section 6-2.2 that if the water surface elevation downstream the weir is increased from 0.20 m to 0.30 m (which corresponds to reduce the drop between the crest of the rectangular notch and the downstream water level from 0.10 m to 0 m) the flow regime passes from a plunging mode to a streaming mode. The velocities at the water surface are then reduced from 2.20 m/s to 1.75 m/s at 0.020 m^3/s and from 2.0 m/s to 1.50 m/s at 0.012 m^3/s. However no amelioration in the number of successful parr was observed when the downstream water level was increased as seen in table 7-2.

According to Stuart (1962), the streaming mode for the surface wave/or breaking wave regime is even less suitable for the passage of salmon because the erratic undulations created by the flow skimming over the water surface disorientate the fish. However this conclusion is not in accordance with the findings of Thompson (1970) on Chinook salmon (*Oncorhynchus tshawytscha*). Thompson carried out a specific study on the effect of the nature of the flow on performance and behaviour of Chinook salmon in a pool and overfall fish pass. He found that Chinook salmon could ascend a pool and overfall pass as well under plunging or streaming mode.

(b) Velocities at orifices

For all the orifices situations studied, the rectangular jet passing through the device was discharged into a pool initially quiescent. The behaviour of this submerged jet into a stagnant environment is similar to the behaviour of three-dimensional jets investigated theoretically and experimentally by Rajaratnam (1976). A plan view of the longitudinal velocity in the vicinity of the 0.20 m width orifice for a discharge of 0.020 m^3/s is given in figure 7-3.

Basically, the jet travels through the pool as a 3-D jet either with two recirculation regions, one on each side of the jet for the orifices located in the middle or with one large recirculation region for the orifices located on the side.

Maximum velocities for the submerged orifices occurred at the vena contracta 0.10 to 0.30 m downstream the opening, along the jet centre line. These were

generally in the range of 0.8 to 1.8 m/s. A comparison of the orifice's efficiency at passing salmon parr with the velocities at their vena contracta is shown in table 7-3 and figure 7-4. The maximum velocity at the vena contracta is obtained for the orifice at the bottom on the side with a 0.10 x 0.10 m opening and it has been calculated to reach 2.88 m/s. A success rate of passage through the orifice of 7.5 % is associated with this high velocity.

Table 7-3: Comparison of orifices efficiency with measured velocities at the vena contracta (* this value has not been measured but calculated)

Orifices design	Success	Velocity at vena contracta
Orifice at the bottom on the side at 12l/s – area orifice = 0.02 m^2	70%	0.97 m/s
Orifice at the bottom on the side at 20l/s– area orifice = 0.02 m^2	80%	1.37 m/s
Orifice at the bottom in the middle at 12l/s– area orifice = 0.02 m^2	87.5%	0.80 m/s
Orifice at the bottom in the middle at 20l/s– area orifice = 0.02 m^2	85%	1.57 m/s
Orifice at the bottom in the middle at 12l/s– area orifice = 0.01 m^2	40%	1.73 m/s
Orifice at the bottom on the side at 12 l/s – area orifice = 0.01 m^2	72.5%	1.60 m/s
Orifice at the bottom on the side at 20l/s – area orifice = 0.01 m^2	7.5%	2.88 m/s*
Orifice at the bottom associated with a weir at 12 l/s – a = 0.01 m^2	62.5%	1.50 m/s
Orifice at the bottom associated with a weir at 20 l/s – a = 0.01 m^2	52.5%	1.62 m/s
Orifice at 5 cm from the bottom at 12 l/s – area orifice = 0.02 m^2	65%	0.80 m/s
Orifice at 5 cm from the bottom at 20l/s - area orifice = 0.02 m^2	40%	1.35 m/s
Orifice at 10 cm from the bottom at 12 l/s – area orifice = 0.02 m^2	25%	0.80 m/s
Orifice at 10 cm from the bottom at 20 l/s – area orifice = 0.02 m^2	55%	1.20 m/s

(i) Location of the orifice: side or middle

Figures 7-5 to 7-7 show the longitudinal variation of the non-dimensional velocity along the jet centre line of the orifices at the side or in the middle, for a small or a large opening (area = 0.01 m^2 or 0.02 m^2) at discharges of 0.012 or 0.020 m^3/s. In these figures, the velocity at the cross-section V_o is used as a velocity scale and the height of the orifice b_o is used as the length scale. Accordingly to the theory of turbulent jet (Rajaratnam, 1976), the longitudinal velocity stays constant within the potential core region and then decreases continuously. From Fig. 7-5, 7-6 and 7-7, it can be observed that V_x/V_o shows some increase near the orifice. This corresponds to the location of the vena contracta. Then V_x/V_o decreases more or least rapidly between x = 2bo-3bo and x = $6b_o$ (length of the potential core for a plane turbulent jet). At a distance greater than 6bo, V_x/V_o levels out. If the orifice is at the side, V_x/V_o is around 0.6-0.7 at low or high flow [0.012 or 0.020 m^3/s] and for the large or small opening [0.01 or 0.02 m^2] whereas if the orifice is in the middle, V_x/V_o is around 0.1-0.2.

It is clear from these figures that the decay of the longitudinal velocity in the jet centre line of the orifices is faster when the orifices are located in the middle. However this phenomenon has no significant influence on the fish passing efficiency.

(ii) Location of the orifice: at the bottom or at 0.05/0.10 m above the bed

The jet diffusion pattern is also altered by the elevation of the orifices above the flume bed in the water column. Jets discharging through orifices located at the bottom are comparable with bluff wall jets while jets passing through elevated orifices behave like free bluff jets [see section 2-5.1.3 for more details]. Representations of the jet diffusion pattern for orifices located at the bottom, at 0.05 and 0.10 m from the base of the pool are shown in figure 7-8. It is clear from these representations that even if the velocities at the cross-section or at the vena contracta are similar for the three orifices elevations, a fish moving near the bottom of the pool might experience dramatically different velocity flow patterns.

The longitudinal variation of the non-dimensional mean velocity along the jet centreline for the orifice at 0, 0.05 and 0.10 m from the bottom of the flume is shown in figure 7-9. In this figure, the velocity at the vena contracta V_{vc} is used as a velocity scale and the height of the orifice is used as the length scale. Figure 7-9 shows clearly that velocity vector patterns in the plane of the jet centreline for the orifices elevated at 0.05 and 0.10 m are similar to those of the bottom orifice. High velocities have been measured to be around 0.80 m/s at 0.012 m^3s^{-1} and 1.35 m/s at 0.020m^3s^{-1}.

By considering the three representations of the flow pattern in figure 7-8, it can be seen that fish near the bed of the pool and moving upstream were confronted with velocities going in the opposite direction and increasing as they were progressing toward the device for the orifice located at the bottom while they were confronted with turbulent flows facing upstream at longitudinal distance lesser than 0.30 and 0.60 m from the device for the 0.05 and 0.10 m elevated orifices. As it was been explained earlier in chapter 2, salmon tend to swim against the flow to find their way upstream. If they are caught in a flow facing upstream,

a certain confusion may arise. As the flow under the main jet, passing through the elevated orifices is also turbulent this is also not an ideal holding area for the fish.

The nature of the different flow conditions near the bed of the flume due to the elevation of the orifice in the water column also corroborates findings presented in section 5-4. It has been observed that fish passed significantly more easily through jets low in the water column and that the height of the orifice from the base of the flume influenced the time it took for fish to move through them. However this decrease in efficiency was not linearly proportional to the elevation of the device relative to the bottom of the flume, for the range of designs tested. Figure 7-4 shows at least a general reduction in efficiency of at least one third.

Photographic observations show parr generally stayed close to the bottom of the flume. This behaviour pattern associated with the fact that near the bottom of the pool quite different velocities and flow patterns exist for the different situations may explain the difference in efficiency observed between the bottom and the elevated orifices.

Thompson et al (1967) carried out similar work on the response of migrating adult salmonids (Chinook salmon, Coho salmon and Steelhead trout) to orifices 2 x 5 feet [0.61 m by 1.525 m] in a vertical or horizontal position at two depths: at a centreline submergence of 3 feet [0.915 m] and 9 feet [2.745 m], the overall approach area being 19 feet deep [5.795 m]. Migrating salmonids were presented with a choice between two orifices with both a 1-foot [0.305m] head. In shallow water, there was equal use of the horizontal and vertical orifice but the vertical orifice was used more than the horizontal orifice in deepwater. There was also an equal use of the vertical orifice when positioned in shallow and deep water but the horizontal orifice was used more when in shallow water than in deep water.

The preference of the vertical orifice over the horizontal orifice might be due to the fact that the vertical orientation allows the fish to swim through the device over a wider range of depth. The second point, which might be concluded from Thompson et al (1967), is that elevated orifices are more suitable than deep orifice and yet this conclusion appears in opposition with our own findings that bot-

tom orifices are more suitable than elevated orifices. But there are great differences between the set up of the two experiments. In Thompson et al (1967), the centreline of all the orifices tested is equal or over 10 feet [3.05 m] from the bottom of the bed and the ratio depth of the water over the size of the fish is equal to 5:1 whereas in this study, the centreline of the orifices tested is less than 0.10 m from the bottom of the bed and the ratio depth of the water over the size of the fish is equal to 2:1. The targeted species for these two experiments are also different as Thompson et al (1967) investigated Pacific salmon whereas this work studied Atlantic salmon.

(iii) Orifice: associated or not with a weir

The overall efficiency of an orifice over a range of flow might be improved by introducing a weir in parallel operating mainly at high flows as shown in figure 7-12. At high flow, the efficiency of a narrow orifice as well as the length of time needed by fish to negotiate it improves significantly by combining with it an overflow weir (Chi-square test, $p = 0.005$). The efficiencies of the 0.10 by 0.10 m bottom side orifices with and without weir combination are shown in figures 7-10 and 7-11. By considering the orifice at the bottom side and the orifice at the bottom side associated with a weir for a discharge of 0.012 m^3/s, it can be seen that the velocity at the vena contracta has been reduced by 8% due to the presence of the weir. This effect is even more apparent for a discharge of 0.020 m^3/s as the velocity at the vena contracta is reduced from 2.88 m/s to 1.61 m/s. This reduction by 45% of the velocity at the vena contracta is also correlated to an efficiency improvement of the 0.10 by 0.10 m bottom side orifice by 45%. From figure 7-12, it is clear that for an average water temperature of 15°C, a water velocity of 2.88 m/s exceeds the swimming capabilities of parr whereas a water velocity of 1.61 m/s is within the maximum swimming speed range (1.5 to 2.1m/s) of parr 0.08 to 0.12 m long.

The introduction of a weir allows the reduction of the velocities downstream the opening just enough to keep the orifice attractive and therefore increases the

range of flow for which the design is passable by the migrating fish as shown in figure 7-12.

(c) Velocities at vertical slots

The great advantage of vertical slots over weirs or orifices is the fact that fish are able to swim through the slot at any desired depth. This is particularly important for non-salmonids species in tropical and subtropical rivers, which have lower swimming capabilities and/or do not have jumping abilities (Stuart and Mallen-Cooper, 1999).

For the 4 vertical slot situations tested [table 7-4], the incoming jet travels towards the end of the flume as a 2-D jet with one recirculation region. Velocities higher than 0.20 m/s concentrate inside a band 0.25 m wide include between y = 0 and 0.25 m and a weak recirculation pattern occurs in the rest of the flume as shown in figure 7-13.

The flume is clearly divided in to two regions: a region of high velocities and turbulence around the axis of the vertical slots and a region of low velocities occupying between 70 and 80% of the total volume of the flume. This flow pattern is similar to the flow pattern observed by Wu for its "simple and effective "vertical slot as shown in figure 2-16 with a slope of 5% (Wu et al, 1999).

Near the bottom of the flume, the velocities for the vertical slot were around 0.50-0.80 m/s. The comparisons of the efficiency of the vertical slots with the maximal velocity they recreate in the flume are shown in table 7-4.

Table 7-4:comparison of the vertical slots efficiency with their maximal velocity:

Design	Success	Velocity near bed	Maximum velocity at slot (calculated)
Vertical slot, 0.05 m wide, 12l/s	50%	0.78 m/s	1.34 m/s
Vertical slot, 0.05 m wide, 20 l/s	22.5%	0.30 m/s	1.82 m/s
Vertical slot, 0.10 m wide, 12 l/s	60%	0.71 m/s	0.81 m/s
Vertical slot, 0.10 m wide, 20 l/s	45%	0.55 m/s	1.18 m/s

The longitudinal variation of the depth-averaged velocity [z =0.01, 0.067 and 0.125] is shown in non-dimensional form in figure 7-14. This figure is similar to figures 7-5 to 7-7 and illustrates that jets from vertical slots can be considered as

plane turbulent jets (Wu et al; 1999). The maximum velocity at the slot V_{sm} [=$\sqrt{2g\Delta h}$] is used as the velocity scale and the half-slot width $0.5b_o$ is used as the length scale. The choice of the velocity scale and the length scale was influenced by the work done by Wu et al (1999). As with the results obtained by Wu et al, V_{av}/V_{sm} shows some increase in the vicinity of the slot for the 0.10m wide vertical slots at a discharge of 0.0.20 m^3/s. For the four situations shown in figure 7-14, V_{av}/V_{sm} decays rapidly up to a distance equal to $6b_o$. At this distance that corresponds to the length of the potential core for a plane turbulent jet, V_{av}/V_{sm} is less than 0.3 for the four situations tested. At this point it is important to note the very low dip occurring for the 0.05 m wide slot in particular not observed by Wu et al. It is effectively clear from figure 7-14 that the V_{av}/V_{sm} seems to increase before levelling out around 0.3 for the 0.10 m wide slot and around 0.2 for the 0.05 m slot. The depression of V_{av}/V_{sm} is due to the fact the trajectory of the jet when passing through the slot is not exactly parallel to the X-axis as shown in figure 7-13.

(d) Turbulence at Orifices, Weirs and Vertical slots

The influence of turbulence on the efficiency of fish passage structures has long been recognised (Clay, 1995; Stuart, 1962). High turbulence might effectively disorientate the migrating salmon or inhibit their jumping abilities. The great difficulty in assessing the direct impact of turbulence on fish pass efficiency lies in the difficulty in dissociating the influence of turbulence from velocity in field and laboratory studies.

The contours of turbulence intensity differ from one device to another but for most of the weirs/orifice/vertical slots situations tested, the level of turbulence (less than 5%) was low in most parts of the flume.

For the weir designs, high turbulence concentrates in the zone of impact near the water surface and are as high as 50%. Turbulence intensity contours shown in chapter 6 also revealed a circular spread and a rapid decrease of the turbulence from the zone of impact.

For the orifice designs, high turbulence occurs along the jet centreline, 0.10 to 0.30 m downstream of the orifice in the vicinity of the vena contracta. The turbulence intensity varies between 20 and 30%, which corresponds to RMS longitudinal velocities between 0.30 and 0.40 m/s. Turbulence values for orifices are less concentrated in one area of the flume and more radially spread than for the weir situations.

For the vertical slot designs, high turbulence occurs 0.10 m downstream the slot. They reach an intensity of 25% for the 0.10 m wide slot and an intensity of 35% for the 0.05 m wide slot. The turbulence concentrates within a very small area (x = [0.10 m; 0.30 m] and y = [0 m; 0.15 m]) in particular for the narrow slot in a similar manner to weirs.

By comparing the contours of turbulence intensity for the three designs: weirs, orifices and vertical slots, it is clear that turbulence patterns differ greatly between the weirs and the orifices while the vertical slots appear to be an intermediate pattern. The maximum turbulence intensity is also greater for the weirs (50%) than for the orifices (20-30%) and the vertical slots (25-35%). However no conclusive evidence was found of the direct and sole influence of the turbulence on the efficiency of the various designs.

7-2.3 *Comparison of orifice and vertical slot efficiency*

a) Correlation of slots efficiency with opening size

Orifice and vertical slot efficiencies at passing salmon are directly correlated with the velocities existing in their vicinity and therefore to the size of the opening and the range of flow at which they were tested.

The efficiency of the orifice varies significantly with the size of the opening (Fisher's exact test, $p = 0.022$). For the orifice with an opening of 0.02 m^2, the velocities at the vena contracta have been measured to be around 0.80 m/s while for the orifice with an opening of 0.01 m^2, the velocities reach 1.60 m/s for a 0.012 m^3s^{-1} flow. In fact, the number of parr passing through the orifice decreases as the velocities in the vicinity of the orifice increase.

Like the orifice, vertical slot efficiency changes significantly with the width of the opening at high flow but not at low flow (Fisher's exact test, p = 0.04 and 0.58 respectively). A significant gap exists between the 0.012 m^3s^{-1} and 0.020 m^3s^{-1} situations for the narrow slot (Fisher's exact test, p= 0.02) that does not occur for the wide slot (Fisher's exact test, p= 0.53).

The size of the orifice/width of the slot and hence the velocities in the vicinity of the orifice/vertical slot have an important effect on the efficiency of the device. The opening has to be calculated to create attractive velocities within the abilities of the targeted fish, but not too high so the fish have difficulty passing. The window of suitable velocity is therefore an important parameter.

b) Orifice versus vertical slot efficiency at similar velocities

It was already been shown in section 5-3.2 that the efficiency of the 0.05 m wide vertical slot is significantly lower than the efficiency of the 0.10 by 0.10 m orifice for a discharge of 0.012 m^3/s.

Figure 7-15 clearly demonstrates that for both the vertical slots and the orifices, their efficiencies decrease as the maximal velocity in the flume increases. The relation between the efficiency and the maximal velocity for the orifices and the vertical slots are expressed in equation 7-1 and 7-2 respectively. It is reminded that in this study, the efficiency of a device corresponds to the percentage of salmon parr passing successfully through it. At similar velocities, the efficiency of the vertical slots is lower than the one of the bottom orifices.

$$Efficiency = -0.4026V_w + 1.2602 \quad \textbf{(7-1)}$$

$$Efficiency = -0.359V_w + 0.906 \quad \textbf{(7-2)}$$

Equations 7-1 and 7-2 are valid for value of V_w greater than 0.60 m/s, V_w being the calculated maximal velocity at the slot for the vertical velocities and the velocity at the vena contracta for the orifices.

It has been explained in chapter 2 that although the slot could be regarded as a plane jet as a first approximation, the velocities at a slot are neither uniform nor perpendicular to the slot (Wu et al, 1999). The results represented in chapter 6 are also in accordance with the findings by Wu et al (1999) that the decay of the maximum velocity in the jet passing through a slot as it travelled through the pool is quicker than that of a jet passing through an orifice.

Hence, it might be postulated than the lower efficiency of vertical slots in comparison with bottom orifices at similar maximal velocities near the device is related to the rapidity of the decay of the jet velocities. This postulate is in accordance with the observations reported by Bates (2000).

7-2.4 *Space occupation in the flume*

To reach the tested devices, parr followed in general the sides of the arena, which provided them with low velocities and cover. In all situations, parr tended to avoid the centre of the flume by swimming along the sides. The comparison of the degree of attractiveness between the "side" and "middle" areas significantly proves that parr tend to avoid the centre of the arena as seen in figure 7-16 (Mann-Whitney, $p = 0.0009$).

This observation is in accordance with the "line swimming" behaviour documented for salmon in large rivers (Clay, 1961; Powers, 1985; Hinch and Rand, 2000). Salmon effectively often stay near the shore when migrating upstream.

7-2.5 *Conclusion*

From a simple comparison between the success rate of weir/orifice/vertical slot devices and the hydraulic conditions existing in their vicinity, the following points have been postulated:

1. Weirs, orifices and vertical slots create very different hydraulic conditions (velocity, flow pattern and turbulence) in the flume, which can be correlated to differences in efficiency at passing parr.

2. The willingness of parr at jumping over weirs can be inhibited by factors completely different from hydraulic characteristics such as the risk of damage.

3. Orifices are suitable devices to attract and pass parr as long as the velocity at the vena contracta is within the swimming capabilities of the fish.

4. Combining the orifice with a weir can increase the range of flow for which orifices are efficient.

5. The position of an orifice from the flume bed in the water column influences the nature of the flow just downstream of the orifice and affects its efficiency.

6. At equal velocity, orifices are more suitable than vertical slots because the decay rate of velocities within a jet is higher for slots than orifices.

7-3 Paths chosen by parr

7-3.1 *Introduction*

The paths chosen by parr are also good indicators of the way they handle the various hydraulic conditions created by the different designs. The choice of path may be influenced by the location of the pass (side/middle) as well as by the nature of the design (orifice/vertical slot) as well as the flow rate (0.012 or 0.020 m^3/s).

The paths are divided into 6 groups noted as path A, B and C as well as "around the flume", "no motion" and "others". For path A, the fish moves straight along the side of the flume from the point of its introduction to the weir or orifice outlet as shown in figure 7-17. For path B, the fish moves first along the downstream end of the flume, then moving upstream along the edge and to the pass device. For path C, the fish starts along path A crossing over to take path B. For the path noted "around the flume", the fish goes round the flume staying

near the wall and returning to its point of introduction. For "no motion" the fish stays in the vicinity of the location of introduction of the flume. "Other", groups together the paths that do not fit in the other categories.

7-3.2 *Comparison of paths chosen:*

7-3.2.1 *Orifice - vertical slot comparison*

A sketch of the narrow 0.05 m slot and smallest orifice 0.01 m^2 is shown in figure 7-18. Table 7-5 summarises the paths taken by the parr at the two flow rates 0.012 and 0.020 m^3/s.

Path A is the most commonly taken path for both designs, followed by path B and then path C but the proportions vary with the designs: 65% of the parr choose path A for the orifice against 46.5% for the vertical slot.

There is no significant influence of the flow rate for the range of flow tested on the path chosen by parr. The results obtained for the two different flows have therefore been regrouped. The proportion in which parr chose path A, B or C varies significantly with the design (Chi-square test: Chisq = 7.347, df = 2, p = 0.026).

By comparing the contours of mean velocity for the two designs at 0.012 and 0.020 m^3/s, it is obvious that the velocities in the jet centre line of the vertical slot are lower than for the 0.01 m^2 side orifice: along the jet centre line, 1.50 m downstream the orifice/slot, the mean velocity is between 0.60-0.80 m/s for the orifice and only around 0.40 - 0.60 m/s for the slot. As fish use the orientation and the strength of the flow to select their path, the slightly higher velocities in the orifice jet centre line might account for the increase by 15% of the selection of path A between the narrow vertical slot and the bottom side orifice. It is also possible to observe a slight tendency of the orifice/slot jet to turn towards the opposite side of the flume. This phenomenon might also have an impact on the path's choice.

The success of the parr confronted with orifices is directly connected to their movements as shown in table 7-6. Around 87.5% of the parr which choose path

A, succeeded, while only 57.1% of the parr which choose path B or C, succeeded (Chi-square test, Chsq = 4.508, df = 1 and p = 0.034).

Table 7- 5: Only the 3 most taken paths are considered for the statistical analysis.

Code		Path A	Path B	Path C
$ObS_{12\text{-}0.01}$	BOTTOM	60%	30%	5%
$ObS_{20\text{-}0.01}$	ORIFICE	70%	15%	0%
$V5_{12}$	VERTICAL	45%	35%	8%
$V5_{20}$	SLOT	48%	18%	15%

It has already been stated in previous paragraphs that for the bottom side orifice and for the vertical slot designs a recirculation phenomenon occurs and that velocities are below 0.40 m/s over most of the flume with high velocities occurring only along the jet centreline. Therefore path A can be seen as the "high velocity" path, and path B as the " low or even reverse velocity". This preference of this "high velocity path " over the " low or even reverse velocity" path can be explained if we take into account the fact that water velocity has been recognised as the major stimulus instigating the upstream movement of salmon (Winstone et al, 1985), hence the expression "attraction flow".

Table 7-6: Number of parr choosing a path as a function of the situation - the number of successful and unsuccessful parr is also given for each path at each situation

	No motion		Path A		Path B		Path C		Turn		Other	
$ObS_{12\text{-}0.01}$	1		24		12		2		1		0	
Y/n	0	1	21	3	7	5	1	1	0	1	0	0
$ObS_{20\text{-}0.01}$	3		28		3		0		0		0	
Y/n	0	6	3	25	0	6	0	0	0	0	0	0
$V5_{12}$	4		18		14		3		1		0	
Y/n	0	4	11	7	6	8	2	1	1	0	0	0
$V5_{20}$	6		19		7		6		2		0	
Y/n	0	6	7	12	1	6	1	5	0	2	0	0

7-3.2.2 *Orifice alone and weir/ orifice combination comparison*

The paths chosen by the parr for the small bottom side orifice ($0.01m^2$) and the combination weir-small bottom side orifice are compared. Sketches of the two designs are shown in figure 7-19 and the proportions of parr choosing between the different paths are shown in table 7-7.

Path A was the most commonly taken path for the two designs, both registering around 64-65%. Path B was the second most chosen path with 23% in both cases, followed by path C with less than 5%. The percentage of parr, which do

not move or stay at the downstream end of the flume varied between 5 and 15 %, the greatest proportions being obtained at 0.020 m^3/s.

There is no significant influence of the flow rate (for the range tested) on the path chosen by parr for the two designs compared. There is also no significant difference between the orifice and the weir/orifice combination (Chi-square test: chsq = 0.305, df = 3, p = 0.959). However the success of the parr confronted with orifice designs is directly connected to their movements: 78.7% of the parr, which choose path A, succeeded, while only 47.1% of the parr, which choose path B or C succeeded (Chi-square test, Chsq = 10.890, df = 1 and p = 0.001).

These results are comparable to those found in the earlier comparison of bottom side orifice and vertical slot. Path A is again the most desirable and the most efficient path. There is also no difference in the behaviour/ movement of the parr for the two designs. This is in accordance with the hydraulic results stating that the combination of the bottom side orifice with a 0.62 m wide and 0.40 m high weir did not alter the flow pattern conditions in the pool even if the velocities at the vena contracta were reduced.

Table 7-7: Only the 4 most taken paths are considered for the statistical analysis.

Code		Path A	Path B	Path C	No motion
$ObS_{12\text{-}0.01}$	ORIFICE	60%	30%	5%	3%
$ObS_{20\text{-}0.01}$		70%	15%	0%	15%
$WOb_{12\text{-}0.01}$	WEIR/	68%	20%	5%	5%
$WOb_{20\text{-}0.01}$	ORIFICE	60%	23%	3%	15%

7-3.2.3 *Pathway as a function of elevation of orifice*

It has already been shown that the elevation of an orifice above the flume bed in the water column affects its efficiency. This section will concentrate on the influence of the orifices elevation on the movement of the parr. In this case we compare an orifice at the bottom, one 5 cm off the bottom and one 10 cm off the bottom of the flume as shown in figure 7-20. It is important to note that the devices are located in the middle and not at the side. The proportions of parr choosing the different path are shown in table 7-8.

For all three devices together, the percentage of parr taking path A, B and C is 25%, 31% and 18% respectively. Parr appeared to choose in almost equal proportion to move along the window (right) side or to move first along the left side of the flume.

The flow rate does not have a significant influence on the path chosen (*Chi square = 0.570, df = 2, p = 0.752*) and the elevation of the opening from the bottom of the pool does not seem to influence significantly the path chosen by parr (*Chi- square test = 7.128, df = 6, p = 0.310*).

Table 7-8: Number of parr choosing a path

Code	Path A	Path B	Path C	Return	No motion	Others
$ObM_{12\text{-}0.02}$	6	9	2	0	1	2
$ObM_{20\text{-}0.02}$	4	9	3	1	1	2
$OFM_{12\text{-}0.02}$	6	3	7	0	2	2
$OFM_{20\text{-}0.02}$	3	7	4	1	2	3
$OTM_{12\text{-}0.02}$	6	2	3	4	2	3
$OTM_{20\text{-}0.02}$	5	7	3	3	0	2

It is interesting to note that even if the hydraulic conditions in the vicinity of an orifice change with its elevation (§ 7-2.1 a), and even if this change affects the orifices' efficiency, this does not significantly affect parr in their choice of path. It might be extrapolated from this observation that parr chose their path not in relation to the hydraulic conditions existing in the vicinity of the orifice but according to the hydraulic conditions existing where they are located in the flume/pool.

7-3.2.4 *Choice of Pathway as a function of the size of the opening*

It has already been shown that the size of an orifice has a major role on its suitability for fish passage. In this paragraph, the influence of size on the movement of the parr is considered. The behaviour of four groups of 20 parr confronted with two bottom orifices of different sizes as shown in figure 7-21 for the two usual discharges of 0.012 and 0.020 m^3/s is compared. The proportions of parr choosing the different paths are shown in table 7-9.

All the parr in this experiment responded to the flow. 22 moved first along the path A, 14 choose the opposite side of the flume (path B), three chose path C and five did one or more circuits of the flume.

Parr choose mainly paths A and B, without either being significantly predominant. A chi-square test shows that the choice of path (between A, B & C) does not vary significantly between the two orifices (Chi-square test: chisq = 1.322, df = 2, p = 0.517), but the success rates vary significantly with the path chosen. This difference lies in the fact that fish taking path A for the larger orifice have greater chances of success that fish taking path A for the smaller orifice (2 versus 7 against 10 vs. 3: chisq = 6.418, df = 1, p = 0.011) This might be explained by the fact that the velocities in front of the opening are much higher in the case of the narrow orifice: 1.73 m/s against 0.80 m/s.

Table 7-9: Number of parr choosing a path as a function of the situation – Number of successful and successful parr is also given for each path at each situation

	No motion		Path A		Path B		Path C		Turn		Other	
$ObM_{12\text{-}0.02}$	0		9		8		2		1		0	
Yes/no	0	0	2	7	5	3	0	2	1	0	0	0
$ObM_{12\text{-}0.01}$	0		13		6		1		0		0	
Yes/no	0	0	10	3	5	1	1	0	0	0	0	0

7-3.2.5 *Pathway as a function of the orifice lateral location*

In this case, we compare two identical orifices: one at the side and the other in the middle. The two orifices are 0.20 m by 0.10 m as shown in figure 7-22. Of the 240 parr introduced into the flume, only 3 did not respond to the flow and remain in the corner where they were introduced. The numbers of parr choosing a path as a function of the situation are shown in table 7-10.

Table 7-10: Number of parr choosing a path

Code		Path A	Path B	Path C	Return	No motion	Others
$ObS_{12\text{-}0.02}$	SIDE	7	1	7	2	1	2
$ObS_{20\text{-}0.02}$		2	9	8	0	0	1
$ObM_{12\text{-}0.02}$	MIDDLE	6	9	2	0	1	2
$ObM_{20\text{-}0.02}$		4	9	3	1	1	2

For orifices at the side, path A is the most direct way to the entrance but the most energy demanding (the fish face constantly high velocities). Path B then avoids high velocities. The flow rate, in this condition, influences the choice of the path (Chi-square = 6.392, df = 2, p = 0.041). At 0.012 m^3/s, most parr moved initially directly toward the jets, but half of them veered away from the fast flowing water half way through and approached by the opposite side (Path C). At

0.020 m^3/s, the same proportion opted initially for a direct or lateral way, but almost all of those, which moved directly toward the jet, veered away.

For orifices at the middle, paths A and B offer the same level of difficulties. The flow does not have a significant influence on the path chosen (Chi square = 0.570, df = 2, p = 0.752).

It might be concluded from this comparison that the location of the orifice at the side or in the middle influence the path followed by the parr even if it does not affect the final efficiency of the device.

7-3.2.6 *Choice of pathway as a function of vertical slot width*

In this case, two vertical slots are compared. Both designs are located at 0.10 m from the right side of the flume, but their widths differ as shown in figure 7-23. The first one is 0.05 m wide and the second 0.10 m wide. The numbers of parr choosing a path and succeeding as a function of the situation are shown in table 7-11. In table 7-12, only the 4 most taken paths are considered.

The percentage of parr, which do not move or stay at the end of the flume, varies between 5 and 15 %. Path A was the most commonly taken path with 47.5%. Path B was the second most chosen path 32 % and less than 10 % chose path C.

Table 7-11: Number of parr choosing a path as a function of the situation - the number of successful and unsuccessful parr is also given for each path at each situation

		Path A		Path B		Path C		Turn		No motion	
0.05 m Slot	$V5_{12}$	18		14		3		1		4	
	Y/n	11	7	6	8	2	1	1	0	0	4
	$V5_{20}$	19		7		6		2		6	
	Y/n	7	12	1	6	1	5	0	2	0	6
0.10 m Slot	$V10_{12}$	10		5		3		1		1	
	Y/n	9	1	1	4	1	2	1	0	0	1
	$V10_{20}$	11		6		2		0		1	
	Y/n	6	5	3	3	0	2	0	0	0	1

There is no significant influence of the flow rate on the path chosen by parr for the 0.05 and 0.10 m wide slots (chi-square tests, p>0,05). There are also no significant differences between the 0.05 m wide vertical slot and the 0.10 m wide vertical slot at the flow rate tested (Chi-square test: chsq = 2.305, df = 3, p = 0.512).

Table 7-12: Only the 4 most taken paths are considered for the statistical analysis.

Code		Path A	Path B	Path C	No motion
$V5_{12}$	0.05 m	45%	35%	8%	10%
$V5_{20}$	Slot	48%	18%	15%	15%
$V10_{12}$	0.10 m	50%	25%	15%	5%
$V10_{20}$	Slot	55%	30%	10%	5%

The success of the parr confronted with vertical slots designs is directly connected to their movements. 57.6% of the parr on path A succeeded while only 29.5% of the parr coming from path B and C succeeded (Chi-square test: Chsq = 8.011, df = 1 & p = 0.005). Like for the orifices located at the side, path A is the most desirable and the most efficient path and the width of the slot does not influence the movement of the parr in the flume even if it has a major role on the efficiency of the slot.

7-3.3 *Pathway chosen by fish for the double orifice design*

In this section, a double orifice shown in figure 7-24 is tested for two total discharges 0.012 and 0.020 m^3/s, two flow ratio 1:1 and 1:5 and two locations of introduction of the parr: right or left corner (Table 7-13). Fish are unable to pass through the 0.5 x 0.05 m orifice, as it was covered by a coarse grid.

Table 7-14 shows that if the flow ratio between the two orifices is 1:1, the velocities at the vena contracta of the two orifices are similar and around 0.60-0.80 m/s at 0.012 m^3/s and around 1.00 m/s at 0.20 m^3/s. If the flow ratio is 1:5, then the velocities at the vena contracta of the coarse grid orifice are three times higher than at open orifice [table 7-14]. The numbers of parr choosing a path and succeeding as a function of the situation are shown in table 7-15.

Table 7-13: Situation tested in series 4 and their success rate

Series IV: September 2000		
AR_{12}	Double orifices with ratio 1:1, parr introduced on the right side at low flow	95%
AR_{20}	Double orifices with ratio 1:1, parr introduced on the right side at high flow	60%
AL_{12}	Double orifices with ratio 1:1, parr introduced on the left side at low flow	40%
AL_{20}	Double orifices with ratio 1:1, parr introduced on the left side at high flow	35%
BR_{12}	Double orifices with ratio 1:5, parr introduced on the right side at low flow	55%
BR_{20}	Double orifices with ratio 1:5, parr introduced on the right side at high flow	60%
BL_{12}	Double orifices with ratio 1:5, parr introduced on the left side at low flow	70%
BL_{20}	Double orifices with ratio 1:5, parr introduced on the left side at high flow	80%

Table 7-14: Velocity measurements at the two orifices for the two discharges tested

Situations	Velocity at coarse grid orifice	Velocity at open orifice
AR_{12} & AL_{12}	0.636 m/s	0.815 m/s
AR_{20} & AL_{20}	0.912 m/s	1.080 m/s
BR_{12} & BL_{12}	0.760 m/s	0.242 m/s
BR_{20} & BL_{20}	1.140 m/s	0.358 m/s

Table 7-15: Number of parr choosing a path as a function of situation. The numbers of successful and unsuccessful parr are also given for each path for each situation.

		No motion		Path A		Path B		Path C	
1:1 flow ratio	AR_{12}	1		14		5		0	
	Yes/No	0	1	14	0	5	0	0	0
	AR_{20}	0		12		8		0	
	Yes/No	0	0	9	3	3	5	0	0
	AL_{12}	5		3		8		4	
	Yes/No	0	5	3	0	1	7	4	0
	AL_{20}	2		3		15		0	
	Yes/No	0	2	3	0	4	0	0	0
5:1 flow ratio	BR_{12}	4		4		12		0	
	Yes/No	0	4	3	1	8	4	0	0
	BR_{20}	2		6		12		0	
	Yes/No	0	2	6	0	6	0	0	0
	BL_{12}	2		4		12		0	
	Yes/No	0	2	4	0	8	0	0	0
	BL_{20}	1		8		10		1	
	Yes/No	0	1	8	0	7	3	1	0

17 out of the 160 parr tested either did not move or stayed at the end of the flume. 54 fish moved initially along the window side to go through the 0.10 by 0.10 m orifice and only 5 of them failed. Four of these parr were confronted with situation AR_{20} and one with situation BR_{12}. Seven took path C and succeeded: four in the situation AL_{12}, two for BL_{12} and one for BL_{20}. A majority of 82 parr preferred path B but 45 of them failed.

By selecting path A, parr increase significantly their chances of success (Chi sq = 29.145, df = 1 & p = 0.000). As the first choice of the parr is determined by the flow conditions at its point of introduction, it is necessary to create conditions, which will lead the parr to make a successful decision.

a. Introduction of the parr on the right side of the flume:

The flow rate does not influence the first choice of pathway of the parr at the two flow ratios tested (Chi-square give p-values superior to 0.05). However the ratio

of flow going through the two orifices has an influence on the parr's first motion as seen in table 7-16 (Chisq = 11.343, df = 1 & p = 0.001).

Table 7- 16: number of parr choosing a path when introduced in the right corner of the flume

	Window side path (A)	Dark side path (B)	No motion
1:1 flow ratio	26	10	1
5:1 flow ratio	10	26	4

b. Introduction of the parr on the left side of the flume:

When introduced in the left corner of the flume, a significant majority of the parr (65%) moves first along the dark sidewall. 22.5% cross the flume and move towards the window side and 12.5% stay at the end of the flume or do not move at all [Table 7-17]. The flow ratios at the two orifices or the total flow rate do not seem to influence the decision of the parr.

Table 7-17: number of parr choosing a path when introduce in the left corner of the flume

		Window side path (A)	Dark side (B)	No motion
AL_{12}	Ratio	3	12	5
AL_{20}	1:1	3	15	2
BL_{12}	Ratio	4	14	2
BL_{20}	5:1	8	11	1

This apparent absence of influence of the flow ratio can be explained by the fact that for the four hydraulic conditions tested, the parr are introduced in the zone of influence of the 0.05 by 0.50 m orifice, which issues a jet of equal or higher velocities than the 0.10 by 0.10 m orifice.

7-3.4 *Conclusion*

The observation of fish movements within the pool revealed that the behaviour/movement of the parr could be classified into three basic paths: (A) the fish moves straight along the side of the flume from the point of its introduction to the weir or orifice outlet, (B) the fish moves first along the downstream end of the flume, then moving upstream along the edge and to the pass device and (C) the fish starts along path A crossing over to take path B.

There was no significant influence of the size or elevation of the orifice in the frequency of the three paths.

There was no difference in the movement patterns of the parr between an orifice alone and an orifice combined with a weir.

There was also no significant influence of the width of the side vertical slot in the frequency of the three paths.

There was significant influence of the design: side orifice/ side vertical slot in the frequency of the three paths.

The choice of path seems to be influenced by factors which did not appear to influence the efficiency of the devices tested [see section 7-2], such as the lateral location of the device. If the structure, in particular an orifice, is at the middle, parr tend to swim equally along the window side or the opposite side of the flume, whereas they move, at least initially, directly towards the jet, if they are introduced in its centreline. The proportion of parr veering then away from the flowing water depends on the velocities.

It can also be extrapolated from the "double orifice" situations that when two jets are in competition to attract parr, the influence of the flow ratio over the frequency of the three paths depends on the initial position of the parr.

7-4 Energy used by the fish

7-4.1 *Introduction*

In section 2-5.1 the forces acting on swimming fish have been defined and analysed. Power and energy requirements were also briefly introduced from a hydrodynamic point of view. It was pointed out then that the power and energy required by fish passing through fish passage structures such as orifices or weirs depend on the temperature of the water, the water velocity and fish characteristics such as length, maturation and swimming speed.

7-4.2 *Energy strategy*

When entering their natal river, spawning salmon stop feeding and rely solely on their energy reserves. Salmon might travel relatively long distances up river to reach their spawning areas and yet these migrations are generally energetically expensive. Brett (1995) estimated that long distance migrants deplete between 75 and 95% of their body fat. From a fisheries management perspective, understanding swimming speed and energy use strategies of migrating salmon is therefore critical for establishing fish passage structures criteria, as high velocity and turbulence impose important energy cost and therefore reduce limited stock of energy vital for successful spawning.

In chapter 3, three levels of speed were identified: (1) cruising or sustained speed, (2) prolonged or steady speed and (3) sprint or burst speed. The differentiation between these three levels being based on "the time for which a given speed can be maintained" (Webb, 1975). Despite a good understanding of these three different levels of swimming activity and despite the evidence of Bell (1973) that the speed at which a fish swims depends on the context, relatively little is known about the swimming and energetic strategies used by spawning salmon.

Field studies in British Columbia have been undertaken by Hinch and Rand (1998 & 2000) to investigate the role of local environment and fish characteristics on swim speed and energy use of sockeye salmon migrating up the river Fraser. The study also investigates their swimming strategies and energy-saving tactics. During the first field study conducted in 1993-1995, electromyogram radio telemetry was used to assess swimming activity and a bioenergetics model was used to estimate the energy used per meter. Hinch and Rand (1998) concluded that fish characteristic such as size and sex had an influence on the efficiency of the migration on an energetic point of view. They also found that in region of turbulent flow pattern (near a island, gravel bar or large rock), the energy expended by sockeye salmon was higher because of longer travel times.

During the second field study, Hinch and Rand (2000) concentrated their investigation on the swimming and energy saving tactics employed by three long distance migrating salmon stocks from the river Fraser using stereovideography and bank side observations. They found that sockeye salmon were highly efficient in low currents but less efficient in high current. According to Hinch and Rand, salmon tend to minimise transport costs per unit distance travelled in low currents. This means that they generate high propulsive power (Power = Propulsive forces x Swimming velocity) in order to reduce travel time and therefore the energy cost (Energy = Power x Time).

In general, three different tactics to reduce transport costs during the migration have been observed during field or laboratory experiments by biologists. These strategies include (1) swimming in low speed current or reverse flow current path (Hinch and Rand, 1998), (2) swimming steadily at hydrodynamic speeds (Weihs 1973) and (3) swimming in burst then coast fashion (Weihs, 1974).

a. Swimming in low speed current or reverse flow:

Hinch and Rand (1998) observed that near banks where small reversed flow areas were created, the ground speed of the migration sockeye salmon was higher than their swimming speed. This observation led them to the speculation that the fish exploit these reverse flows to move forward.

This observation is to put in parallel with our own observation of the parr motion in the experimental flume in Almondbank. By choosing path B, parr were effectively using reverse flow (or recirculating flow) to move upstream.

b. Swimming steadily at hydrodynamic speeds;

The steadily hydrodynamic speed is also known as the metabolic optimal speed and is defined as the constant swimming speed at which the rate of energy expended per unit distance is minimal. Weihs (1977) predicted that this metabolic optimal speed depends on the fork length L of the fish and a constant α (around 0.5) as seen in equation 7-3.

$$V_{optimal} = \alpha L^{0.43} \text{ in m/s} \qquad (7\text{-}3)$$

c. Swimming in burst then coast fashion:

Burst and coast swimming or "kick and glide" consists of two phases. In the first phase, the fish swims at burst speed and in the second or coast phase, the fish keeps its body straight and motionless.

According to Weihs (1974) both at low and high speeds, this method of swimming allows savings around 50% in comparison with a steady swimming at the same average speed. This diminution of energy consumption is due to the fact that the drag of a flexing fish body is between 3 and 5 times higher than the body of the same fish while it coasts at the same speed (Webb, 1975).

7-4.3 *Energy expenditure at a fish pass*

In the following section, an attempt will be made to evaluate the energy cost associated with the different devices: orifice/weir/slot and the three major paths chosen by parr to cross the flume. In this research, the examination and calculation of drag coefficient for swimming fish will be mainly conducted from a hydrodynamic point of view and the metabolic approach to the energy expenditure of fish in fish passage structure will not be considered in detail.

7-4.3.1 *Drag coefficient and drag forces acting on the parr*

It was been shown in section 3-5.3 that the Reynolds and Froude number are two important parameters for swimming fish. They depend on L the fish length, U the velocity of the fish with respect to the water, ρ the water density and ν the kinematic viscosity. A representation of their value is shown in figure 7-25 and 7-26 for fish between 0.08 and 0.14 m long and swimming between 0 and 3.0 m/s for an average water temperature of 15°C.

It has also been shown in section 3-5.3 that the drag coefficient could be described by a semi-empirical equation (Webb, 1975; Behlke, 1991):

$$D = 0.036bk\rho\nu^{0.2}L^{1.8}U^{1.8} \qquad (7\text{-}4)$$

where L is the fish length, U is the velocity of the fish with respect to the water, ρ is the water density and ν is the kinematic viscosity of the water and b and k are two dimensionless coefficients depending on the fish.

The dimensionless coefficient k varies between 3 and 5 and relates the drag coefficient of a flat-plate to the drag coefficient of a swimming fish. The dimensionless coefficient b relates the surface area of the fish A with its length through the relation $A=bL^2$. In the following calculations, we will use k = 4 and b = 0.42 (Webb, 1975; Behkle, 1991). For an average water temperature of 15°C, the drag force exerted on a parr by the surrounding water is approximately:

$$D = 3.821L^{1.8}U^{1.8} \qquad (7\text{-}5)$$

At constant water temperature, the drag force and therefore the power and the energy required by a fish swimming at a swimming speed U (m/s) depends primarily on its swimming speed U and its length L. Representations of the variation of the drag coefficient, the drag force and the power the fish need to deliver according to its swimming speed and its length are shown in figures 7-27 and 7-28. It is clear from these figures that the power increases both with the size and the swimming speed of the fish.

From a hydrodynamic point of view, the energy required by a fish with a constant swimming speed U against a flow of constant velocity V_w to cover a distance d is expressed in equation 7-6:

$$E = \int Power \times dt = D \times U \times \frac{d}{U - Vw} = D(1 + \frac{V_w}{V_f})d \qquad (7\text{-}6)$$

with $V_f = U - V_w$ the speed of the fish relative to the ground

The ground speed of the fish can be expressed by the relation $V_f = \alpha V_w$ with α a dimensionless coefficient representing the energetic strategy adopted by the fish. The velocity of the fish with respect to the water U can also be expressed as function of the dimensionless coefficient α and the velocity of the water V_w.

It is clear from equation 7-6 and figure 7-27 that the energy used by a fish of size L swimming against a flow of velocity V_w to cover a distance d, decreases as α increases, while the power (P= DU) increases as α increases.

The energy used by a fish of size L swimming against a flow of velocity V_w to cover a distance d can also be expressed as a function of its length L, the velocity of the water V_w (m/s), dimensionless strategic coefficient α and the time t (s):

$$E = 3.821 L^{1.8} (1+\alpha)^{2.8} V_w^{2.8} t \qquad (7\text{-}7)$$

$$\text{where } t = \frac{d}{\alpha V_w} \qquad (7\text{-}8)$$

It has been explained in section 3-4.2 that endurance is associated with each swimming speed. For a given speed, the endurance is defined as the maximum period of time the fish will be able to swim at this given speed. It has also been demonstrated that the endurance or "endurance time" depends on the length of the fish, its swimming speed and the temperature of the water. For an average water temperature of 15° C, the endurance time is given in equation 7-8:

$$t_m = 19396.44 L^{2.964} \Big/ \left(1.0545(1+\alpha)^{2.8} V_w^{2.8} L^{-1.15} - 48.231 L^{2.964}\right) \qquad (7\text{-}9)$$

Therefore to cover a distance d by swimming against a flow of velocity V_w, a parr of length L need to choose a strategic coefficient α so that:

1) t is smaller than t_m
2) *And (1+α)Vw* is smaller than the parr burst speed.

The weight W of a fish can also be expressed as a function of this length L through a relation $W = c\ L^3$ where c is a dimensionless coefficient depending on fish characteristics. In the case of 1+ parr, we have adopted c = 11.30 (personal communication, MacLean, 2001)

$$W(kg) = 11.30 L^3(m);\ R^2 = 0.95 \qquad (7\text{-}10)$$

7-4.3.2 *Energy expenditure in the flume*

While swimming in the flume, the parr were confronted with drag forces, buoyancy forces, weight and the virtual mass force. When swimming in the freshwater pool, the gravity forces are balanced by buoyancy; the propulsive force or thrust that the fish need to generate to move upstream is therefore the sum of the drag and virtual mass forces only:

$$\vec{P} = \vec{D} + \vec{F}_{vm}$$

$$P = 0.036bk\rho v^{0.2} L^{1.8} U^{1.8} + 1.2\rho gcL^3 \frac{\partial U}{\partial x} \qquad \textbf{(7-11)}$$

where

$$U = (1+\alpha)V_w$$

It is clear from equation 7-11 that the propulsive force generated by parr is function of (1) the size of the fish L (m), (2) three dimensionless coefficients b, c and k depending on the fish and (3) the velocity of the water velocity V_W (m/s) and a dimensionless coefficient α, a measure of the energy strategy adopted by the fish.

7-4.3.3 *Energy expenditure at weirs*

According to Orsborn and Powers (1985), when leaping over a weir, the fish spend more time in air than water and as the density of air is much lower than the density of water the drag forces acting on the fish while in the air can be neglected. Therefore the fish has only to overcome its weight. Thus the total energy the fish need to supply is:

$$E_p = 0.5mV_F^2 \qquad \textbf{(7- 12)}$$

$$E_p = W\frac{\Delta h}{\sin^2 6} \qquad \textbf{(7- 13)}$$

where m is the mass of the fish, W is its weight, Δh is the height it was to jump and θ is the angle of the leap. In a still pool, the angle of the pool is typically around 60/70°. However according to Powers and Orsborn (1985), Hilliard (1983)

found that downstream of a waterfall or a weir, the standing wave rises by 0.024 Δh above the average depth of the pool. Stuart (1962) also observed that the standing wave helps the fish to leap; the angle of the leaping being therefore increased to 75°. The potential energy the fish has to over come when leaping from a standing wave in this air is therefore approximately:

$$E_p = W\frac{\Delta h}{\sin^2 6}(1-\sqrt{0.024})^2 \qquad \textbf{(7-14)}$$

However equation 7-14 is only valid for the time the fish spend in the air while leaping and does not take into account the forces the fish is confronted with at take off and landing. This calculation of energy requirement is also based on the assumption that at a weir a fish will always leap over the falling water and not swim into it.

The weir design was tested for three different head loss between the upstream and downstream pool elevation [(1): Z = 0.1 m & h_l = 0.108 m; (2): Z = 0.1 m & h_l = 0.15 m; (3):Z = 0 m & h_l = 0.108 m]. Representations of the leaping curves for a 0.11 m long parr superimposed on the sketch for the plane nappes falling from the weir are shown for situations (1) and (2) in figures 7-28 and 7-29. The energy required for the three "weir" situations tested at Almondbank has been calculated using equations 7-10 and 7-14 and is shown in table 7-18.

Table 7-18:Energy required to leap Δh as a function of the fish size and its leap angle

Δh	Length of fish	E (J) for θ =60°	E (J) for θ = 80°
0.208 m	0.08 m	1.15E-03	0.89E-03
	0.14 m	6.15E-03	4.75E-03
0.254 m	0.08 m	1.40E-03	1.08E-03
	0.14 m	7.51E-03	5.80E-03
0.108 m	0.08 m	0.60E-03	0.46E-03
	0.14 m	3.19E-03	2.47E-03

Figure 7-30 shows clearly that the energy requirements to leap over a weir increase linearly with the elevation of the leap, with the weight of the fish (= cL^3) and decrease as the angle of the leap increases.

7-4.3.4 *Energy expenditure at orifices and vertical slots*

Powers and Orsborn (1985) and Behkle (1987,1988, 1991 & 1993) also studied energy expenditure at orifices. When swimming through a port, a swimming fish counters pressure forces, drag forces, virtual mass forces and buoyancy forces.

The virtual mass forces are neglected in this analysis on the grounds that the fish has a constant velocity in the vicinity of the orifice/slot and that in the potential core region of a three-dimensional jet, the velocity is constant (Albertson, 1950; Rajaratnam, 1976).

The energy required to pass through a slot is therefore:

$$E = d\sum F_x \qquad \textbf{(7- 15)}$$

$$E = d(B_x + D_x) \qquad \textbf{(7- 16)}$$

$$E = d(W\tan\theta + 0.5\rho bL^2 C_d U_{fw}^2) \qquad \textbf{(7- 17)}$$

$$E = W\Delta h + (0.5\rho bL^2 C_d U_{fw}^2)d \qquad \textbf{(7- 18)}$$

where W is the weight of the fish, ρ is the density of the fish, L is the length of the fish, C_d is the drag coefficient, U_{fw} is the velocity of the fish with respect to water, d is the distance downstream the orifice from where the fish start to dart, θ is the angle at which the hydraulic gradient (HGL) slopes, Δh is the elevation difference between the upstream and downstream of the pool and b is a dimensionless coefficient. If equations 7-5, 7-10 and 7-18 are combined, the energy required to pass through an orifice is:

$$E = 11.30L^3\Delta h + 3.82(1+\alpha)L^{1.8}V_w^{1.8}d \qquad \textbf{(7-19)}$$

The energy, a parr will expend passing through the orifice depends therefore on two types of parameters, respectively designed as "imposed" and "strategic". The imposed designs are its size L (m), the head loss at the orifice Δh (m) and the

velocity of the water in the vicinity of the orifice V_f (m/s). The strategic parameters are the distance d (m), which is the distance downstream the orifice from where the fish start to dart and the dimensionless coefficient α that corresponds to the energetic strategy adopted by the fish.

Figure 7-31 and 7-32 represent the energy needed by a parr, 0.11 m long to pass through an orifice if it starts to dart at a distance d, downstream the device. The hydraulic conditions are characterised by the velocity at the vena contracta V_{vc} and the head difference Δh upstream and downstream the device. The time it took to cover the distance d is also represented in these figures.

Figure 7-31 is based on the assumption that parr made the strategic choice to swim as fast as possible to generate a high propulsive power in order to reduce their travel time. This means in particular that the swimming speeds of a 0.11 m long parr is going to be around 1.8 m/s and therefore the strategic coefficient α is varying in accordance with the water velocity (or velocity at the vena contracta) in the vicinity of the orifice as shown in table 7-19.

Table 7-19: Water velocity, strategy coefficient and fish swimming speed for 3 "orifices" situations

Situation	Δh	Vvc=Vw	α	$U = (1+\alpha)\ Vw$
Bottom orifice 0.01 m2 - 12l/s	0.1528 m	1.73 m/s	0.04	1.80 m/s
Bottom orifice 0.02m2 - 12l/s	0.0360 m	0.84 m/s	1.14	1.80 m/s
Bottom orifice 0.02m2 - 20l/s	0.1001 m	1.40 m/s	0.29	1.80 m/s

It is clear from figure 7-31 that if for the three different situations, the parr swim at the same speed U, the energy to cover a distance d varies only slightly as a function of the situation, while the travel time varies a lot.

It is also obvious that the distance from the orifice at which the fish start to dart plays an important role in the energy cost of swimming through an orifice. It is interesting to recall that salmon parr approaching jets followed the sides of the flume and swam into the orifice at an angle thus minimising the period of time in fast water and their energy expenditure. Juvenile Atlantic salmon seem therefore to display an energy-conserving behaviour similar to upriver-migrating adult salmon (Hinch and Rand, 2000).

7-4.4 *Example of Energy expenditure calculation*

During series 4 tests, the motion of 3 parr following path A was recorded using a digital video camera system. Theses parr were confronted with the same situation: "Double orifices with flow ratio 1:1 and introduction on the left right side of the flume". The use of a digital camera enables to record the exact position of a parr as a function of the time from its introduction in the flume to its passage through the orifice. The movements of the parr in the flume are shown in figure 7-33 to 7-35.

A simple analysis of the energy expended by the parr between the time of their introduction and their passage through the orifice was conducted. The author had only one digital camera at his disposition, which means that only the X and Y location of the parr were recorded. However from previous direct observations, it had been noticed that the parr were moving preferentially near the bed. Therefore in the following calculations, the assumption will be made that the parr moved in the horizontal plane z = 0.01 m.

The hydraulic conditions existing in the pool for this particular situation have been presented in chapter 6. The water was issued in the pool through two orifices: a square orifice [0.10 m by 0.10 m] located directly in front of the point of introduction of the parr and a rectangular orifice [0.05 m by 0.5 m] blocked by a coarse grid on the opposite side. As the flow measurements have only been conducted within an area 1.50 m by 1.10 m wide, the energy used by the parr has been calculated only from 1.50 m downstream the orifice. The results of the calculations are shown in table 7-20: the time, the energy used if the virtual mass forces are neglected and the energy used if the virtual mass forces are included are given for a travel distance 1.50 m downstream the orifice to the cross section of the orifice.

Table 7-20: Energy used by the parr between x = 1.50 and x = 0.0 m downstream the orifice

	Fish 1	Fish 3	Fish 5
Time	3.16 s	1.29 s	1.57 s
E	0.0863	0.218	0.319
E (virtual Mass)	0.0898	0.223	0.344
E (virtual Mass+head)	0.0899	0.223	0.344

Considering table 7-21, it is obvious that the time and the energy used by the three fish to cover 1.50 m vary as a function of the strategy adopted by the fish. The time taken by the three parr to cover 1.50 m varied between 1.29 s and 3.16 s, which represented a variation of 84%. The energy required to cover this distance varied between 0.0898 J and 0.344 J, which represented a variation of 117%. It can be seen that the virtual mass force counted for only 4-5% of the total energy used.

It might be extrapolated from this simple comparison that the energetic strategy adopted by the fish plays a major role on their energy consumption without regard to the path chosen.

7-4.5 *Conclusion*

In this section on the energy used by parr to swim in a flume and pass through an orifice/slot or jump over a weir, only the hydrodynamic point of view was adopted. However this simple approach to the mechanisms of fish propulsion clearly showed that the energy a fish used to swim or pass an obstacle depends not only on the characteristics of the flow (hydraulic, temperature...) or the characteristics of the fish but also on the strategy selected by the fish.

In table 7-21, estimations of the energy parr need to produce to pass through the studied designs are given. The energy expenditure calculations have been made using equation 7-14 for the weir situations and equation 7-19 for the orifice and vertical slot situations. It is clear from this table that for the three designs tested: orifice/weir or vertical slot, the energy expended by parr increases with their size. For the weir situation, it is also evident that the parr will expend less energy if the water level downstream the weir is raised. In this particular case, the energy expenditure is divided by two when the water level downstream the notch is increased from 0.20 m to 0.30 m. The comparison of the small and large orifices also shows that the energy expenditure is multiplied by 3 when the size of the orifice is divided by two. The energy expenditure is also multiplied by 2.5 when the width of the vertical slot is reduced from 0.10 m to 0.05 m.

In general, the weir appears to offer the less energetic route in front of the wide vertical slot, the large orifice, the narrow vertical slot and the small orifice. This apparent superiority of the weir design over the orifice and vertical slot designs is due to the fact that the energy expenditure calculated here takes into account only the actual jump of the fish and ignores the energy expended by the parr to reach the starting point of the jump.

Table 7-21: energy used by parr 0.10 or 0.12 m long confronted by different designs for a discharge of 0.012 m^3/s. For the orifice and vertical slot design the assumption is made that the parr swims 0.10 m against the high velocities with a strategic coefficient α equal to 0.1.

Design	Fish size (m)	Energy (J)
Weir – wsel = 0.3 m	0.10	1.15E-03
	0.12	1.99E-03
Weir – wsel = 0.2 m	0.10	2.22E-03
	0.12	3.84E-03
Large orifice – a = 0.02 m2	0.10	5.27E-03
	0.12	7.46E-03
Small orifice – a = 0.01 m2	0.10	17.2E-03
	0.12	24.5E-03
Narrow vertical slot – b = 0.10m	0.10	12.2E-03
	0.12	17.3E-03
Wide vertical slot – b = 0.05 m	0.10	4.93E-03
	0.12	6.98E-03

If the energy expended by the fish before passing through the orifice/slot is ignored, as shown in table 7-22 (only the first term of equation 7-19 is considered), the energy used by the fish to pass through the orifice/slot devices tested is less than 3.00E-03J and is smaller or of the same order than the energy used by the fish to jump.

Table 7-22: Energy used by parr 0.10 or 0.12 m long confronted by orifice/vertical slot designs for a discharge of 0.012 m3/s when only the first term of Eq (7-19) is calculated

Design	Fish size (m)	Energy (J)
Large orifice – a = 0.02 m^2	0.10	4.07E-04
	0.12	7.03E-04
Small orifice – a = 0.01 m^2	0.10	17.3E-04
	0.12	29.8E-04
Wide vertical slot – b = 0.10m	0.10	3.77E-04
	0.12	6.52E-04
Narrow vertical slot – b = 0.05 m	0.10	10.2E-04
	0.12	17.7E-04

7-5 Conclusions

The objectives of this chapter were to summarise and bring together the hydraulic and biological results of chapter 5 and 6 in order to throw a new light on the design of fish passage structures such as weirs, orifices or vertical slots. The analysis was divided in three sections: the influence on flow characteristics on the efficiency of a device, the influence of the flow characteristics on the paths chosen by parr and the energy expenditure in relation to the device.

It was found that the suitability of a design and/or the movements of the parr in the flume were both governed by the hydraulic conditions existing in the flume (such as the nature of the flow: overflow jet, submerged jet, plunging or streaming flow, high or low velocity...) and by behavioural patterns such as swimming near the bottom of the flume, line swimming or energetic strategy. The predominance of one characteristic over another appears to change following a complex algorithm, which still need to be found. However by multiplying the number of situations tested, a hydraulic/behaviour pattern can be built.

If it can be proven that parr and adult spawning salmon have the same behavioural patterns, then the findings presented in this chapter can be used as a base to improve the design of fish pass structures. Such an attempt will be made in chapter 8.

CHAPTER 8

BEHAVIOUR OF FISH UNDERGOING SPAWNING MIGRATION: A COMPARISON OF PASSAGE THROUGH WEIRS AND ORIFICES

CHAPTER 8:

BEHAVIOUR OF FISH UNDERGOING SPAWNING MIGRATION: A COMPARISON OF PASSAGE THROUGH WEIRS AND ORIFICES FOR MATURE MALE PARR, ANADROMOUS ADULT AND BROWN TROUT

8-1 Introduction

Experimental results of the behaviour of parr at a range of fishpass designs have been presented in Chapter 5. In Chapter 7, these results were combined with detailed hydraulics and hypotheses were made on the behaviour of homing adult salmon using displaced parr as models. The main recommendation from these studies was that submerged orifices or vertical slots are preferable to overflow weirs in a fish pass.

The purpose of this chapter is twofold:

- To test the hypothesis that, like immature salmon, adult trout and mature parr prefer to pass through orifices rather than over weirs.
- To test the hypothesis that adult wild salmon in the field prefer to pass through orifices rather than over weirs.

8-2 Laboratory study at Almondbank with mature parr and adult trout in November 2000

Large movements of salmon parr, the majority being precious males in search of adult females (Buck and Youngson, 1982) occurs in autumn (Calderwood, 1945). These parr are sexually mature without having first migrated to the sea (Jones, 1959). By using mature male salmon parr and mature male brown trout, it was possible to examine how salmonids on spawning migrations chose between options of orifice and weir. In a first experiment, the behaviour of mature male salmon parr approaching a vertical wall where they were offered the alternatives of passing through an orifice or over a weir was studied. In a second experiment, the behaviour of adult male trout was observed in the same experimental set up. Like Atlantic salmon (*Salmon Salar L.*), brown trout (Salmo *trutta L.*) home to their natal stream to spawn (Stuart, 1957; Banks, 1969) or after displacement (Armstrong and Herbert, 1997).

The incentive for the adult male brown trout to move upstream was created by the presence in the upper part of the flume of 6 male-female couples of brown trout in the spawning process. Chemical cues such as pheromones (Moore and Scott, 1991), visual cues (Takeuchi et al, 1987; Rouger and Liley, 1993) and the mechanical disturbance of river gravel bed caused by female cutting redds (Moore and Scott, 1991; Moore and Waring, 1999) influence spawning behaviour of adult salmonids during the spawning season. Moore and Scott (1991) found that the conspecific odours released into the water column by the disturbance of the gravel bed resulted in an upstream migration of mature male parr Atlantic salmon if the odours were detected by their olfactory systems. Moore & Waring (1999) also found that the sounds of a wild female Atlantic salmon cutting a redd had a priming effect on the reproductive physiology of mature male parr.

8-2.1 *Experimental Apparatus*

Tests were conducted in the laboratory of the Almondbank laboratory between 7th and 21st November 2000. The physical model used for this experiment was the same than the one described in section 4-3.

8-2.2 *Design and hydraulics*

A vertical board including a weir and an orifice divided the flume into two pools. Salmon parr/adult trout approaching the vertical board had the alternative of swimming through an orifice or over a weir.

The orifice used in this study was a 0.20 by 10 m rectangular port positioned at the bottom on the right side of the vertical board as shown in figure 8-1. The weir was a contracted rectangular weir with a crest height of 0.20 m and width of 0.20 m. The weir was positioned in the left corner of the vertical board. The water level in the lower part of the flume was 0.20 m.

For this experimental set up, the flow passing through the flume was fixed at 0.020 m^3/s. This total flow was then divided between the flow passing through the orifice [$Q_o = 15\ m^3/s$] and the flow passing through the weir [$Q_w = 5\ m^3/s$]. The orifice and the weir had been designed to produce identical velocity at the vena contracta of the orifice and in the zone of impact of the overflow jet. The velocities have been calculated both at the vena contracta and in the zone of impact and of the overflow jet with the pool using equations 8-1 and 8-2.

The velocity at the vena contracta varies with Δh the head difference as follow:

$$V_{vc} = \sqrt{2g\Delta h} \qquad (8\text{-}1)$$

The velocity at impact with h_1 the head measured above the crest weir and Z the distance between the bottom crest of the weir and the water surface downstream (Z = 0.0 m) can be expressed by the following equation:

$$V_i = \sqrt{2g(Z + h_1)} \qquad (8\text{-}2)$$

For a better understanding of the hydraulic conditions existing in the downstream pool, measurements of the flow rate, the head loss, velocities and turbulences were conducted in a similar physical model at Glasgow University. All water surface measurements were done using a digital pointer gauge. Velocity and turbulence measurements were taken in various horizontal layers [z = 0.01, 0.05 and 0.10 m] through the flow over an area of 1.22 m wide by 1.50 m long located immediately downstream the device. The instrument used for this purpose was a Sontek Acoustic Doppler Velocimeter. The ADV uses remote sensing techniques to simultaneously measure three velocity components (x, y, z) of flowing water using a single sampling volume.

8-2.3 *Protocol*

The experiments were divided in two series: the first series was conducted between the 7th and the 15th of November 2000 using twenty wild adult male trout [length range: 15-35 cm]. The second series using twenty hatchery reared mature salmon parr [length range: 14-18 cm] was conducted between the 20th and the 21st of November 2000. The temperature of the water in the flume varied between 2^0C and 3^0C during the first series and between 4^0 C and 5^0 C during the second series.

The fish were held in two separate tanks (2 m diameter) supplied with a constant flow of aerated water from the river. Each fish was handled only once and placed in another tank subsequently. Fish were fed to satiation, once daily.

The protocol was to capture and release a male fish (parr/trout) as quickly as possible at the downstream end of the flume adjacent to the viewing window. The fish was then observed continually by a network of cameras and records were made of changes in position with time until it passed trough the orifice or jumped over the weir. The positions of weir and orifice were reversed between each run. Video records using a network of cameras in the upstream half of the flume supplemented the direct observations. These cameras focussed particularly on the behaviour of the fish near the pass entrances. Four small waterproof cameras were placed in the upstream zone of observation.

8-2.4 *Experimental Results*

8-2.4.1 *Hydraulic results*

The head difference Δh between the upper and lower pool was 0.06 m. The velocities were circa 1.00 m/s both at the vena contracta and in the zone of impact of the overflow jet.

The mean velocity patterns for the three horizontal planes at 0.01, 0.05 and 0.10 m above the bed of the flume are shown in figure 8-2. The velocity vectors over vertical slides in the vicinity of the orifice and the weir are shown in figure 8-3.

The jet issuing from the orifice was mainly longitudinal with high velocities concentrated inside a band 0.10 m wide around the jet centre line. Maximum velocities occurred in the horizontal plane at 0.05 m from the bottom of the flume along the jet centre line and reached up to 0.99 m/s, around 0.10 m downstream the orifice. In accordance with the theory of the turbulent jets, it can also be noted that the decay of the centre line velocity was linear [V (m/s) = -0.428*X+0.95, R^2 = 0.92]. It is also interesting to note that in the vicinity of the orifice, the vertical components of velocity was negligible particularly near the flume bed [Fig 8-3].

The flow passing over the weir (1) plunges through the atmosphere and (2) diffuses in the downstream pool, (3) hits the flume bed and then rebounds. There was also the suggestion of a submerged roller of standing wave forming in the axis of the weir (Fig. 8-3). Maximum velocities occur near the water surface in the zone of impact of the jet with the pool and were calculated to have reached up to 1.00 m/s. In the horizontal plane at 0.01 m from the flume bed, maximal velocities occurred 0.50 m downstream the weir and reached 0.40 m/s. A weak recirculation phenomenon with velocities reaching 0.20 m/s could also be observed in the lower central part of the flume. Turbulence intensity varied between 0 and 10 % in the majority of pool reaching 20% around 0.30 m downstream the orifice at 0.01, 0.05 and 0.10 m above the flume bed and 15% downstream the weir at 0.10 m above the flume bed.

8-2.4.2 *Passage of Wild brown trout*

When presented with the choice to pass through the submerged orifice or over the weir, 19 out of the 20 wild male trout individually introduced in the flume selected the bottom side orifice over the weir as shown in table 8-1. The time needed by the trout to pass through the orifice averaged 7694 s [01:57:46] and varied between 47 s and 29400 s [8:10:00] as shown in table 8-5. The only trout, which selected the weir, took 19620 s [05:27:00] to pass.

Table 8-1: Choice made by the adult male trout between the orifice and the weir

Number	Date	Temp water (°C)	Fish length (cm)	Device selected	Time to pass device (s)
1	07-Nov	5	30	Orifice	10801
2	09-Nov	5	30	Orifice	2369
3	09-Nov	5	29	Orifice	8101
4	09-Nov	5	23	Orifice	47
5	13-Nov	4	24	Orifice	90
6	13-Nov	4	35	Orifice	2069
7	13-Nov	4	29	Orifice	29400
8	14-Nov	4	23	Weir	19620
9	14-Nov	4	27	Orifice	412
10	14-Nov	4	25	Orifice	172
11	14-Nov	4	24	Orifice	77
12	14-Nov	4	30	Orifice	2547
13	14-Nov	4	28	Orifice	17994
14	14-Nov	4	27	Orifice	7080
15	14-Nov	4	28	Orifice	11456
16	14-Nov	4	28	Orifice	12420
17	15-Nov	4	15	Orifice	8100
18	15-Nov	4	22	Orifice	7304
19	15-Nov	4	40	Orifice	716
20	15-Nov	4	29	Orifice	13101

Table 8-2: Descriptive statistics

Time	*(s)*	*(h)*	*Time*	*(s)*	*(h)*
Mean	7066	01:57:46	Mode	N/A	
Standard Error	1765	00:29:25	Range	29353	08:09:13
Median	7080	01:58:00	Minimum	47	00:00:47
Standard Deviation	7692	02:08:12	Maximum	29400	08:10:00
Sample Variance	59171695		Sum	134256	
Kurtosis	3		Count	19	13:17:36
Skewness	1		Confidence Level (95.0%)	3708	01:01:48

8-2.4.3 *Passage of reared mature parr*

Table 8-3 shows that all the twenty mature salmon parr passed through the submerged orifice and ignored the weir. The time taken by the parr to pass through the devices varied between 5 and 10740 s [2:59:00] with an average of 1162 s [00:19:22] as shown in table 8-4.

Table 8-3: Choice made by the mature male parr between the orifice and the weir

Number	Date	Temp water (°C)	Fish length (cm)	Device selected	Time to pass devices (s)
1	20-Nov	2	14-18	Orifice	325
2	20-Nov	2	14-18	Orifice	1403
3	20-Nov	2	14-18	Orifice	120
4	21-Nov	3	14-18	Orifice	78
5	21-Nov	3	14-18	Orifice	3240
6	21-Nov	3	14-18	Orifice	1080
7	21-Nov	3	14-18	Orifice	800
9	21-Nov	3	14-18	Orifice	24
10	21-Nov	3	14-18	Orifice	5
11	21-Nov	3	14-18	Orifice	7
12	21-Nov	3	14-18	Orifice	8
13	21-Nov	3	14-18	Orifice	157
14	21-Nov	3	14-18	Orifice	18
15	21-Nov	3	14-18	Orifice	228
16	21-Nov	3	14-18	Orifice	10740
17	21-Nov	3	14-18	Orifice	4900
18	21-Nov	3	14-18	Orifice	58
19	21-Nov	3	14-18	Orifice	14
20	21-Nov	3	14-18	Orifice	5
21	21-Nov	3	14-18	Orifice	20

Table 8-4: Descriptive statistics for the mature male parr

Time	*(s)*	*(h)*	*Time*	*(s)*	*(h)*
Mean	1162	00:19:22	Skewness	3	
Standard Error	578	00:09:38	Range	10735	02:58:55
Median	99	00:01:39	Minimum	5	00:00:05
Mode	5		Maximum	10740	02:59:00
Standard Deviation	2584	00:43:04	Sum	23230	06:27:10
Sample Variance	6676638		Count	20	
			Confidence Level		
Kurtosis	10		(95.0%)	1209	00:20:09

8-2.5 *Discussion*

When artificially displaced, stream-dwelling salmonids fishes can return to the point where they were captured (Miller, 1954; Saunders and Gee; 1964; Garcia

de Leaniz, 1989; Armstrong and Herbert, 1997). This upstream movement may be affected by local water characteristics. Earlier in this thesis (Chapter 5) it was shown that a significantly higher percentage of displaced salmon parr moved through orifices than over weirs within a fixed time. In this chapter, the author has shown that both mature salmon and brown trout, probably motivated to move upstream in search of females, chose an orifice in preference to a weir. Therefore, a preference for orifices over weirs is demonstrated by two different species of salmonid and under two different conditions of homing.

The proportions of mature parr and brown trout that chose orifices were very similar. All the mature parr and 95% of the brown trout selected the orifice to move upstream. These results suggest that despite being adult and bigger, brown trout favour the same type of hydraulic characteristics to move upstream as juvenile salmon (mature or immature).

The maximum velocities at the orifice and at the weir were of the same order, 1.00 m/s. The turbulence intensity in the two zones of high velocities was also comparable: 20% at the orifice and 15% at the weir. Therefore the fact that mature parr and brown trout preferred to swim through the orifice rather than to jump over the weir may not be attributed to a difference of difficulty of passage due to velocity or turbulence.

Salmon parr of length 14 and 18 cm at a water temperature of 2-3°C have a maximum burst swimming speed in the region of 1.0 m/s (Beach, 1984). Mature brown trout of length ranging between 15 and 35 cm at a water temperature of 4-5°C have a maximum burst speed ranging between 1.2 and 2.0 m/s (Beach, 1984). The individual brown trout that went over the weir had a predicted maximum burst speed of 1.45 m/s (Beach, 1984). Despite the fact that the velocity at the vena contracta corresponded to their maximum burst swimming, the average time taken by the parr to move through the orifice [0h20 ±0h40] was lower than the average time taken by the mature trout [2h00 ±2h00]. This different in time of passage might be due to the fact that the mature parr were reared whereas the ma-

ture trout were of wild origin and therefore needed more time to recover from their handling.

There was no evidence that context of upstream migration or size/species of salmonid fish influenced the preference for swimming rather than jumping during upstream migration. It would be very surprising if anadromous adults exhibit radically different behaviour to immature and mature male parr and trout considering that their behaviour appears consistent with minimising mortality and energy expenditure (Chapter 5). Therefore it seems to be reasonable to suggest that wild anadromous salmon on homing migrations are likely to prefer submerged orifices to weirs.

8-3 Preliminary Field test at Tongland Dam Fish Pass in July 2001

The logistics of testing fish pass preferences of anadromous adults in the wild are substantial. Nevertheless, as a complement to the comparison of passage through weir or orifice for mature salmon parr and brown trout, an attempt was made to study salmon moving through the Tongland dam fish pass. The purpose of this field test was to assess the hypothesis that adult wild salmon in the field prefer orifices to weir flow situations.

8-3.1 *General background*

Tongland dam is one of five power stations which together comprise the Galloway Hydro-Electric Scheme (Hudson, 1938). This scheme is located in the southwest of Scotland between the estuaries of the Clyde and the Solway and includes the entire catchment of the Galloway Dee plus the catchment area of Loch Doon

The construction of Tongland power station commenced in April 1931 and was completed in the winter of 1936-1937. Tongland is the last power station of the river Dee and is situated on its estuary. Its principal functions are to generate power and provide daily storage. The average net head at the power station is around 32 m. The storage capacity of the reservoir is around 30 millions of cubic

feet; the maximum draw down is 3 m and the water area at spillway level is 106 acres.

Tongland dam consists of an horizontal arch dam together with a tangential gravity dam on the left bank, which is provided with two flood-gates as shown in figure 8-4. A spillway channel along the flank of the hill forming the eastern boundary of the reservoir also deals with floods. The water for power purposes is taken from the Tongland reservoir through an intake chamber on the right bank upstream of the arch abutment. The intake is connected to a 1 km long aqueduct, which goes from the intake gate to the surge tower near the power station. The intake is provided with fixed screens and the flow through it is controlled by a sluice gate 6 m by 5.40 m.

8-3.2 *Fish passage facility at Tongland*

Tongland dam is also provided with a fish pass following the recommendations of the inspector of Salmon Fisheries in Scotland. The design adopted for the fish pass was initially of the submerged orifice type. The fish pass comprises 30 submerged orifice pools and 4 resting pools. It has a height of 20.7 m and the vertical lift between successive resting pools is limited to 6 m. The submerged orifices have a hexagonal shape as shown in figure 8-5. The flow through the pass was controlled by means of sluice gates at each orifice as shown in figure 8-5.

A series of float-controlled sluices are present in the five higher chambers of the pass. They shut off in succession as the reservoir level falls. The hexagonal gates have the capacity to be opened to deliver between 0.25 and 0.3 m^3s^{-1}. The 5 upper pools are also part of the dam itself and are partly covered over. The amount of light in this part of the pass is therefore restricted

According to Hudson and Hunter (1938), the pass was successful when it was first put in service in April 1935. Spring fish " were experiencing no difficulty in finding the entrance to the pass and making the 70-feet ascent to the reservoir".

Due to an increasingly unsatisfactory assessment of the performance over the years, the 17 first submerged orifice pools were subsequently altered to become

pools with overflow weirs. The hexagonal gates were fully closed but their mechanisms were left in place. Rectangular notches were opened into the walls. Each pool is 4.45 m long, 3.00 m wide and 1.70 m deep. The rectangular notches are 0.70 m wide and 0.85 m high. The notches were made on the opposite side of the pool from the orifices. Baffles were added in the eight intermediate pools and the hexagonal gates were left permanently fully opened. The resulting layout of the pass is shown in figure 8-6.

In November 1997, Scottish Power, the owner of the Tongland power station, commissioned an initial desk study to investigate the hydraulic conditions in the upper resting pool and the five upper pools as salmon appeared unable to proceed through them and accumulated in the resting pool. Following this initial desk study by the Carnie Consultancy and Glasgow University, a small-scale physical model study was commissioned to investigate the causes of the problem and to recommend a solution.

The results of the study indicated that surging was excessive and velocities and turbulences reached values of as high as 3.2 m/s and 1.23 m/s (RMS) respectively. The head loss per pool was of 0.55 m. It was recommended that the hexagonal gates be opened to an area of 0.2 m^2 in order to obtain velocities below 2.0 m/s, and turbulences below 0.67 m/s. To maintain a constant head loss of 0.55 m per tank, it was also recommended that additional diagonal orifices be installed, each with an opening of 0.48 by 0.48 m in each of the upper five pools, as shown in figure 8-7. It was also recommended that an additional wooden partition be installed to divide the upper resting into two pools.

The recommended modifications were made in spring 1998 and successfully tested during summer/autumn 1998. Small waterproof cameras were placed in the upper resting pool and the first of the 5 upper pools. The movement of upriver fish has since been constantly recorded. Since the modifications, salmon appear to proceed easily and quickly from the upper resting pool to the reservoir.

8-3.3 *Seasonal return of spawning salmon in the river Dee*

In order to conduct the field experiments at Tongland fish pass at the best time during the spawning season, the return of salmon over the previous eight years was examined. A fish counter had individually recorded all the returning salmon between 1992 and 1999, allowing an estimation of the number of fish negotiating the fish pass per month as shown in figure 8-8.

Table 8-5: Total number of fish passing through the fish pass at Tongland

Year	1992	1993	1994	1995	1996	1997	1998	1999
Total Number	1452	2448	1633	1150	1614	1289	1769	1012

Between 1992 and 1999, the annual number of fish registered passing up over the fish counter varied between 1012 fish for 1999 and 2448 fish for 1993 as seen in table 8-5. The same pattern occurred every year. Between December and April, a very limited number of passes, between 0 and 1% of the yearly total number, were registered by the counter. In May and November, between 3 and 7% of the annual number of registrations were recorded. These two months represent the start and the end of the spawning season. The counter data suggest that most of the fish enter the river between June and October with an important peak occurring in July as shown in figure 8-9.

In the light of these results, it was decided to conduct the field experiment in July in order to have the greatest sample size as possible.

8-3.4 *Set up of experiments*

The objective was to cut an orifice and a weir in one of the wooden partitions at the top of the pass and to attempt to develop PIT tag technology to detect fish moving though the openings. The PIT tag technology and the antennae system associated with it were designed and built by another PhD student at the University of Glasgow, Phil Rycroft who is also the technical director of the company UKID Systems, specialising in the design and manufacture of radio frequency identification systems.

It was determined that the field test would be carried out between the 12th and 31st of July 2001, the month offering the greatest chance of catching and tagging a sufficient number of fish.

Initially plans to install 10 antennae along the whole fish pass were abandoned. Due to access restrictions associated with foot-and-mouth disease, it was not possible to install a trap downstream of the fish ladder. Instead, fish were trapped at the foot of the ladder and transported upstream to the first resting pool [see Fig 8-6]. The experiment was then restricted to a comparison of a weir and an orifice at one location in the pass.

The choice of passing through a submerged orifice or a over a weir at one singular location in the fish pass was similar in concept to the experiments performed at Almondbank with mature parr and adult brown trout (see section 8-2).

To do so, an orifice was added to the wooden weir structure dividing the upper resting pool in two since the alteration made on the upper part of the fish pass in 1998 (Ervine et al, 1999) as shown in figure 8-10. The weir and the orifice were then both fitted with an antenna to record the passage of the tagged fish through the structures.

The dimensions of the orifice were designed so that the flow and the maximal velocity at the weir and the orifice were similar. The average daily flow passing through the fish pass is around 0.27-0.28 m^3/s. This flow was divided almost equally between the flow passing through the orifice (Q_o= 0.13 m^3/s) and over the weir (Q_w = 0.14-0.15 m^3/s). The submergence of the weir varied between 0 and 0.10 m and the velocity had been calculated to be circa 2.0-2.2 m/s both at the vena contracta and in the zone of impact of the overflow jet. This velocity is comparable to the 2.4 m/s mean water velocity at the orifices of Pitlochry fish pass (Webb, 1990) which salmon successfully ascend (Gowans et, 1999).

8-3.4.1 *Passive integrated transponder tags*

The system used to carry out the experiments consisted of a computer, to retrieve the information, readers otherwise known as decoders, antennae, and transponders (tags). A schematic of the system is shown in figure 8-12.

- HP Single Point Decoder

The decoder reads the encoded signal from the transponder (tag) and decodes it into a language the computer can understand.

Housed in a durable die-cast aluminium enclosure as shown in figure 8-13, the HP Single Point Decoder has been designed to permit the use of long antenna cables with minimum effect on read range and also reduces the effects of surrounding materials on the operation of the antenna. The HPSPD operates from a 24vdc-regulated supply.

- Rectangular Tube Antennae

The antennae search for the transponders (tags) and relay the information from the transponder to the decoder. The antennae power the tag, which then sends back an encrypted code unique to each transponder.

Antennae were specifically designed to fit the various orifices and weirs present at Tongland Dam fish pass. The antenna positioned around the orifice was 320 by 320 mm as shown in figure 8-14 whereas the antenna fixed at the weir was 500 by 760 mm. Having an open frame construction allows objects to pass through the antennae centre. The antennae are sealed and can be used in a submerged environment.

- Glass Transponder:

Each transponder has a unique 9-digit code. As explained earlier, the transponders are passive which mean that they require no renewable source of power as the antenna, through which the transponder is passed, generates the power required.

Housed in a biostable glass capsule as shown in figure 8-15, this transponder is suitable for use in biological environments, and can in particular be inserted in the body of adult salmon without causing internal damage (see section 8-4.1.3).

8-3.4.2 *Tagging the fish*

It was agreed at the start of the field test that a total of 20 spawning salmon reaching the entrance of the pass would be trapped and tagged. The fish were caught between the 12 and the 13th of July 2001 in the lower part of Tongland Dam fish pass.

To catch the required number of salmon, a temporary trap was constructed in the lower part of the pass. This temporary trap worked in the following way:

- A mesh grid was put in position to block the weir notch between pool 56 and 58 (see Fig 8-6) for periods lasting from 4 hours (during the day) up to 12 hours (over night). The trap is shown in figure 8-16.

- The salmon coming from the river Dee and moving towards their spawning grounds were blocked in their upstream migration by the mesh grid and therefore cumulated in pools 56 and 54.

- At the end of this 4 to 12 hours period, the passage between pool 54 and 52 was blocked by a mesh grid, which means that some fish were trapped between pool 54 and 56.

- The fish were then caught using electric-fishing equipment as shown in figure 8-17.

The electric fishing equipment comprised a generator, a control box, a transformer and two electrodes (anode and cathode). The generator, the control box and the transformer, shown in figure 8-17, are positioned on the side the fish pass, and the cathode is positioned in the river downstream of the entrance to the pass so that it does not interfere with the fishing operation. The anode is operated

from the scaffolding built across pools 54 and 56. The stunned fish netted out of the water are then transferred to a holding tank prior to the surgical procedure.

For surgery, fish are anaesthetised in a tank containing a solution of benzocaine (7.5 ml of stock solution for 10 l of water). Implantation of the tags was initiated when a slow, irregular opercular rate was observed, generally within four minutes. Individual fish were then measured and weighed before being placed ventral side up in V-shaped surgical table.

A 0.2-0.5cm incision was made on the ventral surface of the fish in a central position, anterior to the pelvic fins. The transponder, sterilised in alcohol, was then pushed through this incision into the body cavity. The implantation procedure lasted approximately 2 to 3 minutes. The fish were then left to recover for a few minutes in fresh oxygenated water tank before being released in the first resting pool of the pass (pool 70).

Of all 20 individuals, 5 fish were tagged and released on the 12th of July and 15 the 13th of July 2001. The age of each fish was measured by the analysis of scales. All the fish were one sea-winter fish of which 25% were male and 75% female. They had a mean fork length of 62.9 cm (± 0.9) and a mean weight of 2.845 kg (± 0.135). Details of each salmon tagged are shown in table 8-6.

The first five fish were caught in the upper part of the ladder (: between pools 90 and 110 (cf Fig 8-6)) while it was drained in order to install the antennae. The fish were caught by electric fishing and released 2 pools down from the weir-orifice structure. The 15 following fish were caught in the trap located at the entrance of the pass and released in the first resting pool of the system (pool 70 (cf Fig 8-6)).

The detectors were activated continuously, except during a period of one day from the evening of the 16/07 to around 4pm the following day when there was a power cut.

Table 8-6: Details of adult Atlantic salmon tagged

Fish Number	Date	Fork length (cm)	Weight (kg)	Sex	Tag code
1	12/07	62.0	2.600	Female	DC0011I606
2	12/07	56.5	1.850	Female	DC0011F249
3	12/07	68.5	3.670	Male	DC0011E705
4	12/07	69.0	3.850	Male	DC0011E299
5	12/07	64.0	2.380	Male	DC0011F29F
6	13/07	55.5	1.850	Female	DC0011EE5A
7	13/07	64.3	2.500	Female	DC0011F3B0
8	13/07	56.0	1.950	Female	DC0011E42F
9	13/07	64.5	3.350	Male	DC0011F1EE
10	13/07	62.0	3.000	Female	DC0011E4F9
11	13/07	61.4	2.850	Female	DC0011E584
12	13/07	63.0	3.350	Female	DC0011E29B
13	13/07	62.0	2.650	Female	DC00F7C2B
14	13/07	70.5	3.800	Female	DC0011E541
15	13/07	65.5	3.200	Female	DC0011E4D8
16	13/07	63.5	3.000	Female	DC0011F1FF
17	13/07	59.5	2.300	Male	DC0011F35A
18	13/07	62.0	2.750	Female	DC0011E6E7
19	13/07	62.5	2.900	Female	DC0011EF9E
20	13/07	65.0	3.100	Female	DC0011EC33

8-3.5 *Results*

8-3.5.1 *General*

Fifteen of the twenty (75%) salmon tagged between the 12th and the 13th of July were recorded by the orifice antenna and/or by the weir antenna between the 12th of July and the 31st of July 2001. 5 fish were not recorded at the antennae during the period that the detectors were recording. Details of detections are shown in table 8-7.

Ten of the fifteen (= 67%) wild salmon recorded at the orifice or/and weir were picked up on multiple occasions. Only 4 (= 27%) were recorded a single time. In these four cases, two were recorded at the orifice (Fish 13 & 18) and two at the weir (Fish 11 & 15).

Five of the fifteen (= 33%) wild salmon recorded were recorded only at the orifice (Fish 4, 12, 13, 18 & 20), eight (= 53%) were recorded both at the orifice and the weir and two were recorded only at the weir (Fish 11 & 15). Eight of the fifteen (=53%) wild salmon recorded at the orifice and/or the weir were recorded first at the orifice (Fish 1, 2, 4, 12, 13, 18, 20).

There was a diurnal variation in the occurrence of the recordings at the antennae. Figure 8-18 clearly shows that the first recording of the fish occurred only between 08h38 and 22h43, the average time of arrival of the fish in the vicinity of the antennae being 17h00 (± 4h00). No fish arrived in the vicinity of the antennae between 12 am and 6 am, 1 fish reached the antennae between 6 am and 12 pm, 7 between 12 pm and 6pm and 7 between 6 pm and 12 am.

8-3.5.2 *Movements of the five fish released in pool 110*

Fish 1, 2, 3, 4 and 5 were captured, tagged and released in pool 110, 2 pools downstream from the orifice/weir antennae cross wall on 12/07/2001 around 3-4 pm. There were multiple recordings at the orifice and/or weir antennae for Fish 1, 2, 3 and 4 while Fish 5 was not recorded at the orifice or at the weir antenna over the tracking period (ending the 31 July 2001). The results for the recorded salmon are shown in table 8-7.

Fish 3 and Fish 4 were both first recorded in the proximity of one of the antennae circa 3 h after their release whereas Fish 2 and Fish 1 were recorded for the first time at one of the antennae 30h and 67h after their release, respectively. The mean time of first detection at one of the antennae was 1.08 days ± 1.27 days and ranged between 0.12 and 2.80 days.

The duration between the first and the last recording varied between 0.38h and 1.4h for Fish 1, 3 and 4 but reached 32.2h for Fish 2. Fish 2 was recorded once in the vicinity of the orifice, 30.6h after its release and a second time, 32.16h later at the weir.

Fish 1 and 2 were both recorded at the two antennae: the first time at the orifice and the second time at the weir. Fish 3 was recorded 4 times at the weir and 2 times at the orifice in a 49 min period. Fish 4 was recorded four times at the orifice in a 23 min period. As fish 4 was only recorded at the orifice, it might be assumed that it did pass through the orifice.

Table 8-7:Fate of Tagged fish between the 12/07/2001 and 31/12/2001 (Fish 5,8,9,14 and 19 are disregarded as there are no recordings available)

Fish Nber	Fork length (cm)	Date of release	Location of release	Date of first recording	Delay between release and first recording	Location of first detection	Nber of detection at weir	Nber of detection at orifice	Date of last recording	Location of last recording	Time between first and last recording
1	62.0	12/07-15:00	Pool 110	15/07-08:38	67:15 (2 days, 19:15)	Orifice	1	1	15/07-11:40	Weir	1:24
2	56.5	12/07-15:00	Pool 110	13/07-21:38	30:37 (1 day, 06:37)	Orifice	1	1	15/07-05:50	Weir	32:12
3	68.5	12/07-16:00	Pool 110	12/07-18:52	02:52	Weir	4	2	12/07-19:41	Weir	00:49
4	69.0	12/07-16:00	Pool 110	12/07-19:09	03:09	Orifice	0	4	12/07-19:32	Orifice	00:23
6	55.5	13/07-10:00	Pool 70	13/07-18:24	08:24	Weir	42	22	13/07 22:23	Weir	04:00
7	64.3	13/07-10:00	Pool 70	18/07-21:52	131:52 (5 days, 11:52)	Weir	5	5	19/07-04:44	Weir	06:52
10	62.0	13/07-10:30	Pool 70	26/07-14:44	316:14 (13days, 04:14)	Weir	13	9	26/07-17:05	Orifice	02:22
11	61.4	13/07-10:30	Pool 70	14/07-13:42	27:12 (1 day, 03:12)	Weir	0	1	*	*	*
12	63.0	13/07-12:00	Pool 70	16/07-12:01	72:01 (3 days)	Orifice	0	5	16/07-12:08	Orifice	00:07
13	62.0	13/07-12:00	Pool 70	19/07-17:36	149:35 (6 days, 05:35):	Orifice	0	1	*	*	*
15	65.5	13/07-12:30	Pool 70	25/07-19:27	294:57 (12 days, 06:57)	Weir	1	0	*	*	*
16	63.5	13/07-15:00	Pool 70	16/07-13:26	70:26 (2 days, 22:26)	Weir	3	2	16/07-13:48	Weir	00:22
17	59.5	13/07-16:00	Pool 70	14/07-17:39	26:06 (2 days, 02:06)	Orifice	1	1	14/07-17:39	Weir	00:02
18	62.0	13/07-20:00	Pool 70	16/07-14:38	66:58 (2 days, 18:38)	Orifice	0	1	*	*	*
20	65.0	13/07-20:30	Pool 70	18/07-22:43	122:13 (5 days-02:13)	Orifice	0	6	18/07-23:15	Orifice	00:32

8-3.5.3 *Movements of the fifteen fish released in the first resting pool*

Fish 6 to 20 were caught in the trap located at the entrance of the pass and released in pool 70. There were no recordings of Fish 8, 9, 14 and 19 during the tracking period. Fish 11 and 15 were recorded only once, at the weir, whereas Fish 13 and 18 were recorded once, at the orifice. There were multiple recording of Fish 6, 7, 10, 16 and 17 both at the orifice and weir antennae and there were also multiple recordings of Fish 12 and 20 but only at the orifice. The results for the recorded salmon are shown in table 8-7.

There was a great variation in the period between the release and the first recording of the fish at one of the antennae. This period varied from less than a day up to 13 days. The mean time until first detection at one of the antennae was 3.69 days ± 4.01 days and the median time is 2.80 days (range 0.3-13.2 days).

The duration between the first and the last recording varied between 0.03h (Fish 17) and 6.87h (Fish 7). It is interesting to note that for Fish 7, in the 6.87h period between the first and the last recording there was a 5.5h period of inactivity corresponding to the night (between 18/07-23:15 & 19/07-04:44).

The tagged salmon were recorded at the antennae an average of 10.7 times (range: 1-64): 5.9 times at the weir and 4.8 times at the orifice. Four fish were recorded only once (Fish 11, 13, 15 and 18), Fish 17 was recorded two times, Fish 12 and 16 were recorded 5 times, Fish 20 6 times, Fish 7 10 times and Fish 10 22 times. Fish 6 was recorded a great number of times: 64 times within a 4 h period.

8-3.6 *Discussion*

Fifteen of the twenty tagged salmon (75%) were recorded in the vicinity of the antennae within 20 days of their release. The 5 fish that were not recorded at the orifice and/or the weir antennae between the tracking period may have approached the antennae after the recording period had ended, dropped downstream into the river Dee before reaching the upper part of the pass or their tag failed. However, it is also possible that the fish moved upstream during the power cut

when recording was not possible. Therefore, I cannot comment on the overall numbers of fish that moved upstream.

There is no data on the effect of the size of tags used in this study on the behaviour of adult salmon (M. Rycroft is currently developing a new PIT tag system). However following release, two of the five fish released in pool 110 [two pools down the antennae], approached the weir/orifice devices within 3h. The short delay between the release and the first recording of these two fish seems to suggest that the recovery time necessary after the capturing and tagging procedure was less than 3h.

In this present study, initial recordings of salmon in the vicinity of the orifice/weir device occurred during the afternoon [12 pm –6pm] and the early part of the evening [6pm-12 am]. All activities ceased, at least in the vicinity of the orifice/weir device, between 11pm and 5am. It also appears that Fish 7 stopped its activity in the vicinity of the antennae late at night (23:15) to resume it early the following morning (04:45). This pattern is in agreement with the findings of a radio-telemetry study conducted at Pitlochry fish ladder in 1995-1996 (Govans et al, 1999). It was found that the movement of the adult salmon ceased at darkness but continued in the following morning.

The salmon released in resting pool 70 ascended 19 weirs-and-pools and 2 resting pools [from pool 70 to pool 112] within a period of time ranging between 8 h and 316 h (13 days). The great variation in the time taken by the salmon to reach the orifice/weir fitted with the antennae seems to suggest that some of the fish either paused within the fish pass (they might rest in one of the resting pools which have low velocity areas) or fell back and paused immediately below the fish pass entrance. As the trap was installed at the two first pools of the pass, it is possible that the salmon were caught during their "acquaintance period" with the lower pool of the pass. Laine (1995) suggested that some fish need to have some kind of initial experience of the lower part of the pass before ascending. Typically the delay observed between the first approach and the final entry is around 14 days (14.8 days in Gowans et al (1999) and 14 days in Laine (1995)).

Unfortunately, it was not clear whether the recordings at the orifice and/or the weir corresponded to a successful passage of the fish through the orifice/weir or simply to an attempt. In the case of a unique recording, it might be assumed either that these salmon succeeded at the first attempt or that they felt back after failing their first attempt. When there were multiple recordings for a same fish, it was also not clear if the second and following recordings corresponded to an upstream or downstream movement.

The multiple recordings of the majority of the fish (67%) at the orifice and/or the weir antennae might suggest either that salmon tended to investigate both options (swimming through the orifice or leaping over the weir) before going through one of them or that they were experiencing some difficulties in the upper part of the pass despite the modifications made in Spring 1998.

As the proportion of salmon recorded first in the vicinity of the orifice or the weir (8 at the orifice - 7 at the weir) are similar and as there are no significant differences in the number of recordings at the orifice and at the weir for the 15 fish registered at least once in the vicinity of one of the antennae (ANOVA, $df = 1$; $F = 0.036$, $p = 0.85$), this study does not establish the preference of adult for submerged or overflow jets.

This difference of results between the laboratory-based experiments with mature parr and mature brown trout and this field test at Tongland dam could be due to the fact that the orifice was in the first case located at the bottom of the flume and in the second case at 1.00 m above the bottom of the pool.

8-4 Conclusion

The purpose of this chapter was to widen the investigation of the effects of water flow characteristics downstream from orifice/vertical slots and weirs devices on upstream movement of displaced Atlantic salmon parr. This was achieved by observing the movements of mature male salmon parr and brown trout at Almond-

bank rearing station and by attempting to monitor wild adult salmon in the field at Tongland fish pass.

This investigation of the effects of flow characteristics on spawning fish (male mature parr, male adult brown trout and adult salmon) was limited to a comparison of a weir and an orifice. In the laboratory, 20 mature parr and 20 mature brown trout were individually confronted with the alternative of passing through a 0.20 by 0.10 m orifice or over a 0.20 m wide weir. In the field at Tongland dam fish pass, 20 wild salmon were trapped and tagged. They were also confronted in the upper region of the pass with the alternative of passing through a 0.32 by 0.32 m orifice or over a 0.76 m wide weir.

The results obtained for the mature parr and the mature brown trout are in accordance with the conclusions drawn in Chapter 5 and 7. All the mature parr and 95% of the mature brown trout preferred the orifice to the weir despite both structures generating similar maximum velocity (c. 1 m/s). The results obtained from the preliminary field study conducted at Tongland dam fish pass are ambiguous as wild adult salmon were equally attracted by the 0.32 by 0.32 m orifice and the 0.76 m weir. The original objective was to switch the orifice and weir around and run a second group of fish through the system. This procedure would have balanced any tendency of salmon to move up one or other side of the pass and so to first encounter one or other of the pass designs. In view of the uncertainties in interpreting the data, it was decided to terminate the experiment. There clearly were differences between the laboratory and field studies in that multiple recording abounded in the field. An important next step will be to determine whether these recordings reflect the behaviour of fish approaching the cross wall or indicate that they were encountering difficulties leaving the pass.

CHAPTER 9:

CONCLUSIONS AND SUGGESTION FOR FUTURE RESEARCH

CHAPTER 9

CONCLUSIONS AND SUGGESTIONS FOR FUTURE RESEARCH

9-1 Introduction

There is little doubt about the importance or need to improve the design of fish passes at dams or natural obstructions in order to maintain or restore populations of fish living out some of their life cycle in rivers. There is also a clear imperative for combining civil engineering and fish biology expertise in controlled environment research (Mitchell et al, 1998) or in the field or through computer model studies (Rivinoja et, 2001), to improve salmonid habitat (Gibbins and Acornley, 2000). In particular to enhance the efficiency of fish passage facilities, which are bioengineering systems based on biological criteria and involving complex hydraulic phenomena.

The key question is whether this research based on the idea of using scale models of fish-passes to conduct both hydraulic and biological experiments (in order to provide direct comparisons of the efficiency of each type of fish pass in terms of upstream migration) brings a significant new insight about how adult salmon may respond to water flow in the vicinity of fish passage facilities.

The ideal situation in attempting to provide direct comparison of the efficiency of each type of fish pass in terms of upstream migration would be to track a statistically sufficient number of upstream migrants in selected field sites over several years. By conducting such a field test, the efficiency of fish pass may be assessed and some insight into the proportions of migrating population moving upstream may be gained (Webb, 1990; Gowans et al, 1999; Rivinoja et al, 2001). However this kind of field survey is time consuming, requires a lot of instrumentation and is dependent on many incontrollable parameters (weather, temperature, precipitations, river discharge, turbidity...). In addition the behaviour of salmon in the field is influenced by so many factors it would be difficult to establish simple behavioural rules related to hydraulic characteristics.

In this respect, the effect of scale model laboratory fishpass structures containing weirs, orifices and vertical slots and combination of all three on the upstream movement of displaced Atlantic salmon parr was investigated in order to develop and refine hypotheses on the behaviour of adult salmon in the vicinity of fish passes (Chapter 5 and 7). An elementary biomechanical model combining hydrodynamics and energetics of fish propulsion was also elaborated (see section 7-4).

To test the hypothesis that salmon prefer orifices to weirs and to extrapolate this hypothesis to fish pass design, further laboratory-based experiments were conducted, this time with mature male parr (to compare the motivation to move of a displaced parr and a homing parr) and with mature adult brown trout (to assess the influence of the fish size). In the last part of this study, a preliminary field test study was conducted during summer 2001 at Tongland Dam to test the hypothesis postulated using salmon parr and brown trout in 1999 and 2000 on wild adult salmon.

The experimental study of the behaviour of displaced juvenile salmon, homing mature parr and brown trout was supported by extensive hydraulic measurements and analysis of the water flow characteristics downstream the scaled down laboratory based fishpass structure containing weirs, orifices and vertical slots and combination of all three. These hydraulic measurements included head-loss, ve-

locity patterns and turbulence structure using WinADV, ADV analysis and Matlab (see chapter 4 for methods and Chapter 6 for results).

9-2 Main conclusions

- *Efficiency*

A significantly higher proportion of displaced parr moved through submerged orifices and vertical slots than through weirs, despite the fact that these were tested at equal flow rates and comparable velocities. Salmon parr were able, both to locate and pass easily through the orifices or the slots within the few first minutes of their introduction in the flume. They were also capable of passing over the weirs but significantly less effectively than through the orifices or slots. The efficiency, defined as the proportion of salmon parr passing through the device in the 20 first minutes of their introduction in the flume, is typically 68% for orifices, 44% for vertical slots and 2.5% for weirs.

These results can be correlated to the fact that the hydraulic conditions downstream differed greatly depending on whether, a free-falling jet discharged over a weir, or a submerged jet passed through an orifice or slot. These results, therefore suggest that the ability of displaced salmon to move upstream is influenced by local water flow characteristics.

- *Velocity and turbulence*

In the pool downstream of the model weir, orifice or vertical slot, parr were confronted in most part of the flume with velocities less than 0.20 m/s. High velocities concentrated in the vicinity of the device tested and/ or along the longitudinal axis downstream of the orifice/slot or weir. For the range of flows tested, the maximum velocity varied between 1.5 and 2.2 m/s [velocity at impact] for the weirs, between 0.8 and 2.9 m/s for the orifices [velocity at vena contracta] and between 0.8 and 1.8 m/s for the vertical slot.

The efficiency of parr passing through orifice and vertical can be directly correlated to the velocities existing in their vicinity, therefore to the size of the open-

ing and the range of flow at which they were tested. The efficiency declined almost linearly with increasing velocities.

$$Efficiency = -0.4026V_w + 1.2602 \quad (9\text{-}1)$$

$$Efficiency = -0.359V_w + 0.906 \quad (9\text{-}1)$$

Equations 9-1 and 9-2 are valid for value of V_w greater than 0.60 m/s, V_w being the velocity at the vena contracta for the orifices (9-1) and the calculated maximum velocity at the slot for the vertical velocities (9-2).

For the orifice and vertical slot devices, the hydraulic measurements have shown that the flow can be considered as two-dimensional as a first approximation. However at high discharge, the flow downstream a vertical slot is three-dimensional if the slot is narrow. On the contrary, the hydraulic conditions created by a flow passing over a weir are, in all circumstances, three-dimensional. Turbulence patterns differed also greatly between orifices and weirs while vertical slots appeared to be an intermediate pattern. The maximum turbulence intensity was also greater for the weir (50%) than for the orifices (20-30%) and the vertical slots (25-35%). However no conclusive evidence was found of the direct and sole influence of the turbulence on the efficiency at passing parr of the various designs.

It was also found that, for a given velocity, bottom orifices were more efficient than vertical slots at passing parr. For example, at a maximum velocity of 0.8 m/s, the bottom orifice and the vertical slot had efficiency of 87.5% and 60% respectively. According to Bates (2000), the attraction of a jet is due to its momentum, therefore, at equal velocity, orifices may be more suitable than vertical slots because the decay rate of velocities within the jet is higher for slots than orifices. On the other hand, vertical slots have the advantage of allowing fish to swim through them at any desired depth (Stuart and Mallen-Cooper, 1999) and orifices have the disadvantage of being more prone to blockage by debris (Gowans et al, 1999).

Orifices at the flume bottom were significantly more efficient (90%) than those elevated 0.05 (52.5%) and 0.10 m (40%) above the bottom. These orifices had similar velocities at their vena contracta but their jet diffusion patterns were different. Jet diffusion patterns change in relation to the elevation of the orifices above the flume bed. Jet discharging through orifices located at the bottom behaved like bluff wall jets while jets passing through elevated orifices were comparable to free bluff jets. As parr tend to stay near the bottom of the flume (observation done during the behavioural study and corroborated by Kallerberg, (1958)), this may have decreased their ability to detect jets above the bottom and may account for the inverse relationship between height of orifice and ease of passage.

The overall efficiency of a bottom orifice was improved by introducing a 0.6 m wide weir in parallel. This weir operated mainly at high flows. The introduction of the weir allowed the reduction of the velocities downstream the opening [by 8% and 45% for a discharge of 0.012 and 0.020 m^3/s respectively]. At high flow, this reduction by 45% of the velocity at the vena contracta was correlated to an efficiency improvement of the bottom orifice of 45% (from 7.5% to 52.5%). Combining orifices with a correctly designed weir can therefore increase the range of flow for which orifices are efficient.

- *Path chosen*

The movement of parr approaching orifice/weir/vertical slot devices could be classified into three basic paths. For path A, fish moved straight along the side of the flume from the point of introduction to the weir or orifice outlet directly toward the weir/orifice/slot. For path B, fish moved first along the downstream end of the flume, then upstream along the side and to the pass. For path C, fish started along path A and then crossed over to take path B. Parr followed in general the sides of the arena, which provided them with cover.

The paths chosen by parr are: path A 35%, path B 33% and path C 11%. The choice of path seems to be influenced by factors that did not appear to influence the efficiency of the devices tested, such as the lateral location of the device. If

the structure, in particular an orifice, is at the middle, parr tended to swim equally along the window side or the opposite side of the flume, whereas they moved, at least initially, directly towards the jet, if they were introduced in its centreline. The proportion of parr veering, then, away from the flowing water depends on the velocities. As the decay rate of velocities within a jet is higher for slots and orifices, it might explain the significant influence of the design: side orifice/ side vertical slot in the frequency of the three paths.

There was no significant influence of the size or elevation of the orifice or of the width of the side vertical slot in the frequency of the three paths and there was no significant difference in the movement patterns of the parr between an orifice alone and an orifice combined with a weir. It can also be extrapolated from the "double orifice" situations that when two jets are in competition to attract parr, the influence of the flow ratio over the frequency of the three paths depends on the initial position of the parr.

- *Energy*

It has been explained that homing salmon use a range of tactics to reduce energy expenditure during migration (Hinch and Rand, 1998; Weihs, 1973). In this study, parr displayed two main tactics to reduce their energy expenditure during their upstream movement. By choosing path B to reach the upstream part of the flume, they were exploiting reverse flow (or more precisely recirculation flow). It had been noticed during the hydraulic measurements that a recirculation phenomenon occurred in almost all situations. Parr approaching the orifice/slot also chose an economical solution as they swam into the device at an oblique angle thus minimising the period of time spent in high jet core velocities.

In chapter 7, an attempt has been made to estimate the energy cost associated with the different devices and the path chosen by the parr to move upstream. In a hydrodynamic point of view, the propulsive force the fish has to generate to swim against the flow has to overcome gravity, pressure, viscosity, virtual mass, surface tension or even water elasticity forces (Webb, 1975). By using hydromechanics and hydraulics concepts (Webb, 1975; Behkle, 1987, 1988, 1991, 1993)

simplified equations of the energy required to pass through an orifice or a slot and of the potential energy associated with a fish leaping over a weir were expressed. They are a function of parameters such as fish length and weight (L & W), velocity of the water (V_w,), distance covered d, height of the leap (Δh), angle of the leap (θ) and a dimensionless coefficient α corresponding to the energy strategy adopted by the fish. The energy required to pass through an orifice and the potential energy the fish has to overcome when leaping from a standing wave into air are expressed in Eq 9-3 and 9-4:

$$E = 11.30L^3\Delta h + 3.82(1+\alpha)L^{1.8}V_w^{1.8}d \qquad (9\text{-}3)$$

$$E_p = W\frac{\Delta h}{\sin^2\theta}(1-\sqrt{0.024})^2 \qquad (9\text{-}4)$$

The energy expended by parr increases with their size. For weir situations, parr expenditure decreases linearly with the height of the leap. For orifices and vertical slots, the energy expenditure is 3 times greater when the size of the orifice is halved and multiplied by 2.5 when the width of the vertical slots is reduced from 0.10 to 0.05m.

In the particular cases tested in this research, for a discharge of 0.012 m^3/s, for a 0.12 m long fish, the potential energy expenditure to leap over a weir is around 3.8E-03 J if the downstream water level is 0.20 m. For a discharge of 0.012 m^3/s, if the assumption is made that the parr swims 0.10 m (=d) against high velocities with a strategic coefficient α equal to 0.1, the energy used by a 0.12 m long parr is around 7.5E-03 J for the 0.20 by 0.10 m orifice and around 7.0E-03 J for the 0.10 m vertical slot. The weir appears to offer the least energetic route, followed by the wide vertical slot and the large orifice. This apparent superiority of the weir design over the orifice and vertical slot designs is due to the fact that the energy expenditure calculated here takes into account only the actual jump of the fish and ignores the energy expended by the parr to reach the starting point of the jump. If the energy expended by the fish before passing through the orifices/slots is ignored, [only the first term of Eq 9-4 is taken into account], the energy used

by the fish to pass through the orifice/slot devices tested is around 6.5-7.0E-04 J and is smaller than the energy used by the fish to jump.

In conclusion, the suitability of a design and/or the movements of the parr in the flume are both governed by the hydraulic conditions existing in the flume and by behavioural patterns hereditary or not. The predominance of one characteristic over another appears to change following a complex algorithm, which still need to be found. However by multiplying the number of situations tested, a hydraulic/behaviour pattern can be built.

- *Mature male parr and adult male spawning trout*

The purpose of using mature male parr and mature brown trout was to widen the investigation of the effects of water flow characteristics downstream orifice/vertical or weir devices on upstream movement of displaced Atlantic salmon parr to fish undergoing a spawning migration.

This investigation of the effects of flow characteristics on spawning fish (male mature parr, male adult brown trout and adult salmon) was limited to a comparison of a weir and an orifice. In the laboratory, 20 mature parr and 20 mature brown trout were individually confronted with the alternative of passing through a 0.20 by 0.10 m orifice or over a 0.20 m wide weir.

All the mature parr and 95% of the mature brown trout preferred the orifice to the weir despite both structures generating similar maximum velocity (around 1 m/s) and turbulence intensity. The results obtained for the mature parr and the mature brown trout are in accordance with the main conclusion drawn on the preference of displaced salmon parr for vertical slots and orifices over weirs when moving upstream.

This experiment showed that the upstream movement of displaced salmon parr was similar to the upstream movement of spawning mature and mature brown trout.

- *Field tests at Tongland Dam*

As a complement to physical model tests using salmon parr, a preliminary field test was undertaken at Tongland Dam fishpass using new field tracking devices designed by UKID designed for adult salmon. The purpose of this field test was to assess the results found with salmon parr and brown trout in the laboratory at Almondbank that fish found orifices (and slots) easier to negotiate than weirs. The particular situation of the Tongland dam fish pass was thought to allow a comparison between the two for migrating adult spawning salmon.

15 of the 20 salmon tagged reached the orifice and/or weir antennae at the up-stream end of the fish pass in the 20 days following their capture. 11 of them had multiple recordings. Only 4 had a single recording, 2 at the orifice and 2 at the weir. 5 of the 14 were recorded only at the orifice and 8 of the 15 were recorded first at the orifice.

The results obtained from the preliminary field study conducted at Tongland dam fish pass are ambivalent as wild adult salmon were equally attracted by the 0.32 by 0.32 m orifice and the 0.76 m wide weir. However, this study provides interesting information on the diurnal activity of the wild salmon. It was found that the movement of the adult salmon ceased at darkness but continued in the following morning in the vicinity of the orifice/weir antennae.

The interpretation of the data obtained was limited by the fact that the an-tennae do not differentiate between successful and unsuccessful approaches or between upstream and downstream movements.

The aims and objectives of this research, explained in section 1.3 have been fulfilled. The effectiveness of major fish pass design principles (such as pools and traverses or vertical slots) has been investigated, and the synergy of com-bining biological and hydraulic studies has been illustrated. It has also been shown that salmon parr may have a key role in identifying behavioural mechanisms by which adult salmon respond to flow conditions.

9-3 Suggestions for future research

A versatile large-scale physical model of a fish pass entrance including power station, dam and river reach should be constructed. This physical model should then be used to carry out hydraulic measurements and to monitor the detailed movement of salmon and trout against a range of flow conditions, entrance locations, entrance orientation and geometry, elevations, and interactions between power station flow and pass flow.

This facility should be versatile. The model should be constructed with three entrance locations for the fish pass in the centre, at the side and an upstream point. The pass in each case should have the flexibility to be angled up to 30 degrees to the river alignment, to be changed from a weir to a slot to a submerged orifice. The model should have the facility to vary the interaction between the power station and pass flows via a series of louvers constructed into the model bed and via flow ratio varying from 1% to 5% to 10% of the power station flow.

This facility should be instrumented with digital water-level recorders, Acoustic Doppler Velocimeters for velocity and turbulence data gathering, together with a network of digital cameras and under-water video equipment for tracking individual fish. Electromyogram-tagging techniques should also be considered.

The use of digital video recording of salmon and trout in conjunction with the recording of their muscle activity using electromyogram-tagging techniques should allow to obtain more information on energetic strategies used by salmon. These kind of physiological telemetry experiments in conjunction digital video recording and hydraulic measurements would also allow to determine the degree of difficulty fish have in ascending various type of fish pass, to record precisely the path they follow and to develop a better understanding of the relation between hydrodynamics and biological energy metabolism principles.

Using this facility, some research could also be carried out on the long-term effect of sedimentation on the hydraulic conditions existing within fish passage structures and also on the behaviour of spawning salmonids.

This experimental work should also be complemented by three-dimensional computer model studies in order to create a comprehensive database on real fish behaviour. The general Computational Fluids Dynamics (CFD) techniques should be implemented to hydraulics conditions in and downstream fish passage facilities. At this effect, the commercial codes, TELEMAC and CFX4 could be used and the data collected at the facility could be used to validate CFD models.

More work should also be carried out in the field at existing fish passage facilities to determine the pass efficiency of these structures. From the experience gained through the field test conducted at Tongland Dam, it would also be worth building a simplified version of the versatile large-scale physical model of a fish pass entrance in the field in order to be able to test hypotheses elaborated with the laboratory facility using wild adult spawning salmon.

To implement this idea, it would be worth developing more sophisticated fish counters and antennae that will allow the differentiation between upstream and downstream movements and between successful passages and attempts.

There are around 40 Borland lift fish passes in operation in Scotland. Therefore some more work, combining hydraulic and behavioural studies, could be carried out at Borland lift fish passes in order to study the relation between their efficiency and the hydraulic conditions existing in their lower chamber. A study conducted in 1996 at a Borland fish pass located on the river Beauly (Smith et al, 1997) showed that few fish found the lower chamber and that only 40% of the fish entering the pass successfully exited the upper chamber.

Although detailed measurements of the turbulence structure existing downstream of the model orifice, slot or weir were made in this research, the influence of turbulence on the efficiency of the fish passage facilities was not dissociated from the influence of the velocity. It would be interesting to do so by sharpening or smoothing the edges of the orifice, slot or weir structures.

REFERENCES

1) **Aaserude, G., 1984.** New concepts in fishway design. M.S. Thesis, dep't of civil and environmental Engineering, Washington State University

2) **Aitken, P.L., Dickerson, and W.J.M. Menzies, 1966.** Fish passes and screens at power works, Proceedings of the Institute of Civil Engineers, 35,26-57

3) **Albertson, M.L., Dai, Y.B., Jensen, R.A., and Rouse, H., 1948.** "Diffusion of sub-merged Jets", Proc. A.S.C.E., Vol 74, pp 639-663

4) **Aleyev, Y.G., 1977.** Nekton, Dr W. Junk, The Hague, 435pp

5) **Armstrong, J.D. and N.A. Herbert, 1997.** Homing movements of displaced stream-dwelling brown trout, Journal of fish Biology, 50, 445-449.

6) **Armstrong J.D., V.A. Braithwaite, F.A. Huntingford, 1997.** Spatial strategies of wild Atlantic salmon parr – exploration and settlement in unfamiliar areas, J. Anim. Ecol. 66:203-211.

7) **Andrew, F., 1990.** The Use of vertical –slot fishways in British Columbia, Canada, Proceedings of the International symposium on Fishways '90 in Gifu, pp: 267-274.

8) **Alabaster, J. S., 1970.** River flow and upstream movement and catch of migratory salmonids. J. Fish Biol. 2:1-13

9) **Alabaster, J.S., 1990.** The temperature requirements of adult salmon, Salmo salar L., during their upstream migration in the river Dee. J. Fish Biol. 37:659-661

10) **Anon., 1942.** Report of the Committee on Fish Passes. Instn. Civ. Engrs, London, 59p.

11) **Anon., 1986.** Report of the working group on North Atlantic Salmon. International council for the exploitation of the Sea, Copenhagen, C.M. 1986/assess:17

12) **Anon., 1995.** Note for guidance on the provision of fish passes and screens for the safe passage of Salmon, Scottish office Agriculture and Fisheries Department, Edinburgh, 38pp

13) **Banks, J.W., 1969.** A review of literature on the upstream migration of adult salmonids, J. Fish. Biol. 1:85-136.

14) **Bates, K., 1991.** Pool and Chute Fishways, American Fisheries Society Symposium 10:268-277

15) **Bates, K., 2000.** Fishways guidelines for Washington State, Draft 4/25/2000, Washington Department of fish and Wildlife, (Ed) Tony Whiley.

16) **Baxter, G.C., 1961.** River utilisation and the preservation of migratory fish life. Proc. Instn. Civ. Engrs. 18:225-244

17) **Beach, K., 1984.** Fish pass design – criteria for the design and approval of fish passes and other structures to facilitate the passage of migratory fish in rivers. Fisheries research Technical Report N78, Lowestoft

18) **Beamish, F.W.H., 1978.** Swimming capacity. In: Hoar, W.S. & Randall, D. J. (eds). Fish physiology volume VII Locomotion. Academic Press, London: 101-187

19) **Behkle, C.E., 1987.** Hydraulic relationships between swimming fish and water flowing in culverts, Proceedings of the Second international cold regions Environmental Engineering Conference, Edmonton, Alberta.

20) **Behkle, C.E., 1988.** Hydraulic effects on swimming fish in fish passage structures, Proceedings of the National Hydraulic Engineering 1988: 1116-1121pp

21) **Behkle, C.E., 1991.** Power and Energy implications of passage structures for fish, American Fisheries Society Symposium10, 289-298pp

22) **Behkle, C.E., D.L. Kane, R.F. McLean, M.D. Travis, 1993.** Economic Design using fish swimming Energy and Power Capabilities, Proceedings of a symposium on fish passage policy and technology, Portland, Oregon, USA

23) **Bell, M.C. 1973,** Fisheries handbook of engineering requirement and biological criteria: Useful factors in life history of most common species. U.S. Army Corps of Engineers, Portland Oregon.

24) **Beltaos, S. and Rajaratnam, N, 1973.** Plane turbulent impinging jets, ASCE Journal of Hydraulic engineering, Vol 100, pp 69-83

25) **Berg, O.K., 1998.** The formation of land locked Atlantic salmon (Salmo Salar L) Dr Scient. Thesis, University Trondheim 36pp+4 papers

26) **Blaxter, J.H.S., 1969.** Swimming speed of fish. F.A.O. Fish. Rep., 62(1):69-100

27) **Boiten, W, 1990.** Hydraulic design of the pool-type fishway with V-shaped overfalls, Proceedings of the International symposium on Fishways '90 in Gifu, 483-490pp

28) **Bonnyman, G.A., 1958.** Fisheries requirements. Hydro-electric Engineering Practice, Vol. 1, chap XXIV, 1126-1155pp

29) **Brett, J.R. & McKinnon, D., 1954.** Some observations of olfactory perception in migrating adult coho and spring salmon. J. Fish. Res. Bd. Can. 11, 310-318.

30) **Brett, J.R., 1964.** The respiratory metabolism and swimming performance of young sockeye salmon, J. Fish. Res. Bd. Can., 21, 1183-226

31) **Brett, J.R., 1995.** Energetics. In Physiological ecology of pacific salmon. Edited by C. Groot, L. Margolis, and W.C. Clarke. University of British Columbia Press, Vancouver, B.C. pp3-68

32) **Buck, R.J.G. and A.F. Youngson, 1982.** The downstream migration of precociously mature Atlantic salmon , *Salmo salar L.*, parr in autumn, its relation to the spawning migration of mature adult fish, J. fish> boil. 20:279-288

33) **Calderwood, W.L., 1906.** Autumn migration of salmon smolts in Scotland, Rep. Fish Board scot. 1905 (11): 70-74

34) **Chanson, H., 1994.** Hydraulic Design of Stepped cascades, channels, weirs and spillways, ISBN: 0080419186, Elsevier Science Ltd

35) **Clay, C.H., 1961.** Design of Fishways and Other Fish Facilities, Dept of Fish. Can., Ottawa, 301pp

36) **Colavecchia, M., Katopodis C., Goosney R., Scruton D.A. &McKinley R.S. 1998.** Measurement of burst swimming performance in wild Atlantic salmon (Salmo salar L.) using digital telemetry. Regul. Rivers: Res. Mgmt. 14: 41-51

37) **Crisp, D.T., 1996.** Environmental requirements of common riverine European salmonid fish species in fresh water with particular reference to physical and chemical aspects. Hydrobiologia 323:201-221.

38) **Crook, P.H., 1991.** Design of Low-cost Fishways, Proceedings of The American Fisheries Society Symposium10: 256-263pp

39) **Deedler, C.L., 1958,** Modern fish pass in the Netherlands, Progressive Fish Culturalist, October 1958, pp 151-154

40) **Denil, G., 1909.** Les echelles a poisons et leur application aux barrages de Meuse et d'Ourthe, Annales des Travaux Publics de Belgique.

41) **Egglishaw, H.J, 1967,** The food, growth and population structure of salmon and trout in two streams in the scottish Highlands ; Freshwat. Salm. Fish. Res, 38, Scotland, 32pp

42) **Egglishaw, H.J. and P.E. Shackley, 1977,** Growth, survival and production of juvenile salmon and trout in a scottish stream, 1966-1975, J. Fish Biol. 11 : 647-672.

43) **Elliot, J.M., 1981.** Some aspects of thermal stress in freshwater teleosts. In: Pickering, A.D. (eds) Stress in Fish. Academic Press, London: 209-245

44) **Elson, P.F., 1975a.** The importance of size in the change from parr to smolt in Atlantic salmon,Canadian Fish Culturist 21, :1-6pp

45) **Elson, P.F., 1975b.** Atlantic almon rivers, smolt production and optimal spawning : an overview of natural production. Int. Alt. Salmon Found. Spec. Publ. Ser. 6, 96-119

46) **Ervine, D.A., 1976.** The entrainment of air in water. Water Power & Dam construction. Dec 1976 pp27-30

47) **Ervine, D.A., 1998.** Air entrainment in hydraulic structure: a review, Proc. Instn Civ. Engrs Wat. Marit. & Energy, 1998, 130, Sept 142-153.

48) **Ervine, D.A., B. Couvel, J. Stuart and C. Carnie, 1999.** Modifications to a fish pass at Tongland dam, 23rd Annual Meeting of the IAHR, Graz, Austria, August 1999.

49) **Evans, W. A. and F. B. Johnston, 1980.** Fish migration and fish passage: a practical guide to solving fish passage problems. USDA Forest Serv., Region 5, 43pp

50) **Fausch, K.D., 1984.** Profitable stream positions for salmonids: relating specific growth rate to net energy gain, can. J. Zool. 62: 441-451

51) **Forthmann, E, 1936,** Turbulent Jet Expansion, English translation N.A.C.A, TM-789, (original paper in German, Ing. Archiv, 5, 1934)

52) **Gibbins, C.N., and Acornley, R.M., 2000,** Salmonid habitat modelling studies and their contribution to tee development of an ecologically acceptable release policy for Kielder reservoir, north-east England, Regul. Rivers: Res. Mgmt. 16:203-224

53) **Gibson, R.J., 1978,** The behaviour of juvenile Atlantic salmon (*Salmo salar*) and brook trout (Salvenius fontinalis) with regards to temperature and water velocity; Trans. Am. Fish. Soc. 107:703-12

54) **Gibson, R.J., 1988,** Mechanisms regulating species composition, population structure and production of stream salmonids: a review, Pol. Arch. Hydrobiolog. 35:469-95

55) **Gibson, R.J., 1993,** The Atlantic salmon in fresh water: spawning rearing and production, Rev. Fish Biol. Fish. 3:39-73

56) **Goertler, H., 1942,** Berechnung von Aufgaben der freien Turbulenz auf Grundeines neuen Naherungsansatzes., ZAMM, 22, 1942, pp 244-254

57) **Gowans, A. R. D., 1998,** Movements of Adults Atlantic Salmon (Salmo Salar L.) in relation to Hydroelectric Schemes in Scotland, PhD thesis, University of Aberdeen, august 1998.

58) **Gowans, A. R. D., Armstrong, J. D., Priede, I.G. 1999.** Movements of adults Atlantic salmon in relation to a hydroelectric dam and fish ladder. J. Fish Biol. 54:713-726

59) **Guiny, E., D.A. Ervine, and J. D. Armstrong,** 2000 (a), Integrating hydraulics and biology to investigate movements of salmon through fish passes, Proceedings of the international conference " New Trends in Water and Environmental Engineering for safety and Life, Capri, Italy, July 2001.

60) **Guiny, E., D.A. Ervine, and J. D. Armstrong, 2000 (b),** Salmon parr as models to explore adult salmon response at fish pass, Proceedings of the international symposium "Fish Migration on Passage", Aberdeen, Scotland, July, 2001.

61) **Guiny, E., D.A. Ervine, and J. D. Armstrong, 2001 (a),** Fish Passes at Dams and Weirs, 13th Annual Seminar of The Scottish Hydraulics Study group "Environmental River Engineer", Glasgow, March 2001.

62) **Guiny, E., D.A. Ervine, and J. D. Armstrong, 2001 (b),** Optimum Design of Fish Passes – Combining Biology with Hydraulics at the Laboratory Scale, Proceedings of the international symposium on Environmental Hydraulics, Arizona, December, 2001

63) **Guiny, E., J.D. Armstrong and D.A. Ervine, 2001 (c),** Movements of juvenile salmon and mature trout through fish pass entrances designed as weirs and submerged orifices, Proceedings of the international symposium Fishways 2001, Reykjavik, Iceland, September 2001 (submitted).

64) **Halvorsen, M., and O.B. Stabell, 1990,** Homing behaviour of displaced stream-dwelling brown trout, Animal behaviour 39:1089-1097

65) **Harden-Jones, F.R., 1968,** Fish Migration, Edward Arnold press, London

66) **Heggberget, T., 1988,** Timing and spawning of Norwegian Atlantic salmon (*Salmo Salar L.*) Can J. Fish Aquat. Sci. 45:845-849

67) **Hellawell, J.M., 1976,** River Management and the migratory behaviour of salmonids. Fish Mgmt. 7: 57-60

68) **Hilliard, D., 1983,** Weir Optimisation: a new concept in fish ladder design, Dept of Civil and Environmental Engr., Washington State University, Pullman, Washington,

69) **Hinch, S.C. and Rand, P.S., 1998,** Swim speeds and energy use of upriver-migrating sockeye salmon (Oncohynchus nerka): role of local environment and fish characteristics. Can. J. Fish. Aqua. Sci. 55: 1821-1831.

70) **Hinch S.C. and Rand P.S., 2000.** Optimal swimming speeds and forward-assisted propulsion: energy-conserving behaviours of upriver-migrating adult salmon, Can. J. Fish. Aqua. . Sci. 57:2470-2478

71) **Hoar, W.S., 1976,** Smolt transformation: evolution, behaviour and physiology, J. Fish. Res. Board. Can. 33:1233-1252

72) **Hoar, W.S. and Randall, D.J. 1978,** Fish biology volume VII, Locomotion, Academic Press, New York

73) **Holloway, G.A., 1991,** The Brule River Sea Lumprey Barrier and Fish Ladder, Wisconsin, Proceedings of The American Fisheries Society Symposium10: 264-267pp

74) **Hudson, W. and J.K. Hunter, 1938,** The Galloway Hydro-Electric Development, Paper presented at the Institution of Civil Engineers, 22nd February 1938.

75) **Huntingford, V. A., Braithwaite, J. D. and Armstrong, D. Aird, P. Joiner 1999.** Homing in juvenile salmon in response to imposed and spontaneous displacement: experiments in an artificial stream, *Journal of Fish Biology*, Vol. 53, No. 4, Oct 1998, pp. 847-852

76) **Huntsman, A.G., 1939,** Salmon angling in the Magaree River. Bull. Fish Res .Bd Canada 57:1-75

77) **Huntsman, A.G., 1945,** Migration of salmon parr, J. fish. Res Board can. 6: 399-402

78) **Hutchings, J.A. and M.E.B. Jones, 1998,** Life history variation and growth rate thresholds for maturity in Atlantic salmon, *Salmo salar*, Can J. Fish. Aquat. Sci. Vol 55(suppl. 1) 22-47

79) **Hynes, A.B.N., 1970,** The ecology of running waters, Toronto, University of Toronto Press, 555pp.

80) **Jordan, W.C. and A.F. Youngson, 1992,** The use of genetic marking to assess the reproductive success of mature male Atlantic salmon parr (*Salmo Salar, L*) under natural spawning conditions. J. Fish Biol. 41:613-618

81) **Jungwirth, M., Schmutz, S., Weiss, S. (Eds), 1998,** Fish Migration and Fish Bypasses, Fishing New Books 19-32, Oxford ISBN: 0-85-238-2537

82) **Kalleberg, H., 1958.** Observation in a stream tank of territoriality and competition in juvenile salmon and trout. Rep. Inst. Freshwater Res., Drottningholm 39:55-98

83) **Katopodis, C. and N. Rajaratnam, 1983,** A review and Laboratory Study of Hydraulics of Denil Fishways, Canadian Technical Report of Fisheries and Aquatic Sciences 1145.

84) **Katopodis, C., 1990,** Advancing the art of engineering fishways for upstream migrants, Proceedings of the International symposium on Fishways '90 in Gifu, 19-28pp

85) **Katopodis, C., 1995,** Recent Fishway Design Problems in Canadian Rivers, Proceedings of the International symposium on Fishways '95 in Gifu, 1-7pp

86) **Katopodis, C., Rajaratnam N., Wu, S., Tovell, 1997,** Denil Fishways of varying Geometry, Journal of Hydraulic Engineering, Vol 123, No 7, July, 1997

87) **Katopodis, C., 1998,** Sustaining Fish migrations: Swimming performance and fish passage /exclusion methods, Proceedings of Nordic Symposium on fish passage, Oslo, Norway, September 9-11

88) **Keenleyside, M.H.A. and F.T. Yamamoto, 1962,** Territorial behaviour of juvenile Atlantic Salmon(salmon salar L.). Behaviour 19, 139-169.

89) **Kumar, G., Nago, H., Maeno, S., Hoshina, T.,** Hydraulics of Ice Harbor Type Fish-way, Proceedings of the International symposium on Fishways '95 in Gifu, 79-86pp

90) **Laine, A., R. Kamula and J. Hooli. 1993.** Fundamental concepts of Fish Passage in Scandinavian Countries. In Proceedings of a symposium on Fish Passage Policy Technology, Ken Bates (Eds).

91) **Laine, A., 1995,** Fish swimming behaviour in finnish fishways, Proceedings of the International symposium on Fishways '95 in Gifu, 323-328pp

92) **Larinier, M.,1984,** Dispositif mixte passe à poisons-glissières à canoe-kayak. Rapp. Préliminaire non publié, 19 p.

93) **Larinier, M., 1990,** Experience in fish passage in France: Fish pass design criteria and downstream migration problems, Proceedings of the International symposium on Fishways '90 in Gifu, 65-74pp

94) **Larinier, M., 1992.** Facteurs biologiques a prendre en compte dans la conception des ouvrages de franchissement, notion d'obstacle a la migration. Bull. Fr. Peche Piscic. 326-327: 20-29

95) **Larinier, M., 1998,** Upstream and downstream fish passage Experience in France, In Fish Migration and fish Bypasses,Eds : Jungwirth, M., Scmutz, S., Weiss, S.,Fishing New Books 19-32, Oxford, ISBN : 0-85-238-2537

96) **Launder, B.E., and Spalding, D.B., 1972,** Mathematics models of turbulence, Academic press london

97) **Lencastre, A., 1961,** Free overflow spillways, Engineering and design Principles, National Laboratory for civil engineering Studies, report No 174, Lisbon, Portugal, 1961

98) **Liepmann, H. W., and Laufer, J., 1947,** Investigation of free turbulent mixing, N.A.C.A. Tech. Note 1257

99) **MacLean, A., 2001,** personnal communications on the weigth of salmon parr

100) **McLeod, A.M. and P. Nemenyi. 1939-1940.** An investigation of fishways, Uni. Iowa, Stud. Eng. Bull. N 24, 63pp.

101) **Metcalfe N.B. and J.E. Thorpe, 1990,** Determinants of geographical variation in the age of seaward migrating salmon (Salmo salar), J. Anim. Ecol. 59:135-145

102) **Mills, D.H., 1991,** Ecology and management of Atlantic Salmon, London: Chapman and Hall. 351 pp

103) **Mitchell, J., McKinley, R.S., Power, G., Scruton, D.A., 1998,** Evaluation of Atlantic salmon parr responses to habitiat improvement structures in an experimental channel in Newfoundland, Canada, Regul. Rivers: res. Mgmt. 14:25-39

104) **Moller Jensen, J., 1980,** Recaptures from the international Tagging Experiments at West Greenland. Rapp. P. V. Reun. Cons. Int. Explor. Mer, 176,122-35

105) **Moore, A. and Scott, A.P., 1991,** Testosterone is a potent odorant in precocious male Atlantic salmon *(salmo salar L.)* parr. Philosophical transactions of the Royal Society of London, series B332, 241-244.

106) **Moore, A. and C.P. Waring, 1999,** Reproductive priming in mature male Atlantic salmon parr exposed to the sound of redd cutting, Journal of Fish Biology, 55, 884-887

107) **Morton, B. R., Taylor, G. I. and Turner, J. S. 1956,** Turbulent Gravitational Convection maintained and instantaneous sources, Proc. R. Soc. London, A234, pp1-23

108) **Myers, R.A., 1984,** Demographic consequences of precocious maturation of Atlantic salmon *(Salmo salar)*, Can. J. Fish. Aquat. Sci. 41:1349-1353

109) **Nakamura, S., Koizumi, N., Kasai, Y., Jikei, N., 2000,** An experimental study on a modified Larinier fishway, New Trends in Water and Environmental Engineering for Safety and Life, Maione, Majone Lehto & Monti (Eds), 2000, Balkema, Rotterdam, ISBN: 90 5809 138 4

110) **Northcote, T.G., 1998** Migratory Behaviour of fish and its significance to movement through riverine Fish Passage Facilities, In "Fish Migration and Bypasses", Eds: Mathias Jungwirth, Stefan Schmutz, and Steven Weiss. Fishing News Books.

111) **Pani, B.S., 1972.** Three dimensional turbulent wall jets. Thesis, Uni. of Alberta, Edmonton

112) **Parrish, D.L., R.J. Behke, S.R. Gephard, S.C. McCormick and G.H. Reeves, 1998,** Why aren't there more Atlantic salmon *(Salmo Salar L.)*? Can J. Fish Aqua. Sci. (Suppl.: 281-287)

113) **Pasche, E., Dauwe L, Blank M., 1995,** New design principles of Fishways, Proceedings of the international symposium on fishways'95 in Gifu, Japan, October 24-26

114) **Payne; P. L., 1988,** The Hydro: A study of the development of the major hydroelectric schemes undertaken by the North of Scotland Hydro-Electric Board, Aberdeen University Press. 354 p

115) **Powers, P. and Orsborn, J., 1985;** Analysis of Barriers to upstream fish migration, An investigation into the physical and biological conditions affecting fish passages success at culverts and waterfalls, US department of energy, Bonneville power administration, Division of fish & wildlife.

116) **Powers, P. and Orsborn, J., Bumstead, T., Klinger-Kingsley S., Mih, W., 1985;** Fishways – An assessment of their development and design, US department of energy, Bonneville power administration, Division of fish & wildlife.

117) **Pyefinch, K. A., 1955.** A review of the literature on the biology of the Atlantic salmon (Salmo Salar L.). Freshwater Salm. Fish. Res. 9:1-24

118) **Rainey, W.S., 1991,** Recent Adult Fish Passage Projects on Tributary of the Colombia River, Proceedings of the American Fisheries Society Symposium10: 278-288pp

119) **Rajaratnam, N. and Subramanya, K., 1967,** Plane turbulent free jet and wall jet. Journal of the royal Aeronautical Society, London, England, pp585-587

120) **Rajaratnam, N., Pani, B.S., 1974,** Three-dimensional turbulent wall jets. IAHR Journal of Hydraulic research, Vol 11, No 1, pp 69-83

121) **Rajaratnam, N., 1976,** Turbulent jets, Ed Elsevier, ISBN: 0-444-41372-3

122) **Rajaratnam, N., Van der Vinne, G., Katopodis, C., 1886,** Hydraulics of vertical slot fishways, Journal of Hydraulic Engineering, Vol 112, N 10,

123) **Rajaratnam, N., Katopodis, C., Flint-Petersen, L., 1987,**Hydraulics of two-level Denil fishway, Journal of Hydraulic Engineering, Vol 113, No. 5, May 1987

124) **Rajaratnam, N., Katopodis, C., Mainali, A., 1988,** Plunging and streaming flows in pool and weir fishways, Journal of Hydraulic Engineering, Vol 114, No. 8, August 1988.

125) **Rajaratnam, N., Katopodis, C., Mainali, A., 1989,** Pool-orifice and poll-orifice-weir fishways, Canadian Journal of Civil Engineering, Vol 16, No. 5, pp: 774-777.

126) **Rajaratnam, N. and Katopodis, C., 1991,** Hydraulics of steeppass fishways, Canadian Journal of Civ. Eng. Vol 18:1024-1032

127) **Rajaratnam, N., Katopodis, C., Solanski, S., 1992,** New designs for vertical slot fishways, Canadian journal of civil Engineering, Vol 19, N 3, pp: 402-414

128) **Rajaratnam, N., 1995,** Almanac of energy dissipation mechanisms, in Energy Dissipators, Eds: Vischer and Hager

129) **Rajaratnam, N., Katopodis, C., Wu, S., Sabur, M.A., 1997,** Hydraulics of resting pools for Denil fishway, Journal of Hydraulic Engineering, Vol 123, No. 7, July 1997

130) **Reichardt, H., 1942,** Gesetzmassigkeiten der freien Turbulenz ,**VD1-Forschungsheft, 414**

131) **Reynolds, O., 1894,** On the dynamical Theory of Incompressible fluids and the determination of the Criterion. Philosophical Transactions of the Royal Society, Vol 186

132) **Rivinoja, P., McKinnell, S., Lundqvist, H., 2001,** Hindrances to upstream migration of Atlantic salmon (Salmo salar) in a northern Swedish river caused by a Hydroelectric power-station, Regul. Rivers: Res. Mgmt. 17:101-115

133) **Rosen, M. W., 1959,** Waterflow about a swimming fish, U.S. Naval Ordnance Test Station, TP 2298, China Lake, California, 96 pp

134) **Rouger, Y. and Liley, N.R., 1983,** Effect of social environment on plasma hormones and availability of smilt in spawning male rainbow trout. Canadian Journal of Zoology 71, 280-285

135) **Rouse, H., 1938,** Fluid mechanics for hydraulic engineers, engineering societies monograms, 1st ed. McGraw-Hill Bool Co., New York, NY, 415pp

136) **Saunders, R.L. and J.H. Gee, 1964,** Movements of young atlantic salmon in a small stream, J.Fish. Res. Board can. 21:27-36

137) **Scimeni Ettore, 1930,** Sulla forma delle vene tracimanti, L'Energia Elettrica, Aprile

138) **Schlichting, H., 1968,** Boundary layer theory, Pub: McGraw-Hill, New York, 6th edition

139) **Shearer, W.M., 1992,** The Atlantic Salmon: Natural history, exploitation and future management, fishing News books, ISBN: 0-85238-188-3

140) **Smith, G. W., I. P. Smith, S. M. Armstrong, 1994.** The relationship between river flow and the entry to the Aberdeenshire Dee by returning adult salmon. J. Fish Biol. 45:958-960

141) **Smith, G.W., A.D.F. Johnstone, W.M. Shearer, T.J. Carter, 1997,** " The behaviour of adult Atlantic salmon (Salmo salar L.) in a Borland lift pass as determined by underwater television observations" Fisheries Research Services Report N0 10/97

142) **Smith I.R., 1975,** Turbulence in lakes and rivers, Freshwat. Biol. Ass. Sci. Publ. Anbleside, UK, FBA 79pp

143) **Stradmayer L. and J.E. Thorpe, 1987,** The response of hatchery-reared Atlantic salmon, salmo salar L., parr for pelleted and wild prey; Aquaculture Fish. Management; 18:51-61

144) **Struthers, G., 1993.,**Facilities and Requirements for The Migration of salmonids in Scottish Waters Harnessed for Hydro-Electric Generation, Proceedings of a symposium on fish Passage and Technology, 75-80pp

145) **Struthers, G., 1996.** Hydroelectric development in Scotland and its effects on fish.

146) **Stuart, I.G. and M. Mallen-Cooper, 1999.** An assessment of the effectiveness of a vertical slot fishway for non-salmonid fish at a tidal barrier on a large tropical/subtropical river, Regul. Rivers: Res. Mgmt. 15: 575-590

147) **Stuart, T.A., 1957.** The migration and homing behaviour of brown trout (Salmo trutta L.). Freshwater Salm. Fish. Res. 18:1-27.

148) **Stuart, T.A., 1962,** The Leaping Behaviour of Salmon and Trout at Falls and Obstructions DAFS Freshwater Fisheries and Salmon Fisheries Research, N 28, 46pp.

149) **Takeuchi, H., Takei, K., Satou, M., Matsushima, T., Olumoto, N. & Ueda, K., 1987,** Visual cues as key stimuli for courtship behaviour in the male hime salmon. Animal behaviour 35, 936-939.

150) **Thompson, C. S., 1970;** Effect of flow on performance and behaviour of Chinook salmon in fishways, USFWS bur. Comm., Fish. Spec. Sci. Rpt. Fisheries No 601, 1970

151) **Thompson, C. S., Davis, W. S., Slatick, E., 1967;** Response of migrating adult salmonids to vertical and horizontal rectangular Orifices at two depth; USFWS bur. Comm., Fish. Spec. Sci. Rpt. Fisheries No 547, 1967

152) **Tollmien, W., 1926,** Berechnung Turbulenter ausbreitungsvorgange, ZAMM, 6, pp468-478, (English translation, NACA TM-1085, 1945)

153) **Travade, F. and M. Larinier, 1992,** Ecluses et ascenseurs a poissons, Bull. Fr. Peche Piscic. 326-327:95-110

154) **Travade, F., Larinier, M., Boyer-Bernard, S., Dartiguelongue, J., 1998.** Performance of four fish pass installations recently built on two rivers in South West France. In Fish Migration and fish Bypasses;Eds : Jungwirth, M., Scmutz, S., Weiss, S.,Fishing New Books 19-32, Oxford, ISBN : 0-85-238-2537

155) **Trentacoste, N., and Sfortza, P.M., 1966.** An experimental investigation of three-dimensional free mixing in incompressible turbulent free jets. Rep. 81, Department of Aerospace Engineering, polytechnic Institute of Brooklyn, New York.

156) **Trentacoste, N., and Sfortza, P.M., 1967.** Further experimental results for three-dimensional free jets. J.A.I.A.A., 5:885-891.

157) **Tsujimoto T., T. Kitamura, S. Murakami, 1995,** Numerical calculation of flow in vertical slot and its application, Proceedings of The International Symposium on Fishways'95 in Gifu, 57-63pp

158) **Uedda, M., 1990,** Proposal of Optimum fishway system Based on field Investigations, Proceedings of The International Symposium on Fishways'90 in Gifu, 313-319pp

159) **Videler, J.J., 1993,** Fish swimming, Eds: Chapman and Hall, fish and Fisheries series 10, ISBN: 0 412 40860 0

160) **Vischer, D.L. and W. H. Hager, 1995,** Energy Dissipators, Ed A.A. Balkema, ISBN: 90 5410 198 9

161) **Wardle, C. S., 1978.** Non-release of lactic acid from anaerobic swimming muscle of plaice *pleuronectes platessa*: a stress reaction. Journal of biology, 77: 141-155

162) **Wardle, C.S., 1975.** Limit of fish swimming speed. Nature, London.255: 725-727

163) **Webb, J., 1989,** The movements of adult Atlantic salmon in the river Tay, Scottish fisheries Research Report, 44, 32pp

164) **Webb, J., 1990.** The behaviour of adult Atlantic Salmon ascending the rivers Tay and Tummel to Pitlochry dam. Scottish fisheries Research report N 48, 27pp

165) **Webb, J. and H.M. Mclay, 1996,** Variation in the timing of spawning of Atlantic Salmon (Salmo salar) and its relation to temperature in the Aberdeenshire Dee Scotland. Can J. Fish Aquat. Sci. 53:2739-2744.

166) **Webb, P. W. 1975.** Hydrodynamics and energetics of fish propulsion. Bull Fish Res. BD., 190, 158pp

167) **Webb, P.W. and D. Weihs, 1983,** Fish biomechanics, Eds: Praeger, ISBN: 0030594618

168) **Weihs, D., 1973,** Optimal fish cruising speed. Nature 245:48-50

169) **Weihs, D. 1974,** Energetic advantage of burst swimming of fish; J. Theor. Biol. 48: 215-229

170) **Weihs, D., 1977;** Effects of size on sustained swimming speeds of aquatic organisms in scale effects in animal locomotion, edited by Pedley, 333-338. New York: Academic press

171) **Winstone, A. J., A.S. Gee and P.V. Varallo, 1985,** The assessment of flow characteristics at certain weirs in relation to the upstream movement of migratory salmonids, J. Fish Biol., 27:75-83

172) **Wu, S. and Rajaratnam, N, 1996,** Submerged flow regimes of rectangular sharp-crested weirs, Journal of Hydraulic Engineering, Vol 122, No 7, July, 1996, pp 412-413.

173) **Wu, S., Rajaratnam, N. and Katopodis, C., 1999,** Structure of flow in vertical slot fishways, Journal of Hydraulic Engineering, Vol 125, No 4, April, 1999, pp 351-360

174) **Xu Duo-Ming and Yu Chang-Zhao, 1983,** Pingmian shuisheliu dui caodide changji yaquiang ji qi maidong texing. Shuili xuebao, Beijing, (5), 1983, pp52-58

175) **Yates, G.T., 1983,** Hydrodynamics of body and caudal fin propulsion, chapter 6 in "Fish Biomechanics", Eds: P.W. Webb and D. Weihs, Praeger, London

176) **Yevdjevitch, V.M., 1966.** Diffusion of slot jets with finite orifice length-width ratios. Hydraul. Pap., 2, Colorado State University, Fort Collins.

177) **Youngson, A. and Hay, D., 1996,** The live of salmon: an illustrated account of life history of Atlantic salmon, Swan Hill Press, England

178) **Zhou, Y., 1982,** The swimming behaviour of fish in towed gears; a re-examination of the principles. Scott. Fish. Work. Paper. Dept. Agric. Fish. Scotl, (4), 1-55

179) **Ziemer, G.L., 1961.** Fish transport in waterways, Alaska dept. of fish and Game, 10p.

180) **Ziemer, G.L., and Behlke, C.E., 1966,** Analysis of salmon in steep fish ladders, Proceedings of the 2nd Annual American Water Resources Conference, pp328-339

181) **Zijnen, B.G. and Van der Hegge, 1958.** Measurements of the velocity distribution in a plane turbulent air jet. Appl.Sci.Res. Sect. A, 7:256-276

HYDRAULIC AND BIOLOGICAL ASPECTS OF FISH PASSES FOR DAMS

VOLUME II OF II (FIGURES)

Eliane M. Guiny
(Eng. ESTP Paris, M.Sc.)

Thesis submitted for the degree of
Doctor of Philosophy
In the Department of Civil Engineering,
The University of Glasgow

Department of Civil Engineering
University of Glasgow
Rankine building
Oakfield Avenue
Glasgow G12 8LT

September 2001

CHAPTER 2:

LITERATURE REVIEW OF FISH PASS DESIGN

CHAPTER 3

BIOLOGY OF ATLANTIC SALMON (*SALMO SALAR L.*)

CHAPTER 4:

EXPERIMENTAL FACILITIES

CHAPTER 5:

EXPERIEMENTAL RESULTS OF THE BEHAVIOUR OF PARR AT WEIR/ORIFICE/SLOT DEVICES

As Numbered in

ORIGONAL

No

Vi

CHAPTER 6:

HYDRAULIC MEASUREMENTS AT GLASGOW FLUME

As Numbered in

ORIGONAL

No

XI

CHAPTER 7:

INTEGRATION OF FISH BEHAVIOUR DATA AND HYDRAULIC MEASUREMENTS

CHAPTER 8:

BEHAVIOUR OF FISH UNDERGOING SPAWNING MIGRATION: A COMPARISON OF PASSAGE THROUGH WEIRS AND ORIFICES

Table of figures:

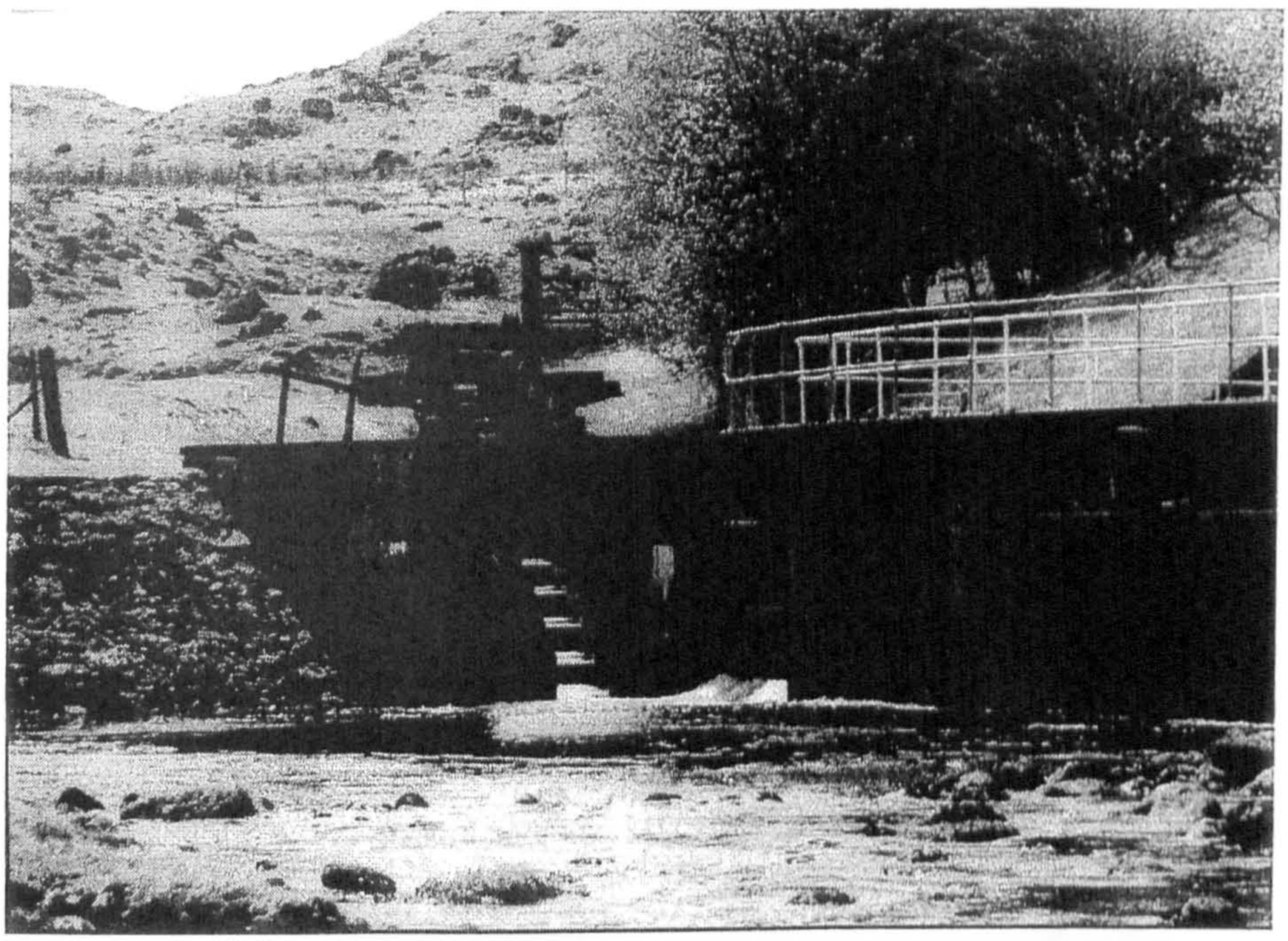

Figure 2-1: Fishpass at dam in Scotland

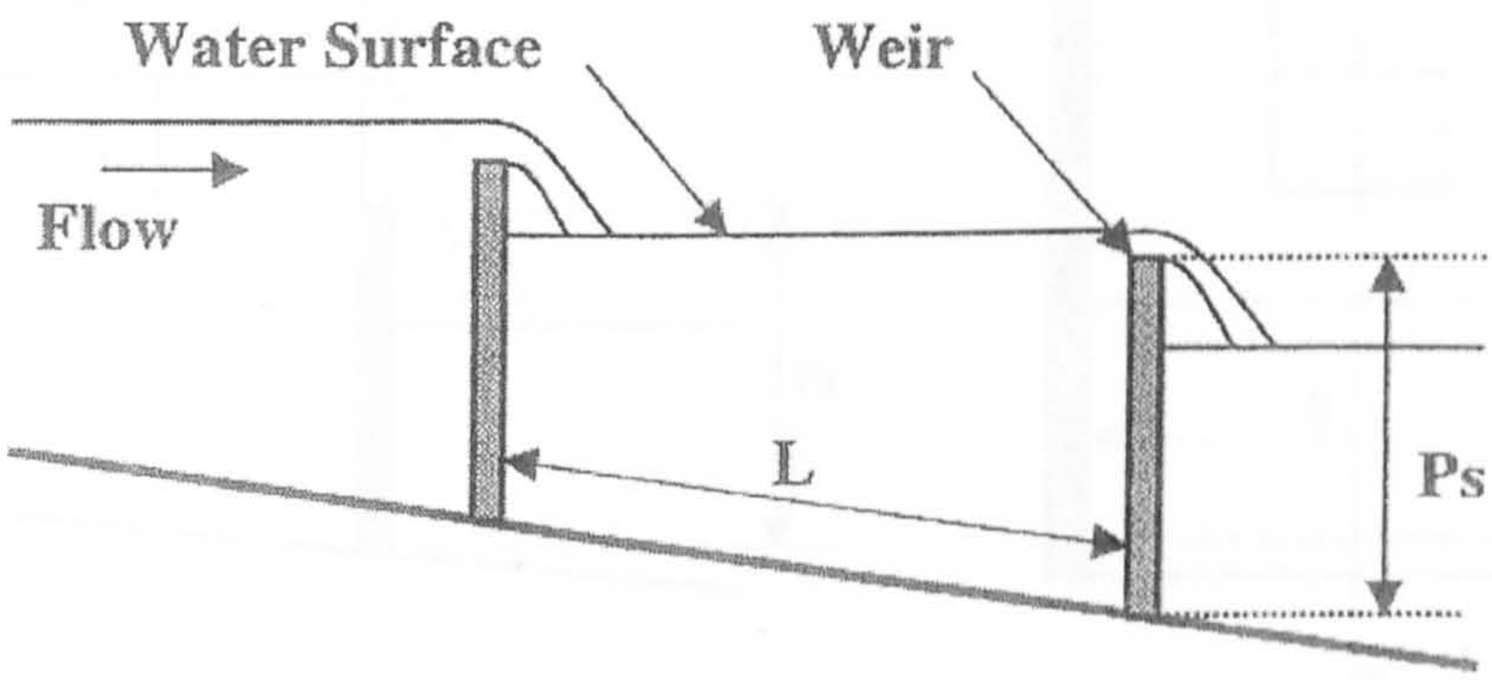

Figure 2-2: Schematic of a weir and pool pass

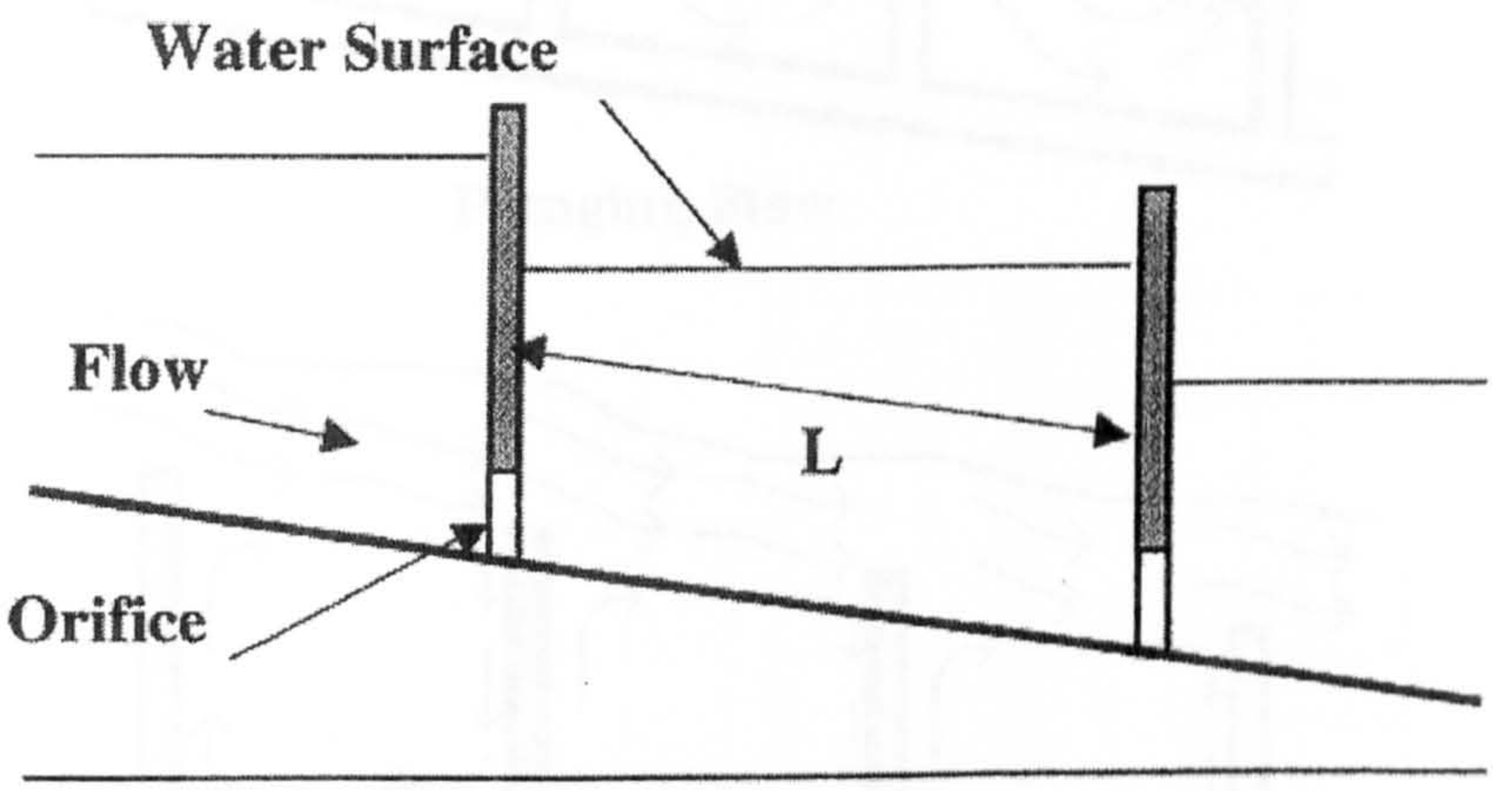

Figure 2-3: Schematic of an orifice of pool pass

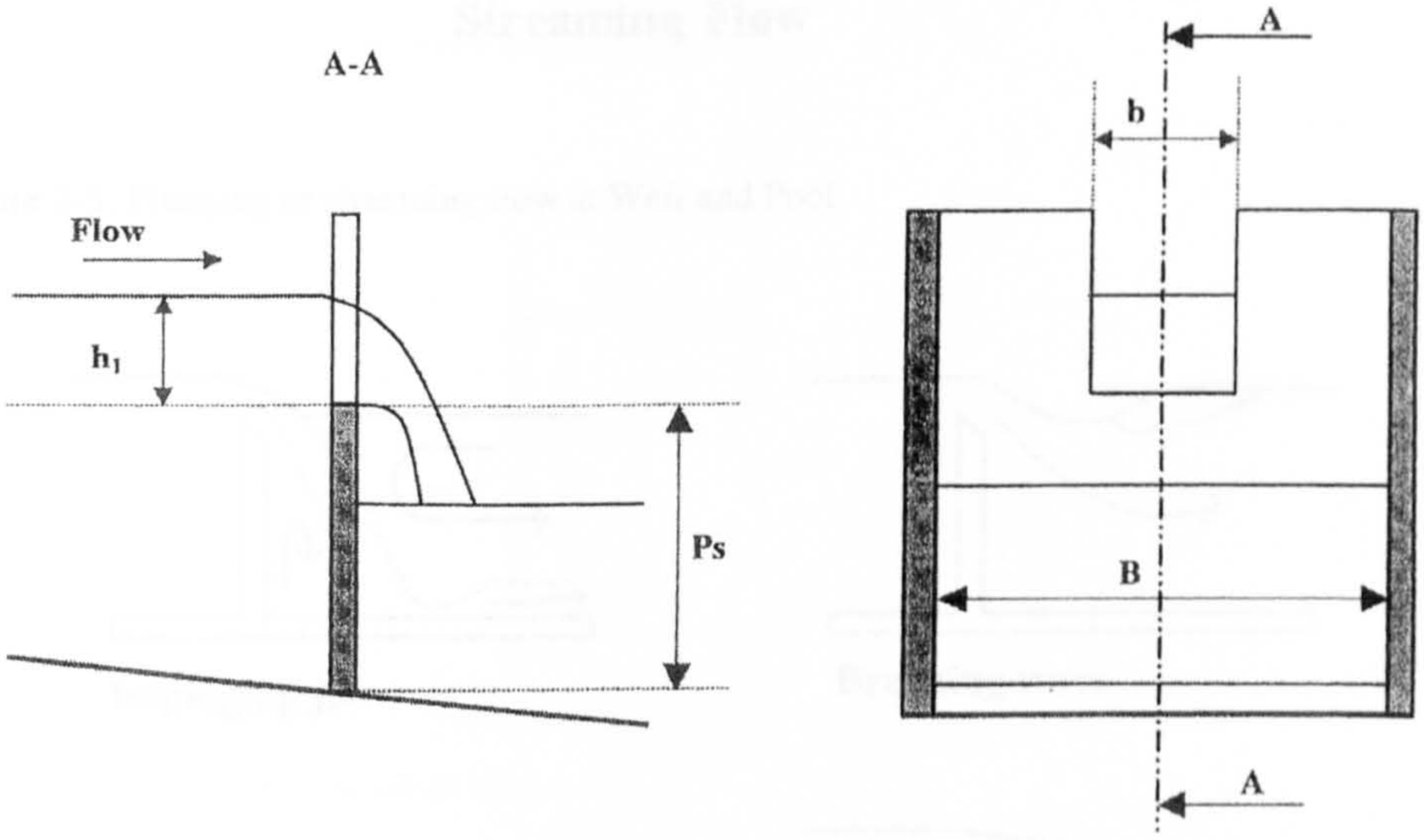

Figure 2-4: Schematic of a weir and pool pass

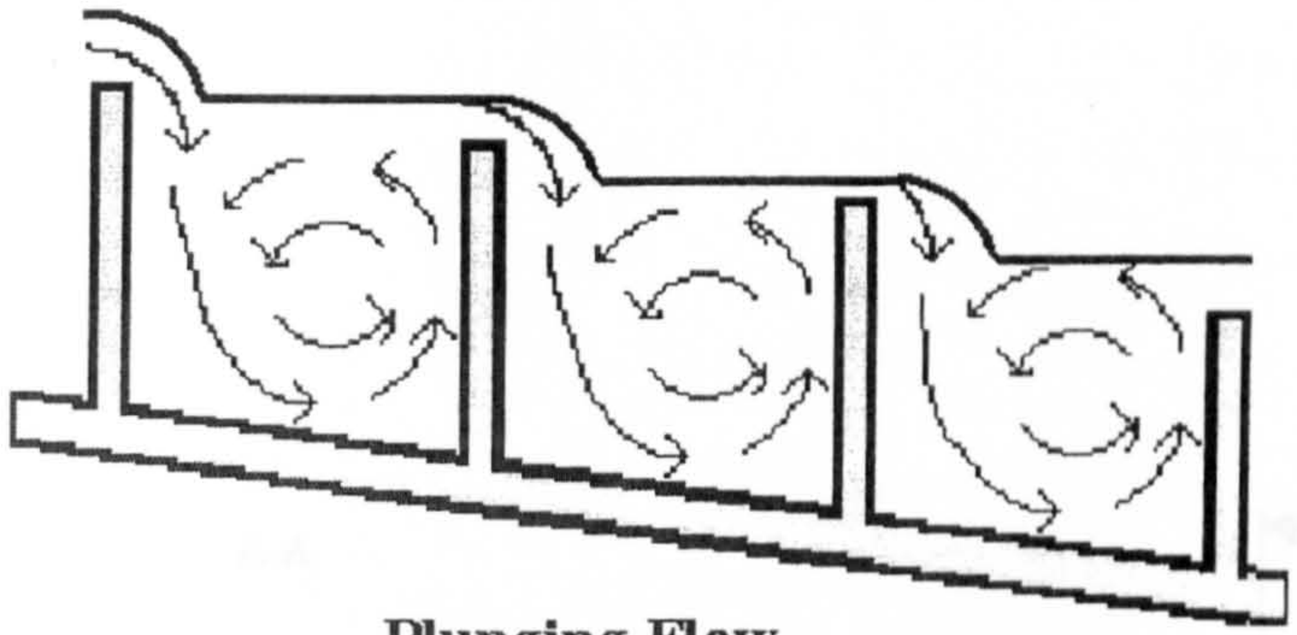

Plunging Flow

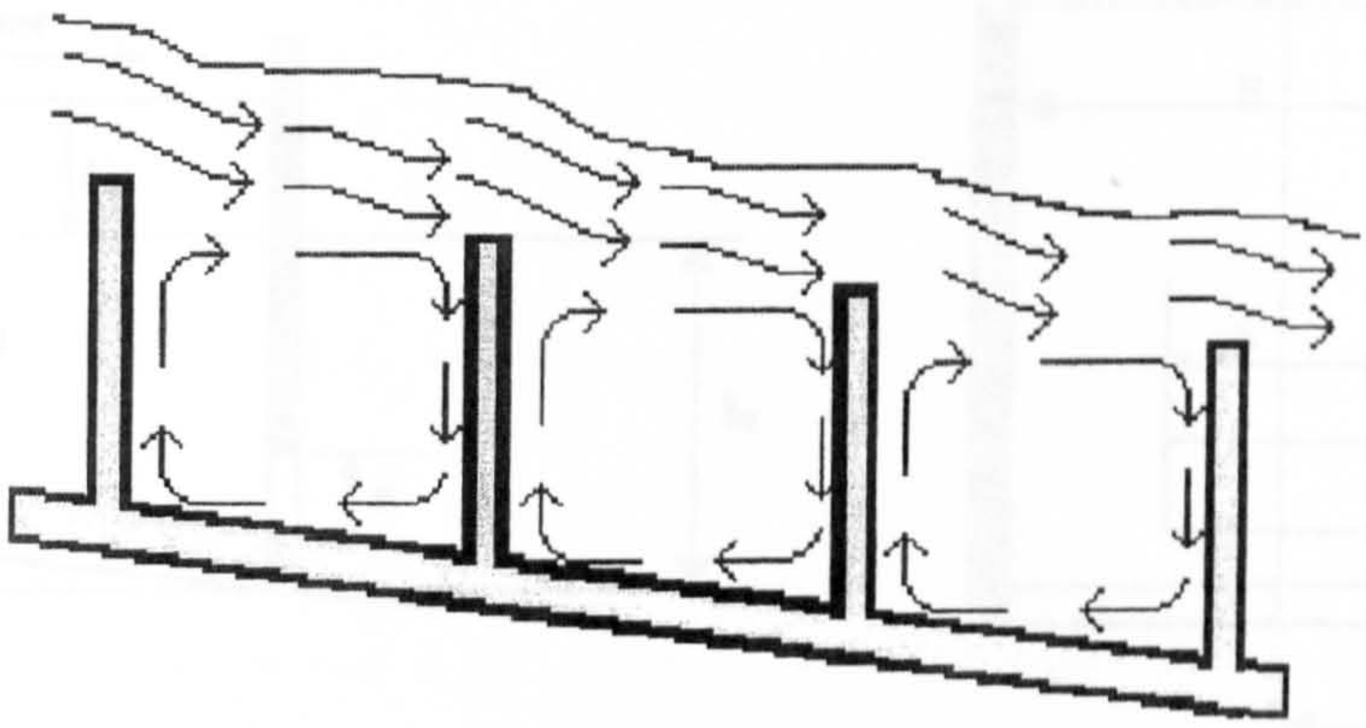

Streaming Flow

Figure 2-5: Plunging or streaming flow at Weir and Pool

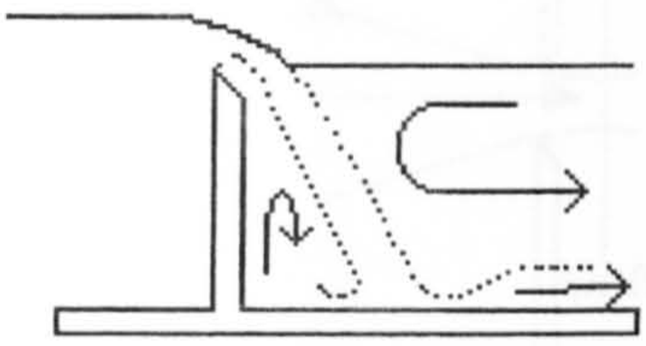

Impinging jet

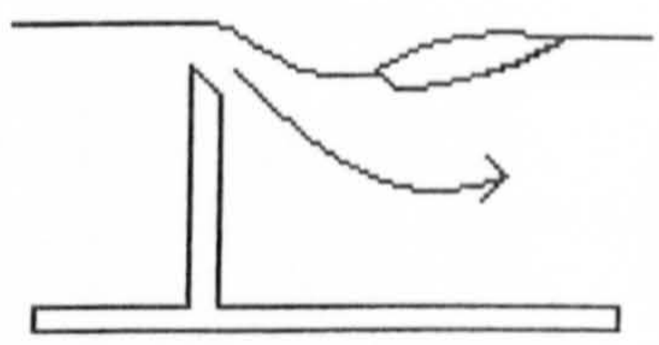

Breaking wave

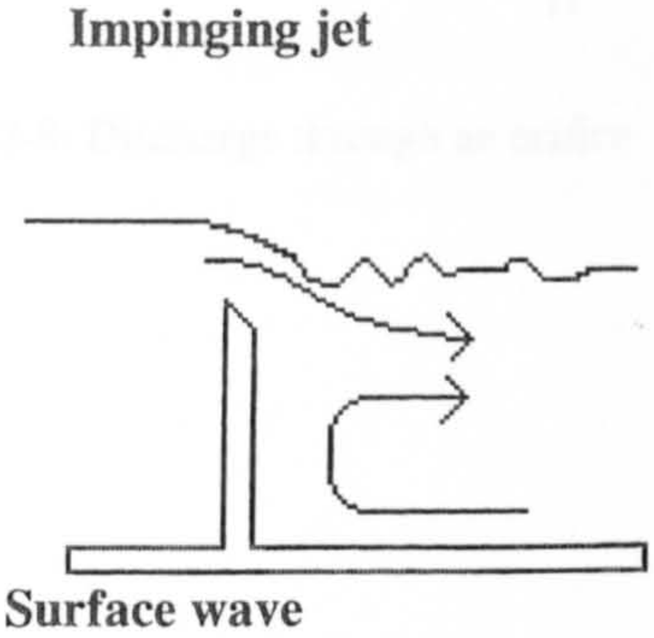

Surface wave

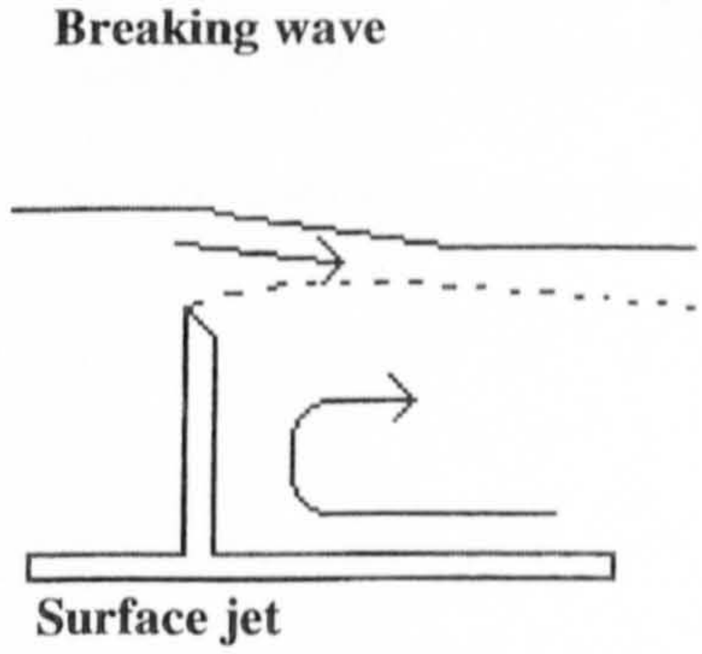

Surface jet

Figure 2-6: The four different regimes for sharp crest weirs (From Wu & al, 1996)

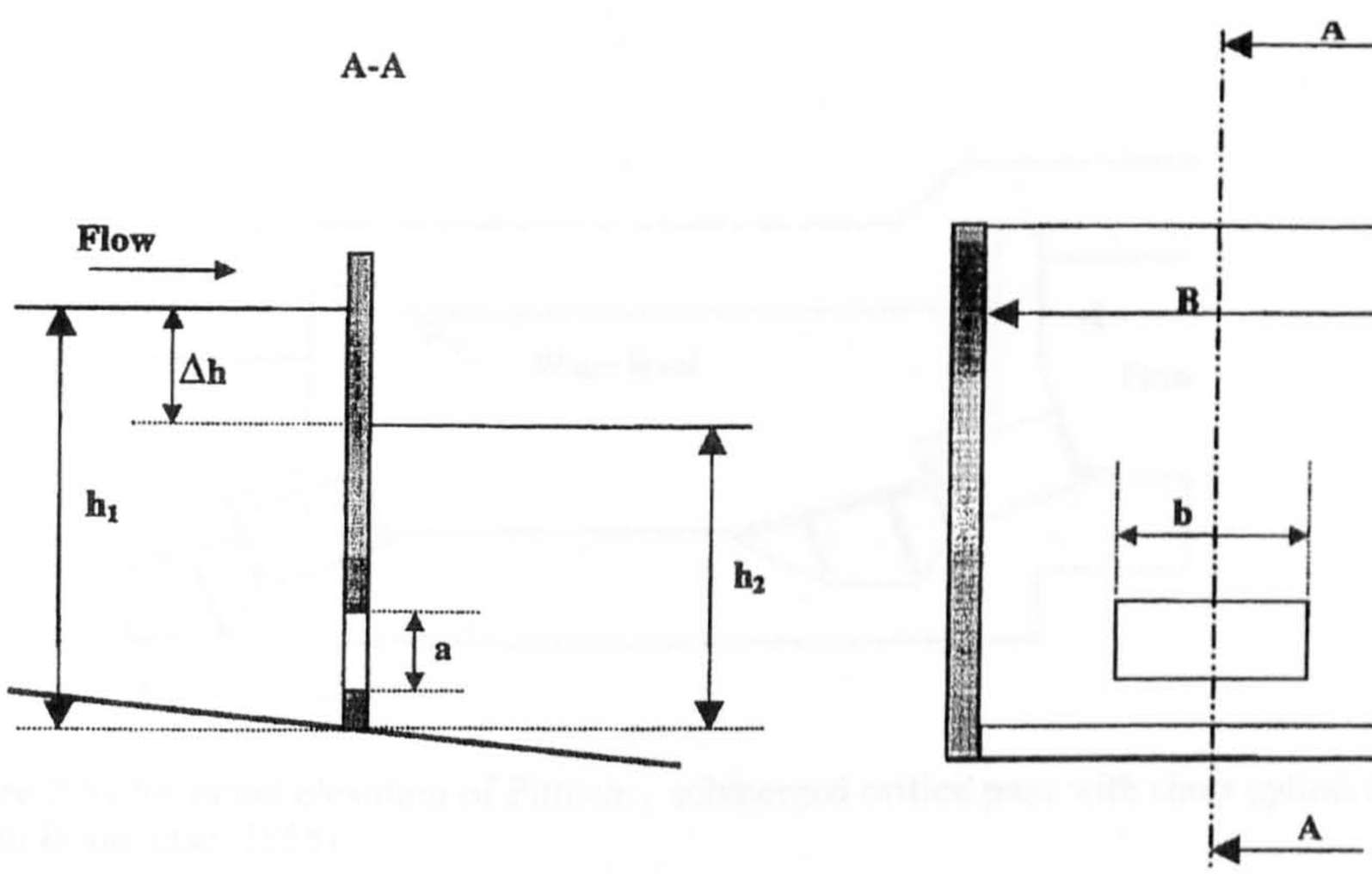

Figure 2-7: Schematic of an orifice and pool pass

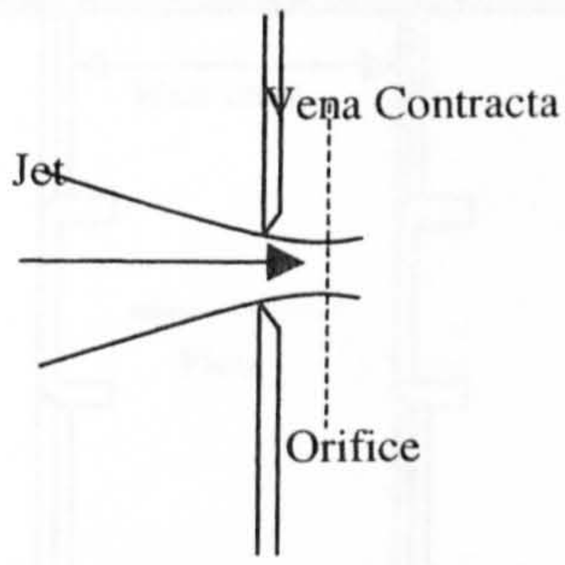

Figure 2-8: Discharge through an orifice

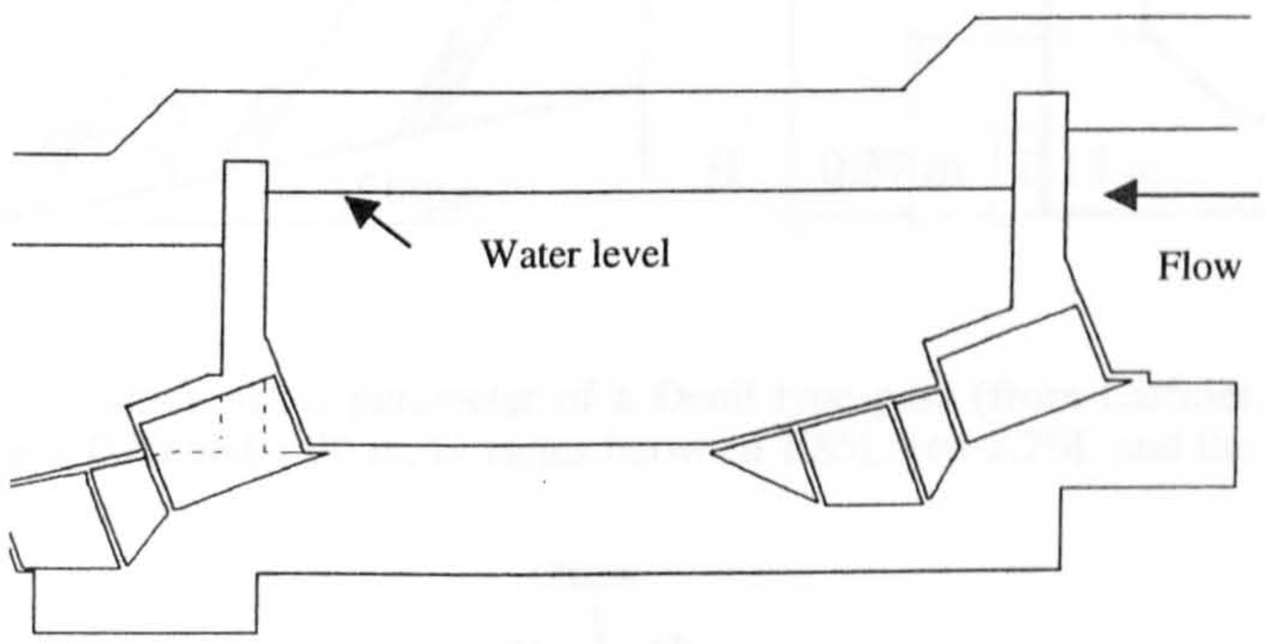

Figure 2-9: Sectional elevation of Pitlochry submerged orifice pass with short cylindrical orifices (From Bonnyman, 1958)

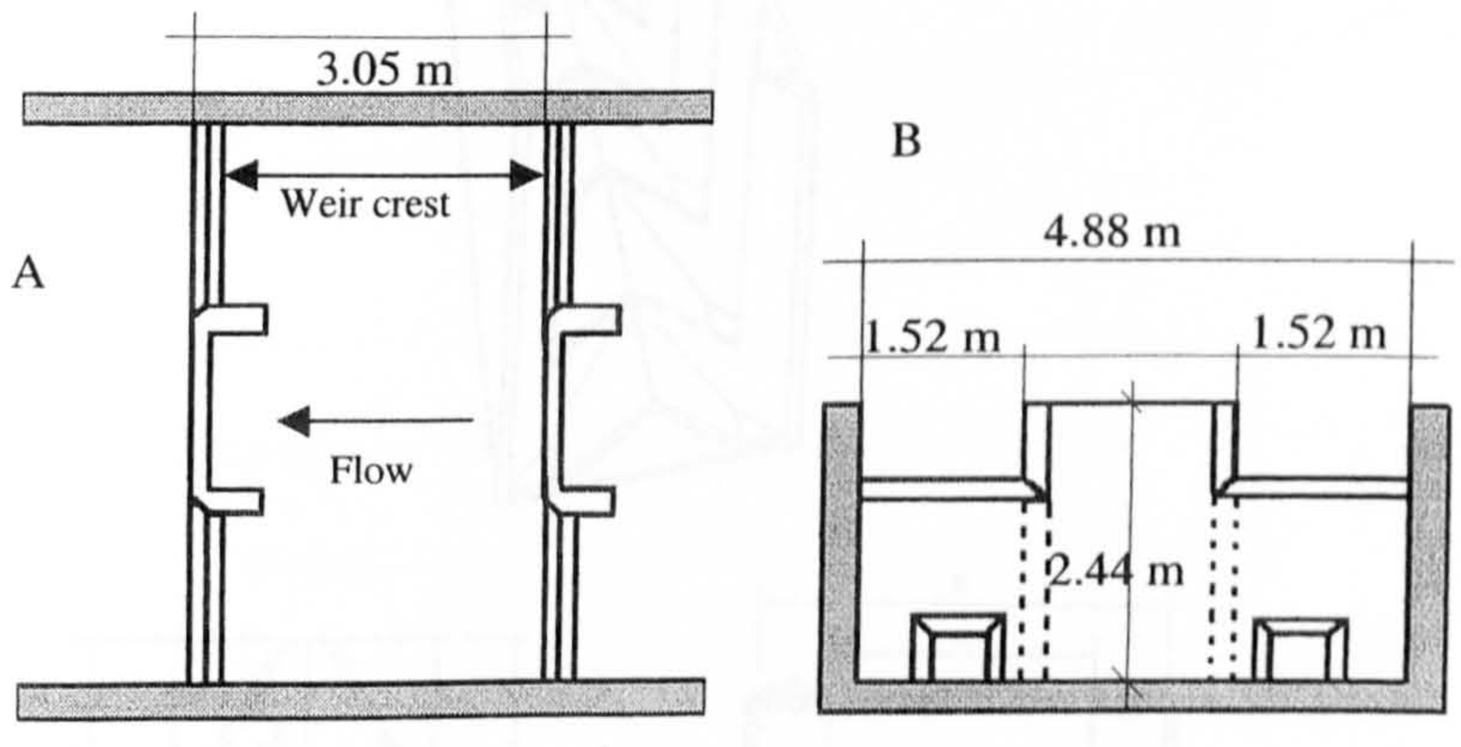

Figure 2-10: Characteristics of the Ice Harbor type: (A) Plan view and (B) Elevation (From Clay, 1995)

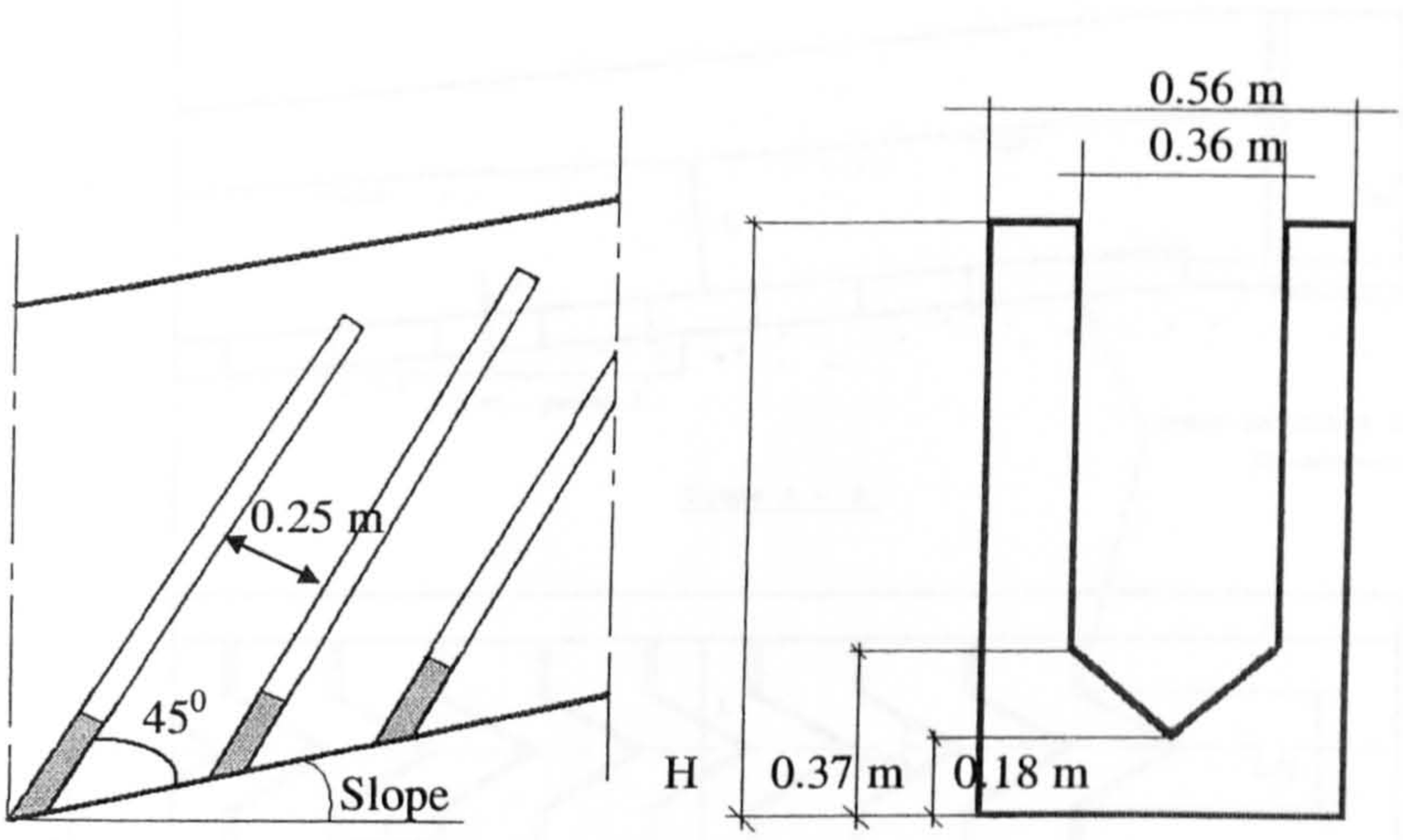

Figure 2-11: Characteristics parameter of a Denil type pass (from Larinier, 1992). The width L varies between 0.60 and 1.00 m, H varies between 1.85L and 2.20L and the slope varies between 12 and 20 %

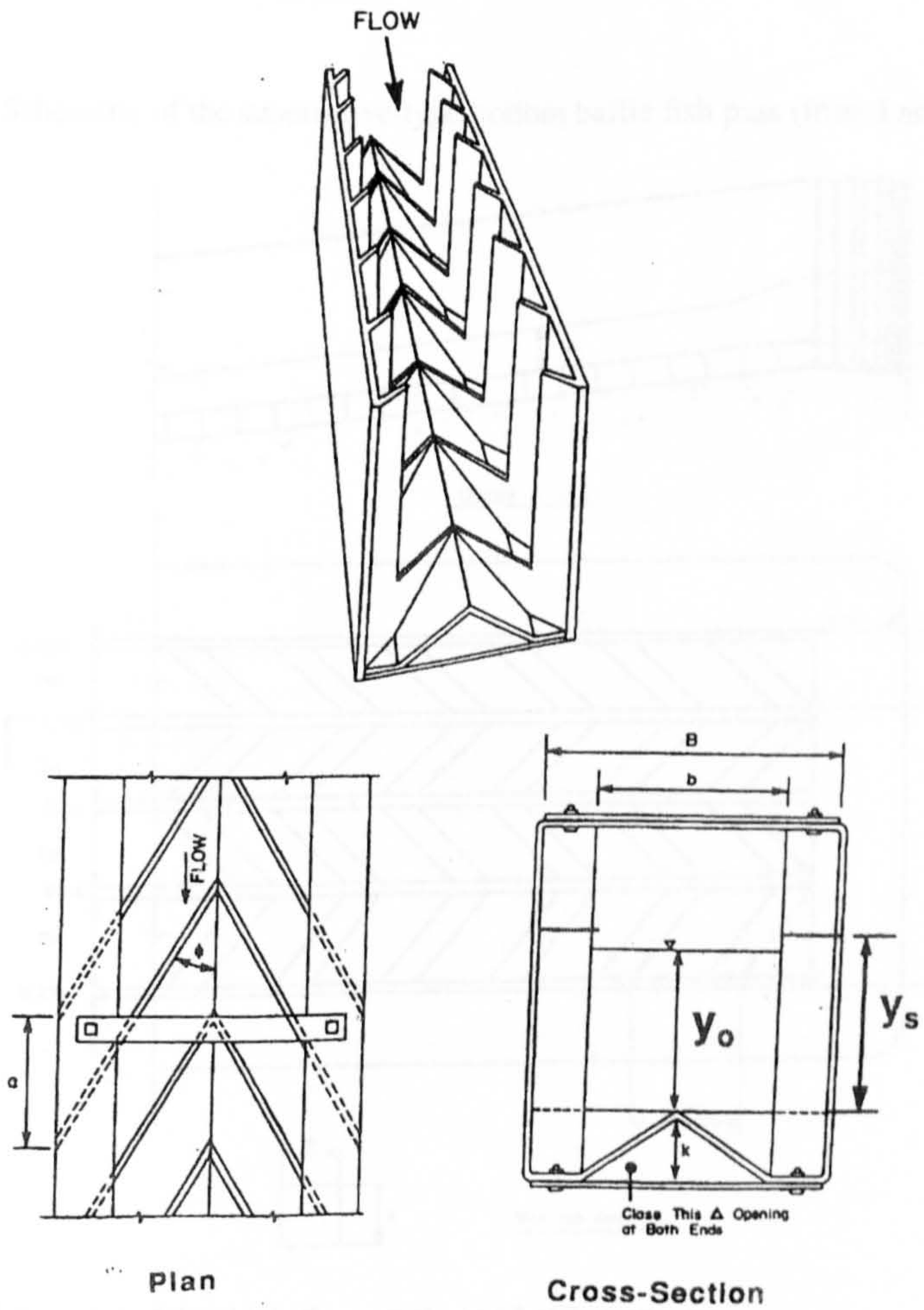

Figure 2-12: Characteristic parameter of the Steep pass (from Rajaratnam & Katopodis, 1991)

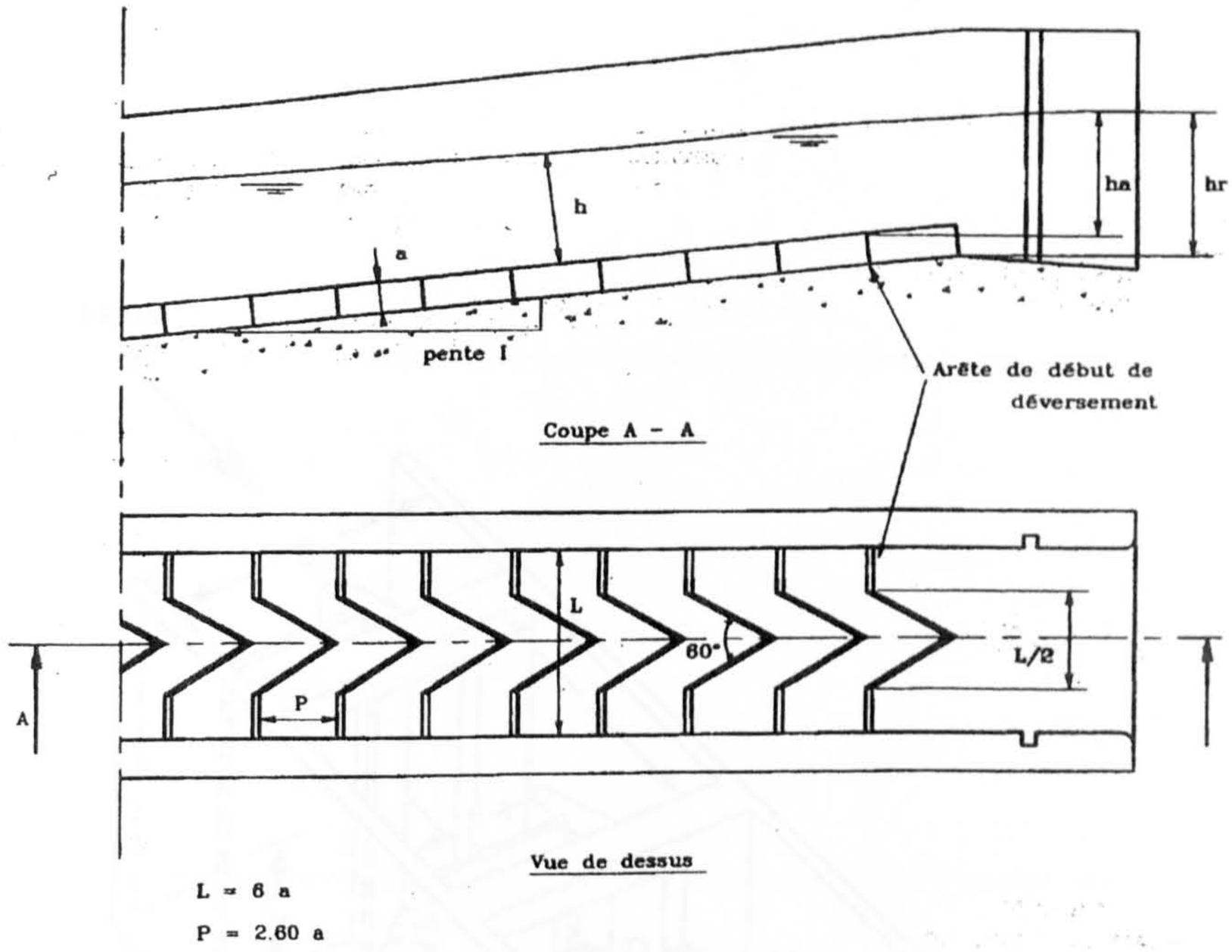

Figure 2-13: Schematic of the superactive-type bottom baffle fish pass (from Larinier, 1992)

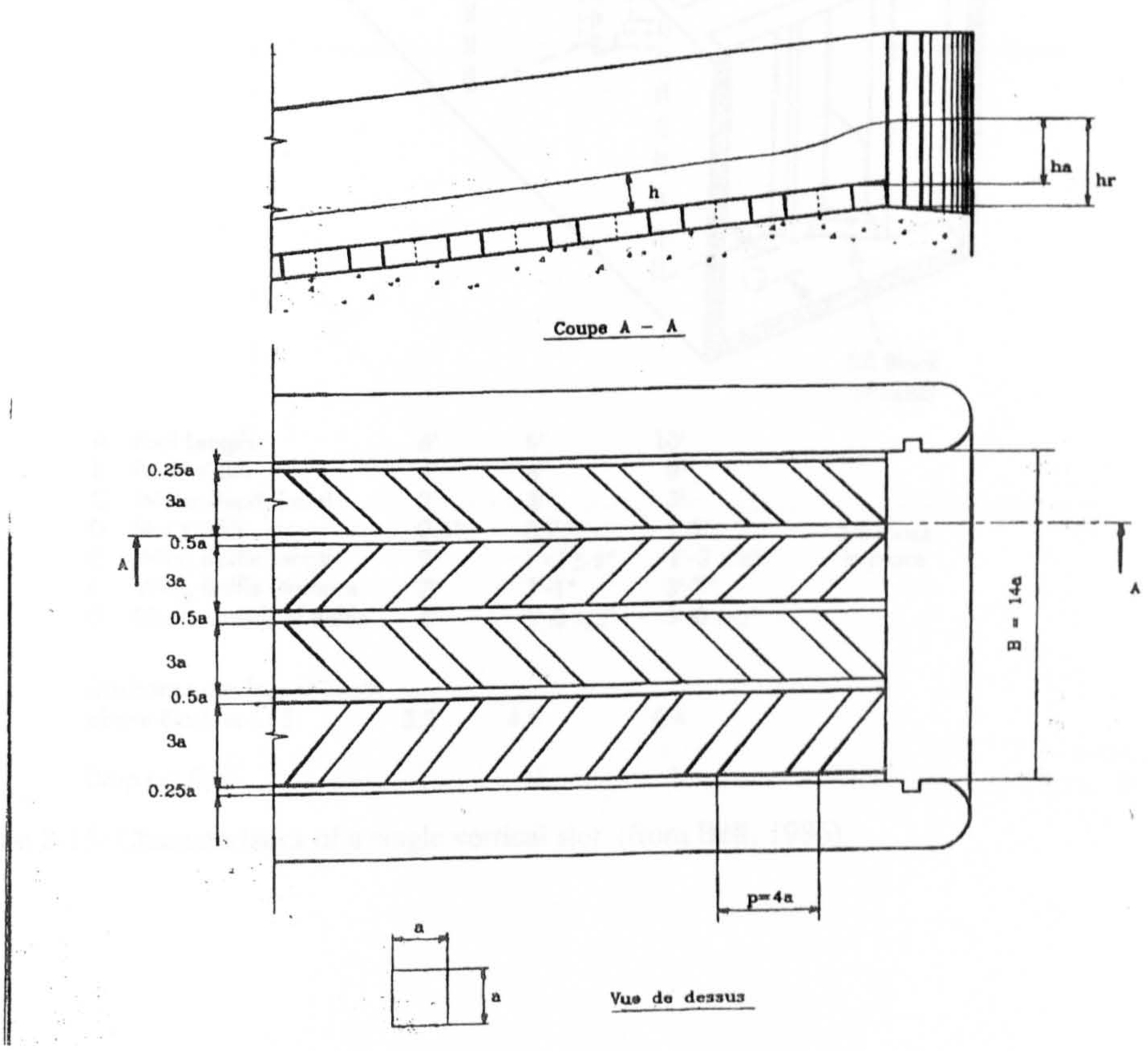

Figure 2-14: Schematic of the thick chevron shaped baffle fish pass

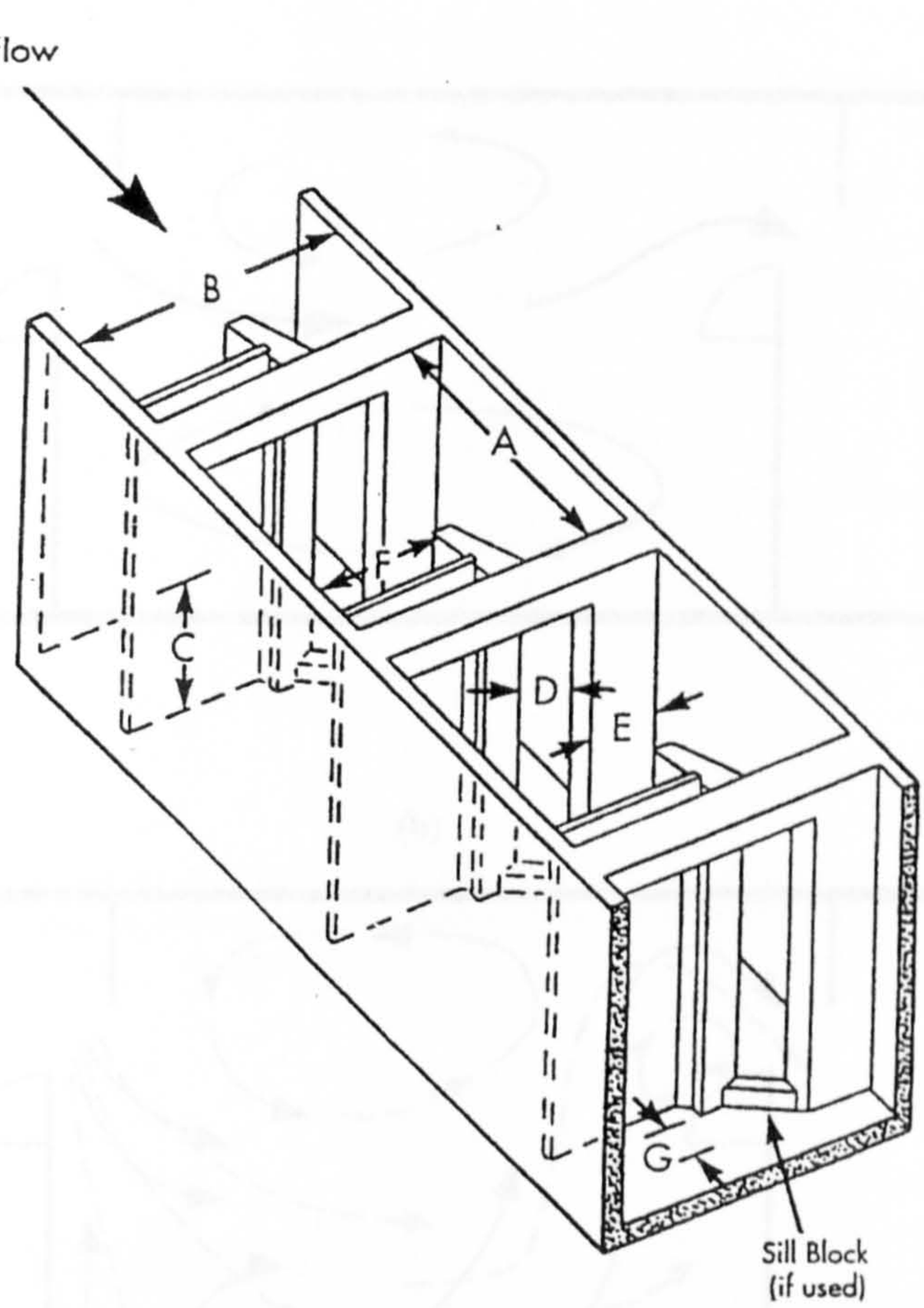

A	Pool Length	6'	8'	10'	
B	Pool Width	4'	6'	8'	
C	Water Depth (min)	2'	3'	3'	
D	Slot Width	0.5"	0.75"	1.0"	* Sill Block in place
E	Wing Baffle Length	9"	1'-3 5/8"	1'-3 5/8"	
F	Wing Baffle Distance	2'	3'-1"	3'-7"	
G	Displacement of Baffle	4'	5'-0 1/2"	5'-0 1/2"	
	Discharge per foot of Depth above Block in CFS	3.2	4.8	6.4	
	Drop per Pool	1'	1'	1'	

Figure 2-15: Characteristics of a single vertical slot (from Bell, 1986)

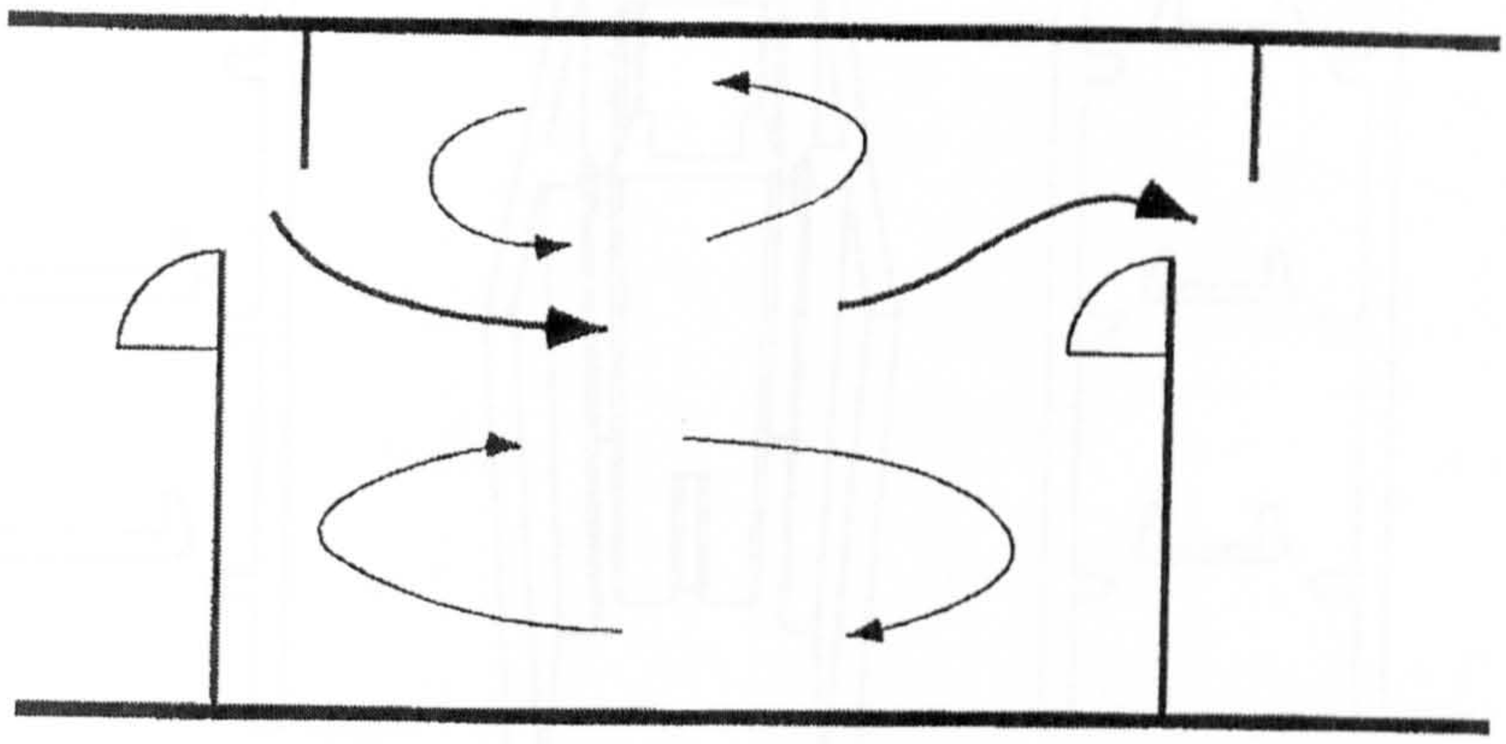

(b)

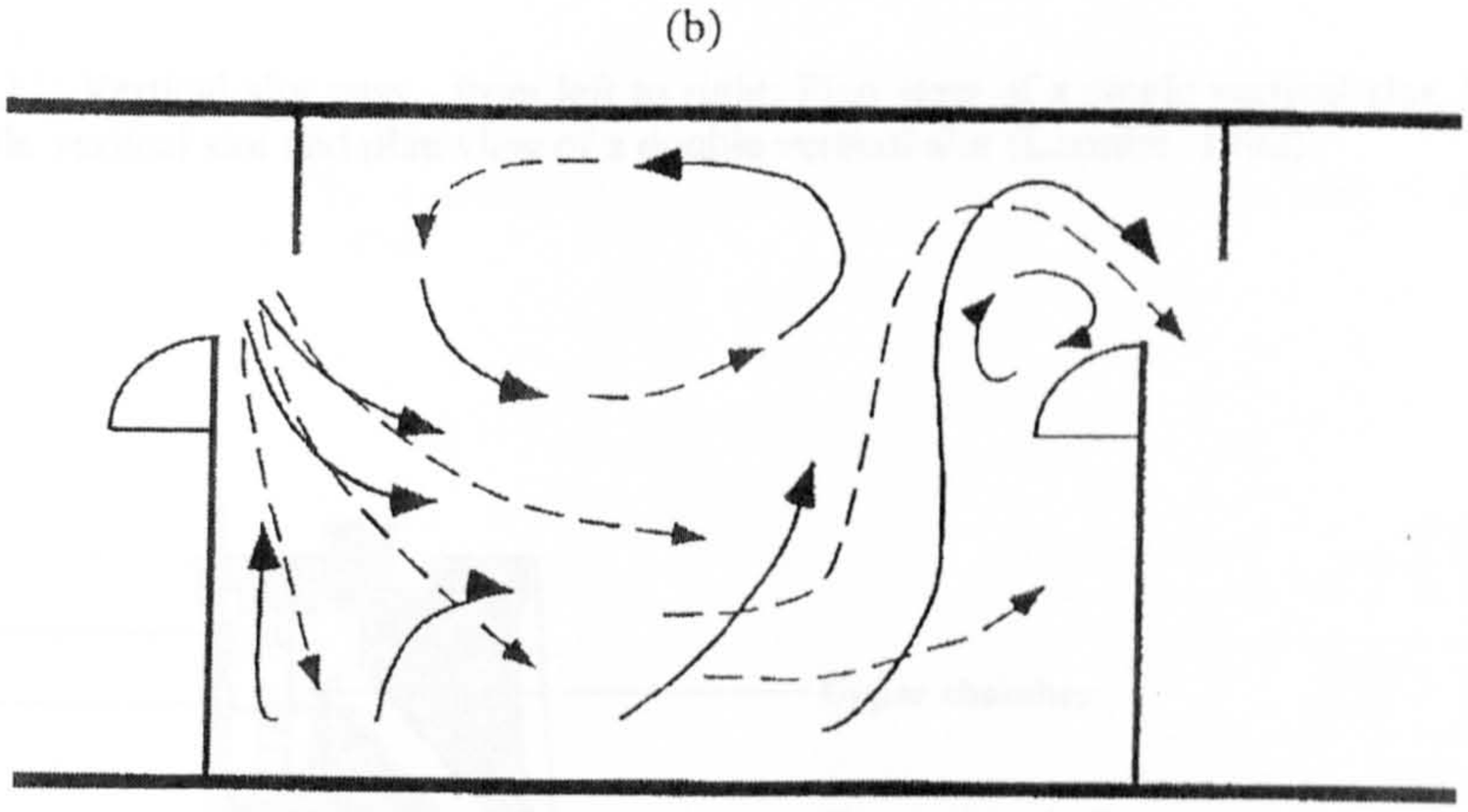

Figure 2-16: Two typical flow patterns in the pools for Vertical Slot fish pass. Flow pattern (a) occurs for slopes of 5%, while flow pattern (b) occurs for slope of 10-20% (from Wu et al, 1999).

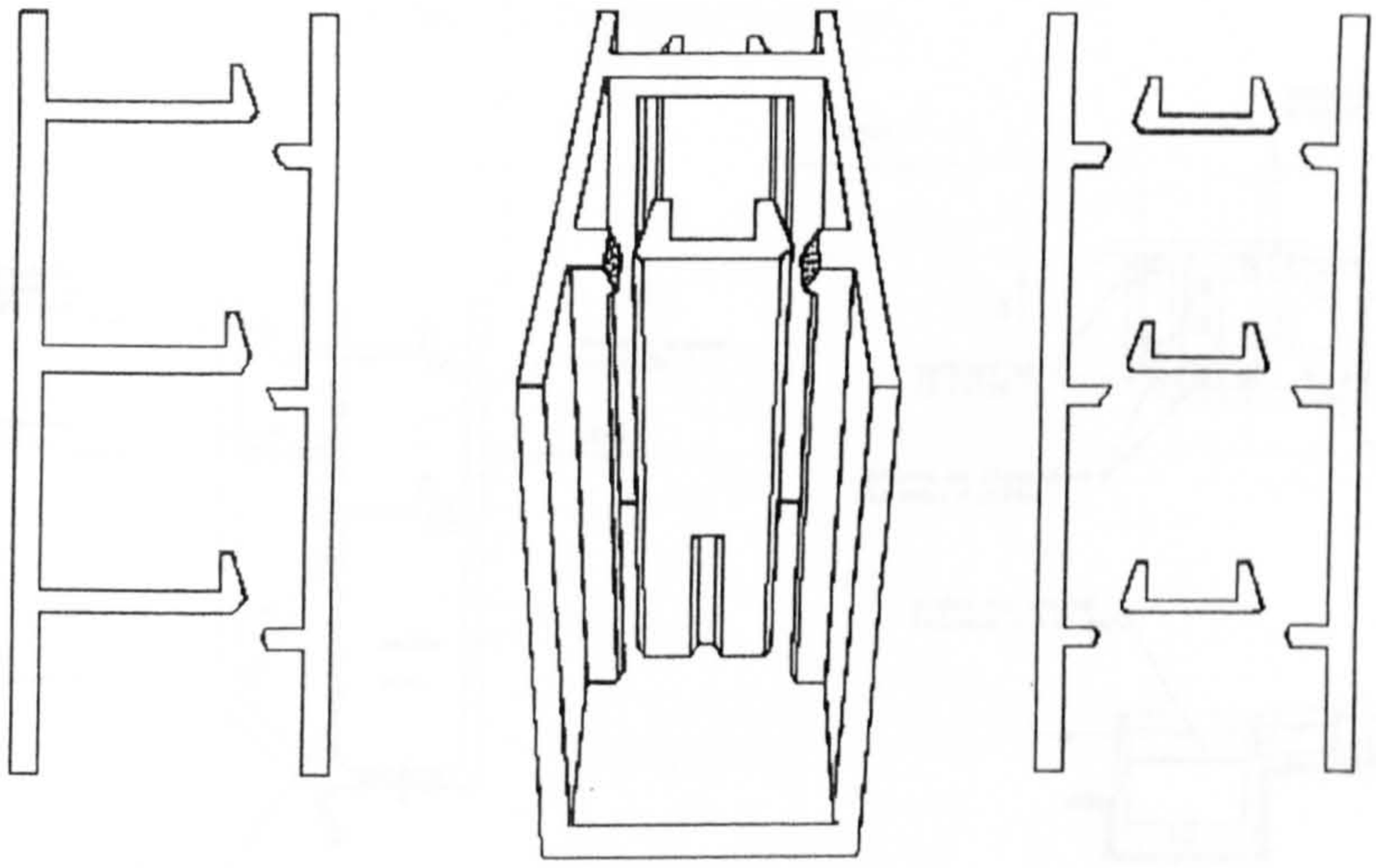

Figure 2-17: Vertical slot pass - from left to right: Plan view of a single vertical slot, Perspective of a double vertical slot and plan view of a double vertical slot (Larinier, 1992)

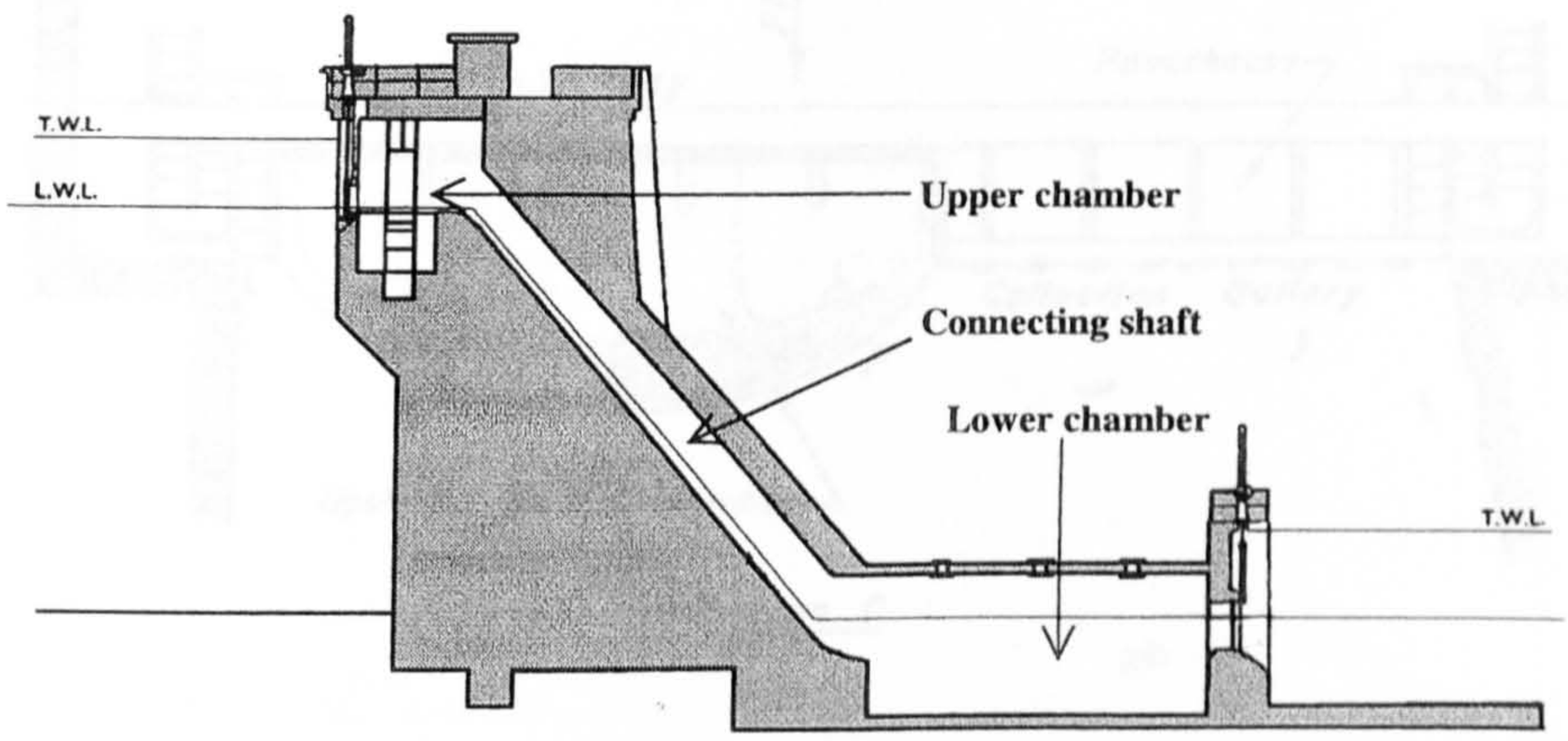

Figure 2-18: Section of Borland fish lock (from Bonnyman, 1958)

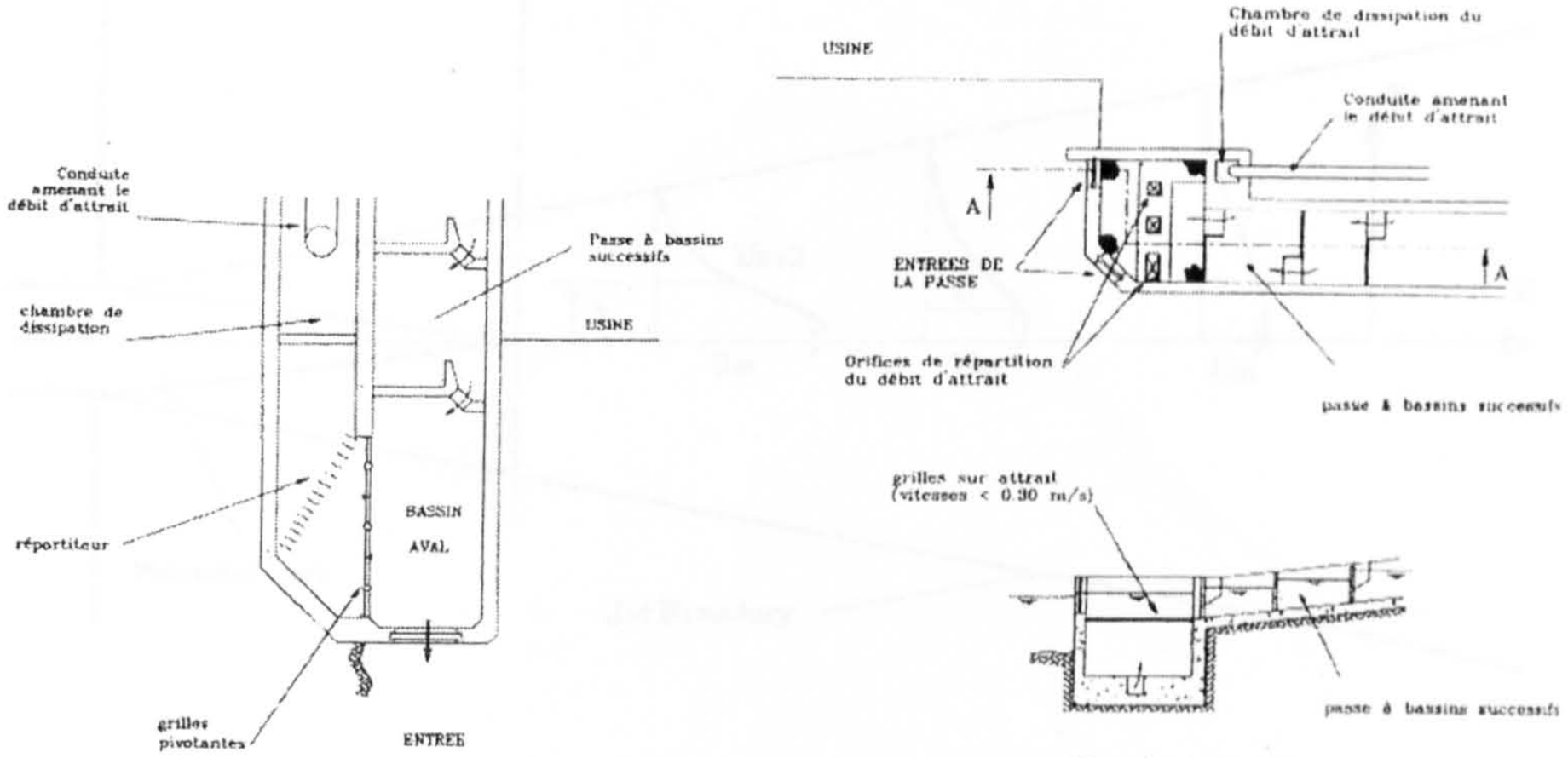

Figure 2-19: Schematic Plan showing the principle of injection of auxiliary water at the fish pass entrance (from Larinier, 1992)

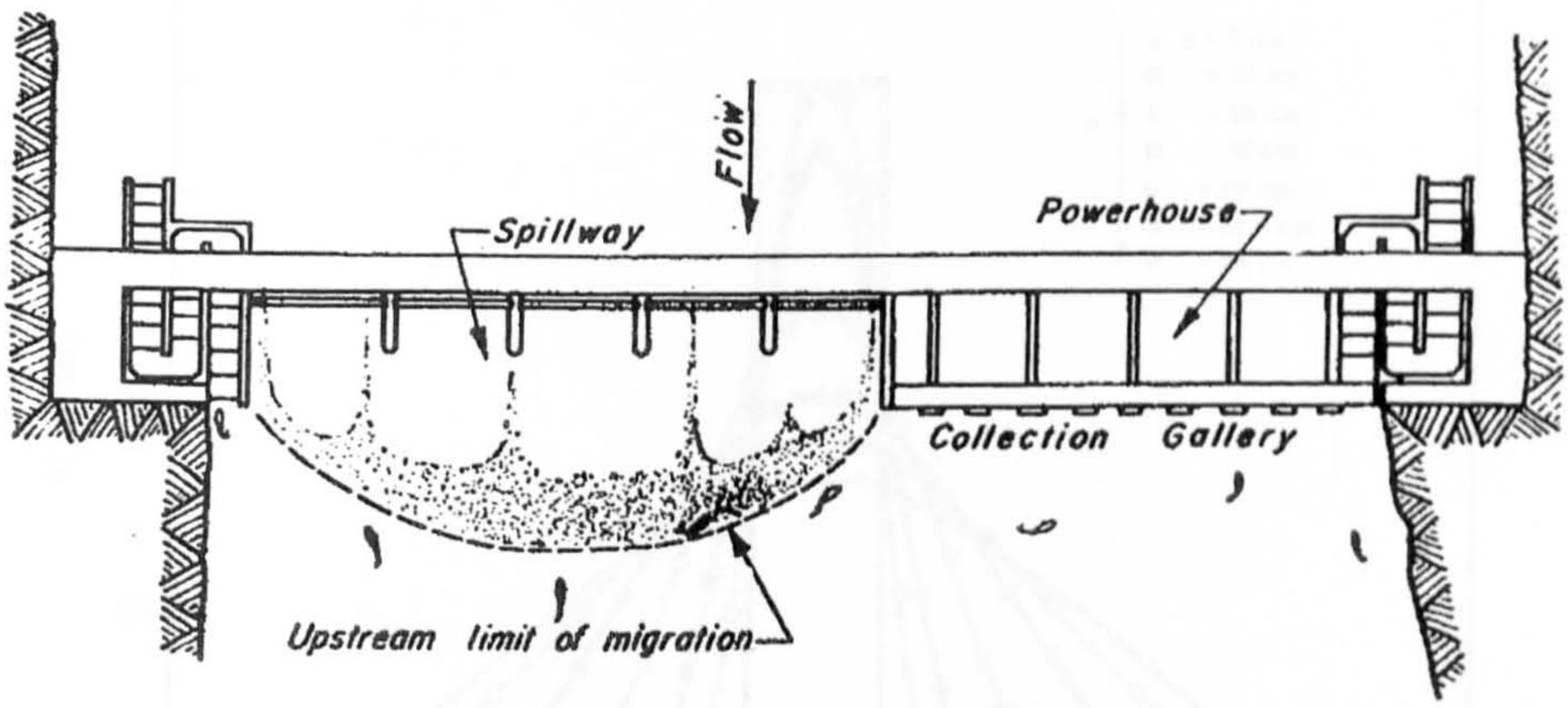

Figure 2-20: Schematic plan near fish pass entrance: combined gated spillways and powerhouse (from Clay, 1995)

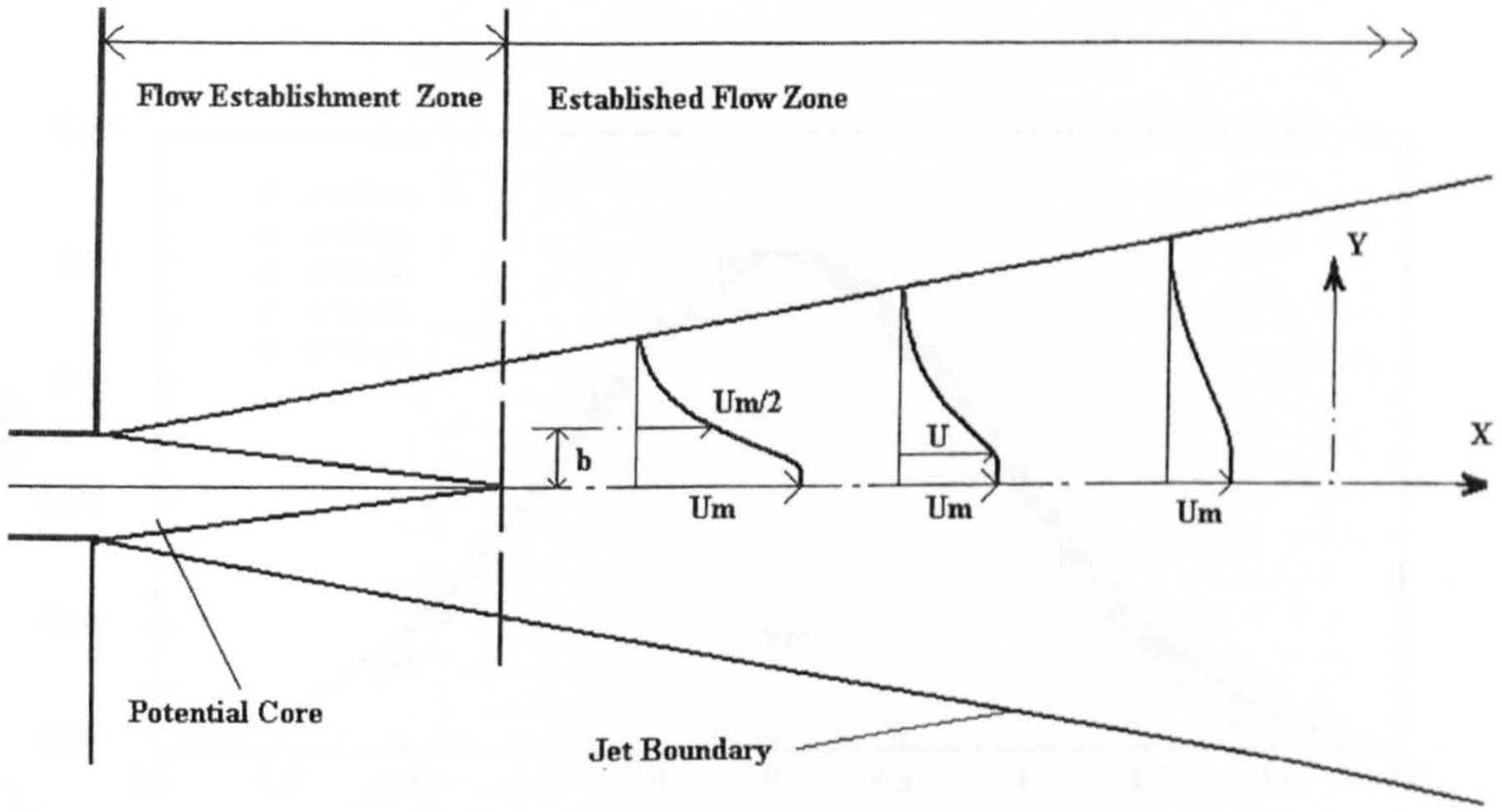

Figure 2- 21: Definition sketch of a plane turbulent jet (from Rajaratnam, 1976)

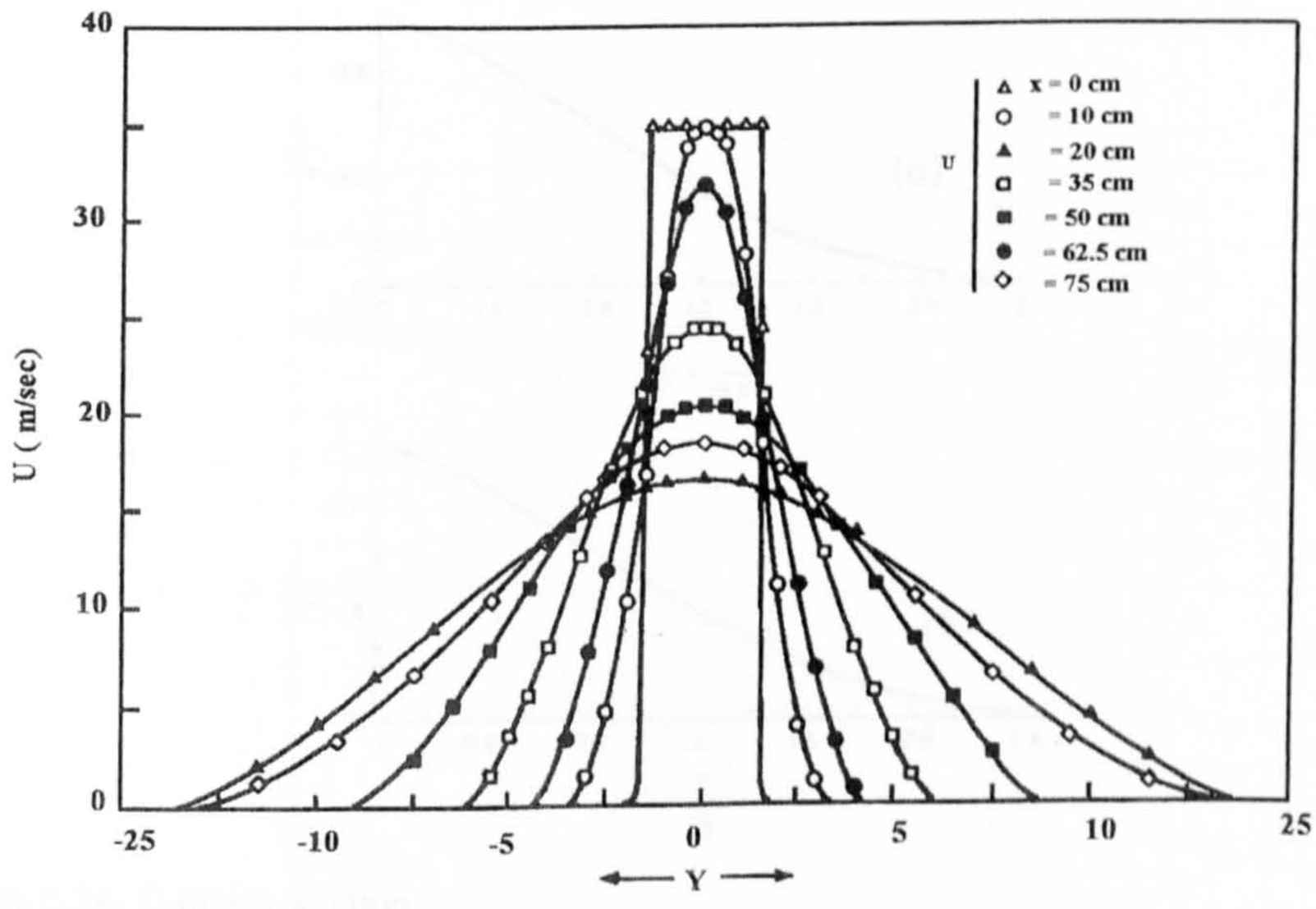

Figure 2-22:Velocity distribution for the plane turbulent jet at various cross-sections (from Forthmann, 1934)

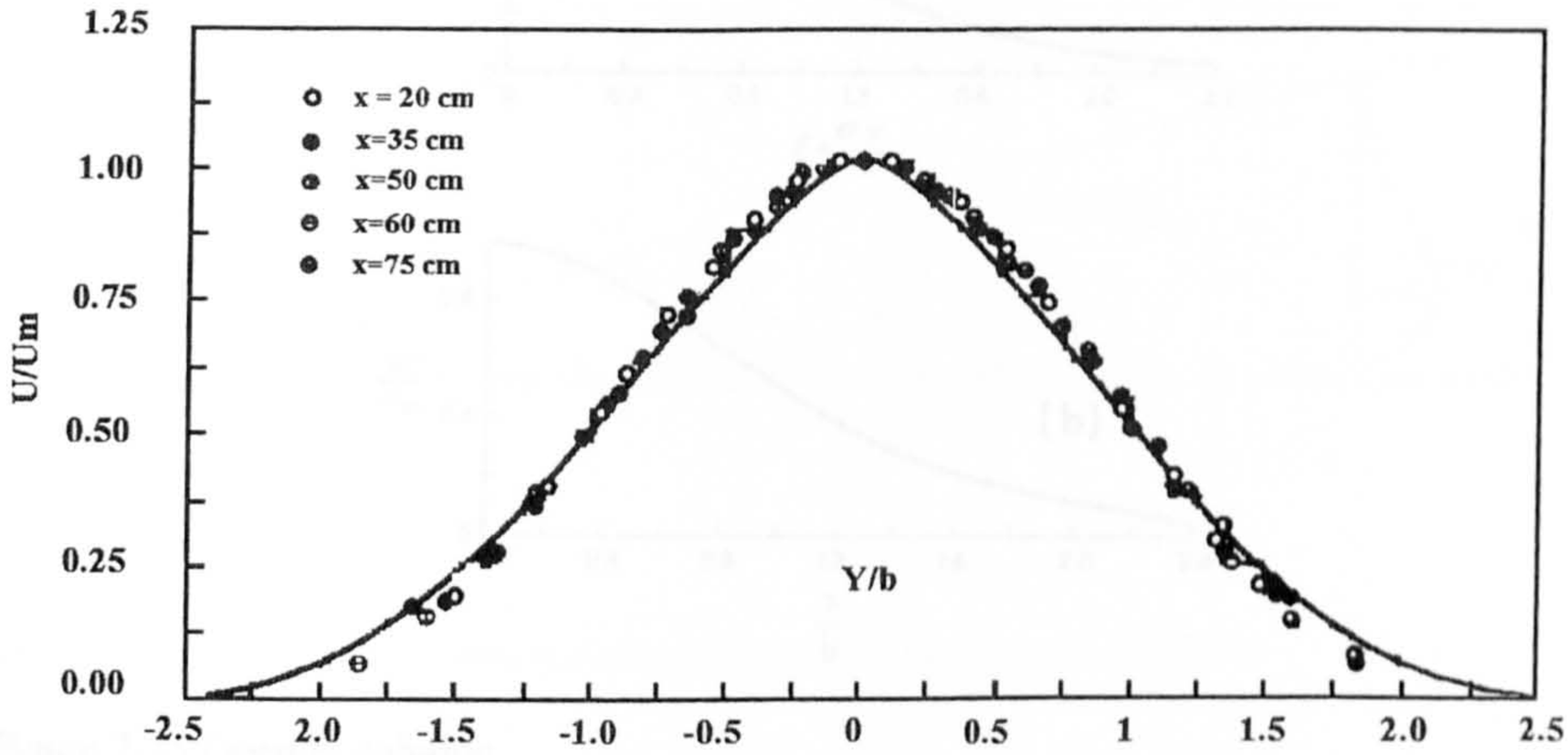

Figure 2-23: Similarity of velocity distribution for plane turbulent free jets (from Forthmann, 1934)

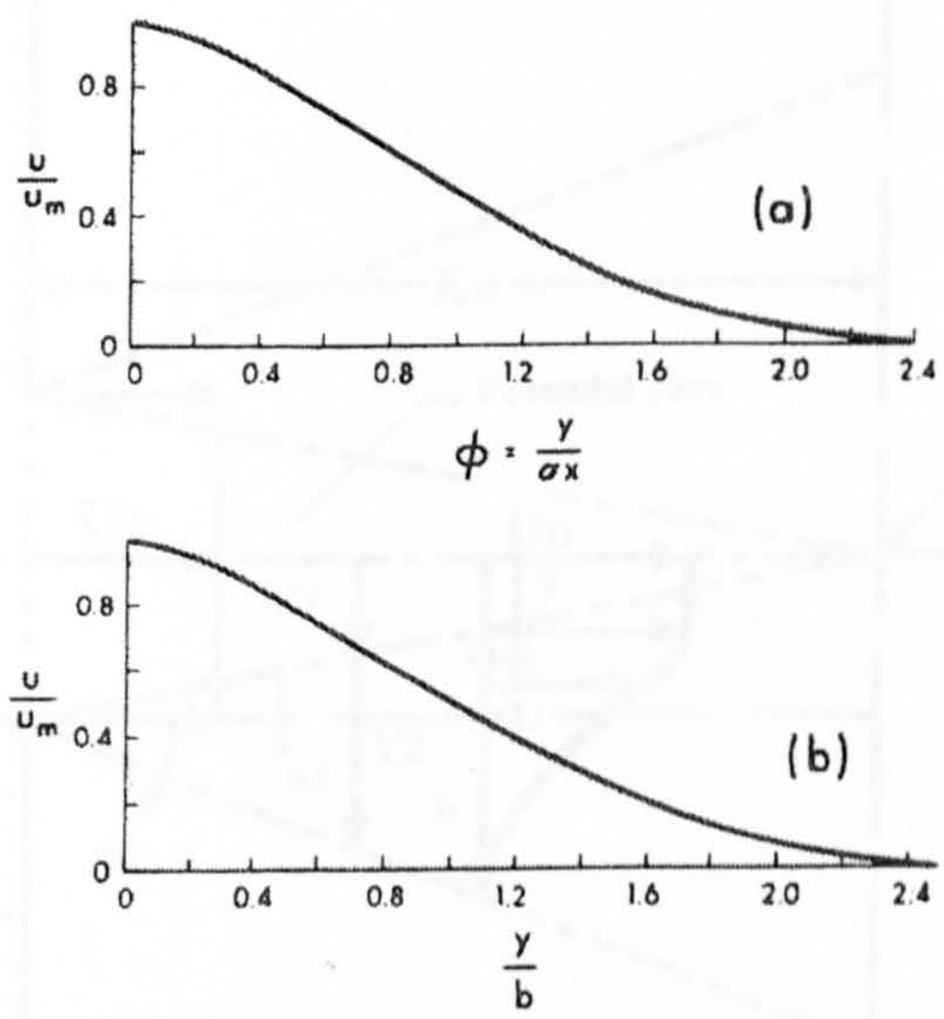

Figure 2-24: Tollmien solution

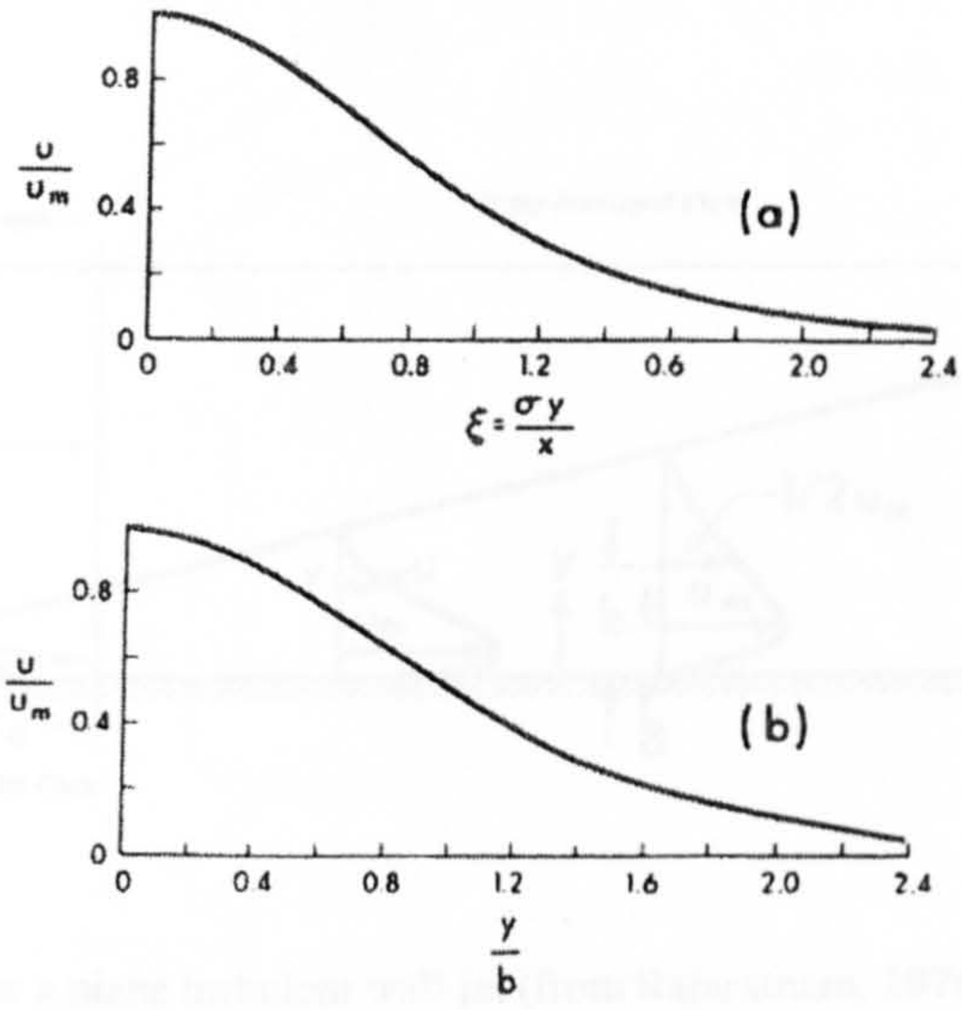

Figure 2-25:Goertler solution

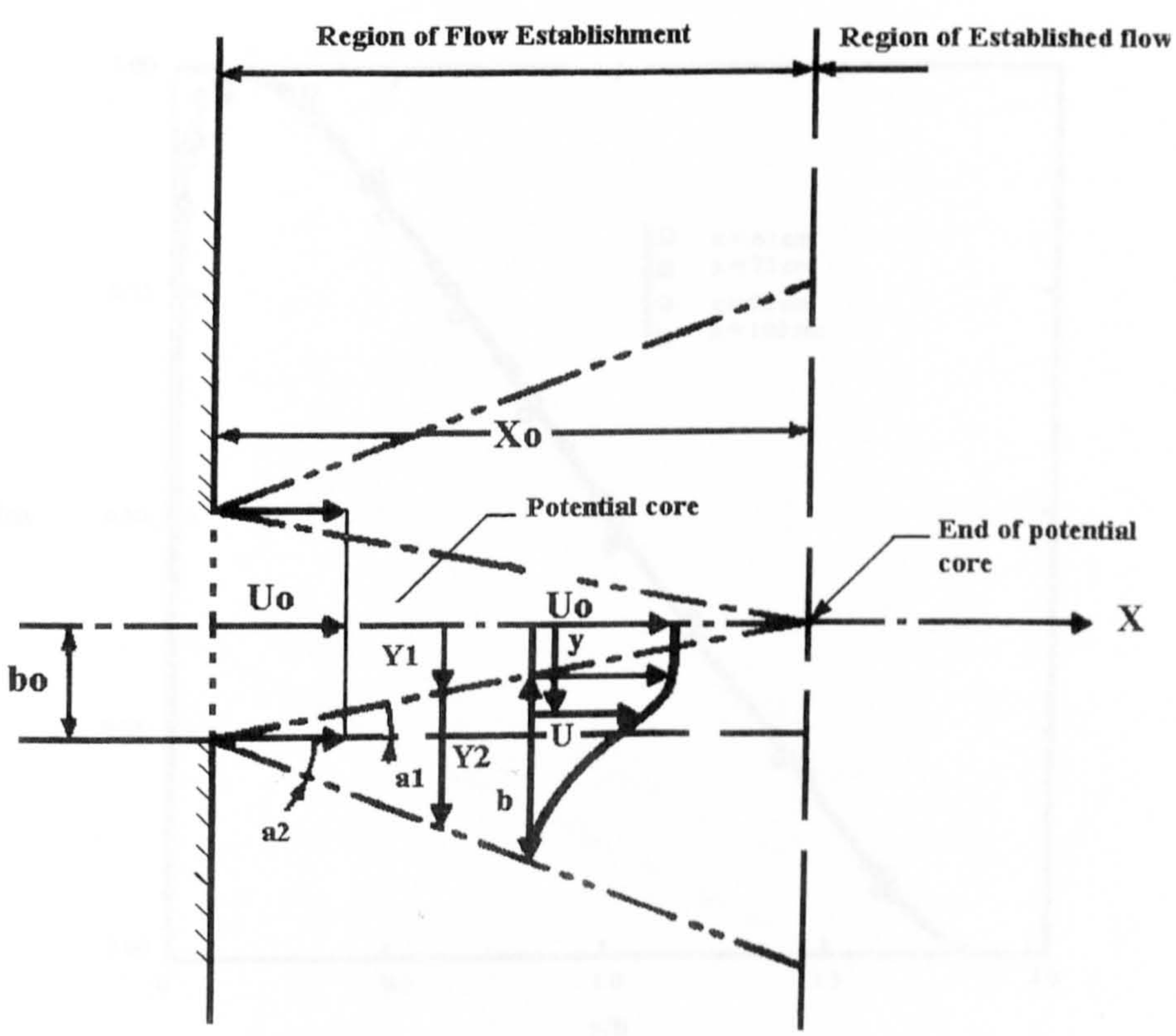

Figure 2-26: Sketch of the flow establishment region for a plane turbulent jet

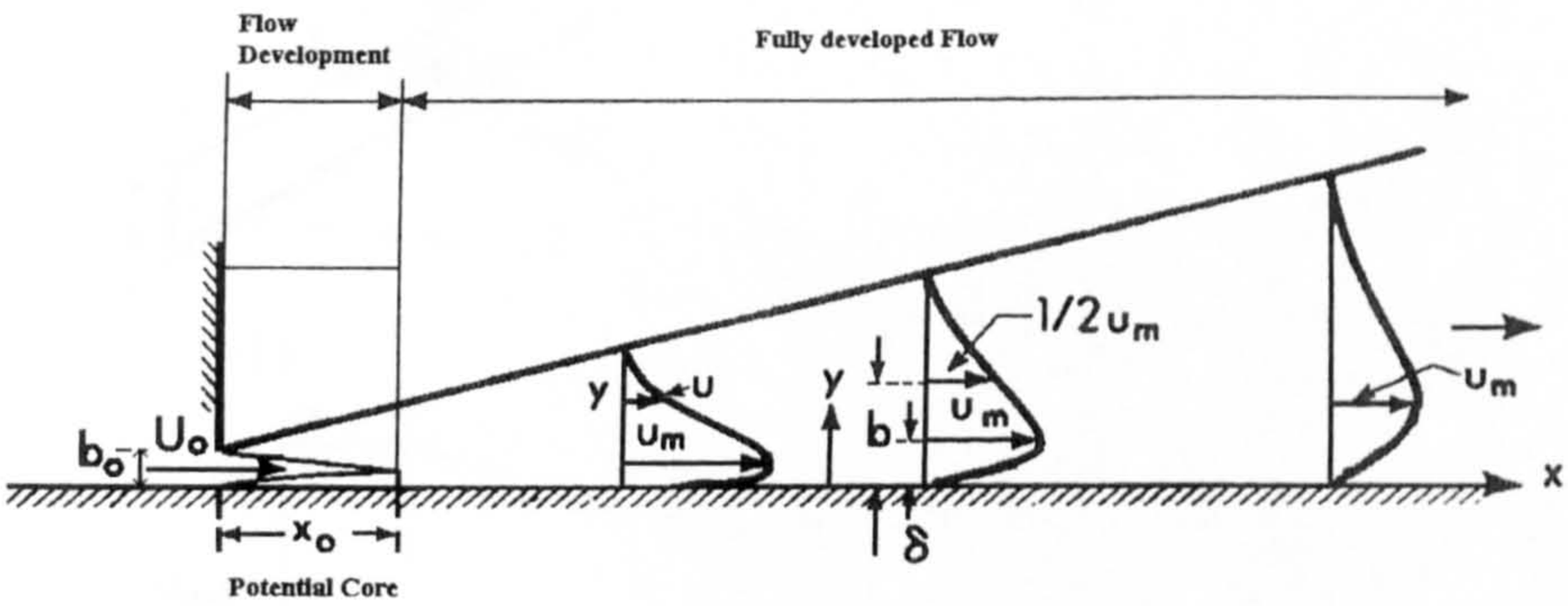

Figure 2-27: Sketch for a plane turbulent wall jet (from Rajaratnam, 1976)

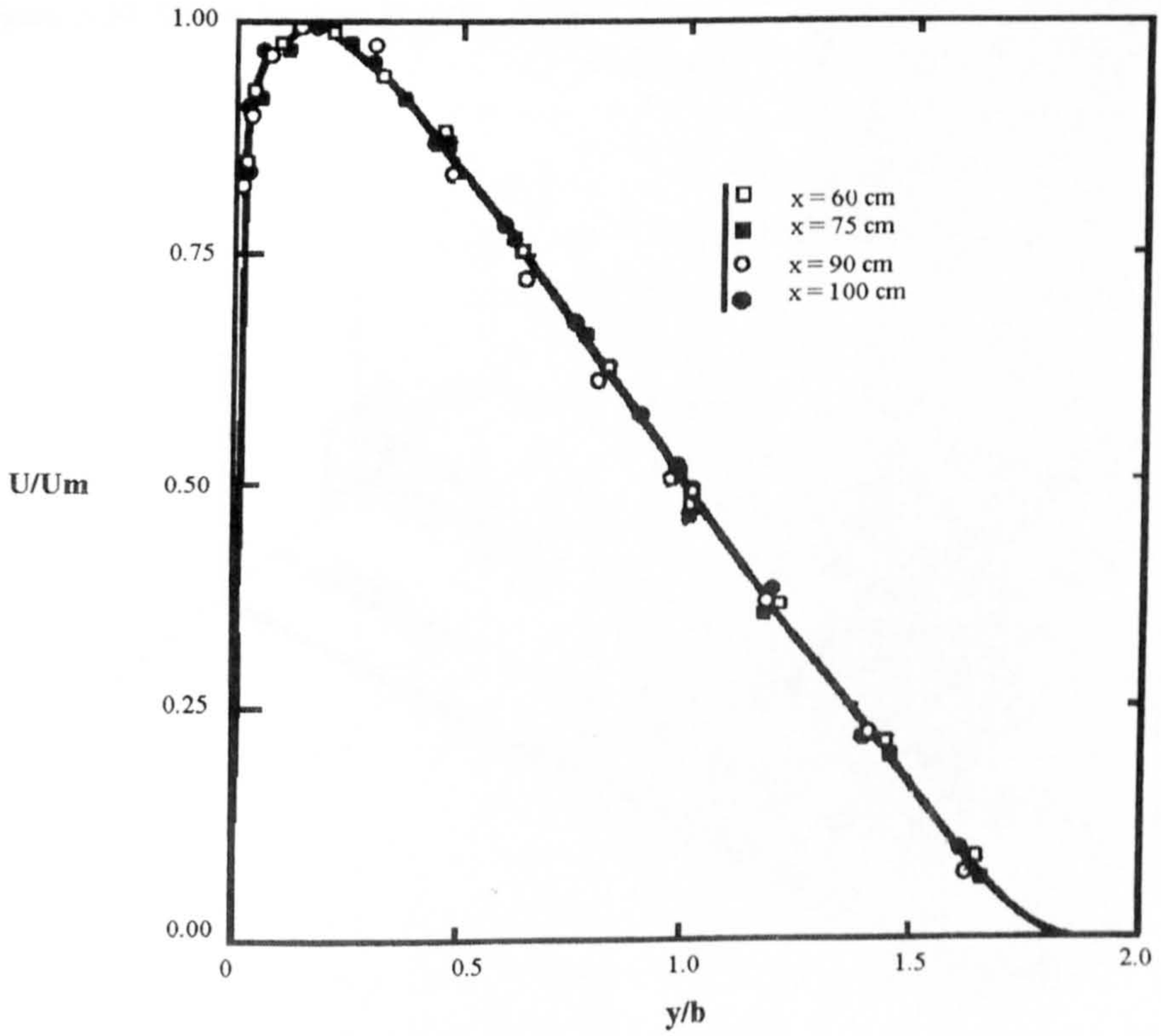

Figure 2-28: Similarity of velocity profiles for plane wall jets (from Forthmann, 1934)

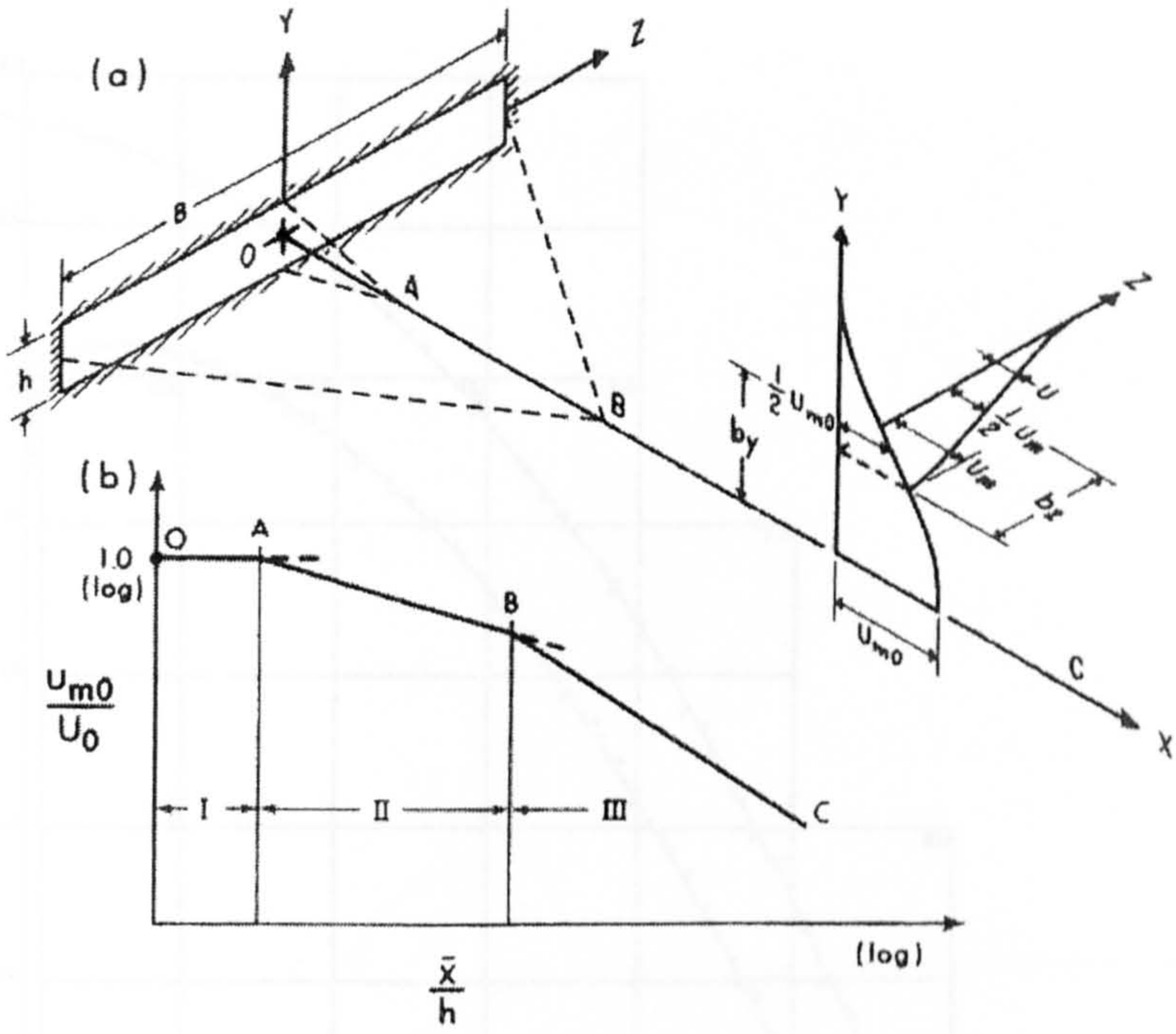

Figure 2-29: Sketch for three-dimensional jets

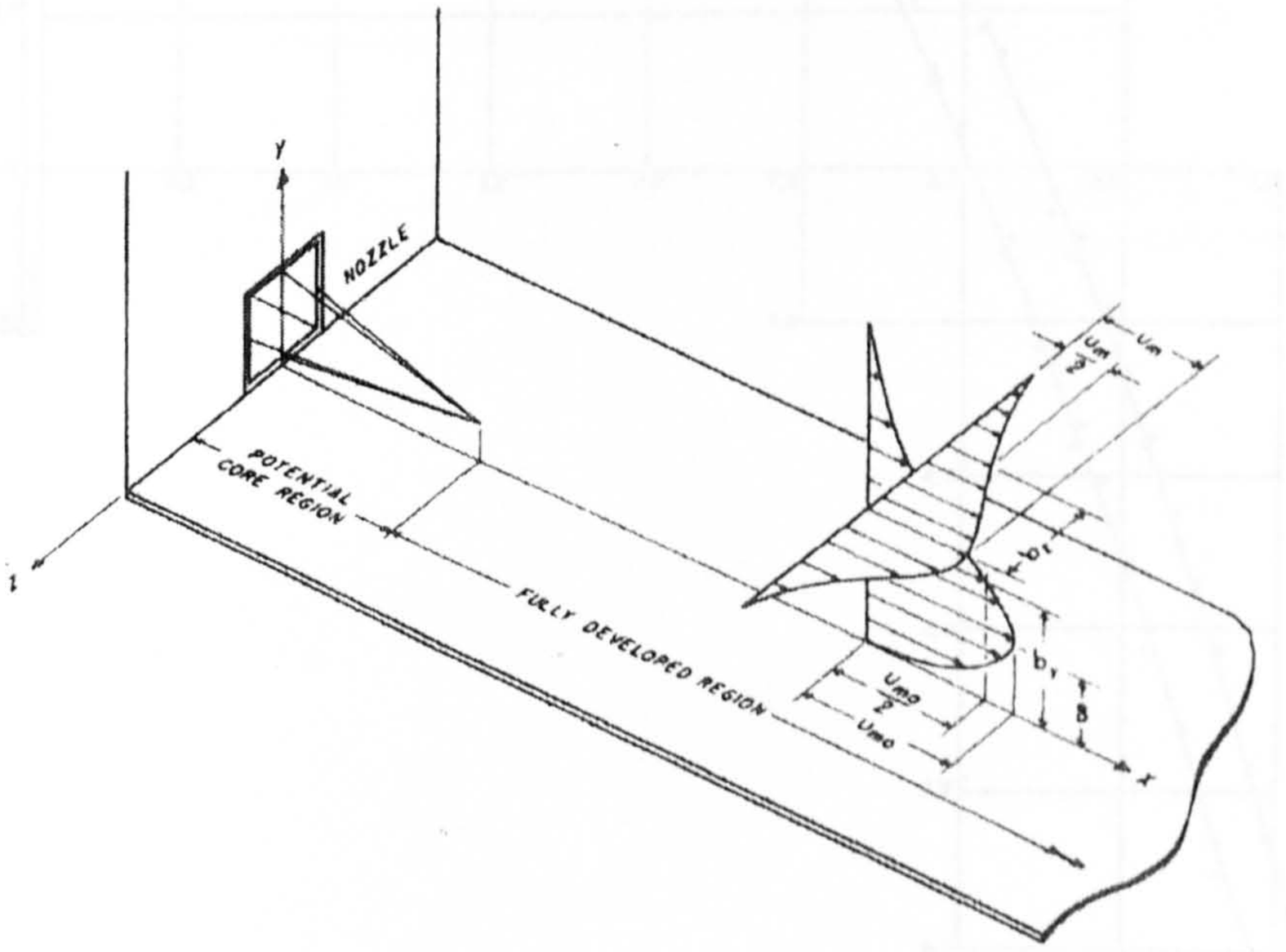

Figure 2-30: Sketch for a square bluff wall jet

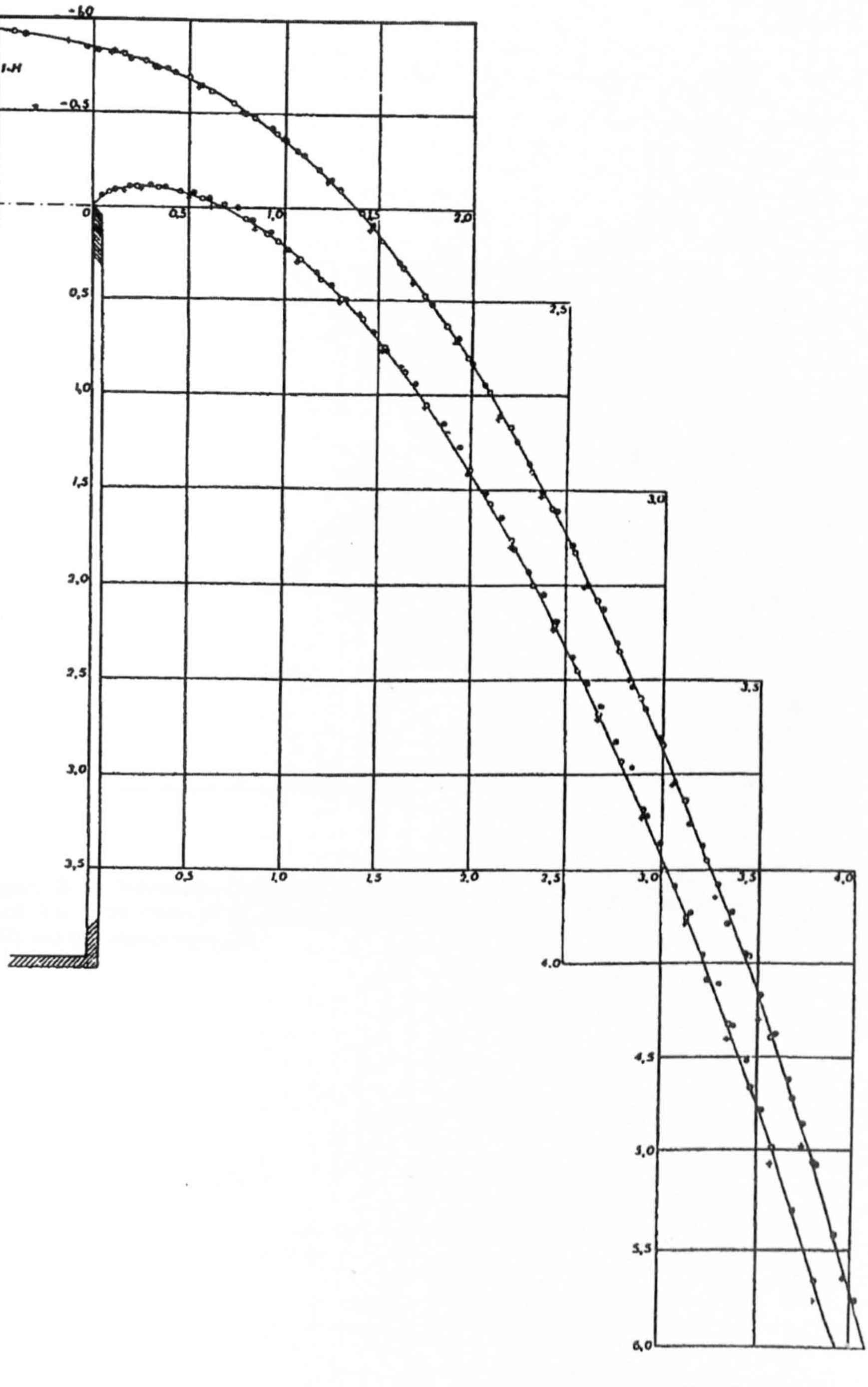

Figure 2-31:Schema of the overflow free jet as studied by Scimeni (1930) (from Armengous, 1991)

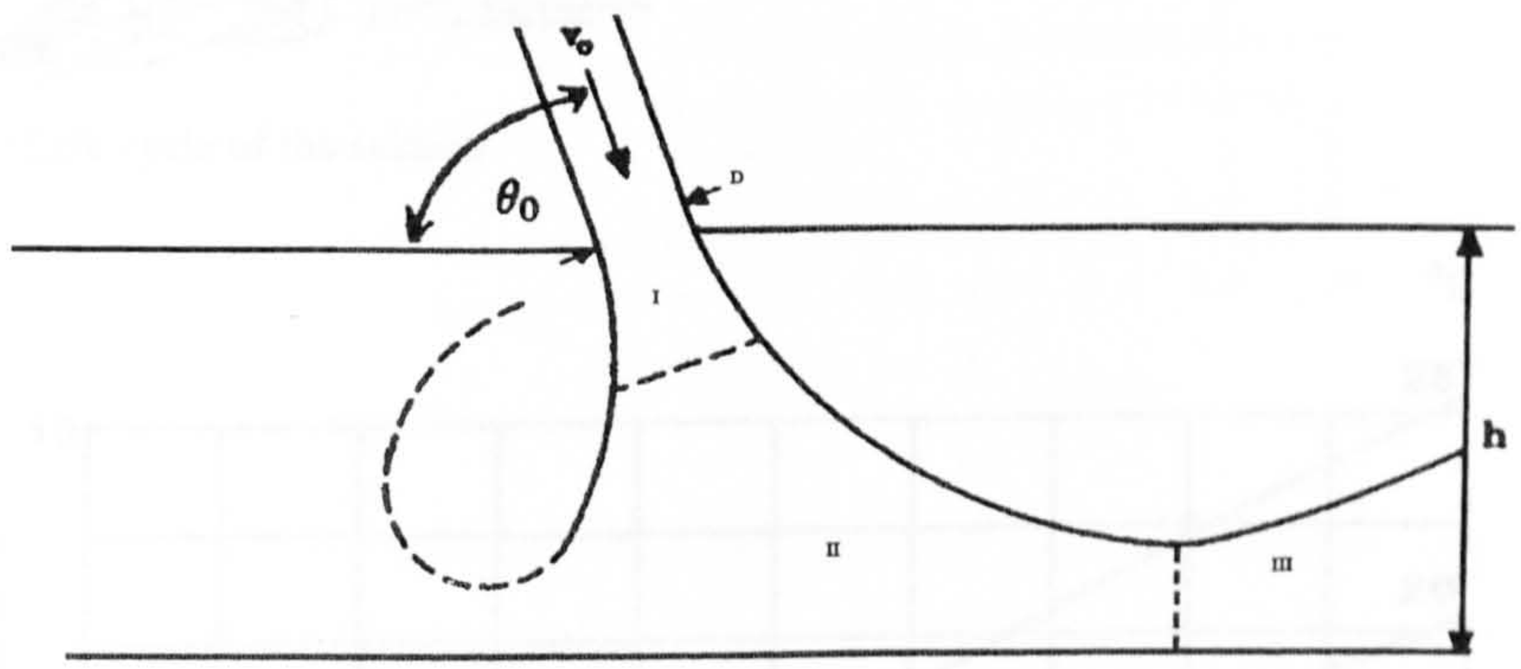

Figure 2-32: Schematic representation of the plunging jet when impacting with the quiescent pool. The three zones of the jet are also represented: the zone of free fall (I), the deflection zone (III) and the impact zone (II)

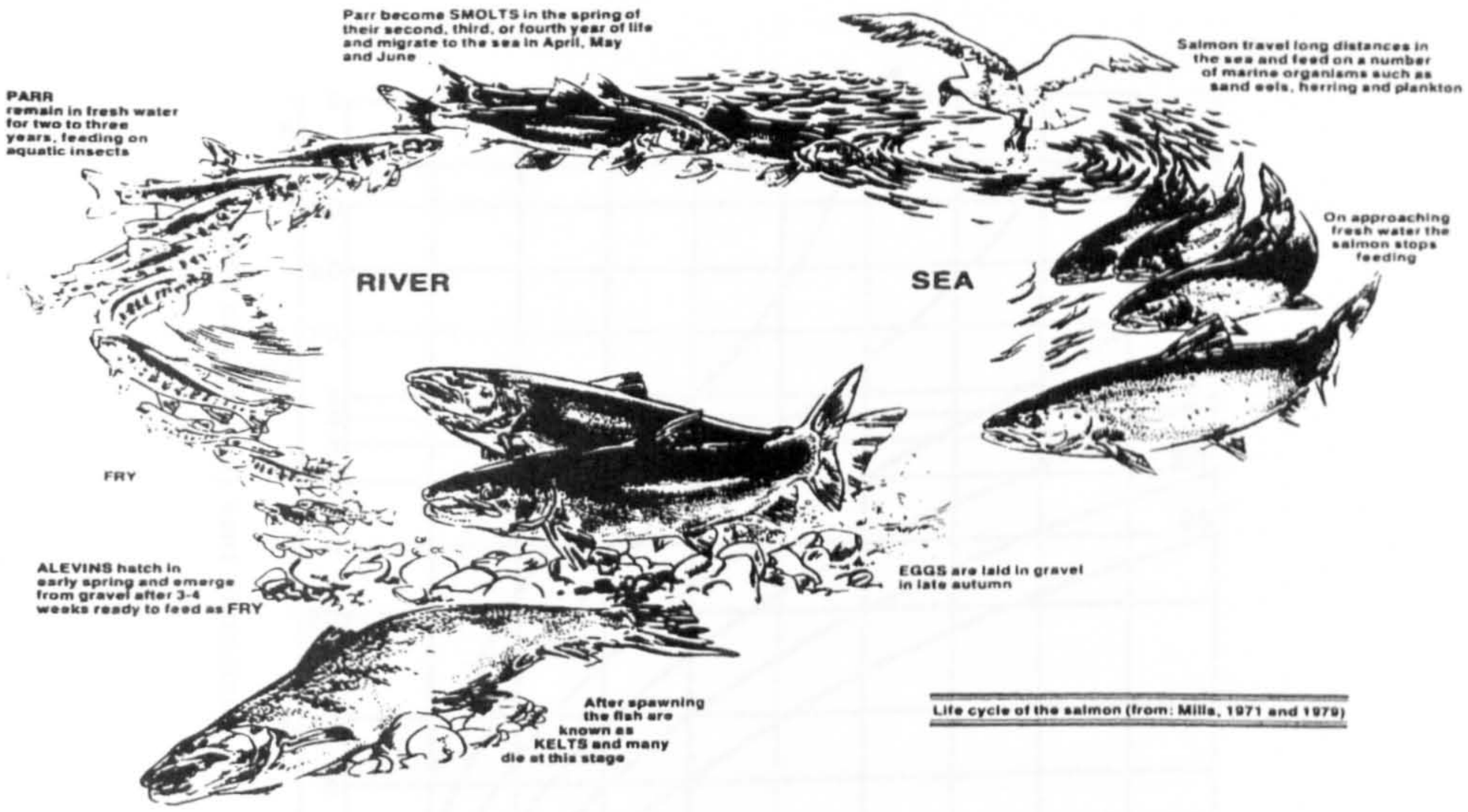

Figure 3-1: Life cycle of the salmon

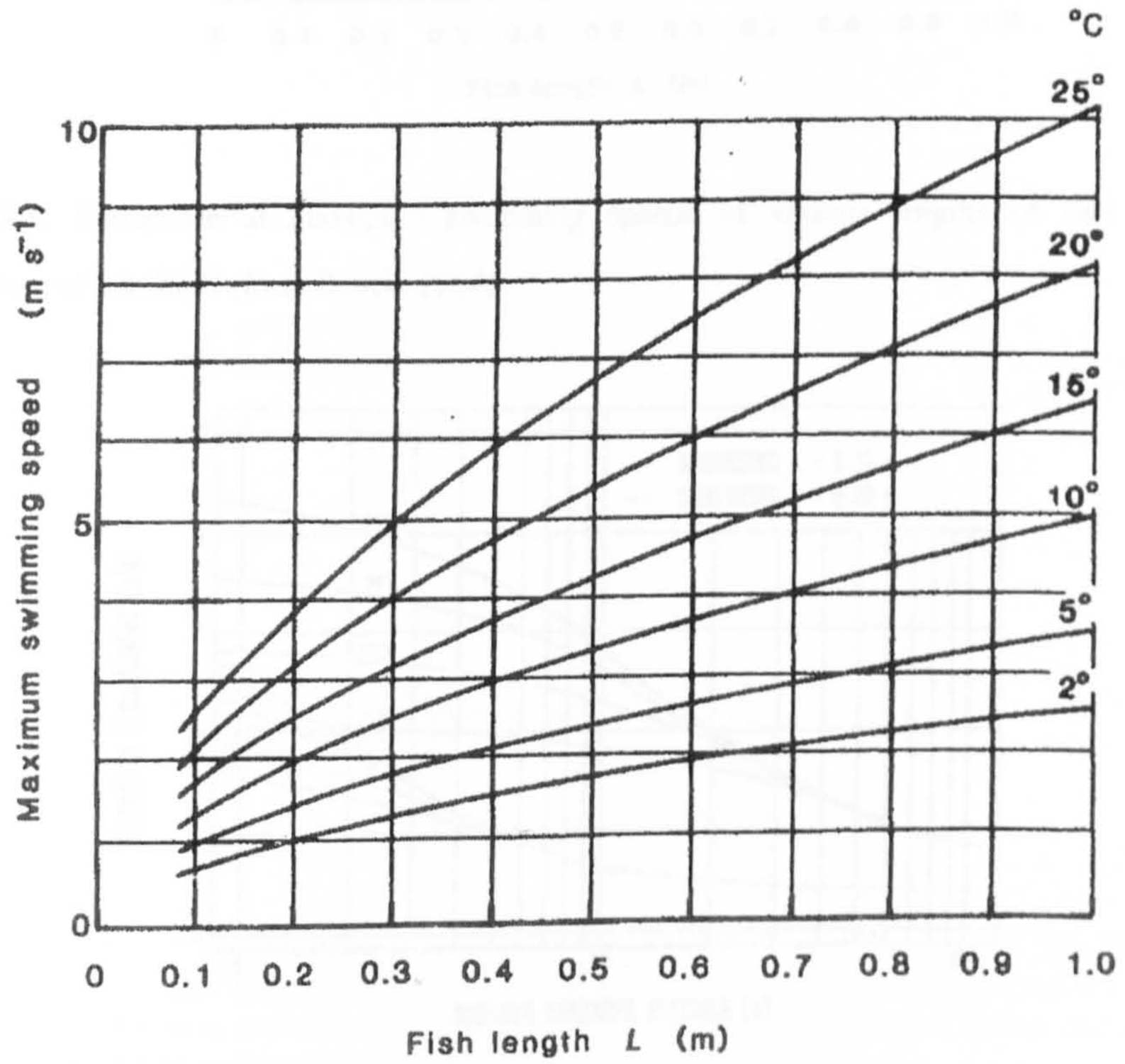

Figure 3-2: Maximum-swimming speeds against fish length over temperature range of 2 to 25 C (from Beach, 1984)

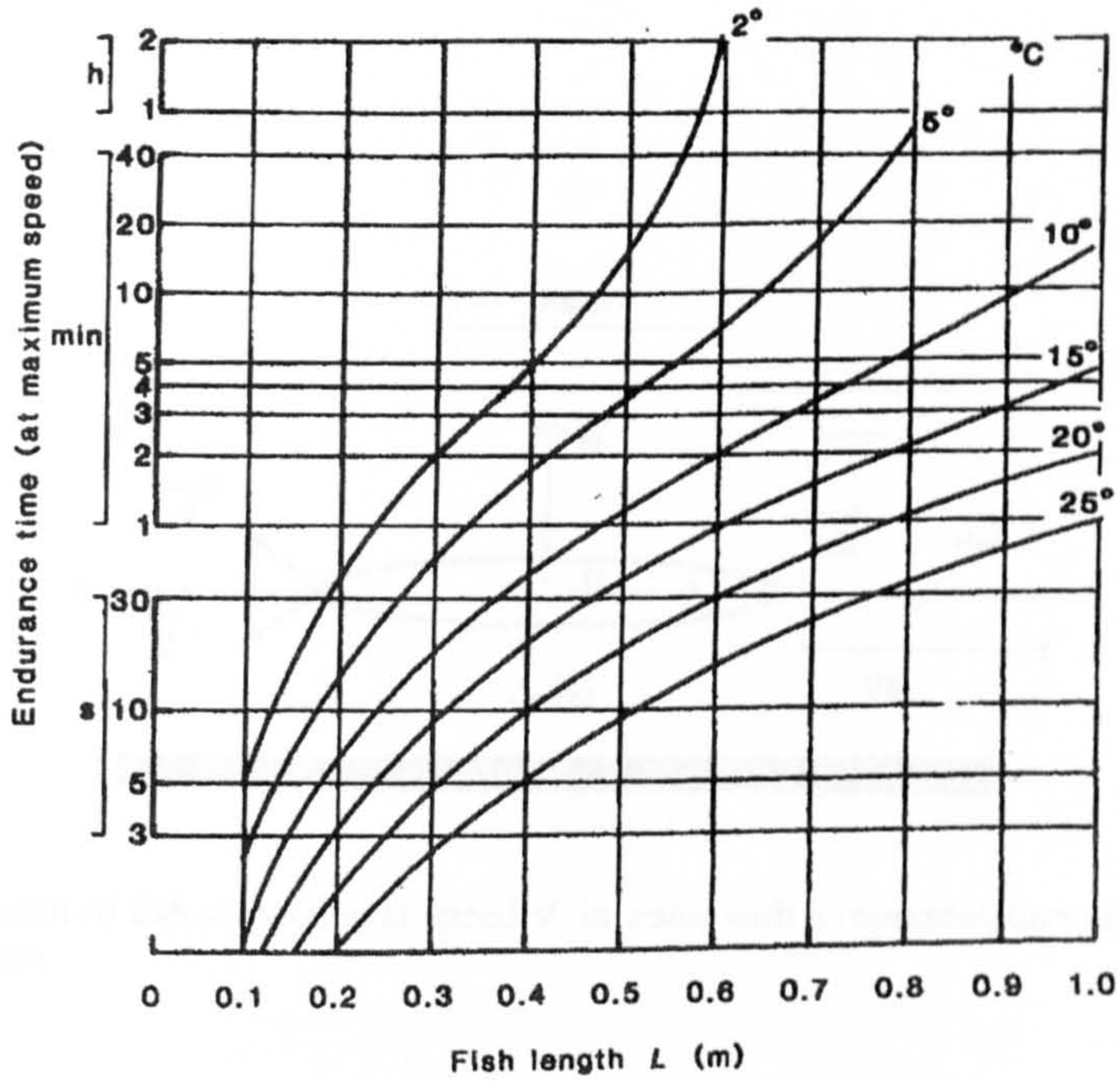

Figure 3-3: Endurance at maximum swimming speeds of various lengths of fish over a temperature of 2 to 25 C (from Beach, 1984)

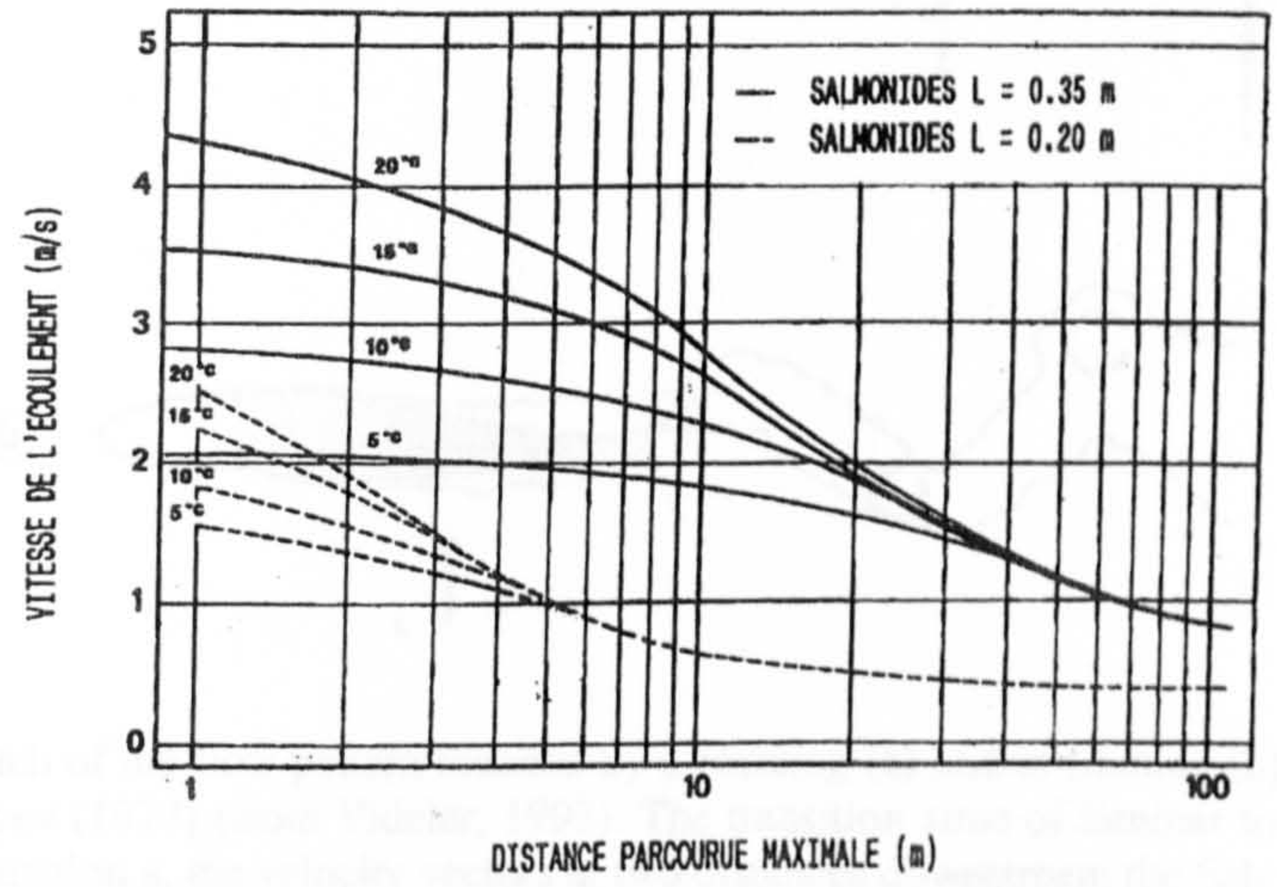

Figure 3-4: Maximum swimming distance versus water velocity and temperature for two lengths of salmonids (Larinier, 1992)

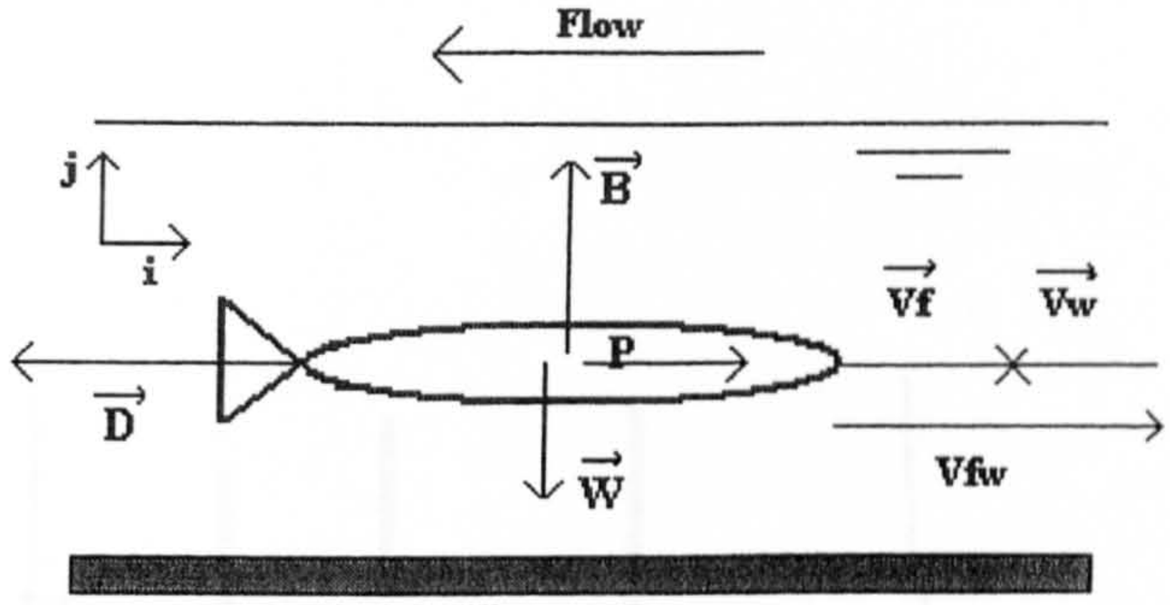

Figure 3-5: Sketch of fish swimming at speed V_f in water with a representation of the main forces acting on the fish

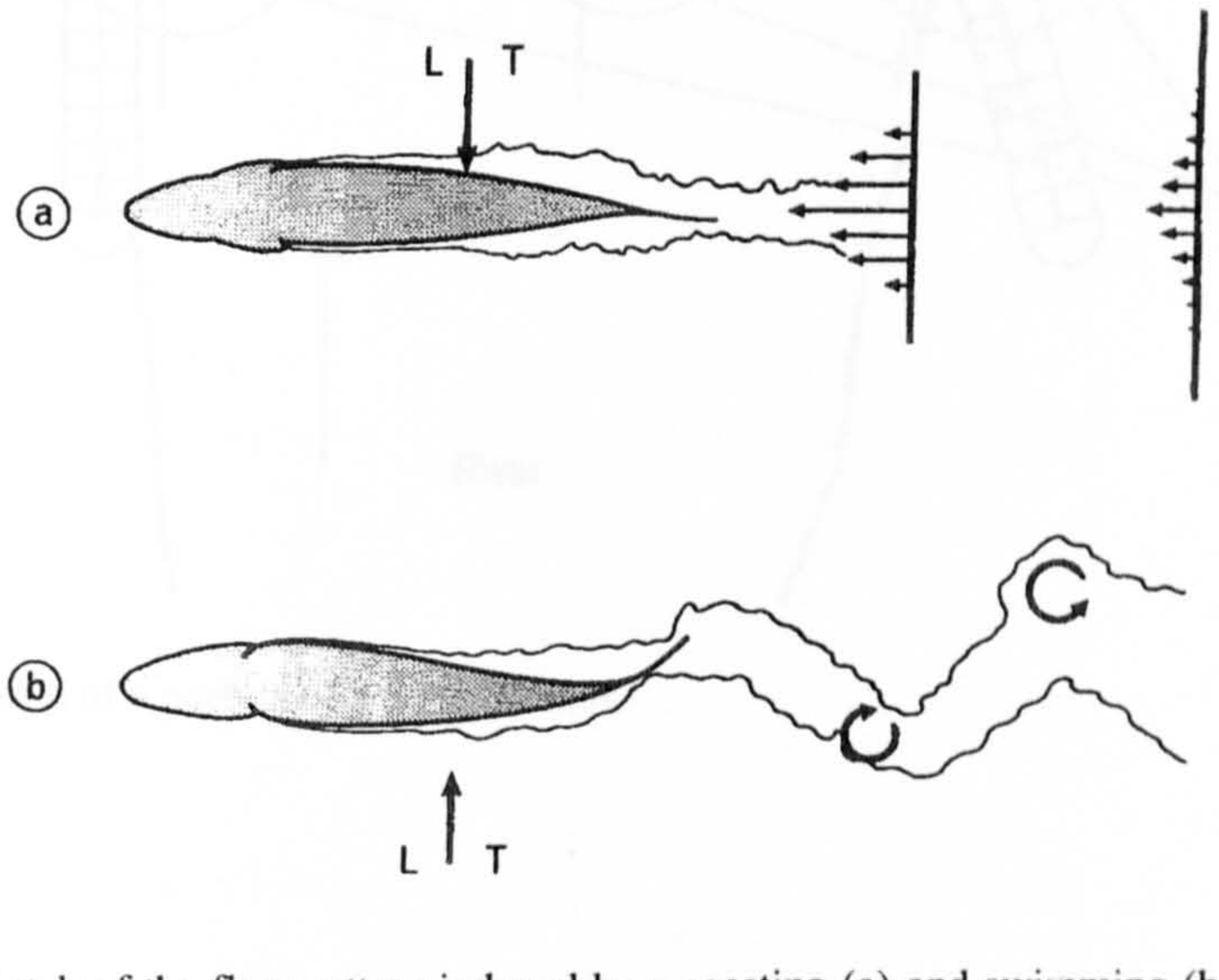

Figure 3-6: Sketch of the flow pattern induced by a coasting (a) and swimming (b) fish, based on pictures by Aleyev (1977) (from Videler, 1993). The transition zone of laminar to turbulent flow is shown. For situation a, the velocity vectors at two distances downstream the fish are shown. For situation b, vortices in the wake are shown.

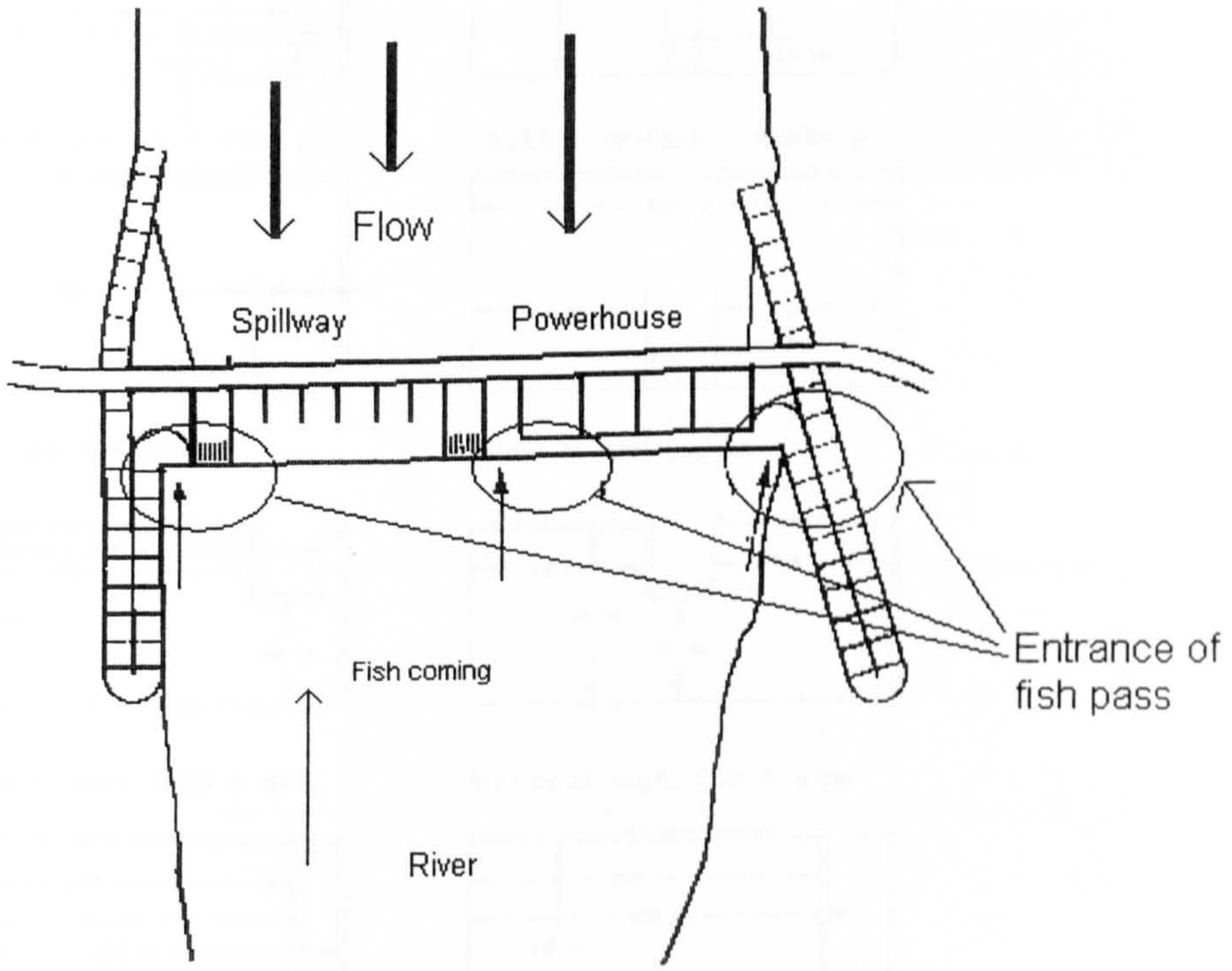

Figure 4-1:Sketch of a portion of a river at a dam

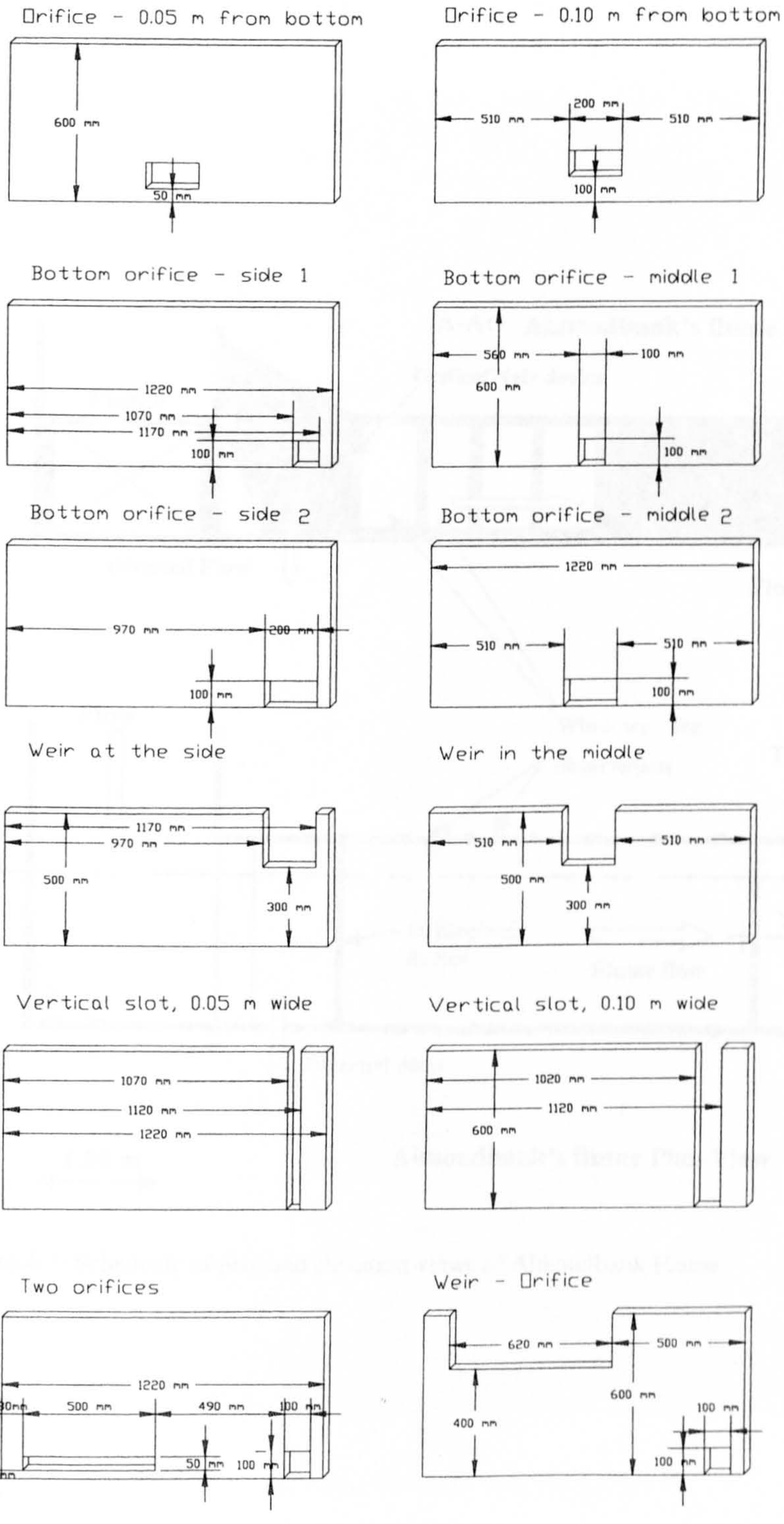

Figure 4-2: Schematic of the tested designs

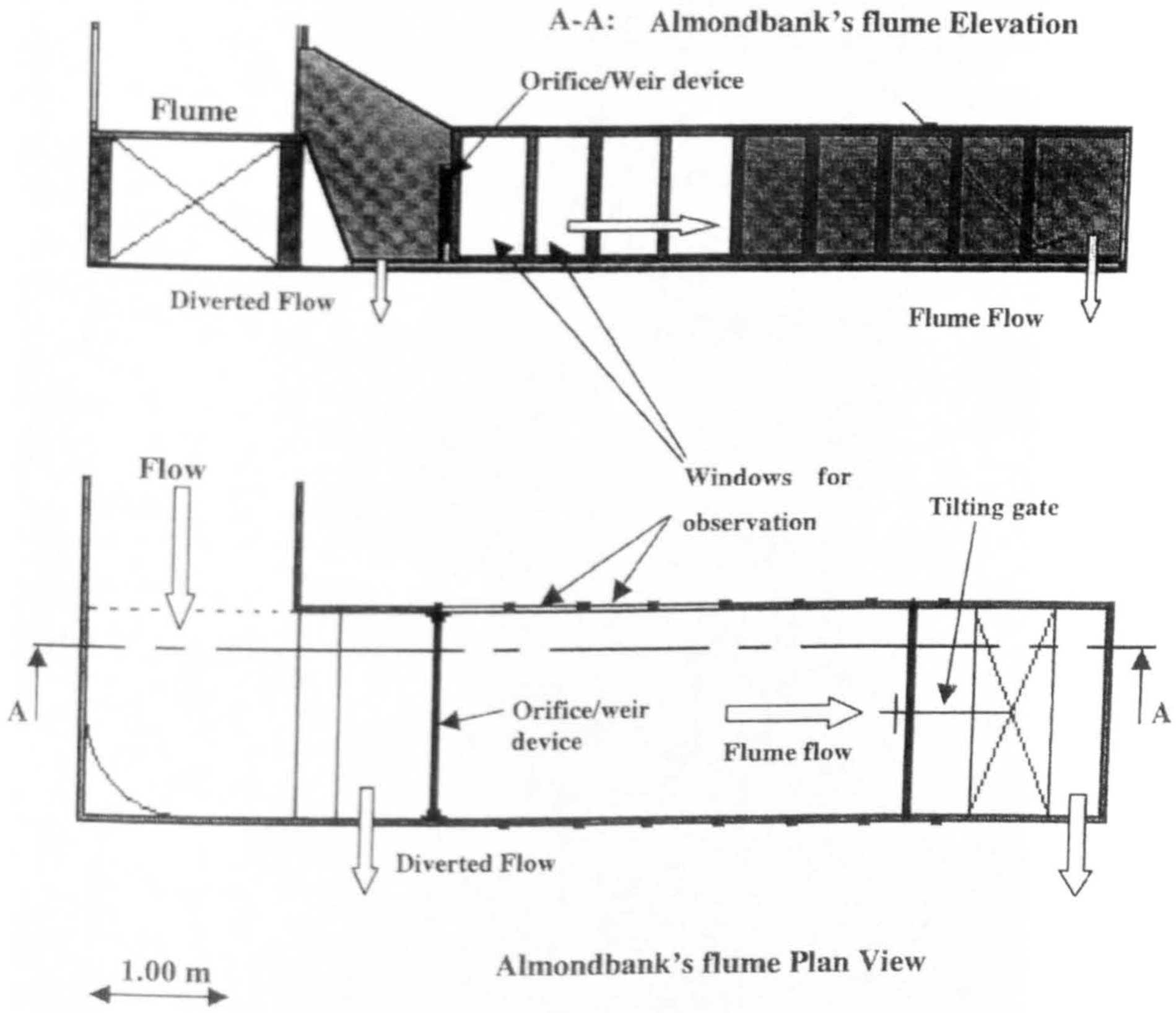

Figure 4-3: Schematic of plan and elevation views of Almondbank Flume

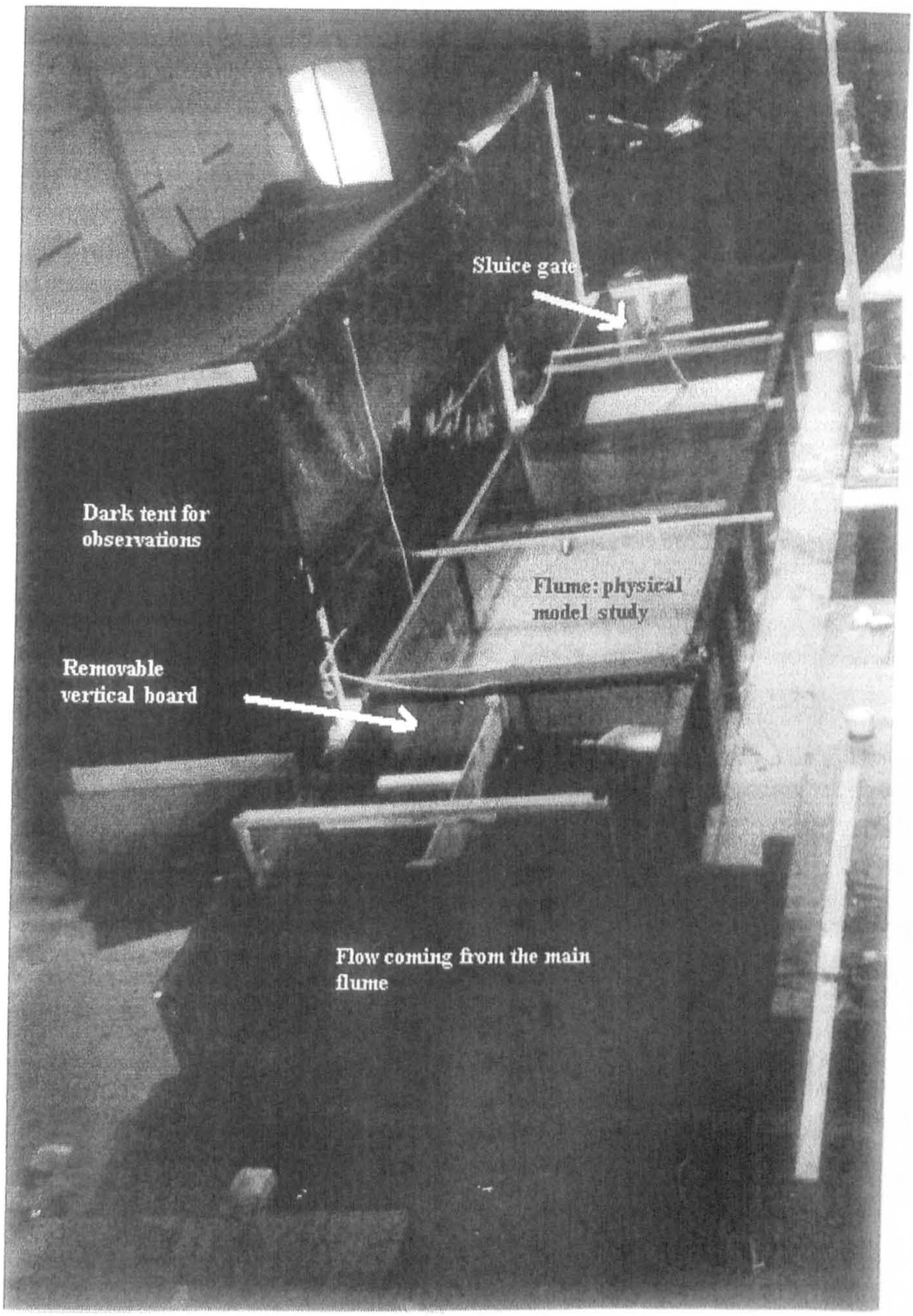

Figure 4-4: General view of the physical model - set up for series IV

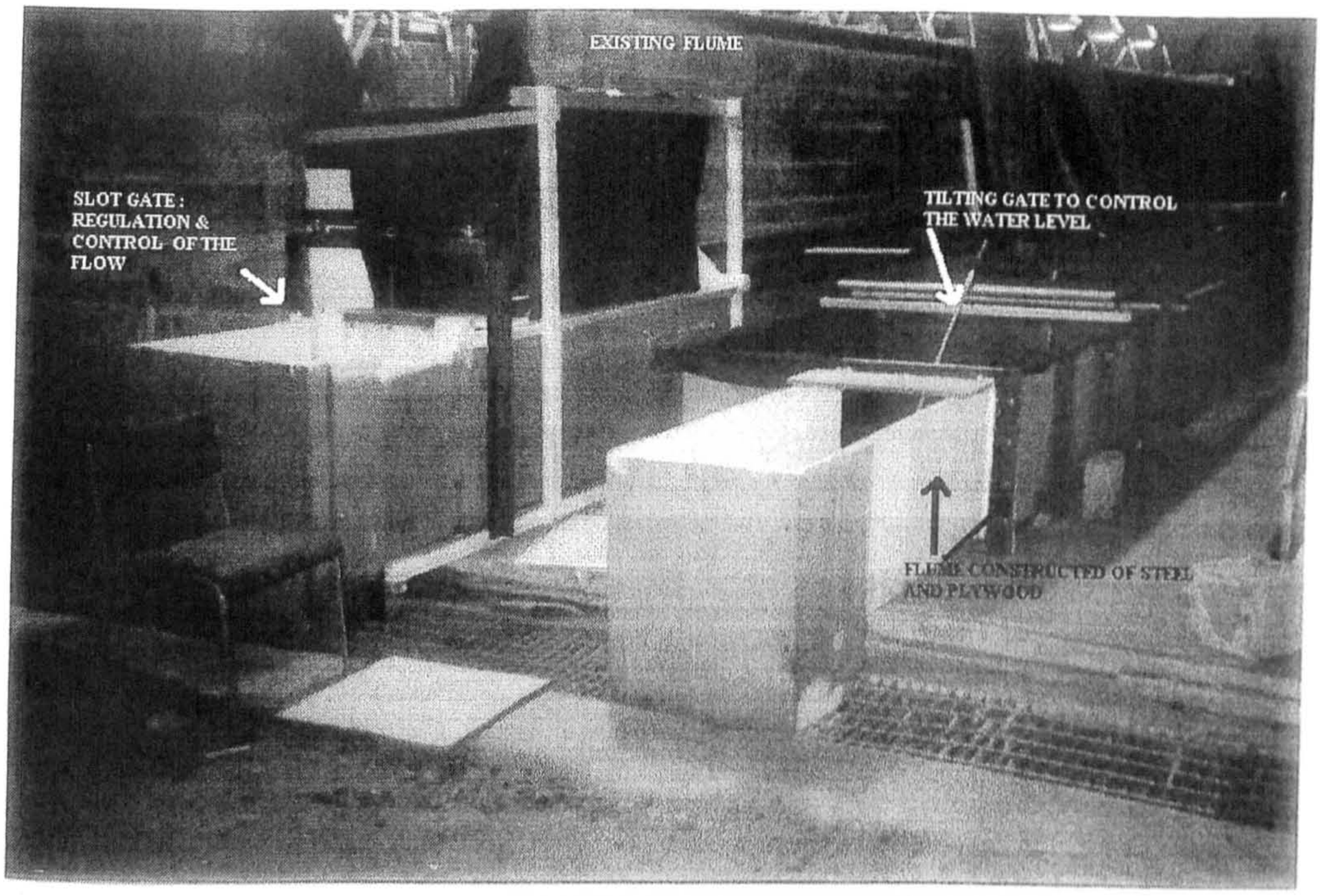

Figure 4-5: photo taken during the reconstruction of the physical model in Spring 2000

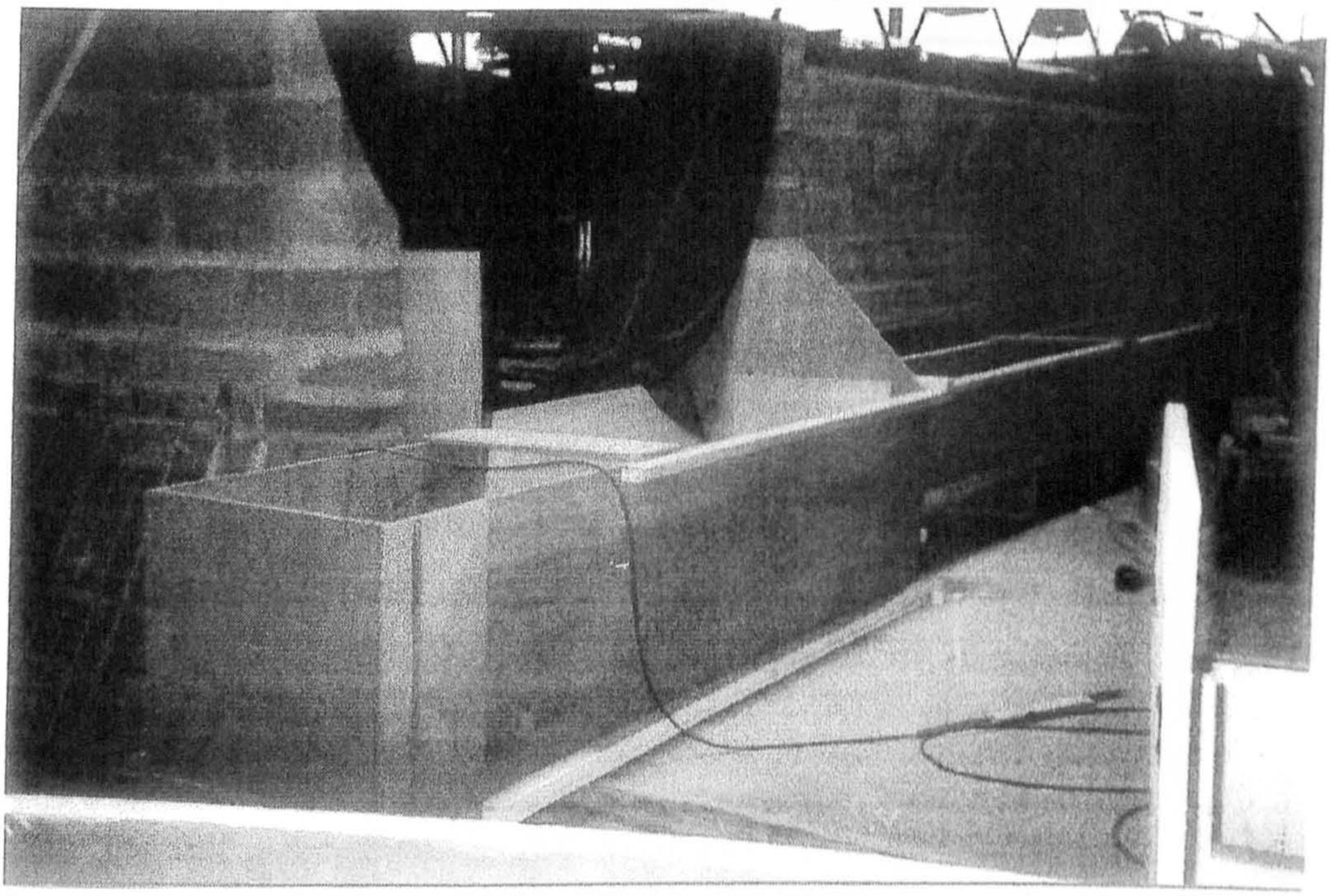

Figure 4-6: Photo showing the connection of the physical model with the existing flume

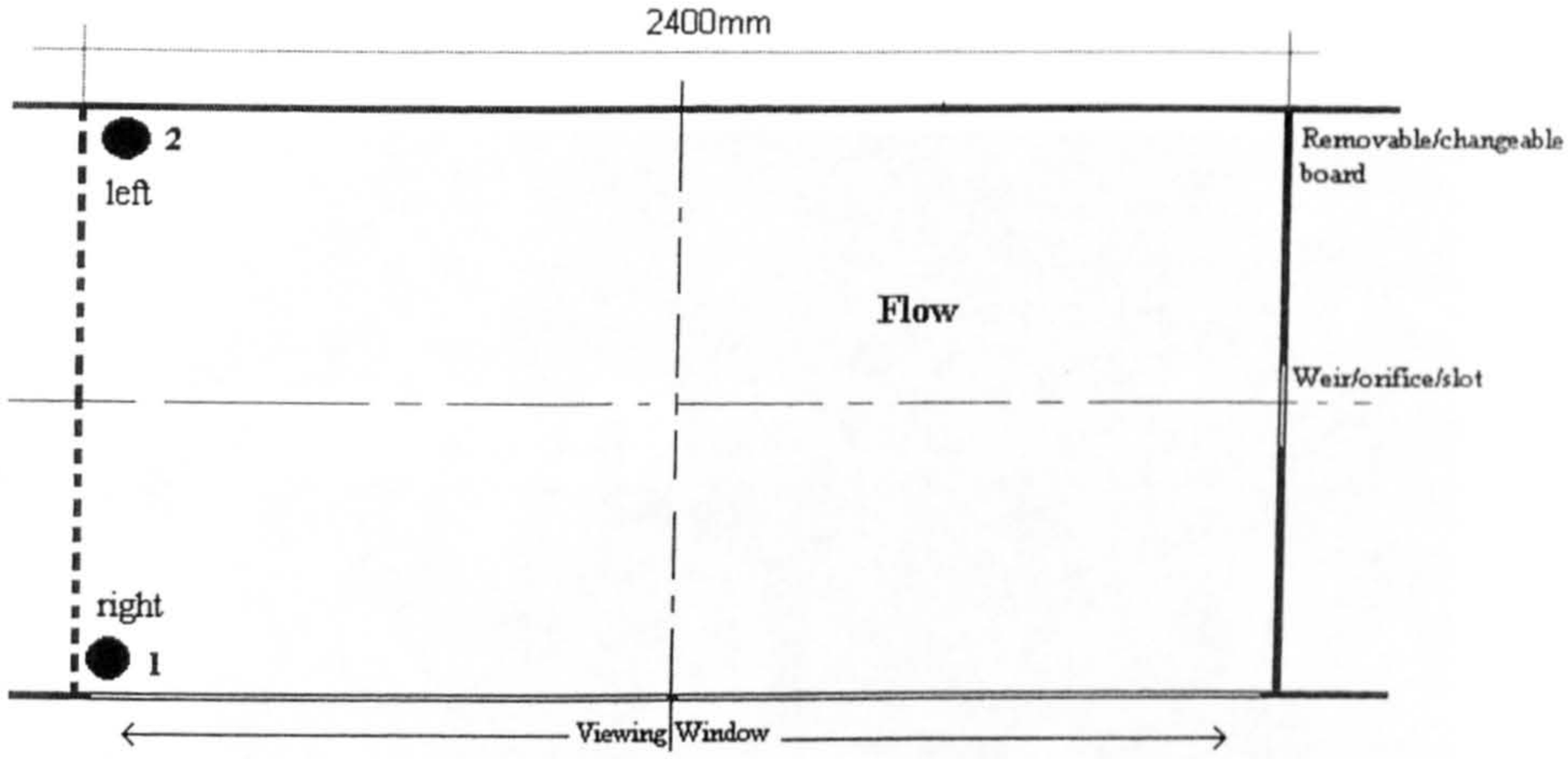

● Location of parr introduction in the flume - 1: Series I to Series III & half Series IV
2: half Series IV

Figure 4-7: Sketch showing location of introduction of parr for series 1 to 4.

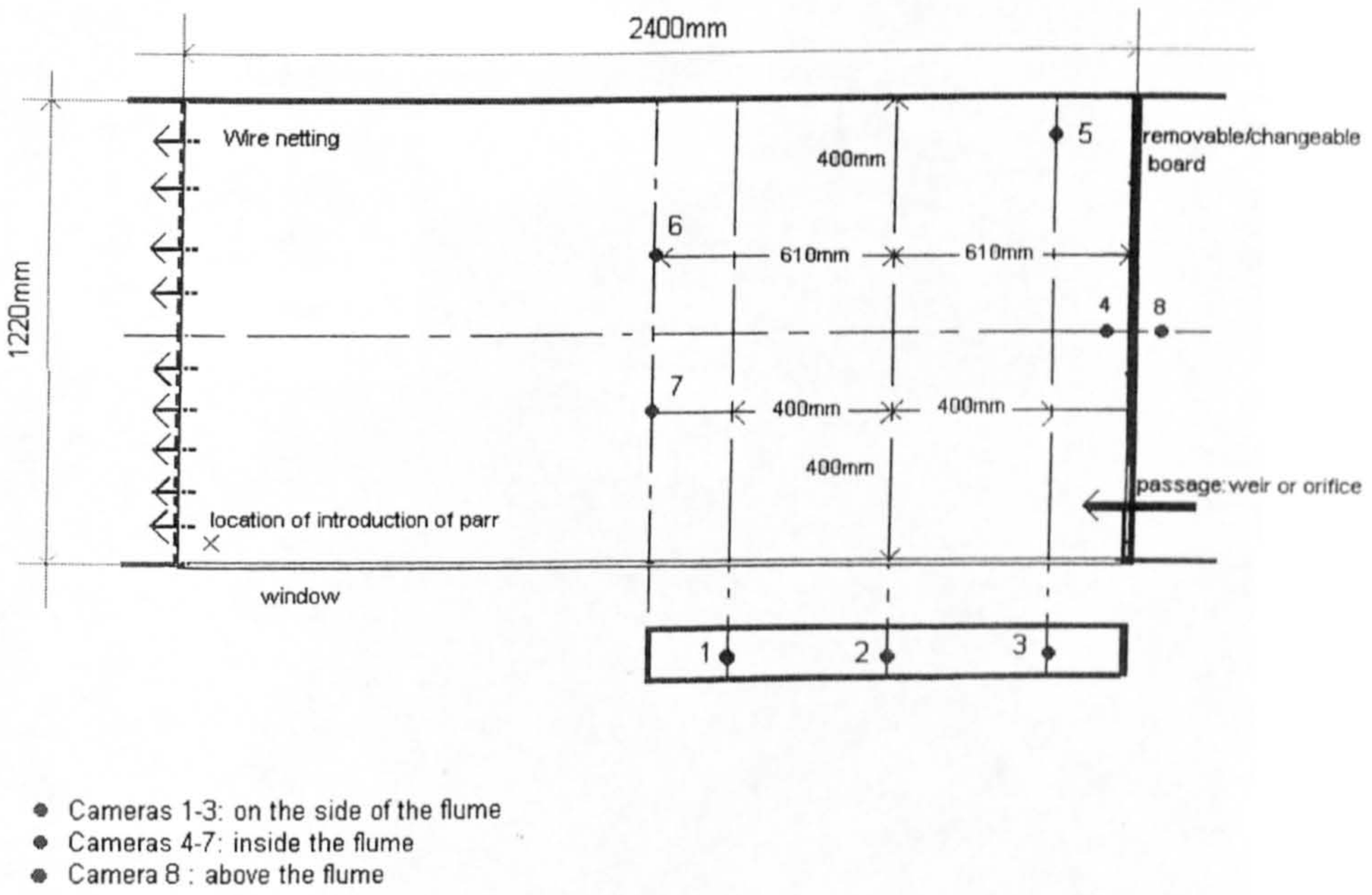

- Cameras 1-3: on the side of the flume
- Cameras 4-7: inside the flume
- Camera 8 : above the flume

Figure 4-8: Position of camera in the flume for the weir/orifice passage on the side. Position of camera 4 changes for the weir/orifice in the middle

Figure 4-9: Video recording system

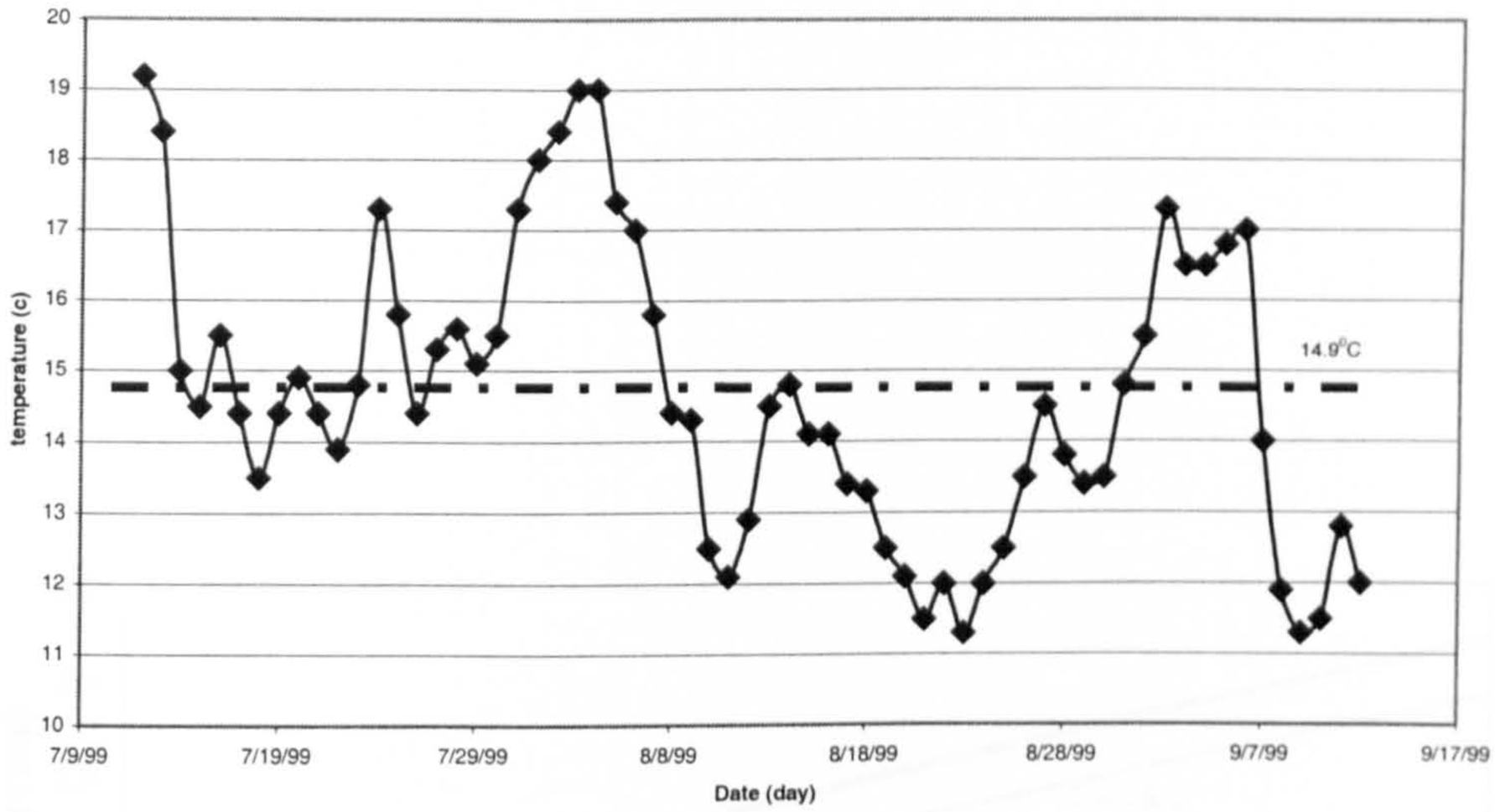

Figure 4-10: Temperature of the water in the flume during the testing period of series I

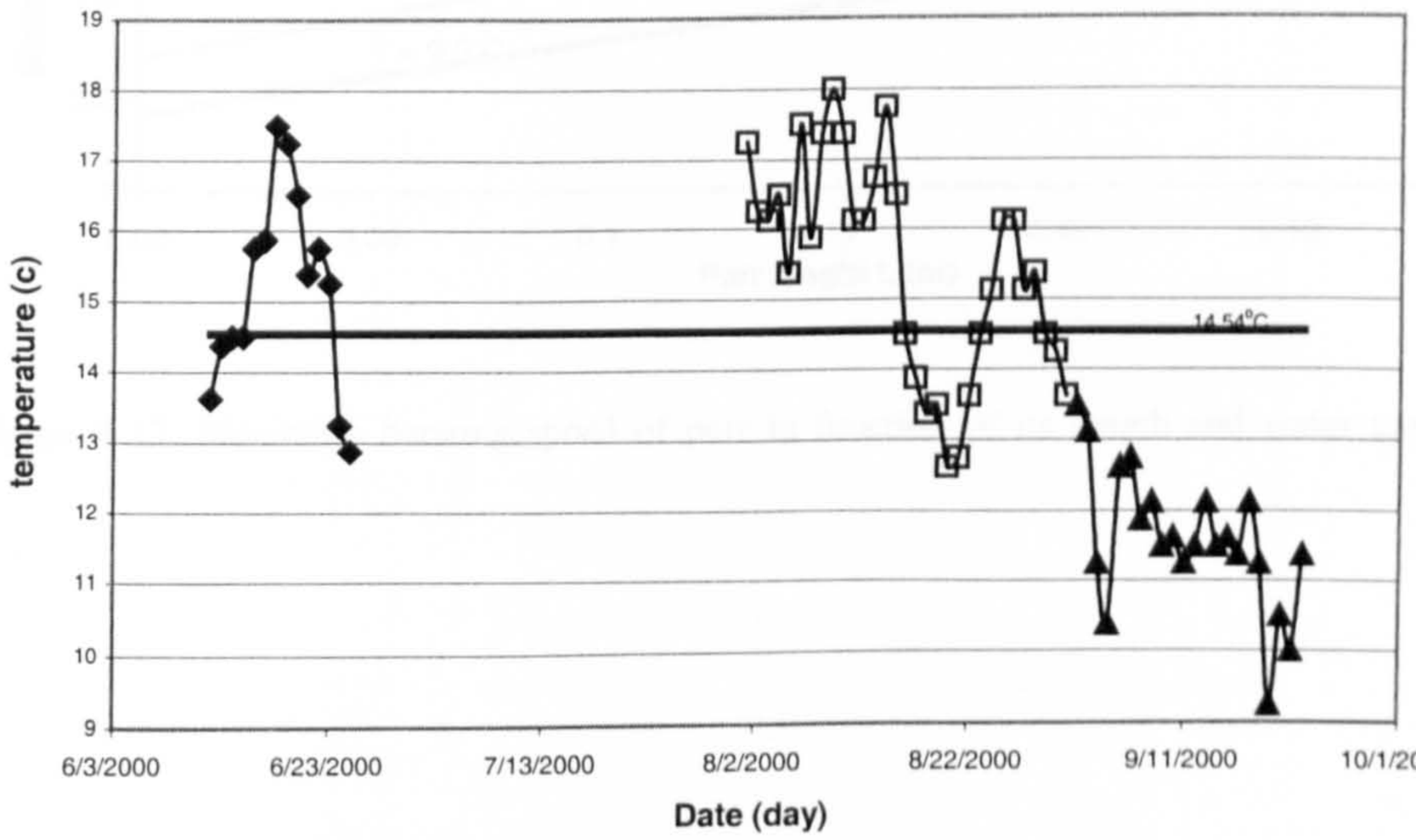

Figure 4-11: Temperature of the water in the flume during the testing period of series II to IV (the mean temperatures for series II, III and IV are respectively 15.34°C, 15.47°C and 11.57°C)

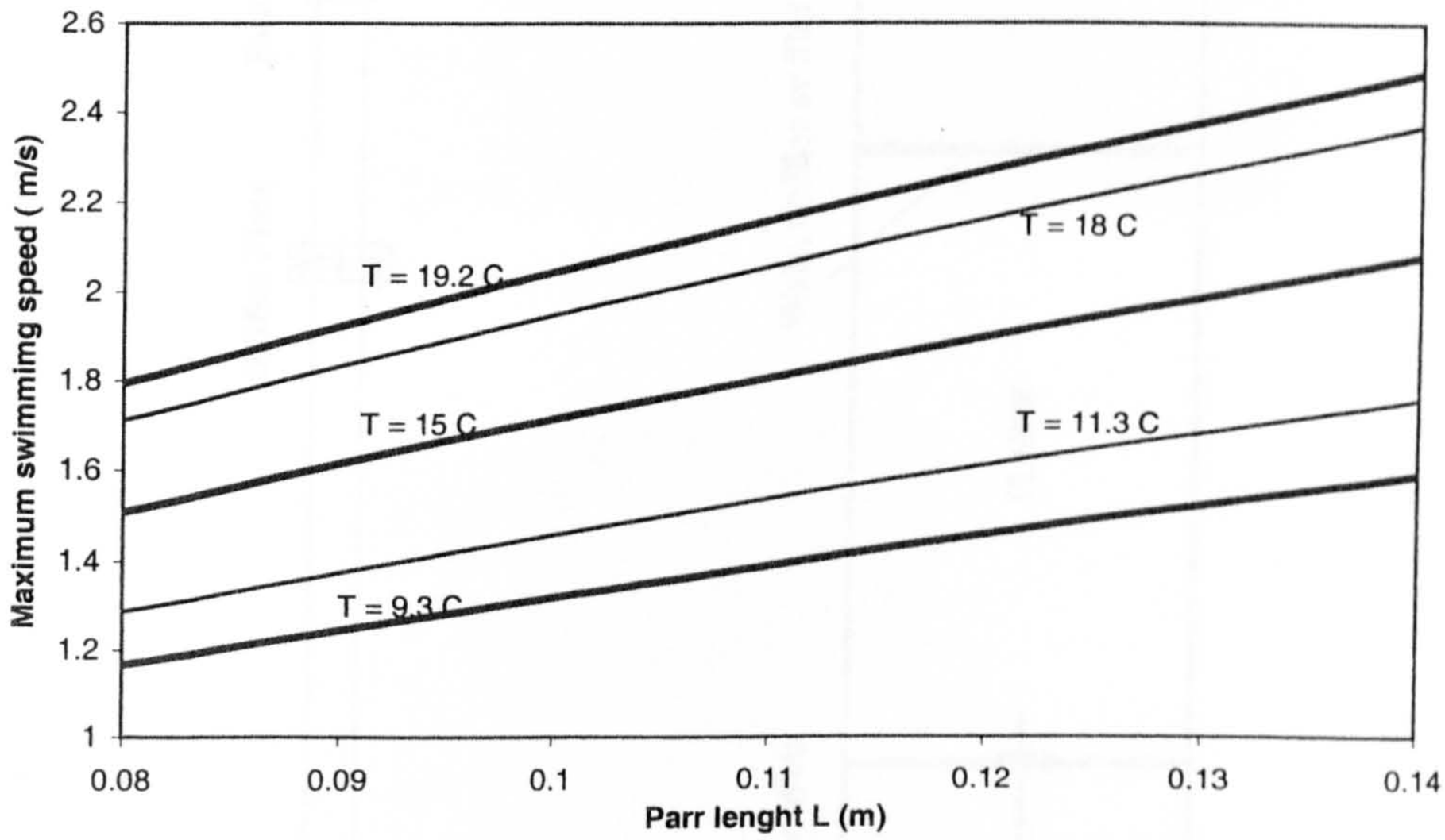

Figure 4-12: Maximum bursting speed of parr in function of its length and water temperature

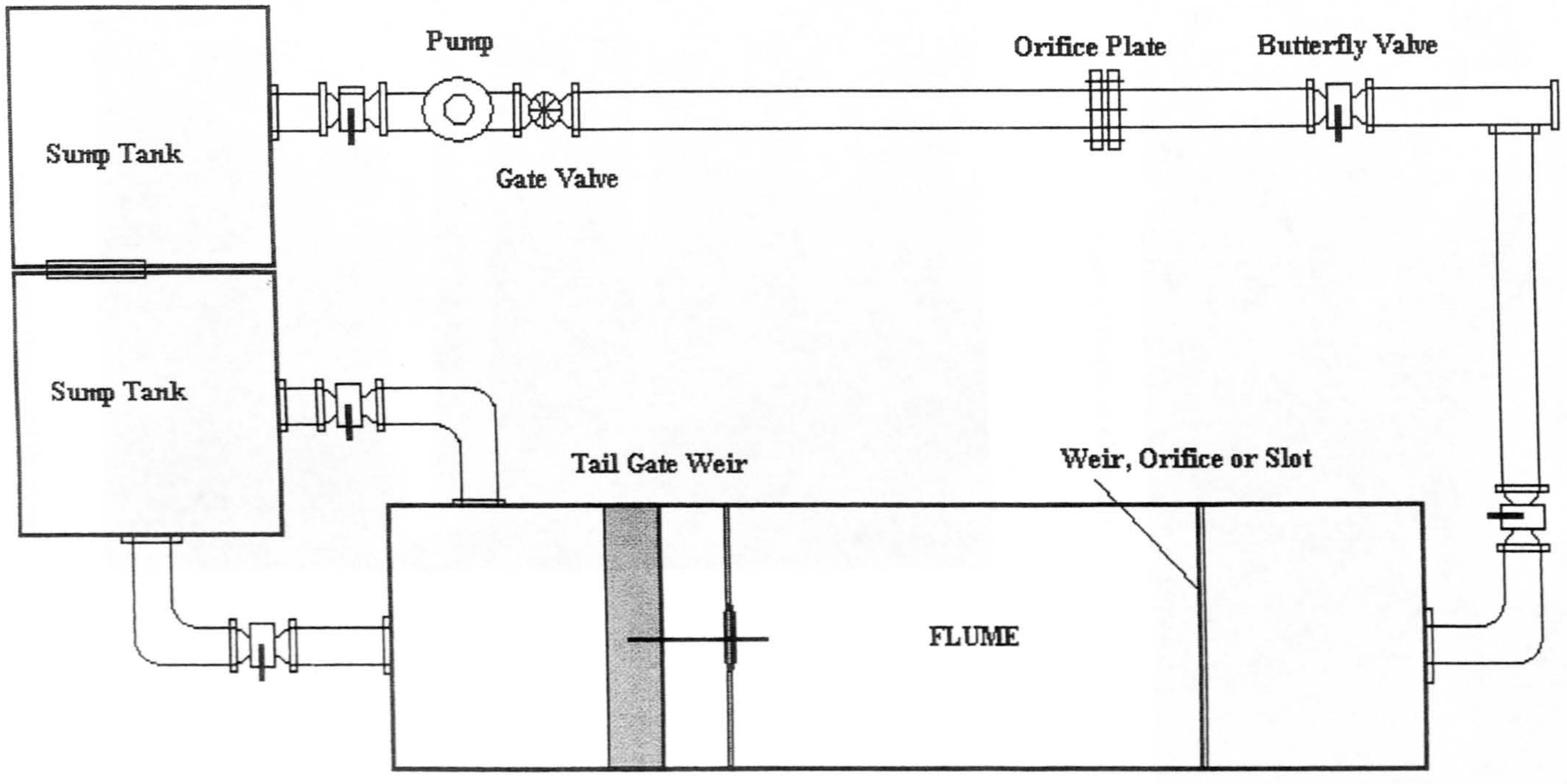

Figure 4-13: Plan of Glasgow Flume – Plan view

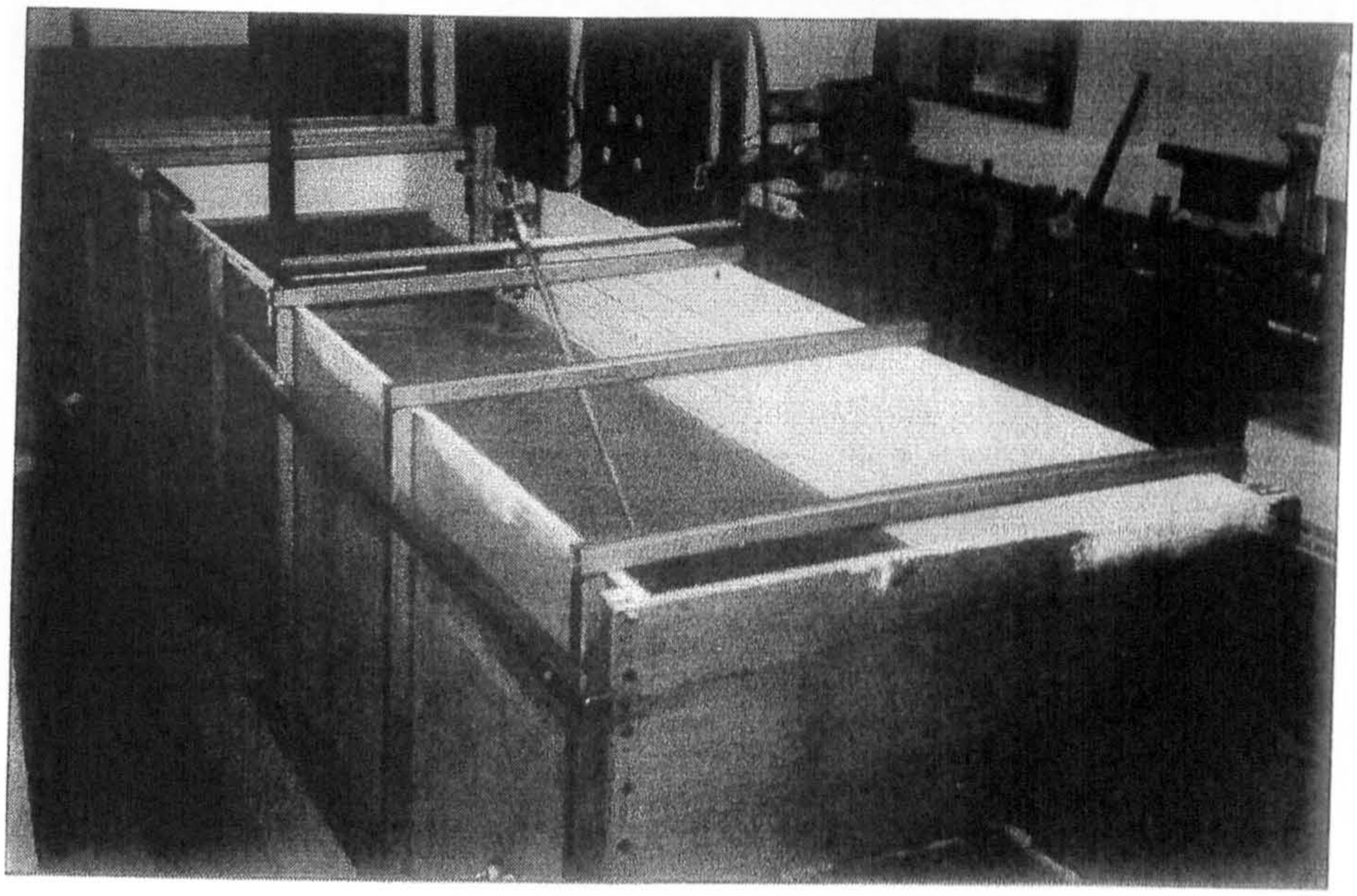

Figure 4-14: General view of experimental flume at Glasgow

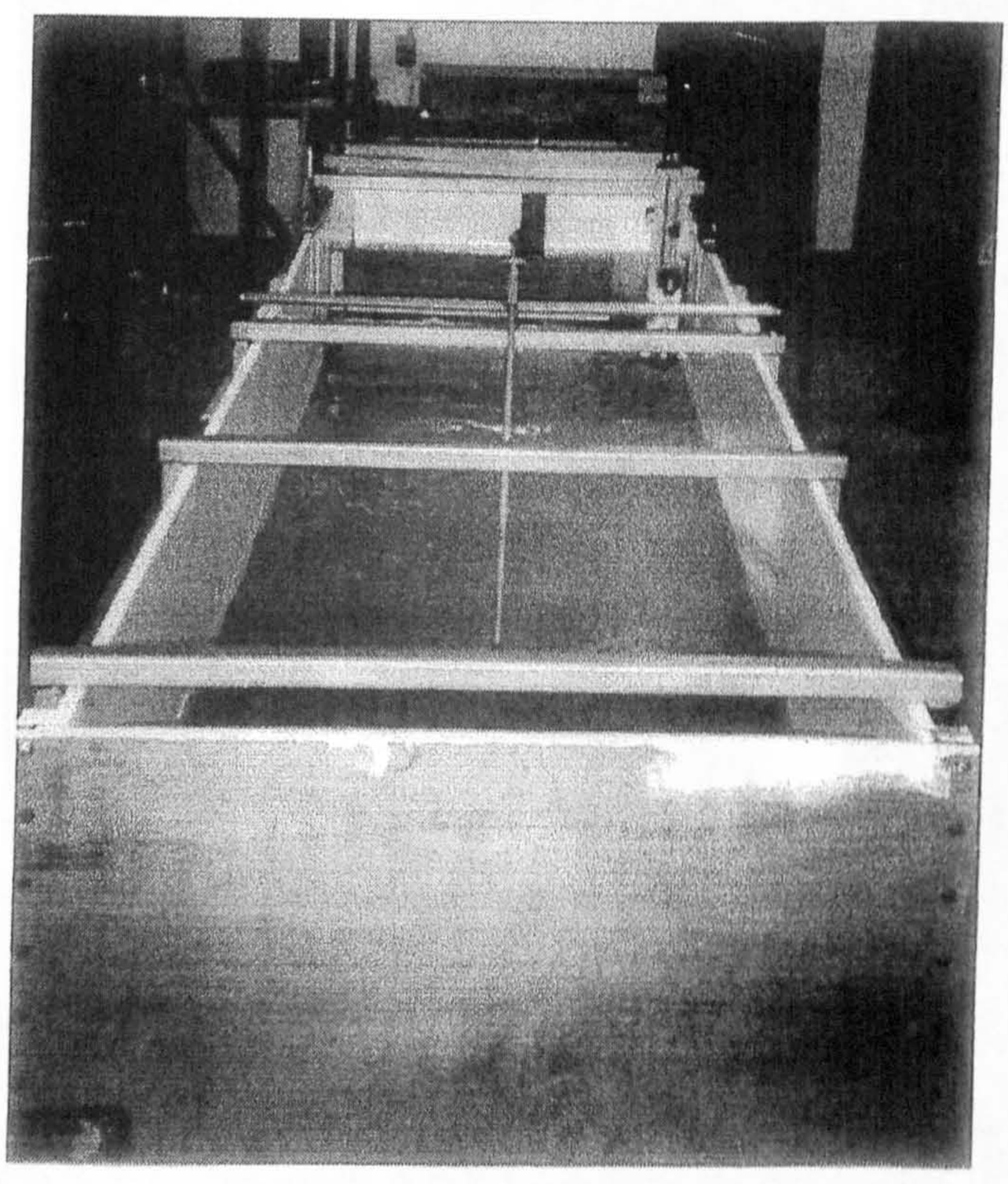

Figure 4-15: General view of experimental flume at Glasgow

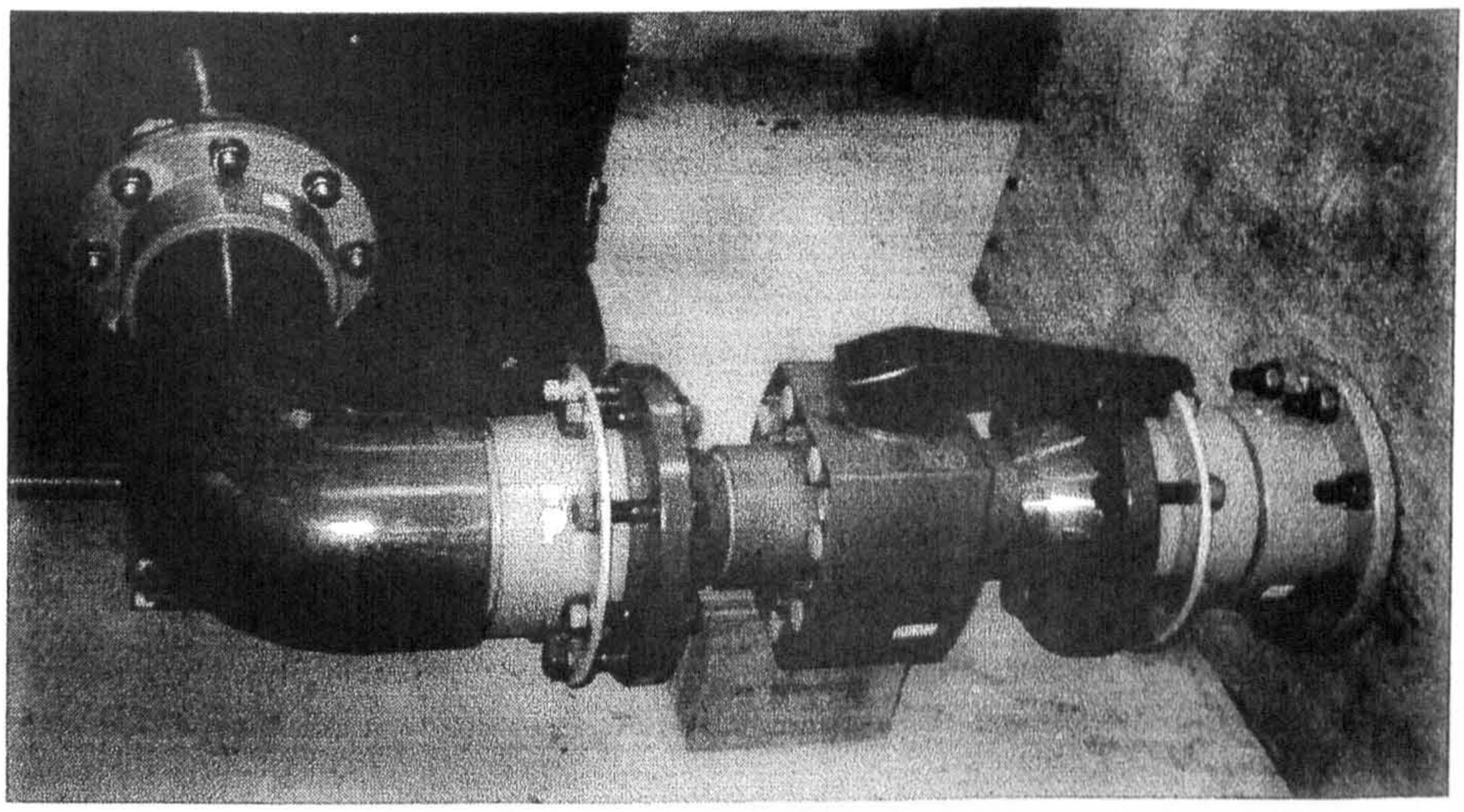

Figure 4-16: Valve between the channel flume and the galvanised steel tanks

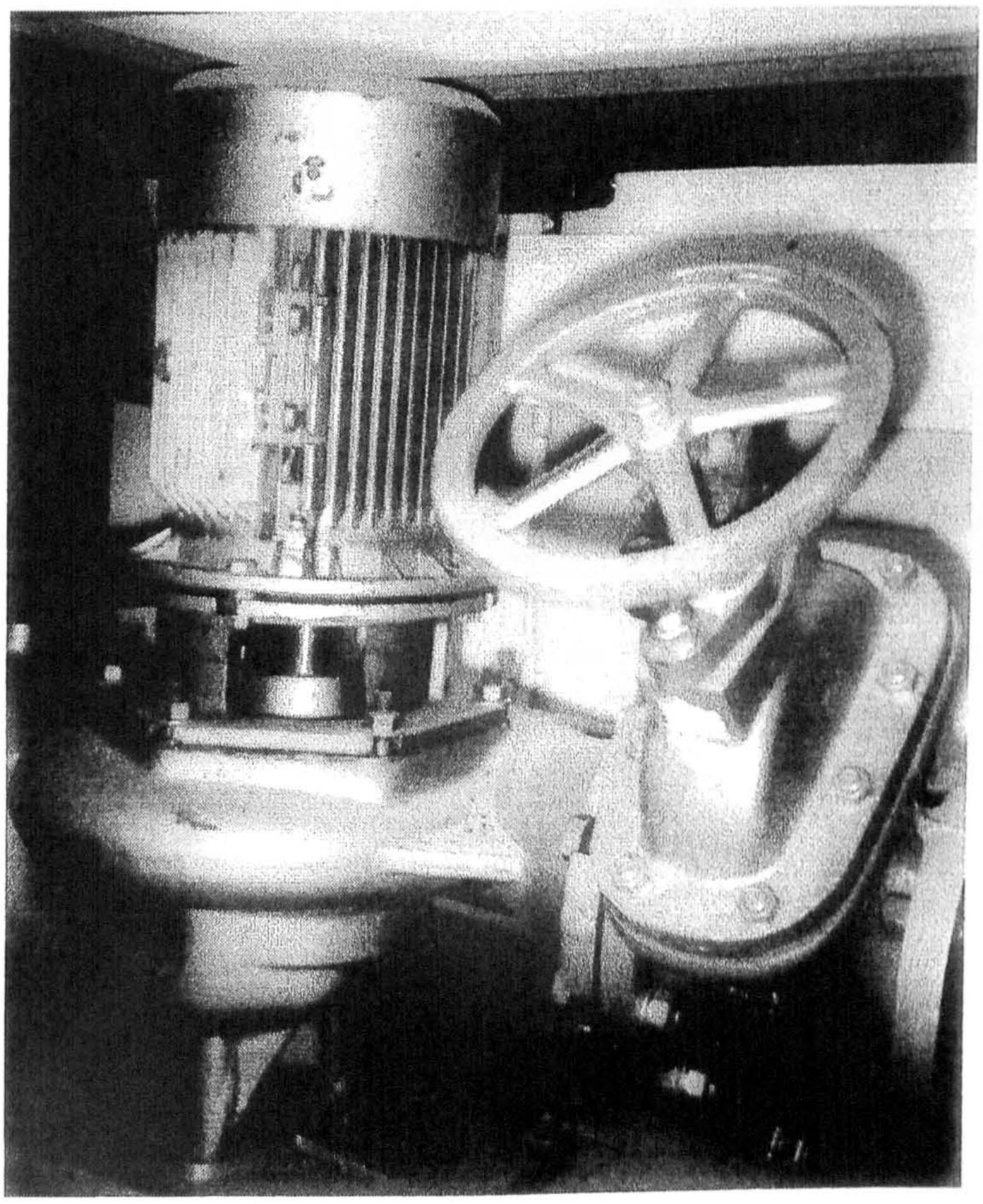

Figure 4-17: Pump MYSON MSK 150-4210

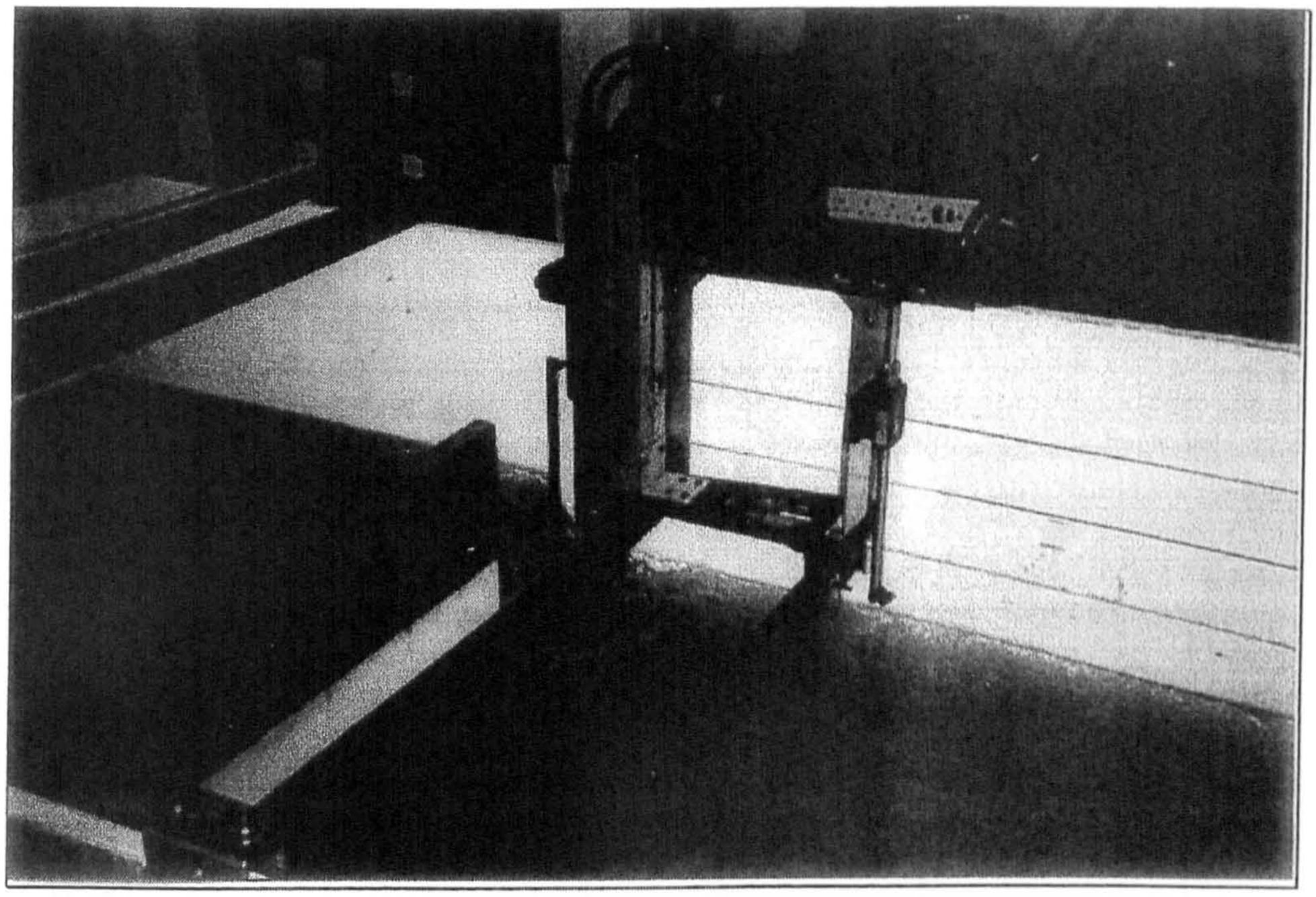

Figure 4-18: Apparatus and ADV probe for velocity and turbulence measurements

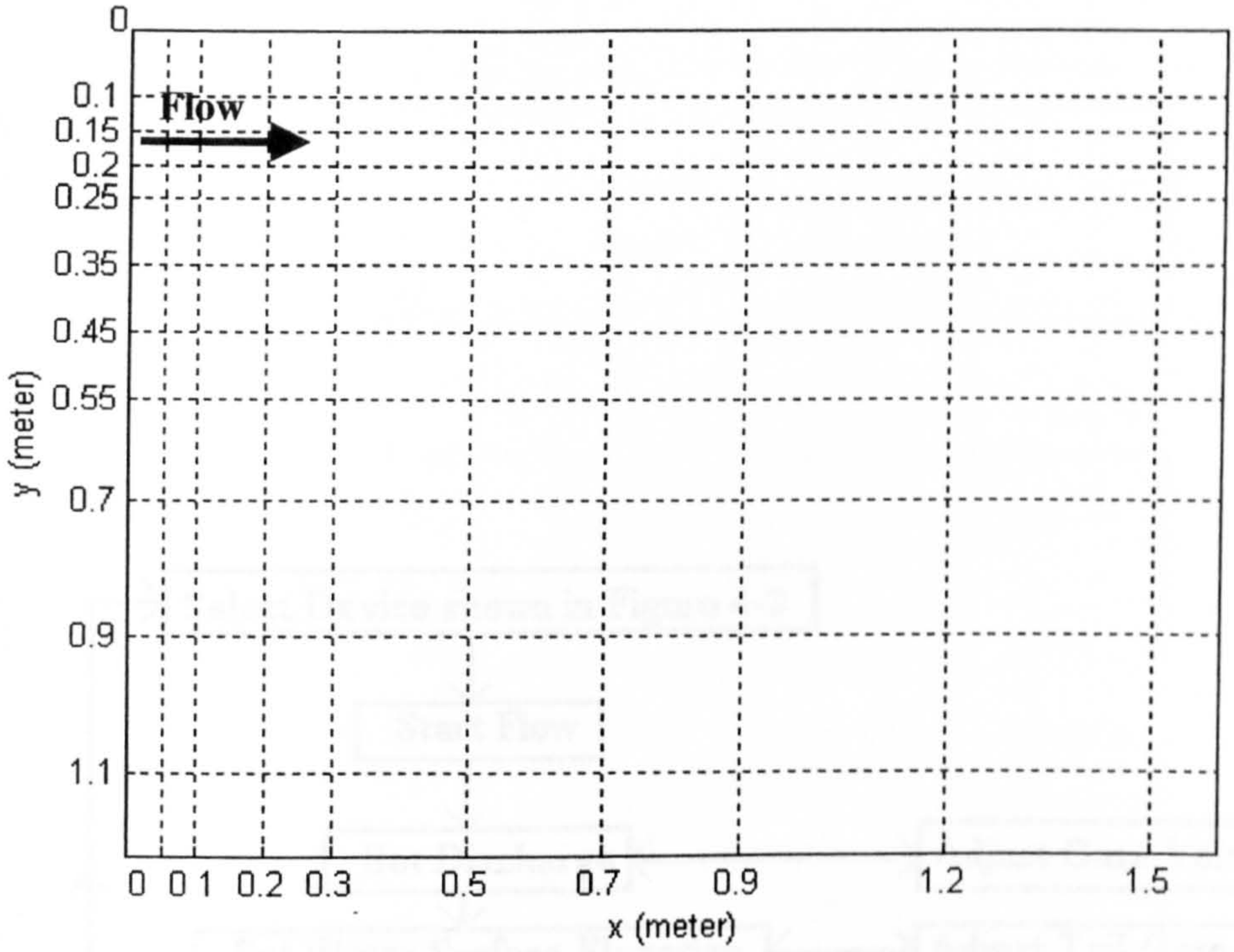

Figure 4-19: Measurement Grid if the weir/orifice is in the corner

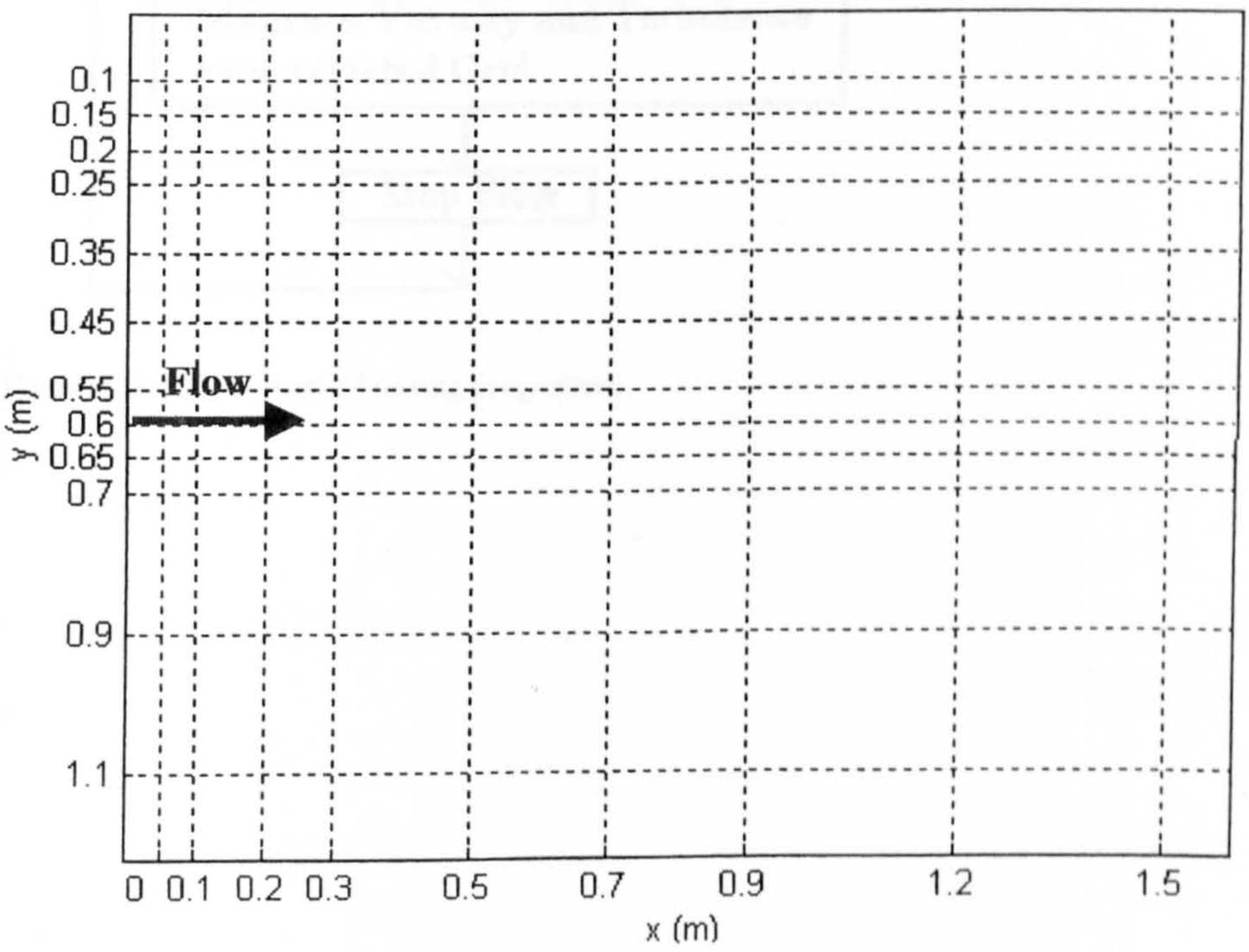

Figure 4-20:Measurement Grid if the weir/orifice is in the middle

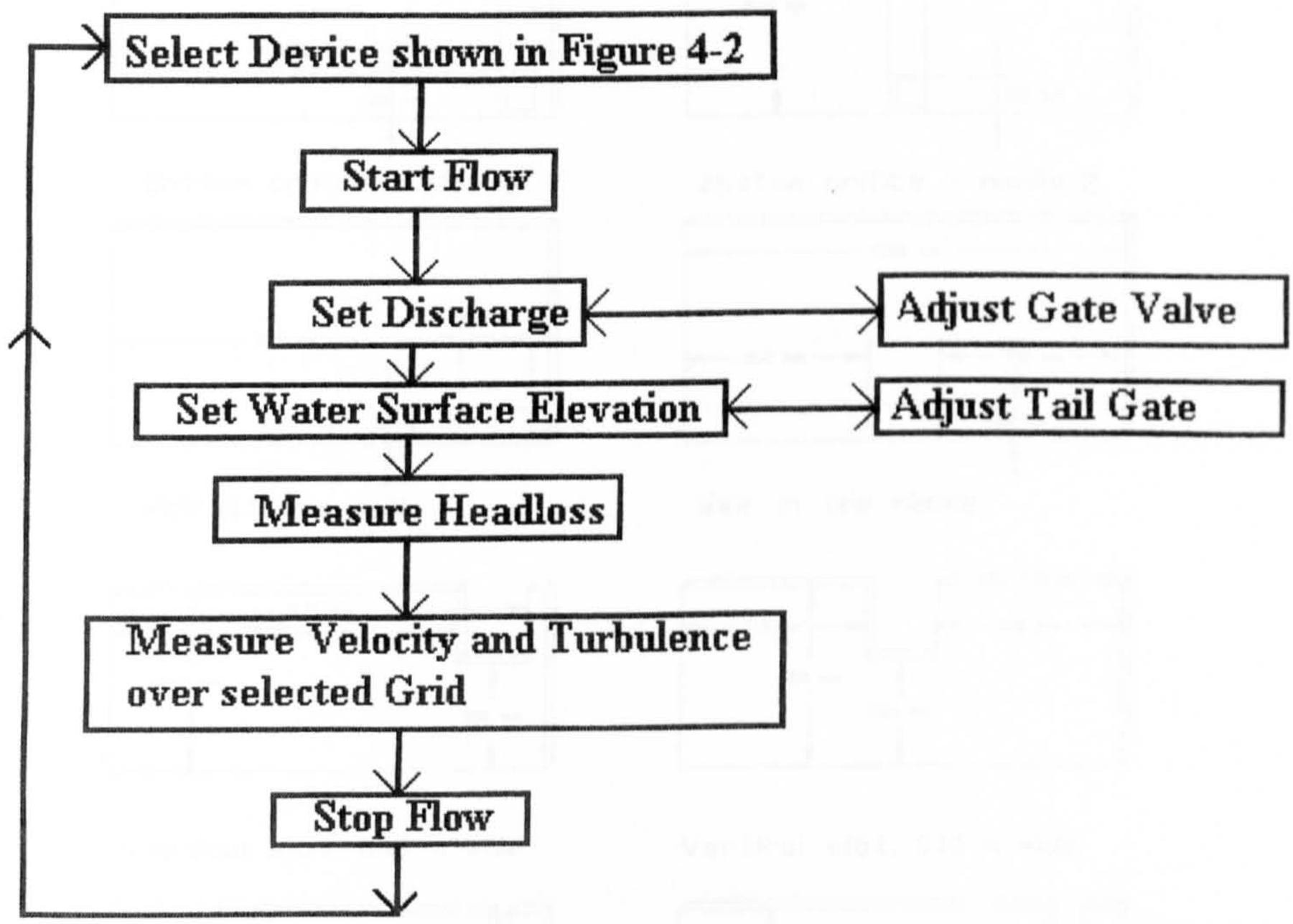

Figure 4-21: Flow chart of testing programme

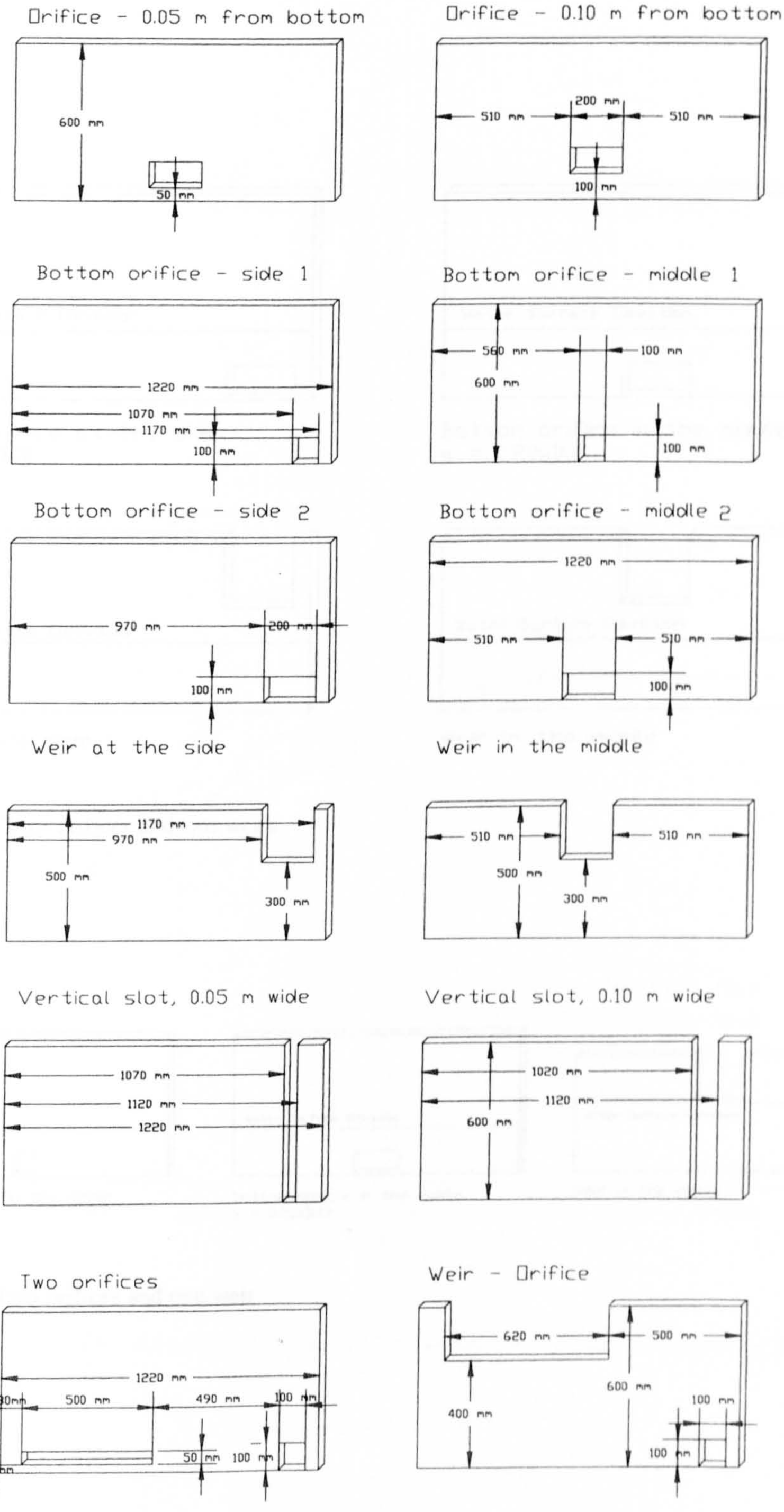

Figure 5-1: Schematic of the designs tested

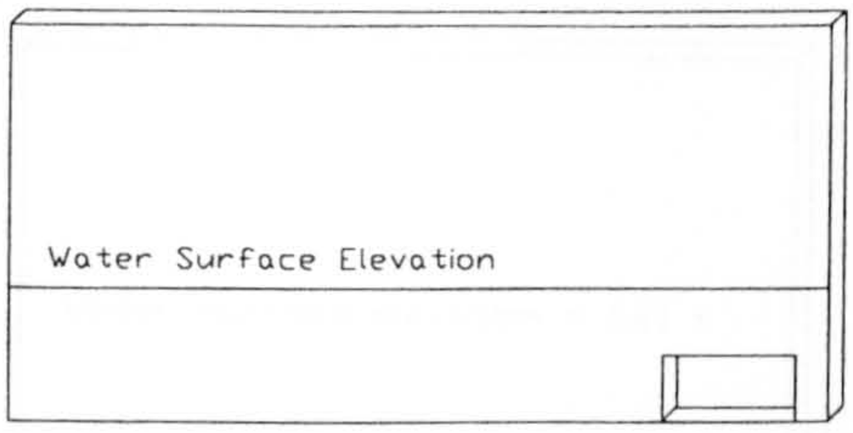

Bottom orifice at the side
a = 0.20×0.10

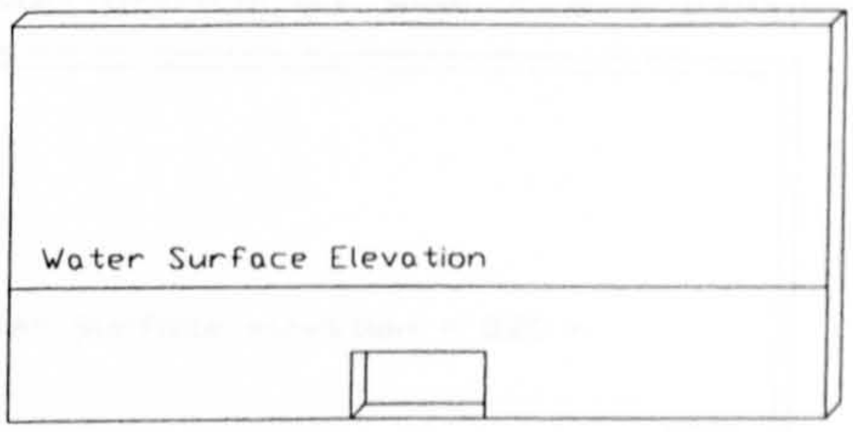

Bottom orifice in the middle
a = 0.20×0.10

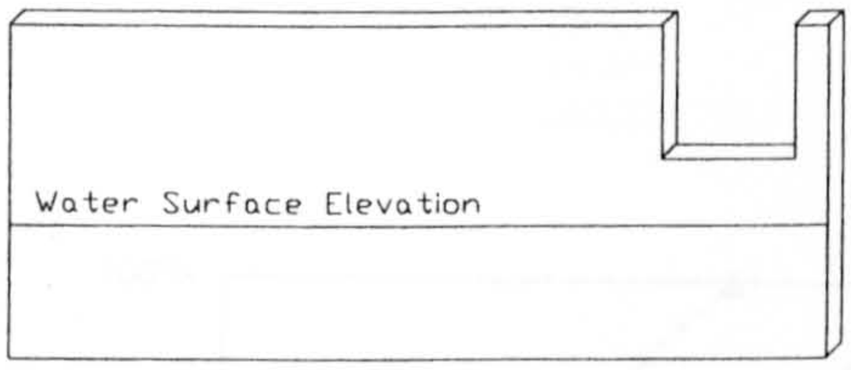

Weir at the side

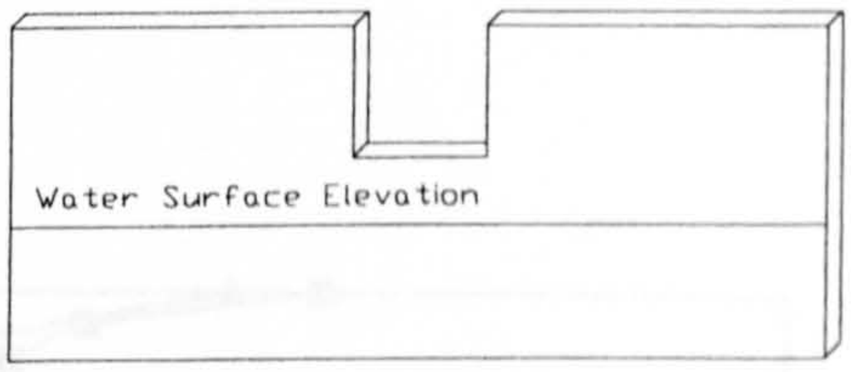

Weir in the middle

Figure 5- 2: Two orifices and two weirs

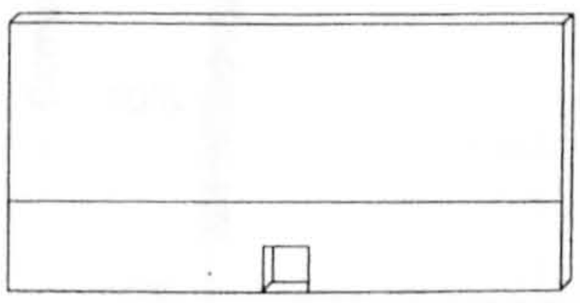

Bottom orifice in the middle
a = 0.10×0.10

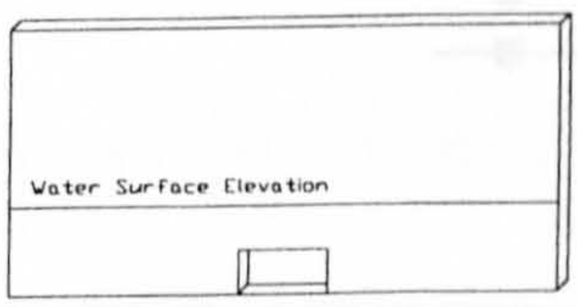

Bottom orifice in the middle
a = 0.20×0.10

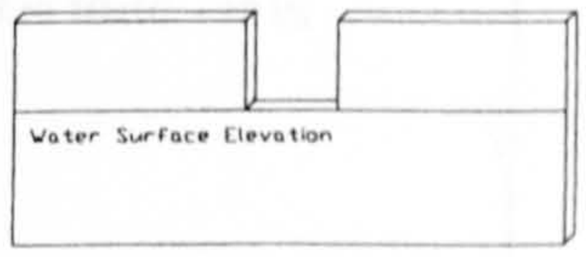

Weir in the middle

Figure 5-3: Two orifices and one weir

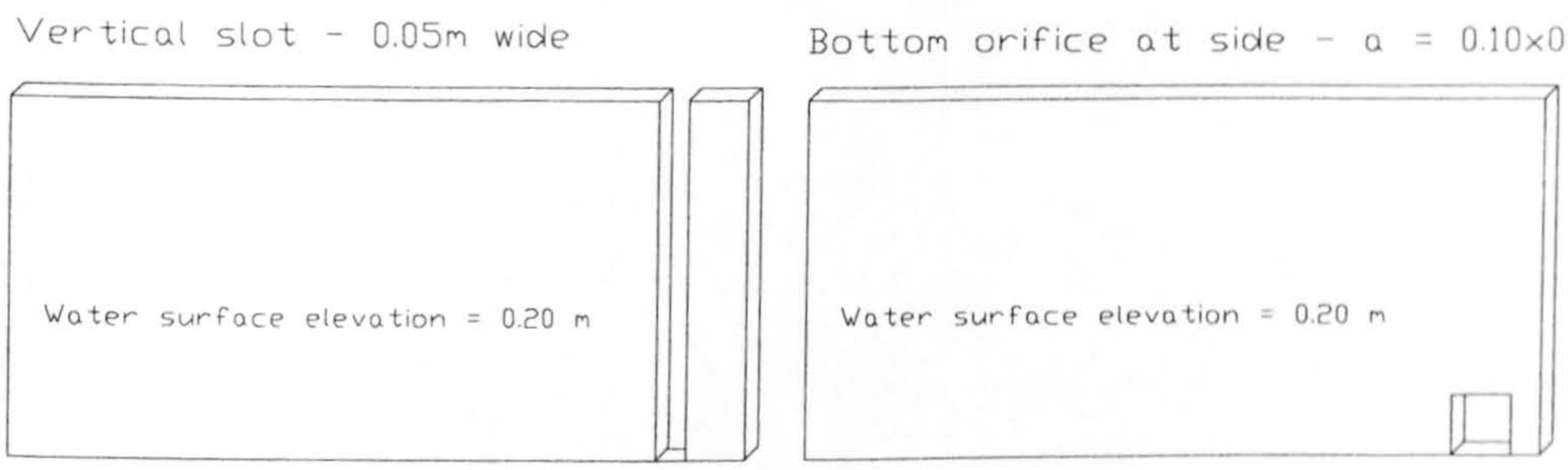

Figure 5- 4: One orifice and one vertical slot

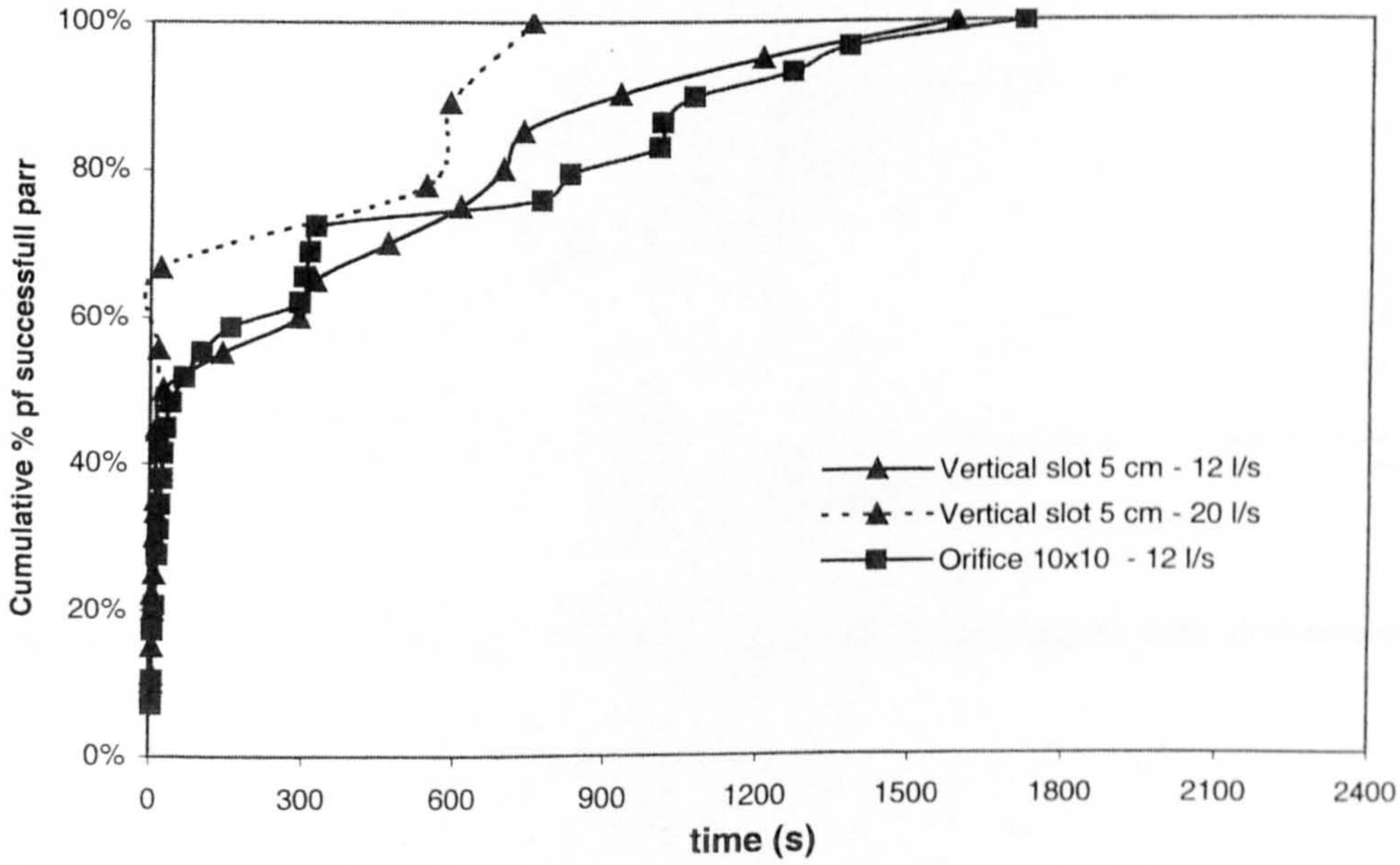

Figure 5- 5: Cumulative percentage of successful fish versus time for the different designs: ObS, WOb & V5 of series III

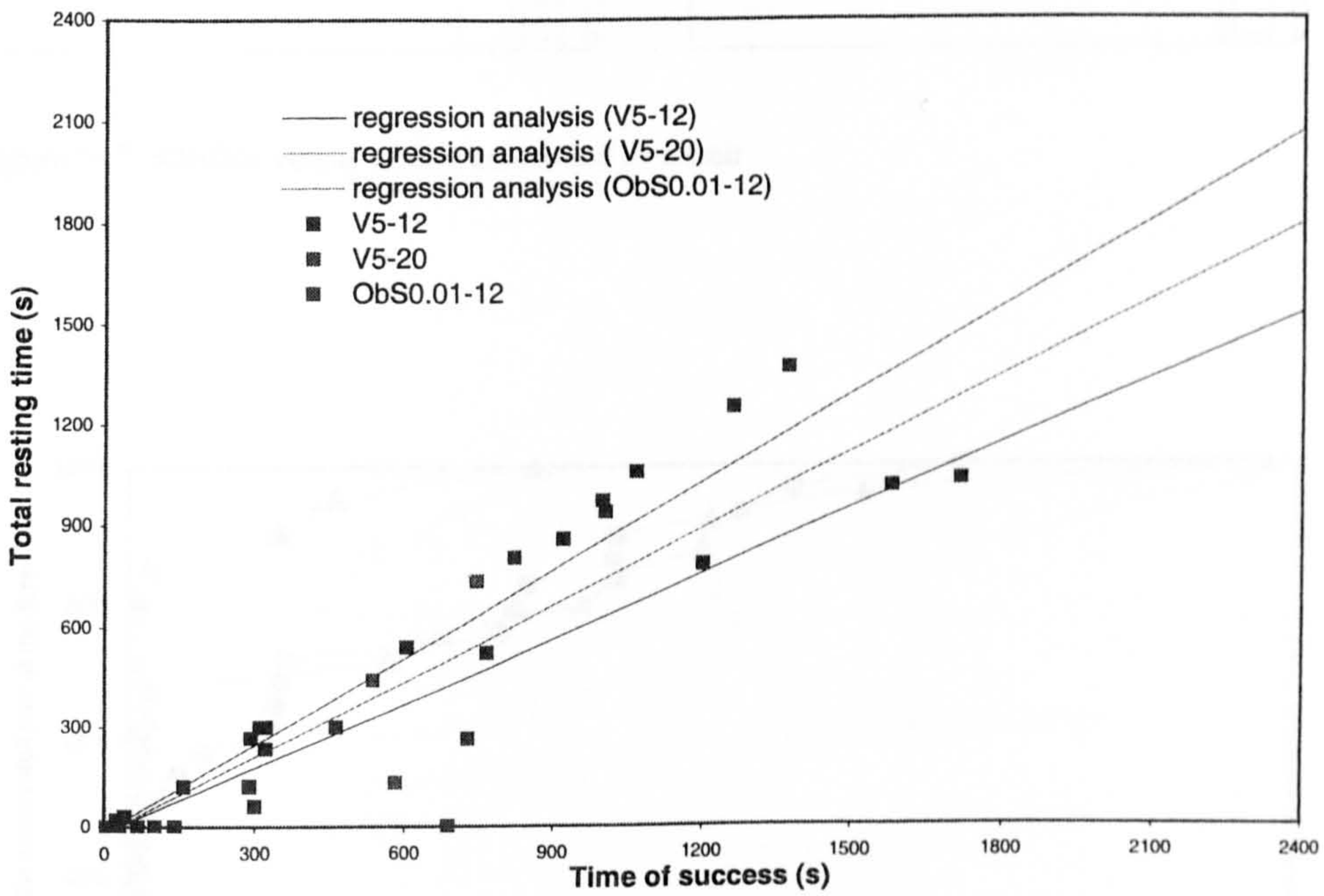

Figure 5- 6: Regression analysis: influence of the time spent in the flume on time spent resting (p = 0.000)

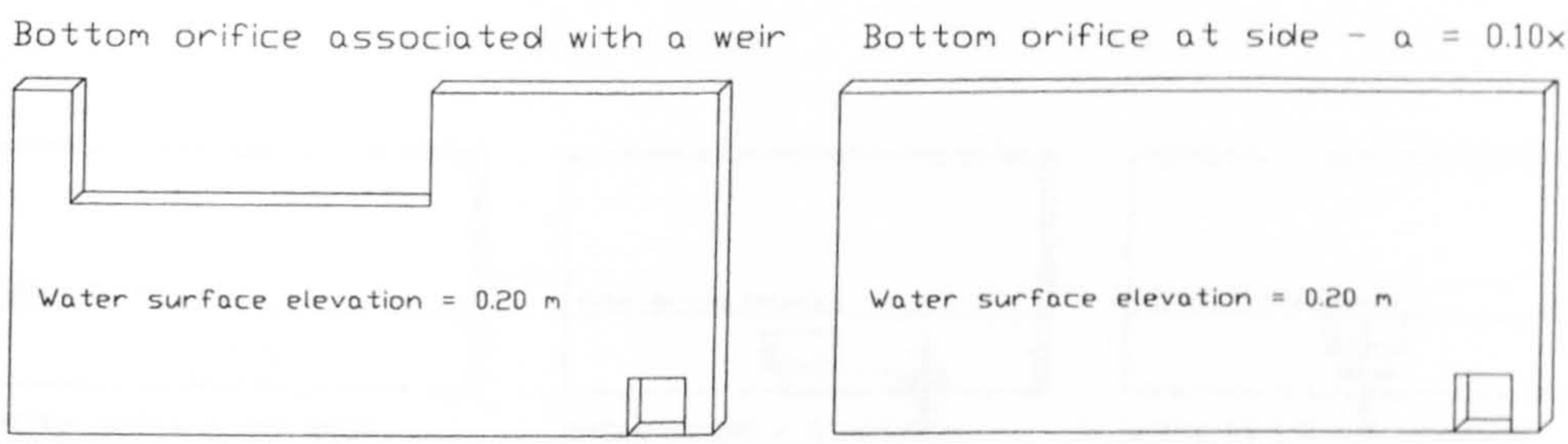

Figure 5- 7: :Orifice versus orifice associated to a weir

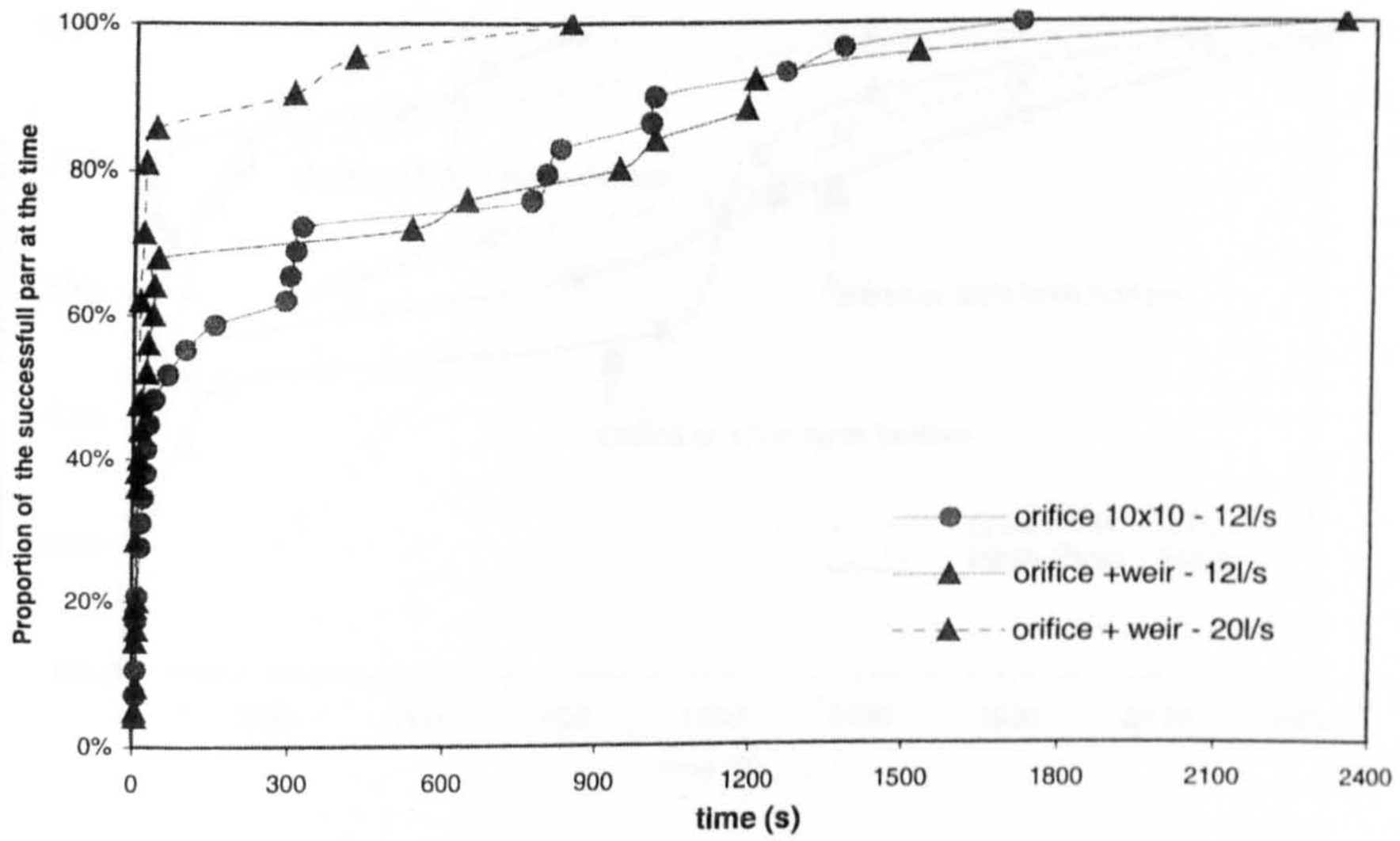

Figure 5- 8: Cumulative percentage of successful fish versus time for the different designs: ObS &WOb of series III

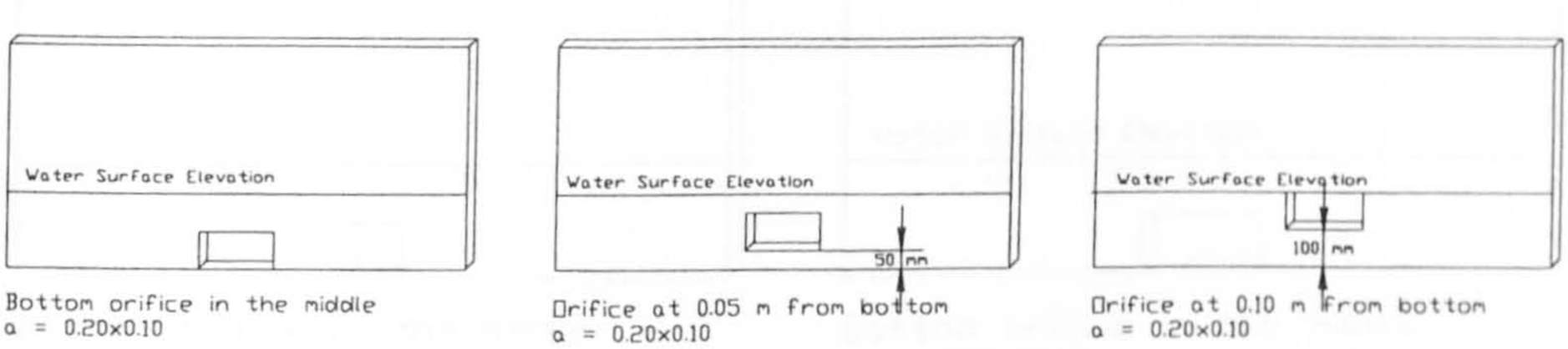

Figure 5- 9: Three orifices at 3 different elevations

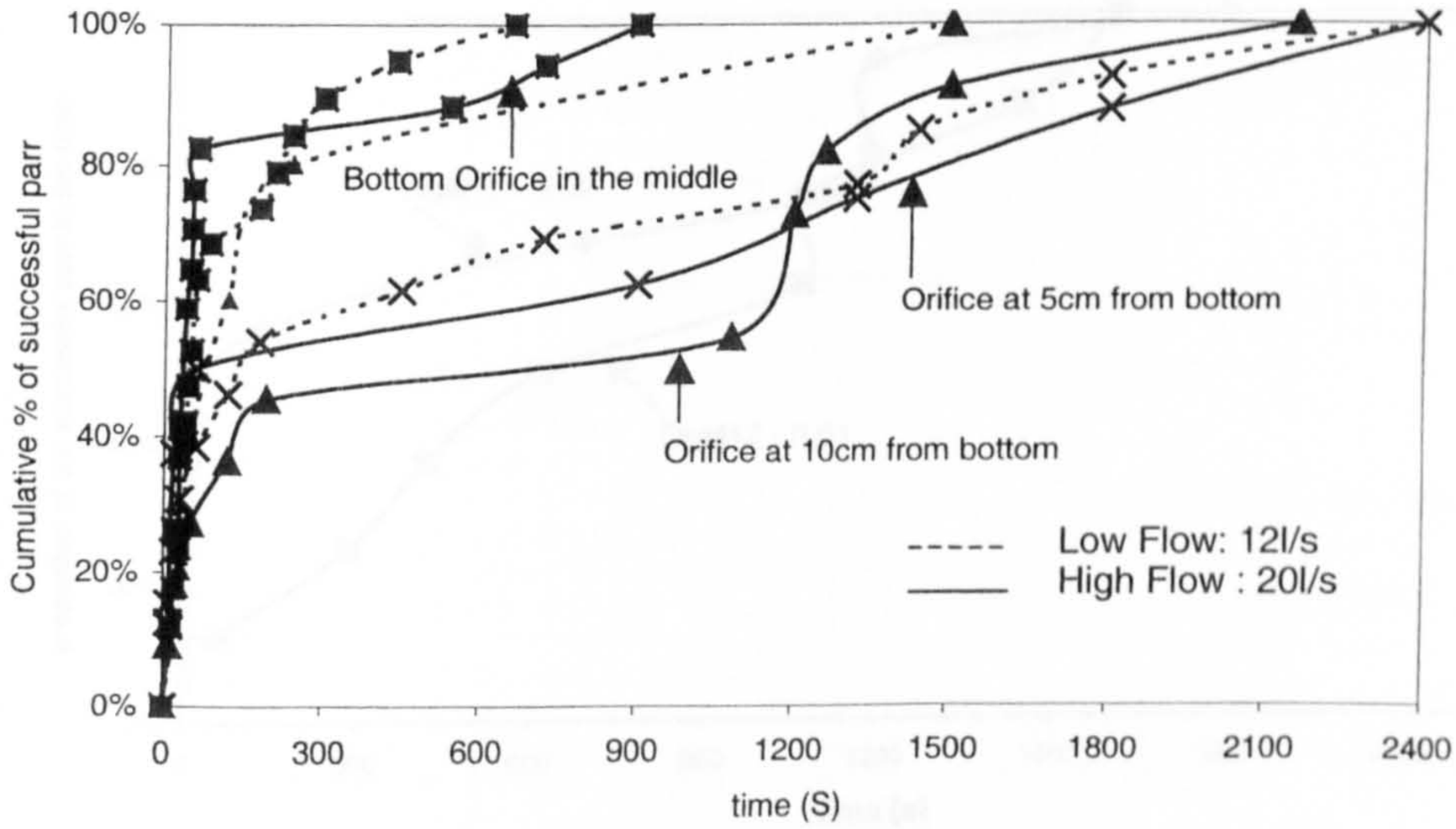

Figure 5-10: Cumulative percentage of successful fish versus time for the different orifice designs

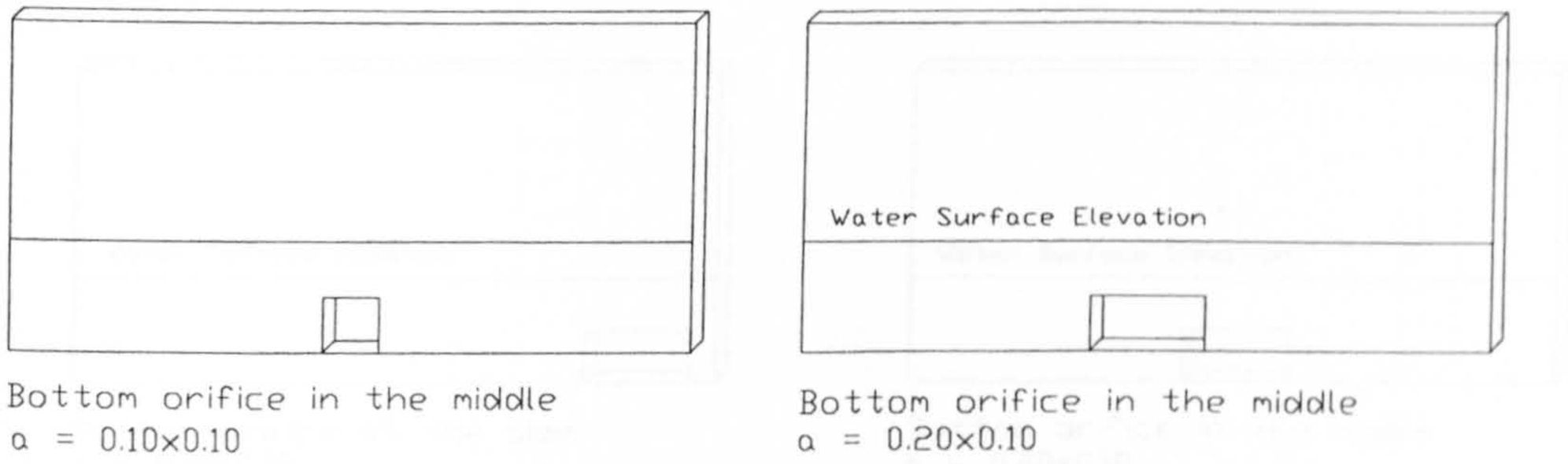

Figure 5- 11: Two bottom orifices in the middle with different areas

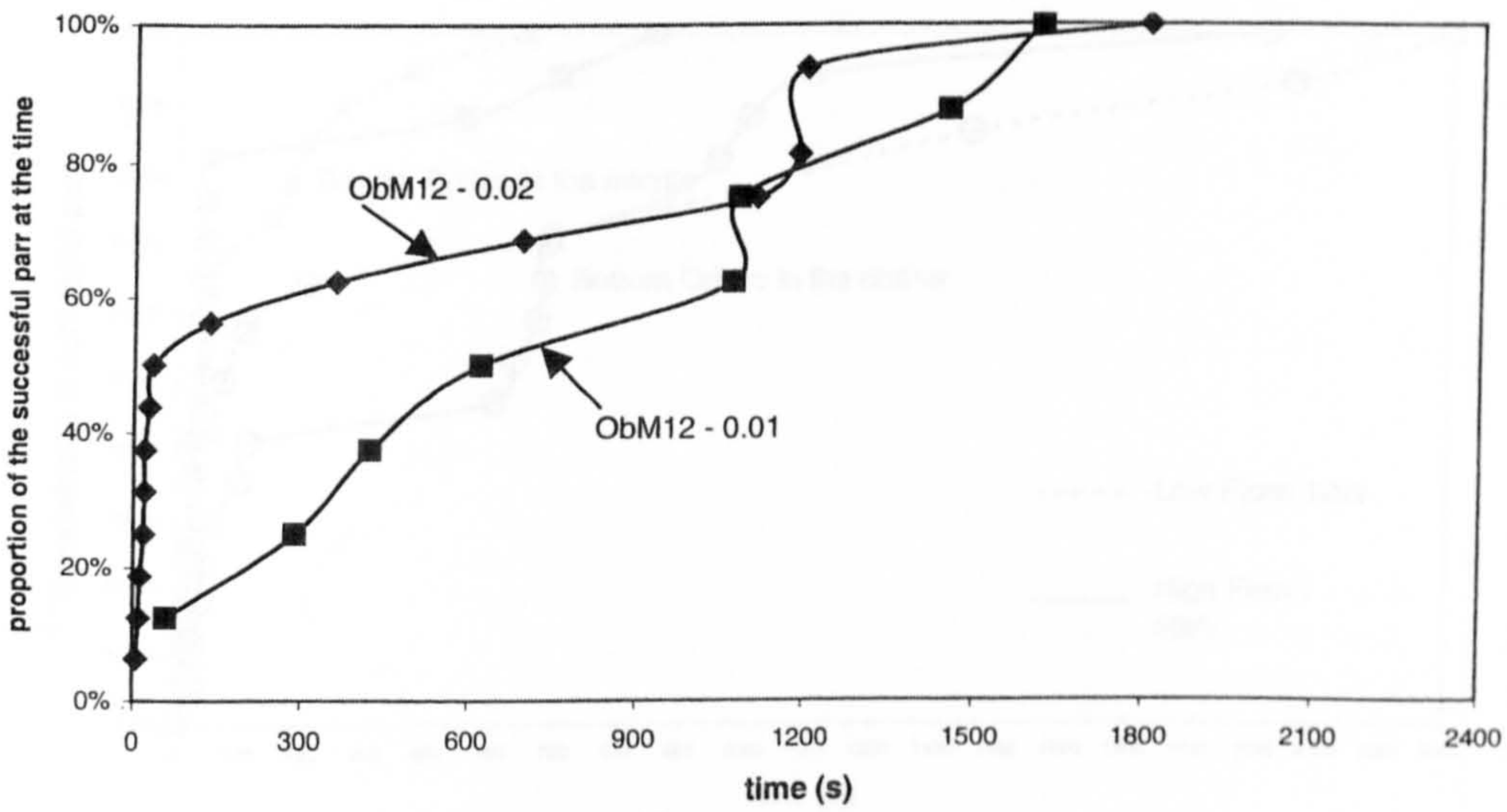

Figure 5- 12: Cumulative percentage of successful fish versus time for the two orifices designs of series II

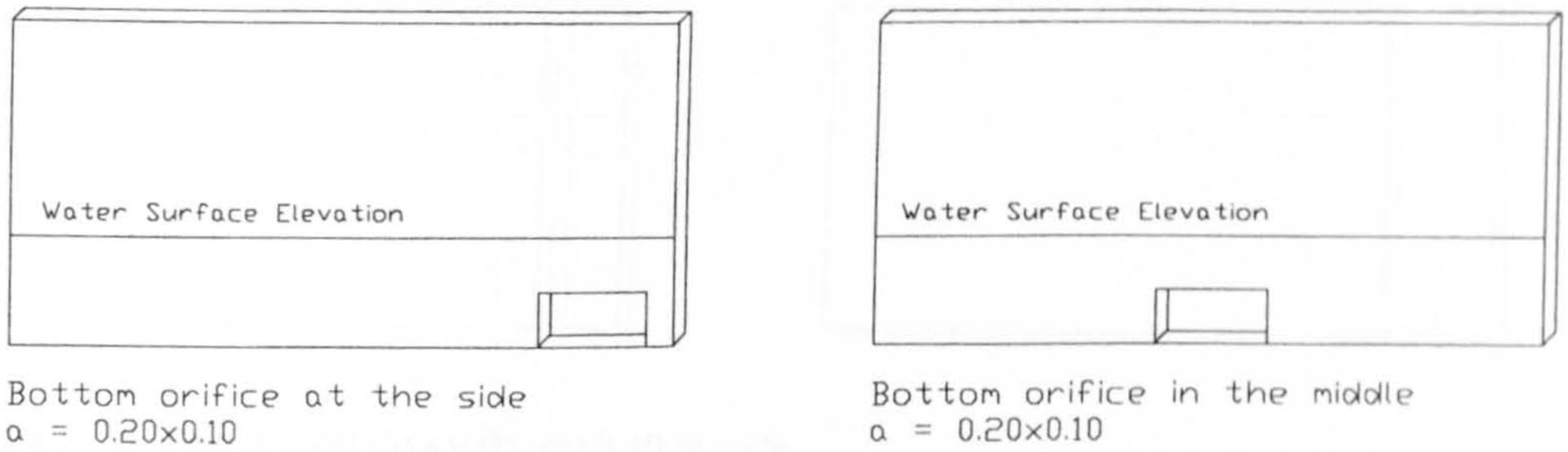

Figure 5- 13:Two 0.20 by 0.10 m orifices at two different locations

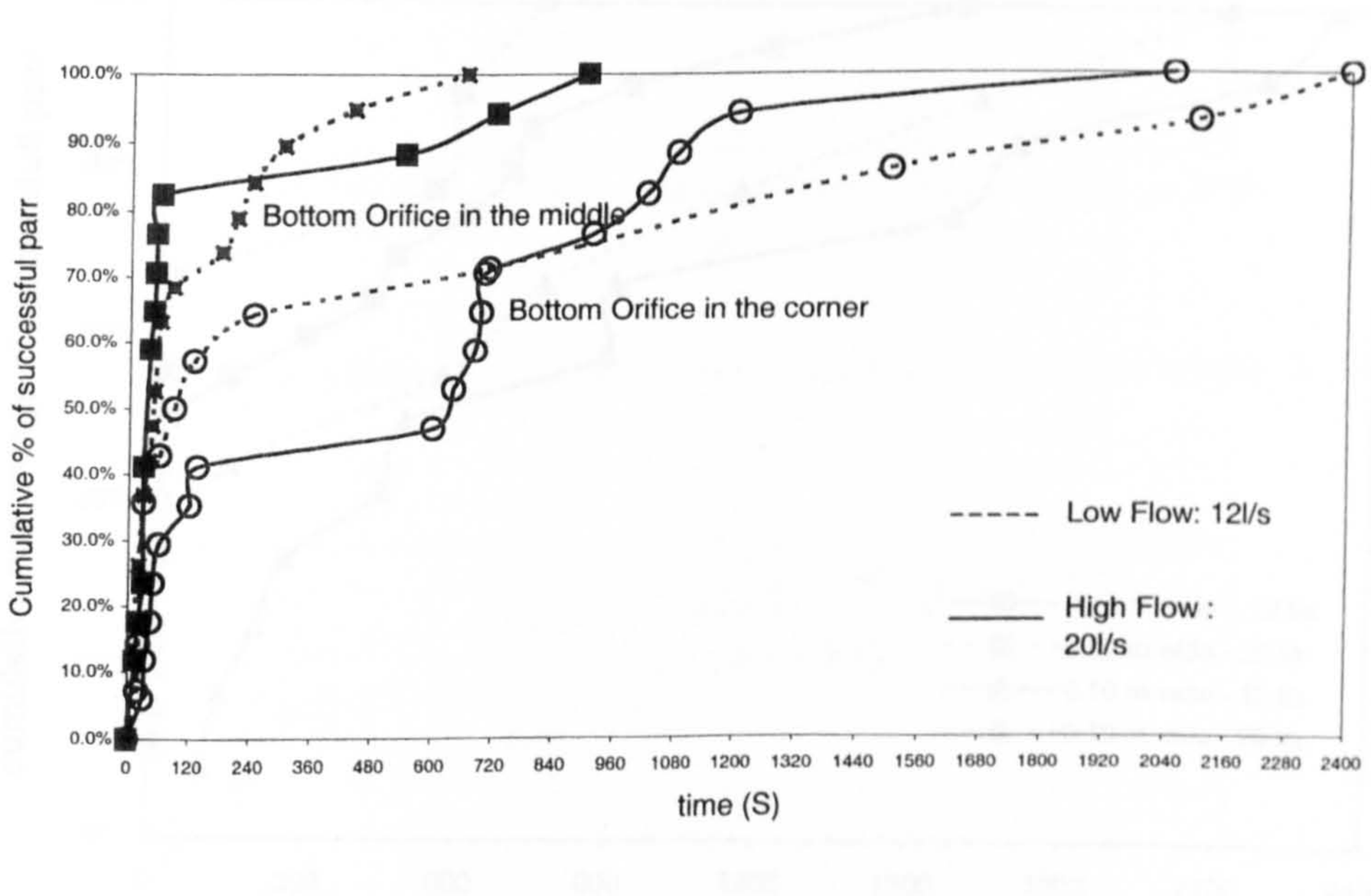

Figure 5-14: Cumulative percentage of successful fish versus time for the different orifice designs

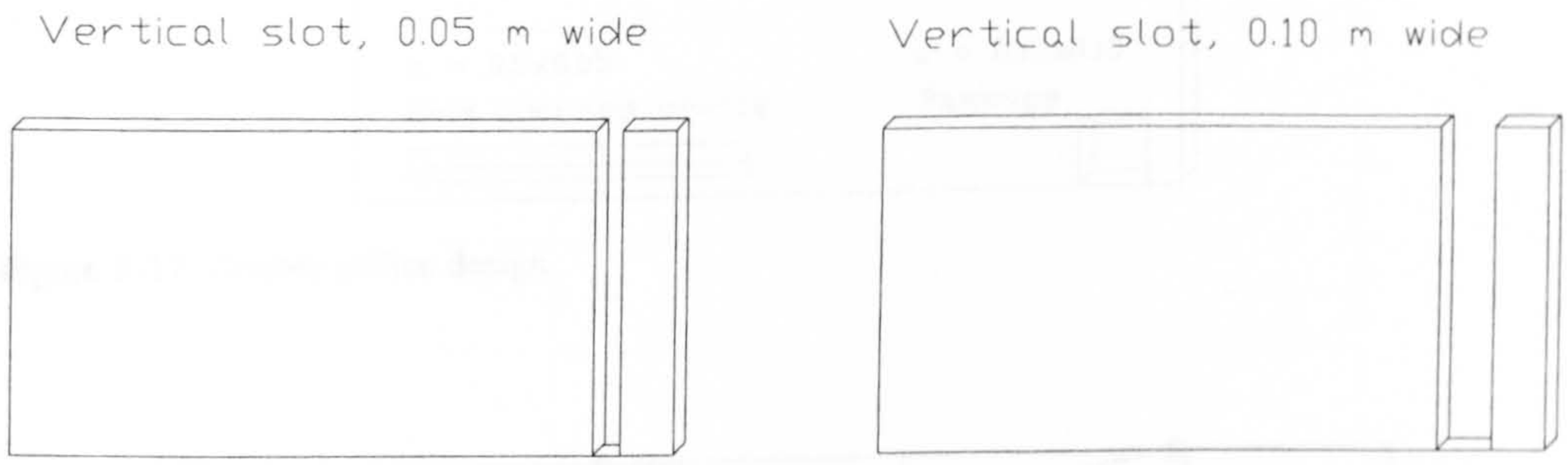

Figure 5- 15: Two vertical slots 0.05 and 0.10 m wide

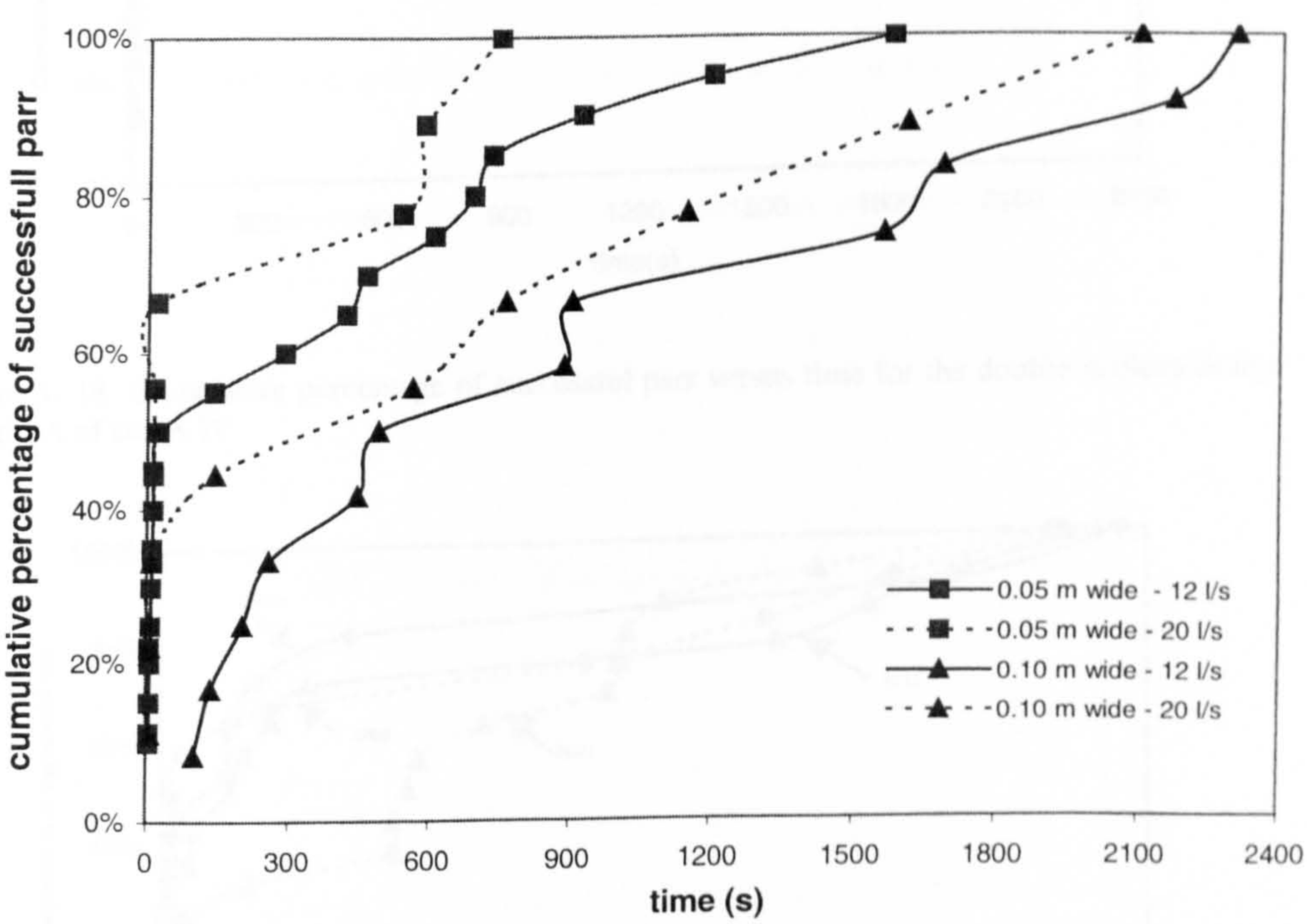

Figure 5-16:Cumulative percentage of successful fish versus time for the vertical slots of series III

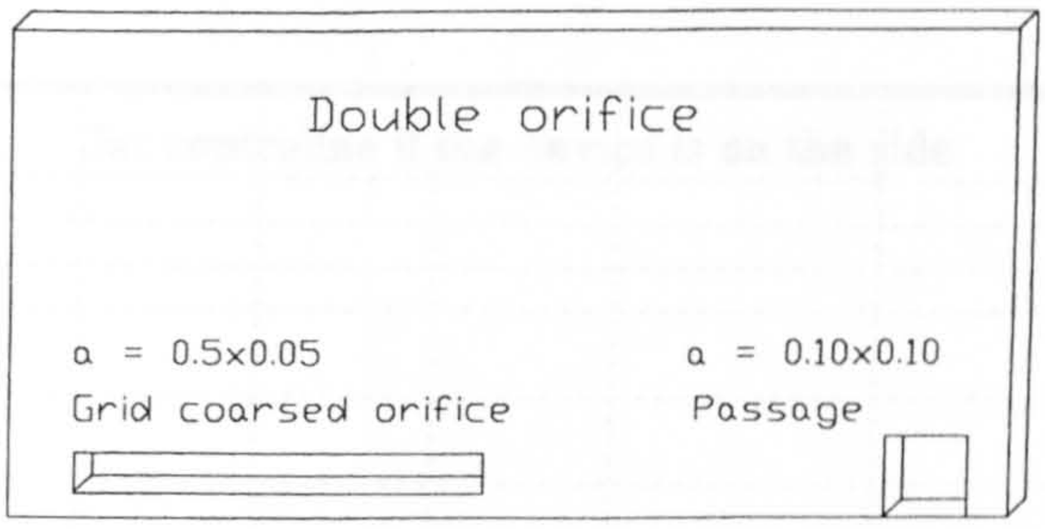

Figure 5-17: Double orifice design

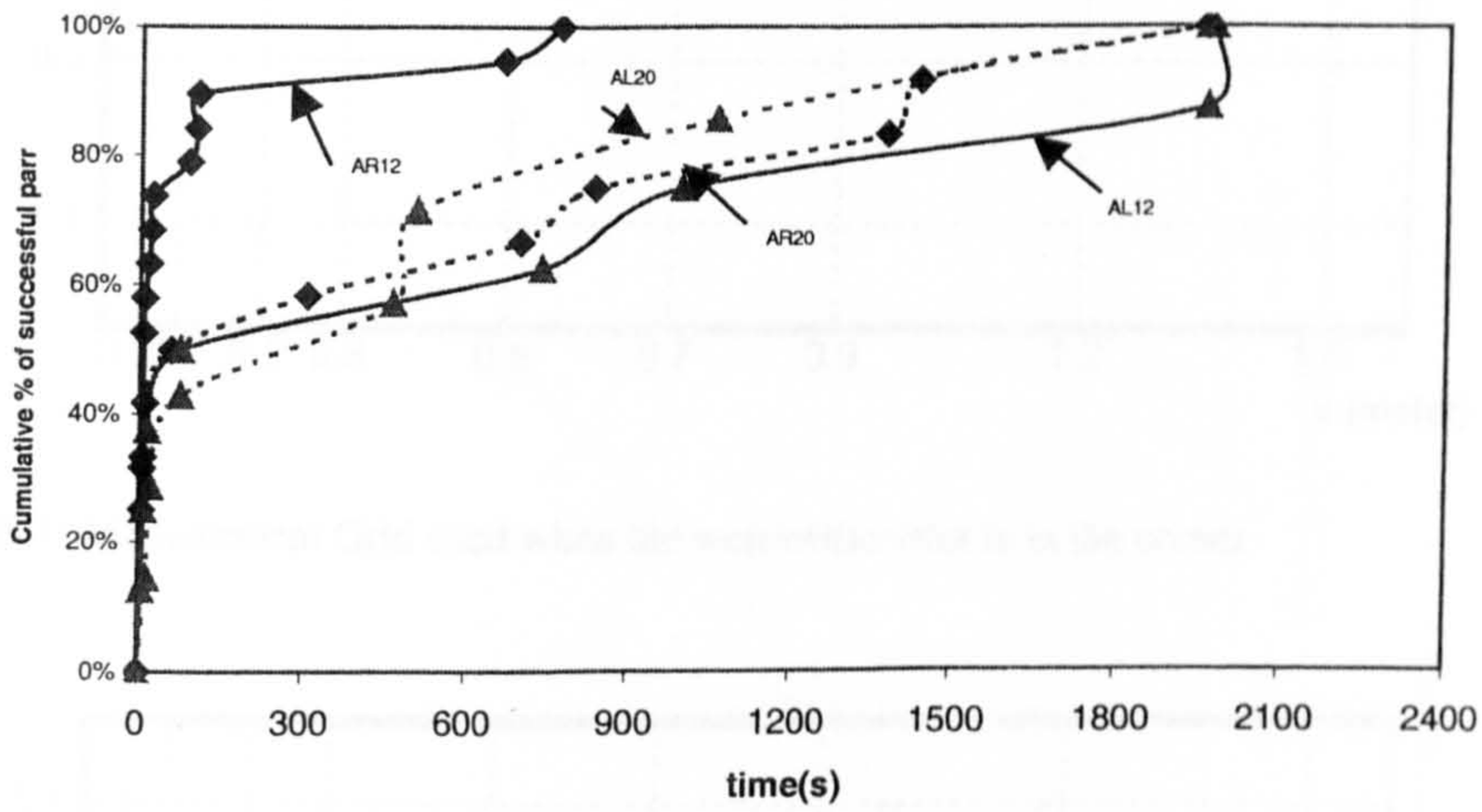

Figure 5- 18: Cumulative percentage of successful parr versus time for the double orifices design at ratio A of series IV

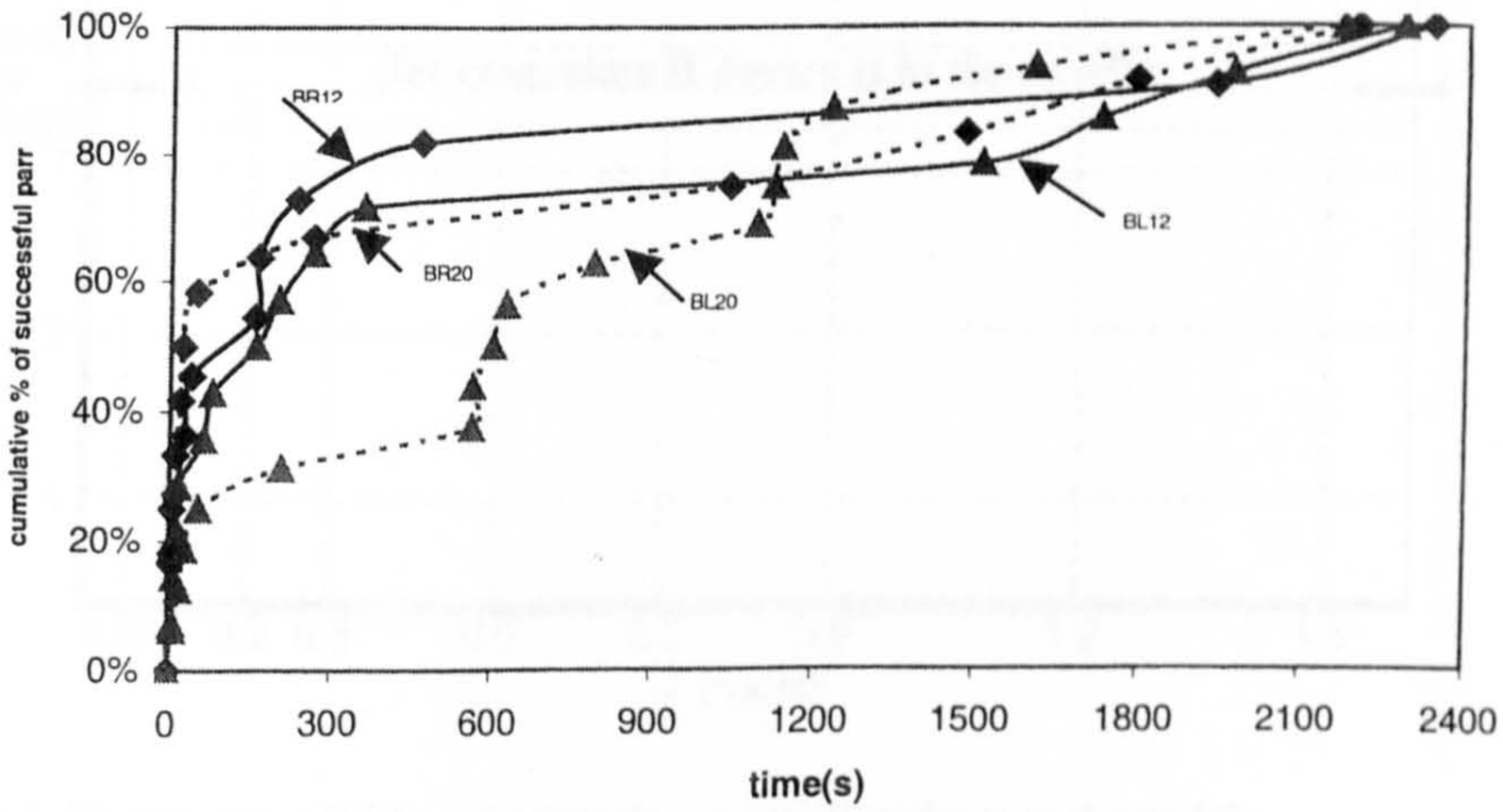

Figure 5-19: Cumulative percentage of successful parr for the double orifices design at ratio B of series IV

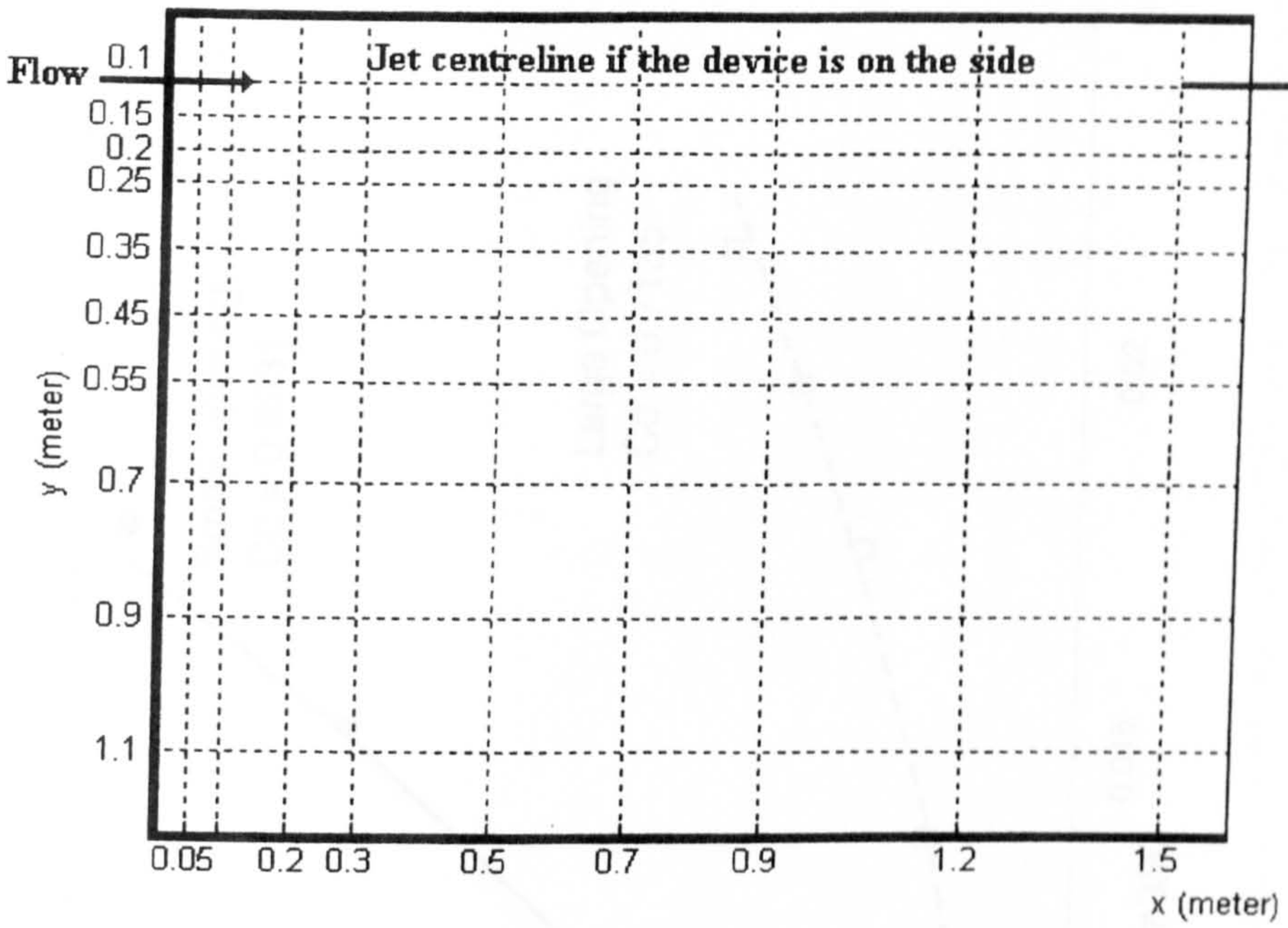

Figure 6-1: Measurement Grid used when the weir/orifice/slot is in the corner

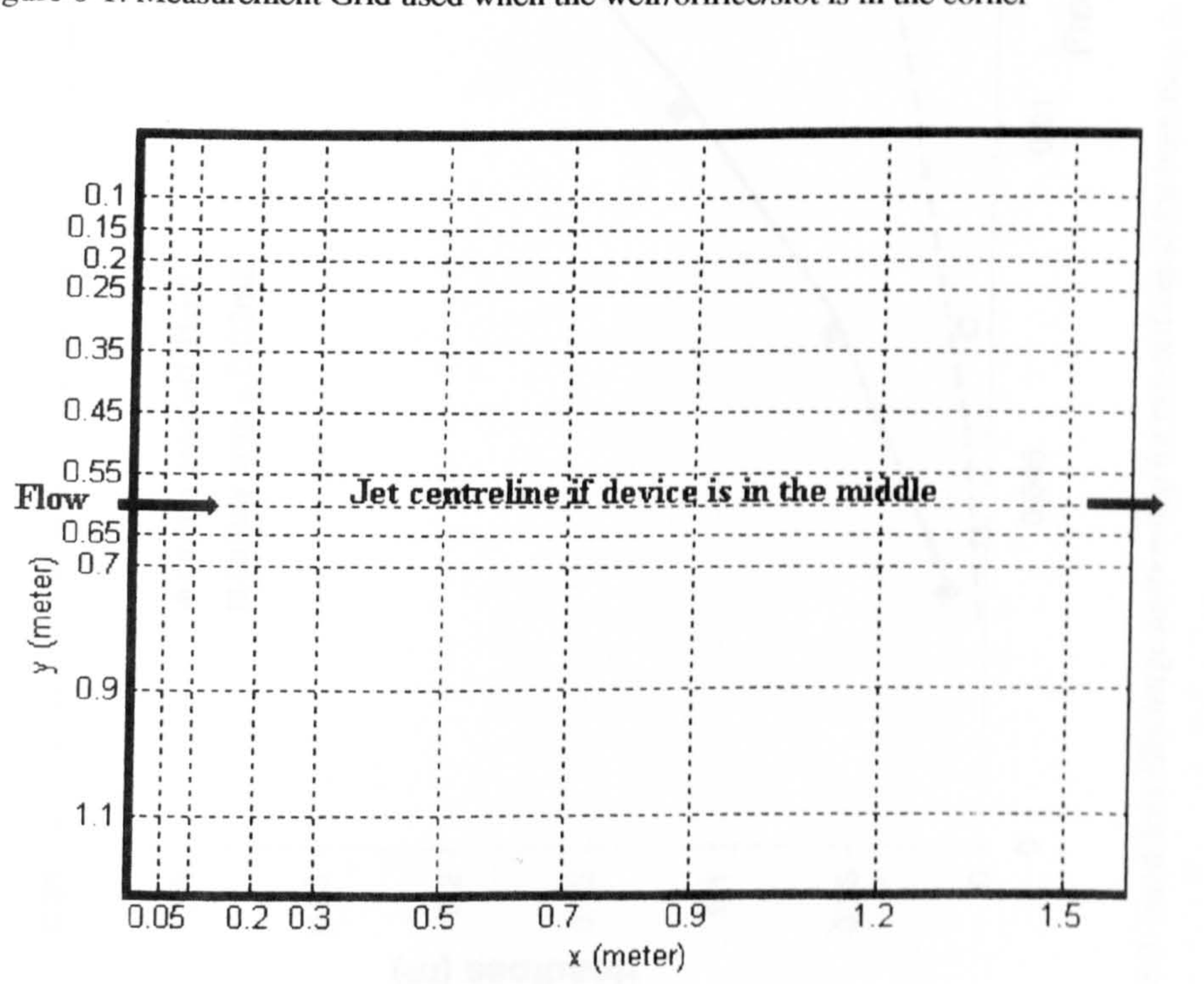

Figure 6-2: Measurement Grid used when the weir/orifice/slot is in the middle

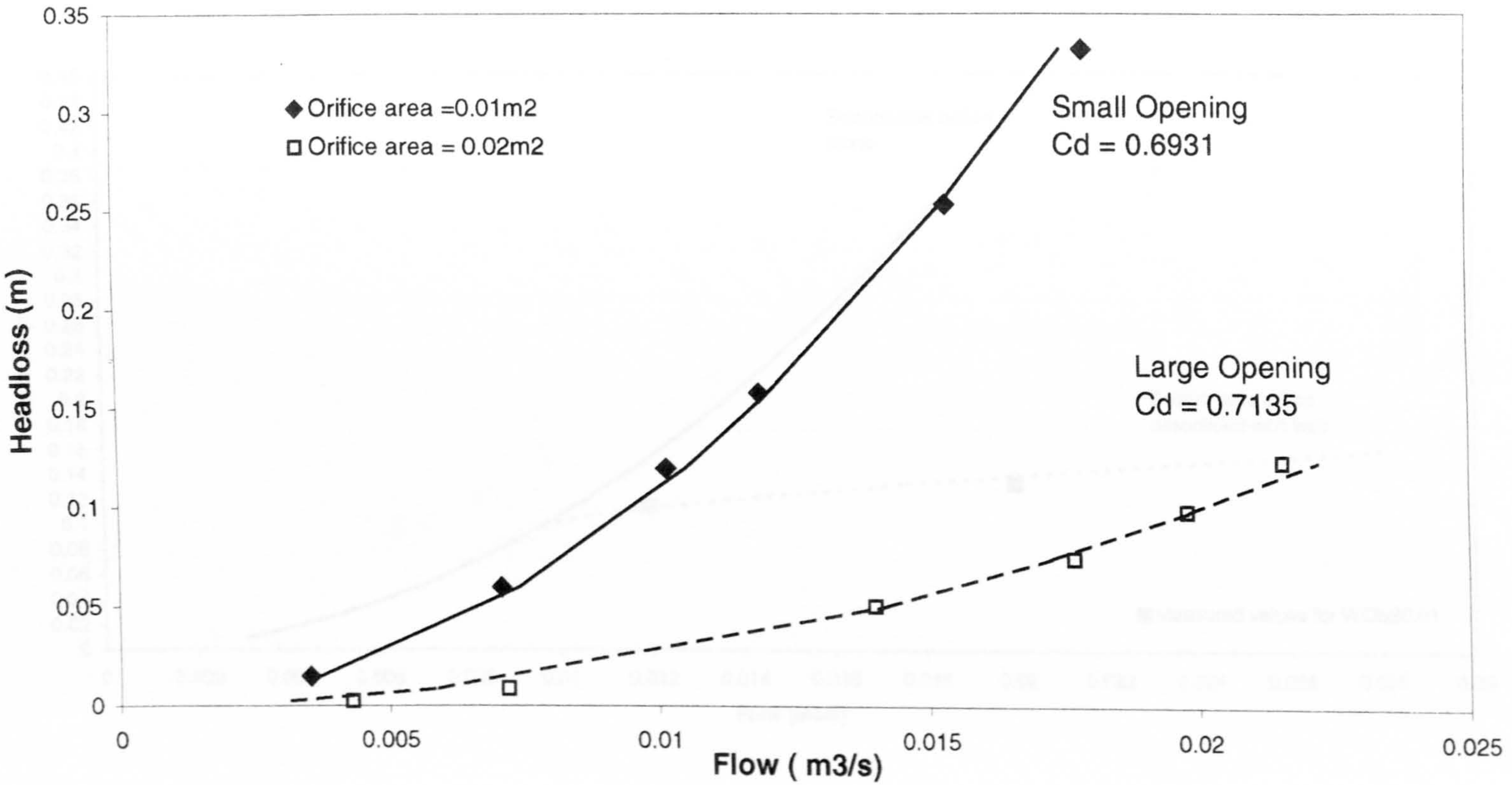

Figure 6-3: Head-loss /discharge relationship for two orifices at the bottom

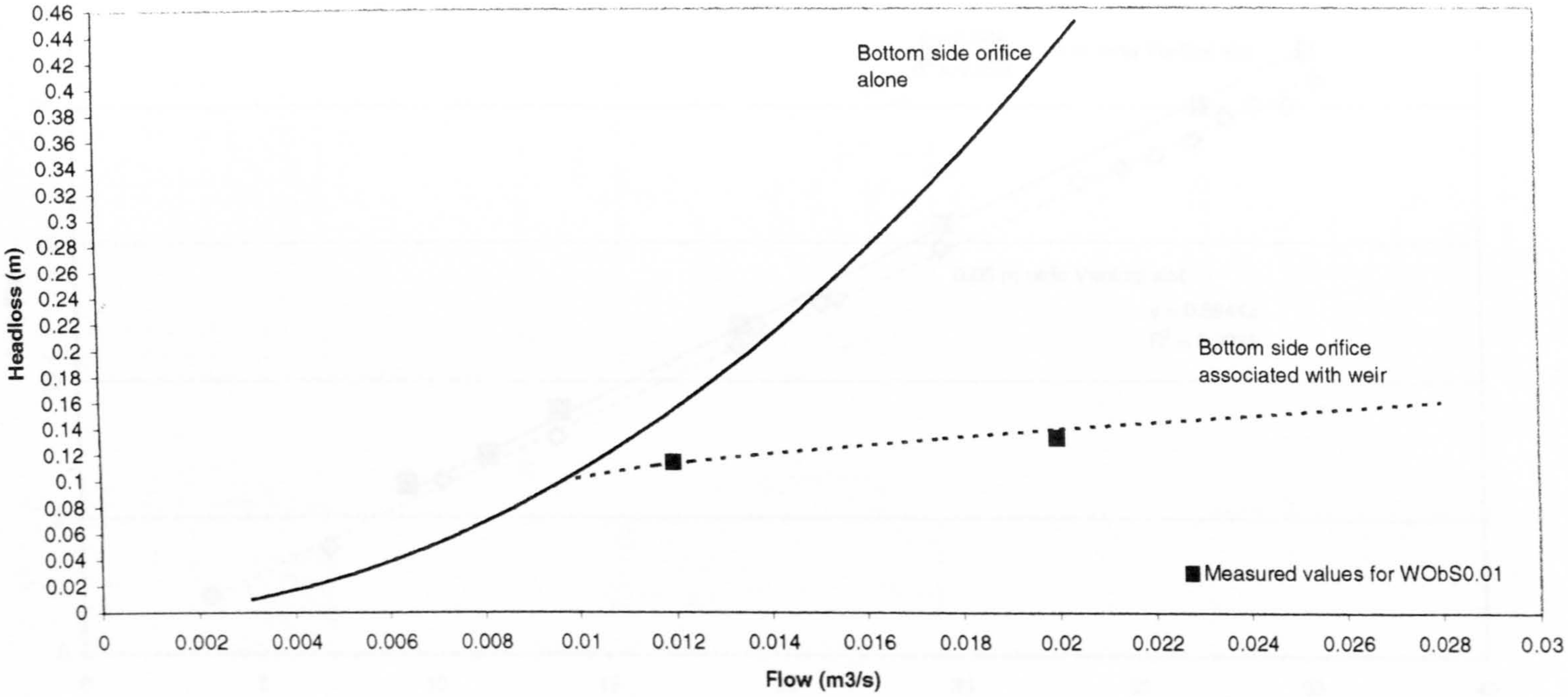

Figure 6-4: Head difference between the upstream and downstream part of the flume in relation to the total discharge Q for the 0.10 by 0.10 m orifice and the 0.10 by 0.10 m orifice associated with a weir.

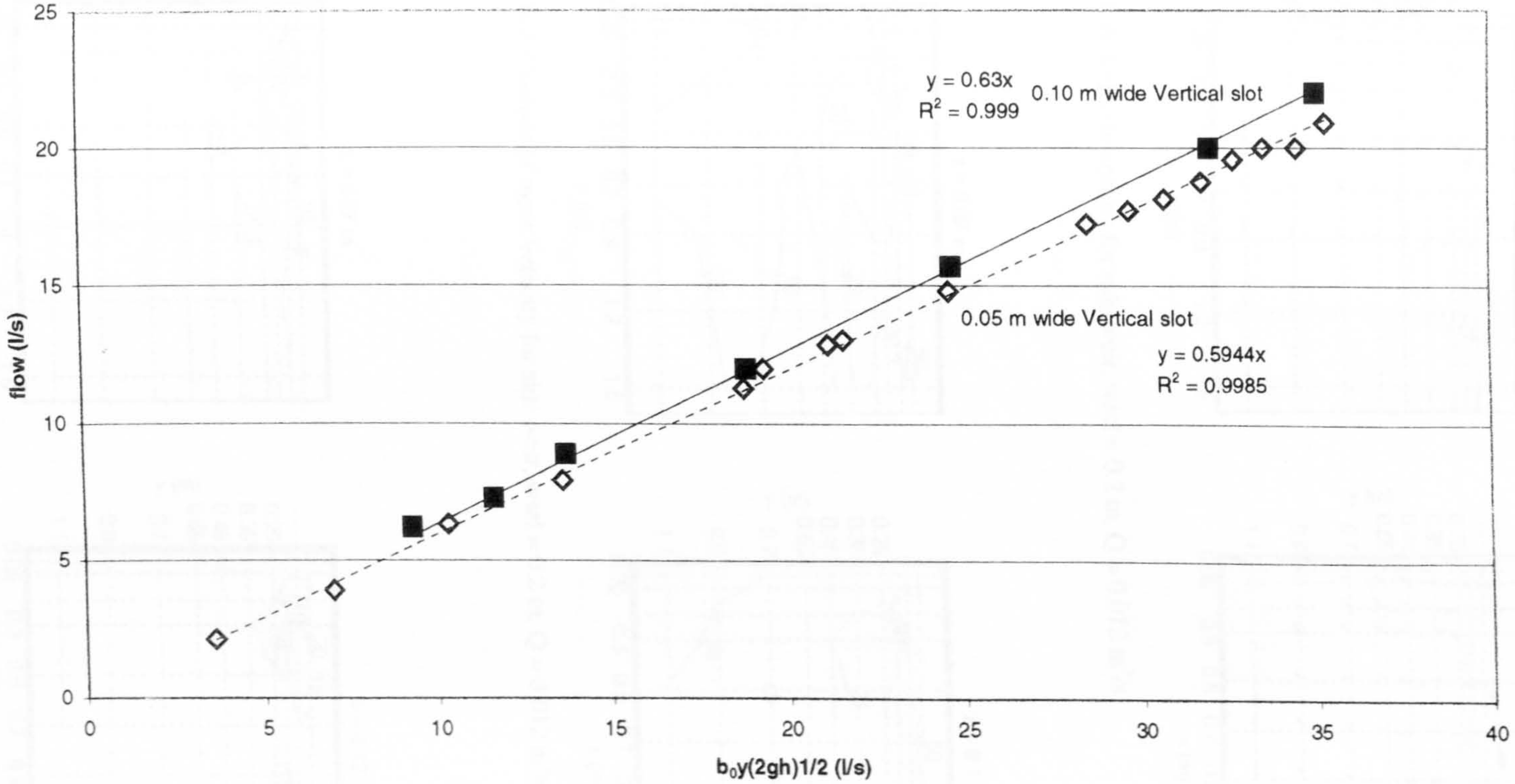

Figure 6-5: Determination of the Discharge coefficients for the 0.05 and 0.10 m wide vertical slots

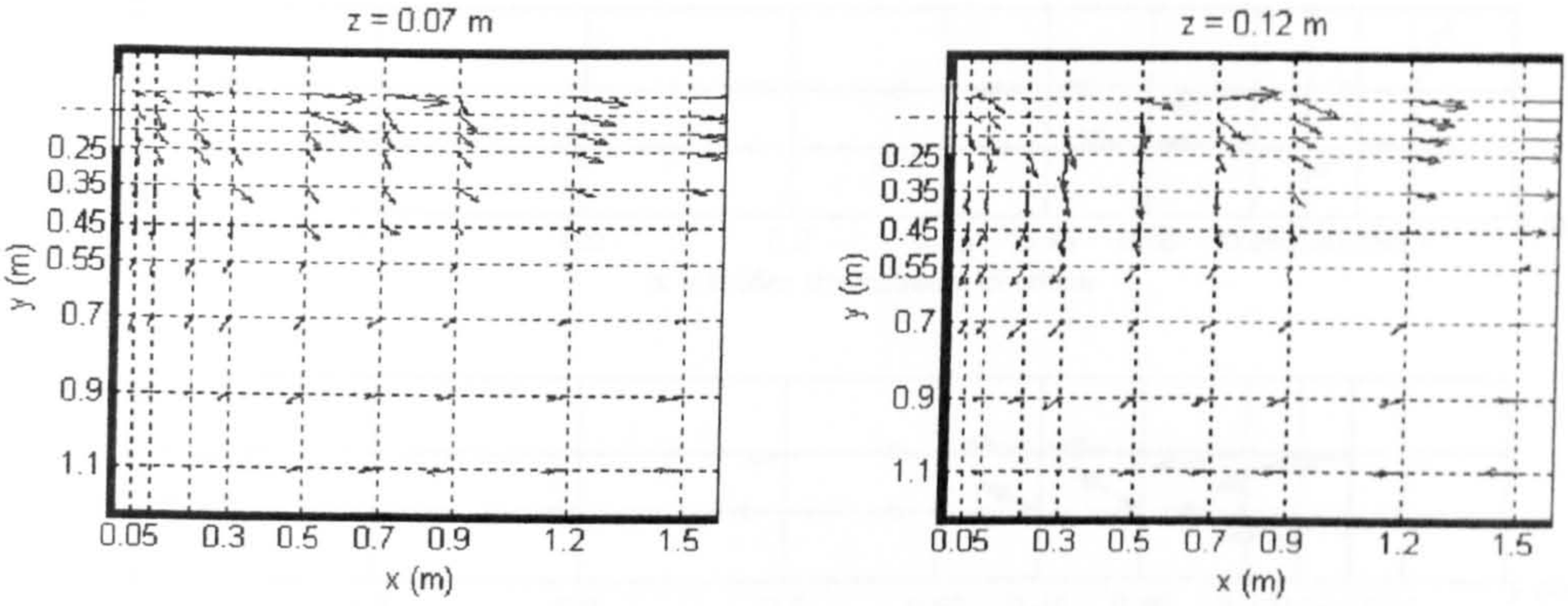

Figure 6-6: Velocity vectors for side weir, wsel = 0.2 m, Q = 0.012 m^3/s

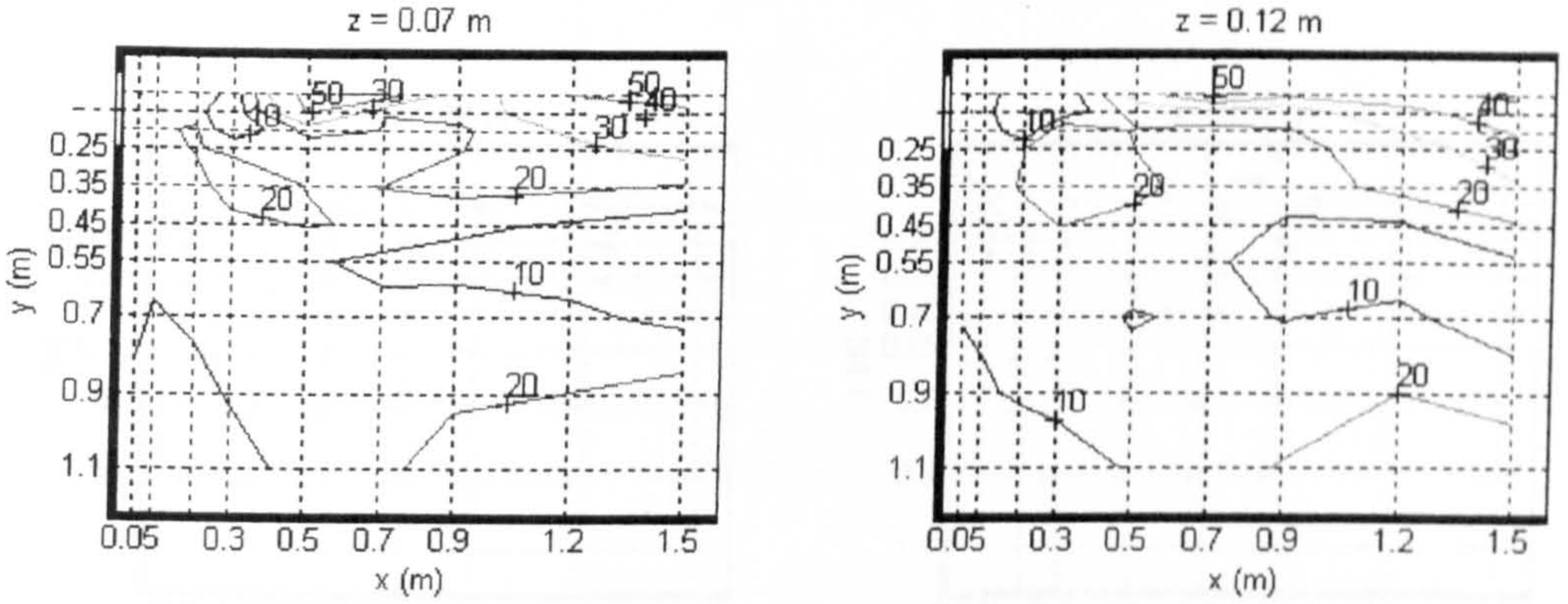

Figure 6-7: Contour of mean velocity for side weir, wsel = 0.2 m, Q = 0.012 m^3/s

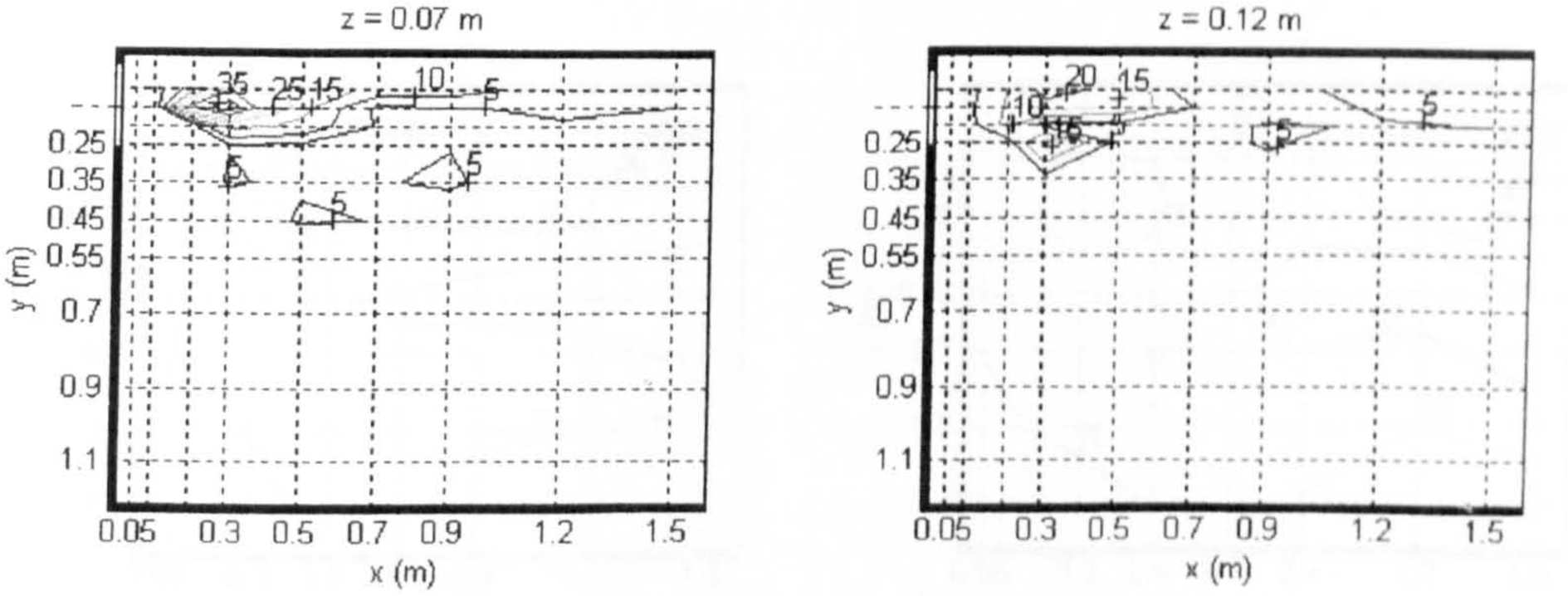

Figure 6-8: Contour of turbulence intensity for side weir, wsel = 0.2 m, Q = 0.012 m^3/s

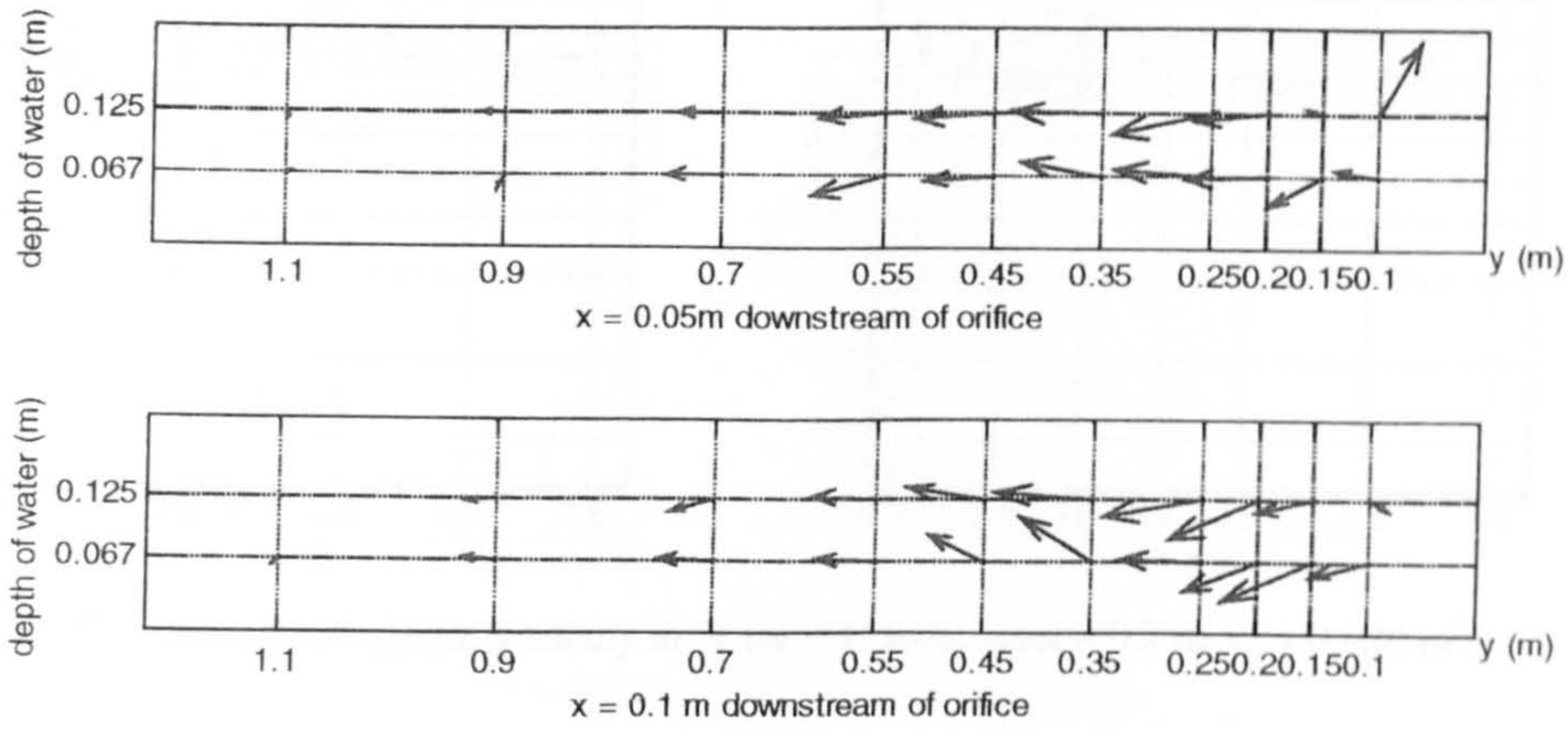

Figure 6-9:Velocity vectors over vertical slides for the side weir, wsel = 0.2, Q = 0.012 m^3/s

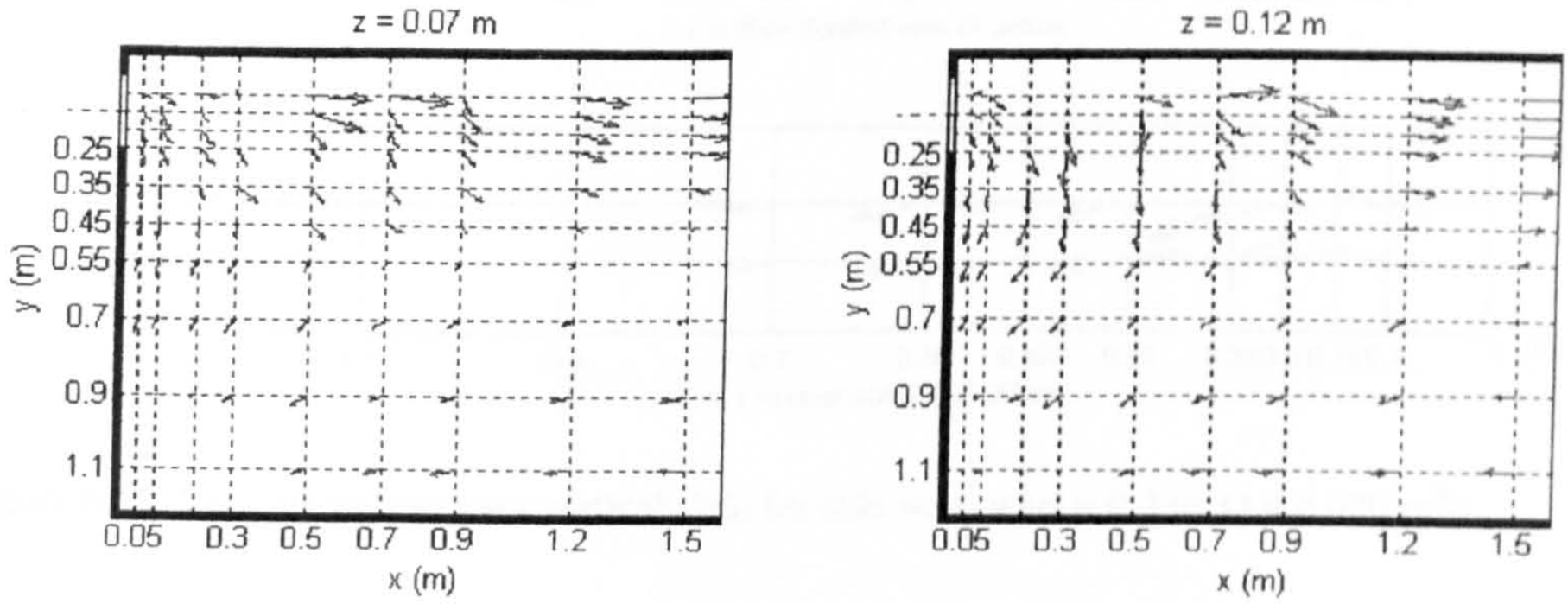

Figure 6-10: Velocity vectors for side weir, wsel = 0.2 m, Q = 0.020 m^3/s

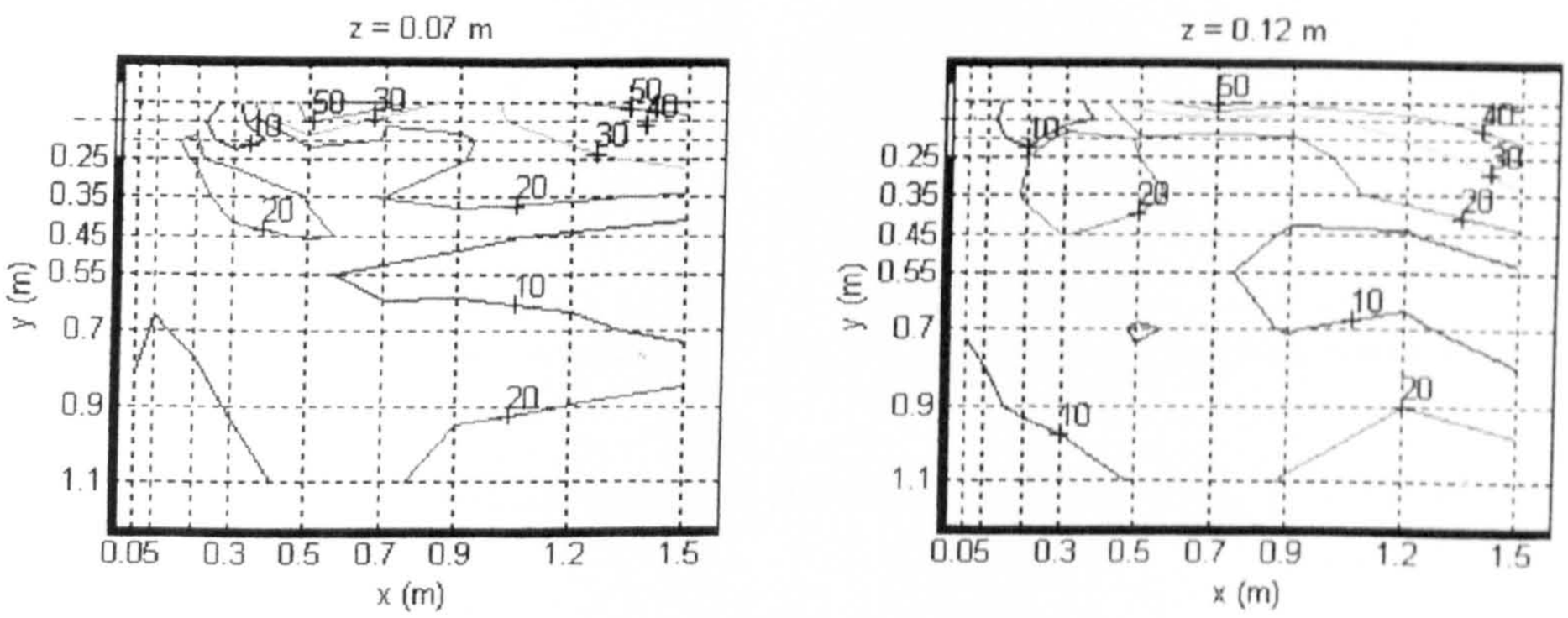

Figure 6-11: Contours of mean velocity in cm/s for side weir, wsel = 0.2 m, Q = 0.020 m^3/s

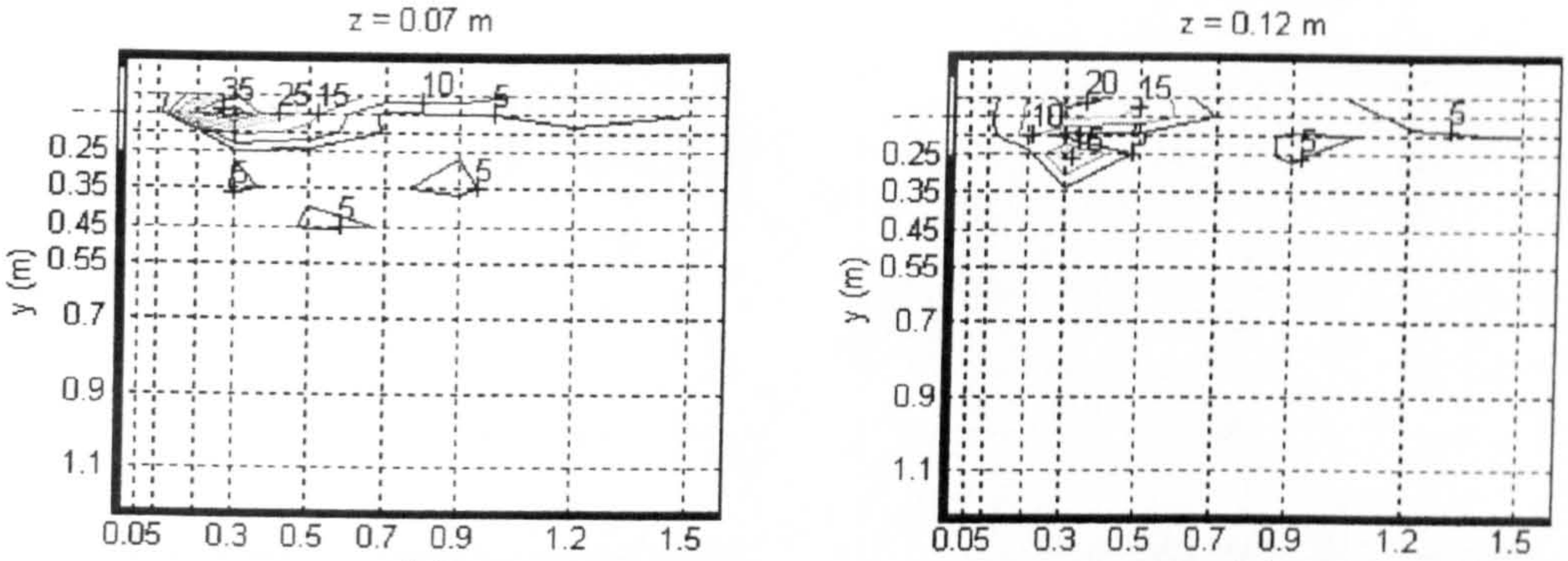

Figure 6-12: Contours of turbulence intensity in % for side weir, wsel = 0.2 m, Q = 0.020 m^3/s

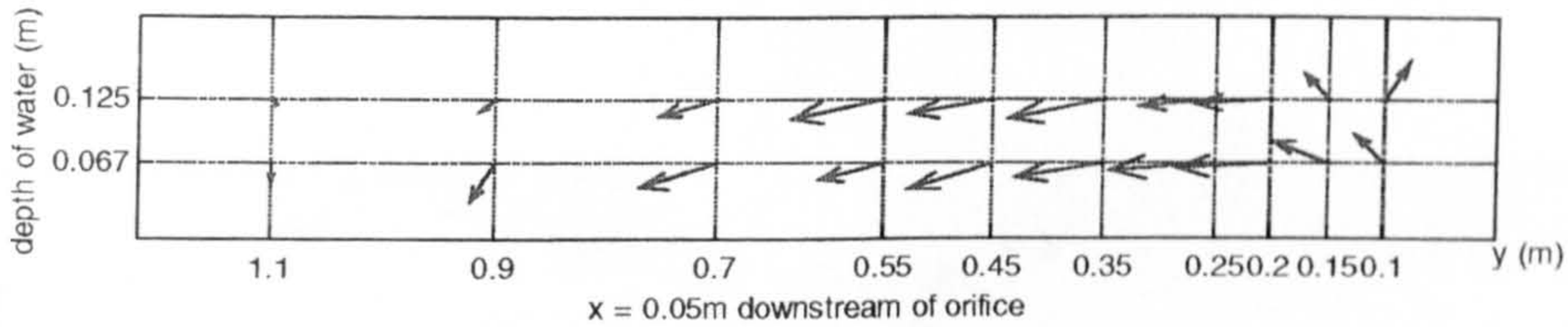

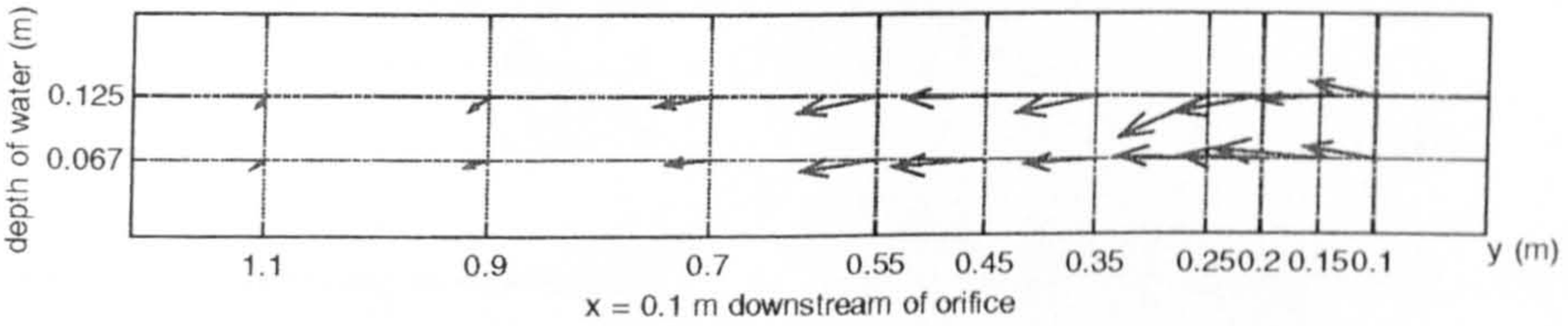

Figure 6-13: Velocity vectors over vertical slide for side weir, wsel = 0.2 m, Q = 0.020 m^3/s

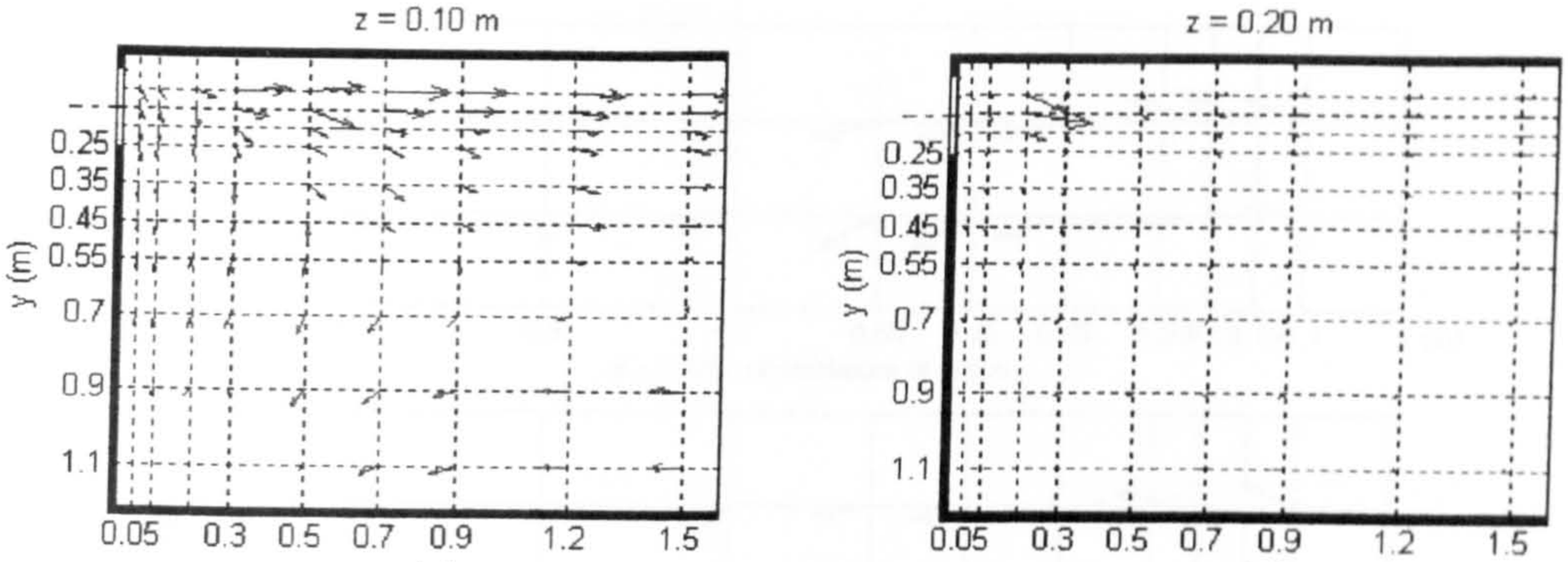

Figure 6-14: Velocity vectors for side weir, wsel = 0.3 m, Q = 0.012 m^3/s

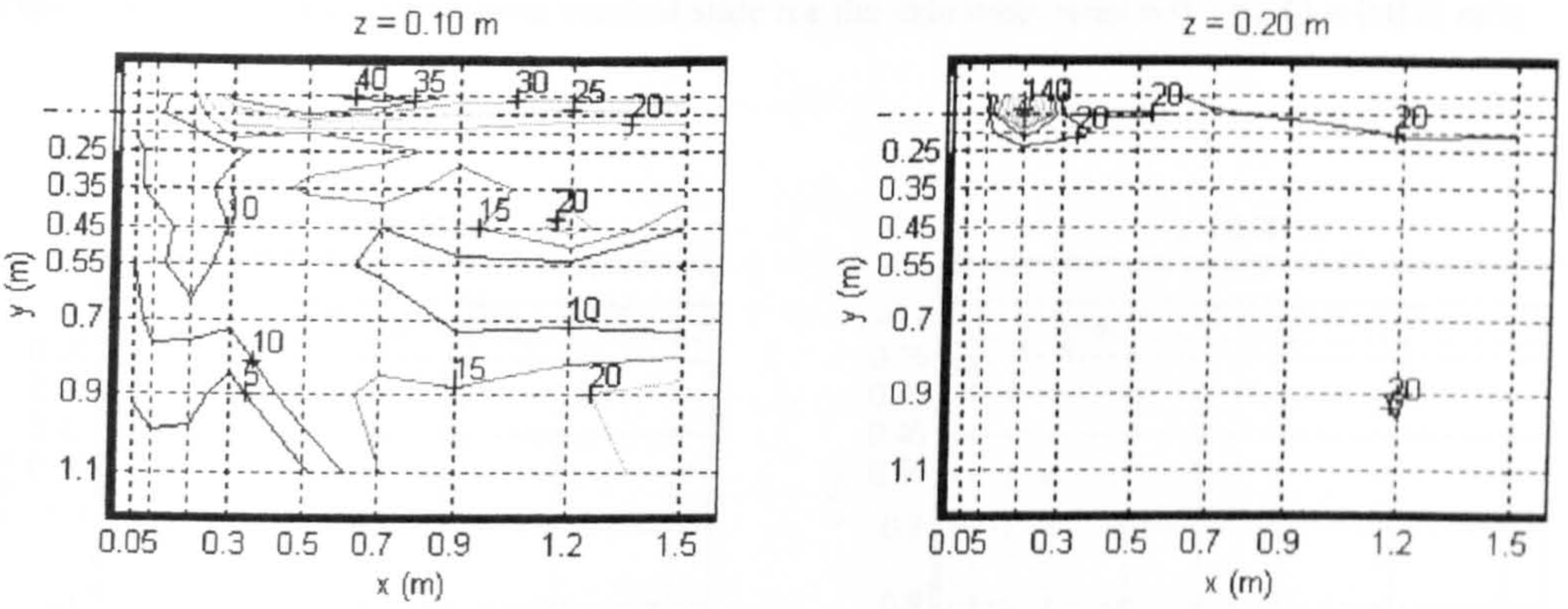

Figure 6-15: Contours of mean velocity in cm/s for side weir, wsel = 0.3 m, Q = 0.012 m^3/s

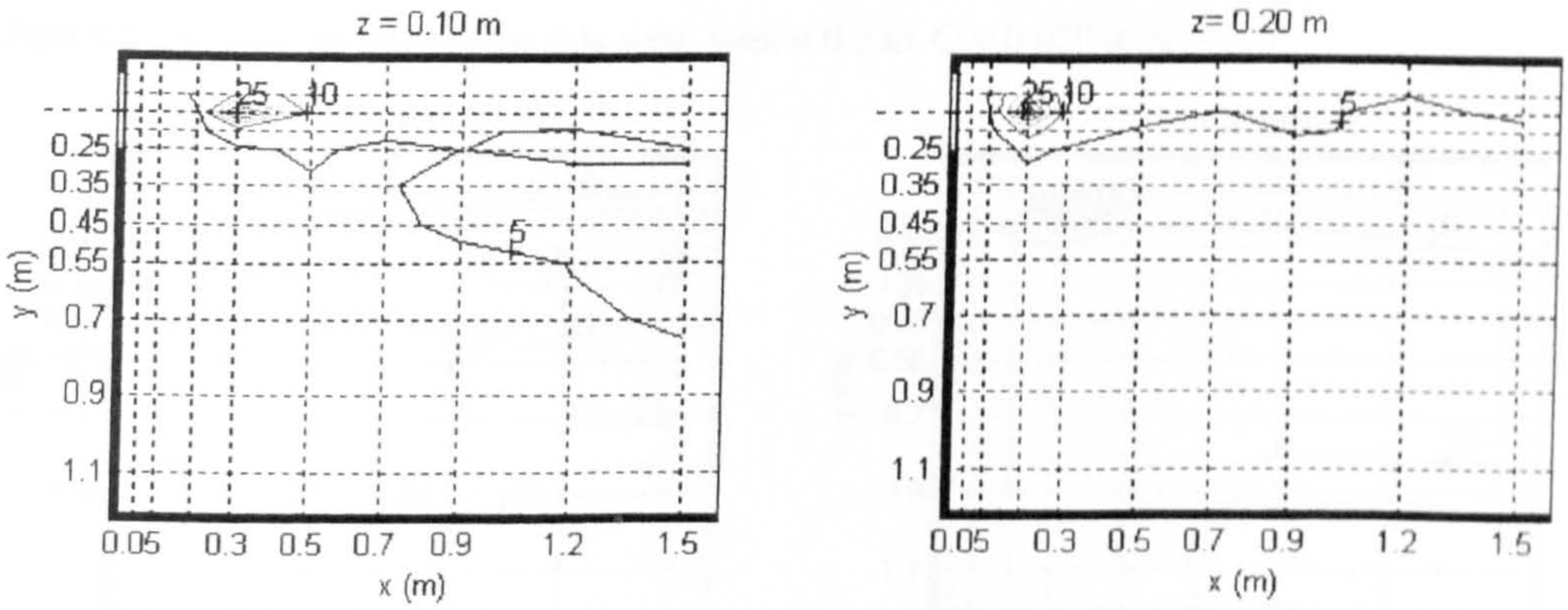

Figure 6-16: Contours of turbulence intensity in % for side weir, wsel = 0.3 m, Q = 0.012 m^3/s

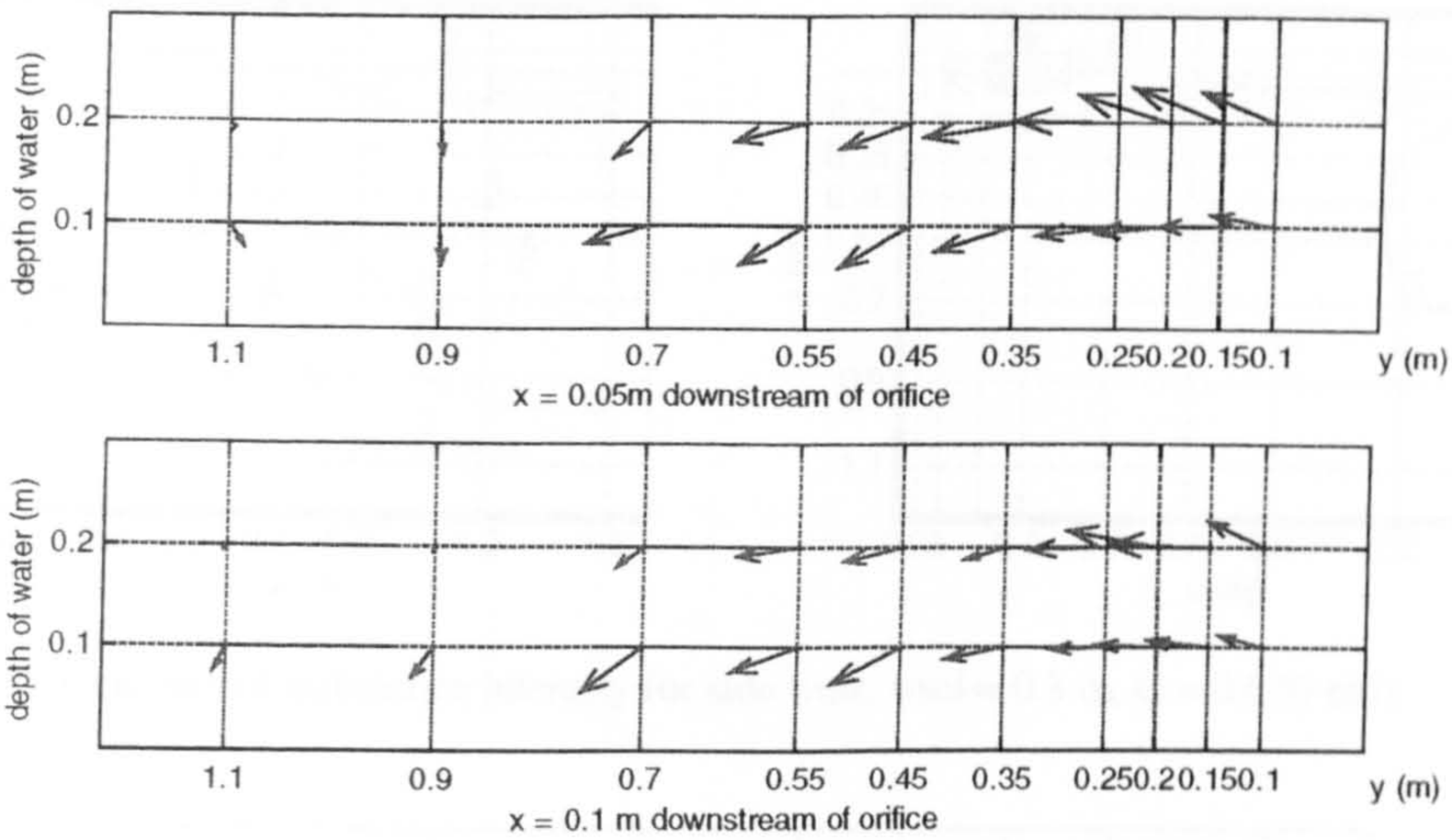

Figure 6-17: Velocity vectors over vertical slide for the side weir, wsel = 0.3 m, Q = 0.012 m^3/s

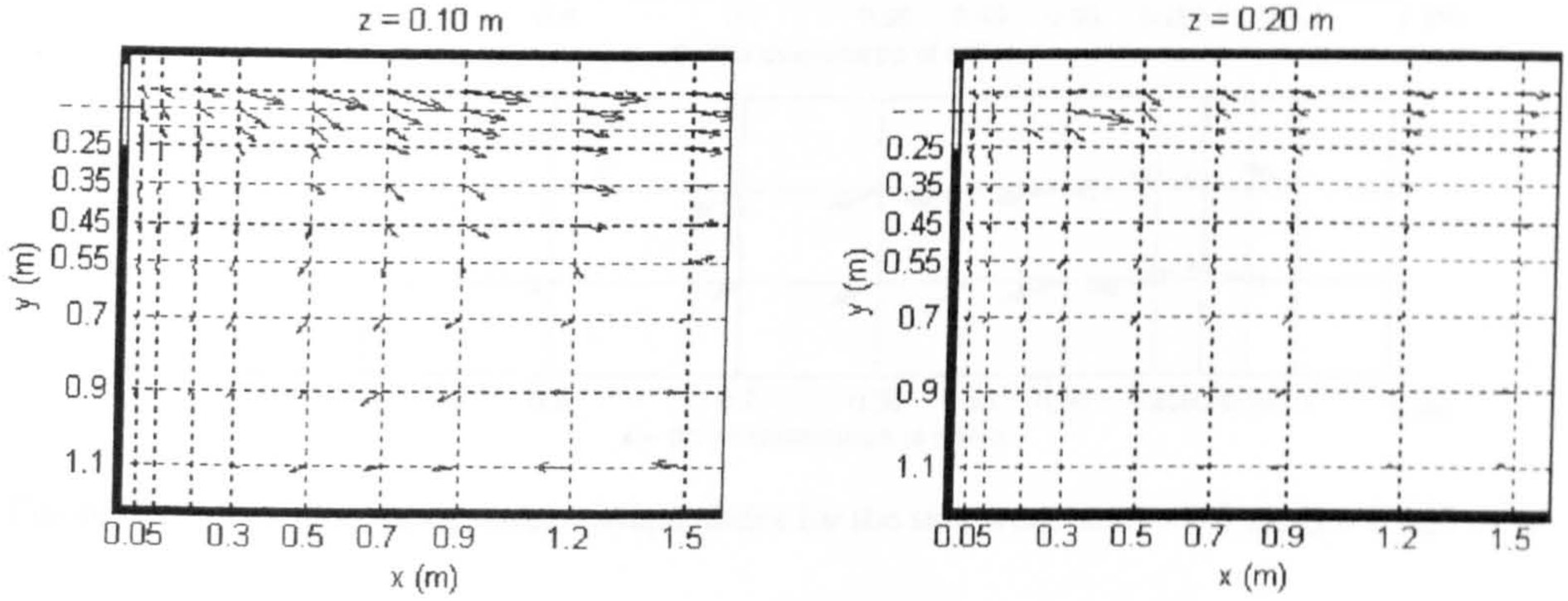

Figure 6-18: Velocity vectors for side weir, wsel = 0.3 m, Q = 0.020 m^3/s

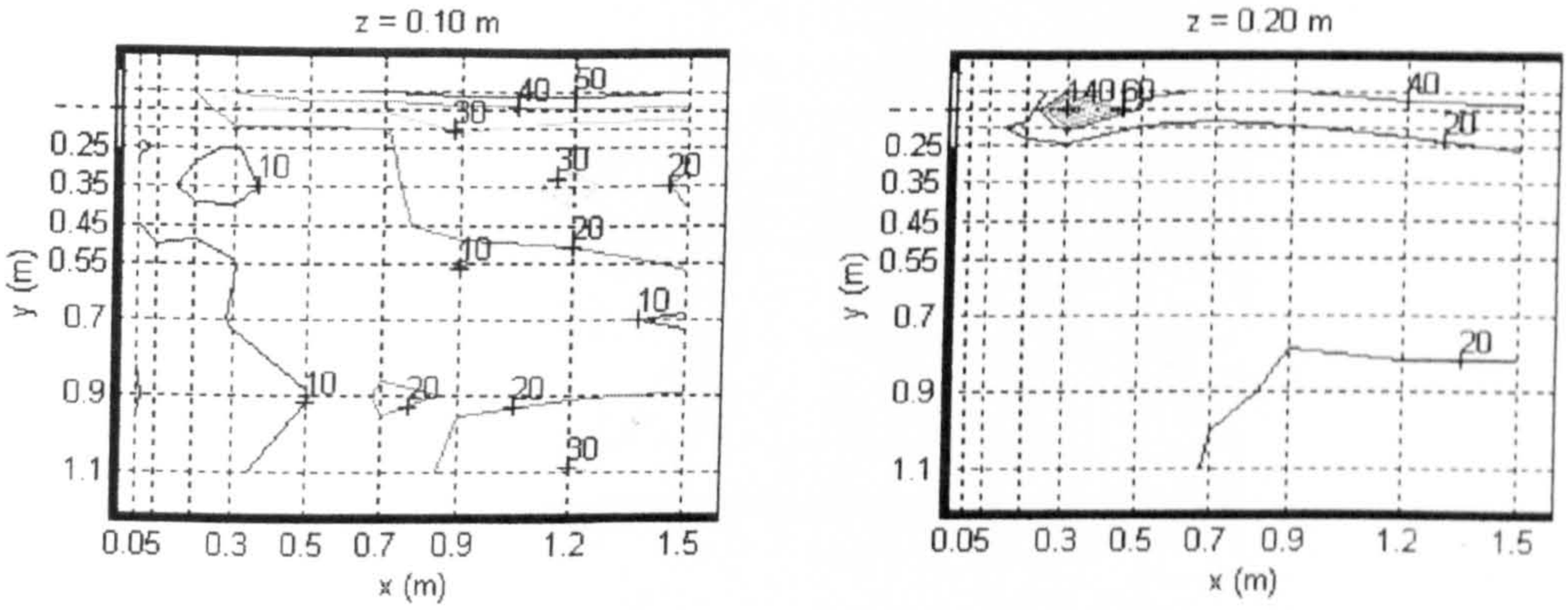

Figure 6-19: Contours of mean velocity for side weir, wsel = 0.3 m, Q = 0.020 m^3/s

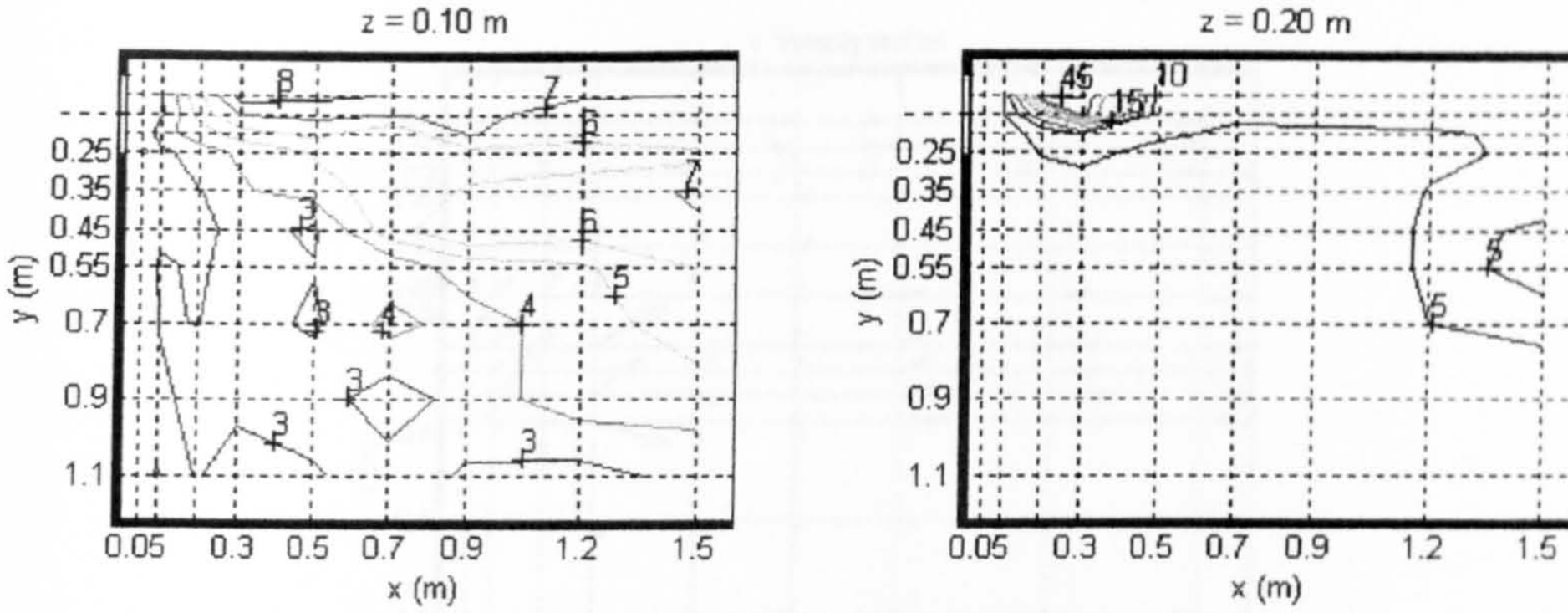

Figure 6-20:Contours of turbulence intensity for side weir, wsel = 0.3 m, Q = 0.020 m^3/s

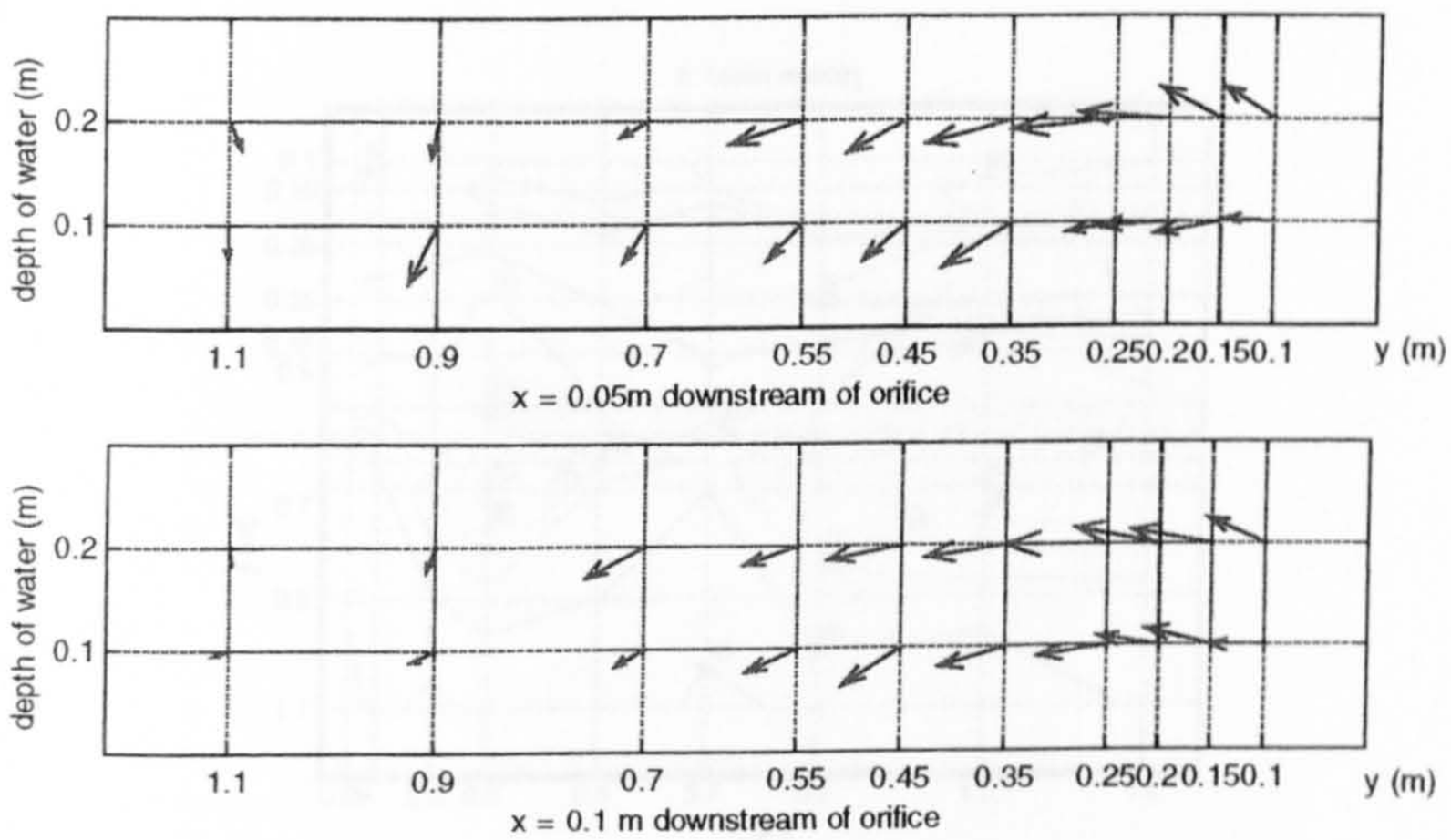

Figure 6-21: Velocity vectors over vertical slides for the side weir, wsel = 0.3 m, Q = 0.020 m^3/s

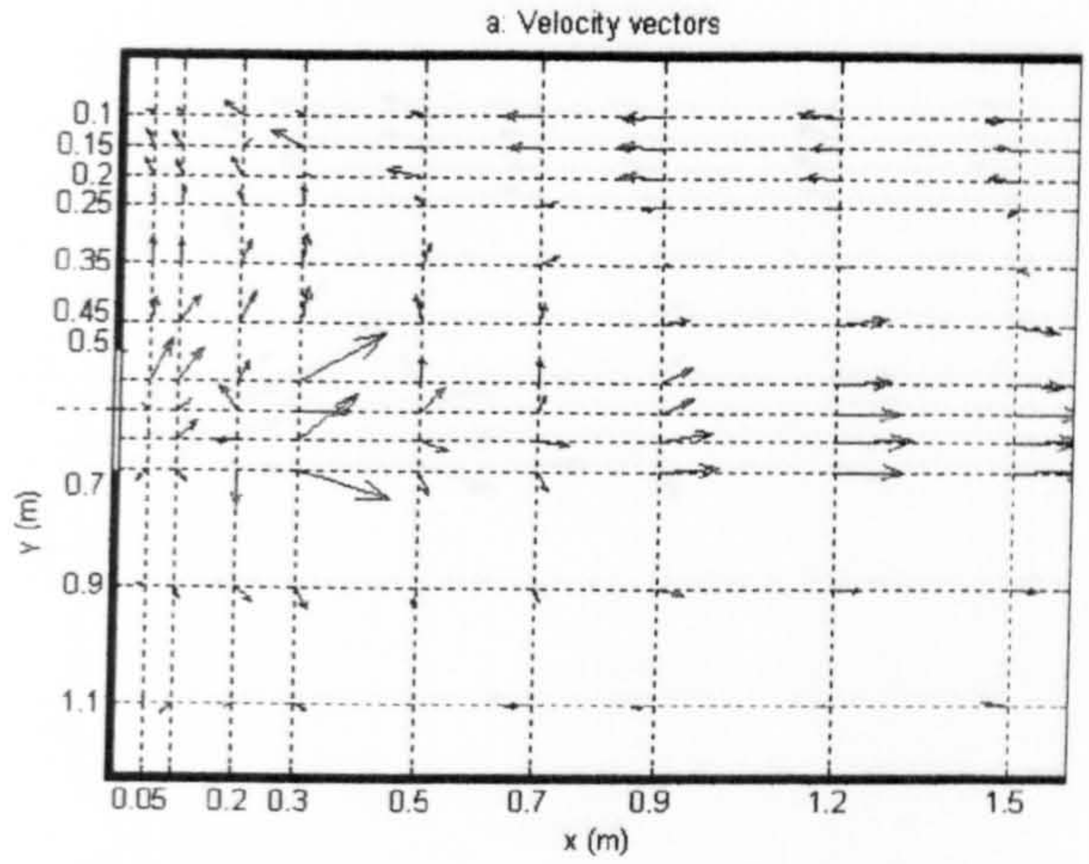

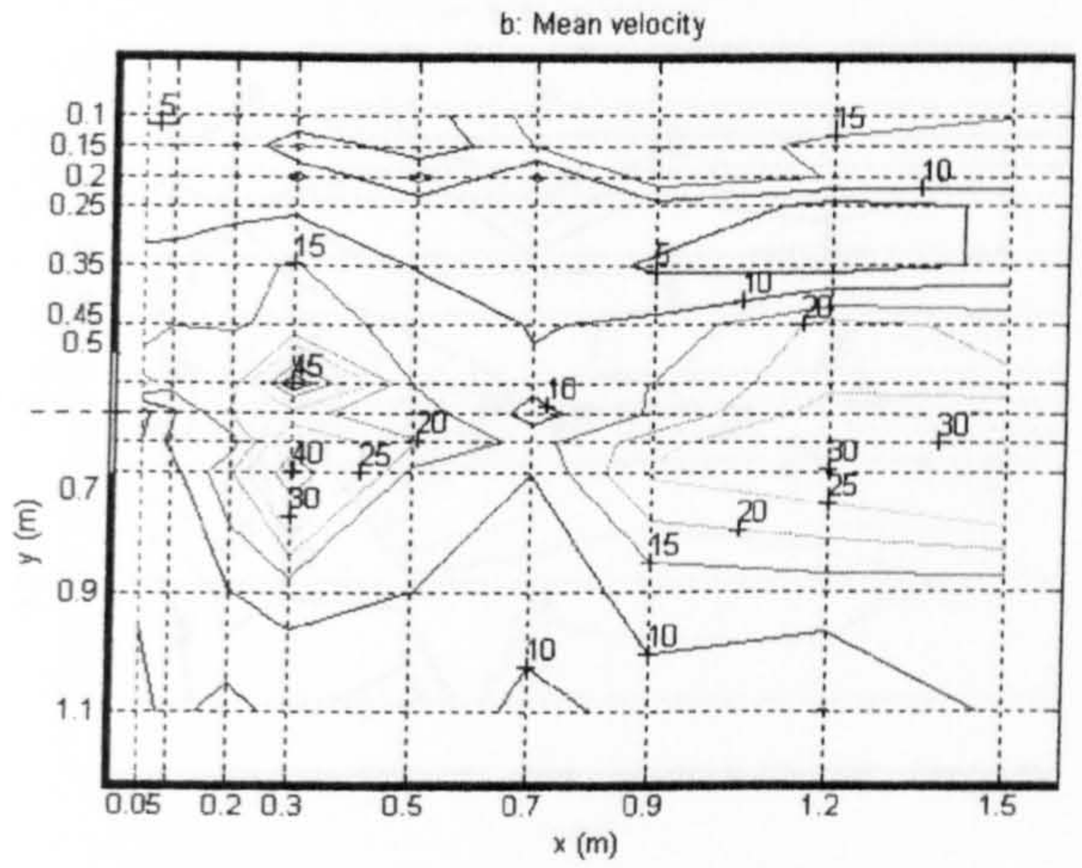

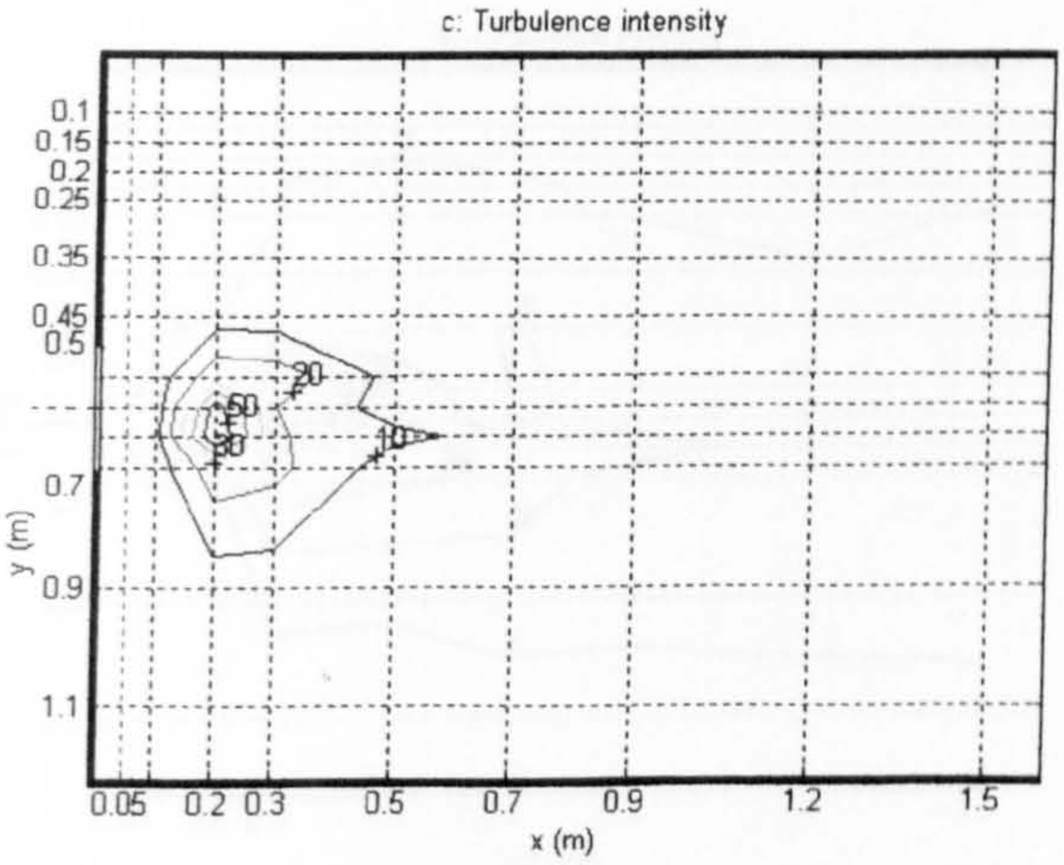

Figure 6-22: Middle Weir, wsel = 0.20m, Q = 0.012m^3/s [$WM_{12\text{-}0..2}$] (a: velocity vectors; b: contours of mean velocity in cm/s and c: contours of turbulence intensity in %)

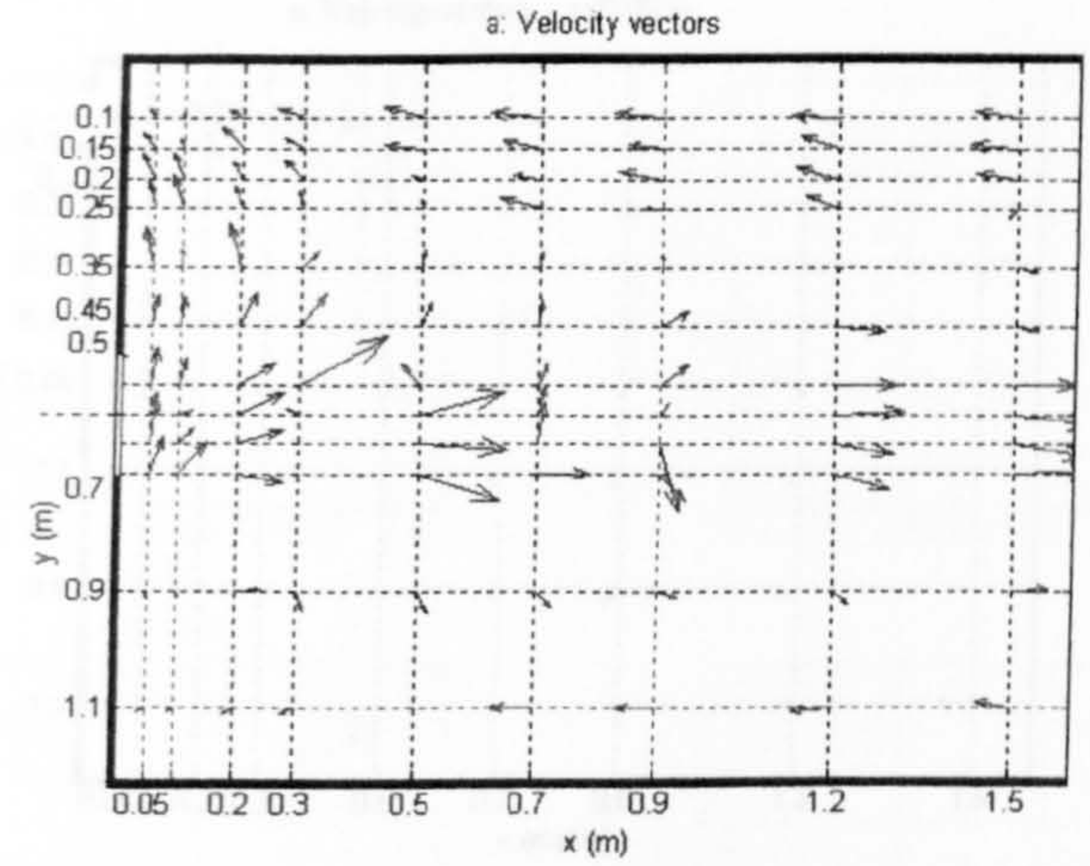

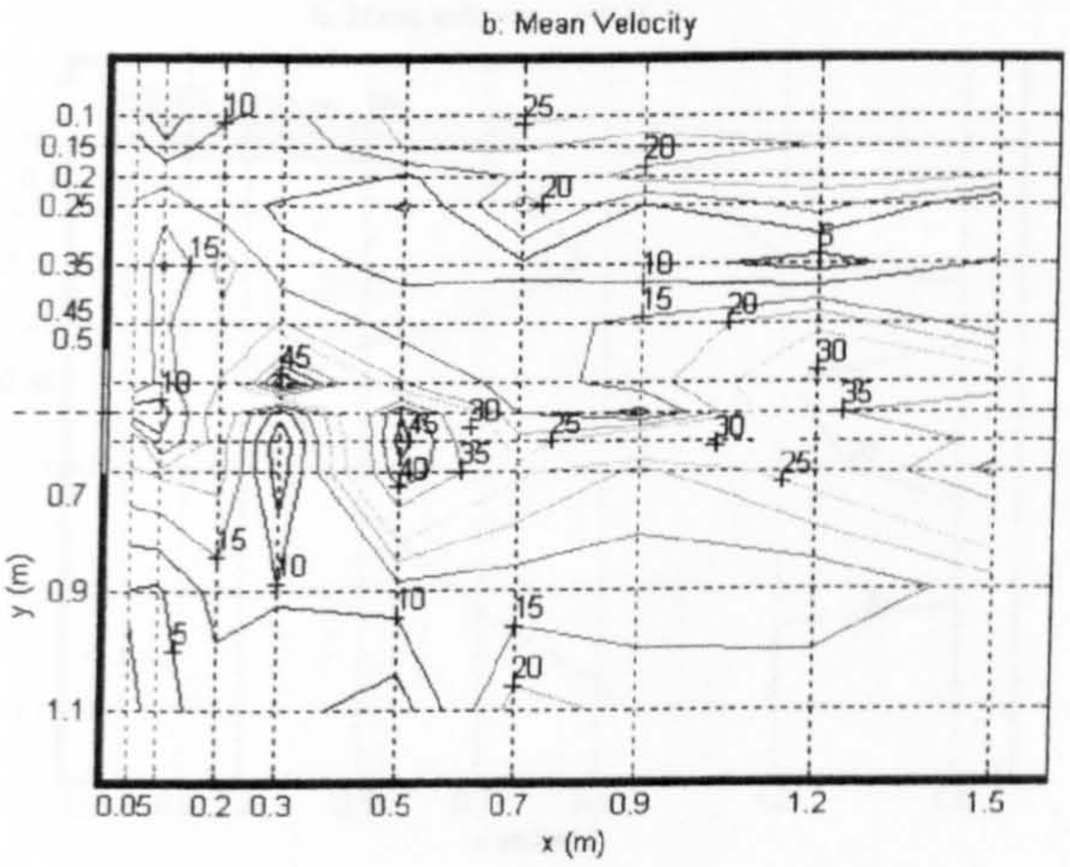

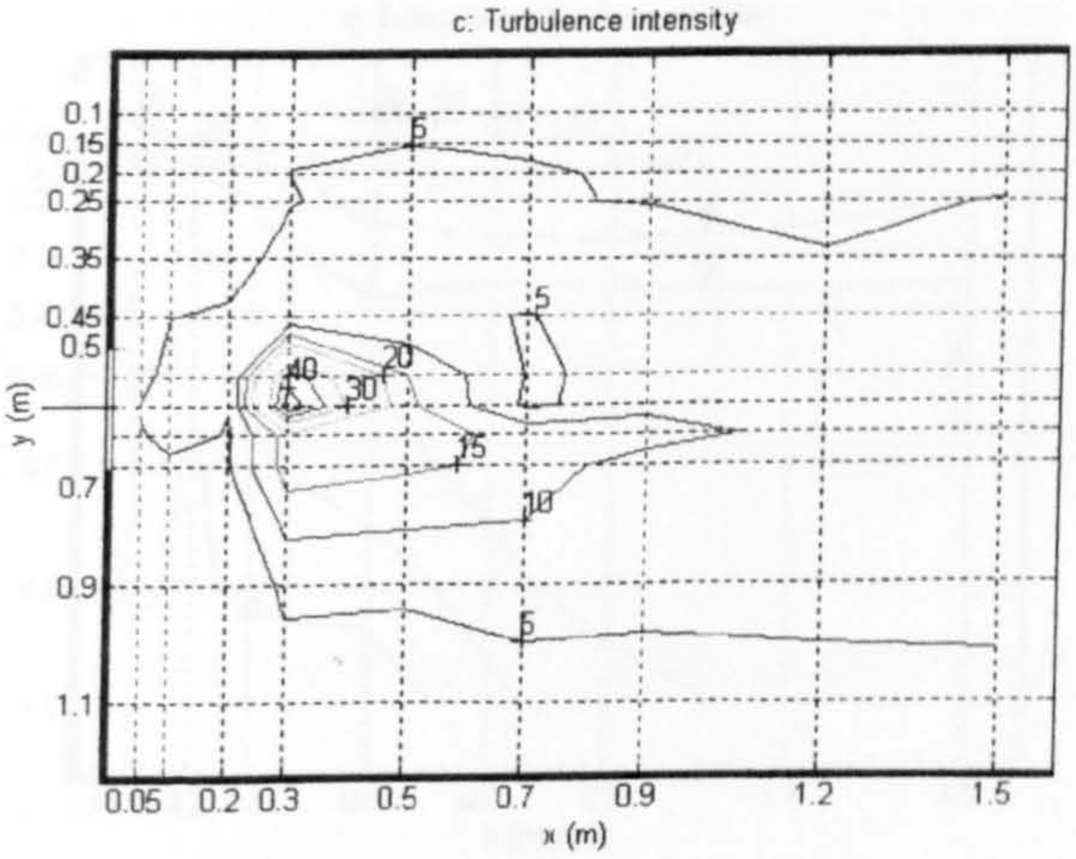

Figure 6-23: Middle Weir, wsel = 0.20m, Q = 0.020m^3/s [$WM_{20\text{-}0.2}$] (a: velocity vectors; b: contours of mean velocity in cm/s and c: contours of turbulence intensity in %)

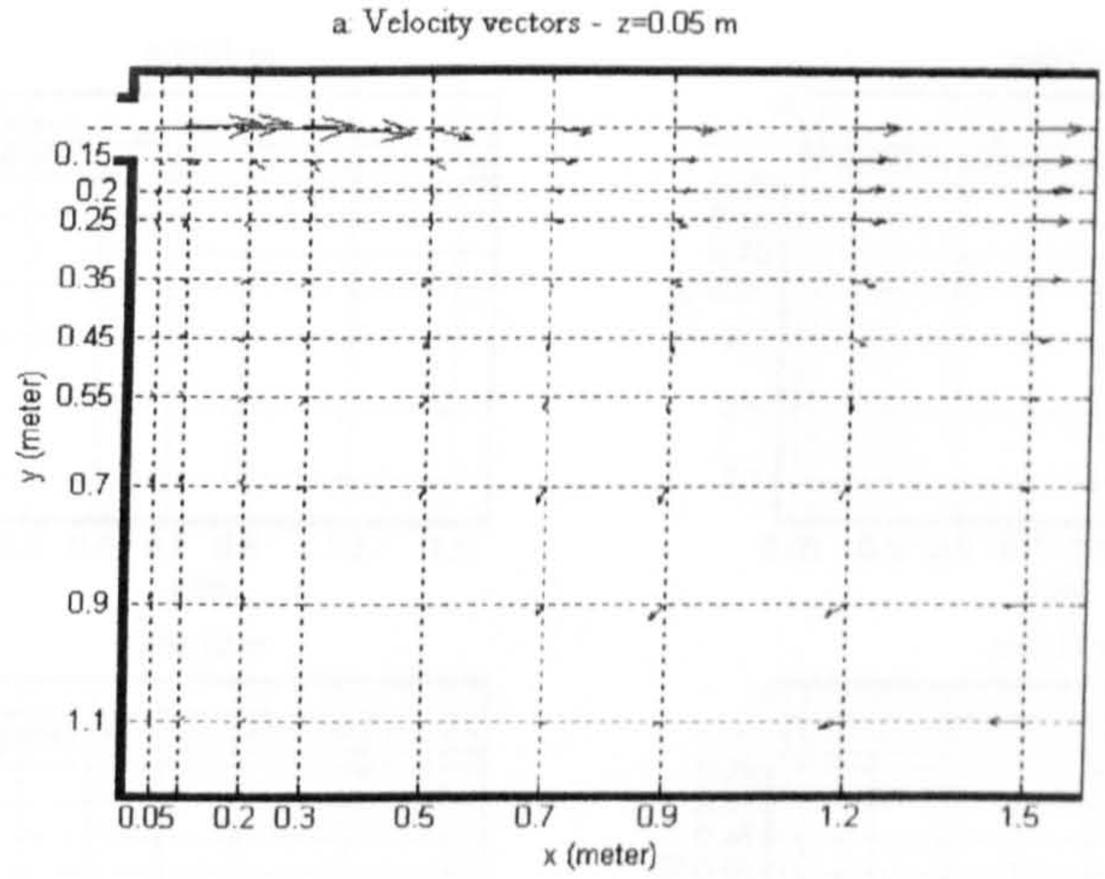

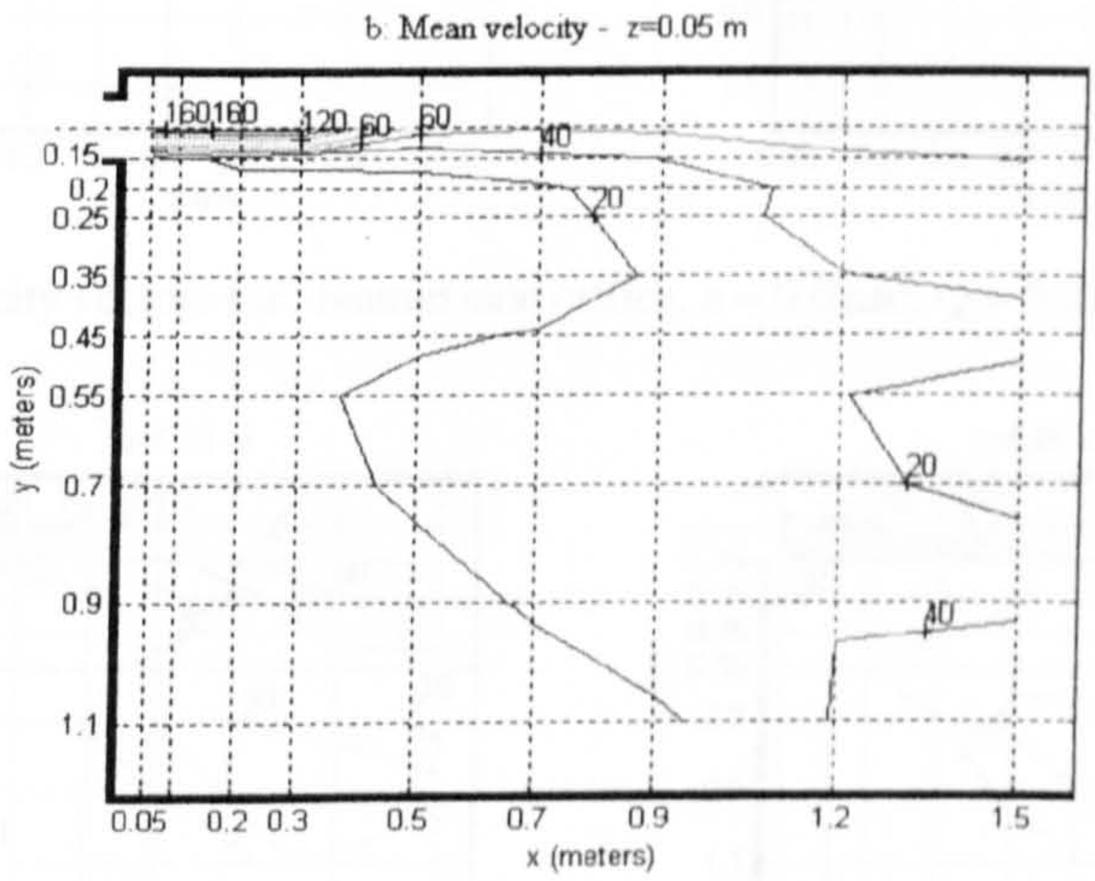

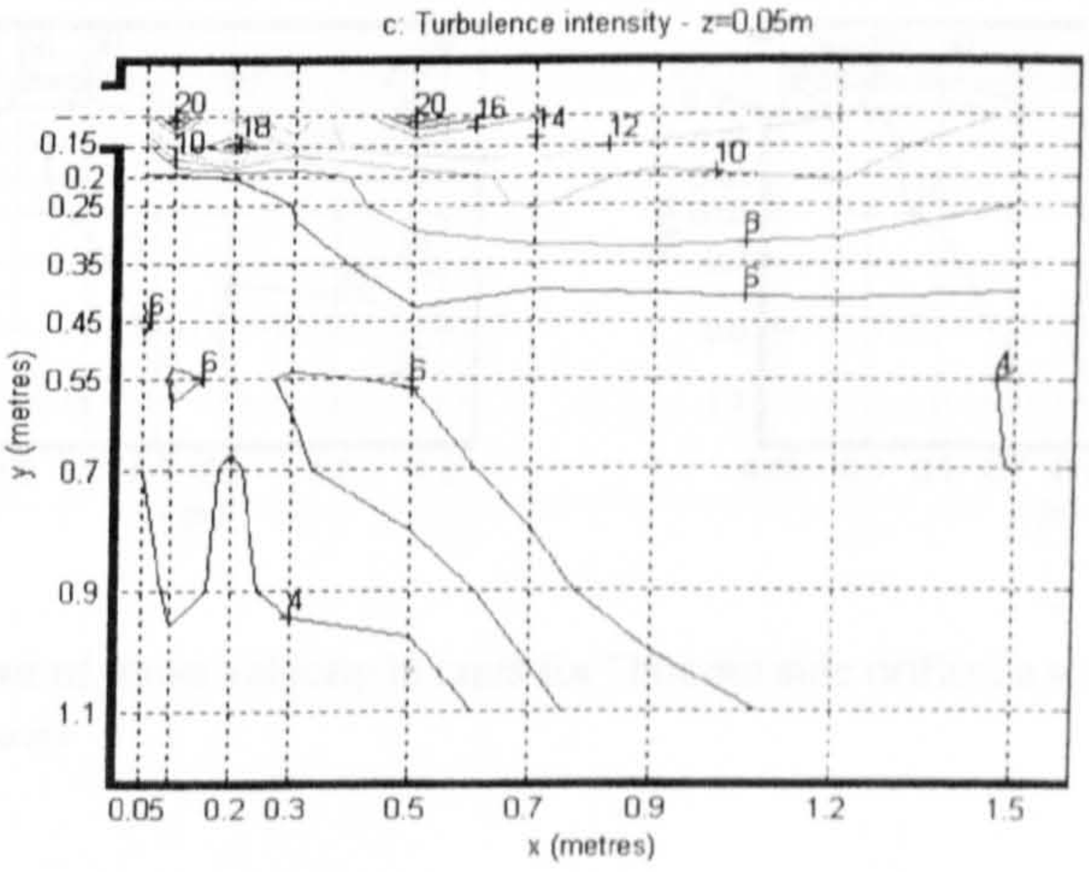

Figure 6-24:Bottom side orifice, a = 0.01m^2, Q = 0.012m^3/s [$ObS_{12\text{-}0.01}$] (a: velocity vectors; b: contours of mean velocity in cm/s and c: contours of turbulence intensity in %)

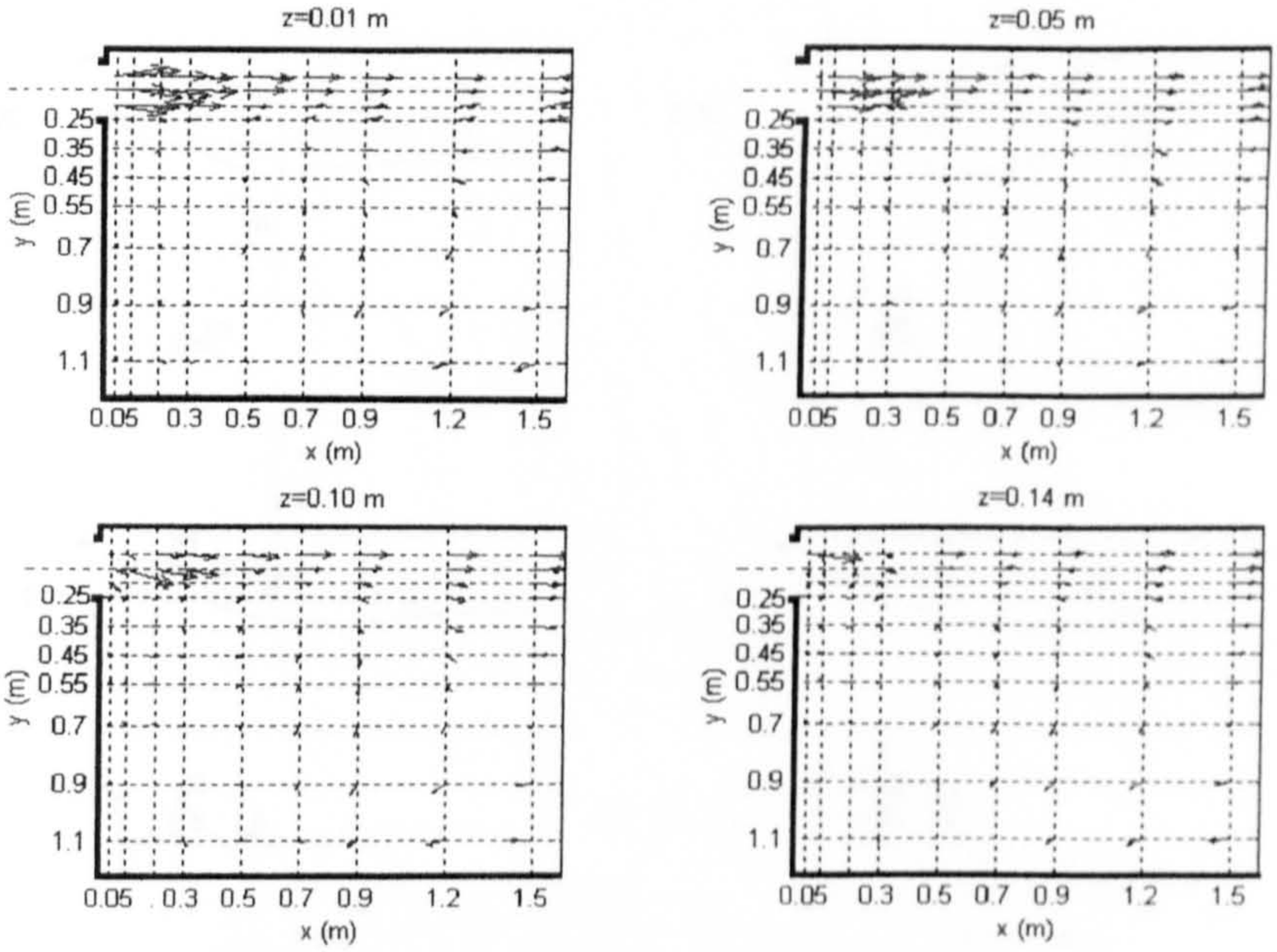

Figure 6-25: Velocity vectors for "bottom side orifice, a = $0.02m^2$, Q = $0.012m^3/s$" [$ObS_{12\text{-}0.02}$]

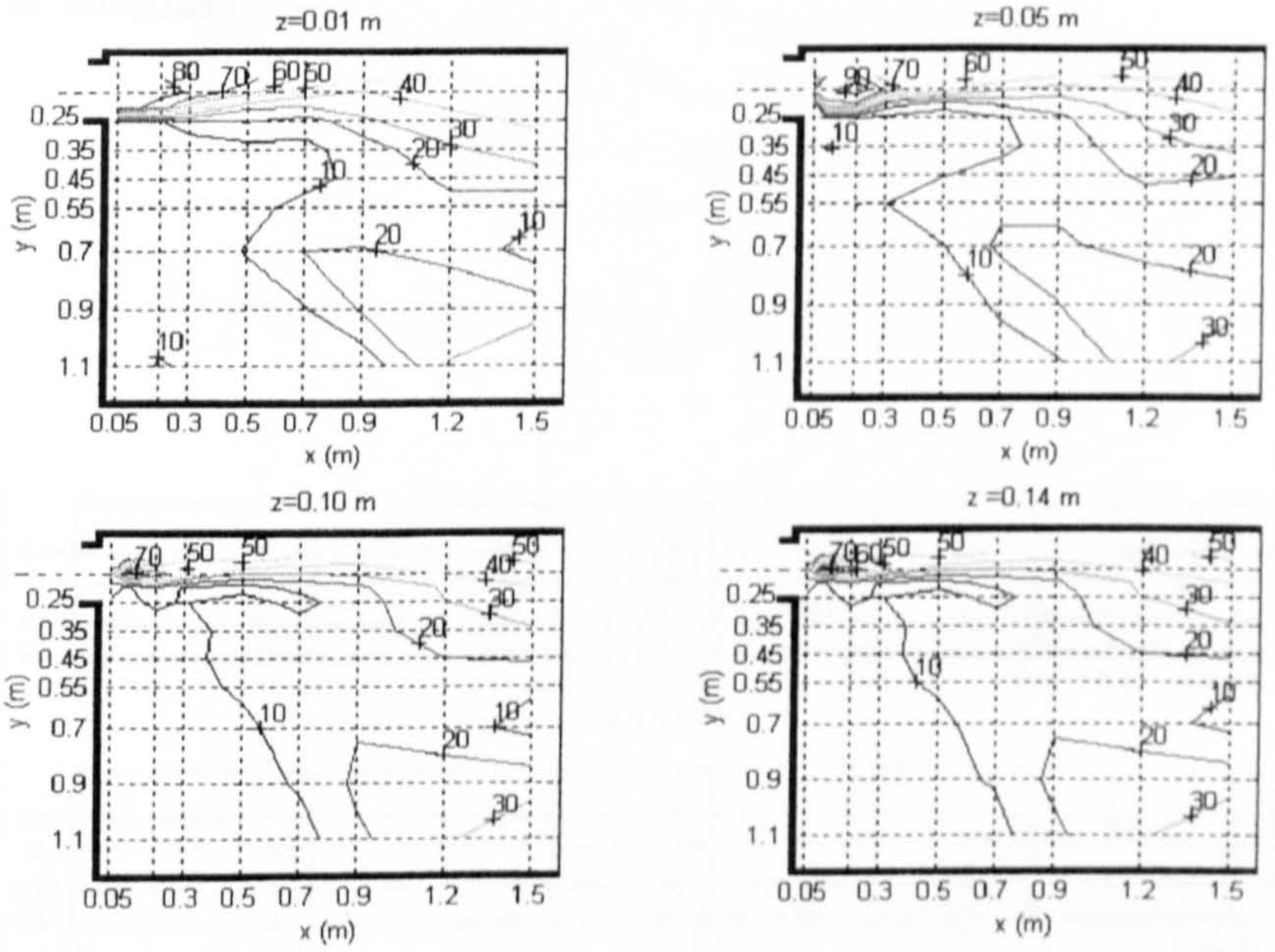

Figure 6-26: Contour of mean velocity in cm/s for "bottom side orifice, a = $0.02m^2$, Q = $0.012m^3/s$" [$ObS_{12\text{-}0.02}$]

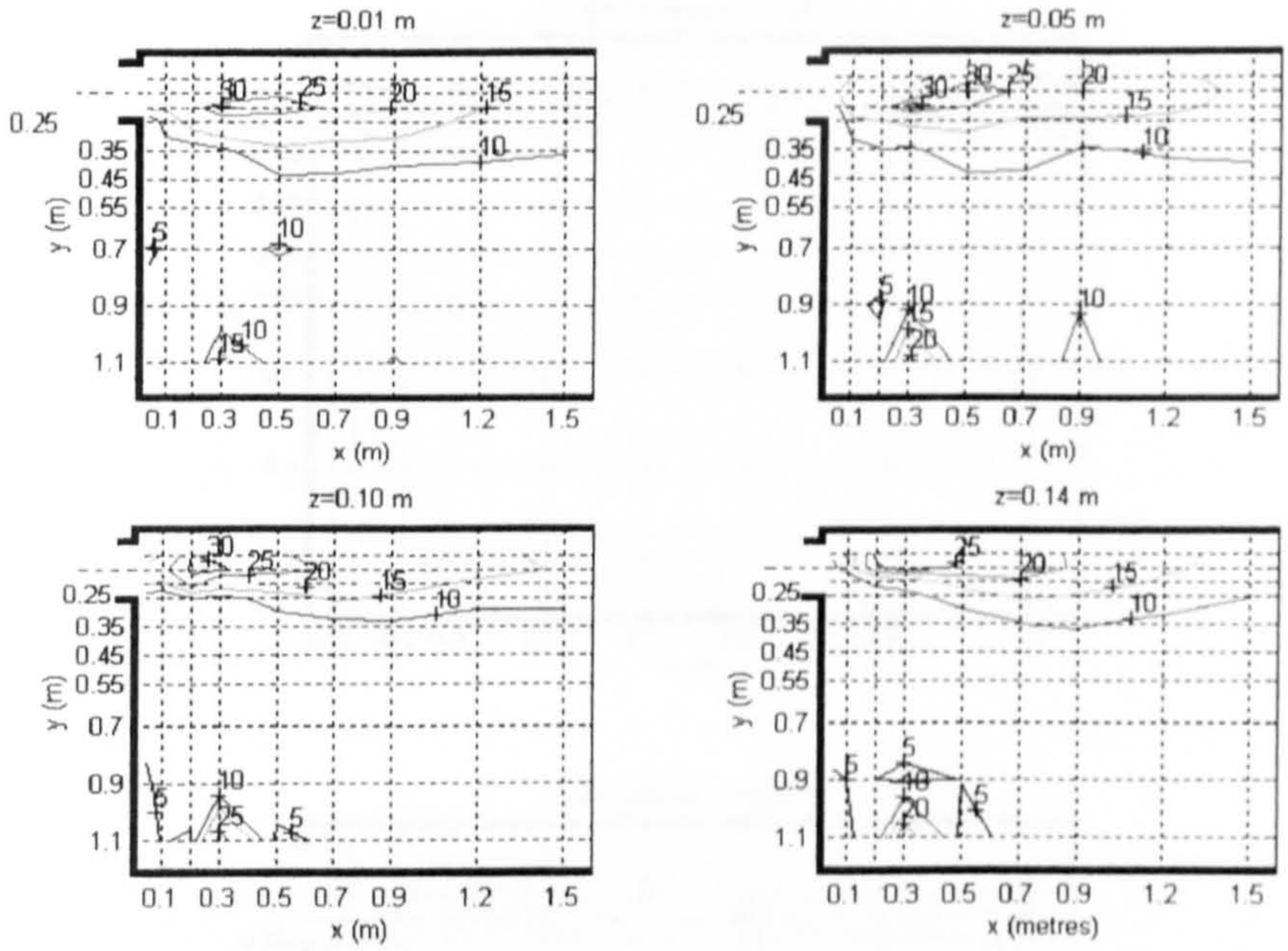

Figure 6-27: Contour of turbulence intensity in % for "bottom side orifice, a = 0.02m^2, Q = 0.012m^3/s" [ObS$_{12\text{-}0.02}$]

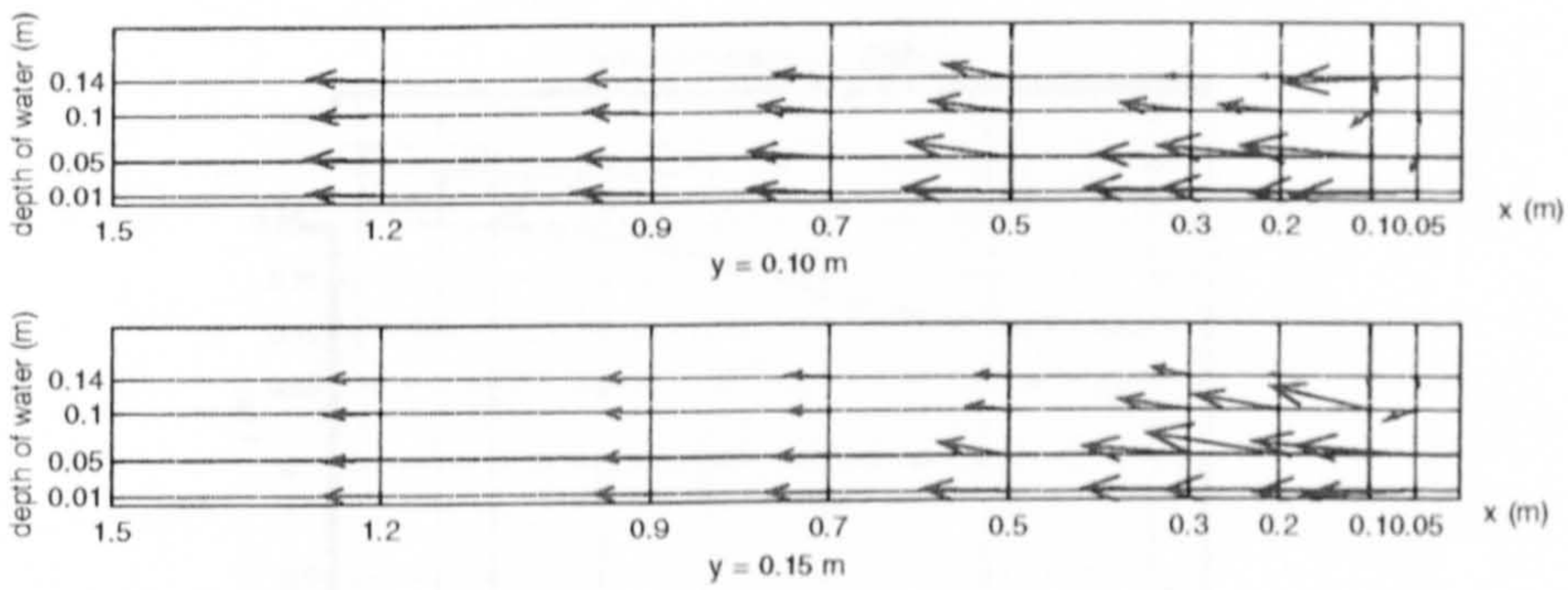

Figure 6-28:Velocity vectors over vertical slides for the bottom side orifice, a = 0.02m^2, Q = 0.012m^3/s

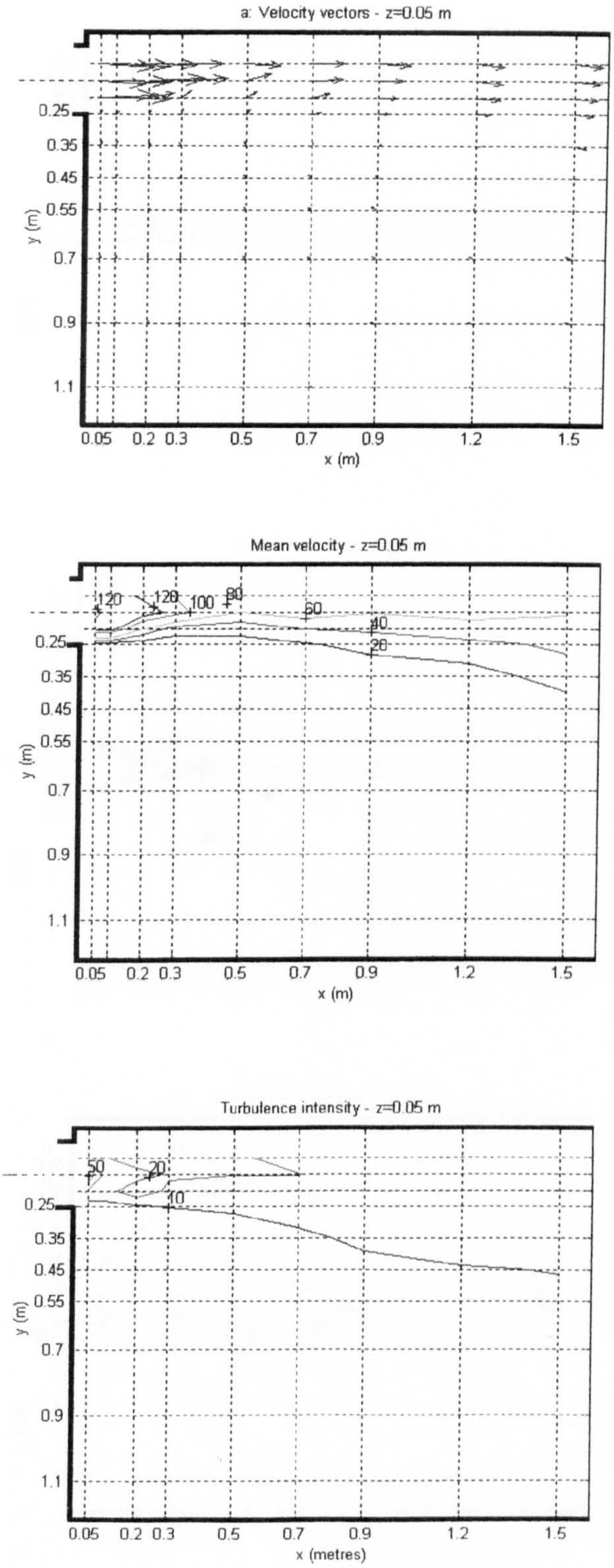

Figure 6-29: Bottom side orifice, a = 0.02m^2, Q = 0.020m^3/s (a: velocity vectors; b: contours of mean velocity in cm/s and c: contours of turbulence intensity in %).

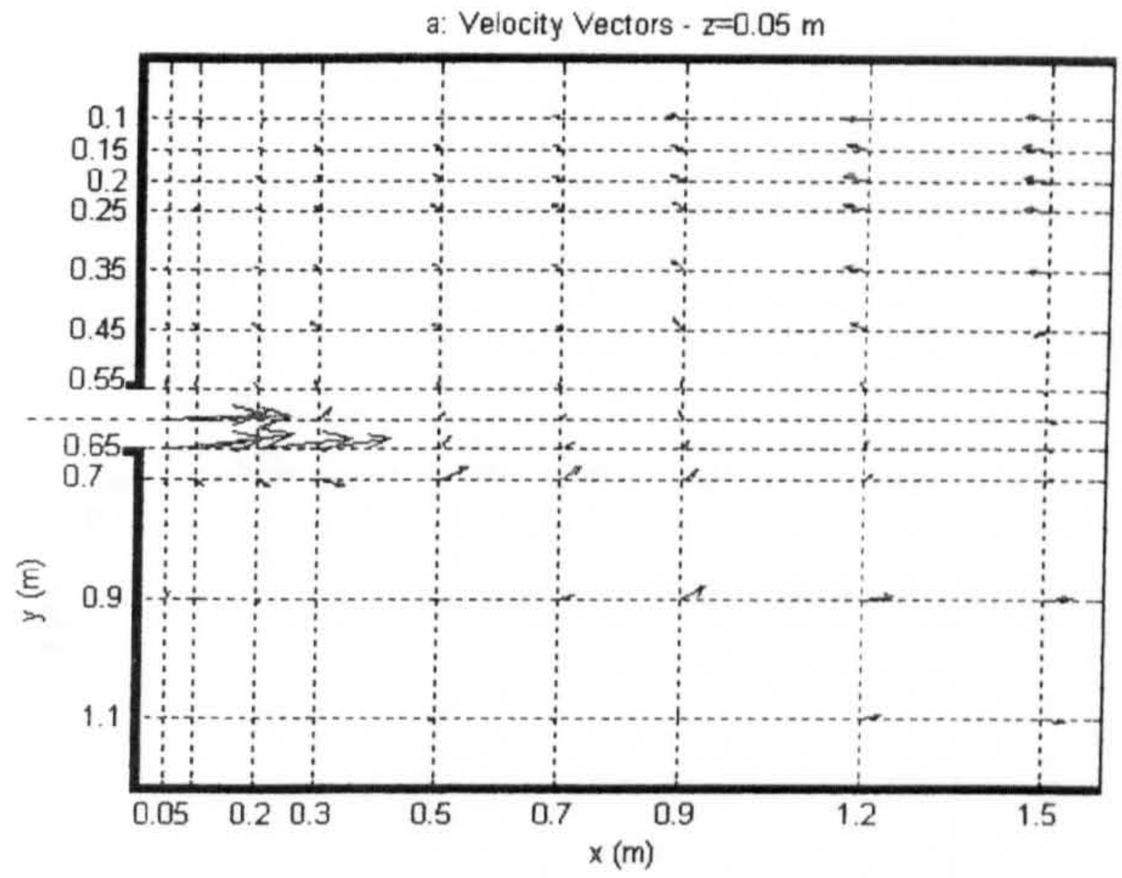

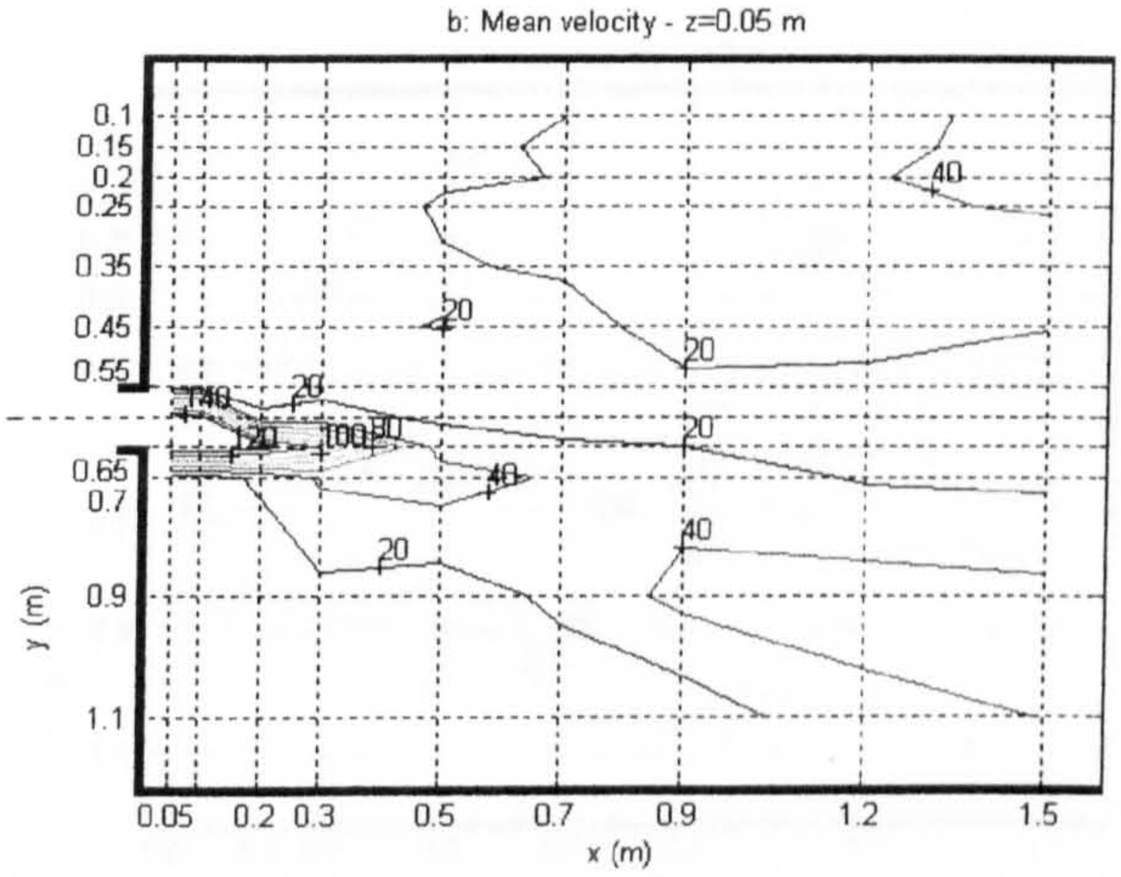

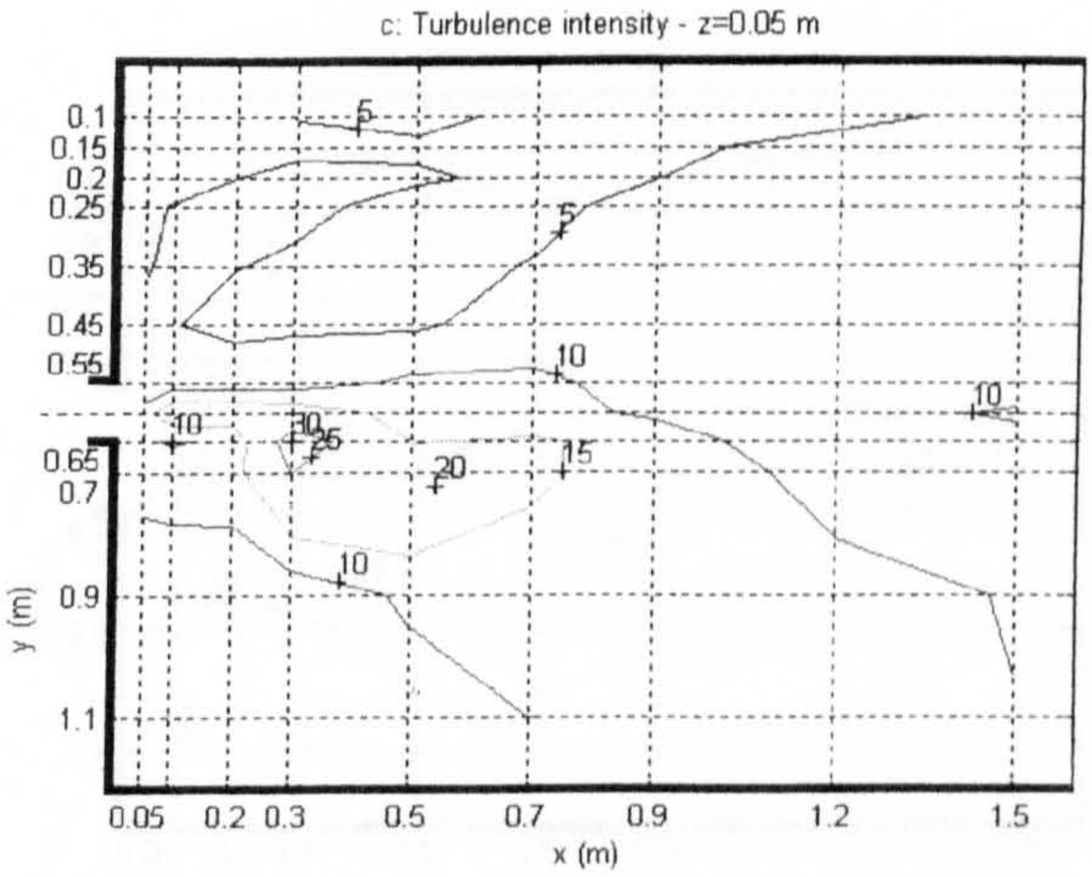

Figure 6-30: Bottom middle orifice, a = 0.01m^2, Q = 0.012m^3/s [ObM$_{12\text{-}0.01}$] (a: velocity vectors; b: contours of mean velocity in cm/s and c: contours of turbulence intensity in %)

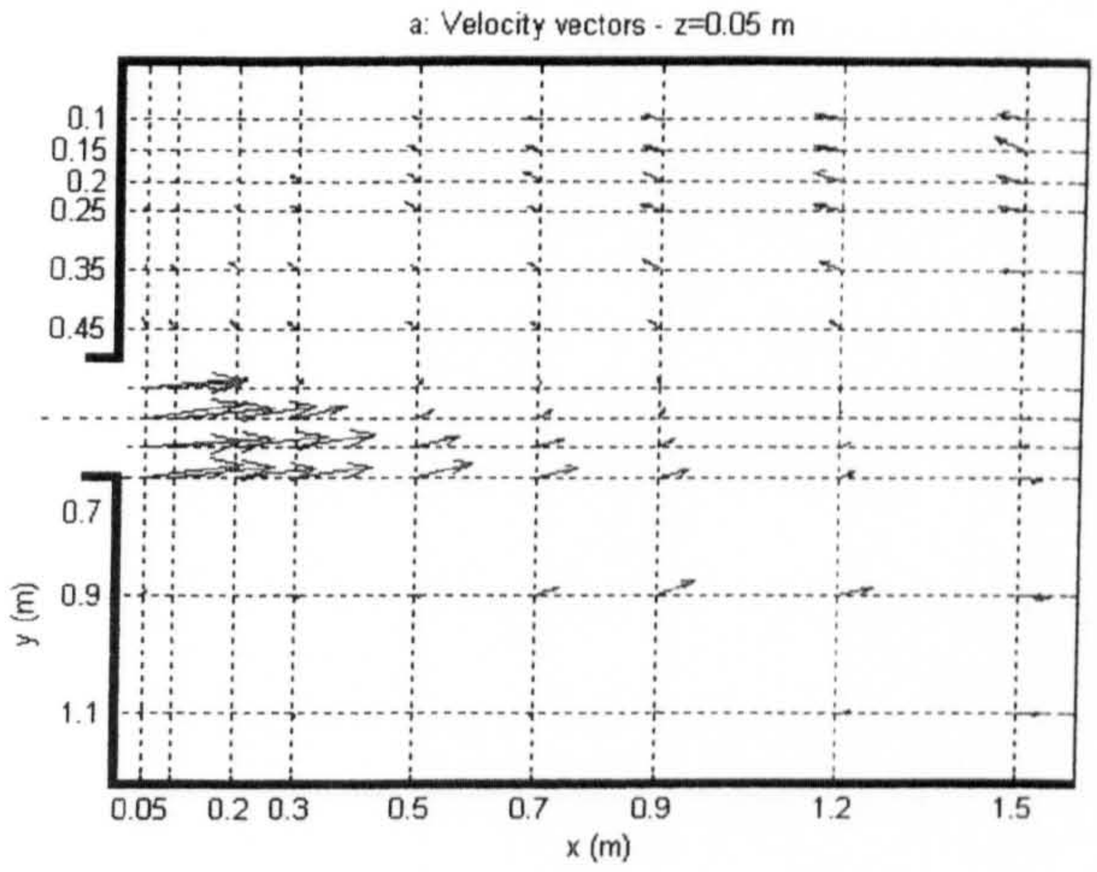

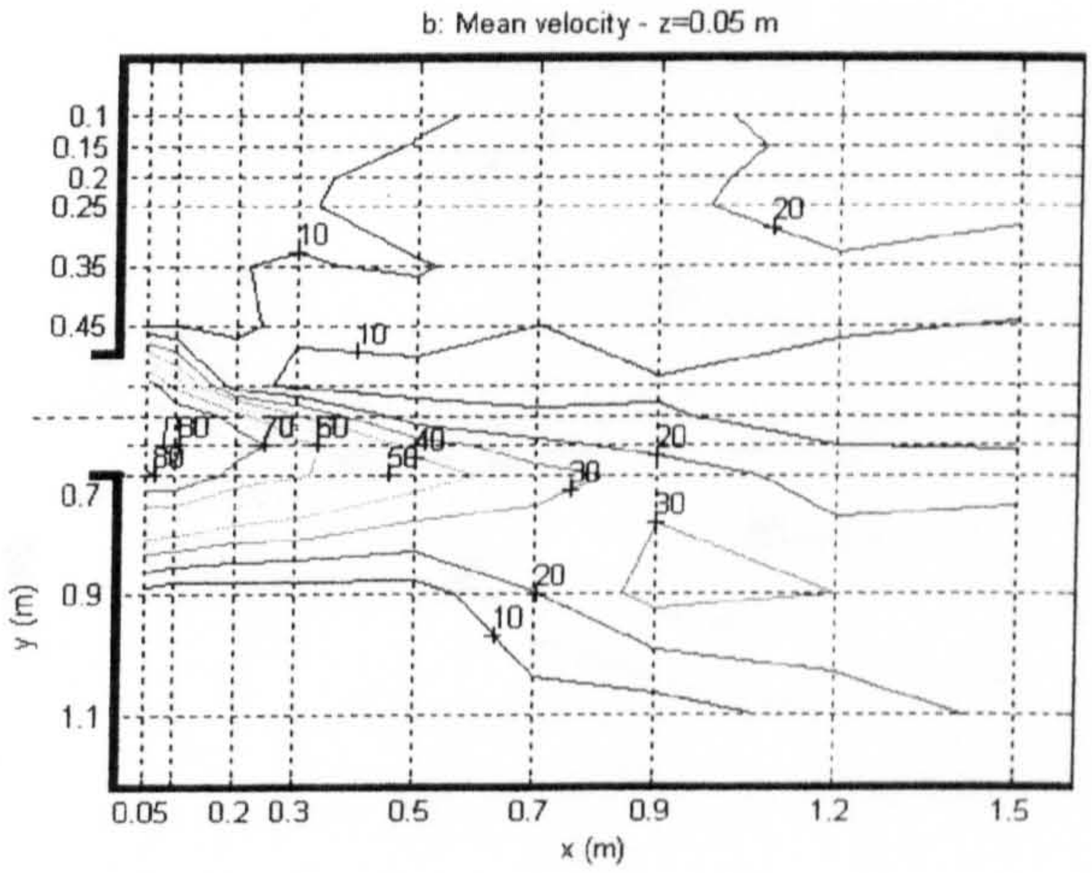

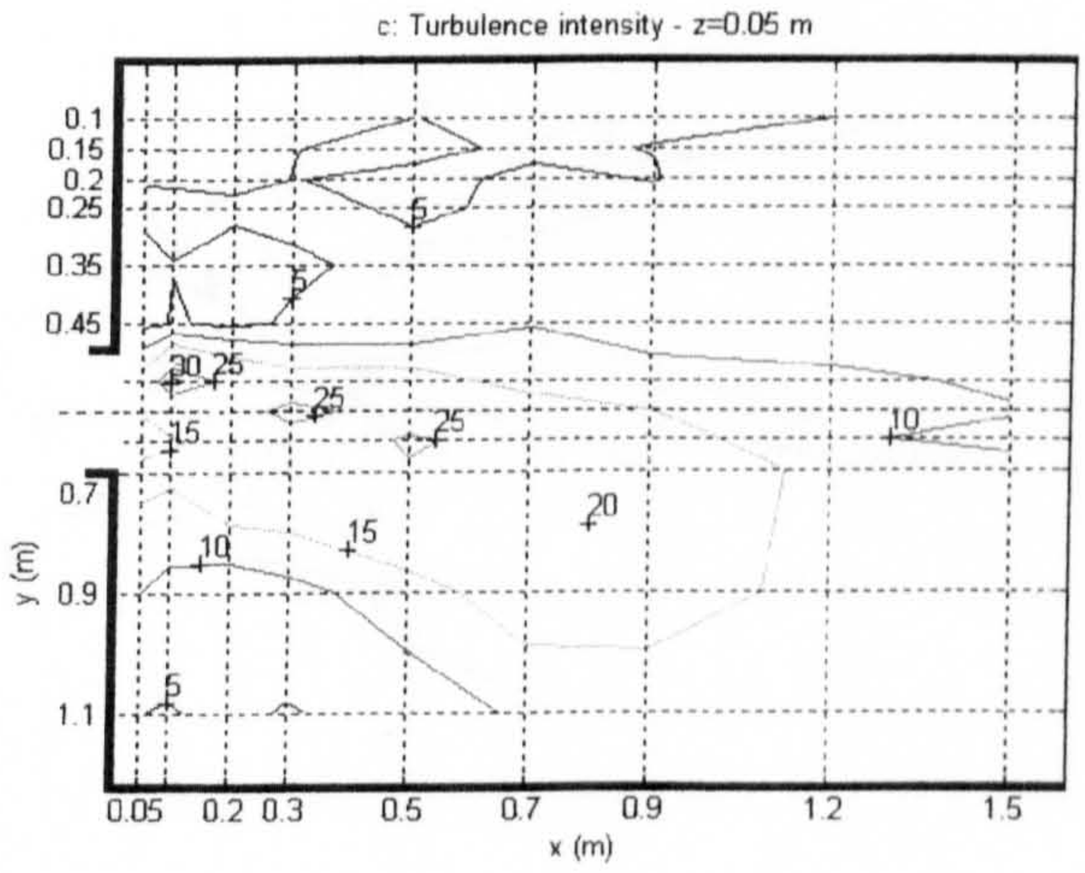

Figure 6-31: Bottom middle orifice, a = 0.02m^2, Q = 0.012m^3/s [ObM$_{12\text{-}0.02}$] (a: velocity vectors; b: contours of mean velocity in cm/s and c: contours of turbulence intensity in %)

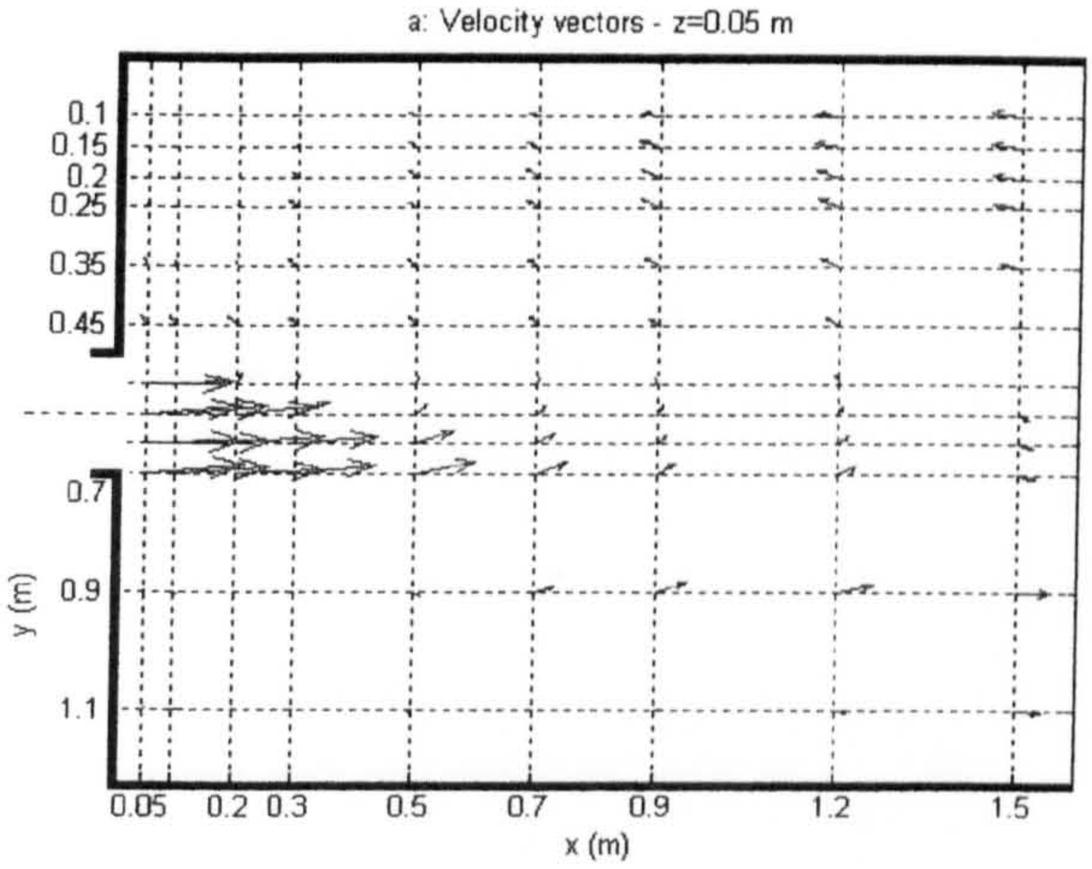

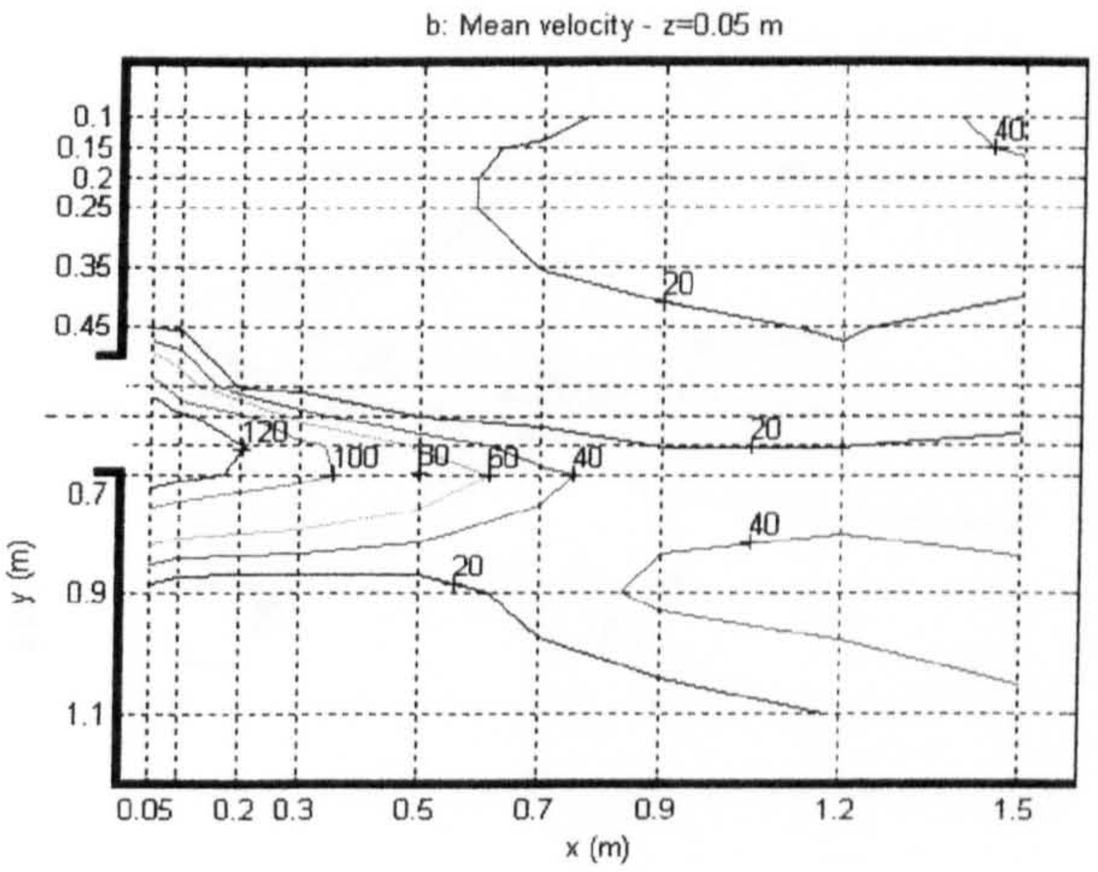

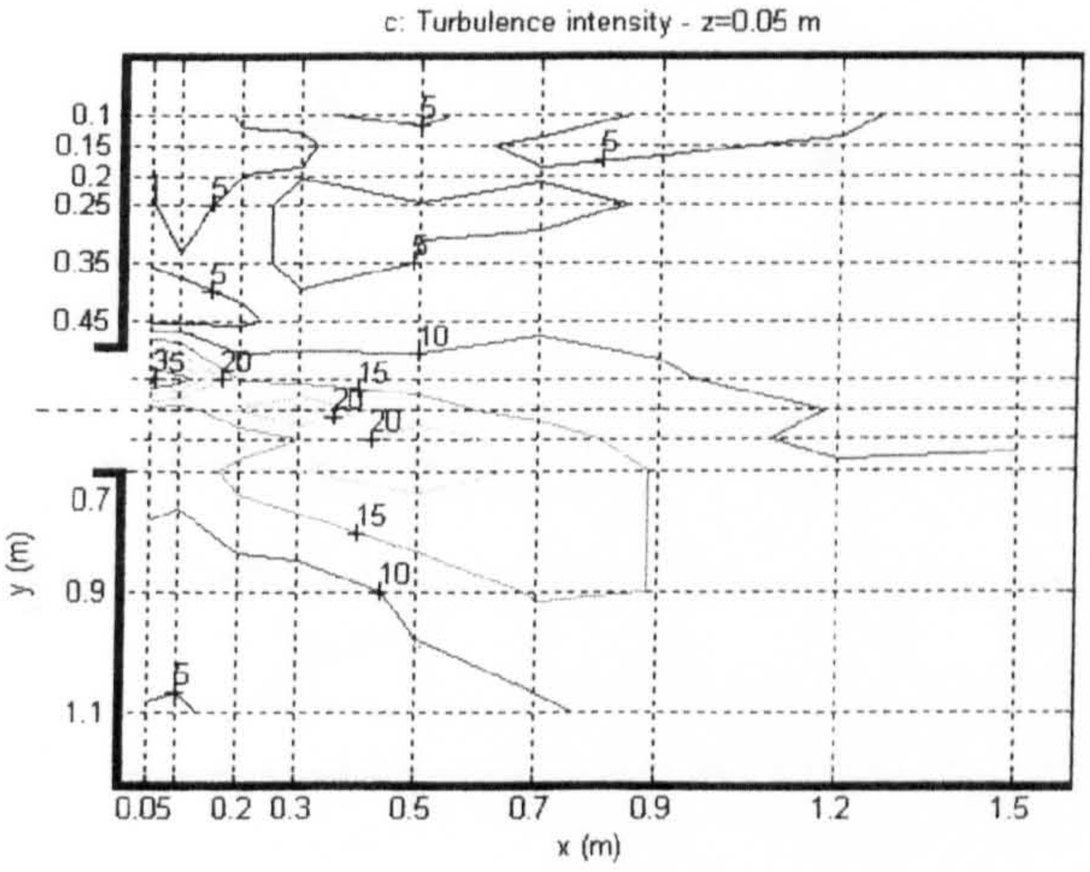

Figure 6-32: Bottom middle orifice, a = 0.02m^2, Q = 0.020m^3/s [$ObM_{20\text{-}0.02}$] (a: velocity vectors; b: contours of mean velocity in cm/s and c: contours of turbulence intensity in %)

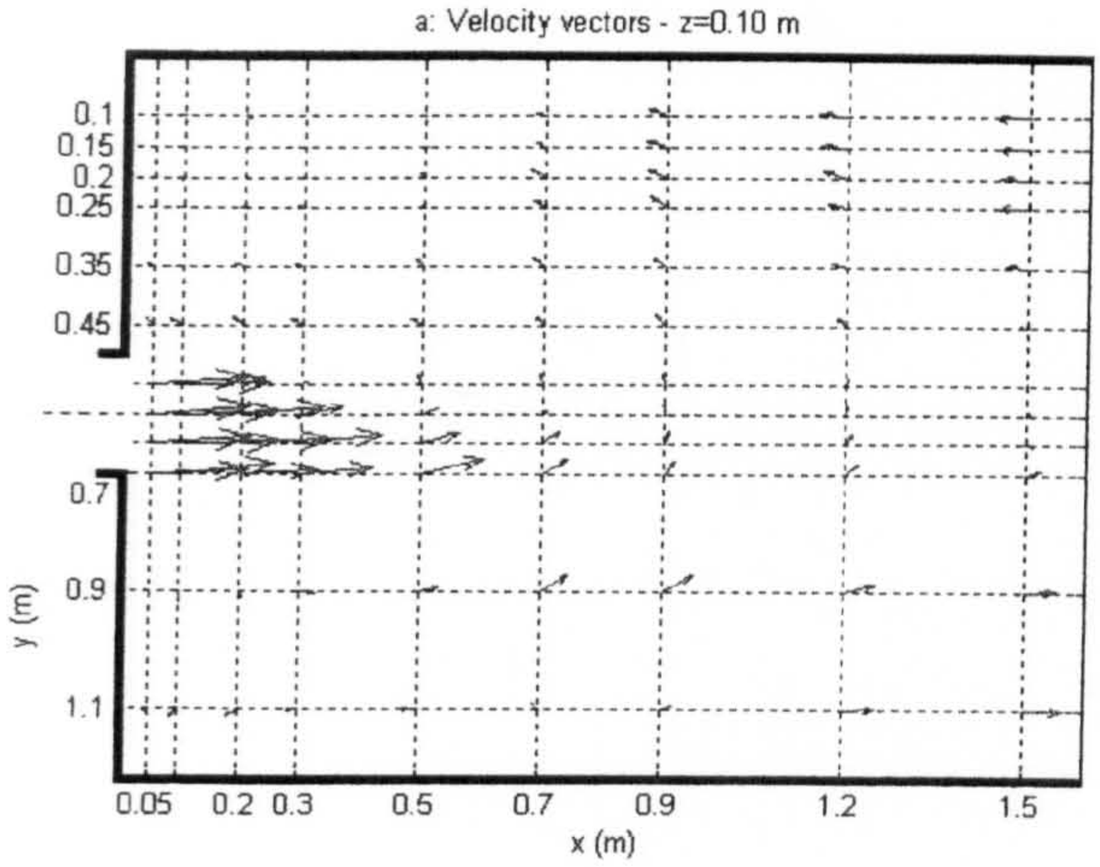

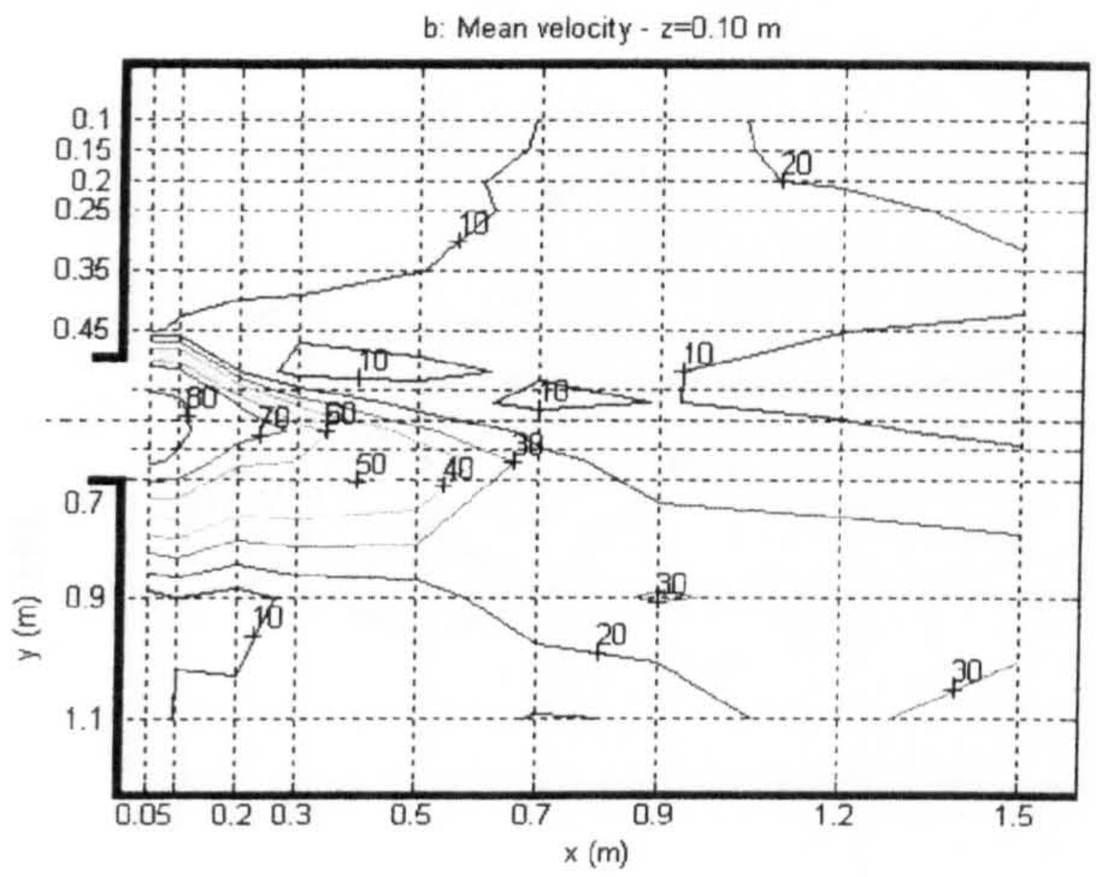

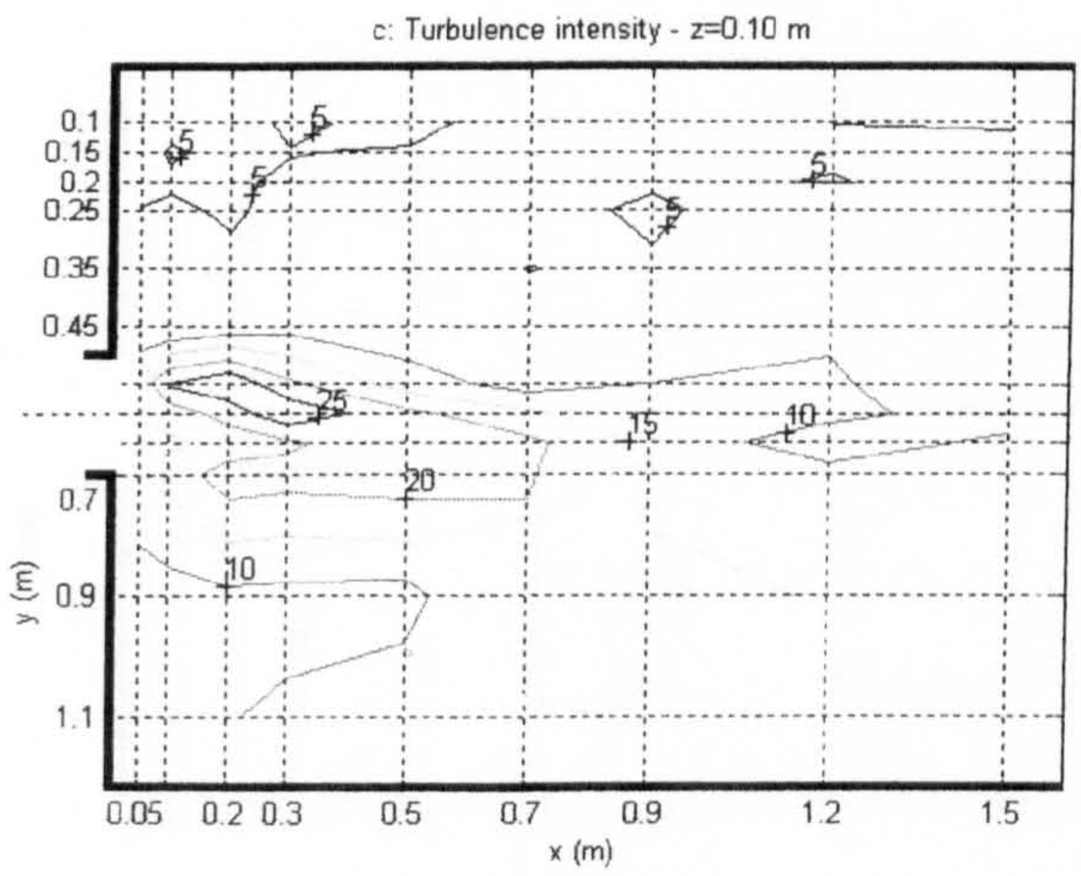

Figure 6-33: Middle orifice at 0.05 m from the bottom, a = 0.02m^2, Q = 0.012m^3/s [$OFM_{12\text{-}0.02}$] (a: velocity vectors; b: contours of mean velocity in cm/s and c: contours of turbulence intensity in %)

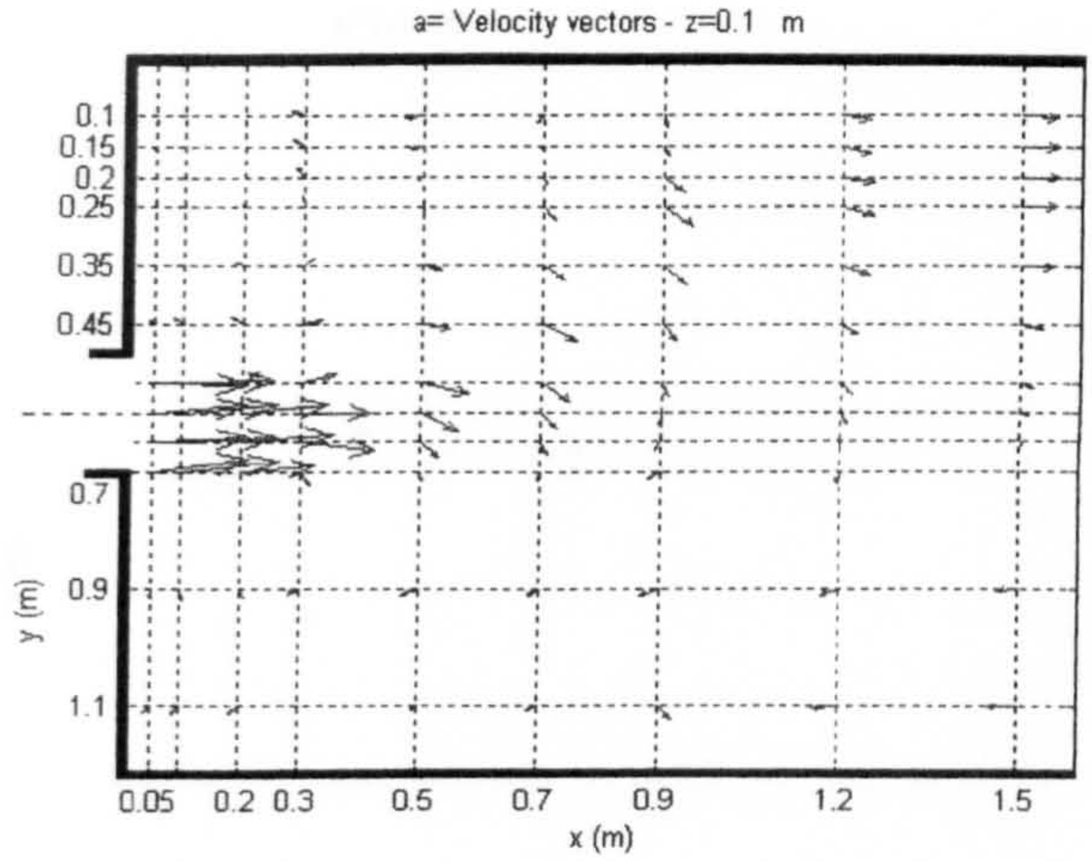

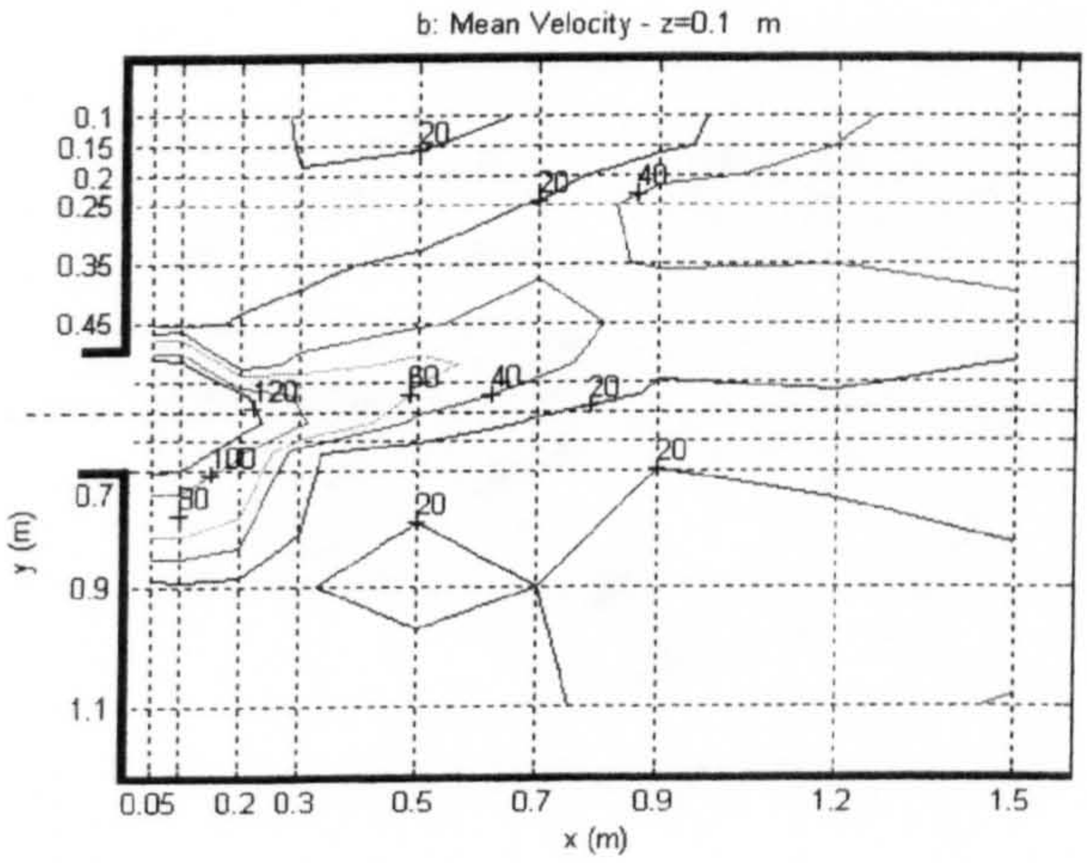

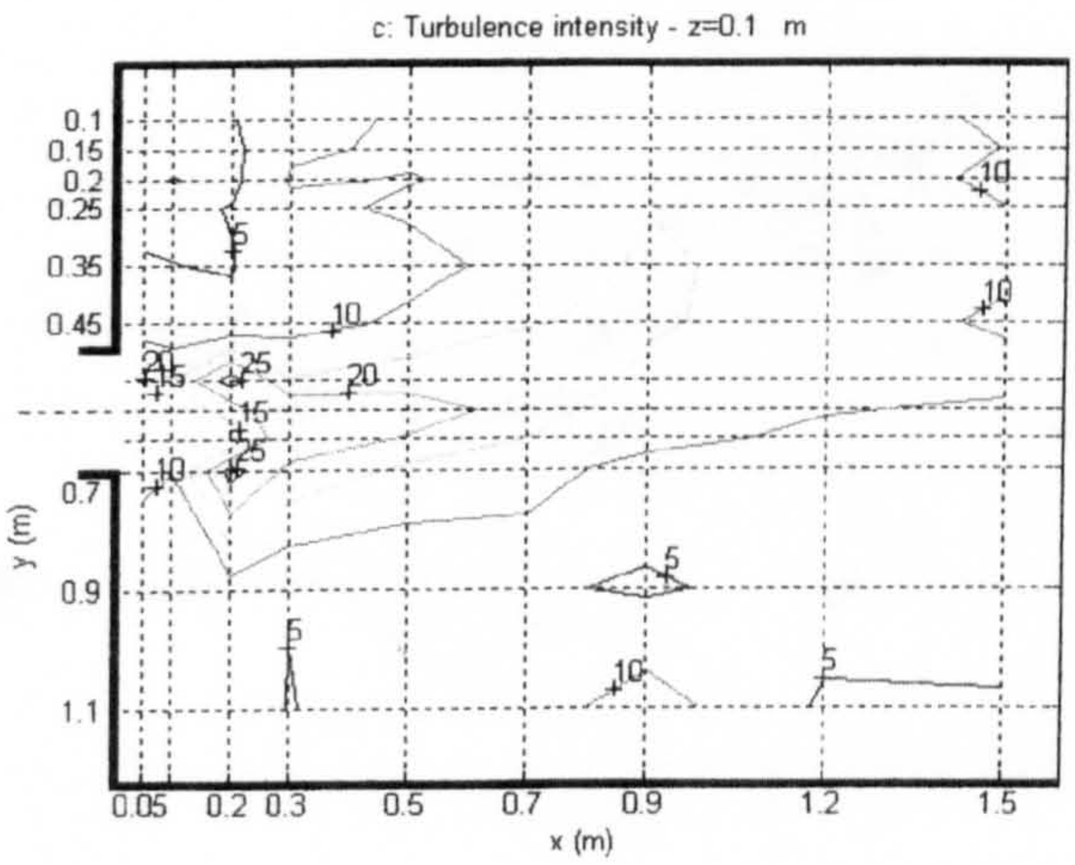

Figure 6-34: Middle orifice at 0.05 m from the bottom, a = 0.02m^2, Q = 0.020m^3/s [OFM$_{20\text{-}0.02}$] (a: velocity vectors; b: contours of mean velocity in cm/s and c: contours of turbulence intensity in %)

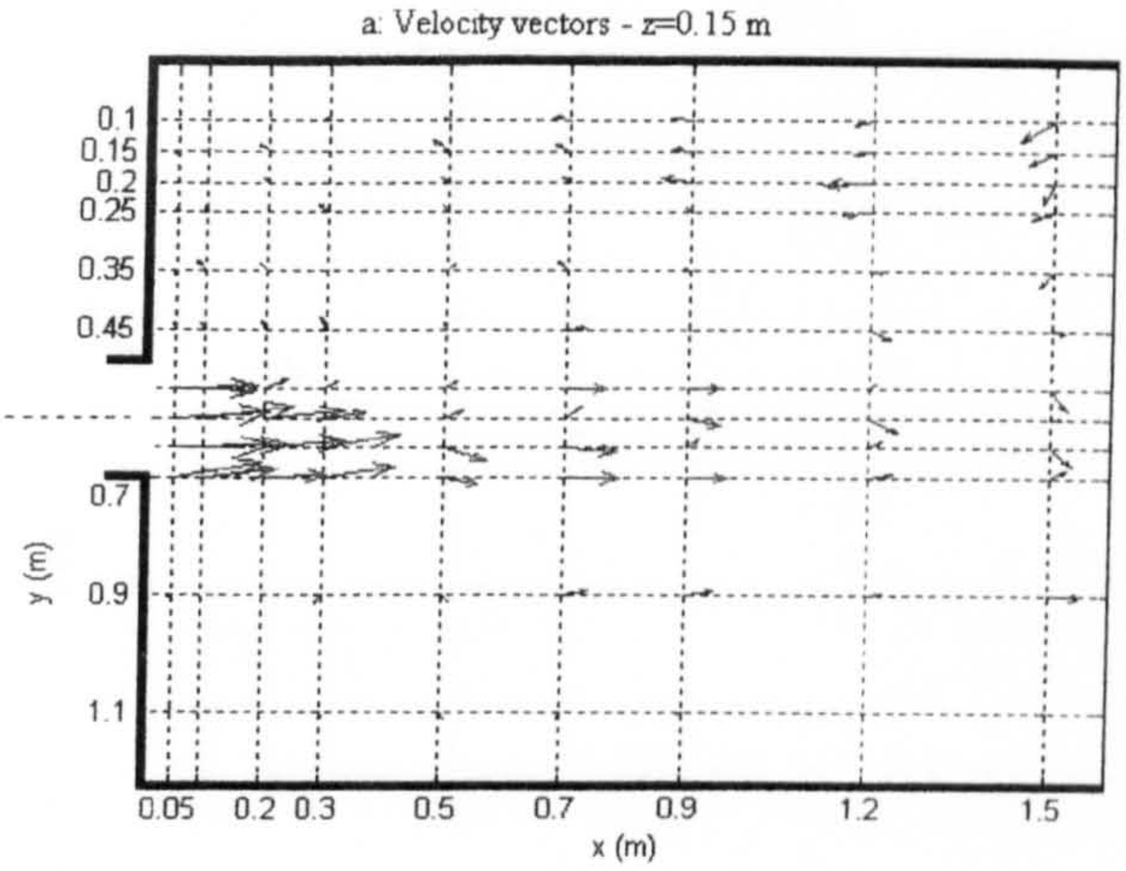

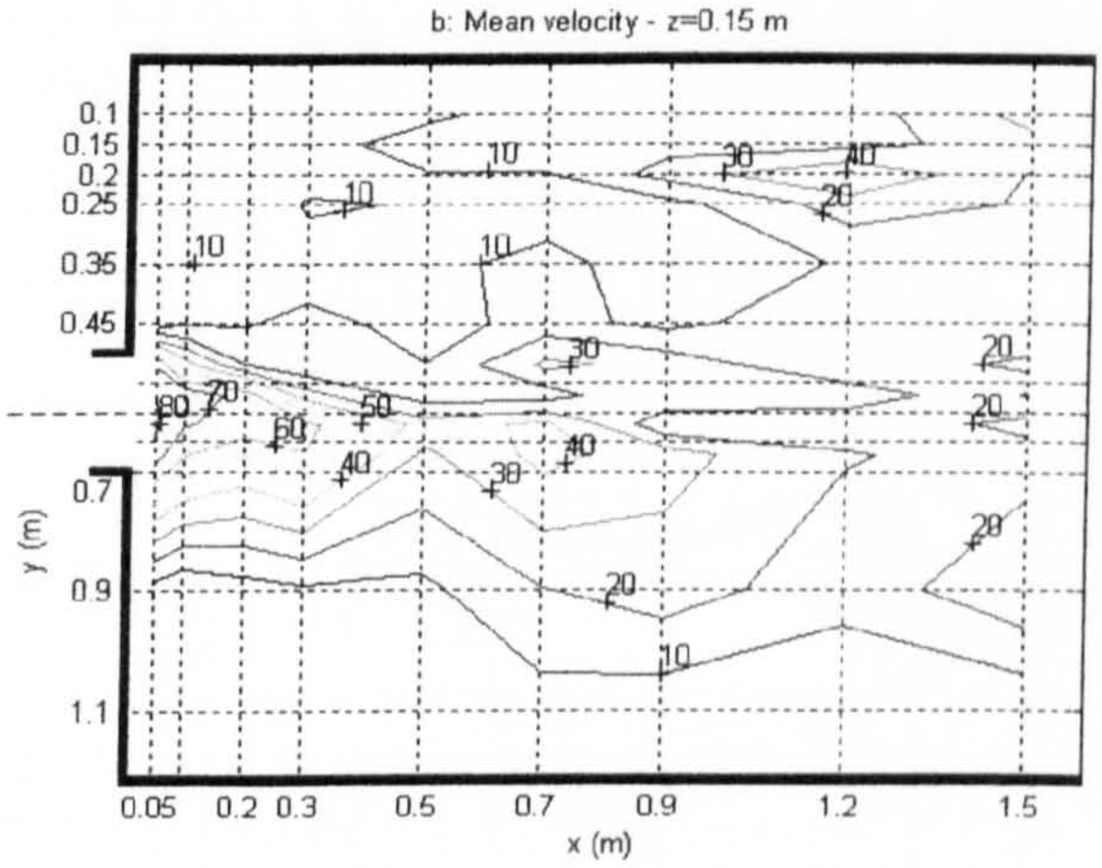

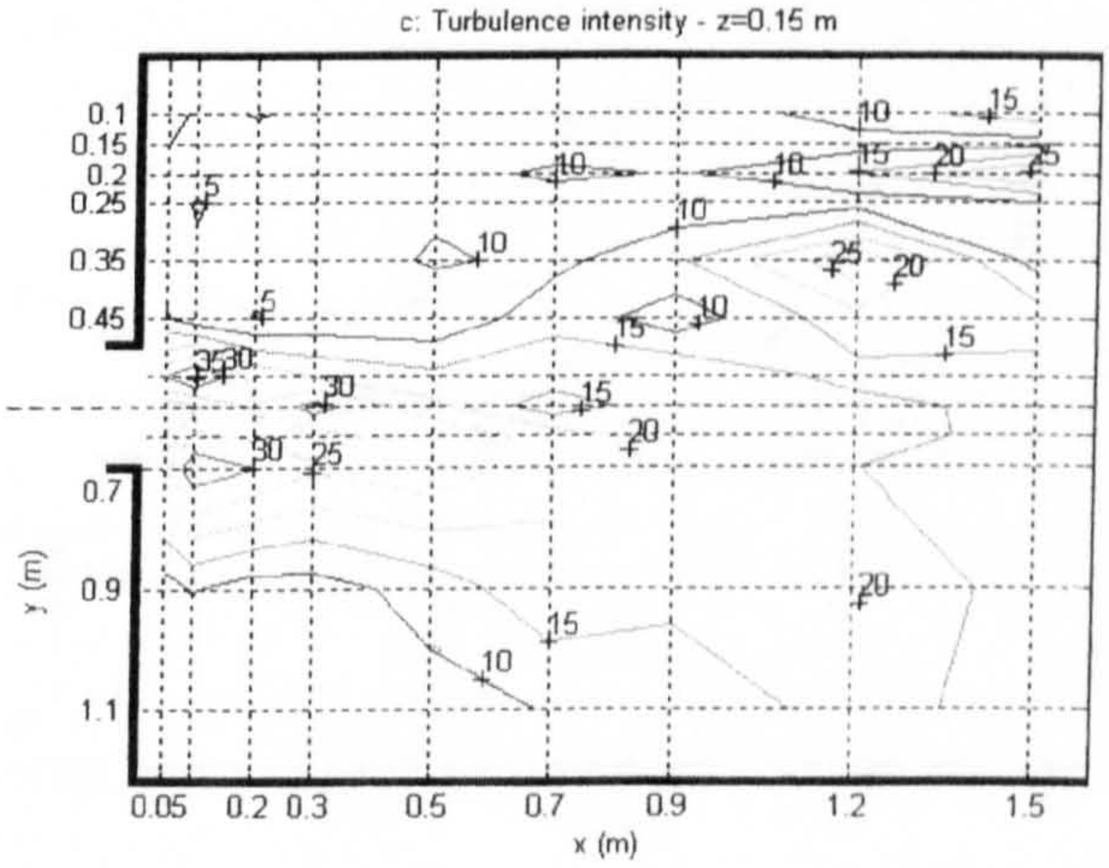

Figure 6-35: Middle orifice at 0.010 m from the bottom, a = 0.02m^2, Q = 0.012m^3/s (a: velocity vectors; b: contours of mean velocity in cm/s and c: contours of turbulence intensity in %)

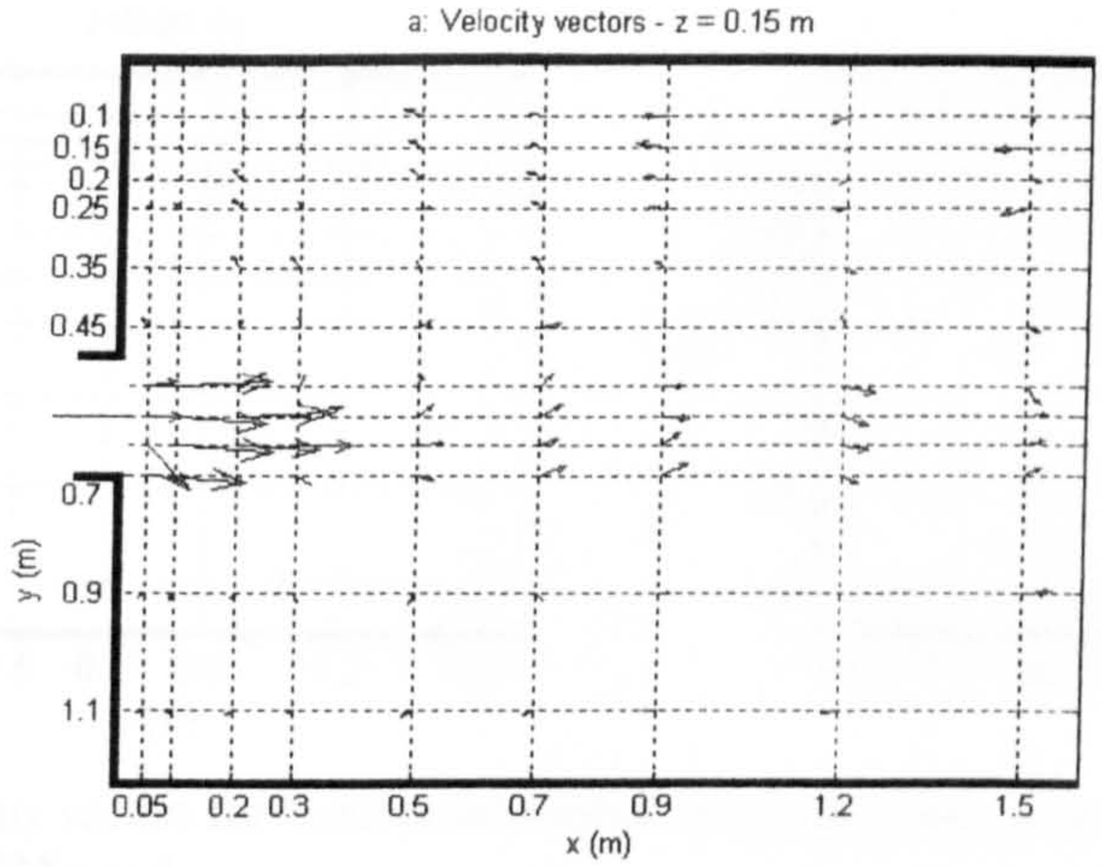

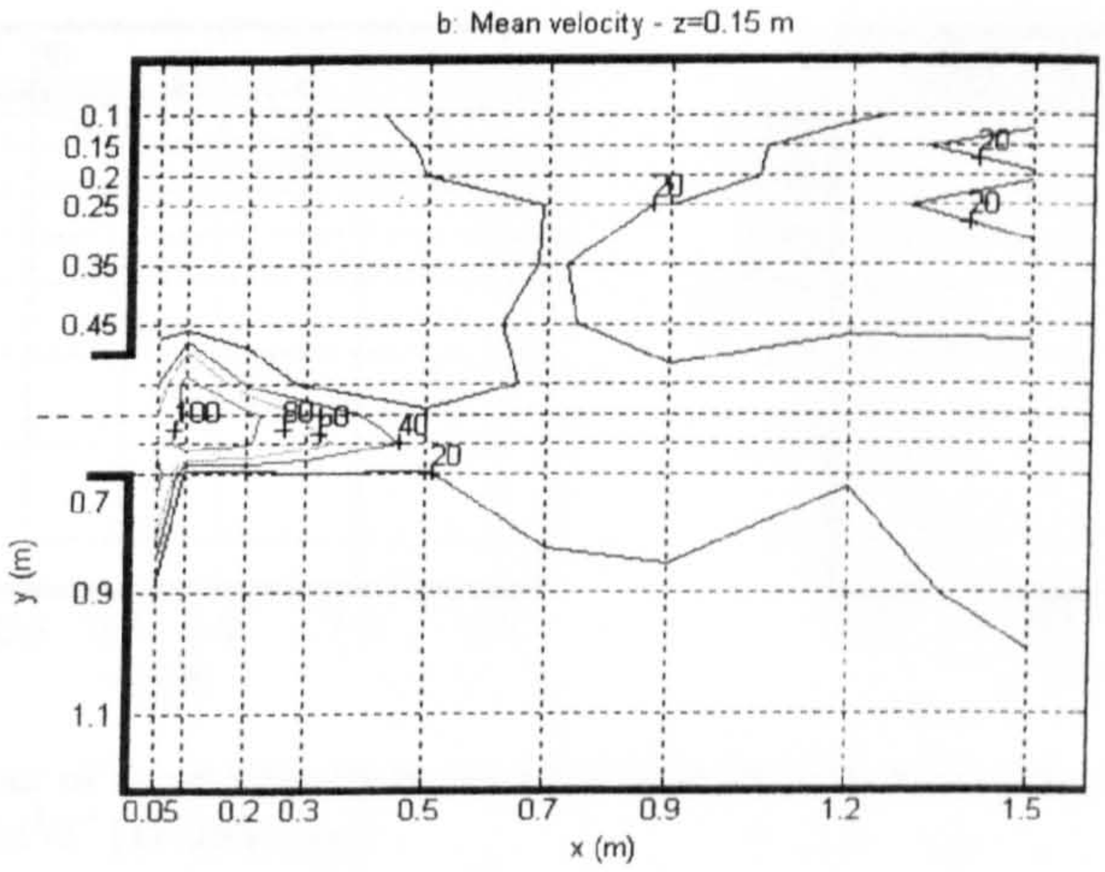

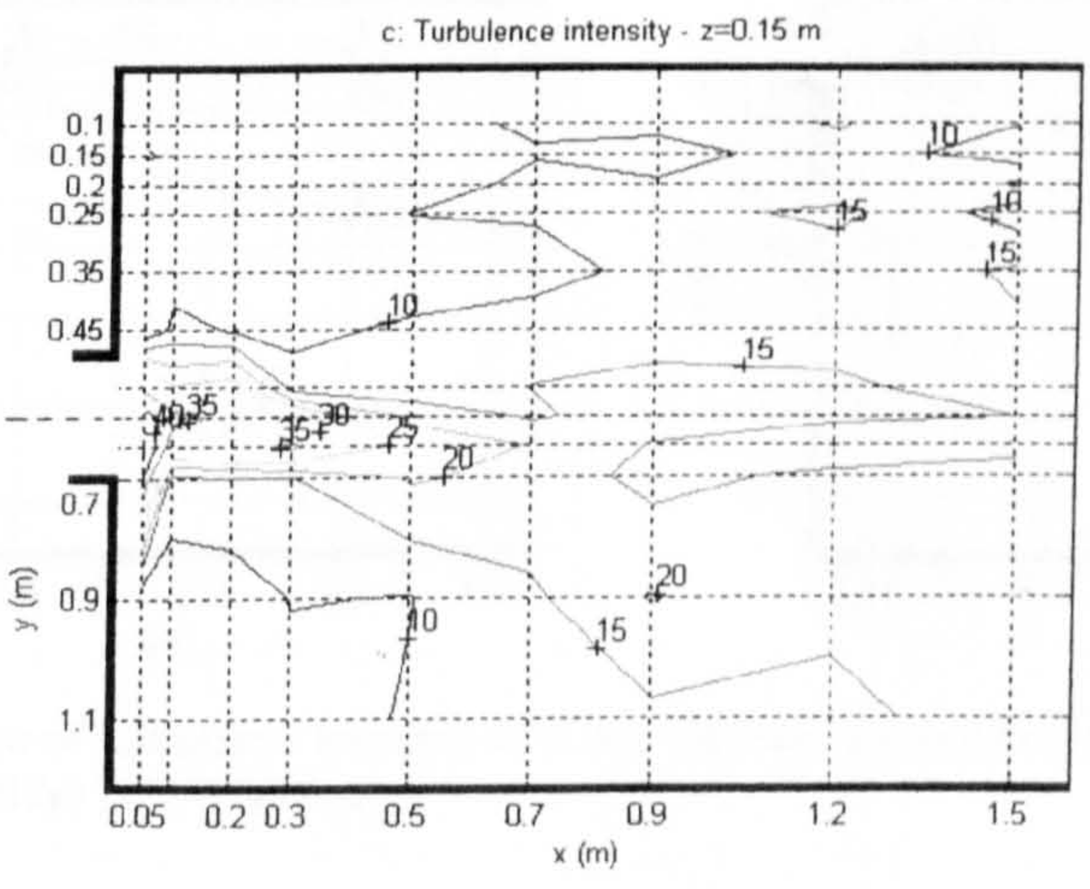

Figure 6-36: Middle orifice at 0.010 m from the bottom, a = 0.02m^2, Q = 0.020m^3/s (a: velocity vectors; b: contours of mean velocity in cm/s and c: contours of turbulence intensity in %)

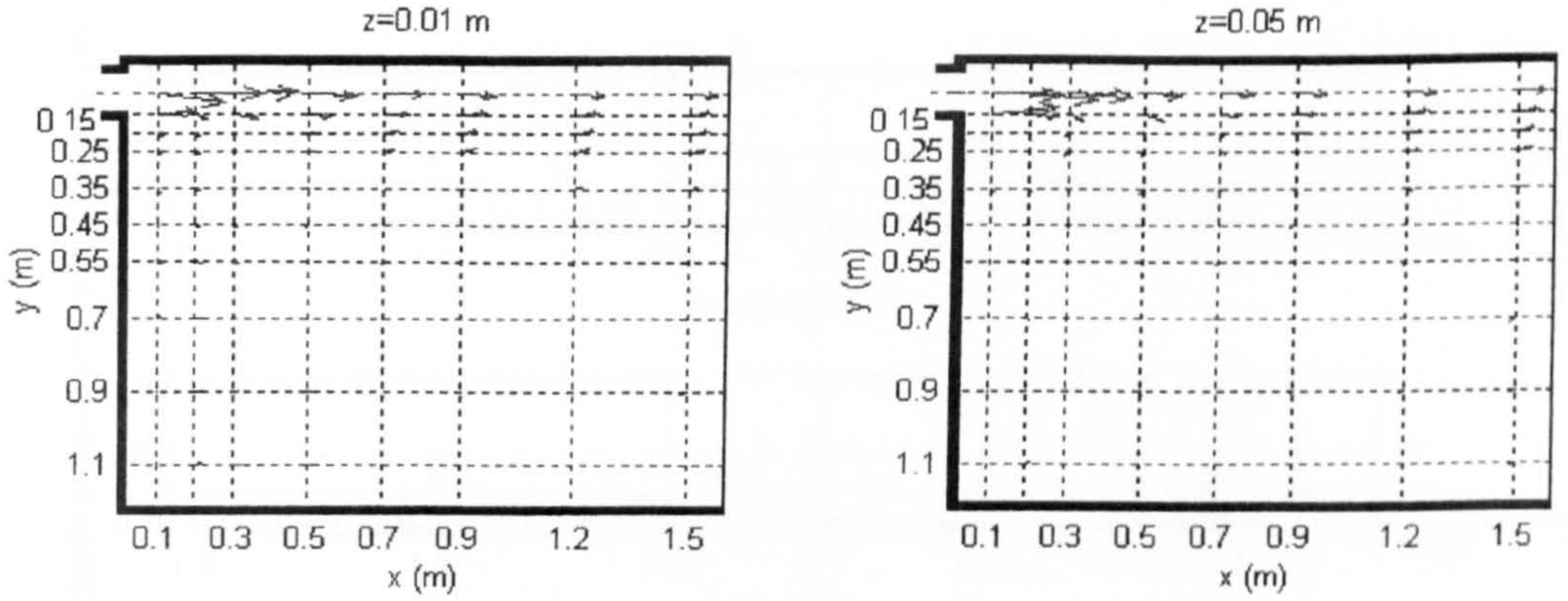

Figure 6-37: Velocity vectors for "bottom side orifice associated with a weir, a = $0.01m^2$, Q=$0.012m^3/s$" [$WObS_{12\text{-}0.01}$]

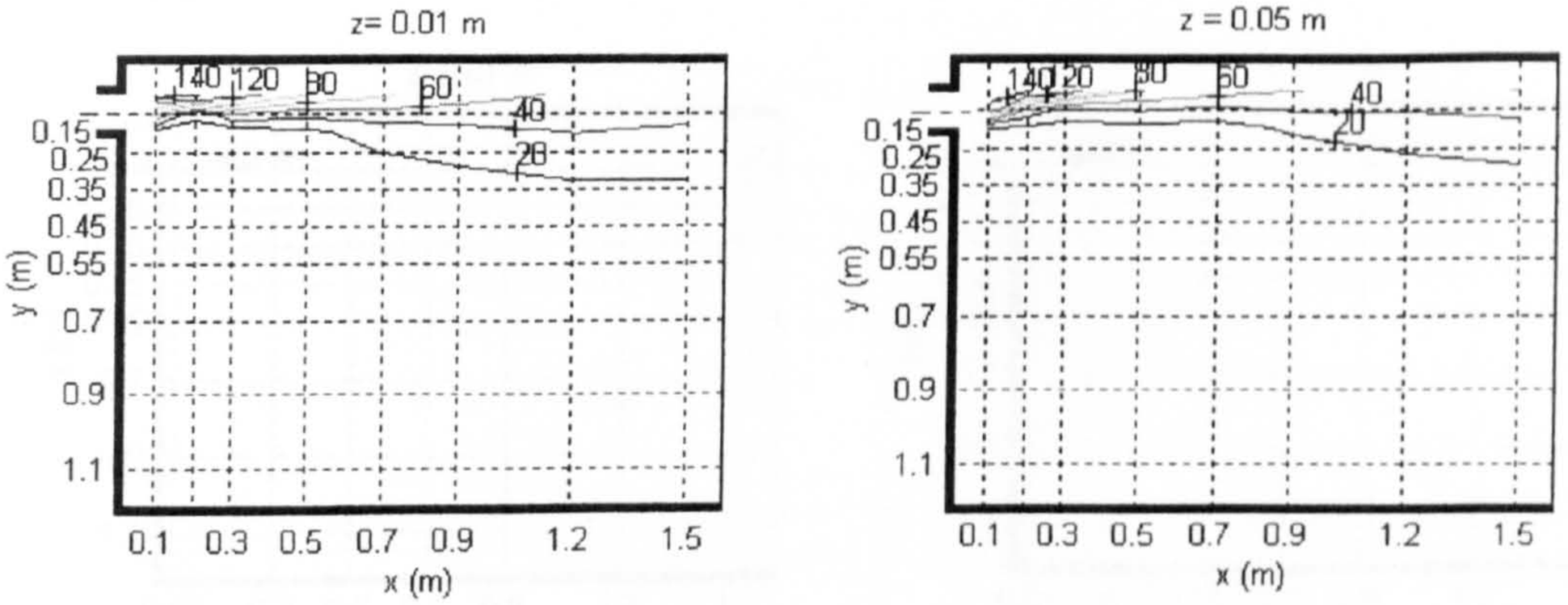

Figure 6-38: Contour of mean velocity in cm/s for "bottom side orifice associated with a weir, a = $0.01m^2$, Q = $0.012m^3/s$" [$WObS_{12\text{-}0.02}$]

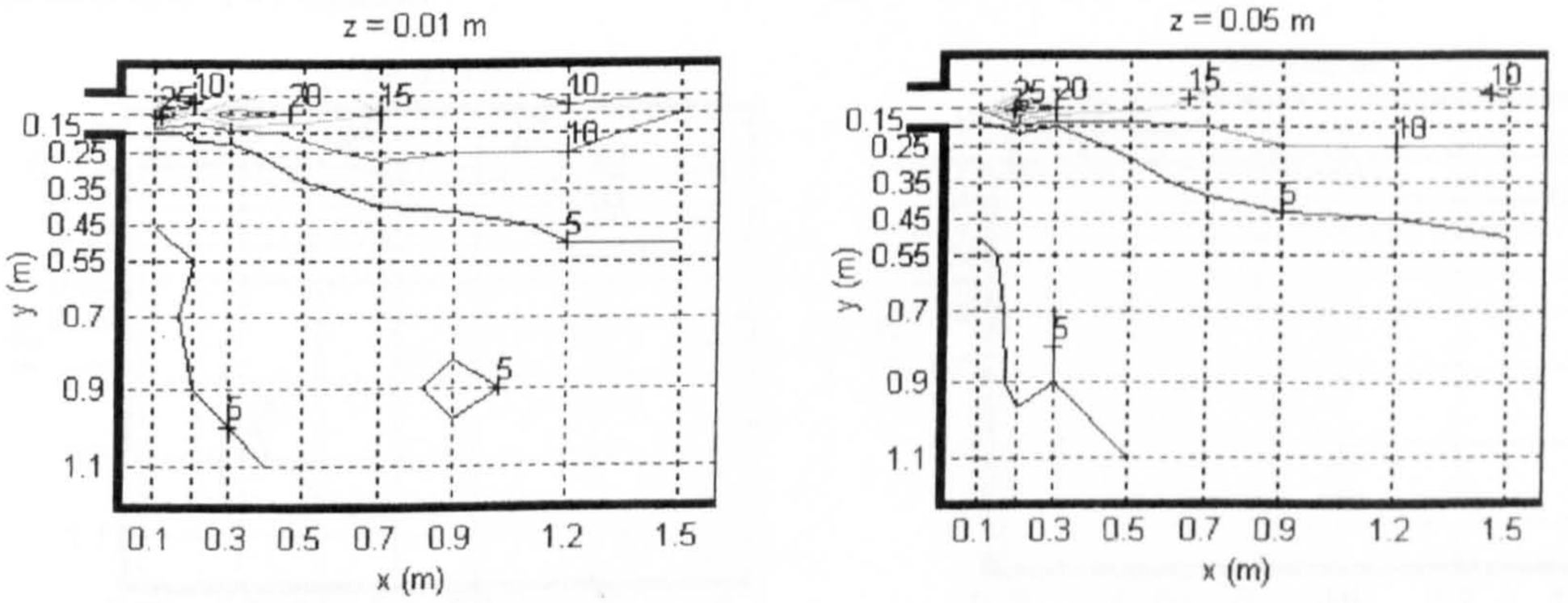

Figure 6-39: Contour of turbulence intensity in % for "bottom side orifice associated with a weir, a = $0.01m^2$, Q = $0.012m^3/s$" [$WObS_{12\text{-}0.02}$]

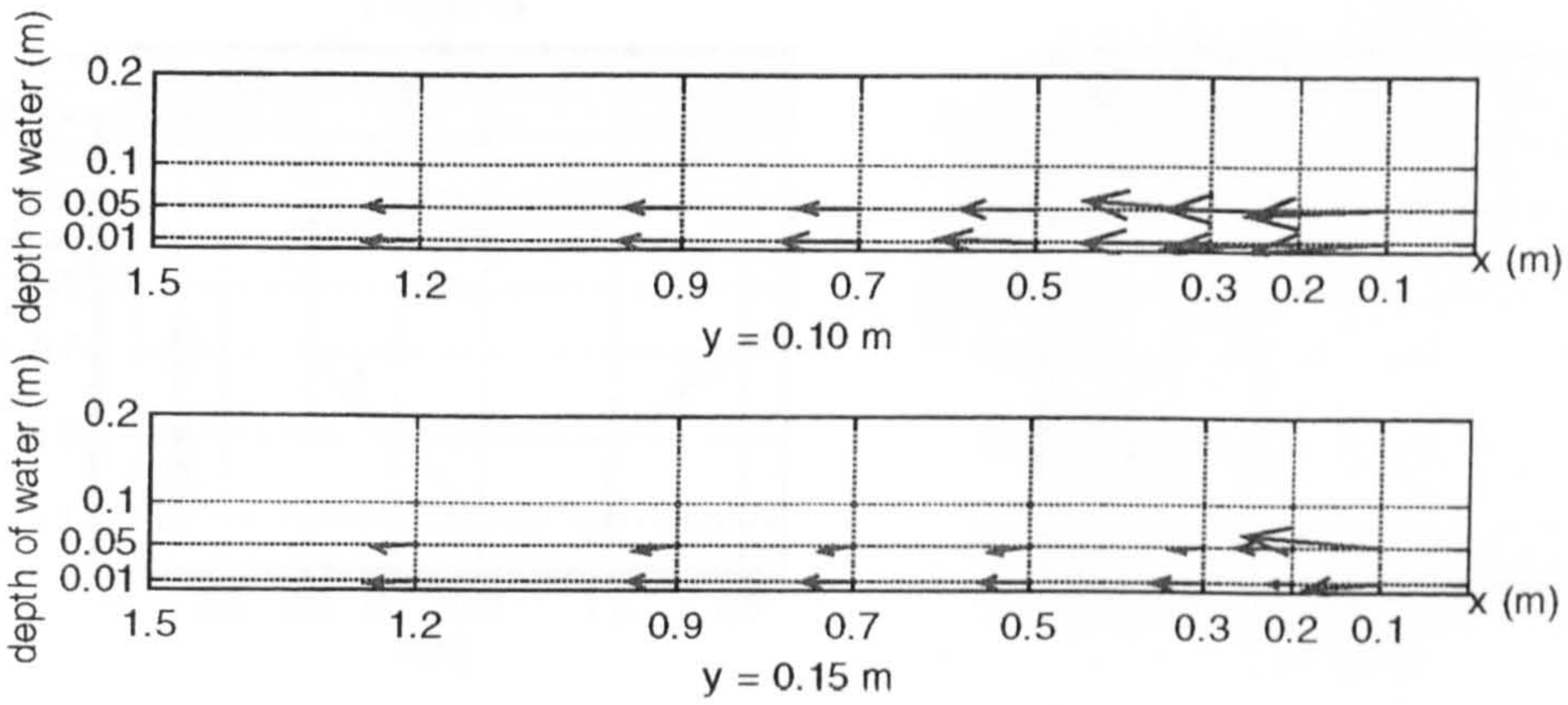

Figure 6-40: Velocity vectors over vertical slide for "bottom side orifice associated with a weir, a = 0.01 m2, Q = 0.012 m3/s"

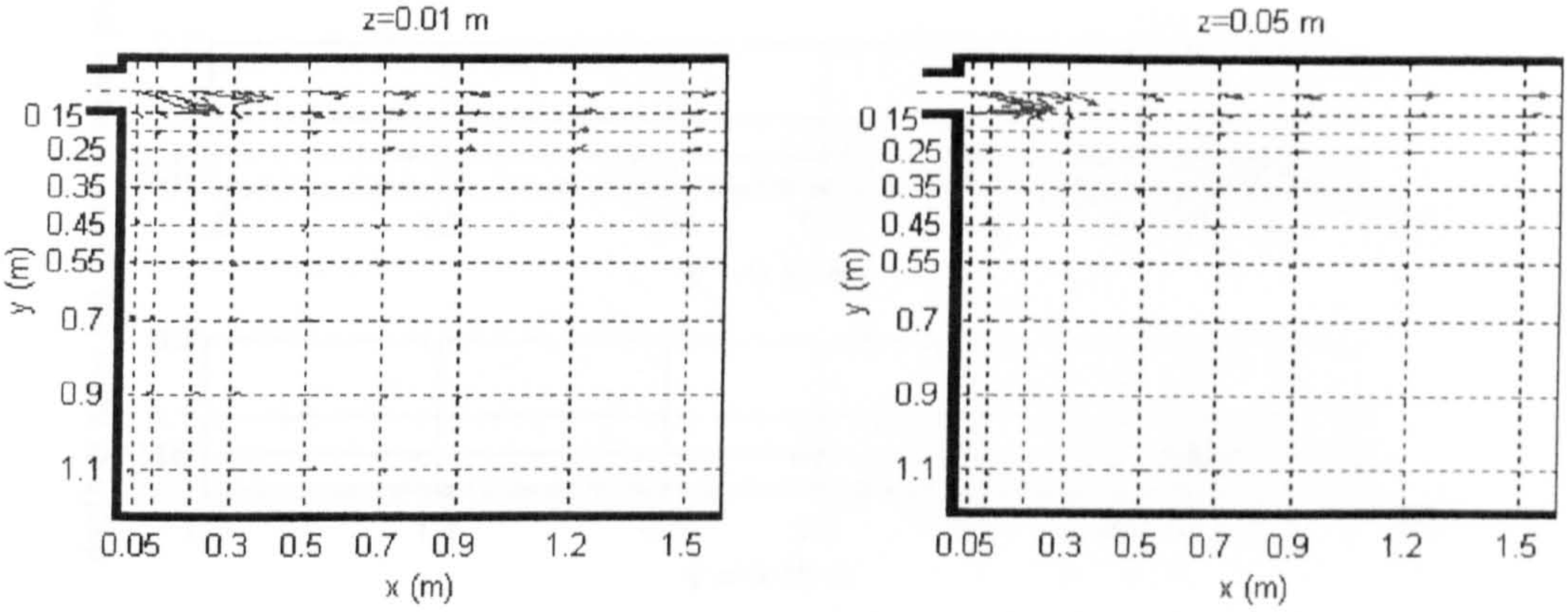

Figure 6-41: Velocity vectors for "bottom side orifice associated with a weir, a = $0.01m^2$, $Q=0.020m^3/s$" [$WObS_{20\text{-}0.01}$]

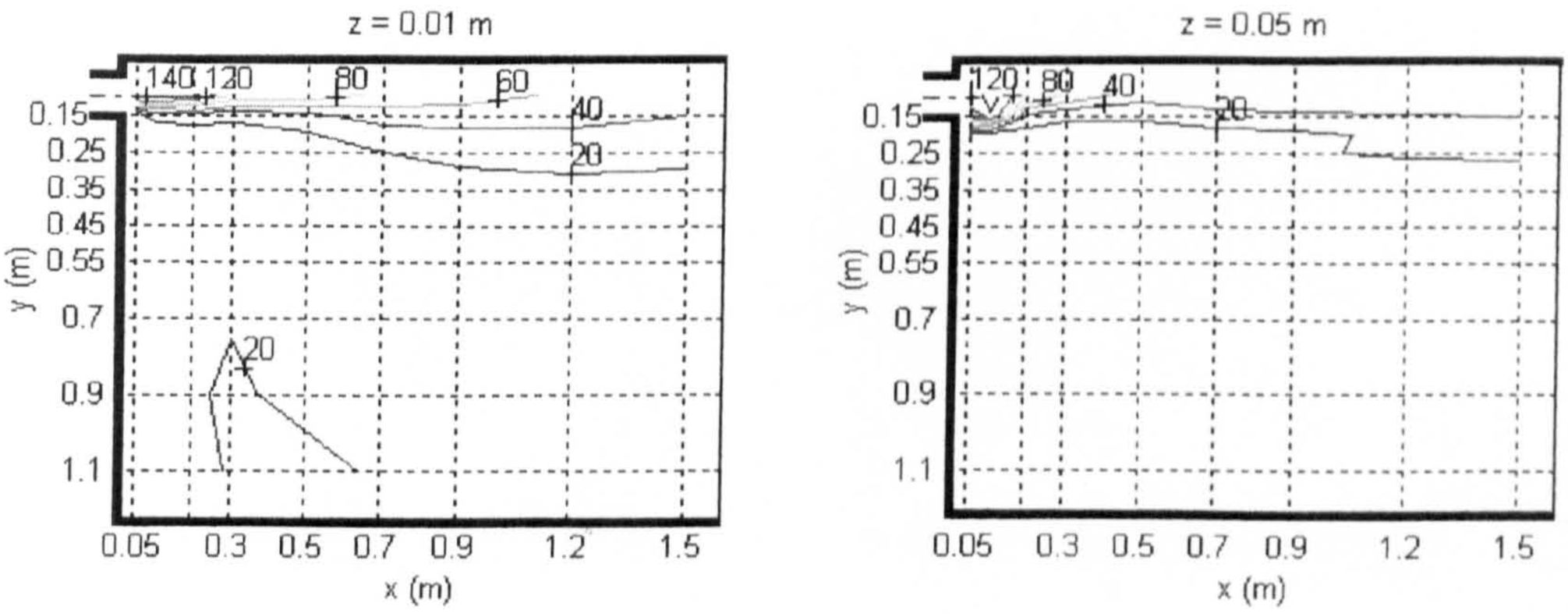

Figure 6-42: Contour of mean velocity in cm/s for "bottom side orifice associated with a weir, a = $0.01m^2$, $Q = 0.020m^3/s$" [$WObS_{20\text{-}0.02}$]

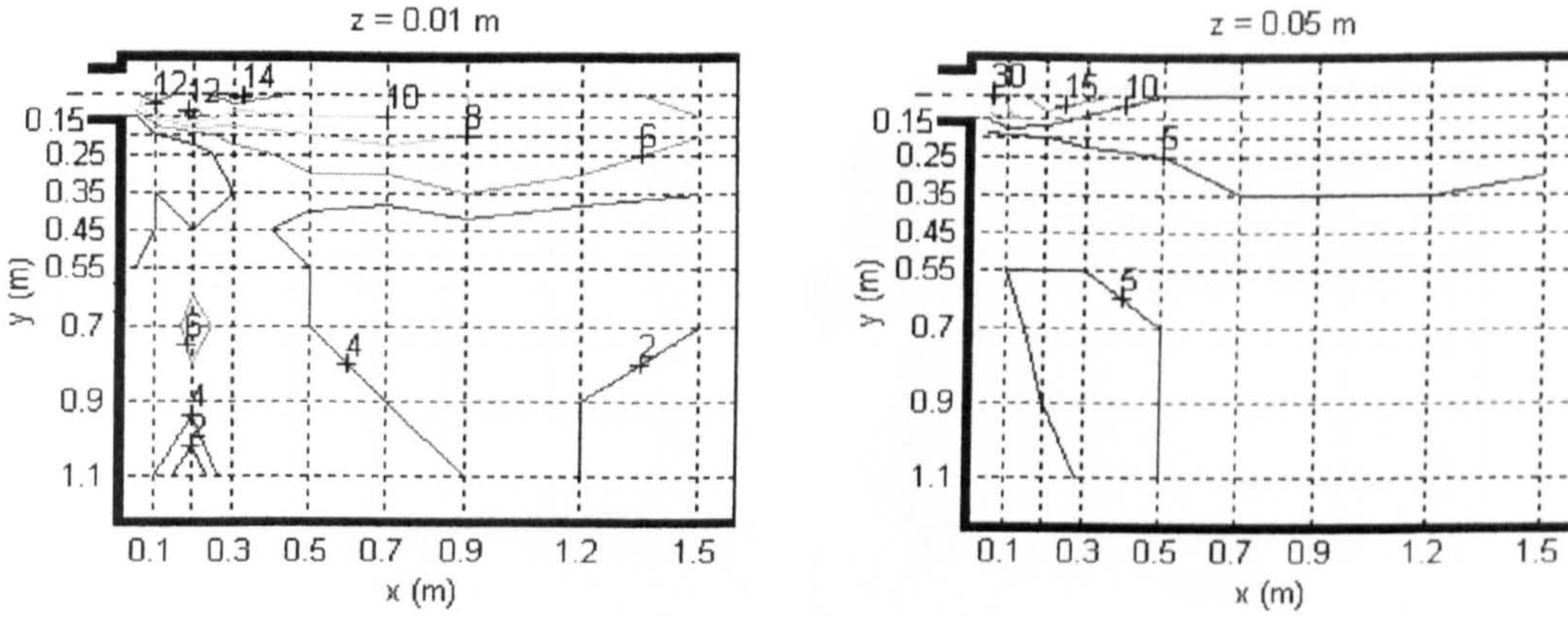

Figure 6-43: Contour of turbulence intensity in % for "bottom side orifice associated with a weir, $a = 0.01m^2$, $Q = 0.020m^3/s$" [$WObS_{20\text{-}0.02}$]

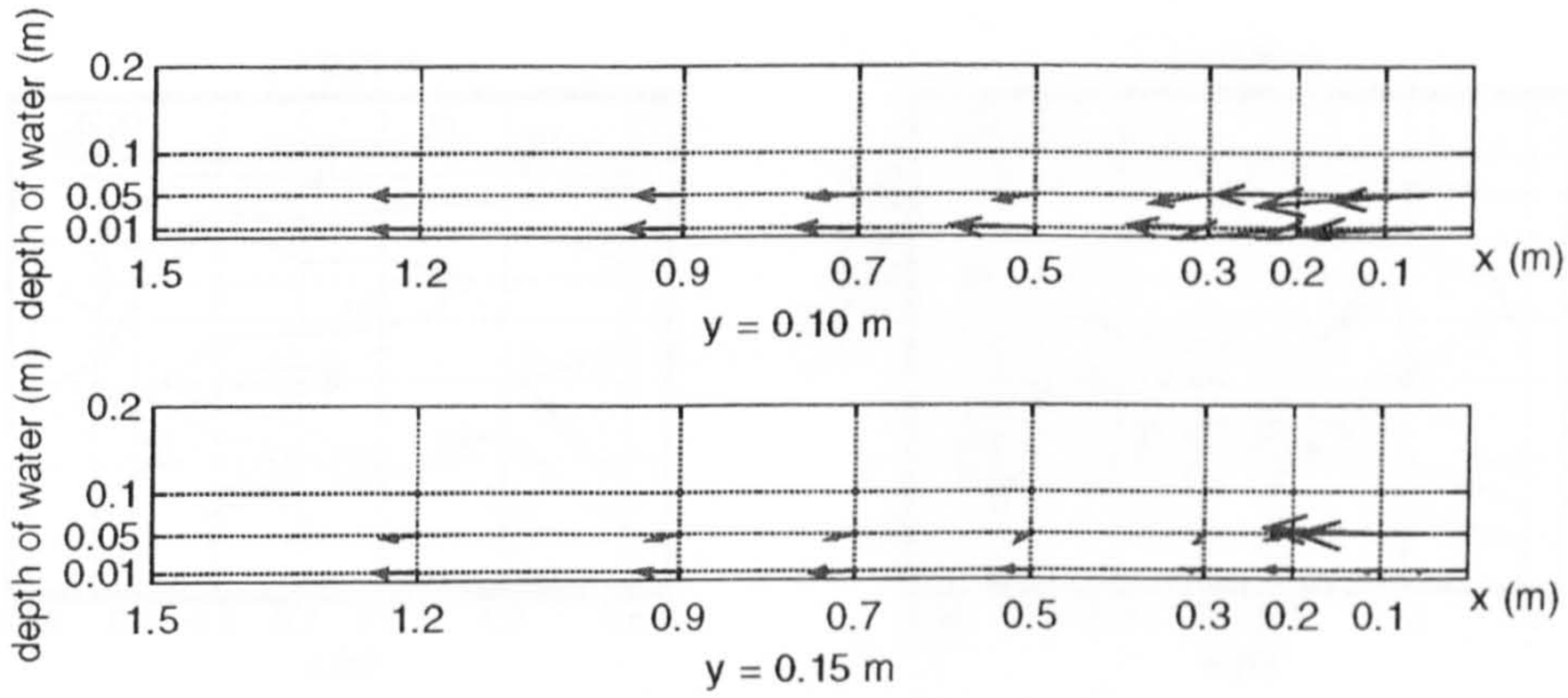

Figure 6-44: Velocity vectors over vertical slides for the bottom side orifice associated with a weir, $a = 0.01\ m^2$, $Q = 0.020\ m^3/s$

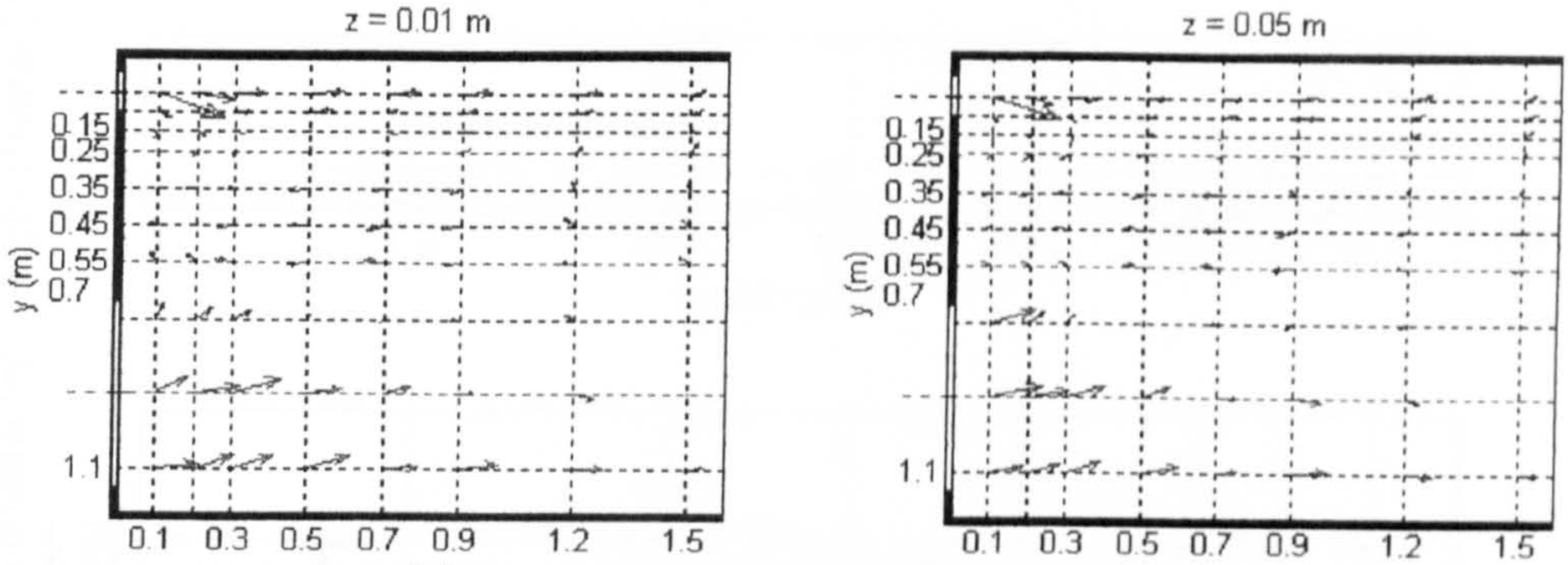

Figure 6-45:Velocity vectors for the double orifice, ratio 1:1, Q = 0.012 m^3/s

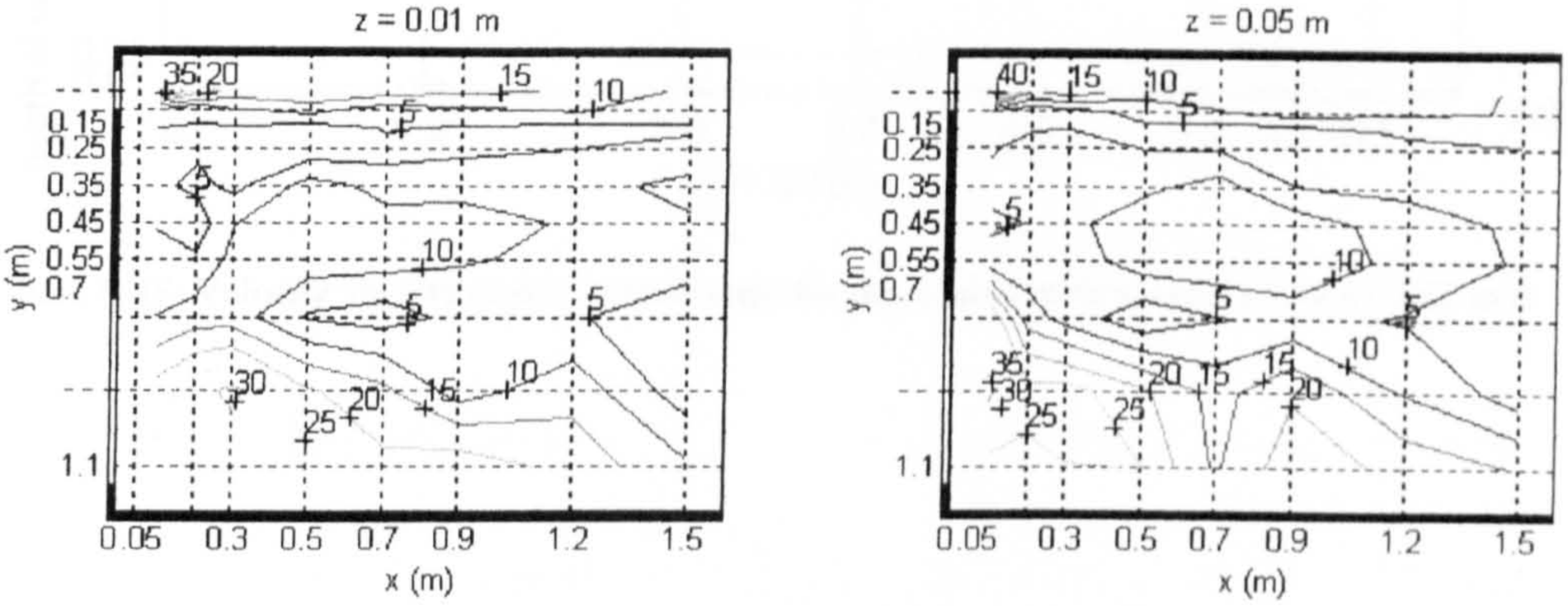

Figure 6-46: Contours of mean velocity in cm/s for the double orifice, ratio 1:1, Q = 0.012 m^3/s

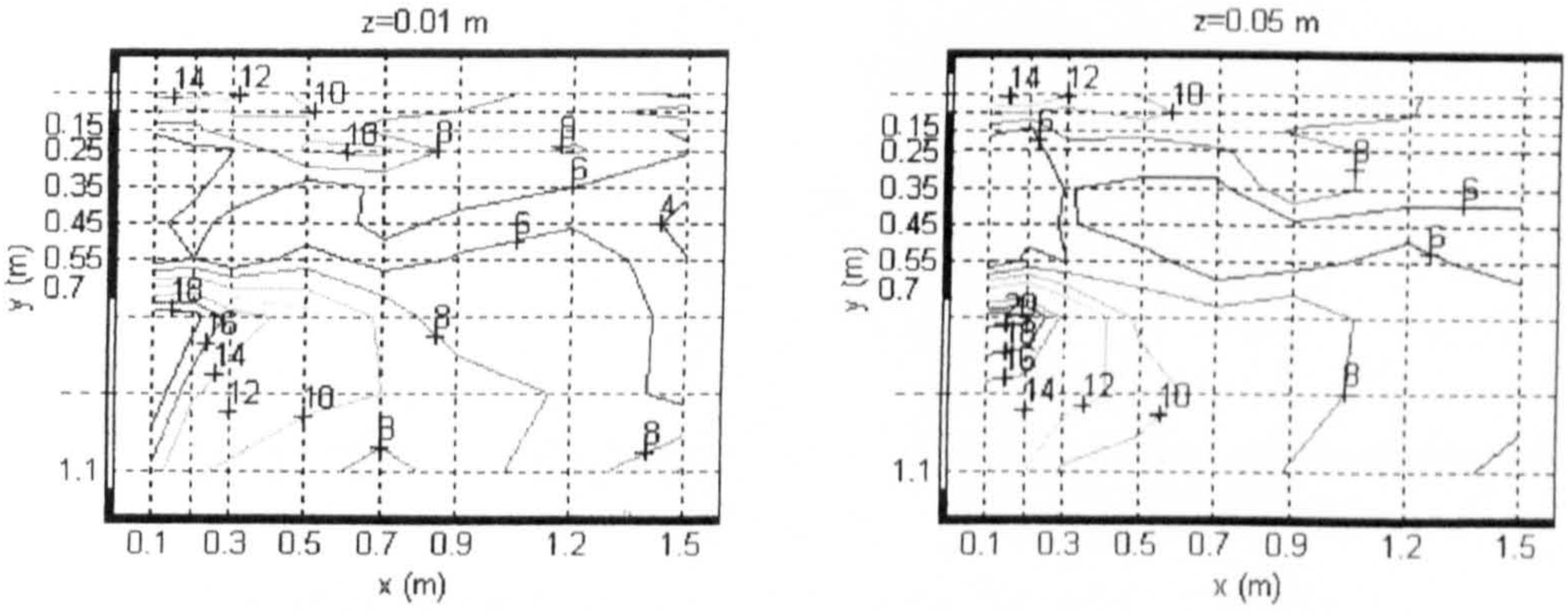

Figure 6-47: Contours of turbulence intensity in % for the Double orifice, ratio 1:1, Q = 0.012 m^3/s

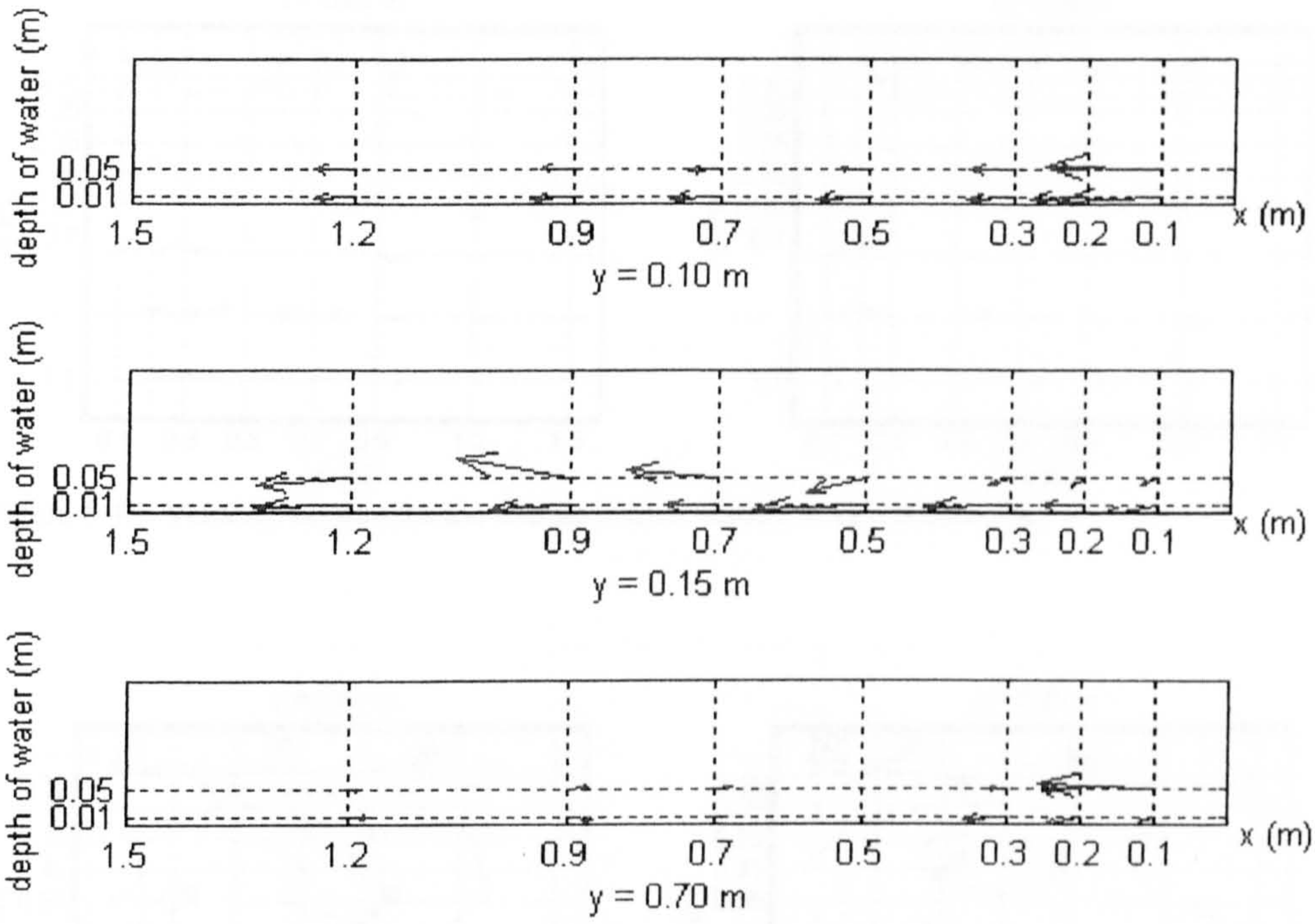

Figure 6-48: Velocity vectors over a vertical slide for the double orifice, ratio 1:1,Q = 0.012 m^3/s

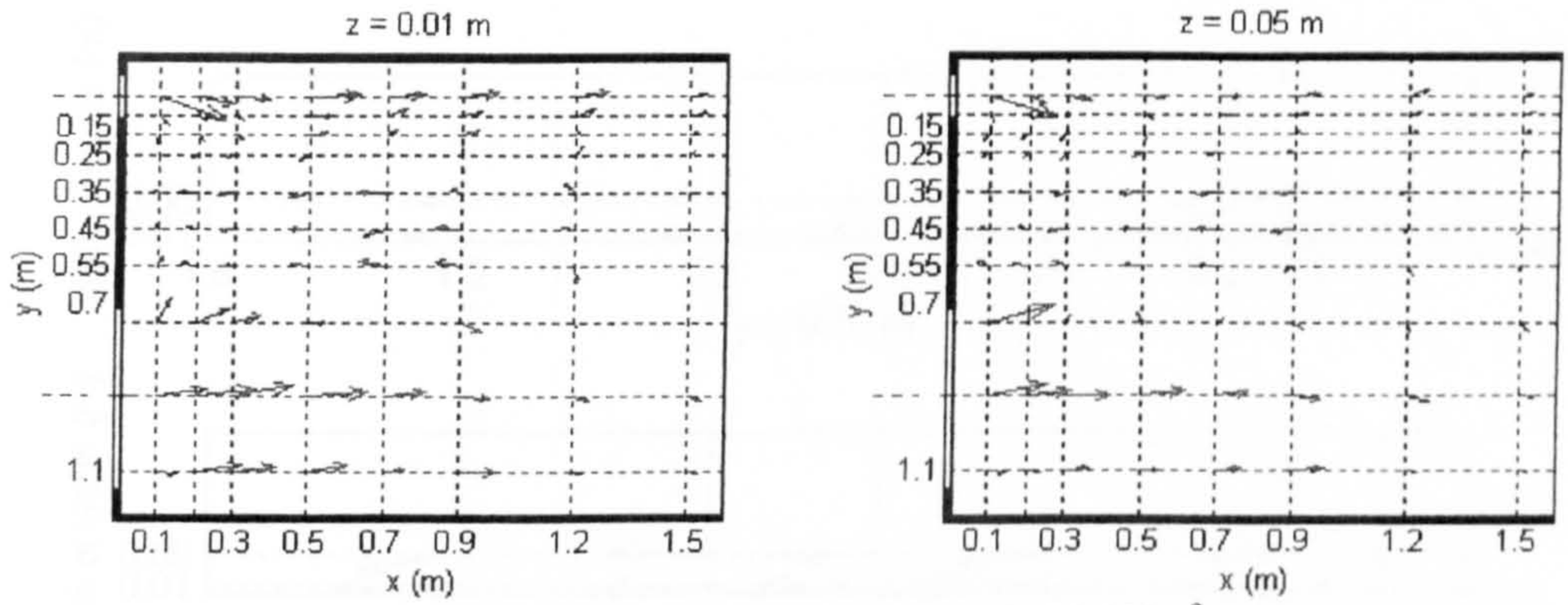

Figure 6-49: Velocity vectors for the double orifice –ratio1:1, Q = 0.020m^3/s

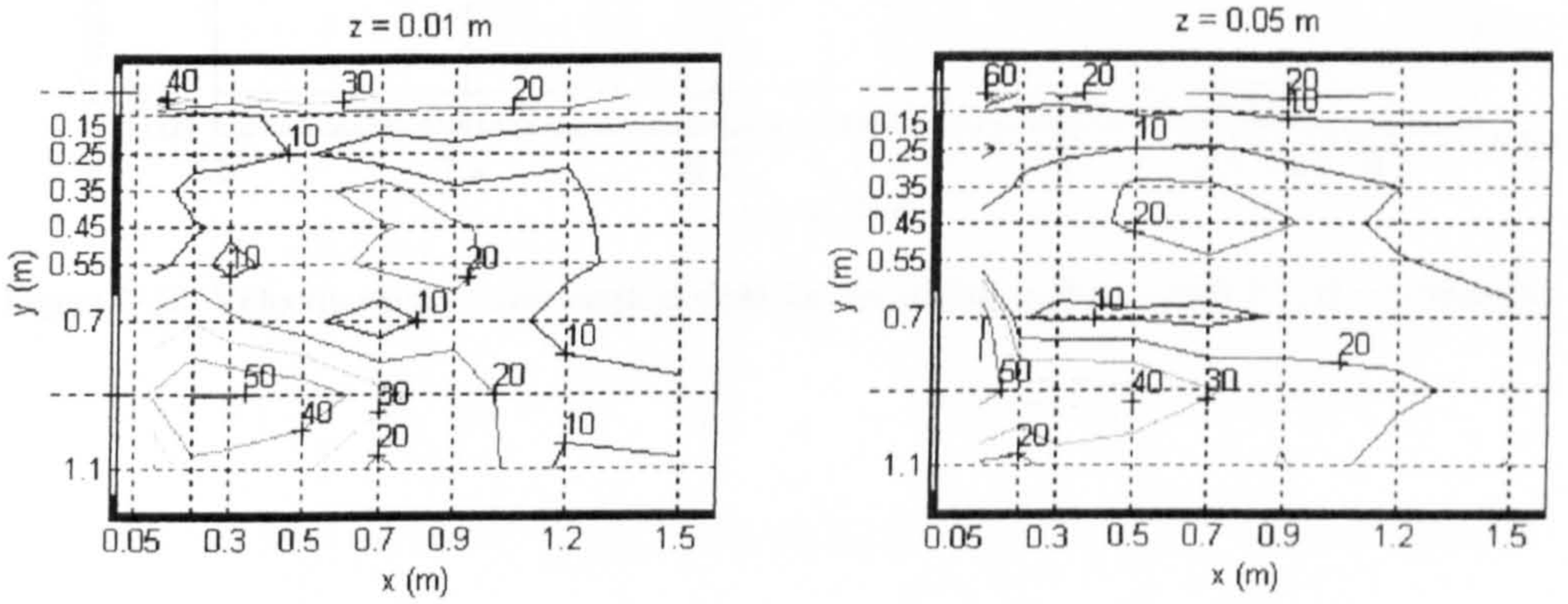

Figure 6-50: Contour of mean velocity in cm/s for the Double orifice – ratio 1:1, Q = 0.020m^3/s

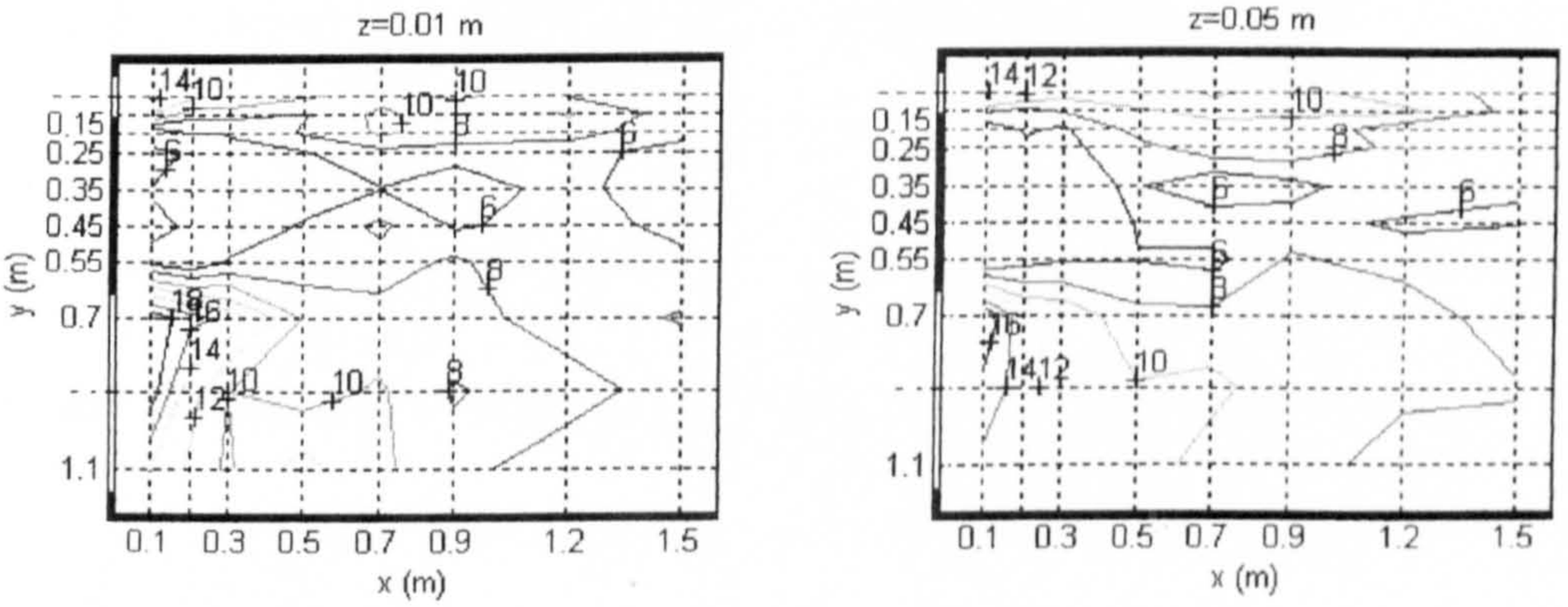

Figure 6- 51: Contour of turbulence intensity in % for the Double orifice – ratio 1:1, Q = 0.020m^3/s

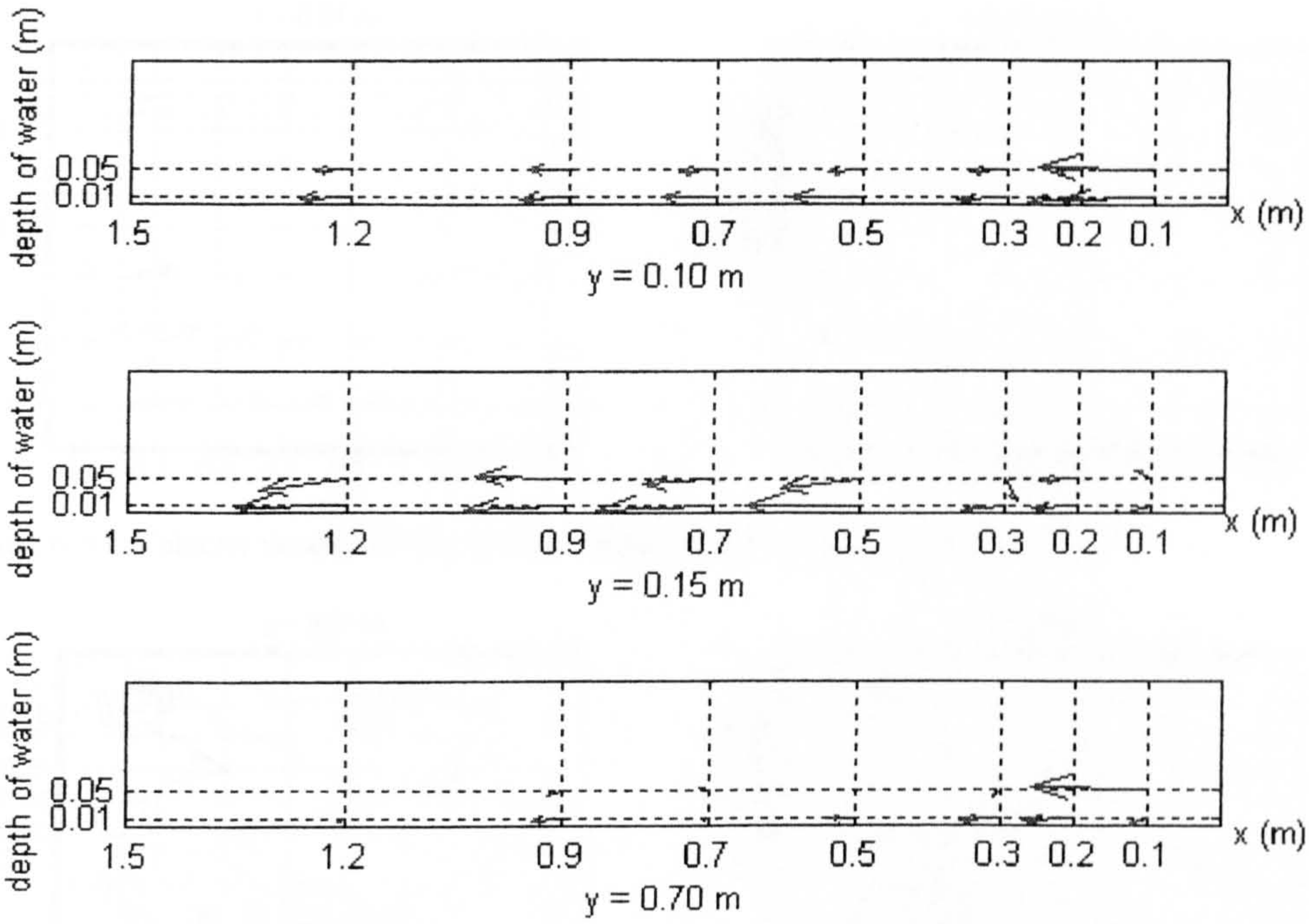

Figure 6-52: Velocity vectors over vertical slide for the double orifice – ratio 1:1, Q = 0.020m^3/s

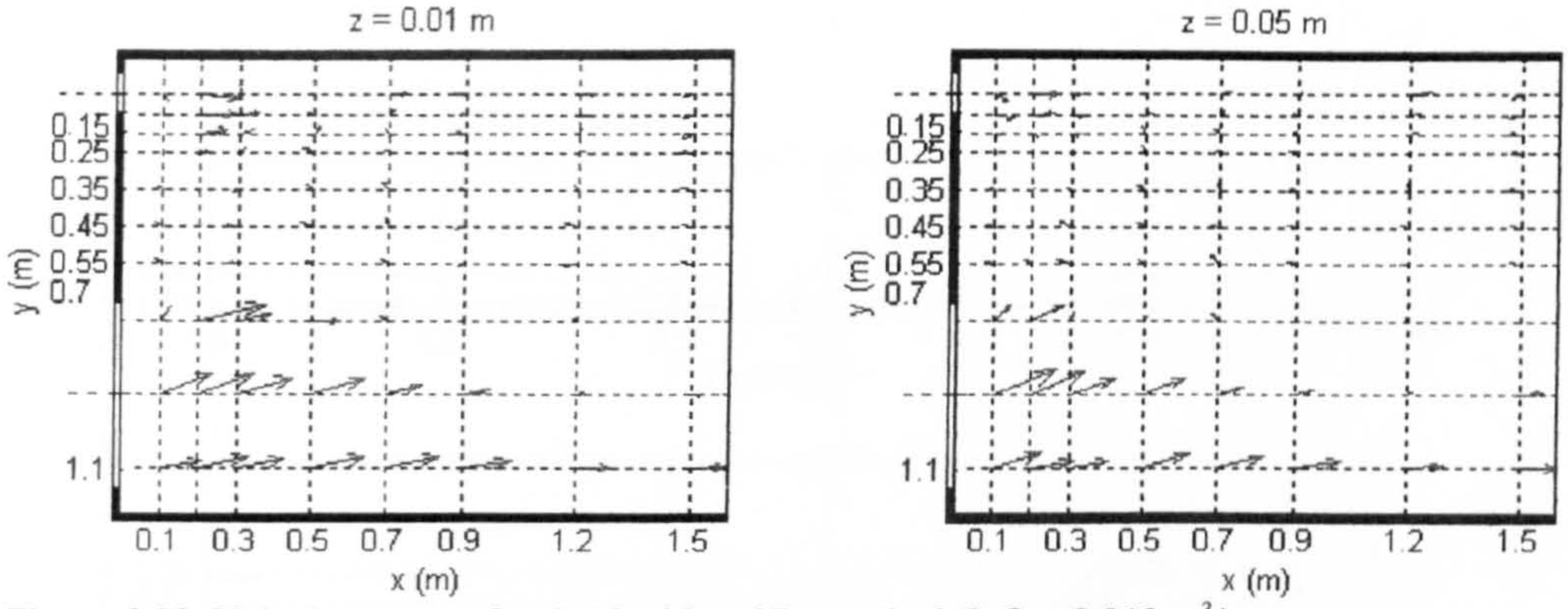

Figure 6-53: Velocity vectors for the double orifice, ratio 1:5, Q = 0.012 m^3/s

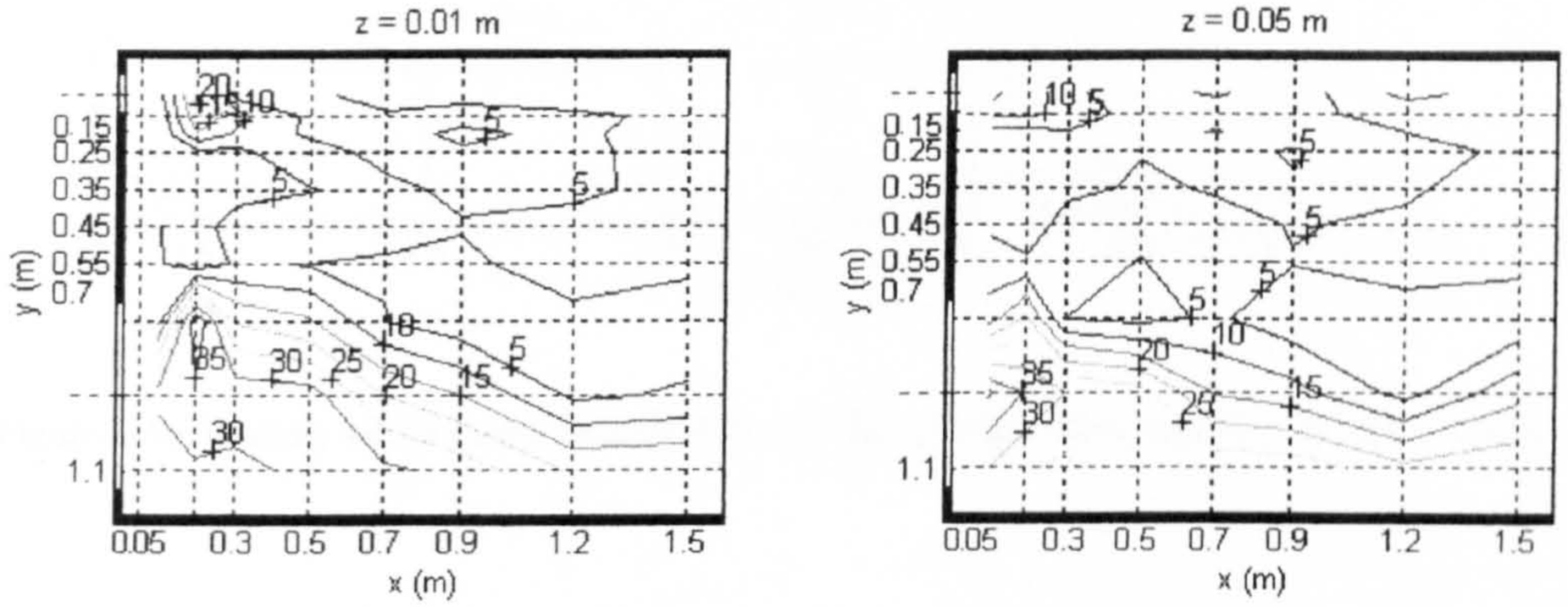

Figure 6-54: Contours of mean velocity in cm/s for the double orifice, ratio 1:5, Q = 0.012 m^3/s

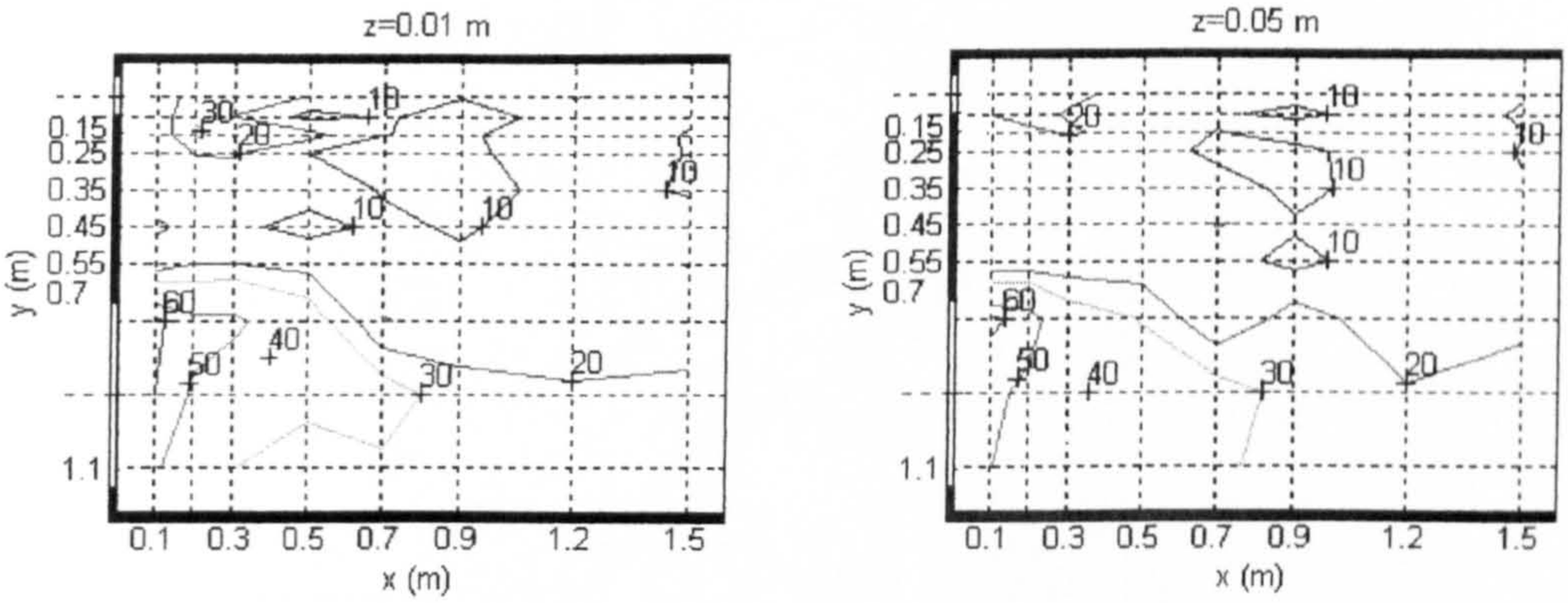

Figure 6-55: Contours of turbulence intensity in % for the double orifice, ratio 1:5, Q = 0.012 m^3/s

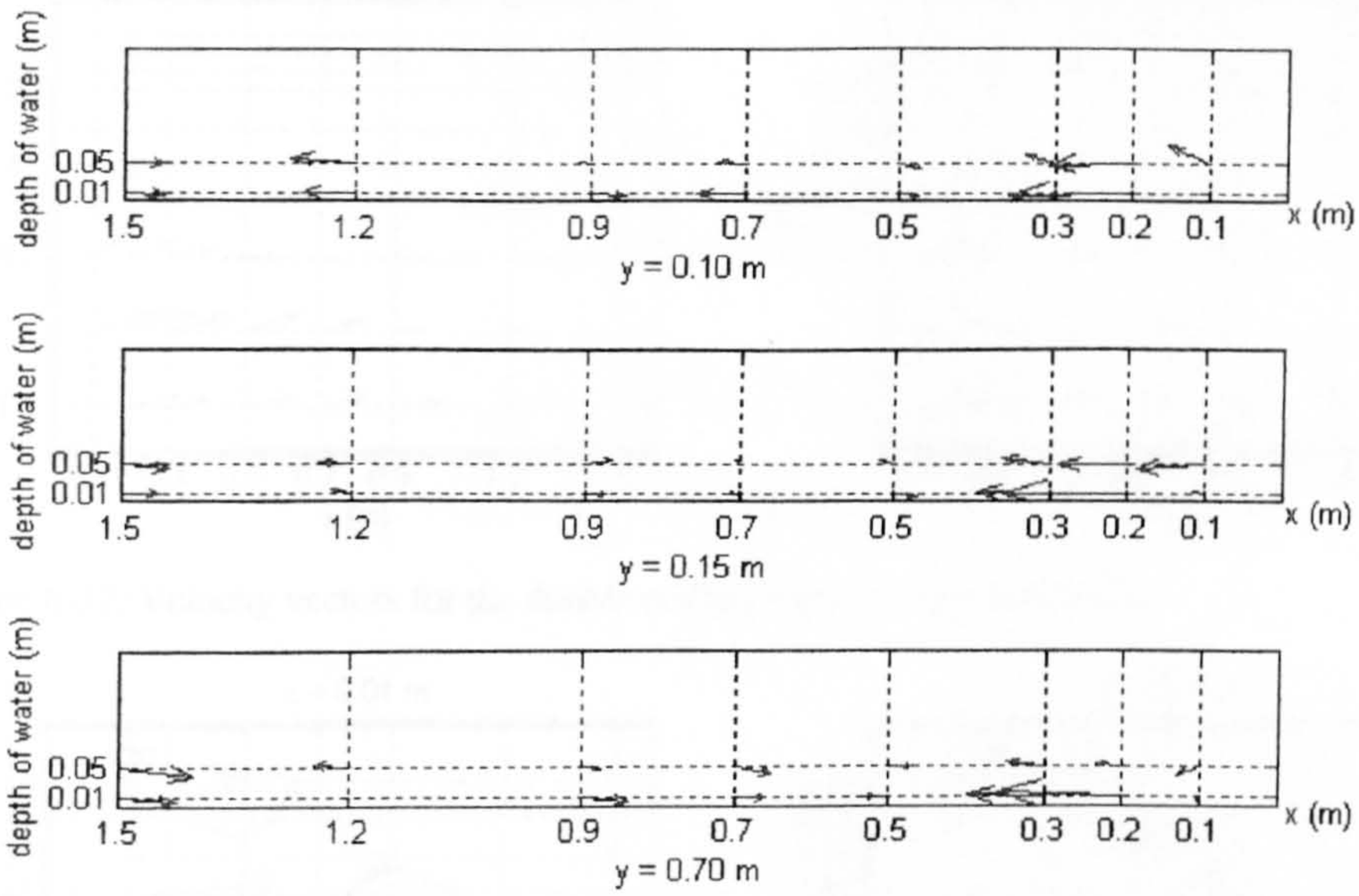

Figure 6-56: Velocity vectors over vertical slides for the double orifice, ratio 1:5, Q = 0.012 m^3/s

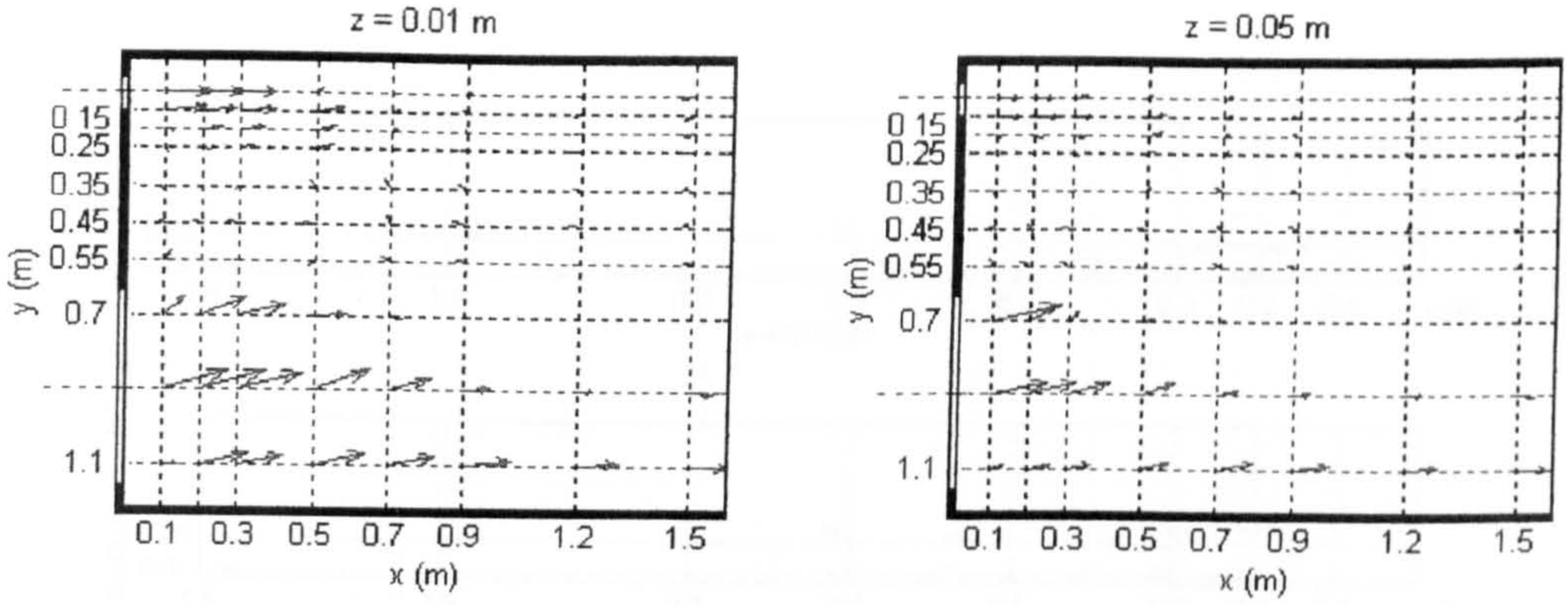

Figure 6-57: Velocity vectors for the double orifice, ratio 1:5, Q = 0.020 m^3/s

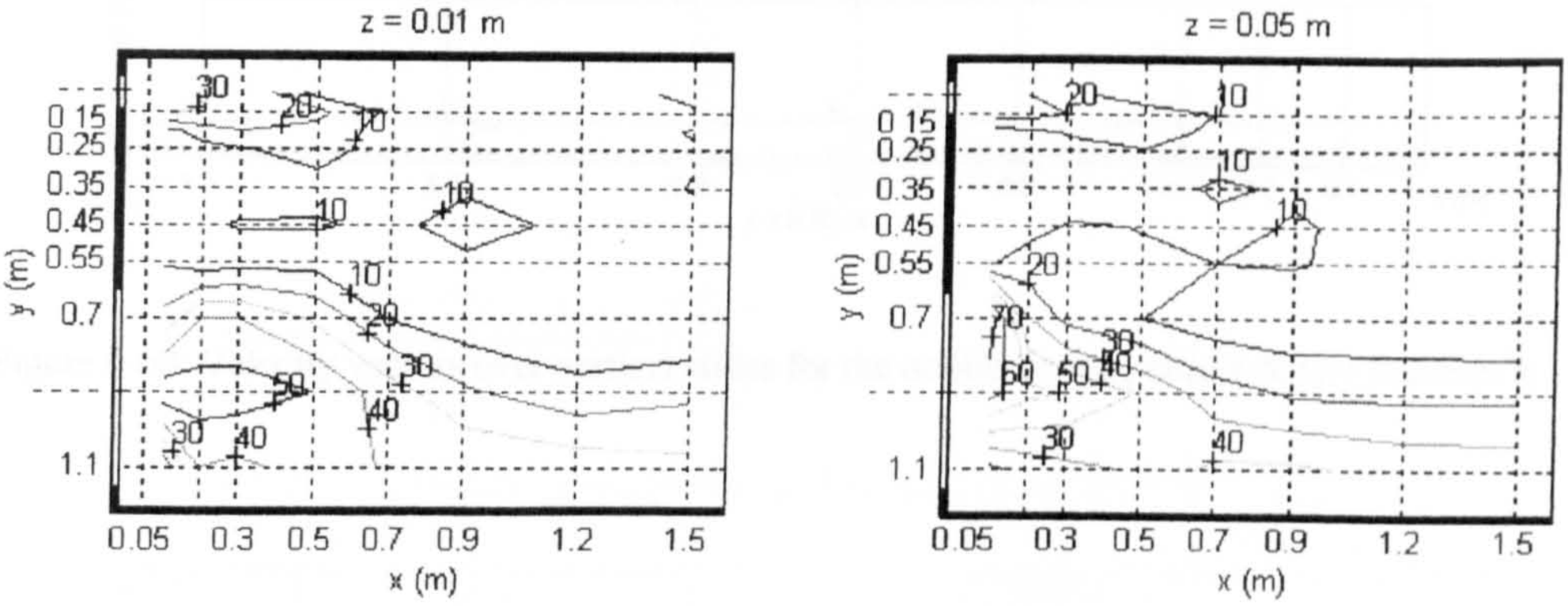

Figure 6-58:Contours of mean velocity in cm/s for the double orifice, ratio 1:5, Q = 0.020 m^3/s

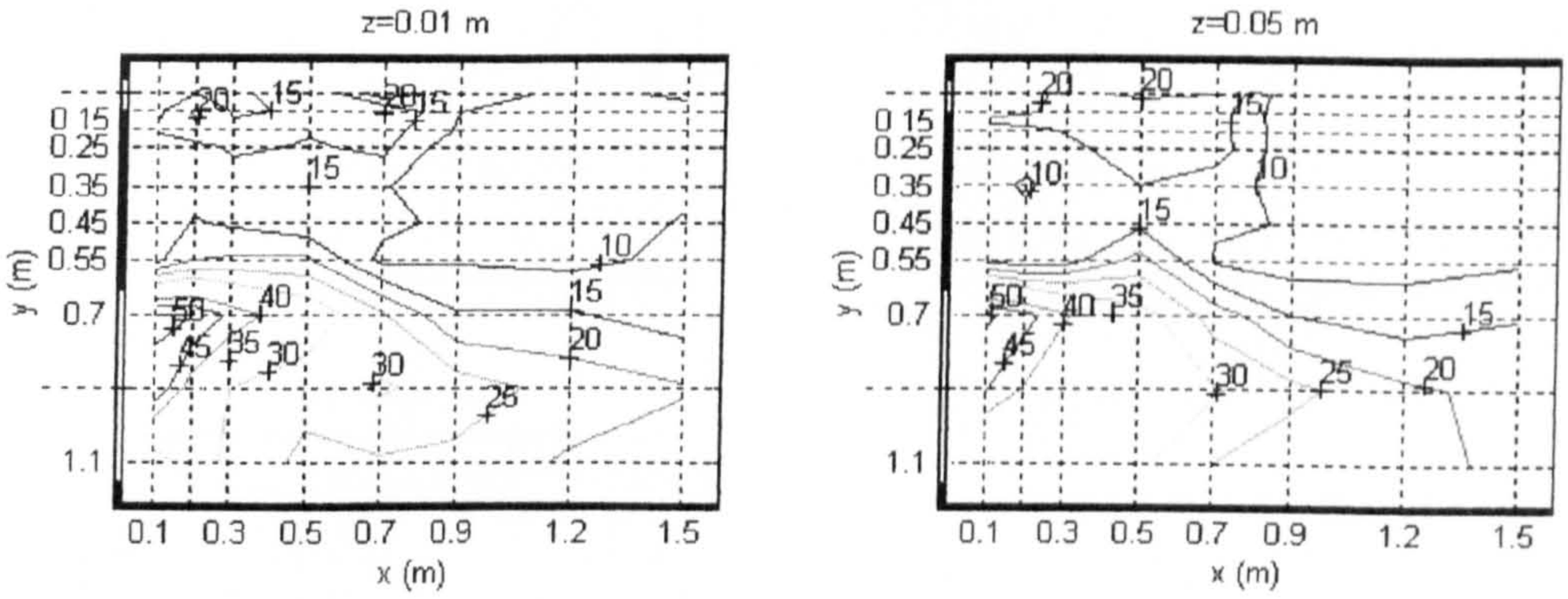

Figure 6-59: Contours of turbulence intensity in % for the double orifice, ratio 1:5, Q = 0.020 m^3/s

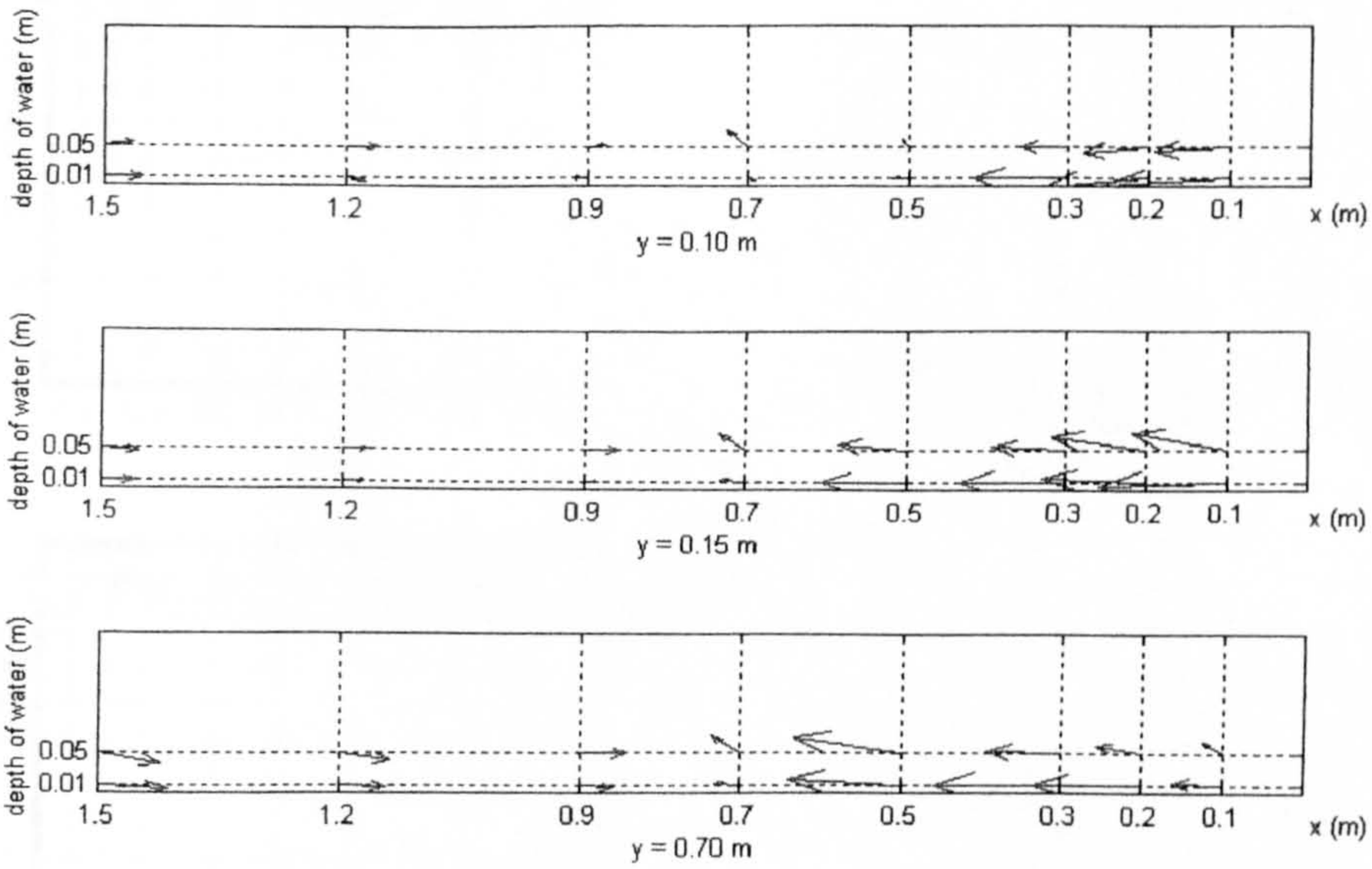

Figure 6-60: Velocity vectors over vertical slides for the double orifice, ratio 1:5, Q = 0.020 m^3/s

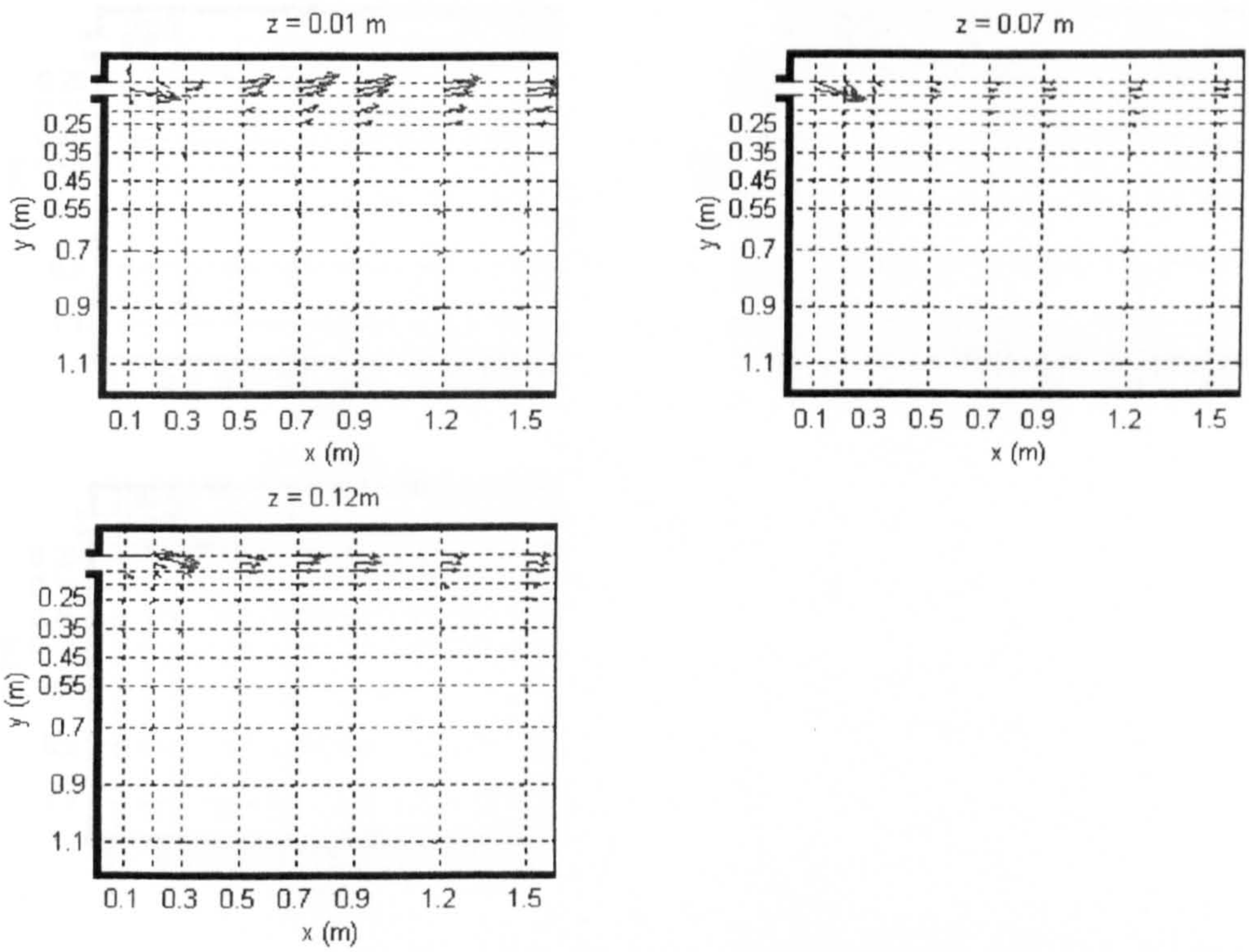

Figure 6-61: Velocity vectors for "vertical slot, 0.05 m wide, Q = 0.012m^3/s" [$V5_{12}$]

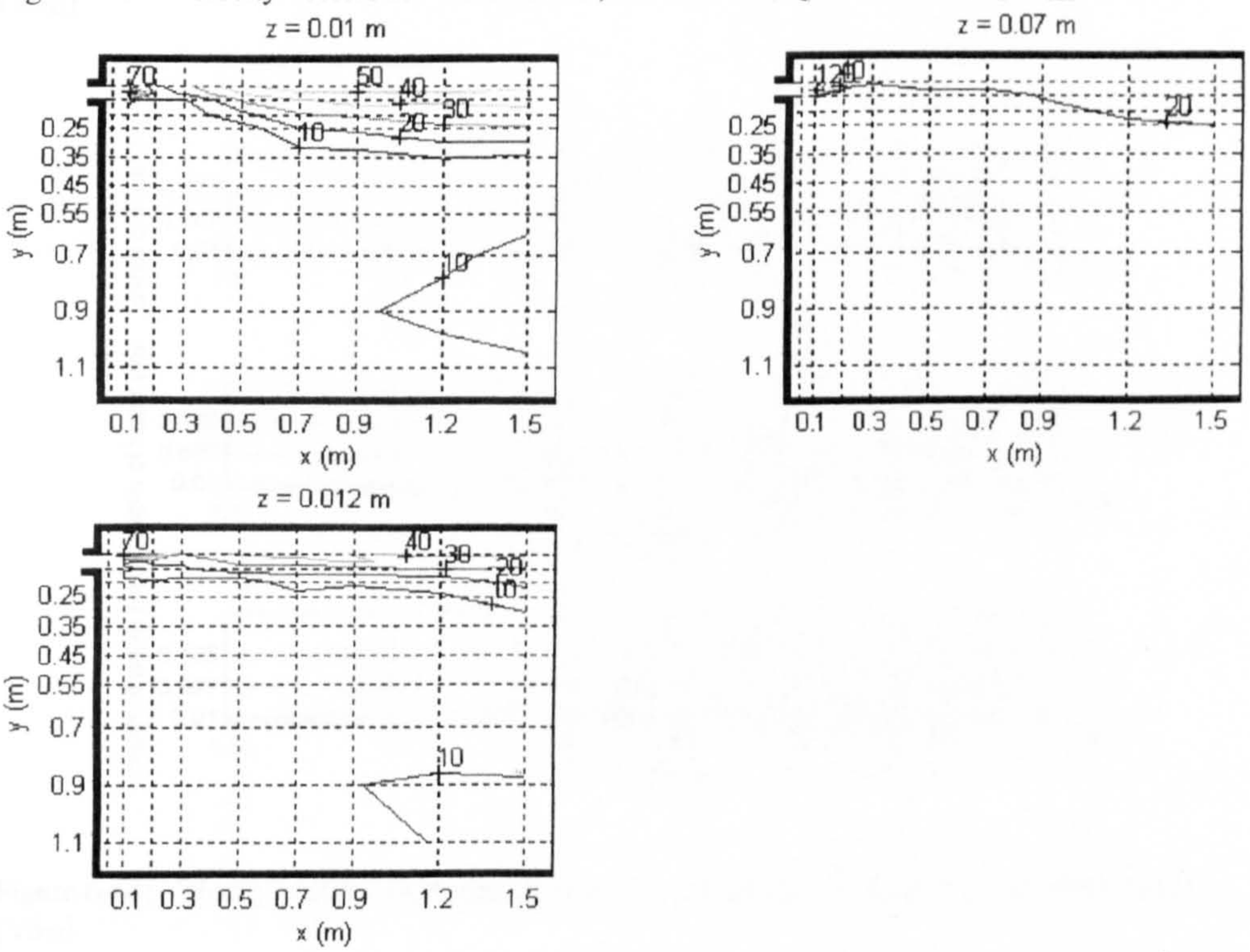

Figure 6-62: Contour of mean velocity in cm/s for "Vertical slot, 0.05 m wide, Q = 0.012m^3/s" [$V5_{12}$]

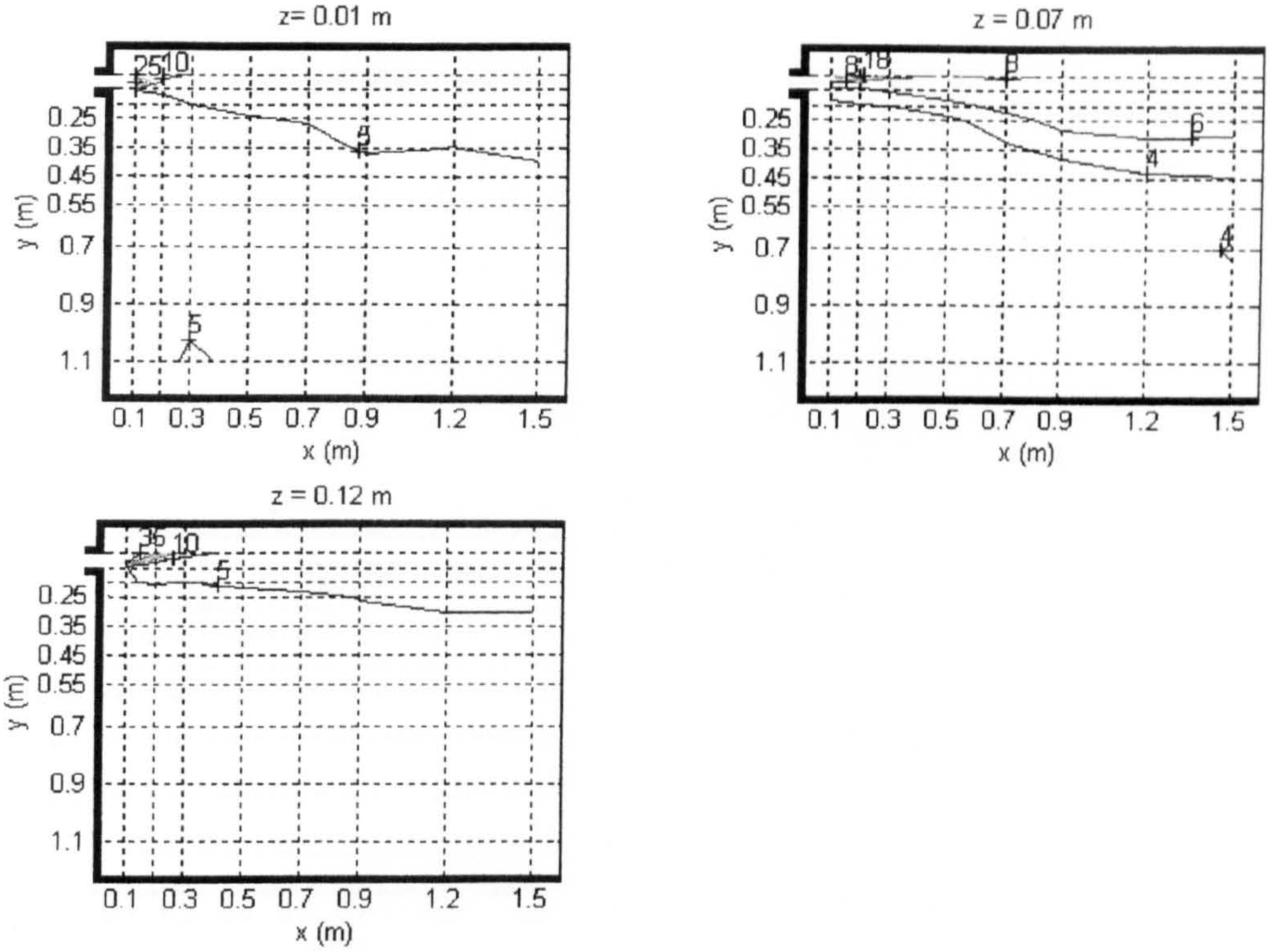

Figure 6-63: Contour of turbulence intensity in % for "vertical slot, 0.05 m wide, Q = 0.012m^3/s" [$V5_{12}$]

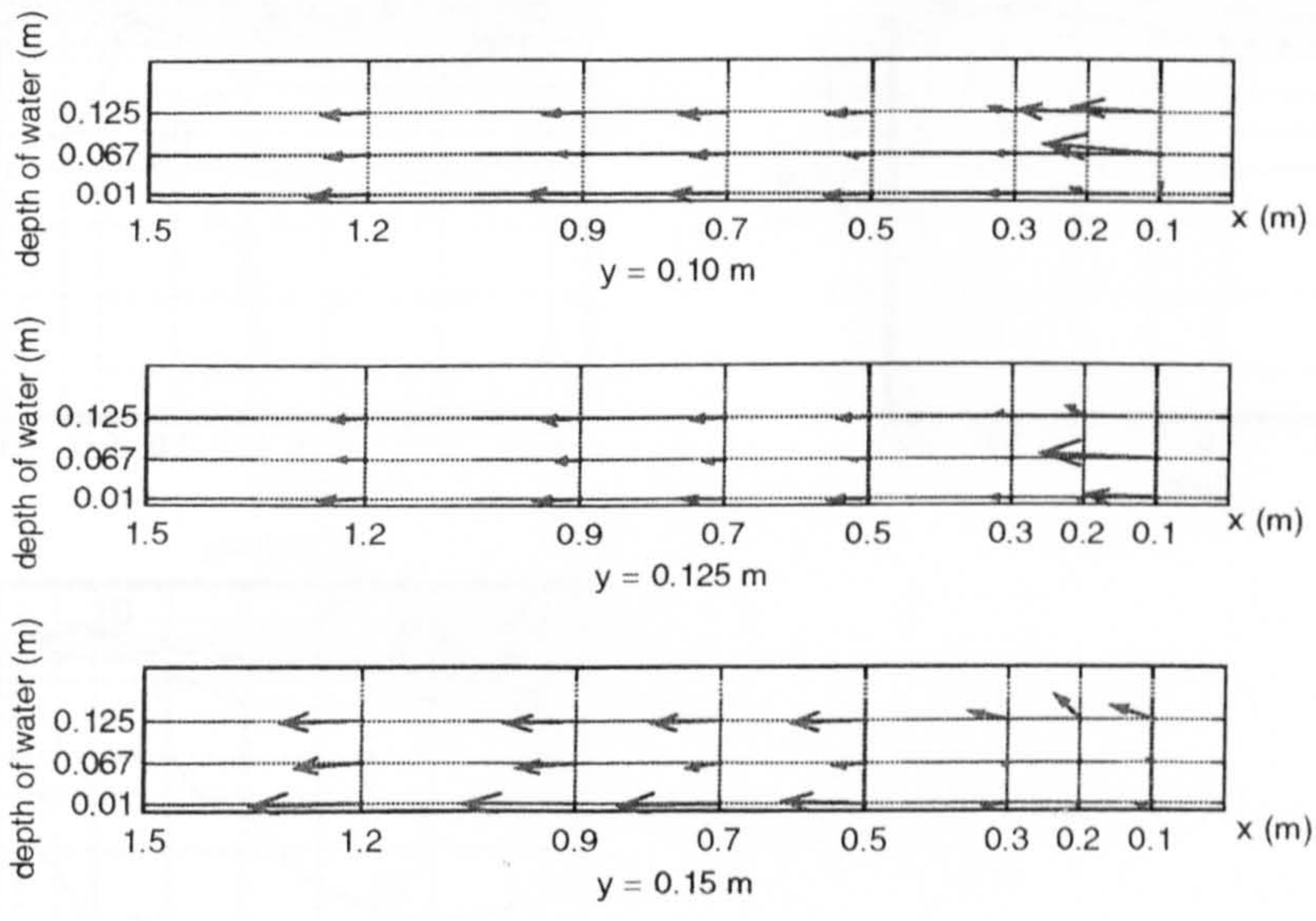

Figure 6-64: Velocity vectors over vertical slot for "vertical slot, 0.05 m wide, Q = 0.012m^3/s" [$V5_{12}$]

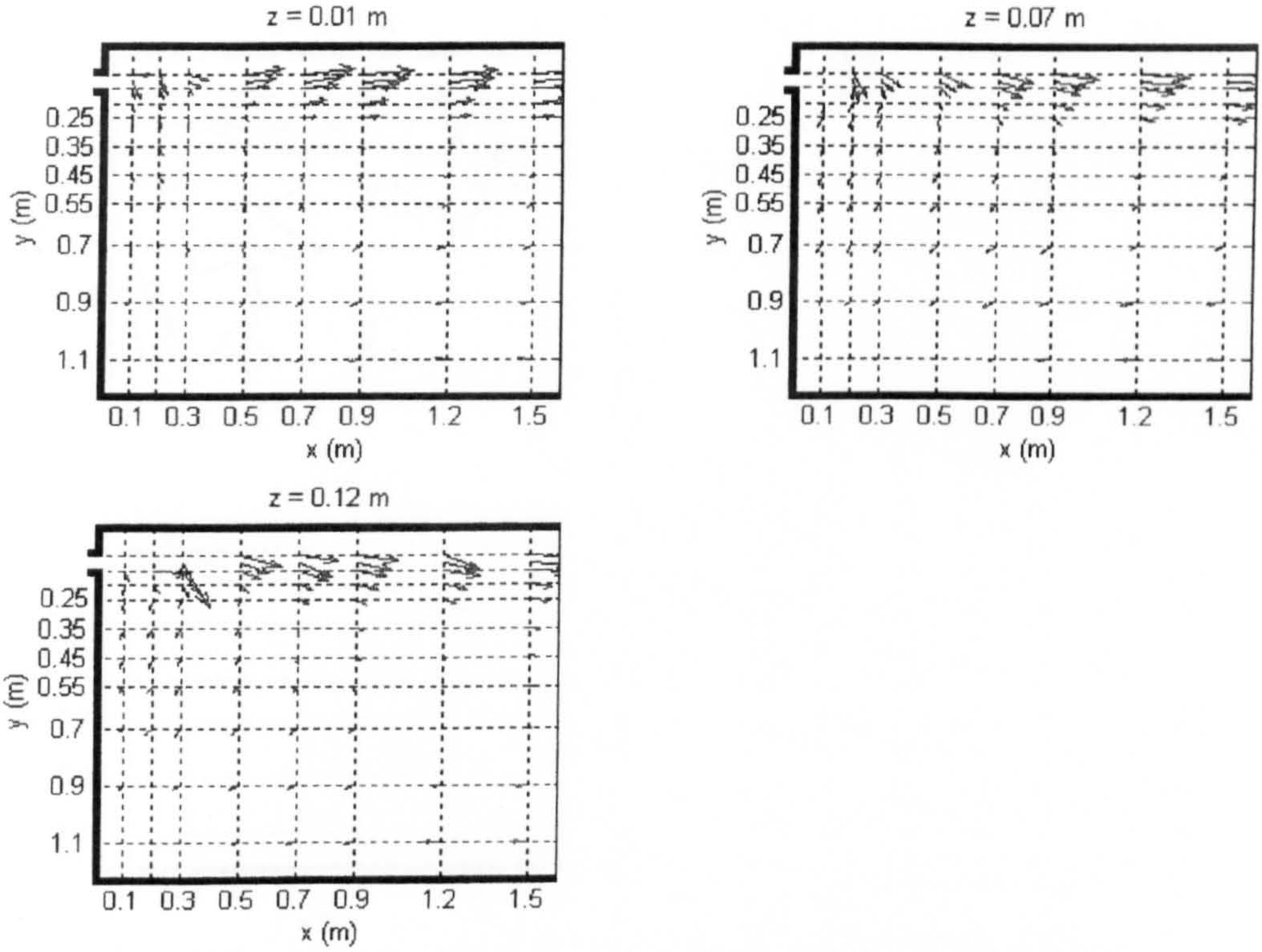

Figure 6-65: Velocity vectors for "vertical slot, 0.05 m wide, Q = 0.020m^3/s" [V5$_{20}$]

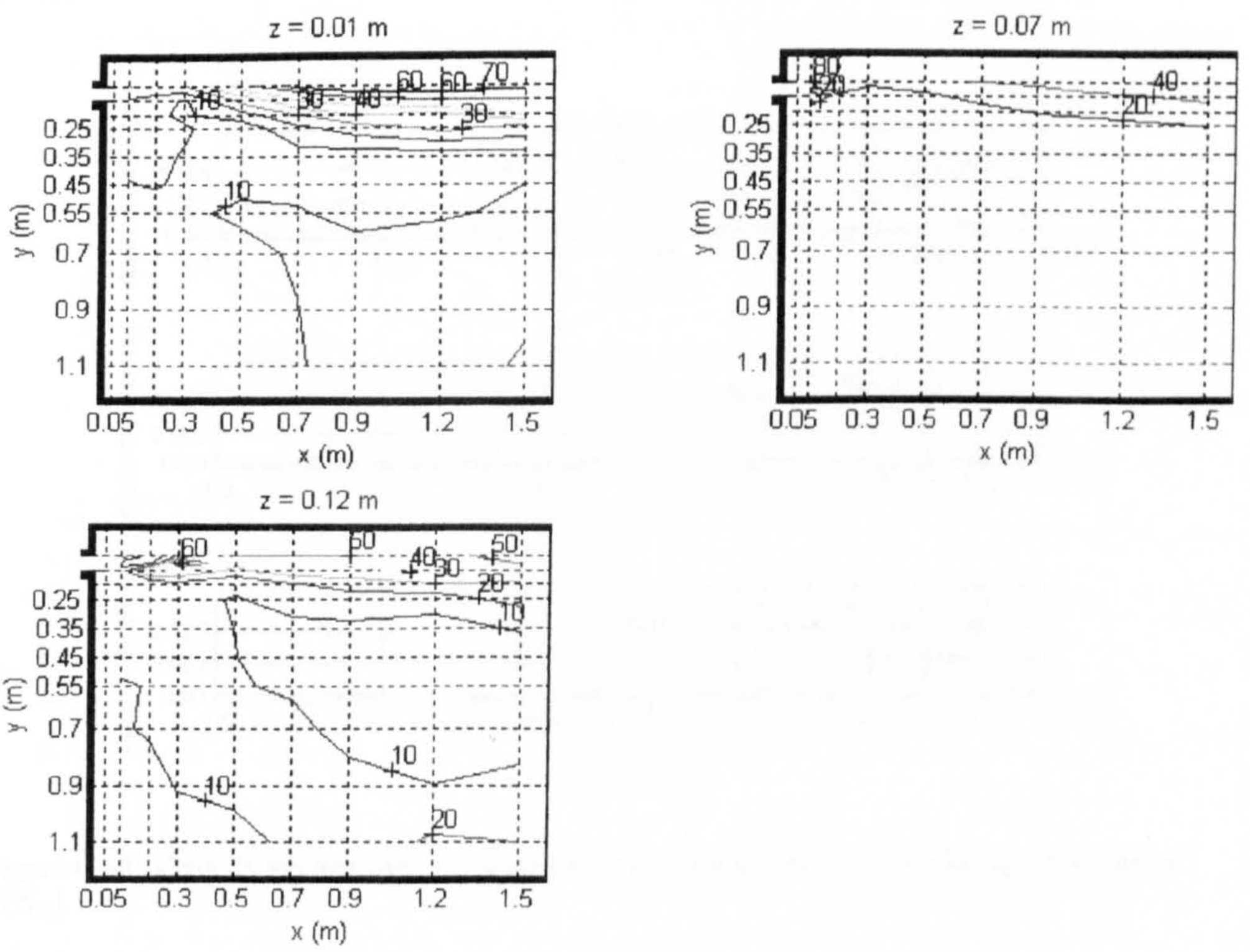

Figure 6-66: Mean velocity contours for "vertical slot, 0.05 m wide, Q = 0.020m^3/s" [V5$_{20}$]

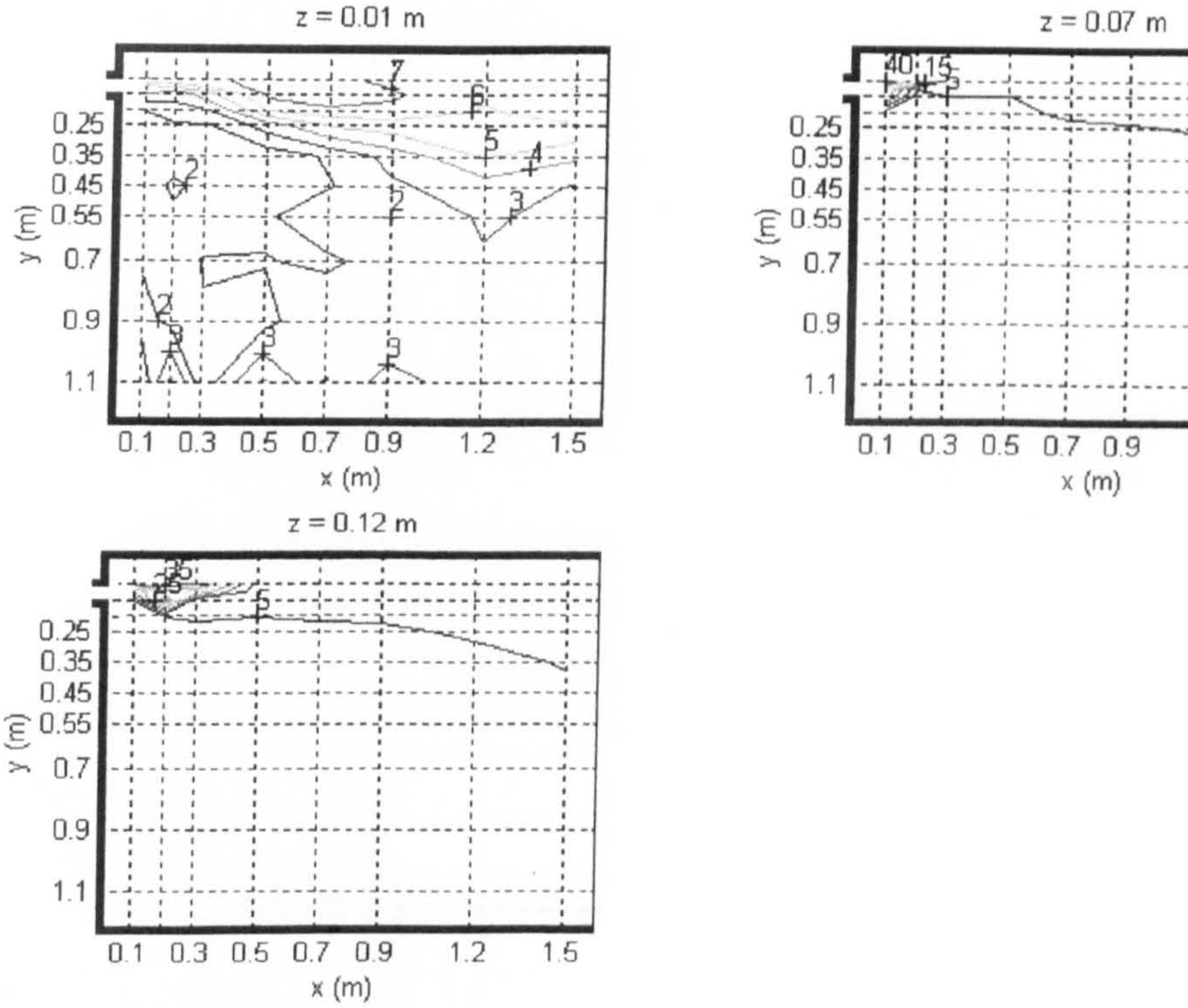

Figure 6-67: Contour of turbulence intensity for "vertical slot, 0.05 m wide, Q = 0.020m^3/s" [$V5_{20}$]

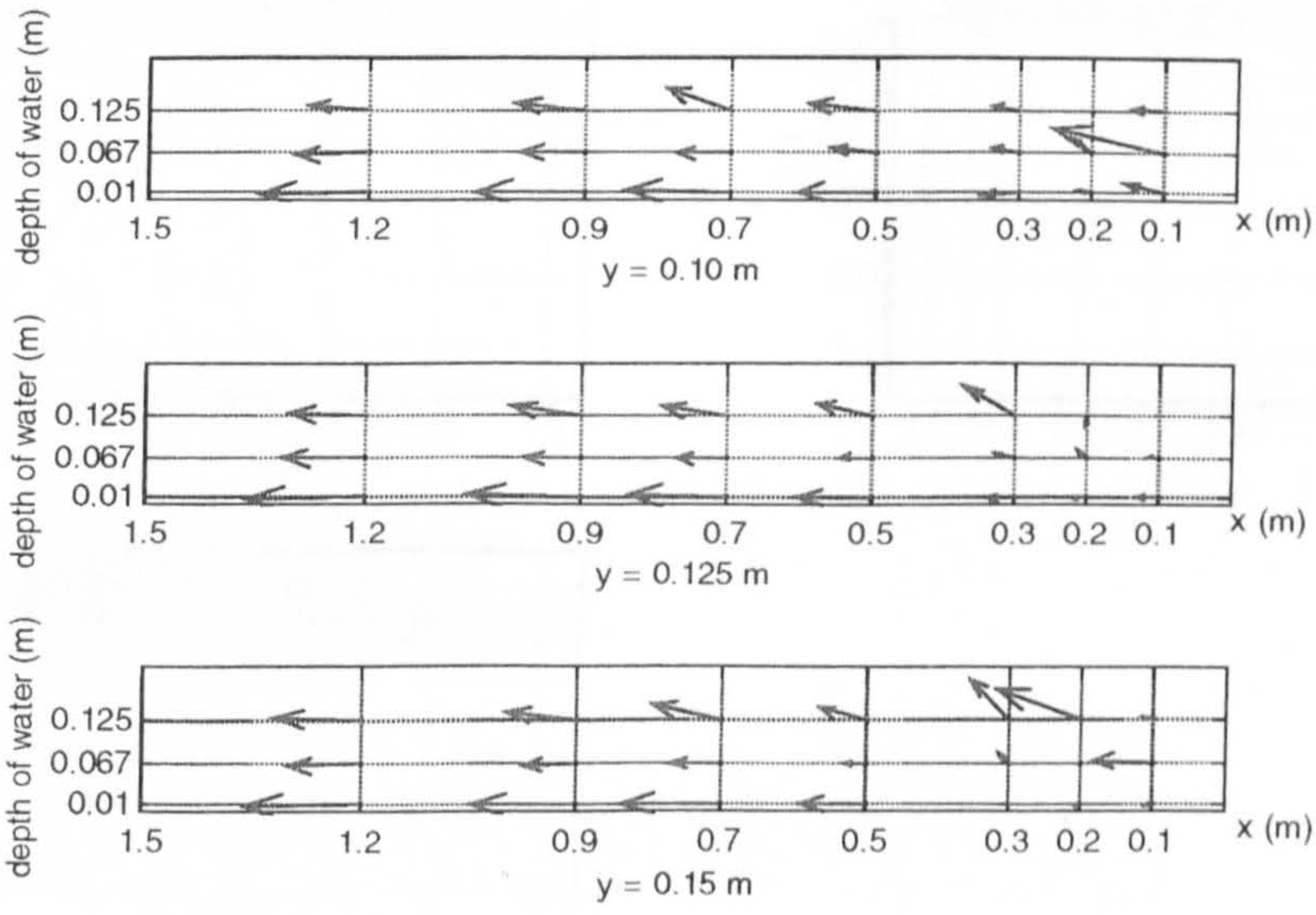

Figure 6-68: Velocity vectors over vertical slide for "vertical slot, 0.05 m wide Q = 0.020m^3/s" [$V5_{20}$]

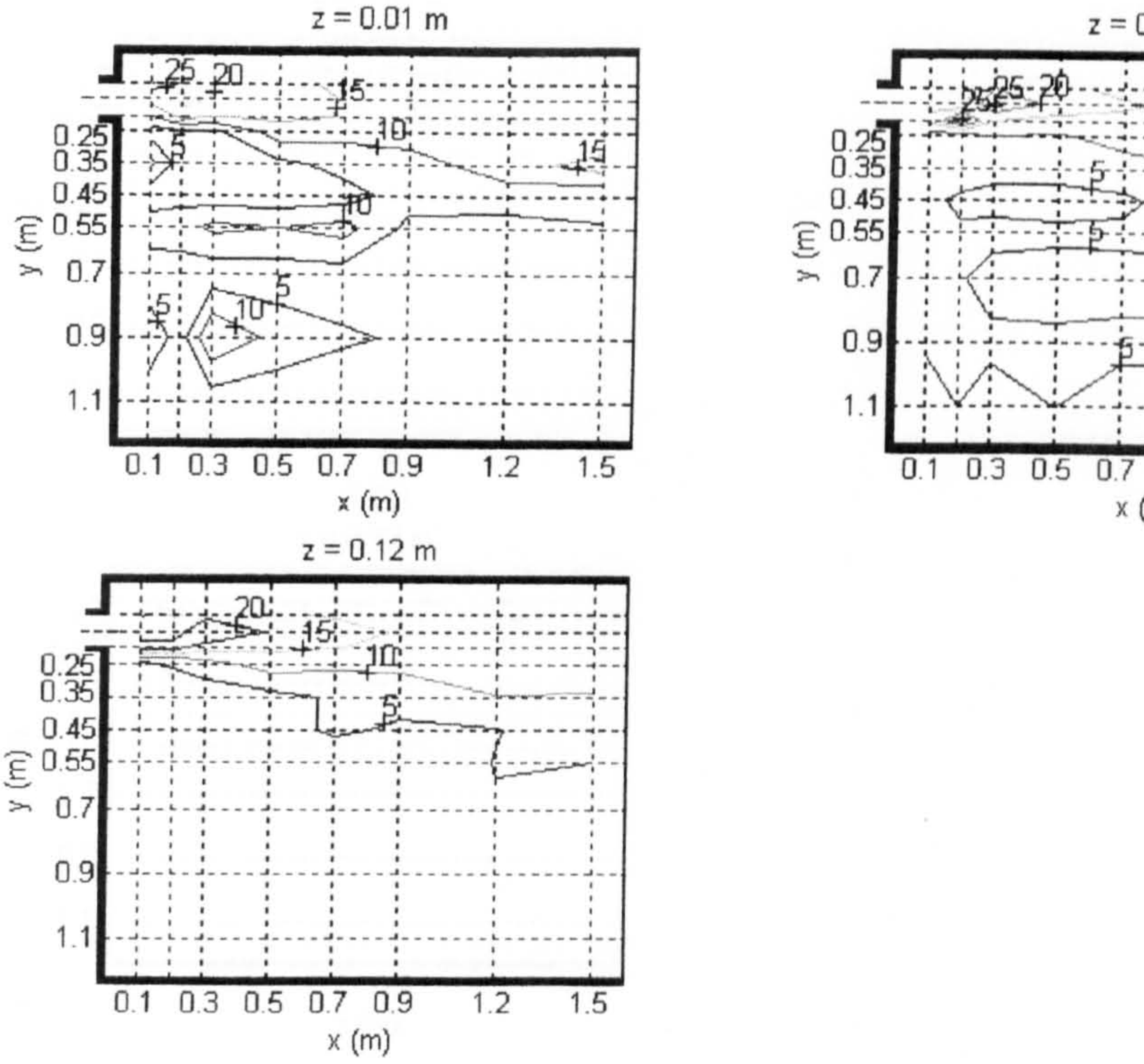

Figure 6-71: Contours of turbulence intensity in % for "vertical slot, 0.010 m wide, Q = $0.012 m^3/s$"

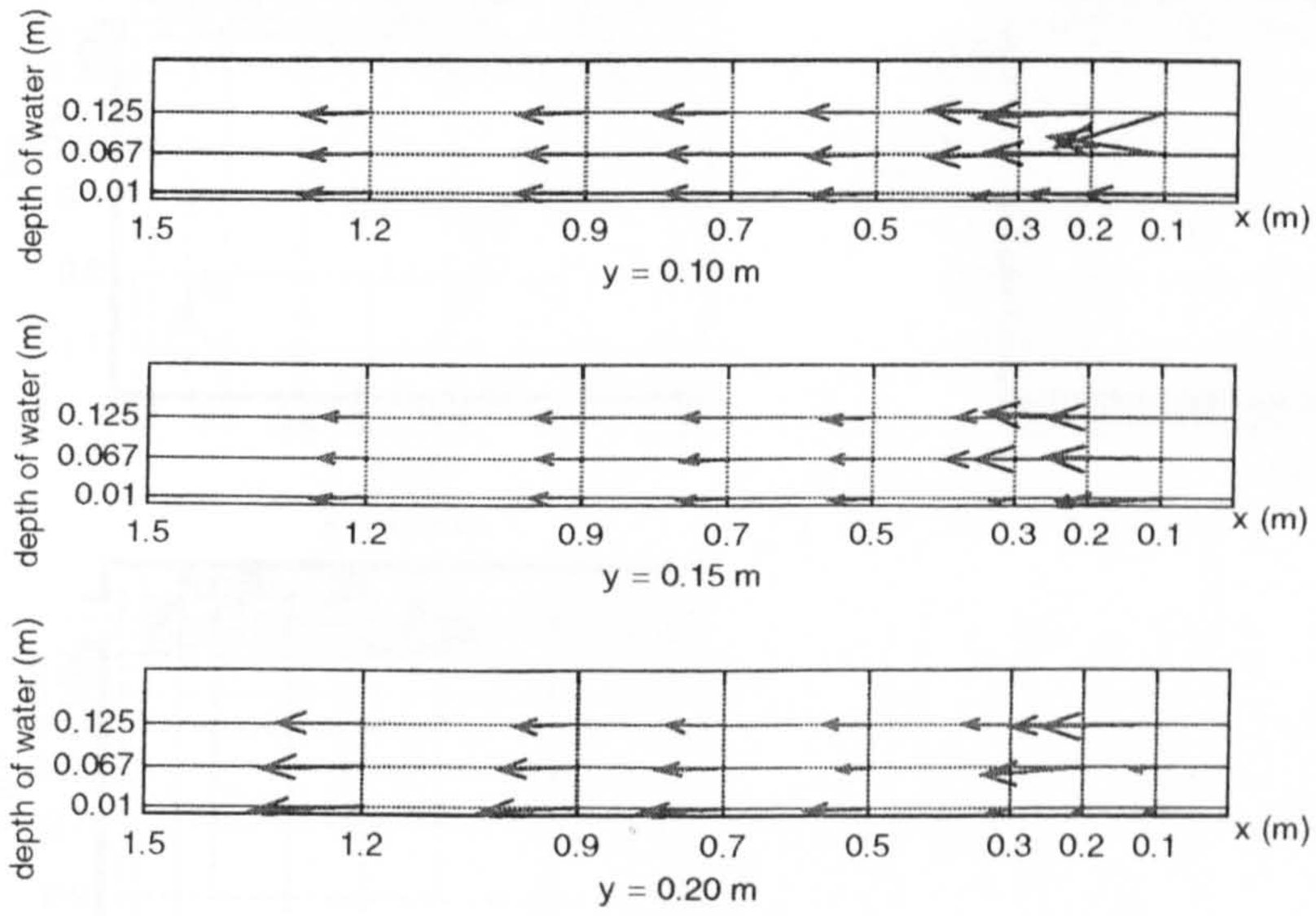

Figure 6-72: Velocity vectors over vertical slide for "vertical slot, 0.010 m wide, Q = $0.012 m^3/s$" [$V10_{12}$]

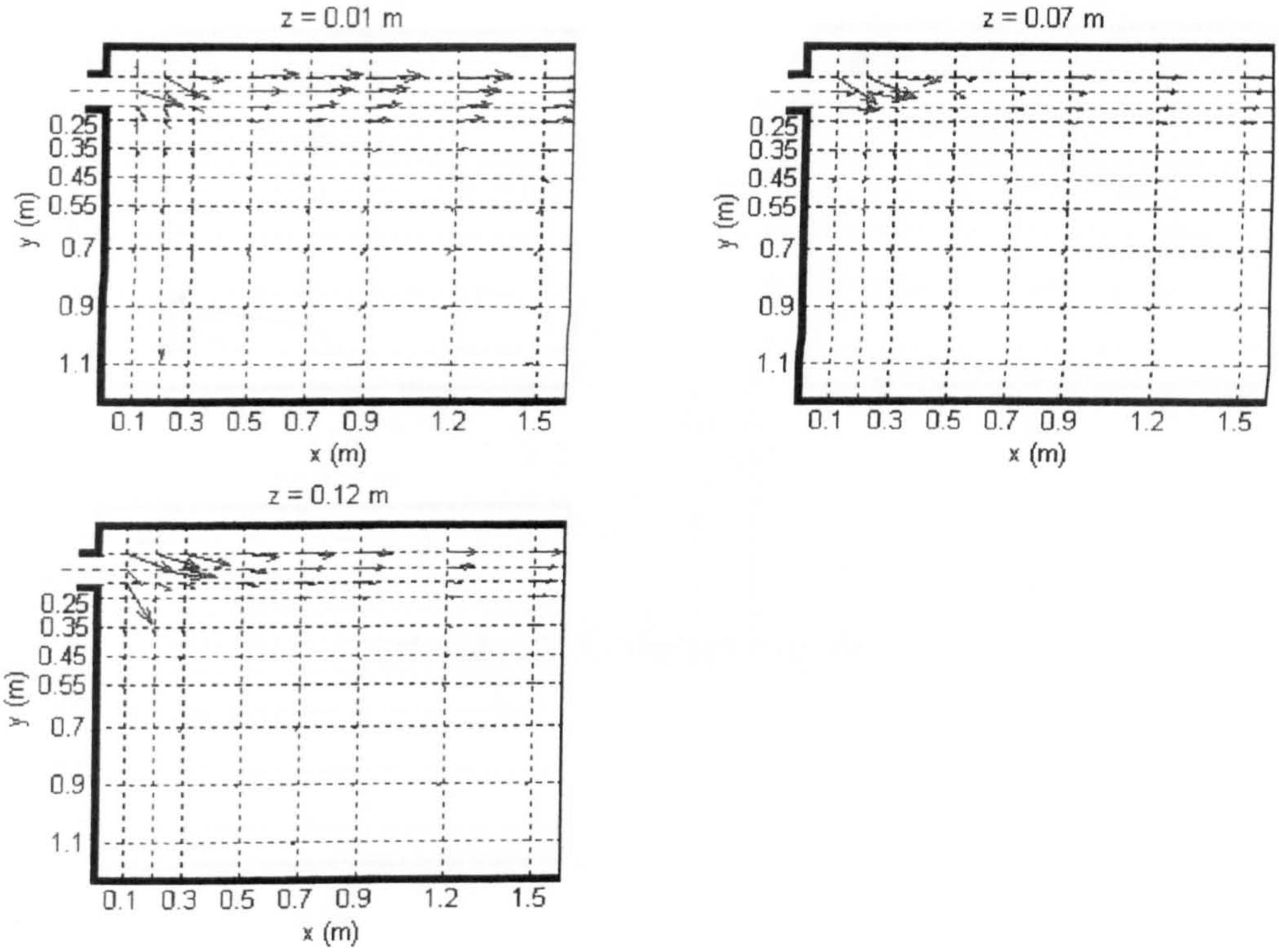

Figure 6-73: Velocity vectors for vertical slot, 0.010 m wide, Q = 0.020m^3/s" [V10$_{20}$]

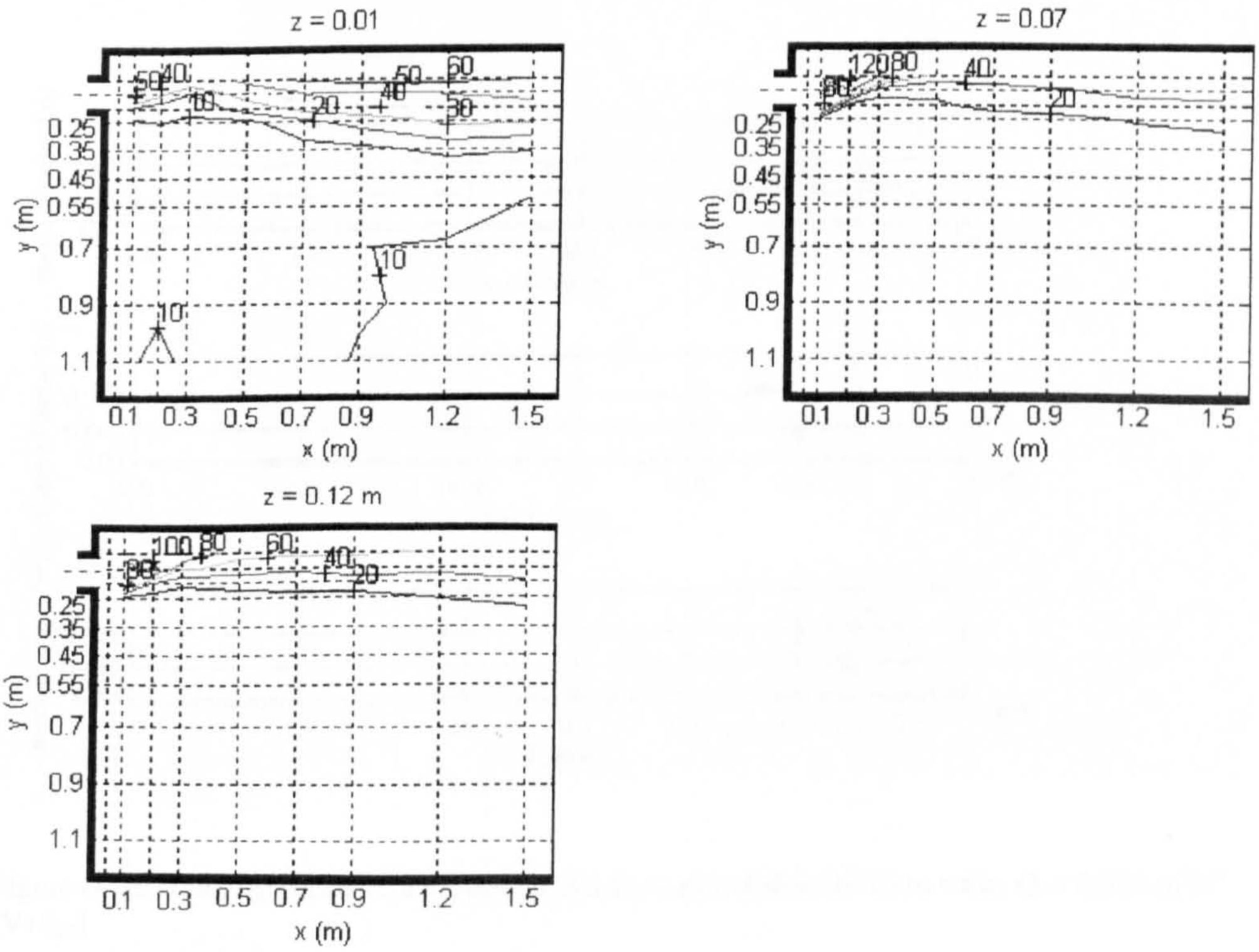

Figure 6-74: Contours of mean velocity for vertical slot, 0.010 m wide, Q = 0.020m^3/s" [V10$_{20}$]

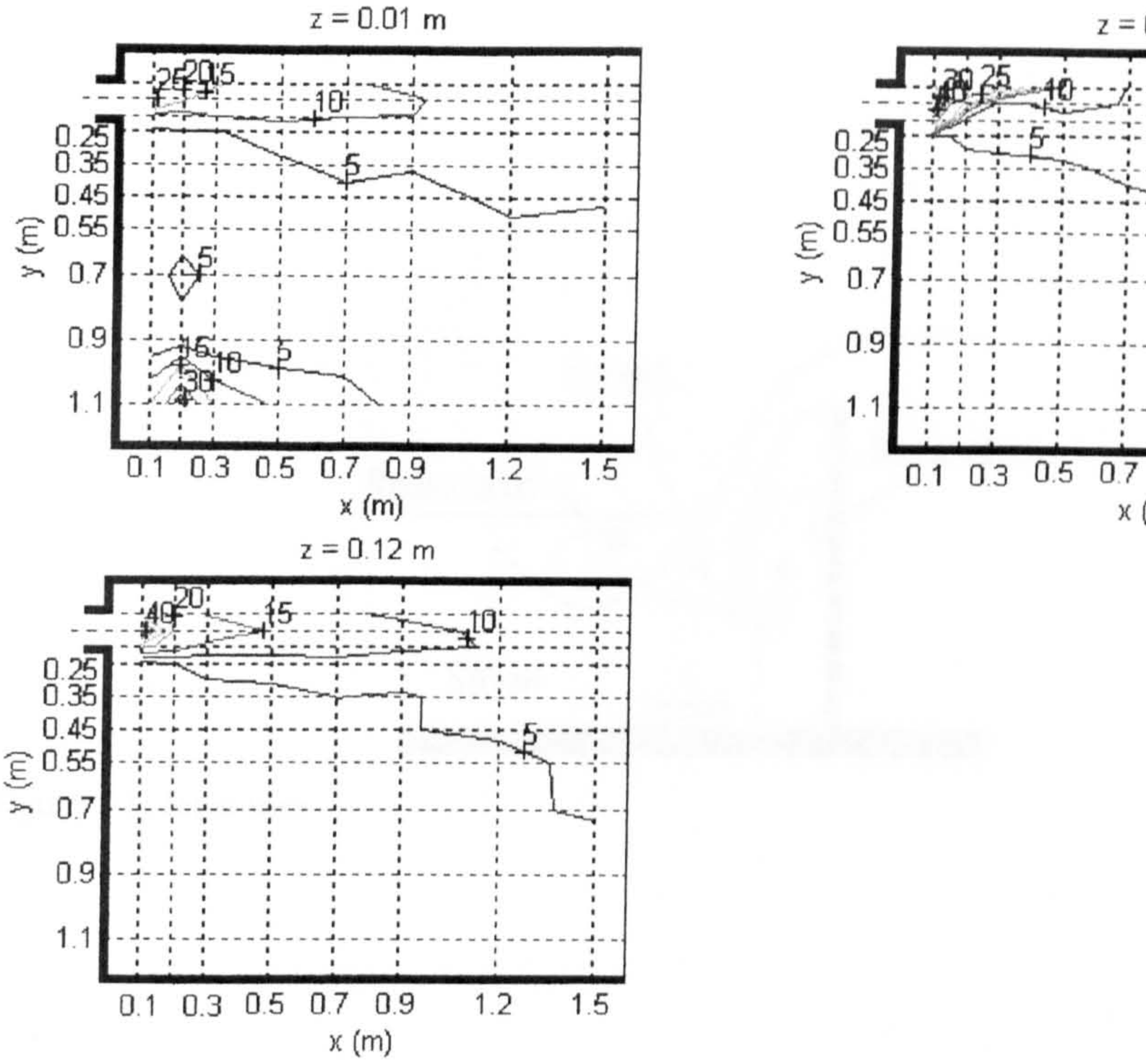

Figure 6-75: Contours of turbulence intensity in % for vertical slot, 0.010 m wide, Q = 0.020m^3/s" [$V10_{20}$]

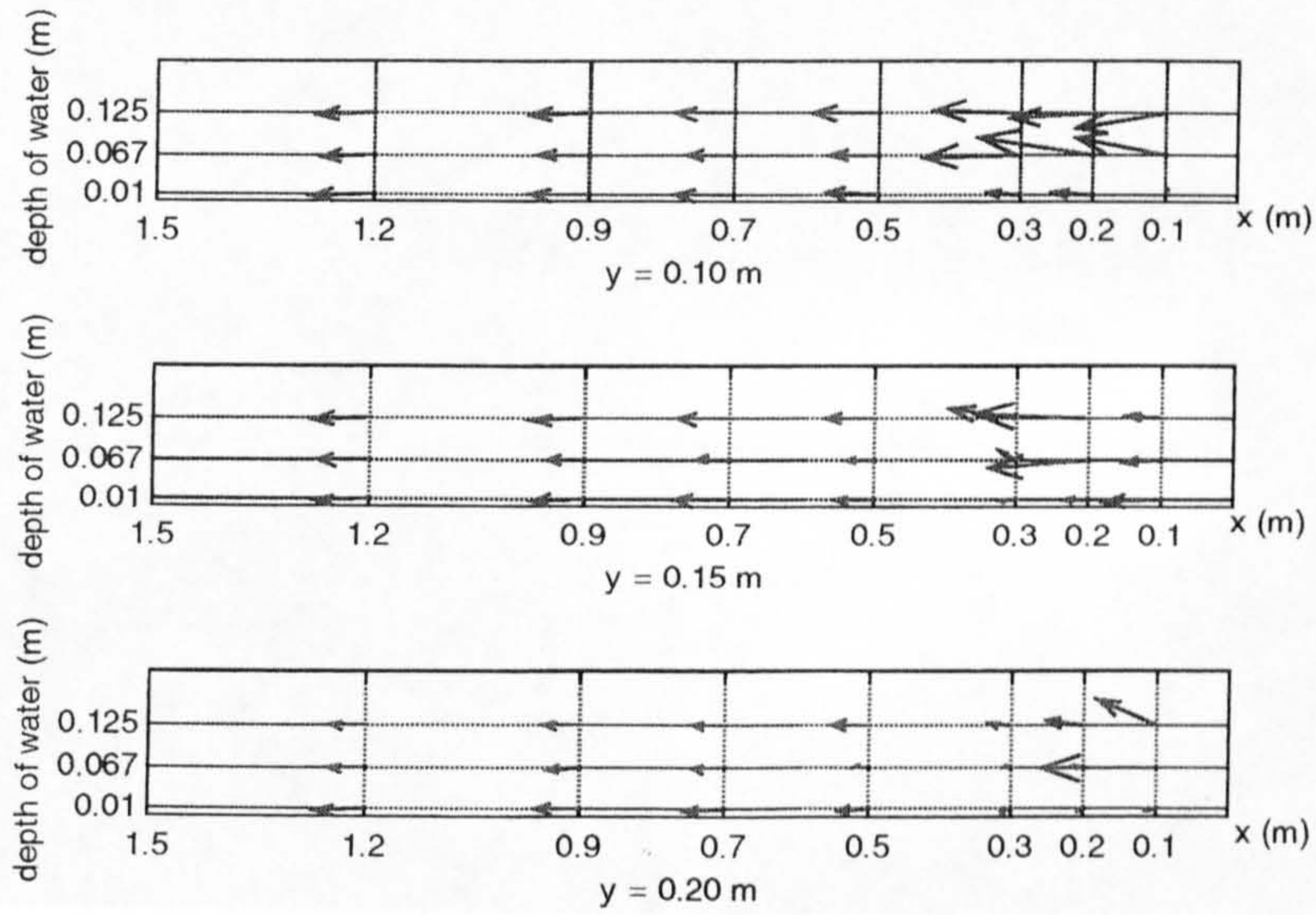

Figure 6-76: Velocity vectors for vertical slides for vertical slot, 0.010 m wide, Q = 0.020 m^3/s" [$V10_{20}$]

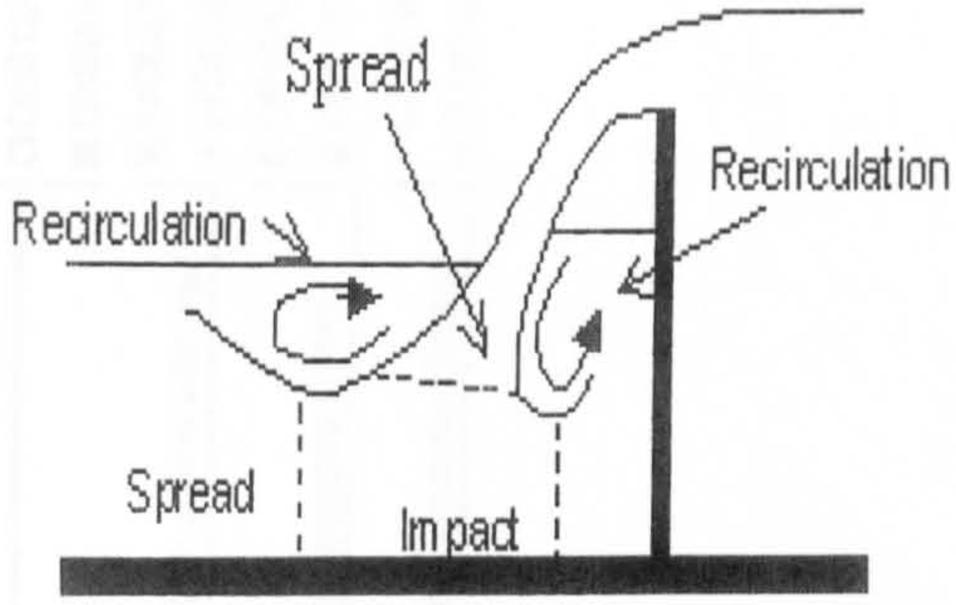

Figure 7-1: Jet at weir

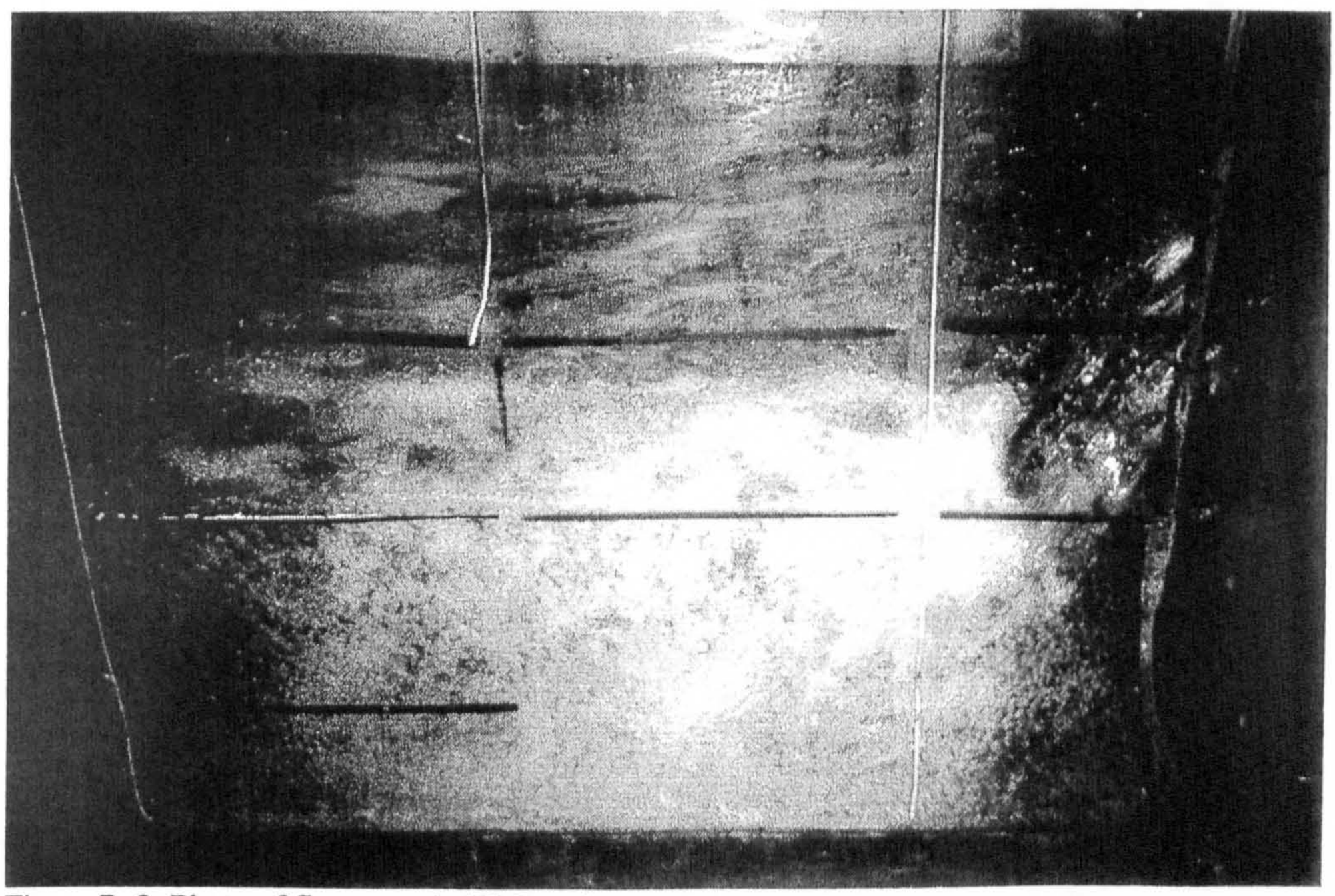

Figure 7- 2: Photo of flow at weir ($ObS_{20\text{-}0.2}$)

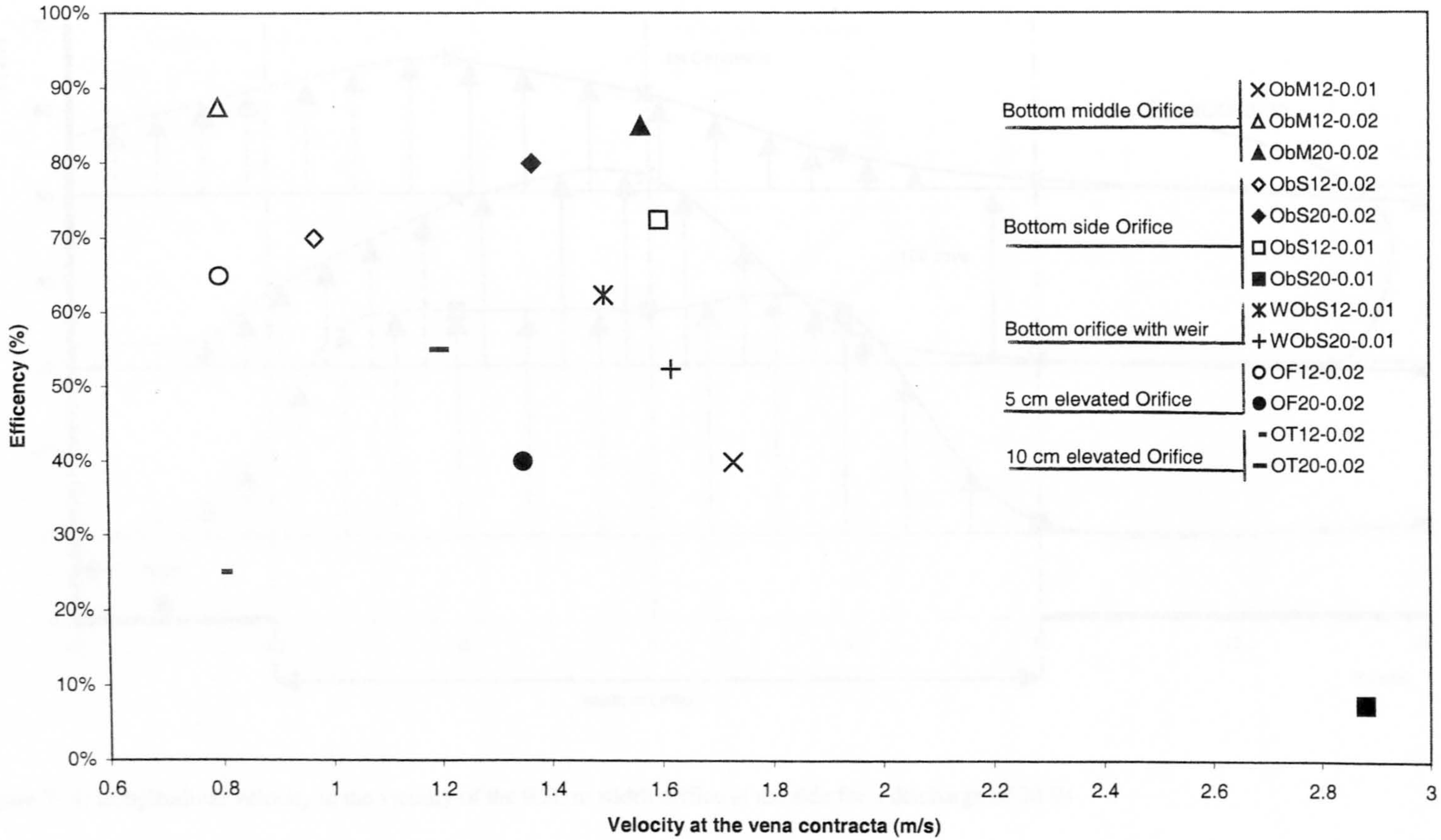

Figure 7- 3: Efficiency of the different orifices designs in relation to the velocity at their vena contracta. 1.80 m/s is the maximum bursting speed of a parr 0.11 m long for a water temperature of 15°C.

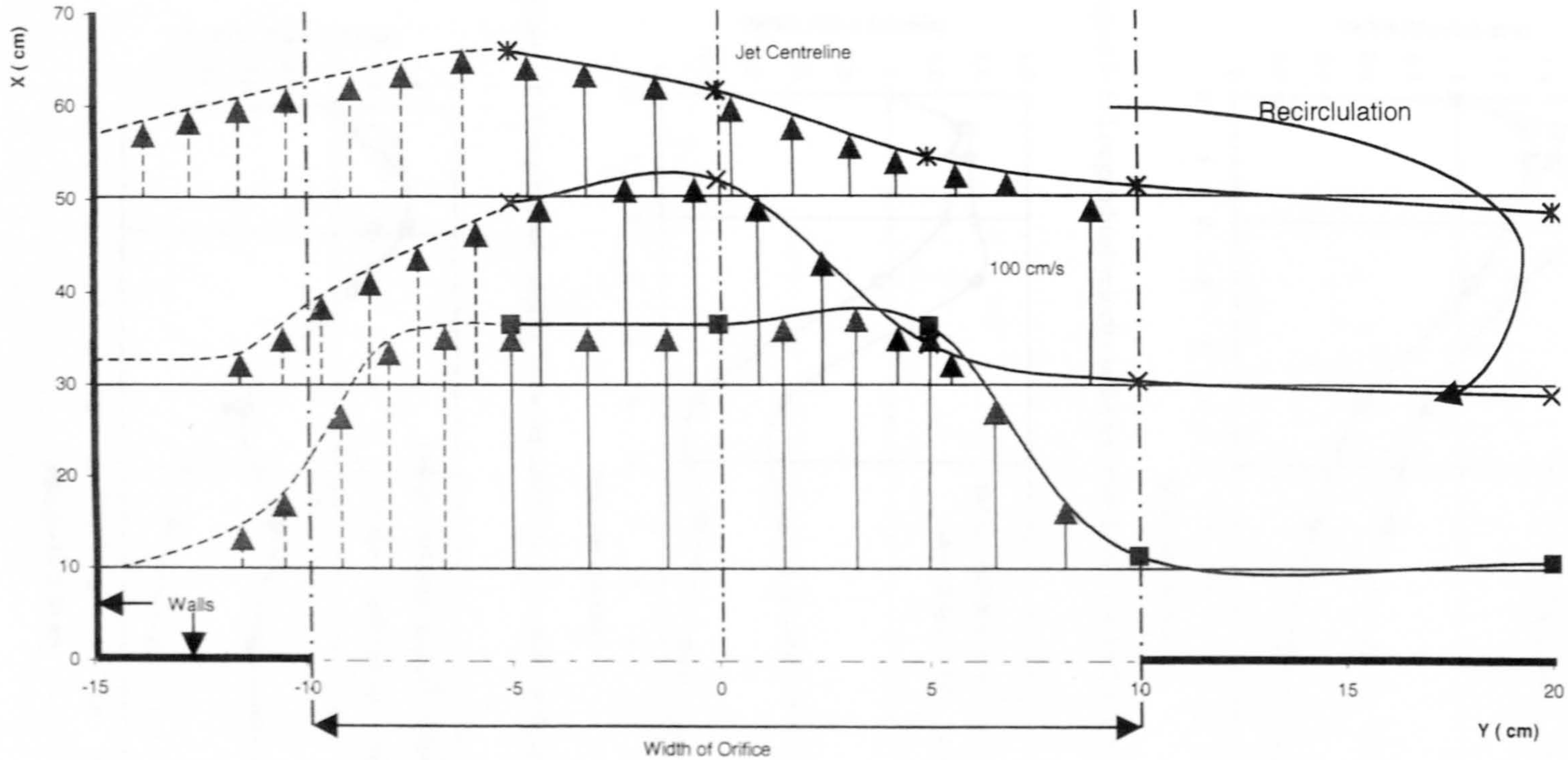

Figure 7- 4: Longitudinal velocity in the vicinity of the 0.20 m width orifice at the side for a discharge of 20 l/s

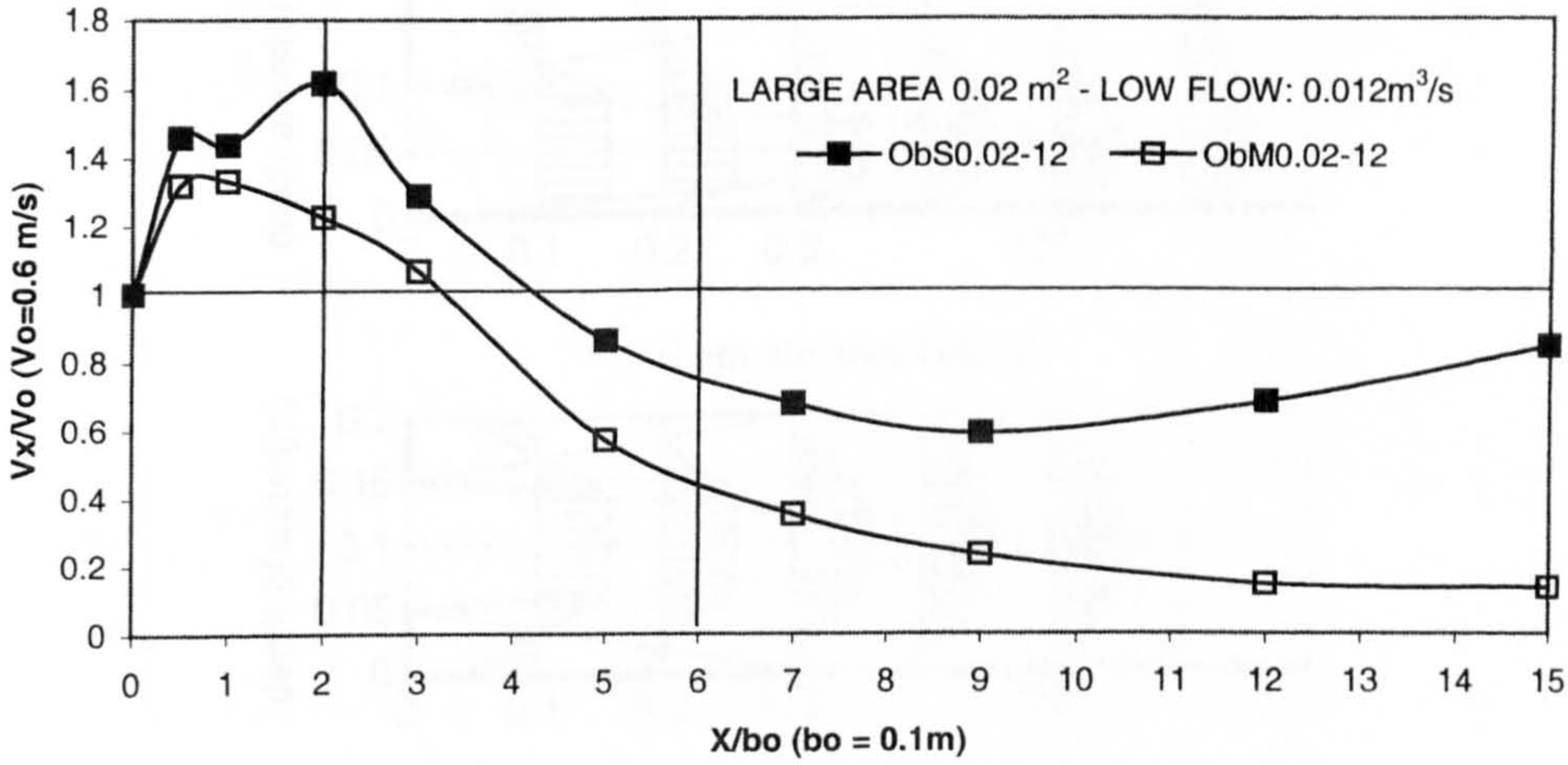

Figure 7- 5: Longitudinal velocity in the jet centreline at z = 0.05 m for a discharge of 0.012m^3/s

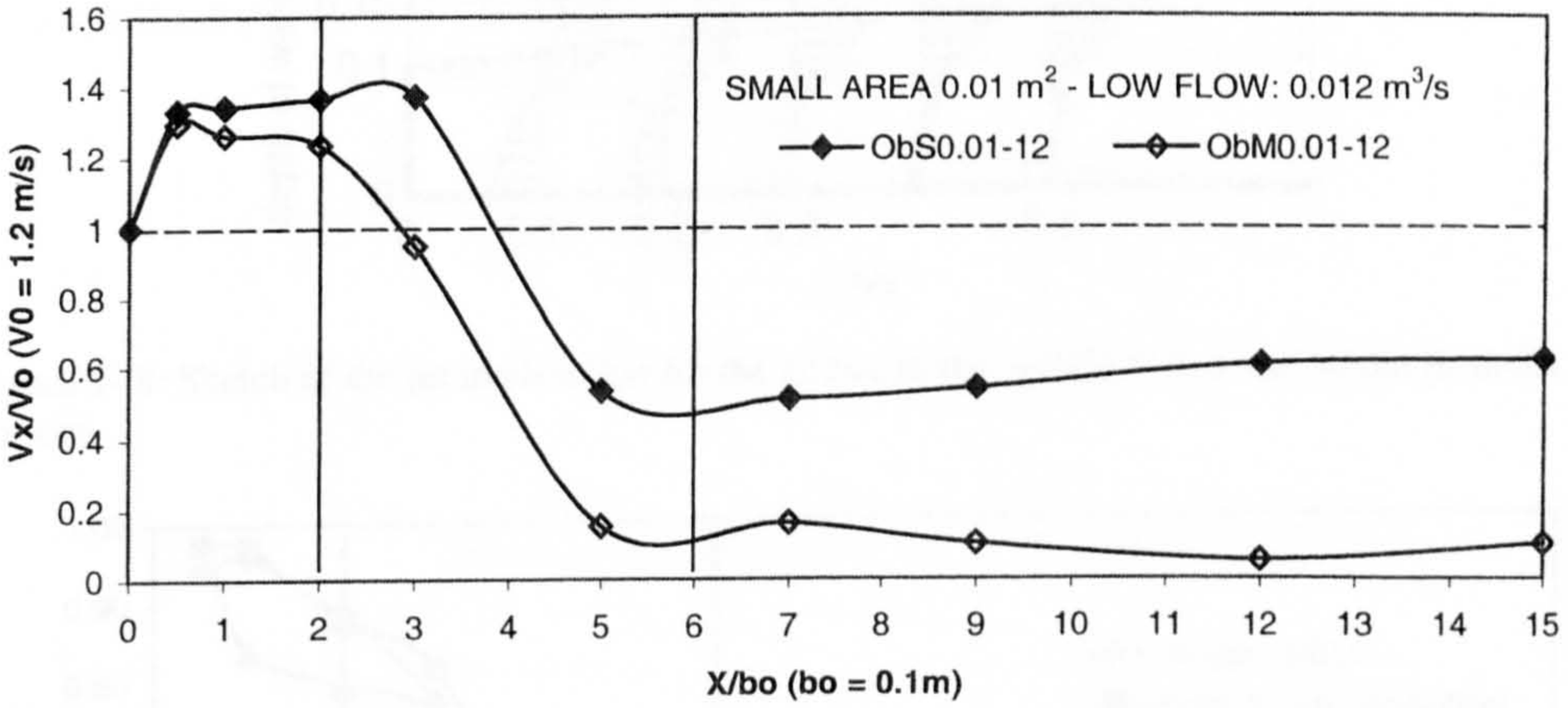

Figure 7- 6: Longitudinal velocity in the jet centreline at z = 0.05 m for a discharge of 0.012 m^3/s.

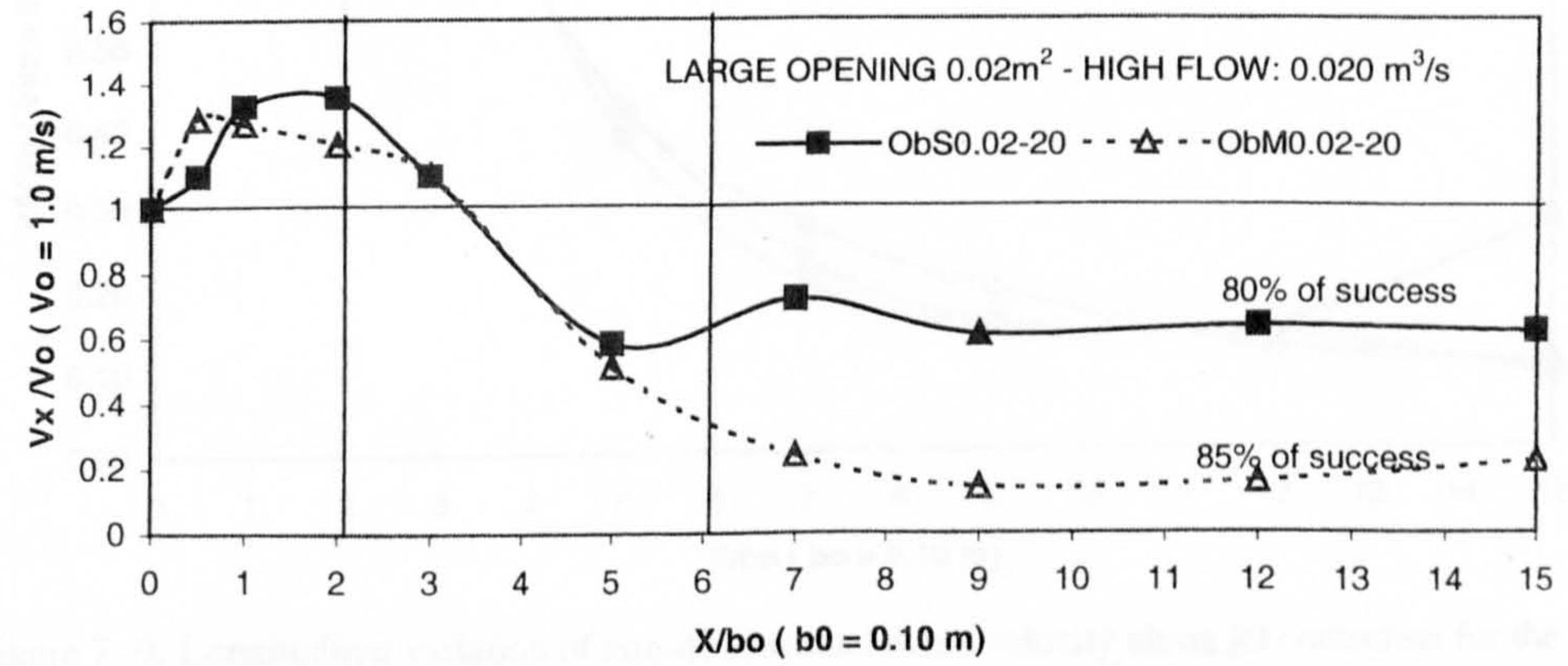

Figure 7- 7: Longitudinal velocity in the jet centreline at z = 0.05 m for a discharge of 0.020 m^3/s

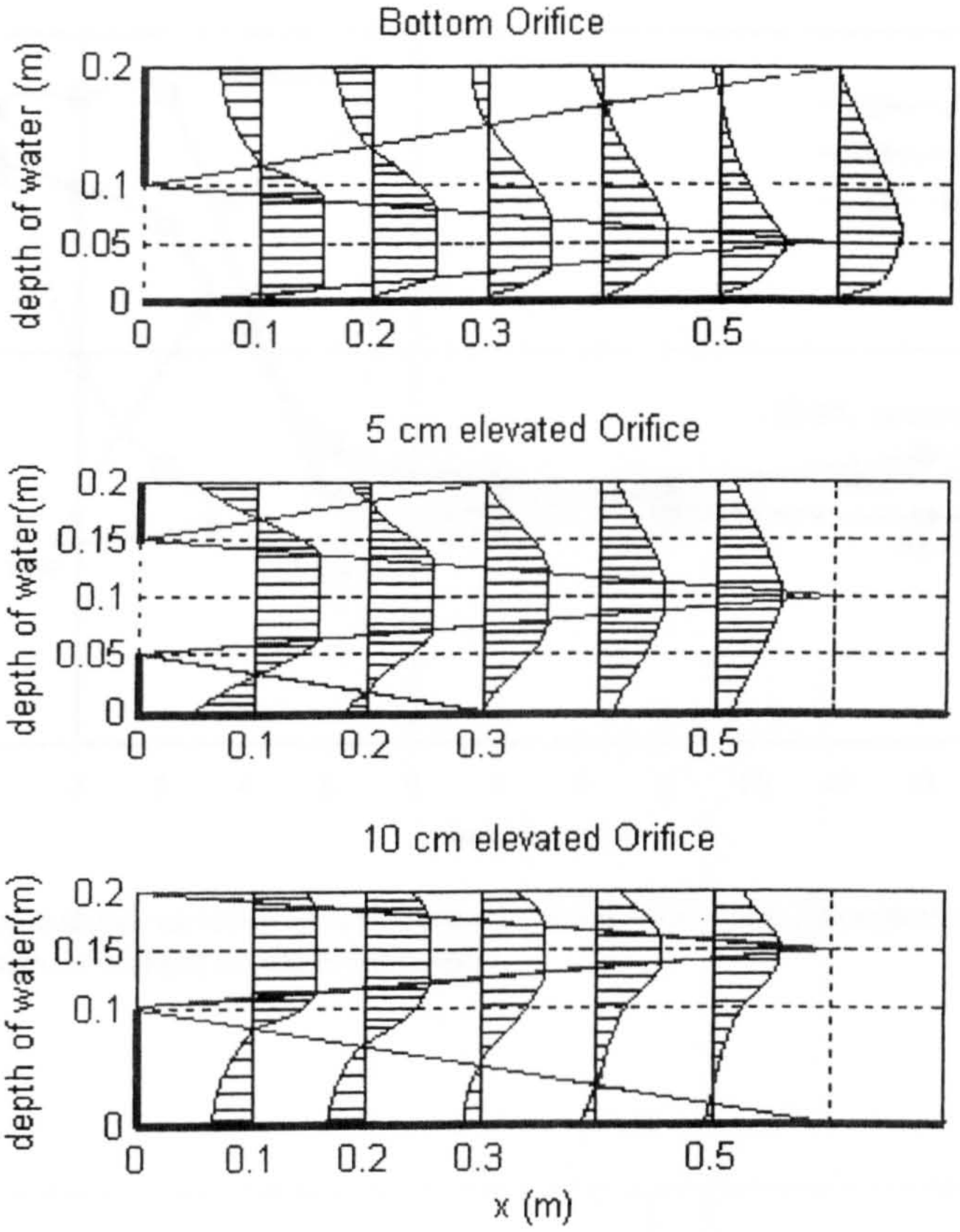

Figure 7- 8: Sketch of the jet in elevation for the orifice in the middle at 0, 5 and 10 cm from the bottom.

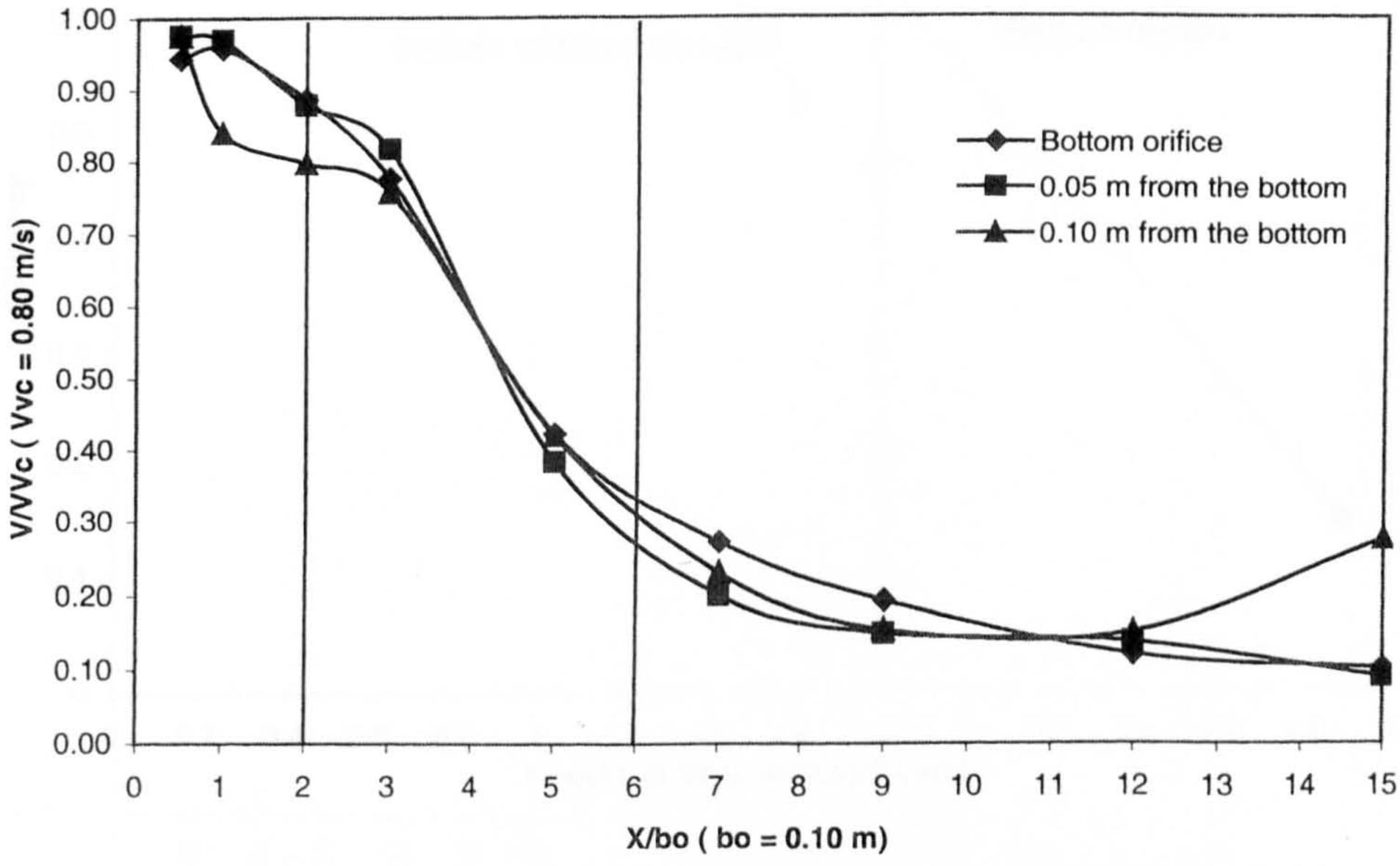

Figure 7- 9: Longitudinal variation of non-dimensional mean velocity along jet centreline for the orifices at 0, 5 and 10 cm from the bottom for a discharge of 0.012 m^3/s and an opening of 0.02m^2

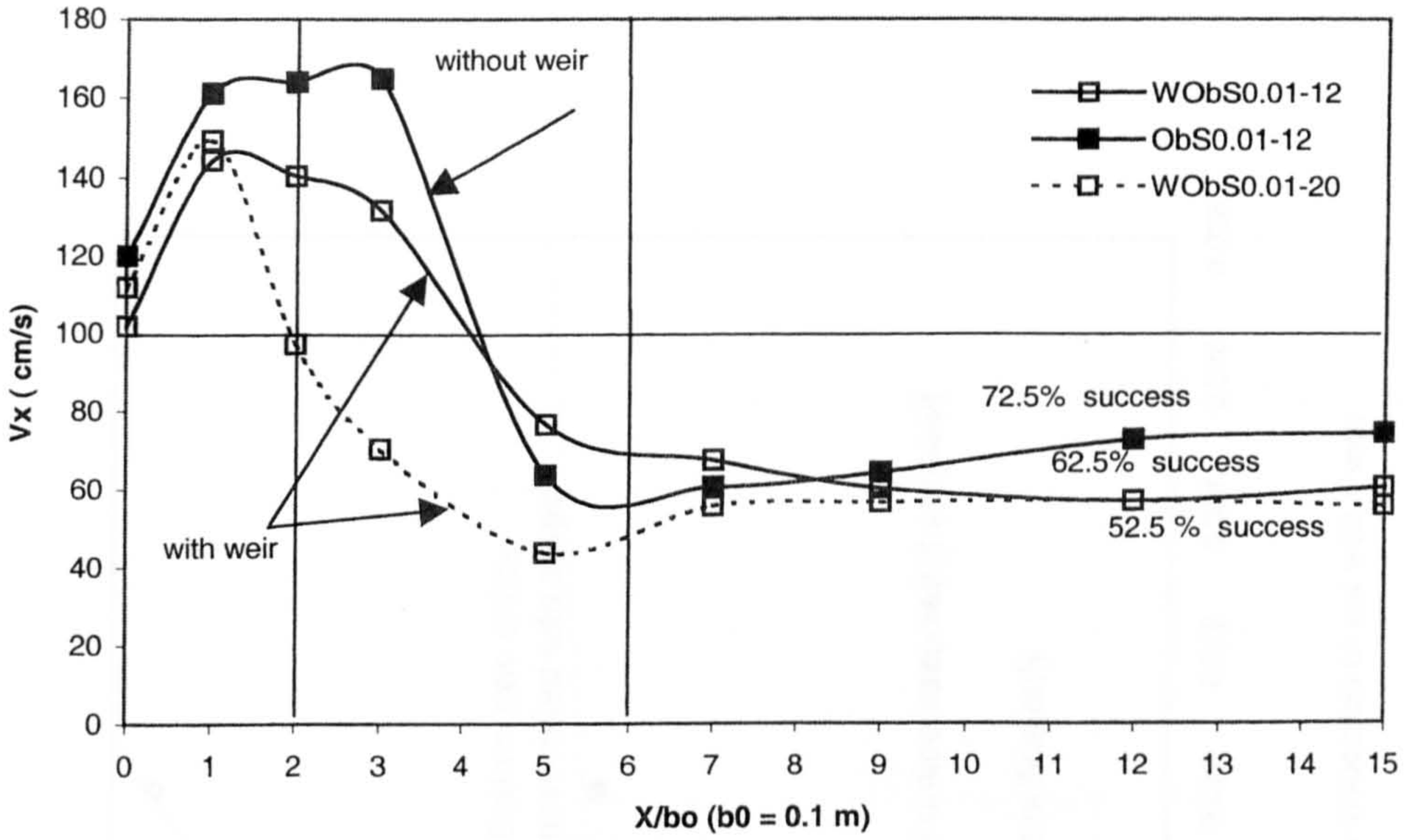

Figure 7- 10: Longitudinal variation of longitudinal velocity Vx along jet centreline for the bottom orifices with or without a weir combination

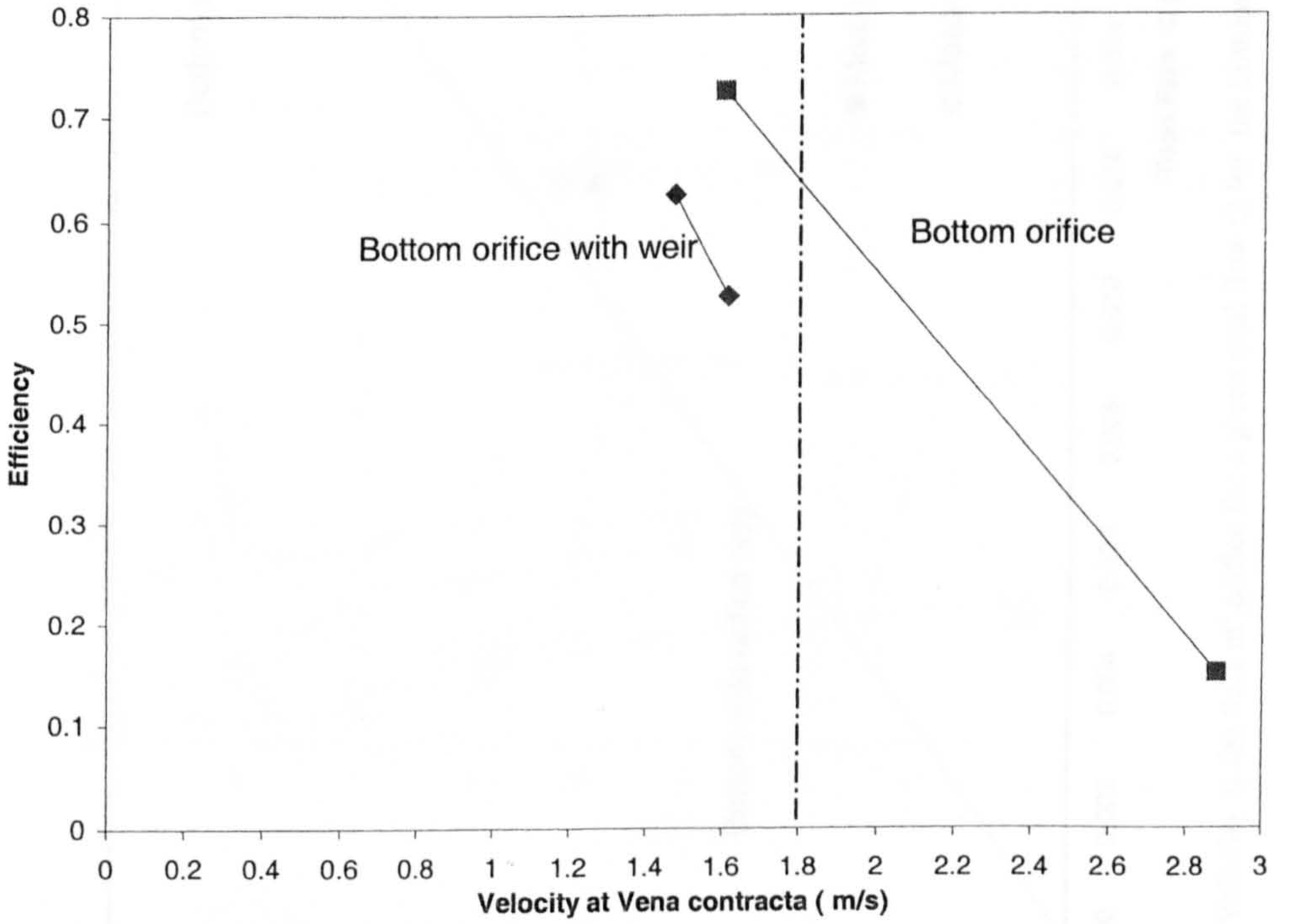

Figure 7- 11: Efficiency of the 0.10 x 0.10 side orifices in relation to the velocity at the vena contracta. 1.80 m/s is the maximum bursting speed of a parr 0.11 m long for a water temperature of 15°C

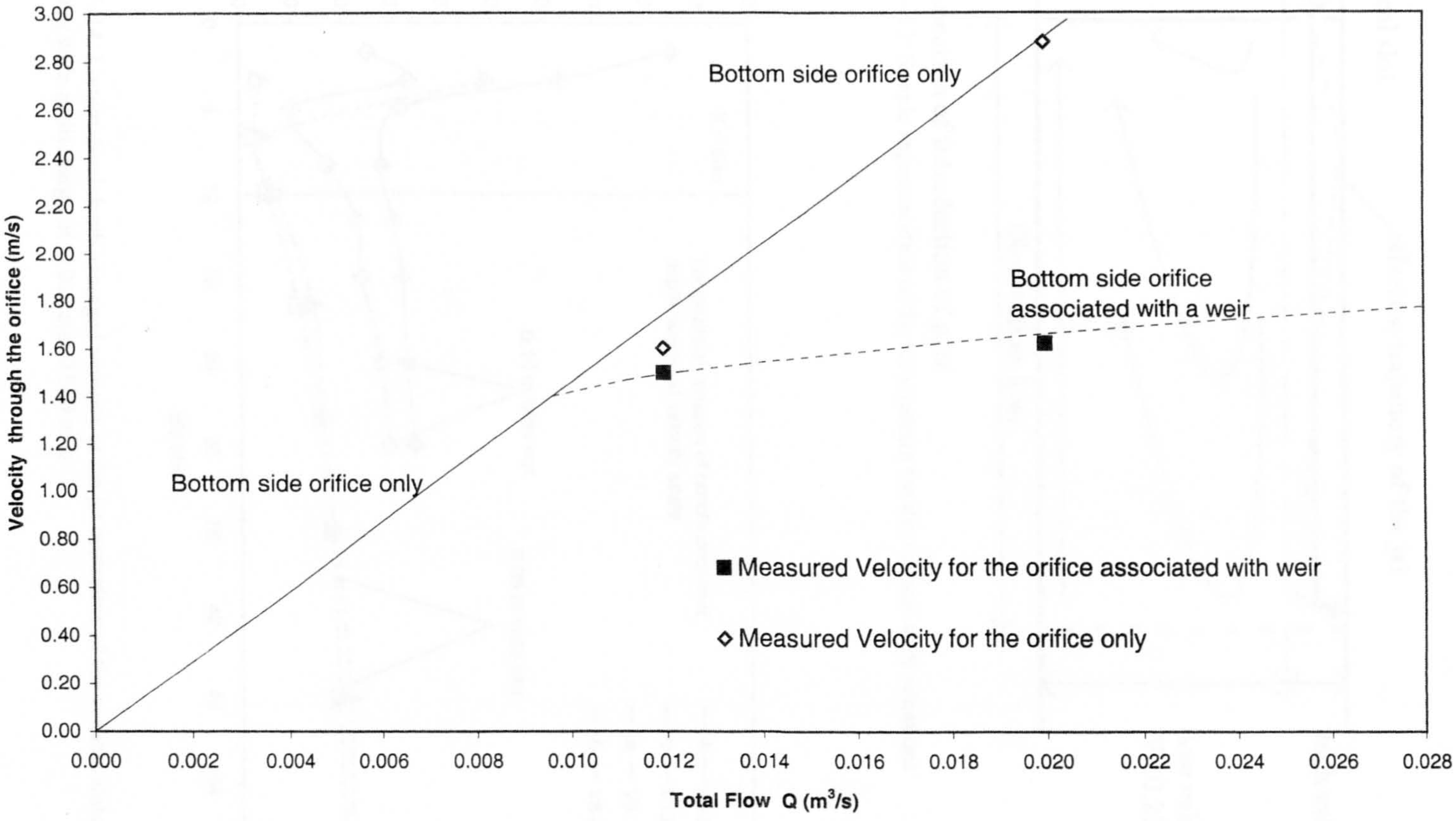

Figure 7- 12: Velocity at the 0.01 m^2 orifice for a given total flow Q for the bottom side orifice situation associated or not with a weir

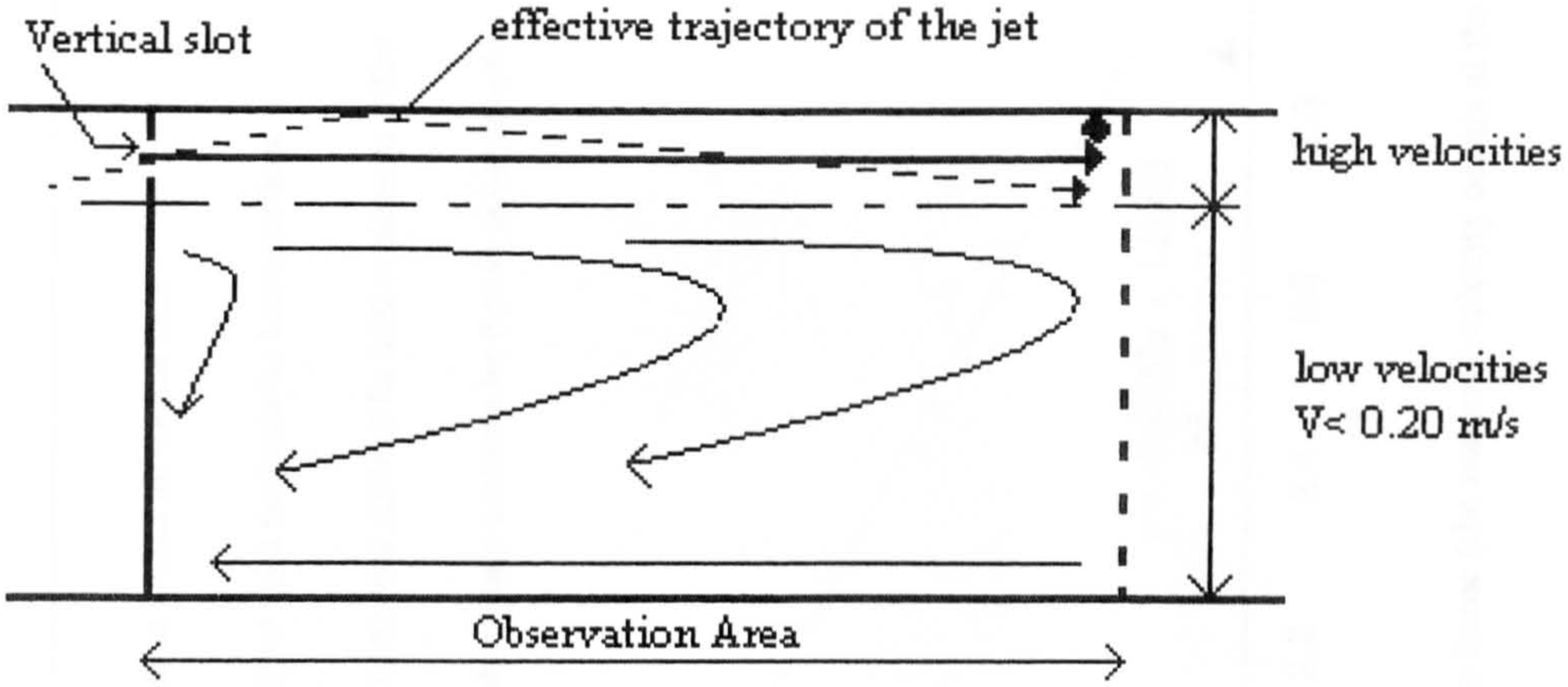

Figure 7- 13: Simple representation of the flow pattern for the vertical slots situations

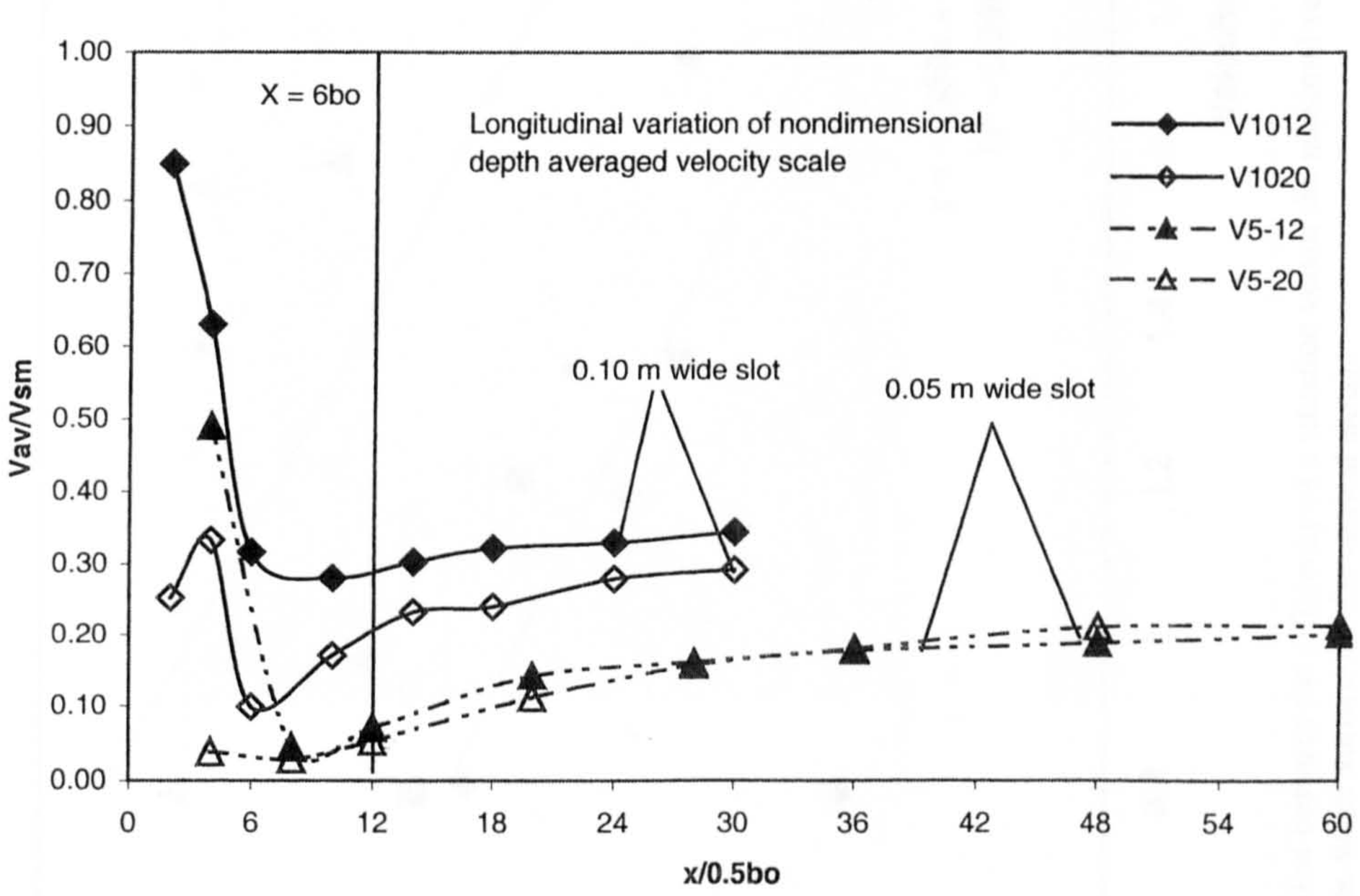

Figure 7- 14: Longitudinal depth averaged velocity in the jet centreline of the vertical slots 0.05 and 0.10 m wide at discharge of 0.012 and 0.020 m^3/s

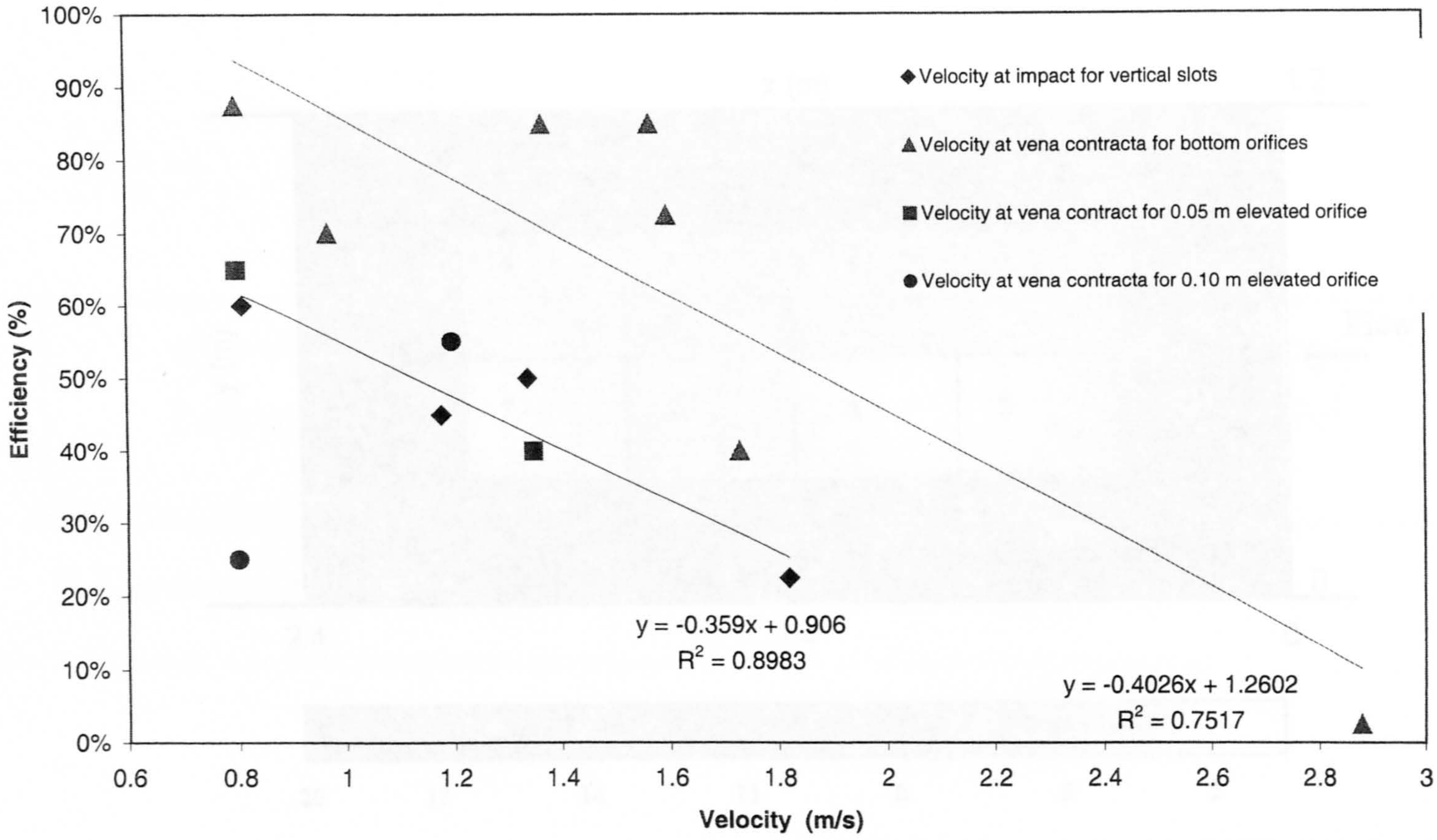

Figure 7- 15: Relation between the efficiency of a situation versus the maximal velocity existing in the flume (the maximal velocity occurs at the vena contracta for orifices and near the water surface for the vertical slots)..

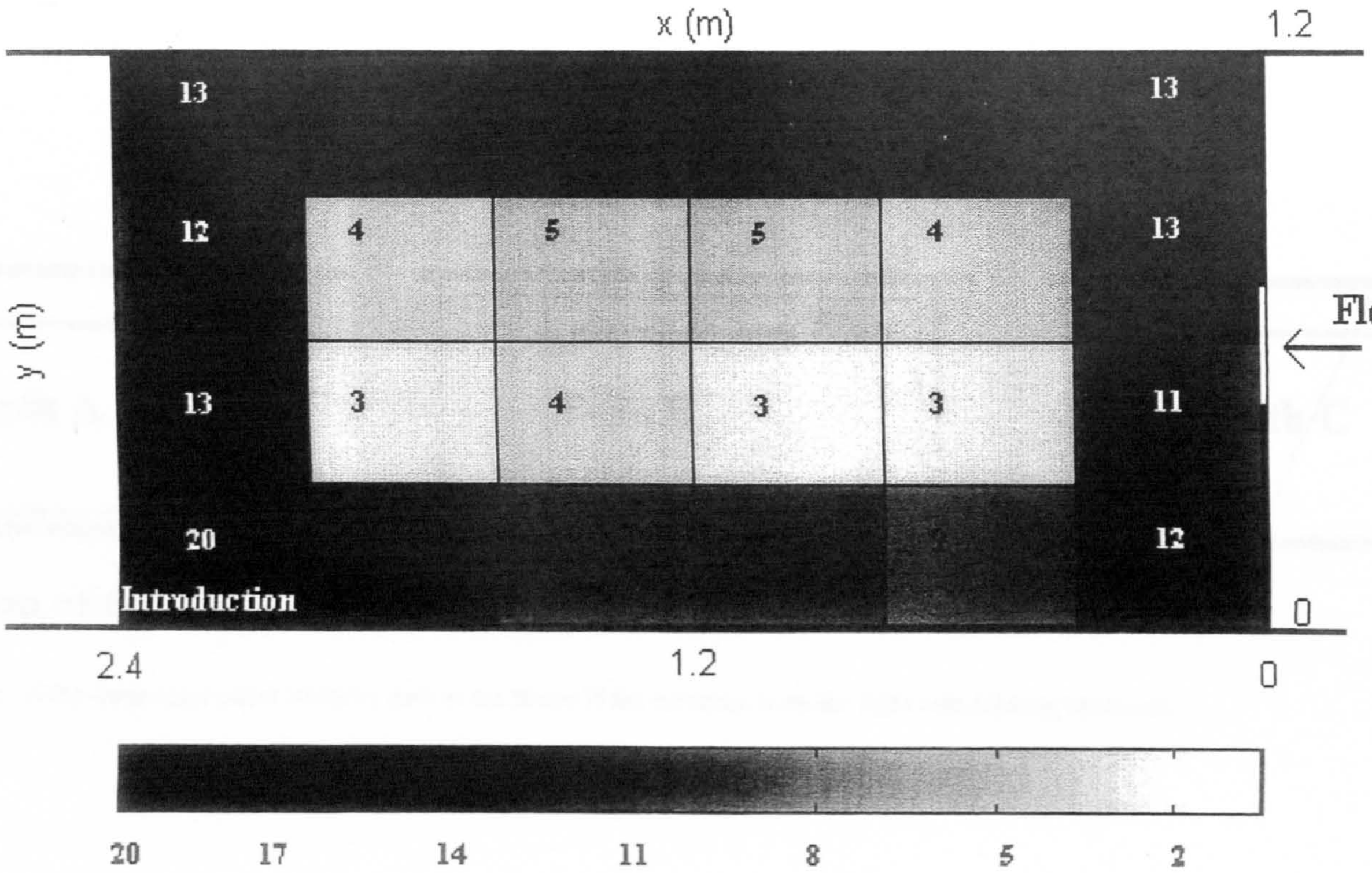

Figure 7- 16: Average space occupation for series I. A dimensionless number varying between 0 and 20 represents the intensity of the occupation of a portion of the flume by the parr.

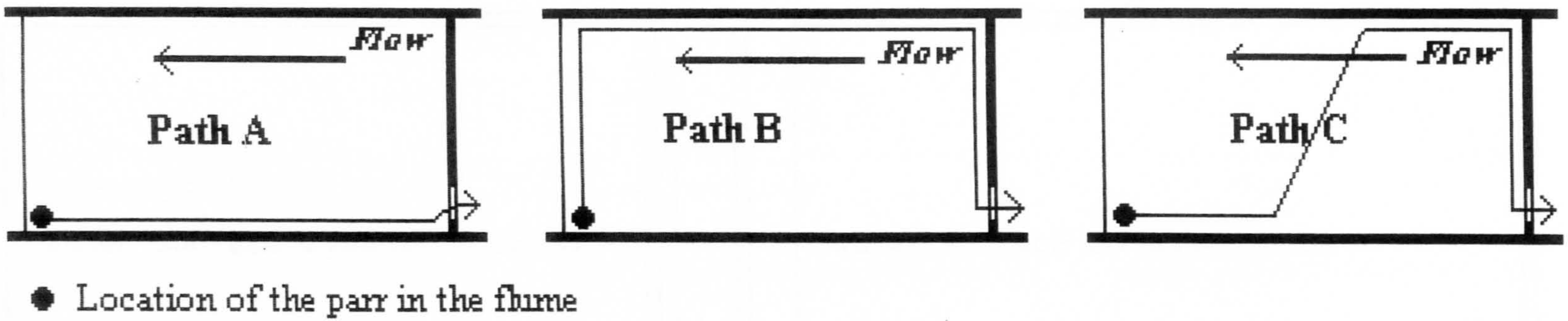

Figure 7-17: Schematic of the three main paths taken by parr in the flume if the entrance is on the right side looking upstream

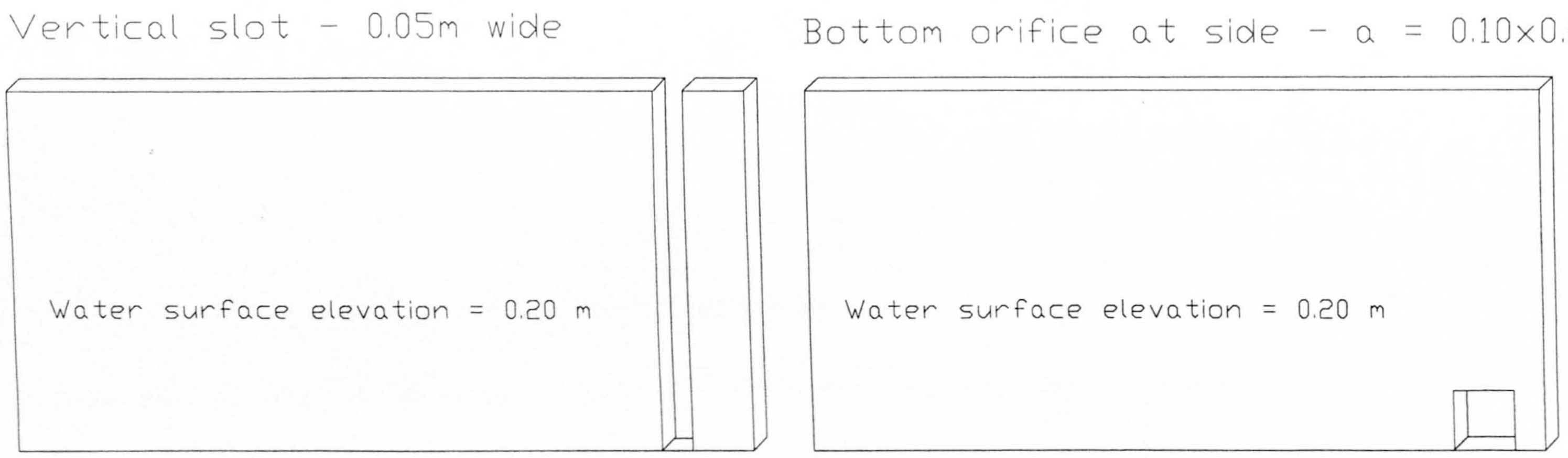

Figure 7-18: One 0.10 x 0.10 m orifice versus 0.05 m wide vertical slot

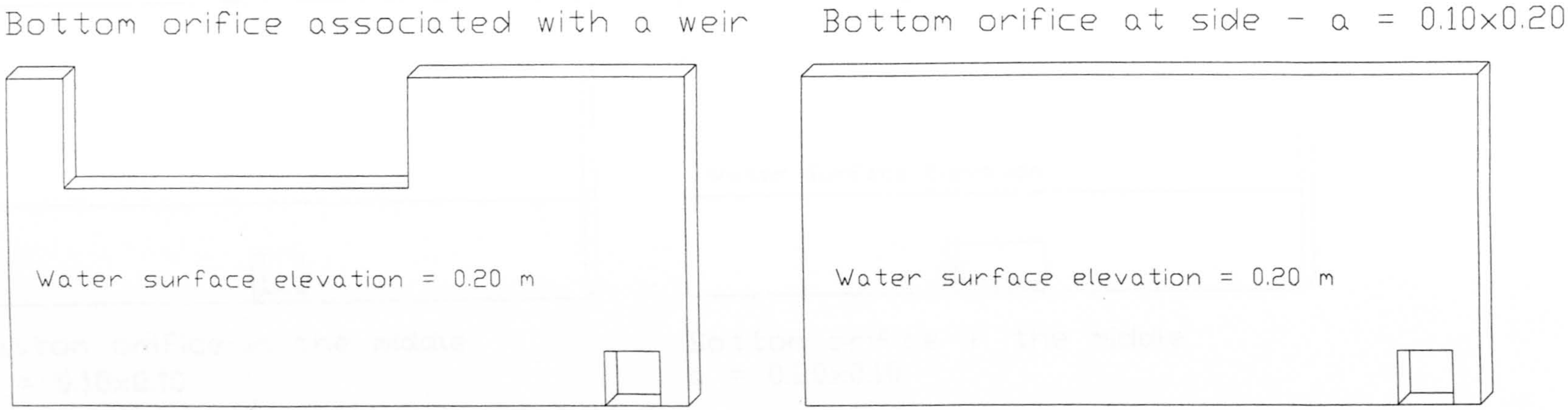

Figure 7-19: One 0.10 x 0.10 m orifice versus 0.10 x 0.10 orifice associated with a weir

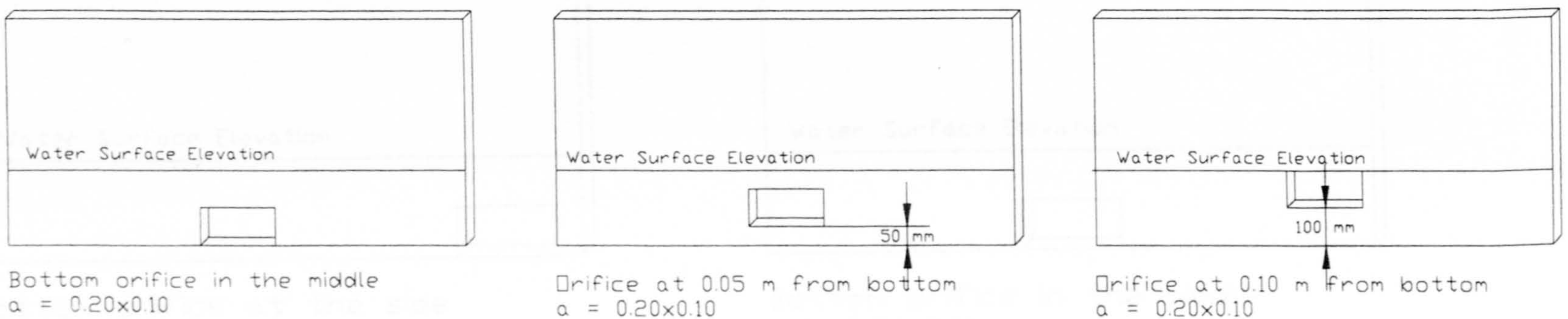

Figure 7-20: Three orifices at three elevations in the water column

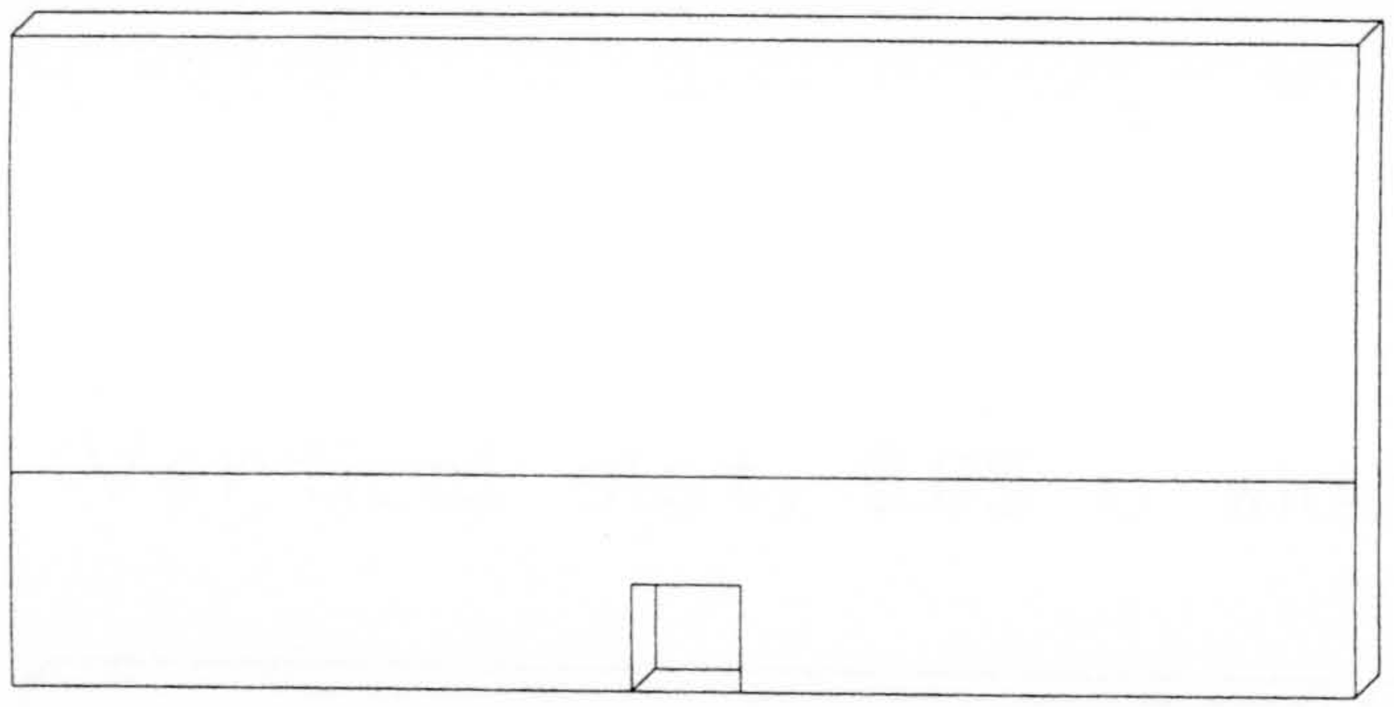

Bottom orifice in the middle
a = 0.10×0.10

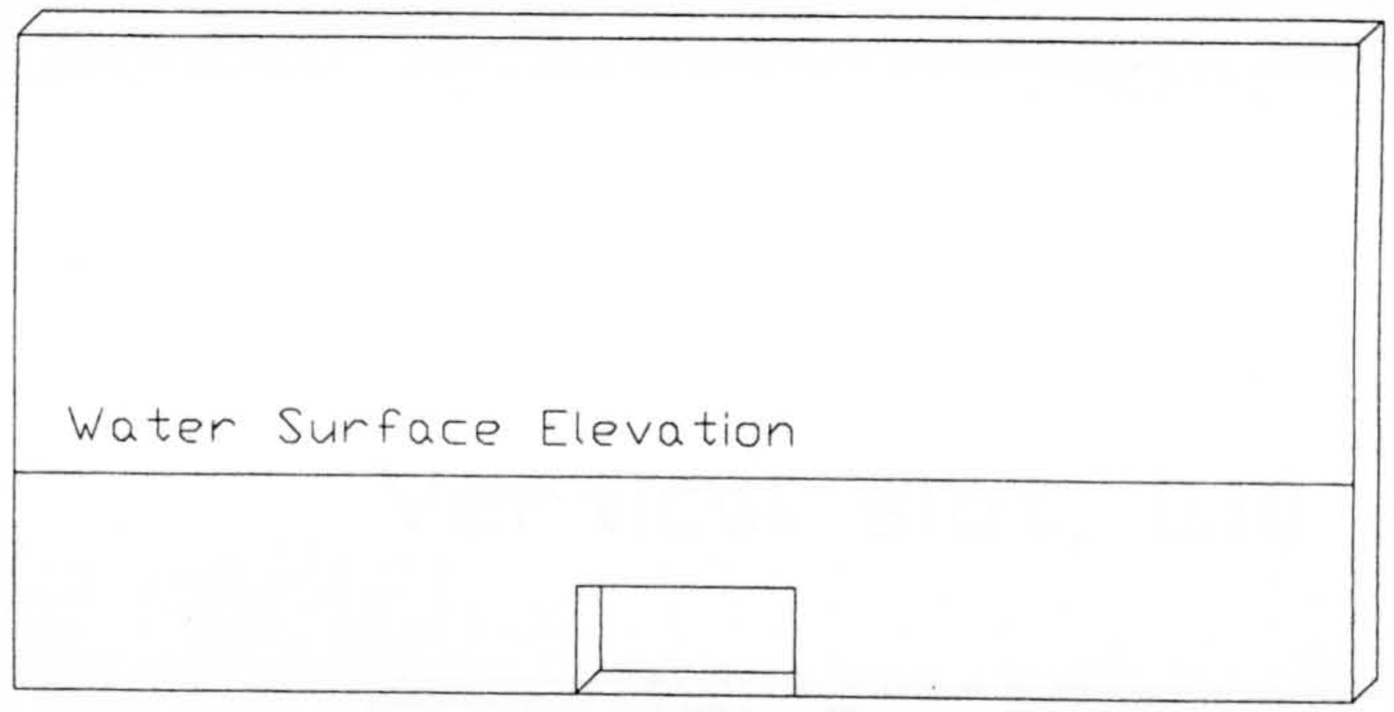

Bottom orifice in the middle
a = 0.20×0.10

Figure 7-21: Two middle orifices with different opening sizes

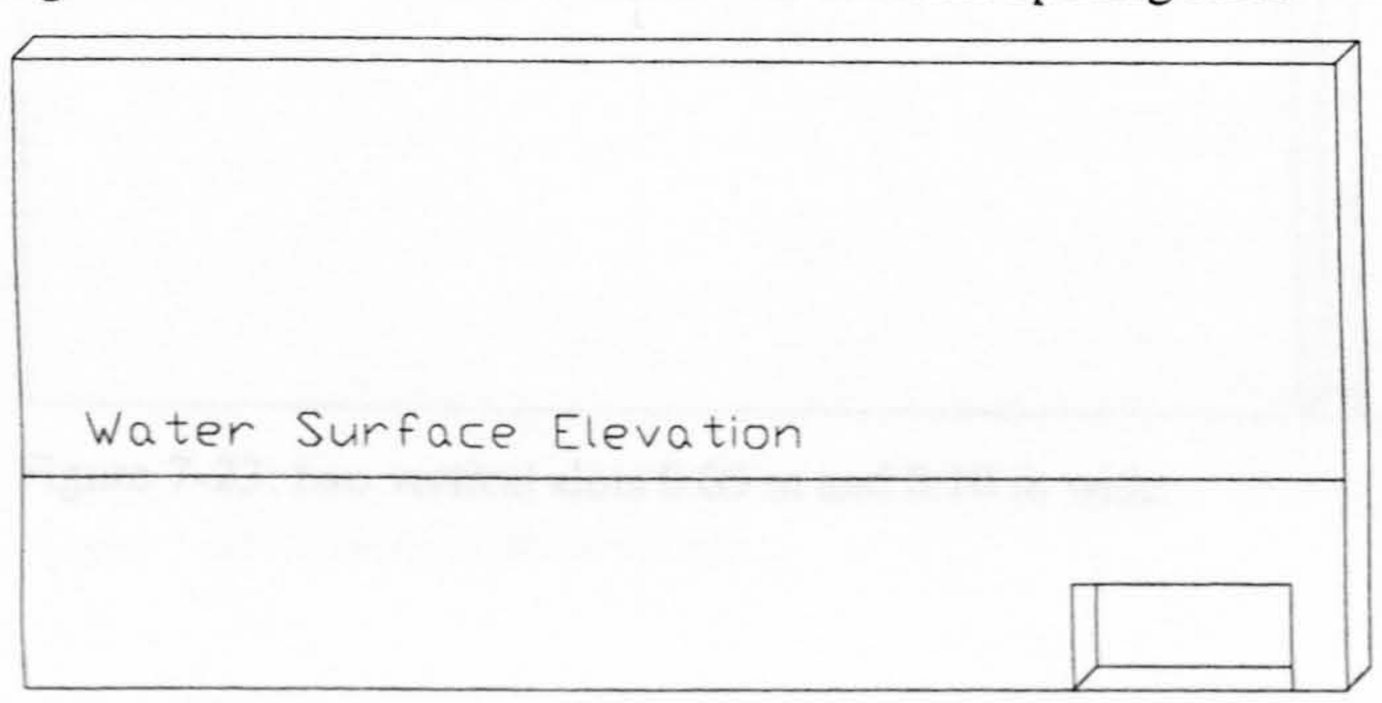

Bottom orifice at the side
a = 0.20×0.10

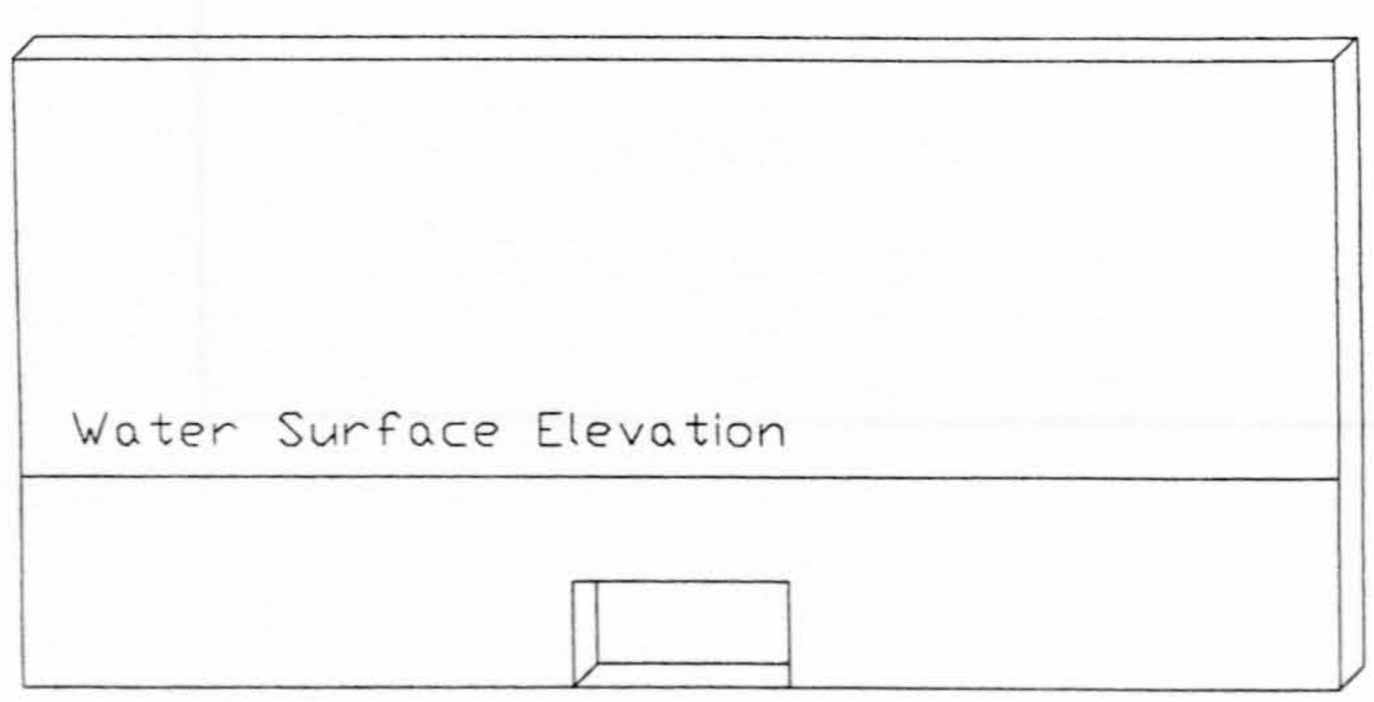

Bottom orifice in the middle
a = 0.20×0.10

Figure 7-22:Two orifices with different lateral location : middle or side

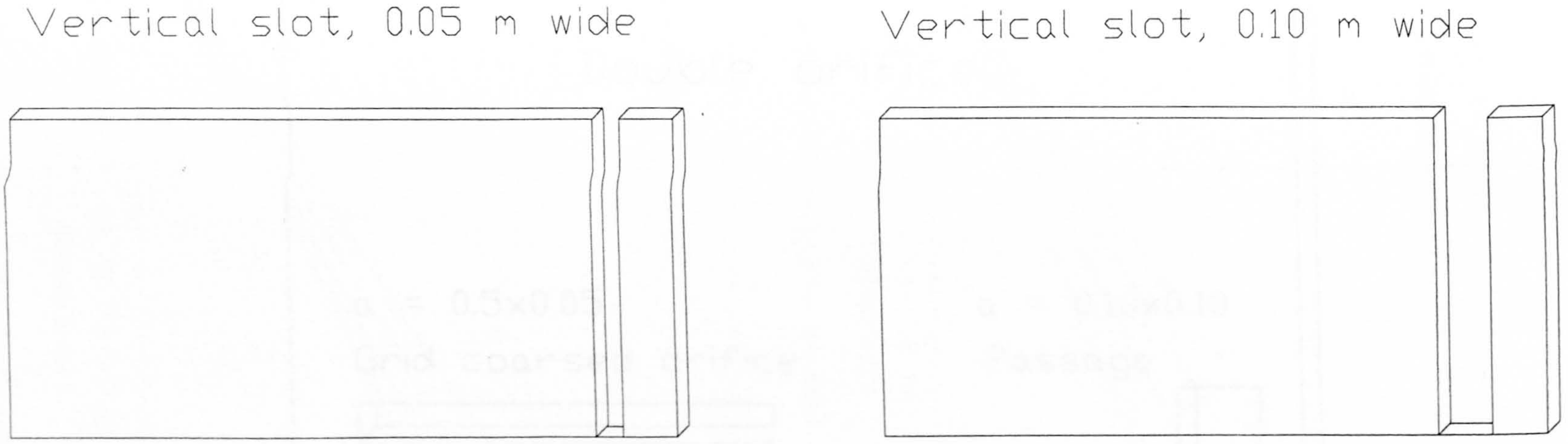

Figure 7-23: two vertical slots 0.05 m and 0.10 m wide

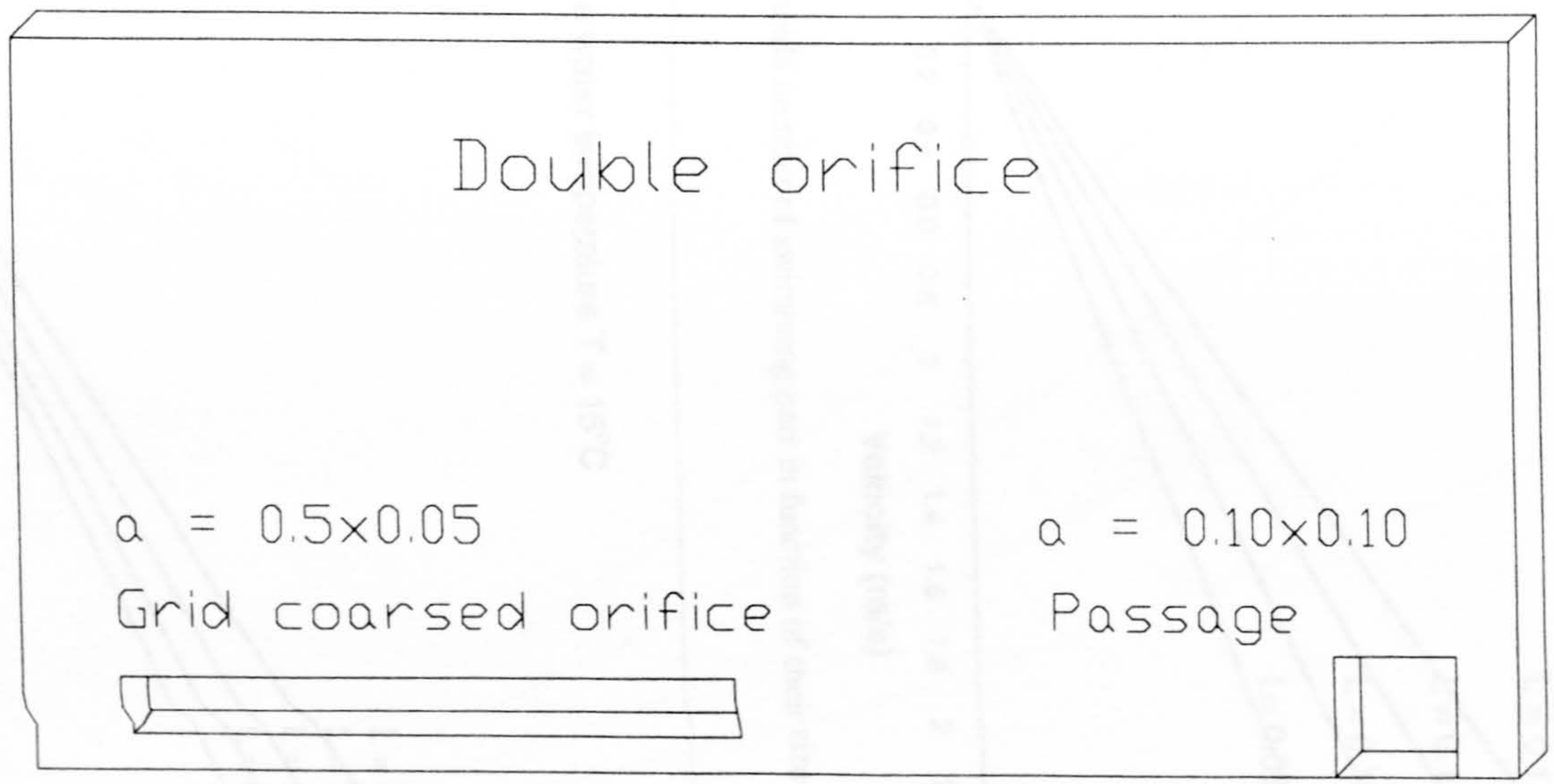

Figure 7-24: Double orifice design

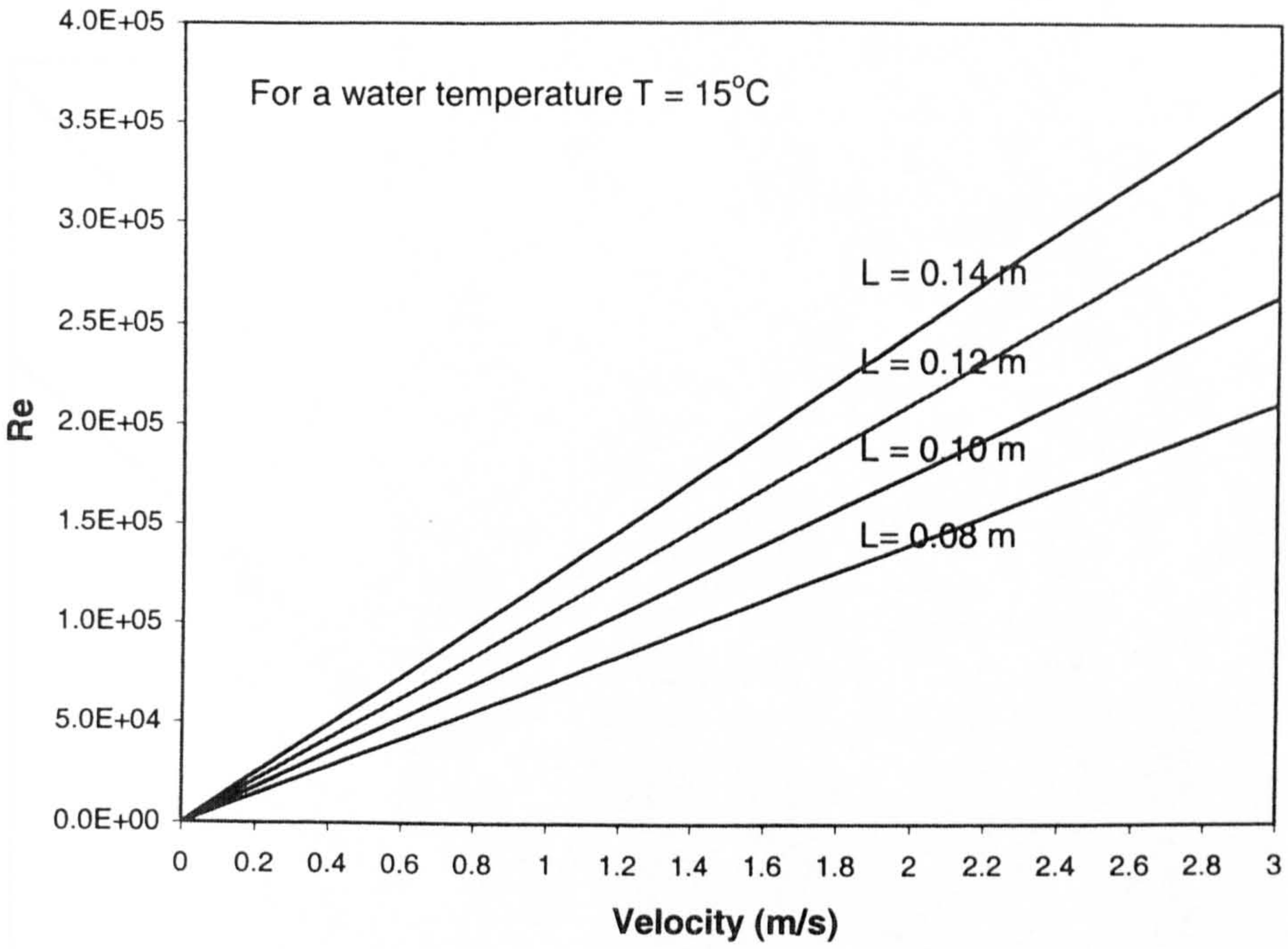

Figure 7-25: Reynolds number of swimming parr in function of their size and swimming speed.

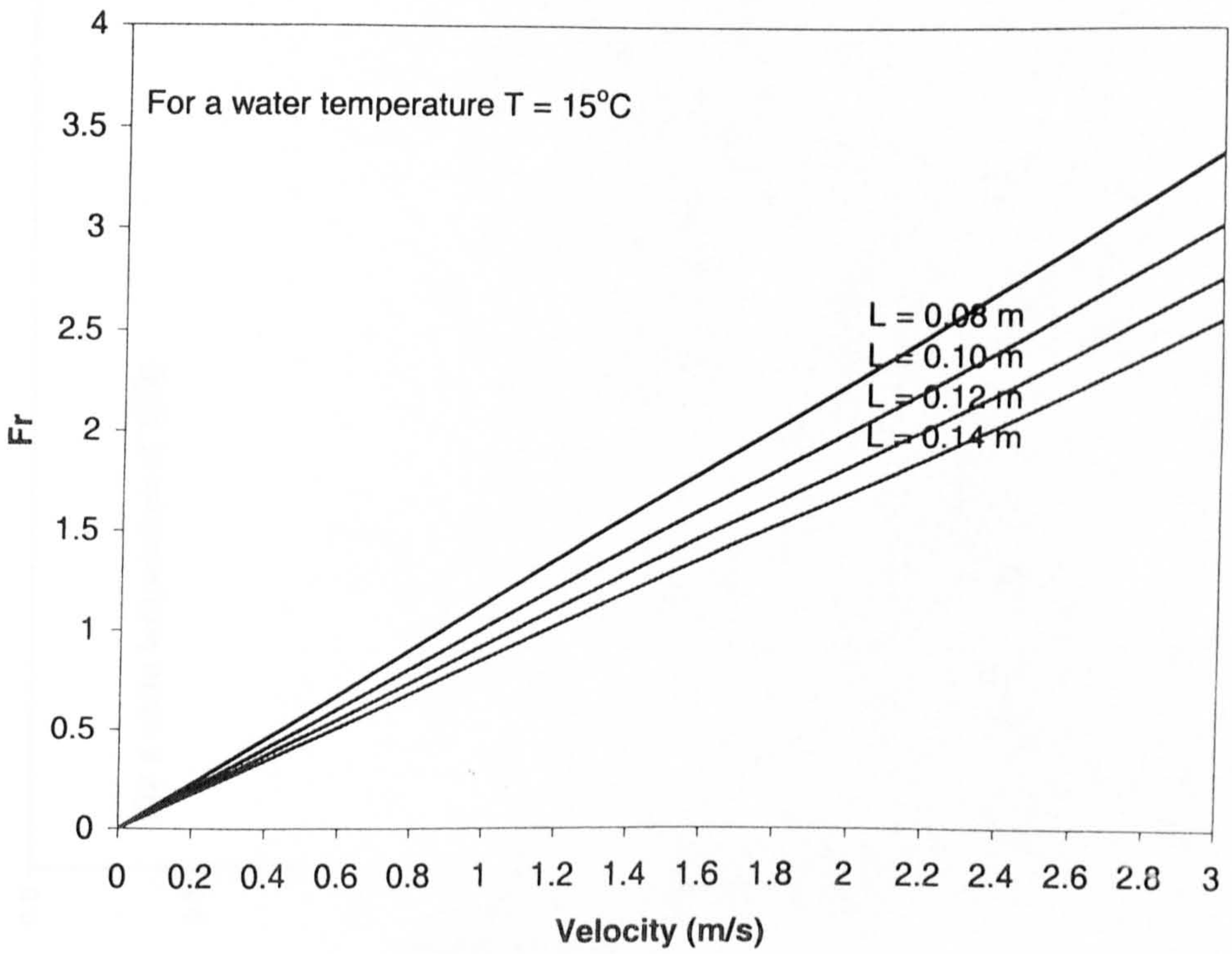

Figure 7-26: Froude Number of swimming parr in function of their size and swimming speed.

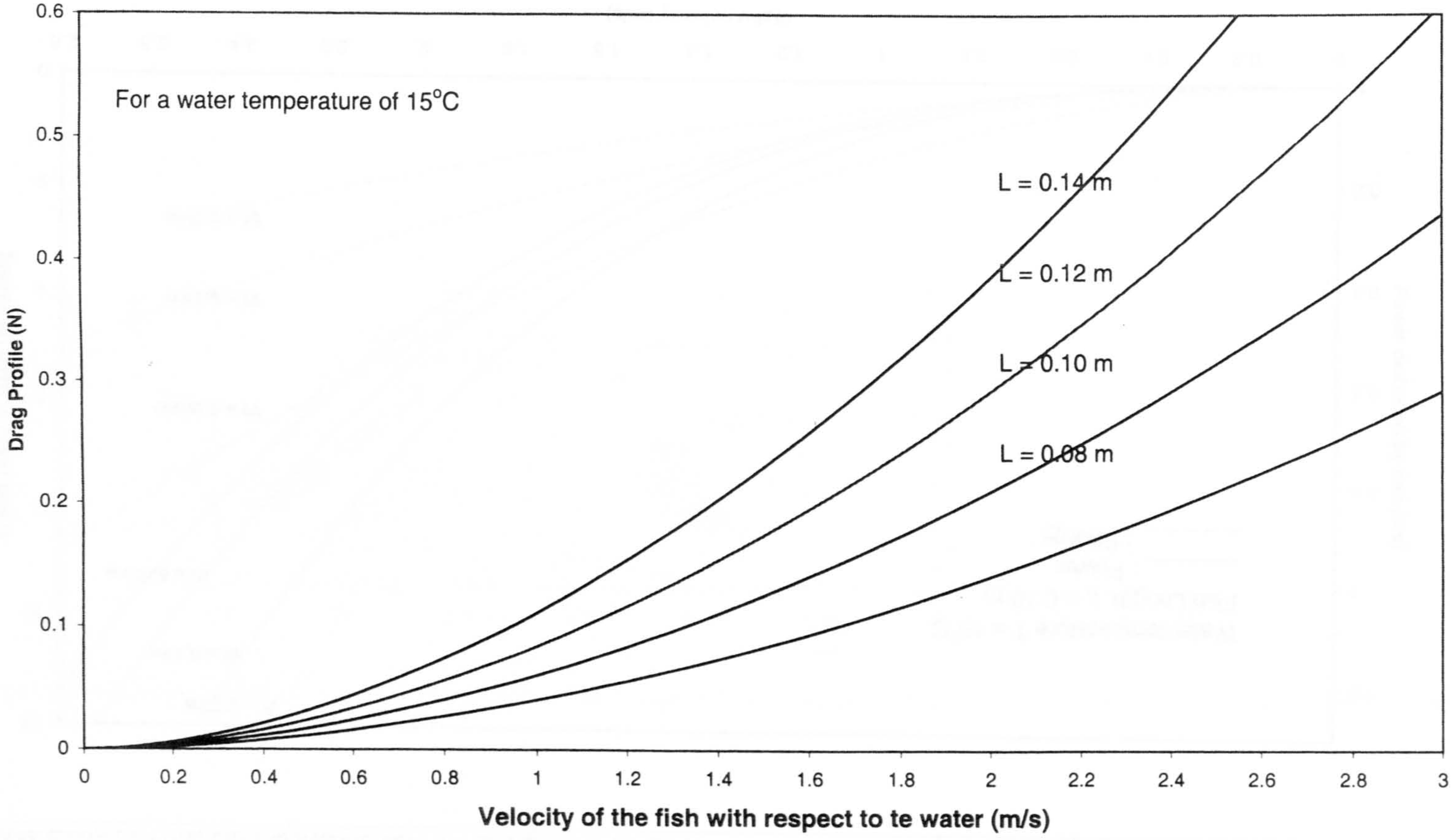

Figure 7-27:Drag forces acting on a swimming parr in function of its size and its swimming speed for a water temperature of 15°C

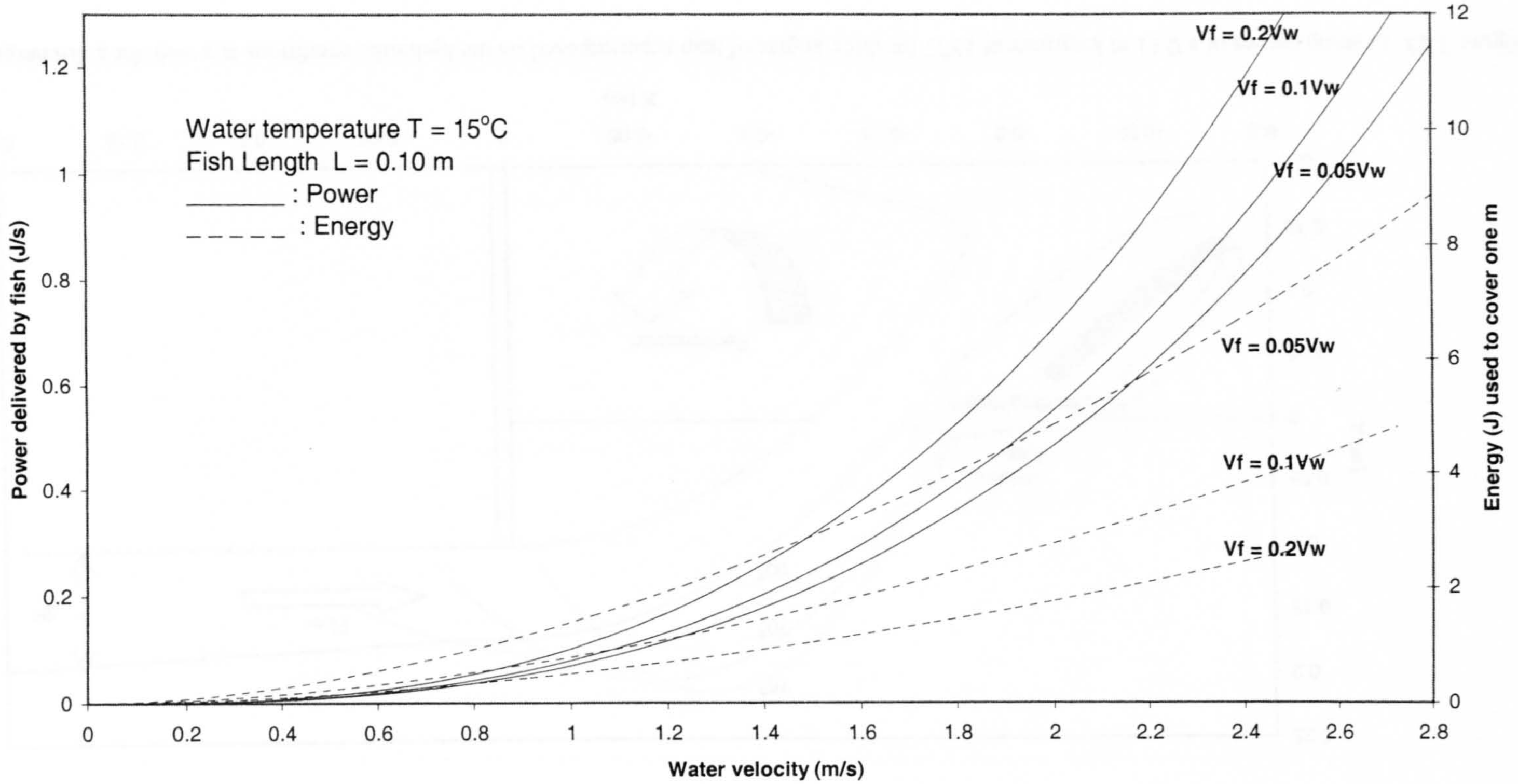

Figure 7-28: Power and Energy, a swimming parr need to provide from a hydrodynamic point of view if it swims at a ground speed Vf against a flow of velocity Vw.

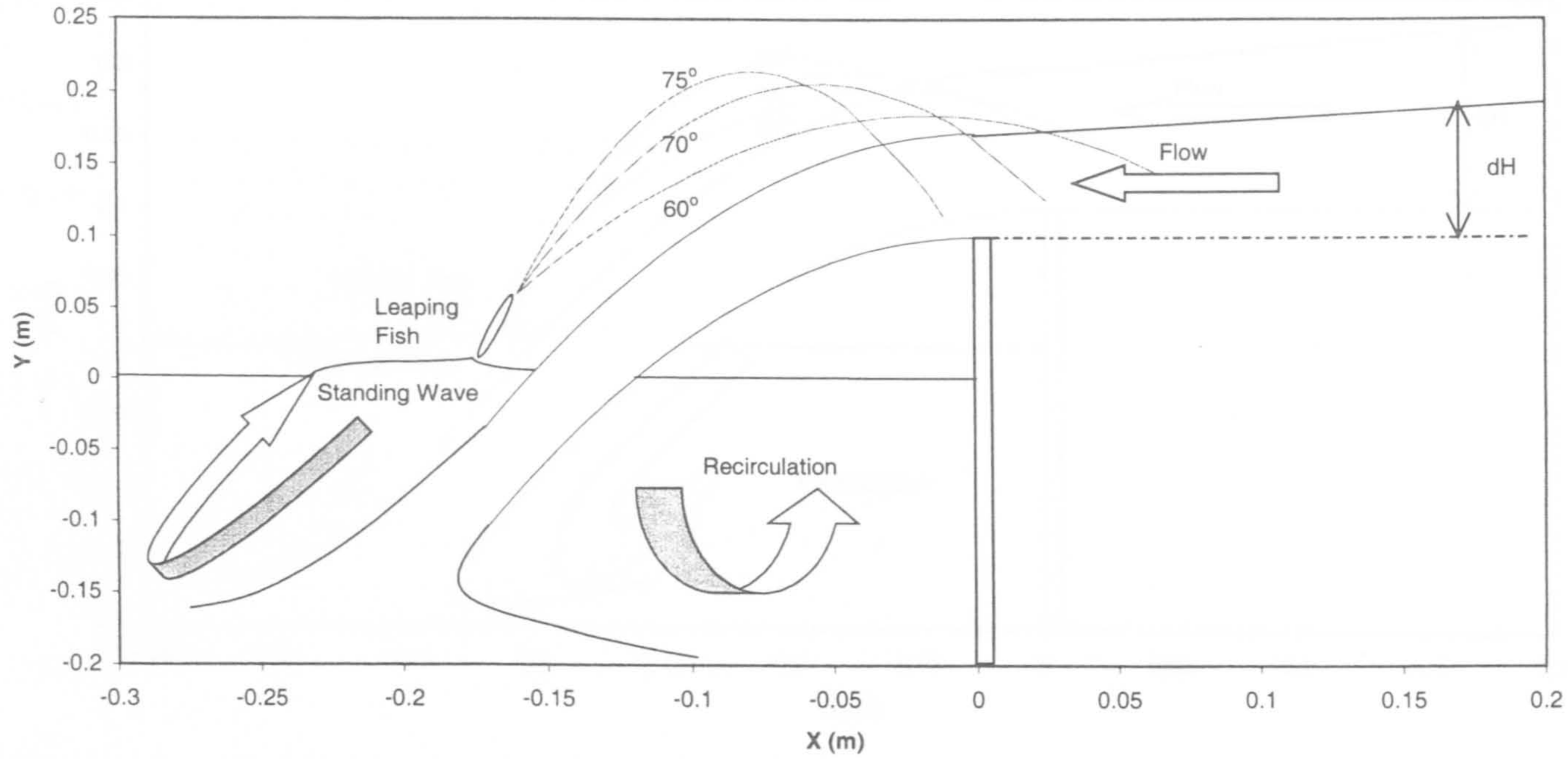

Figure 7-28: Leaping curves of a 0.11 m long parr at 15°C for three angles of leap superimposed on the hydraulic conditions at a weir for a discharge of 0.012 m3/s

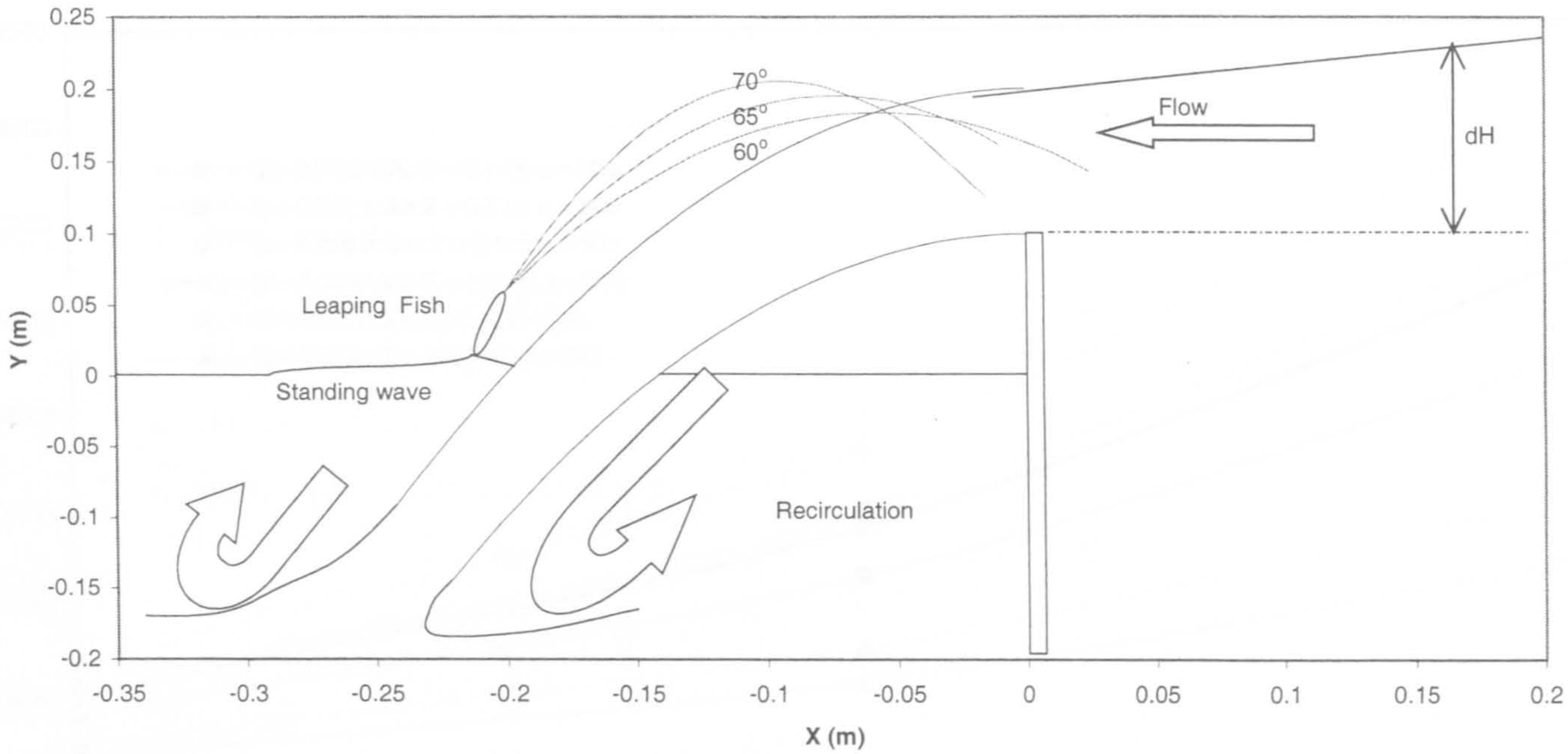

Figure 7-29: Leaping curves of a 0.11 m long parr at 15°C for three angles of leap superimposed on the hydraulic conditions at a weir for a discharge of 0.02 m3/s.

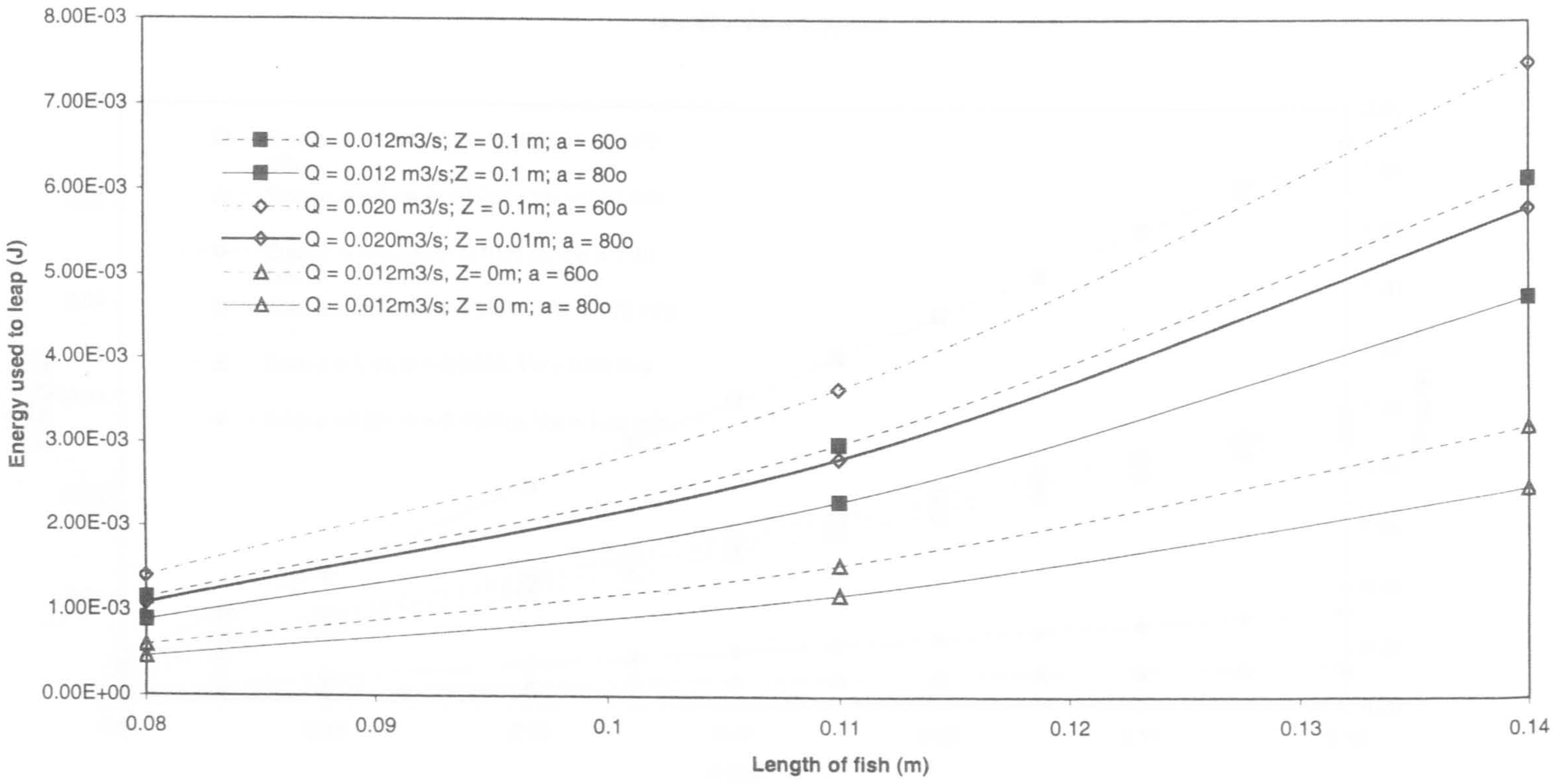

Figure 7-30: Energy used to leap over a weir by a parr in function of its size, the angle of the leap (60 or 80°) and the hydraulic conditions: discharge Q and the height of the crest Z in relation to the water lever.

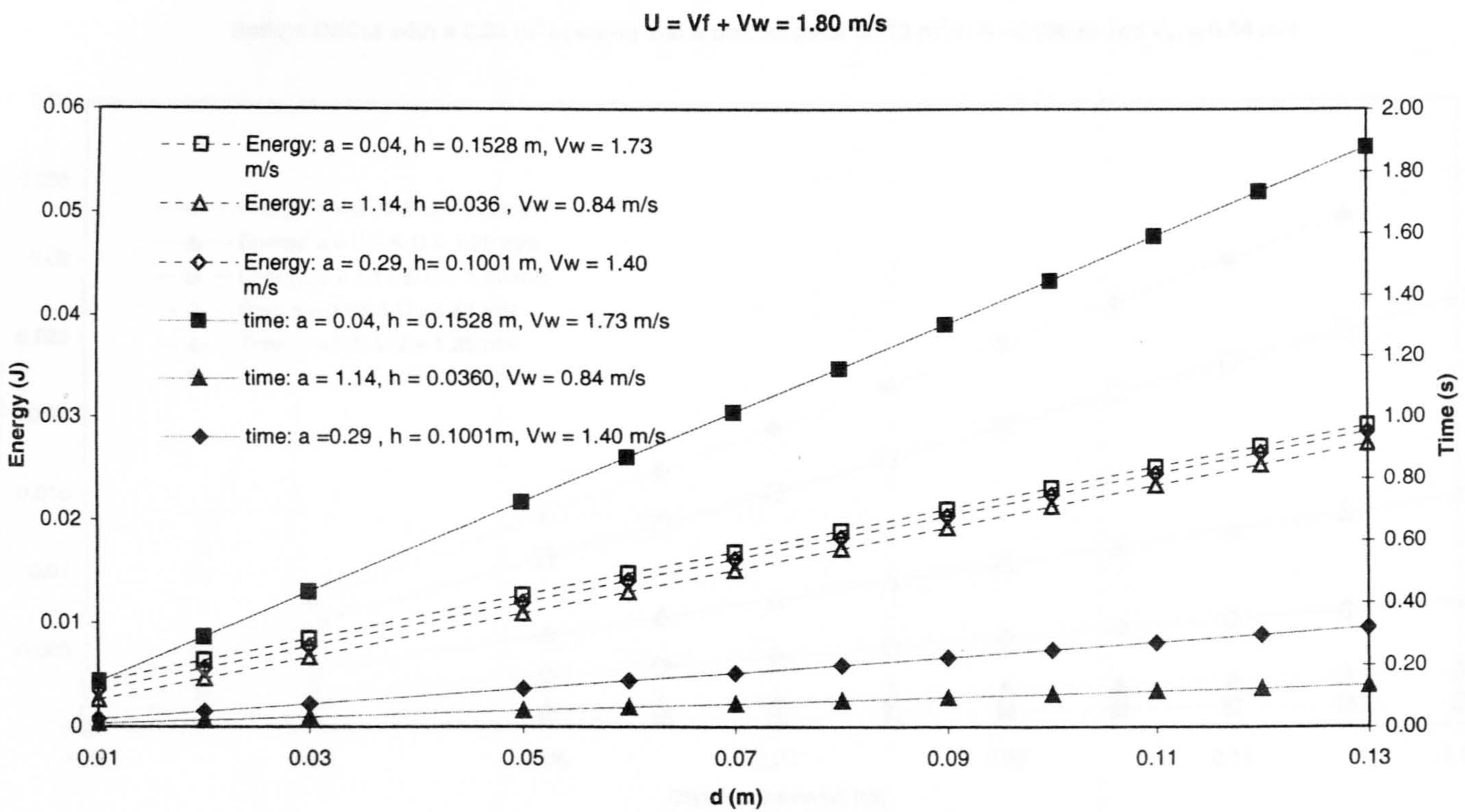

Figure 7-31: Energy and time needed by a parr swimming through a slot in relation the hydraulic conditions (h, Vw), its ground speed (αVw) and the distance covered.

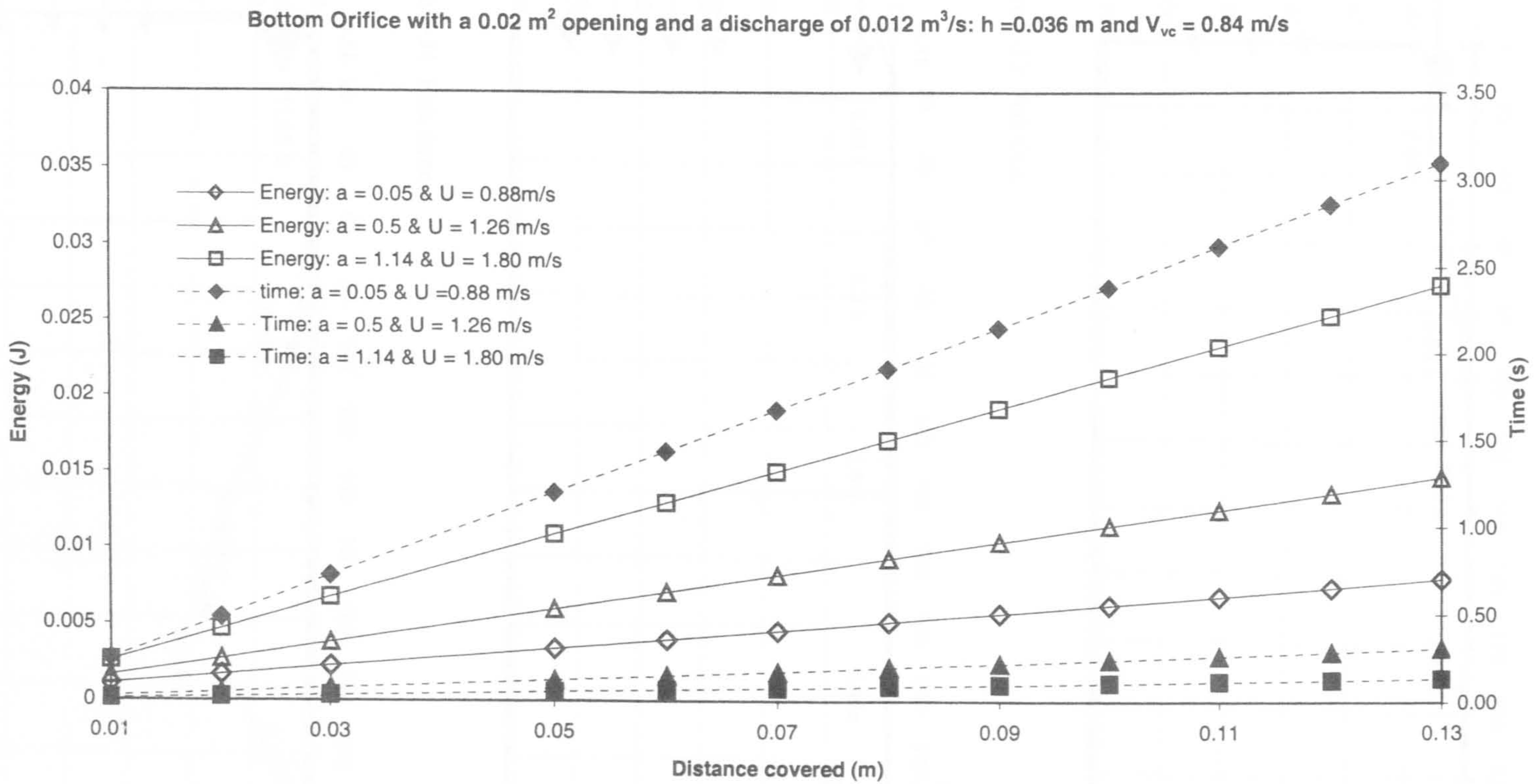

Figure 7-32: Energy and time needed by a parr swimming through a slot in relation to the strategic coefficient chosen.

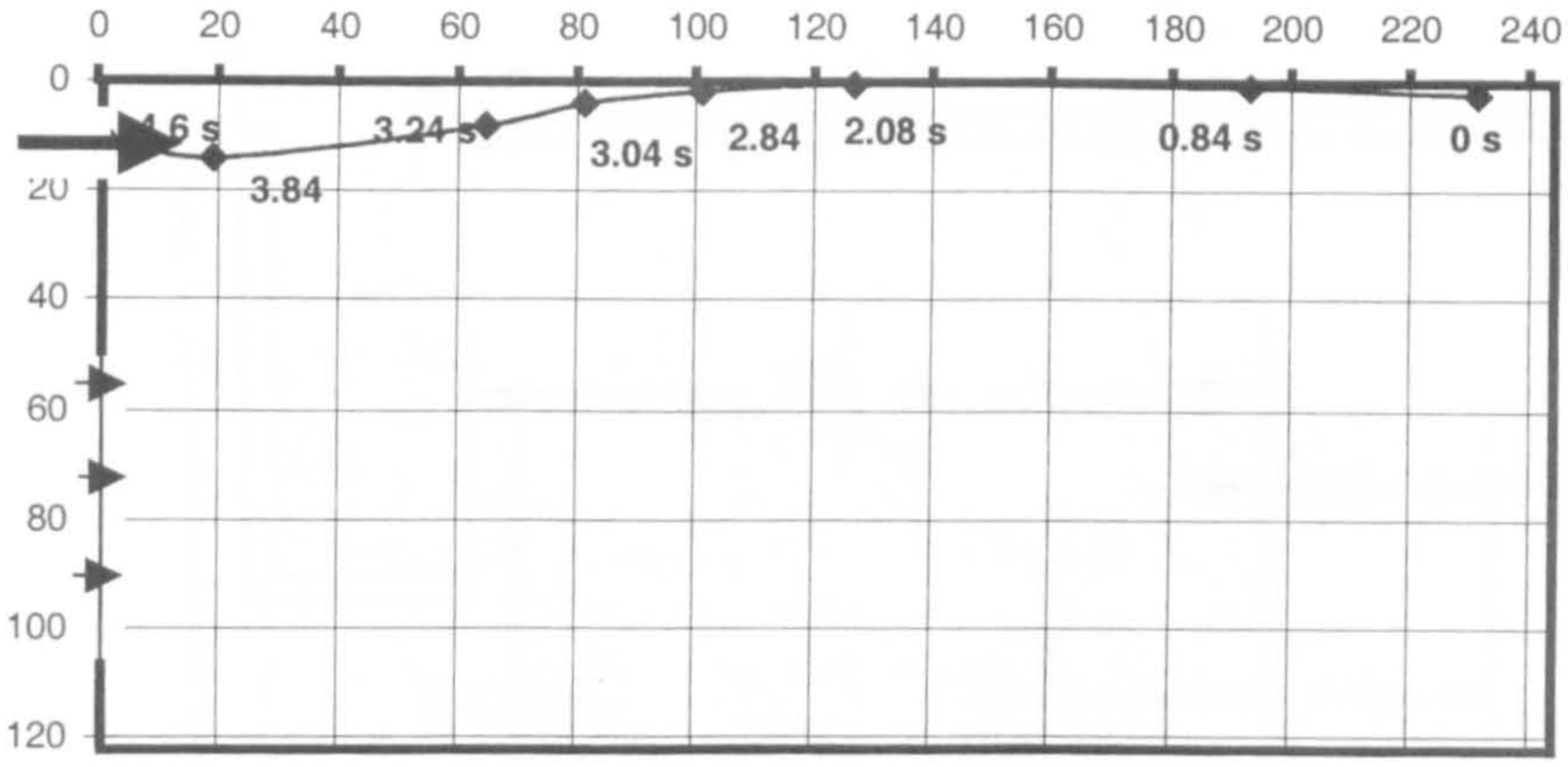

Figure 7-33: Fish One

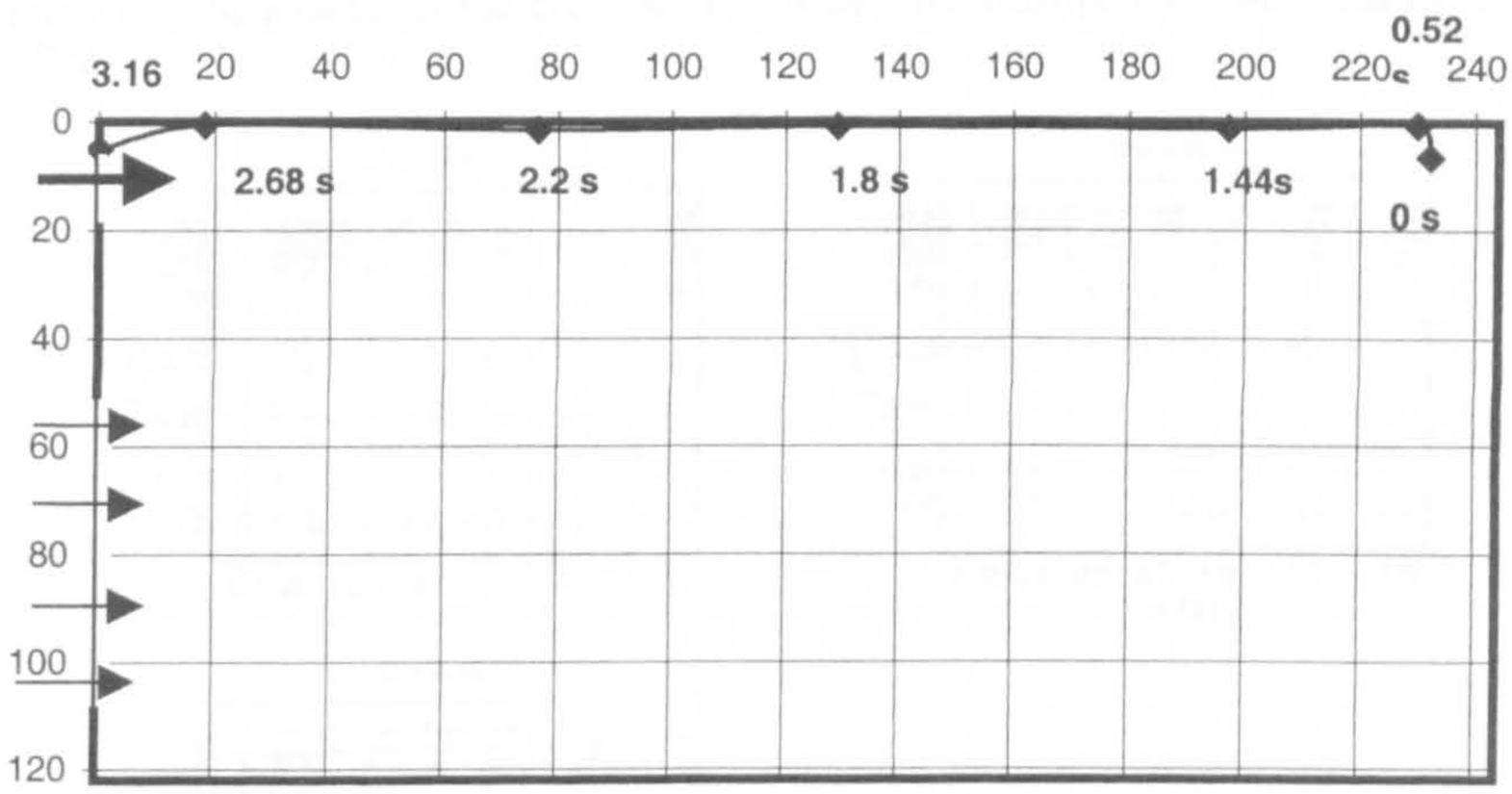

Figure 7-34: Fish three

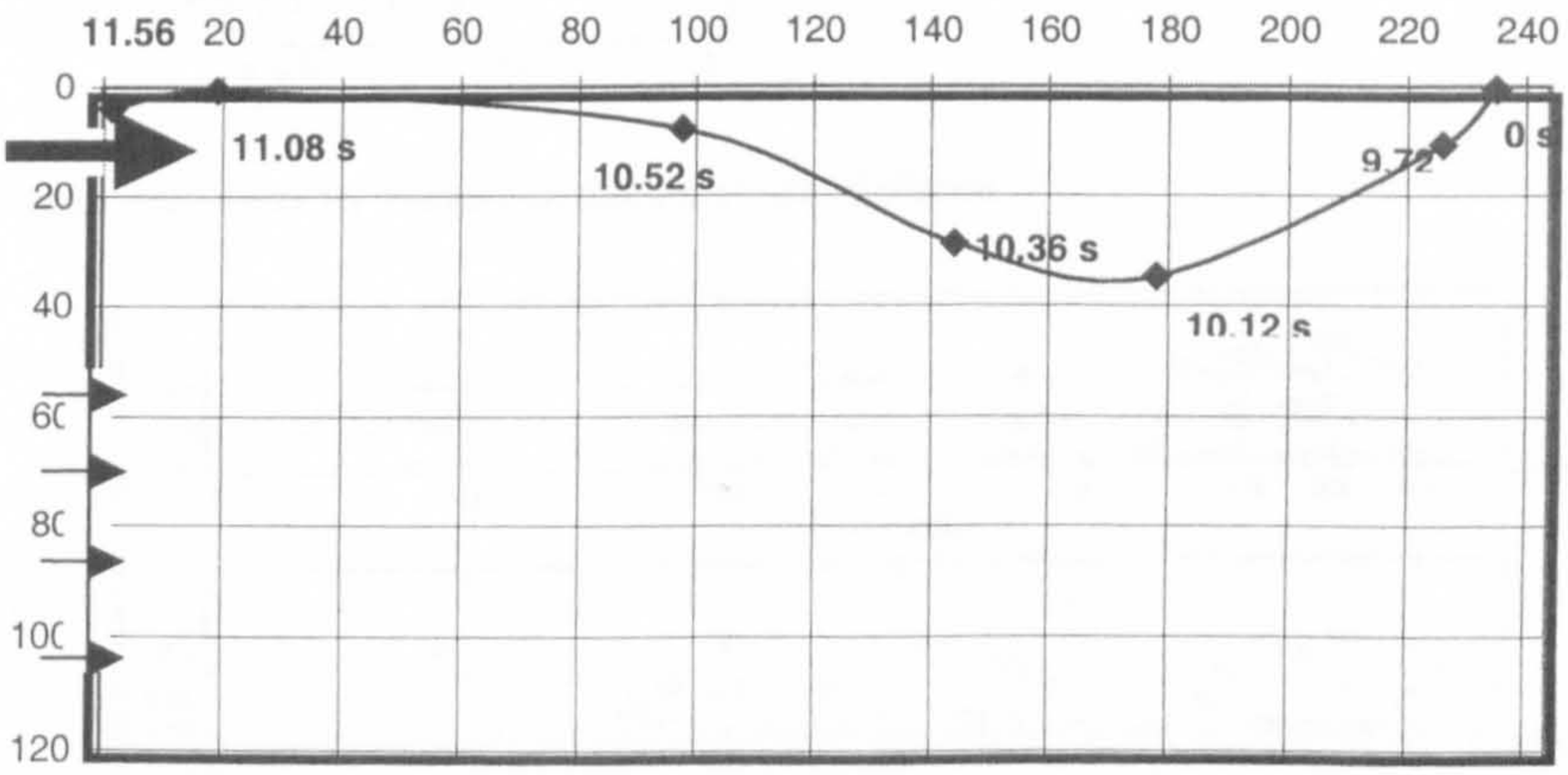

Figure 7-35: Fish six

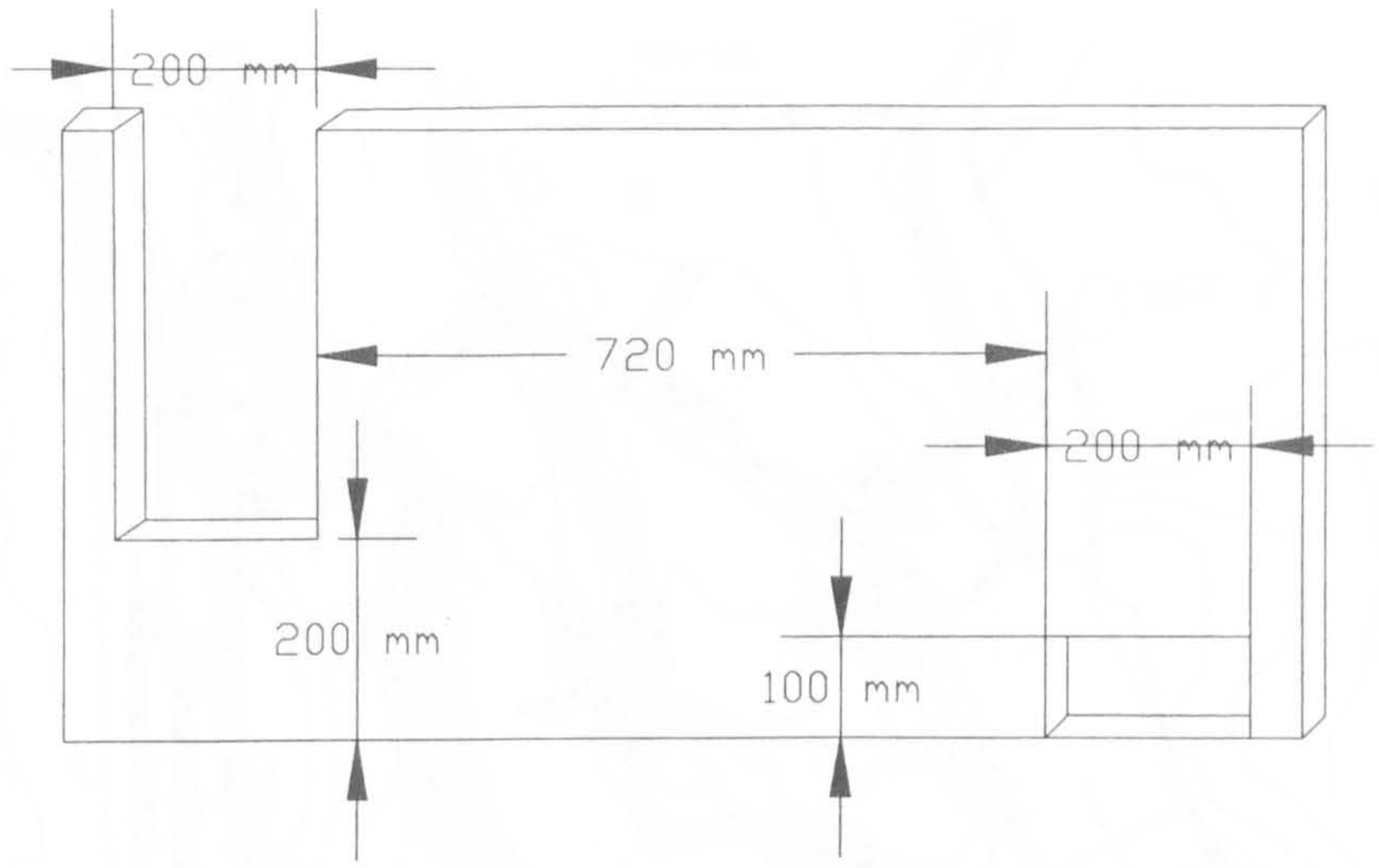

Figure 8-1: Schematic of the cross wall including the 0.20 m wide weir and the 0.10 by 0.20 m orifice.

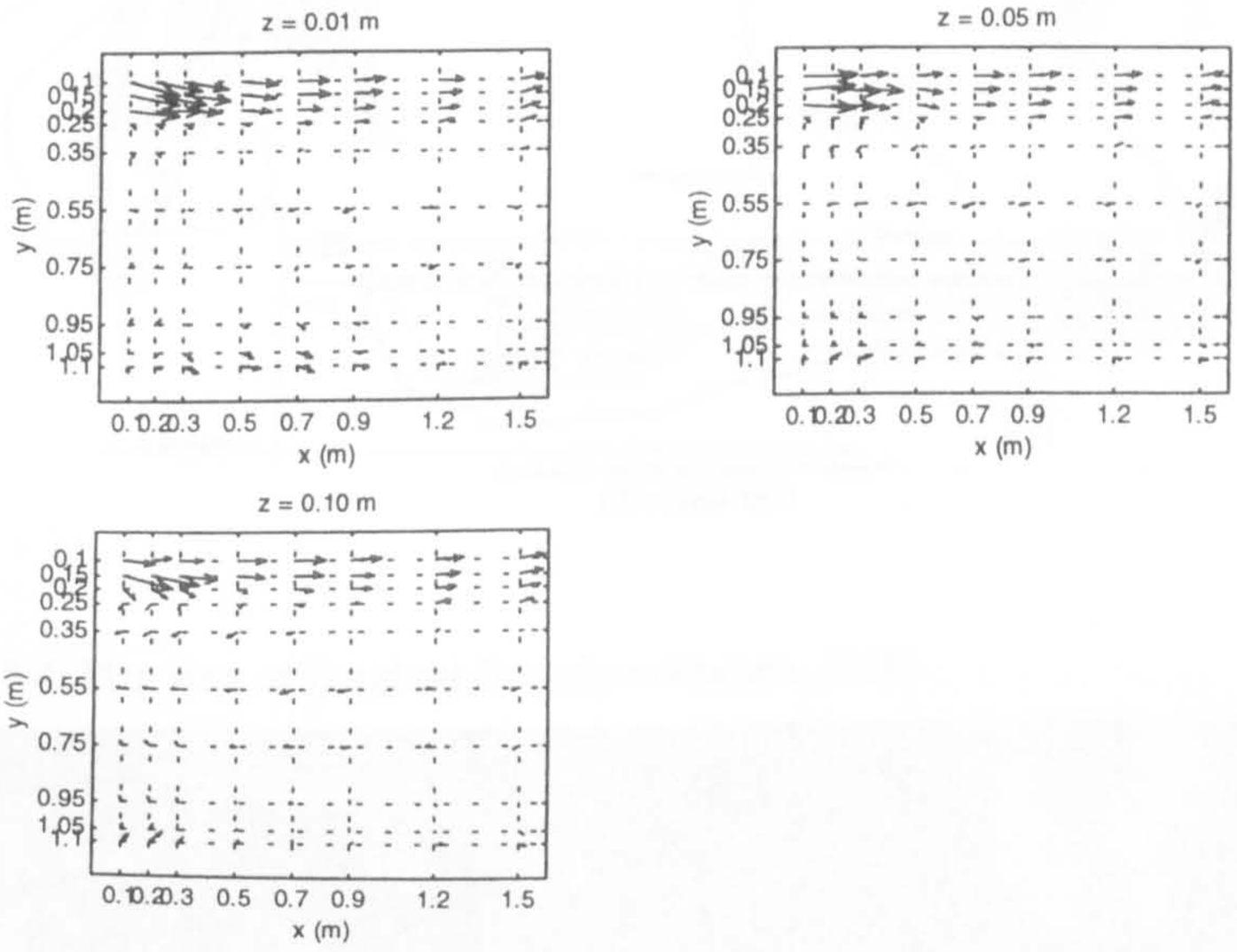

Figure 8-2: Velocity vectors in three horizontal planes

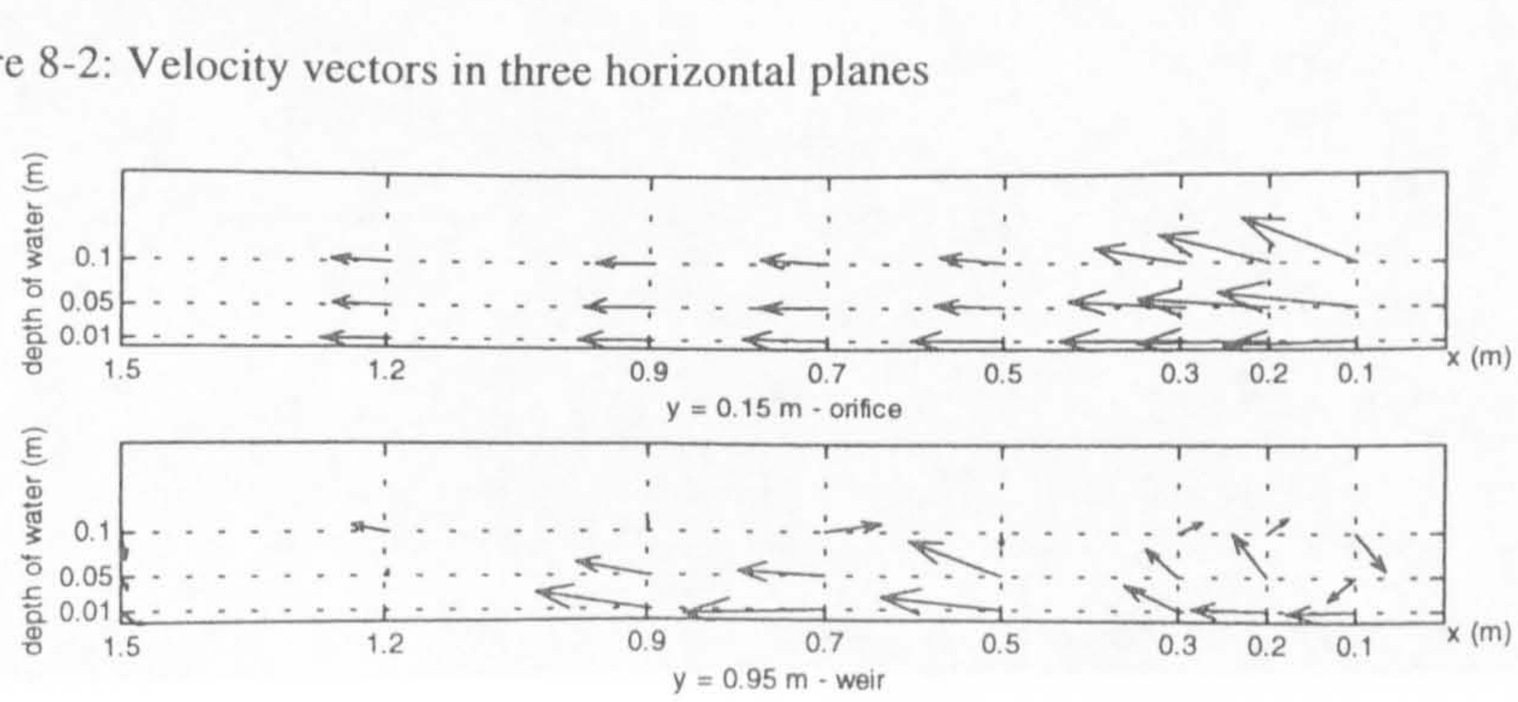

Figure 8-3: Vertical slices in the vicinity of the orifice and the weir

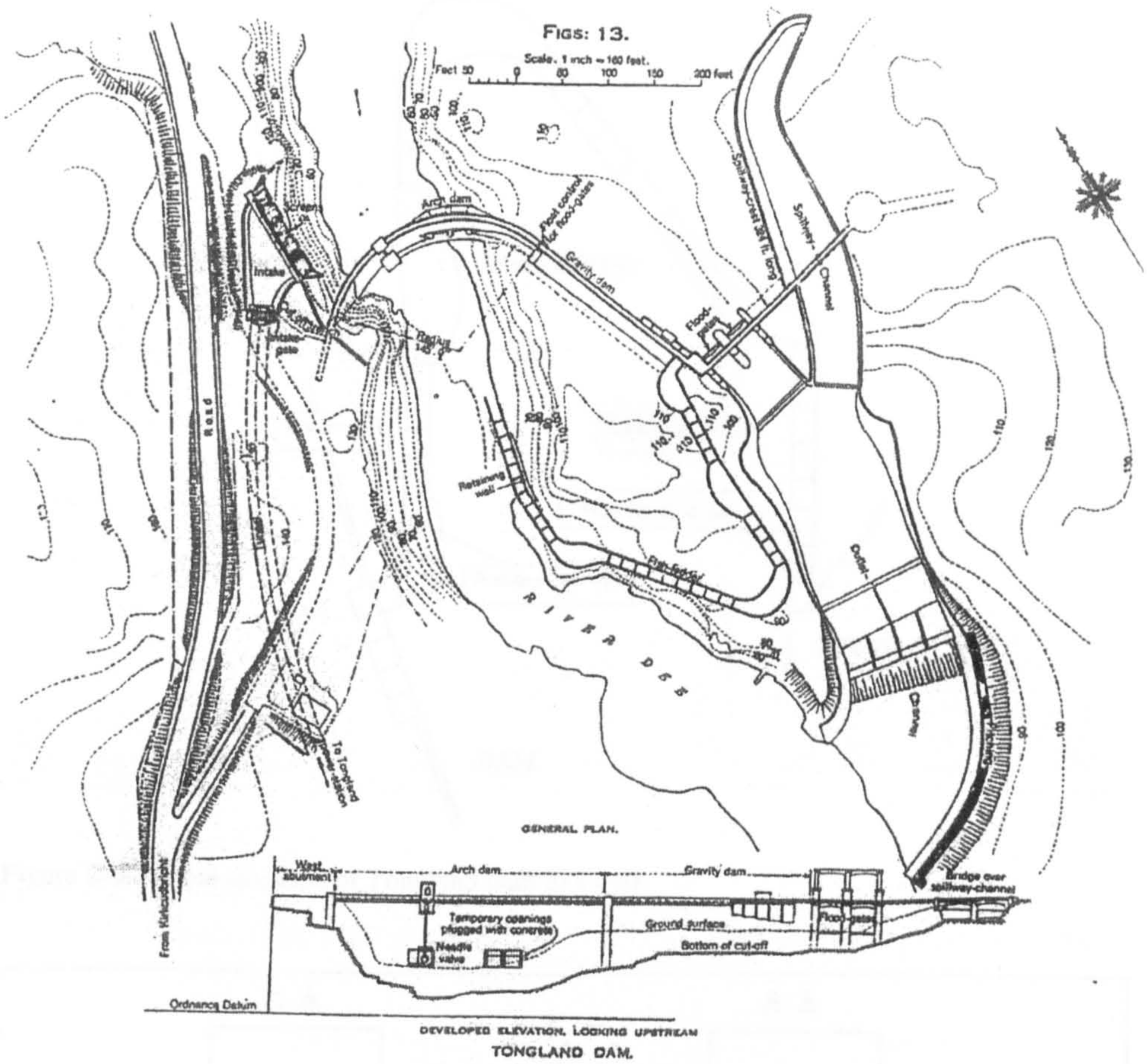

Figure 8-4: Plan view of Tongland Dam (from Hudson, 1938)

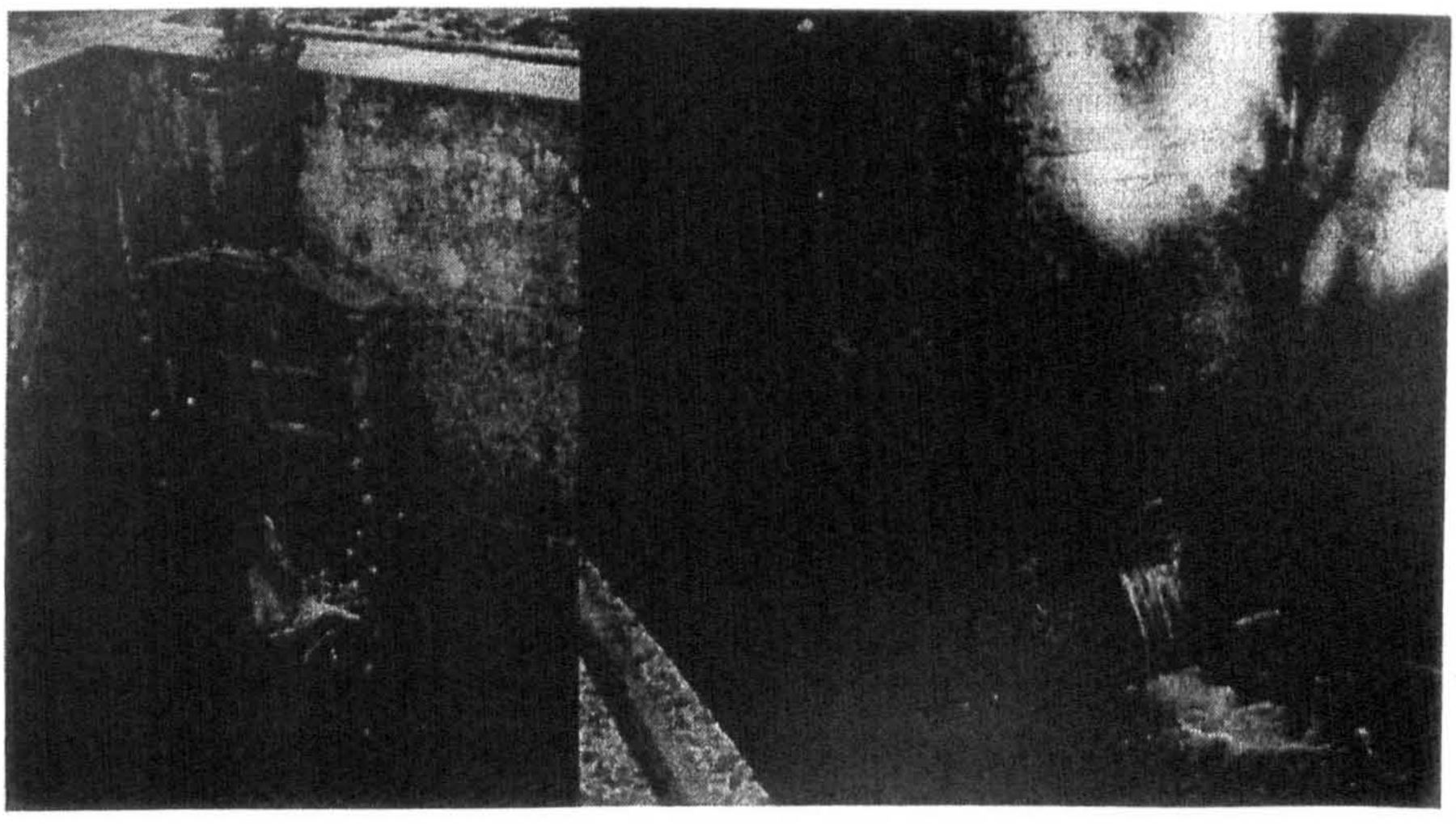

Figure 8-5: Photo of the submerged orifice design with the closing system

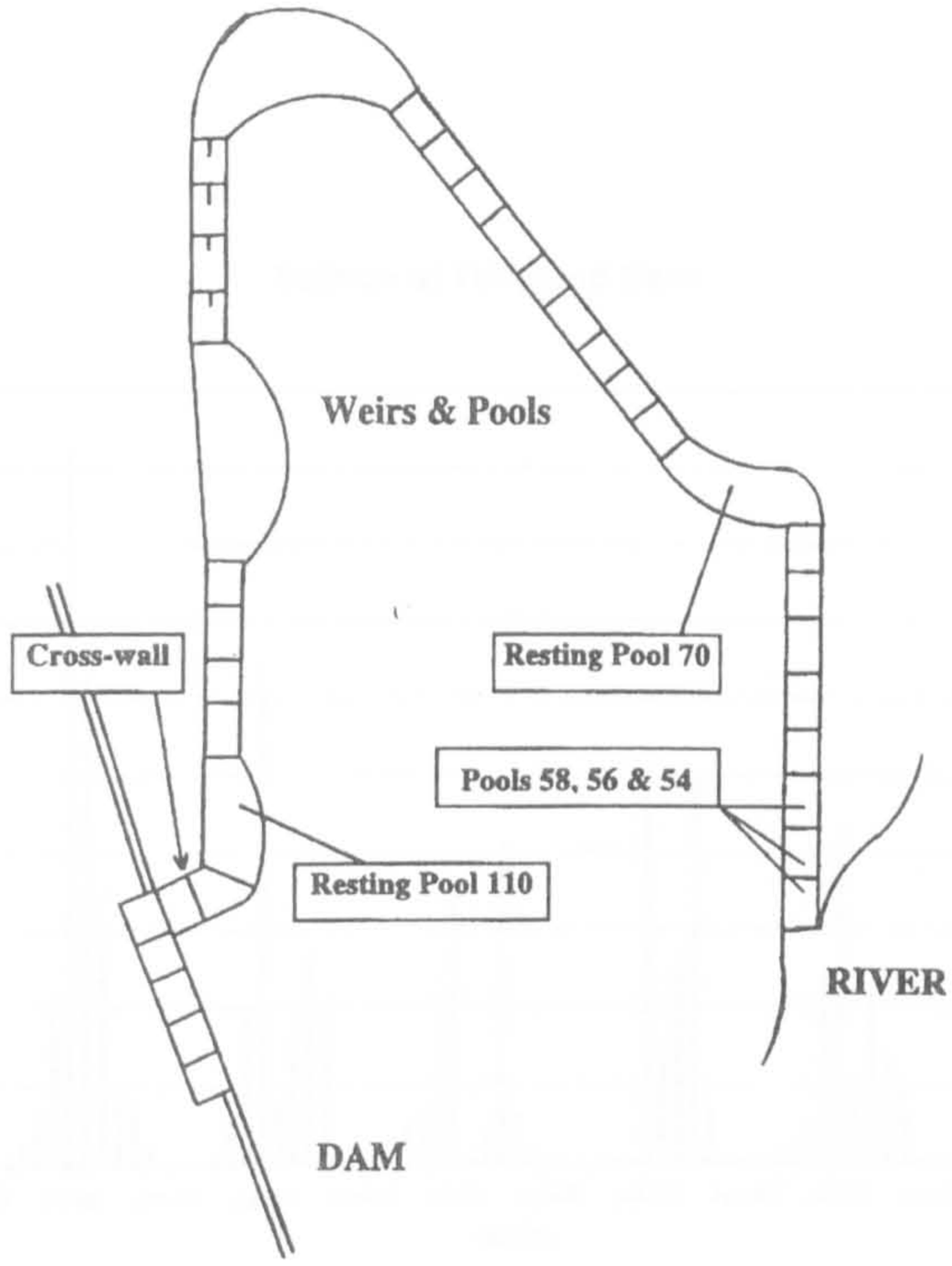

Figure 8-6: Actual situation of Tongland dam fish pass

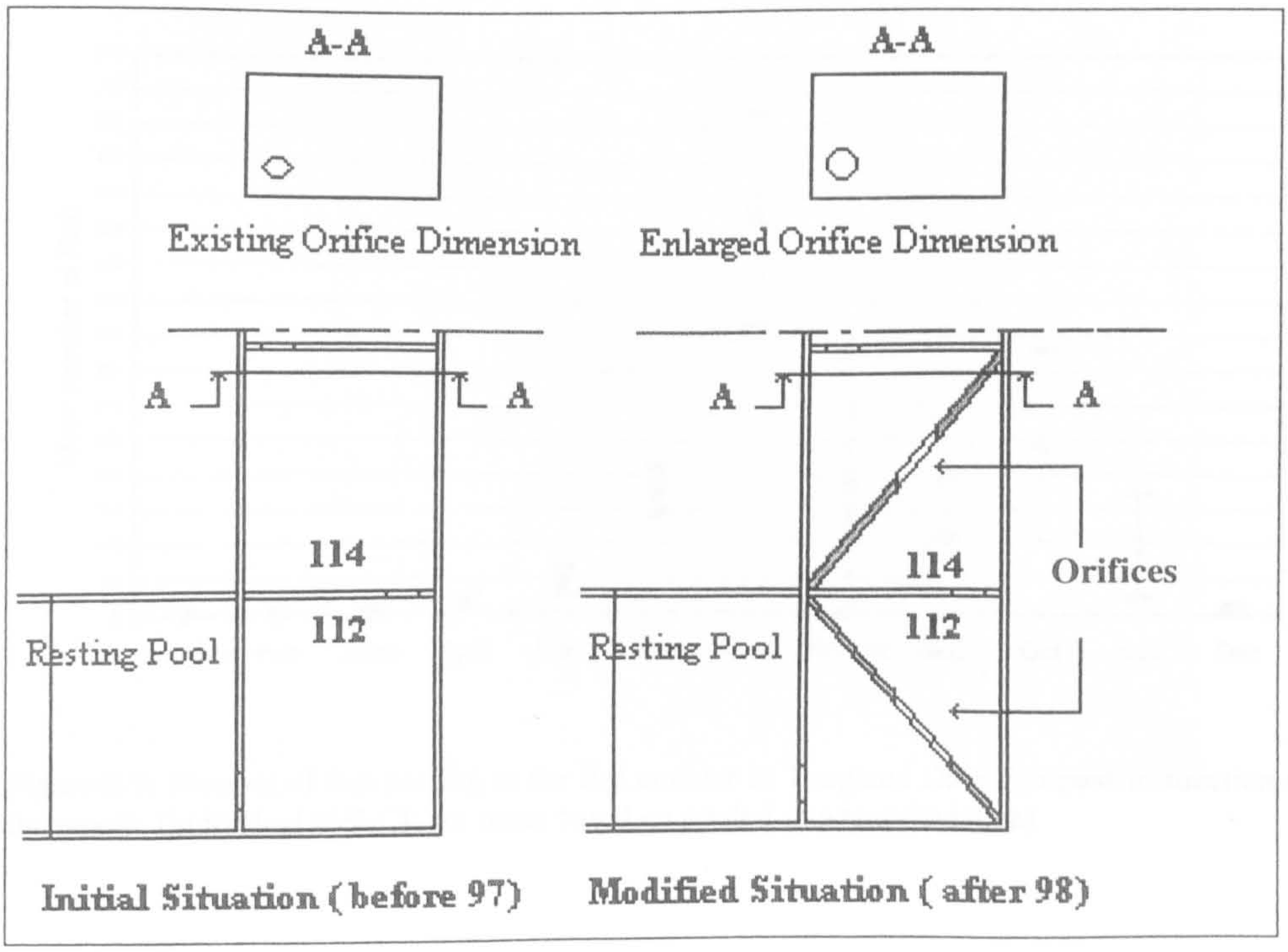

Figure 8-7:Situation at the upper pools before and after alteration in winter 98

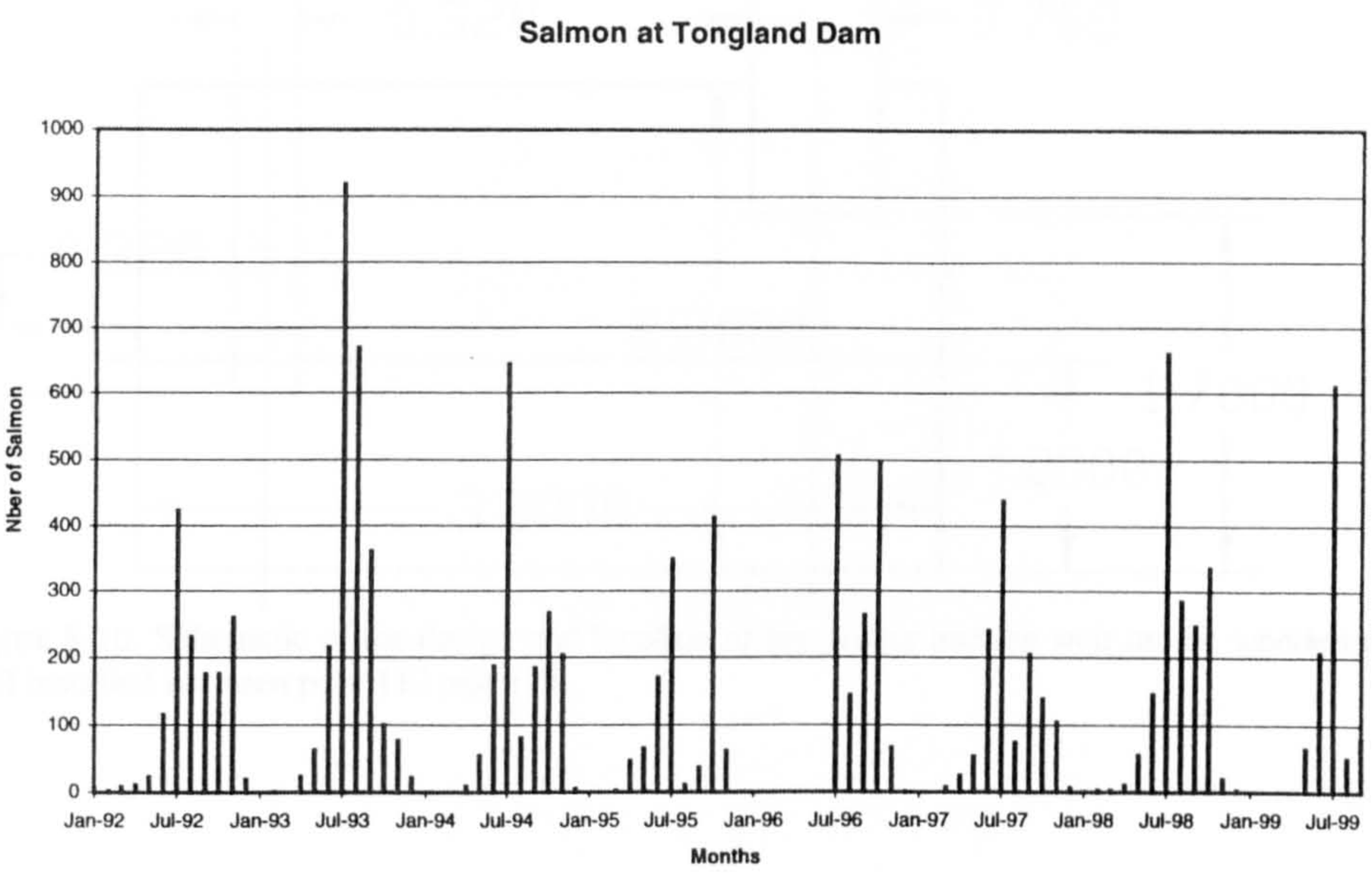

Figure 8-8: Total number of parr passing through the fish counter per month for Jan 92 to Sept 99

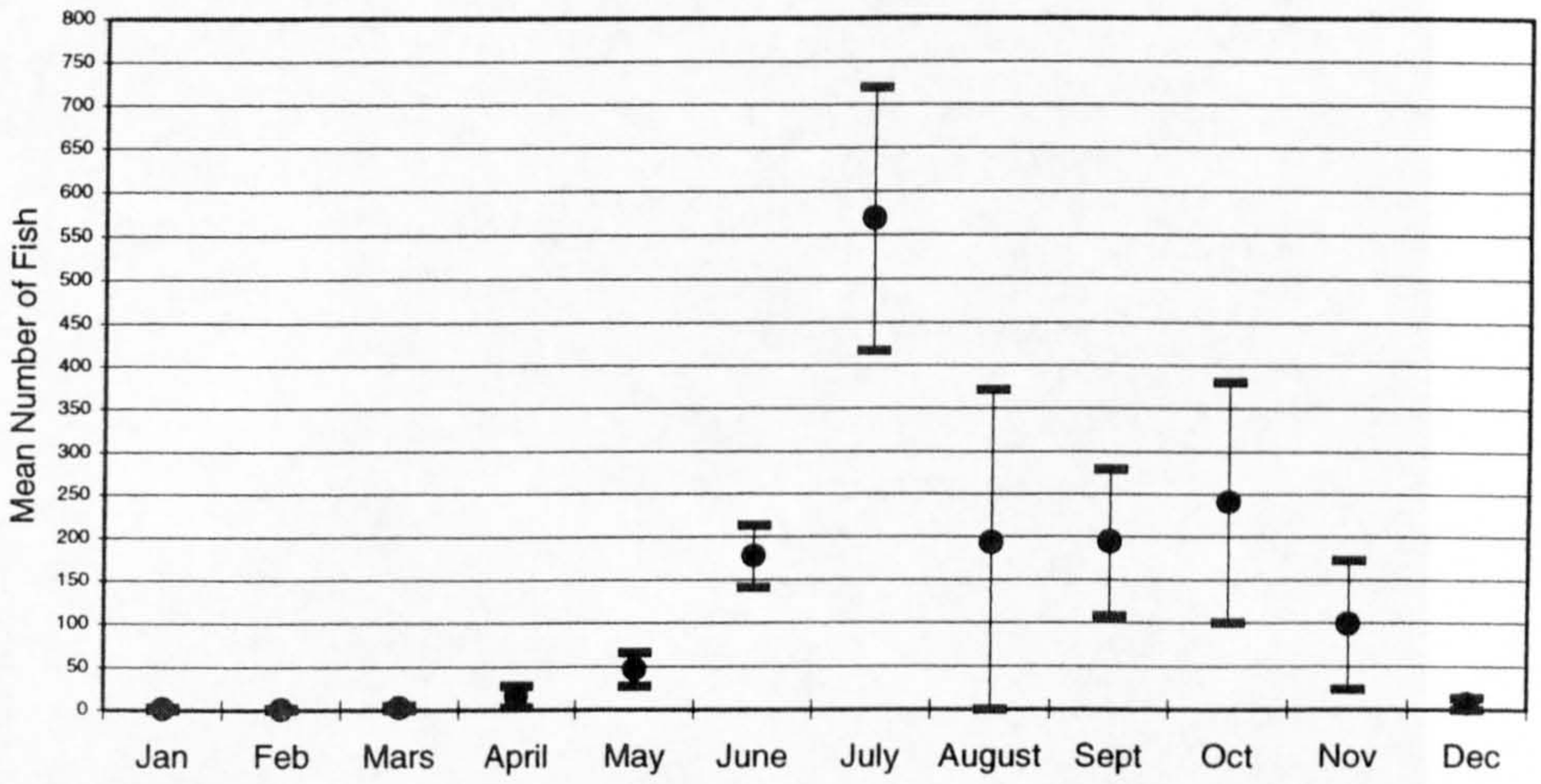

Figure 8-9: Number of fish passing at the fish counter at Tongland Dam fish pass in function of the month. (Individual 95% CIs for mean based on pooled standard deviation)

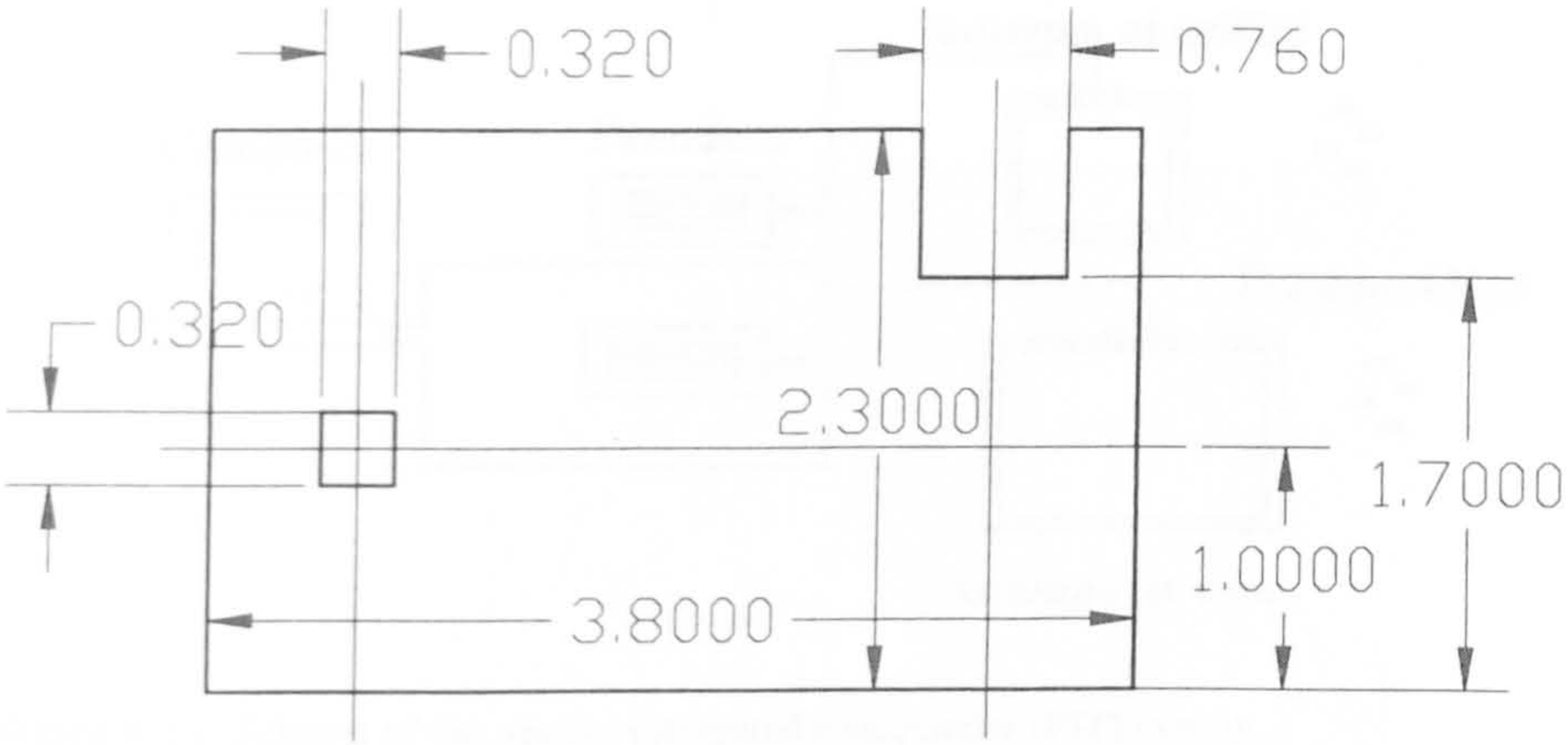

Figure 8-10: Schematic of the design and location of the orifice and the weir on the wooden cross wall installed between pool 112 and 113.

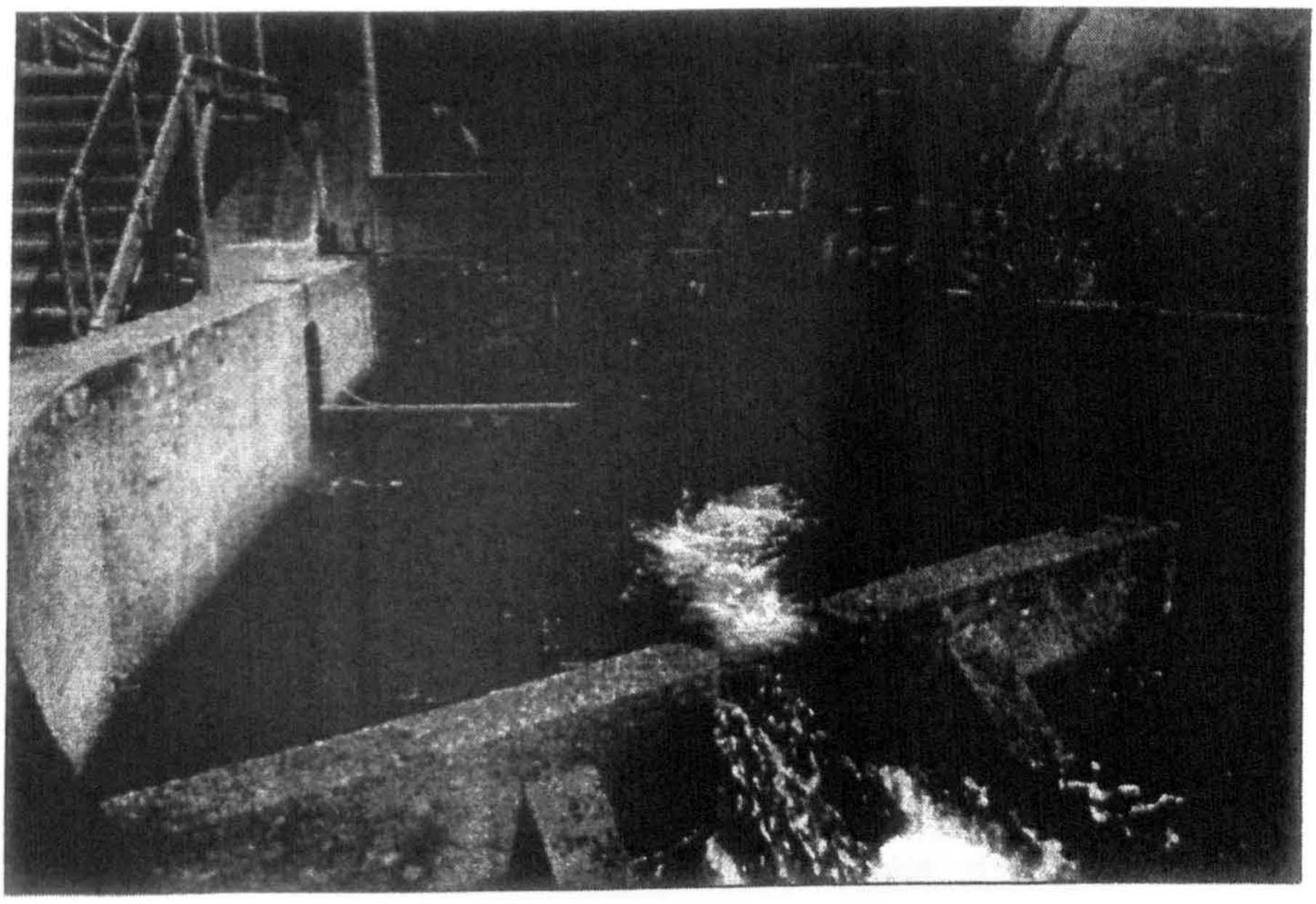

Figure 8-11: Location of the comparison weir/orifice

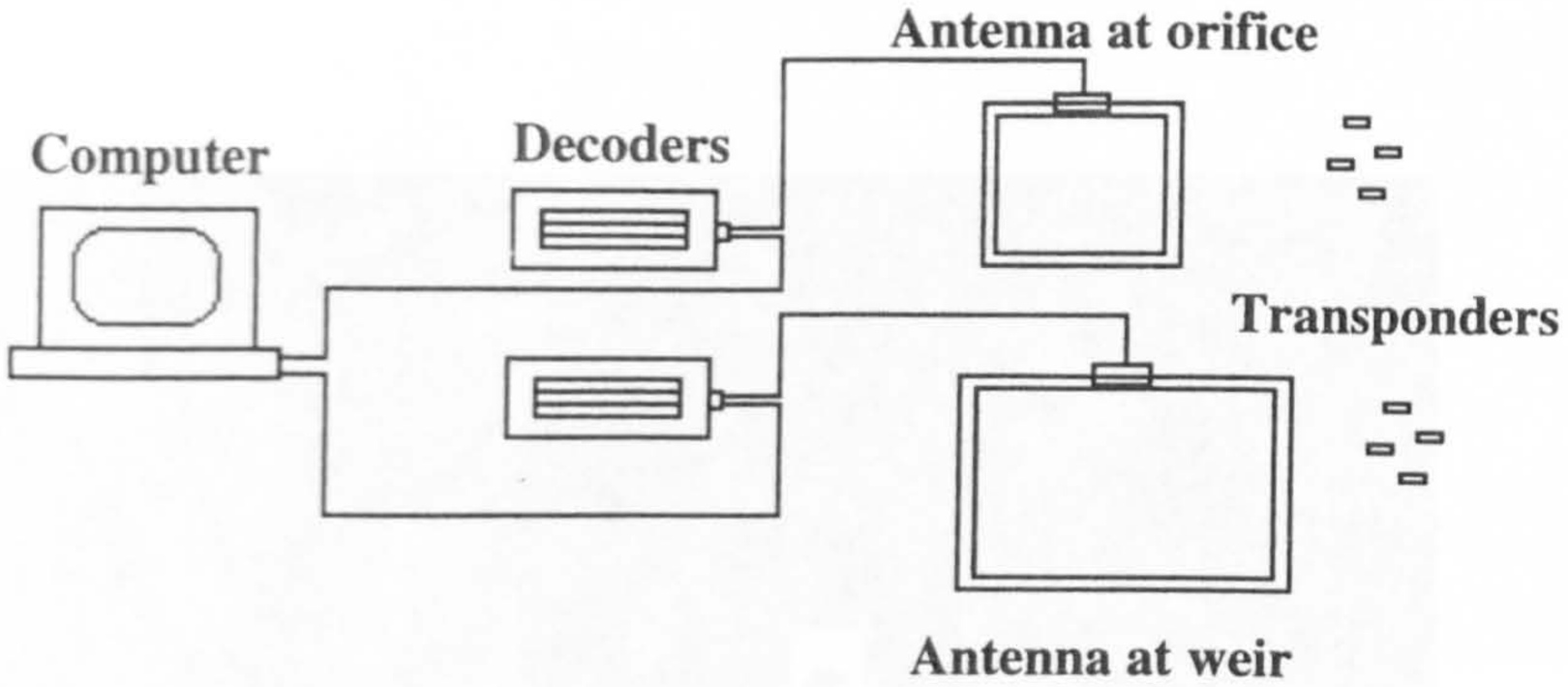

Figure 8- 12: Schema of the passive integrated transponder (PIT) system

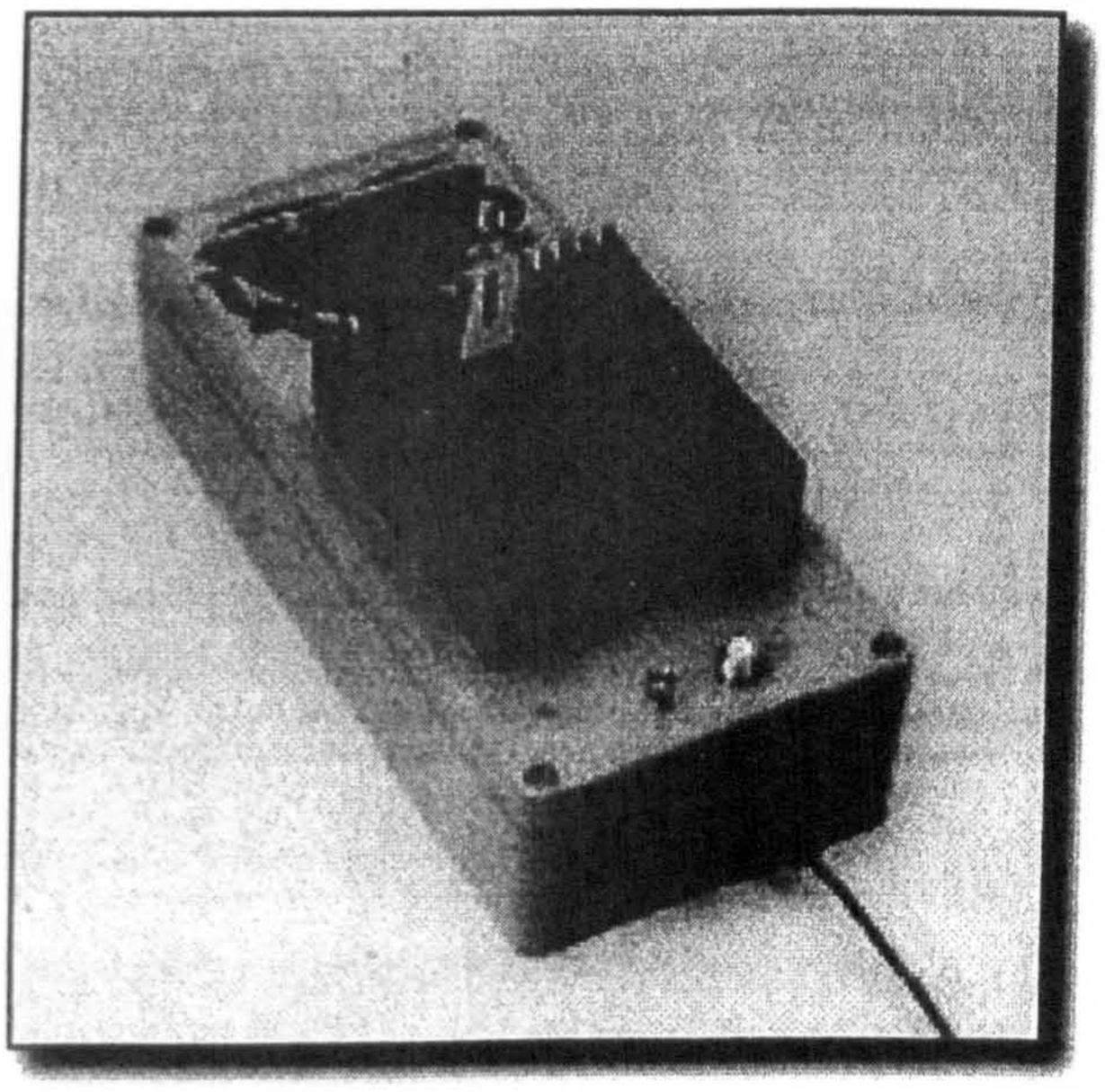

Figure 8- 13: HP SINGLE POINT DECODER: Part No. 81-01-03-01-000

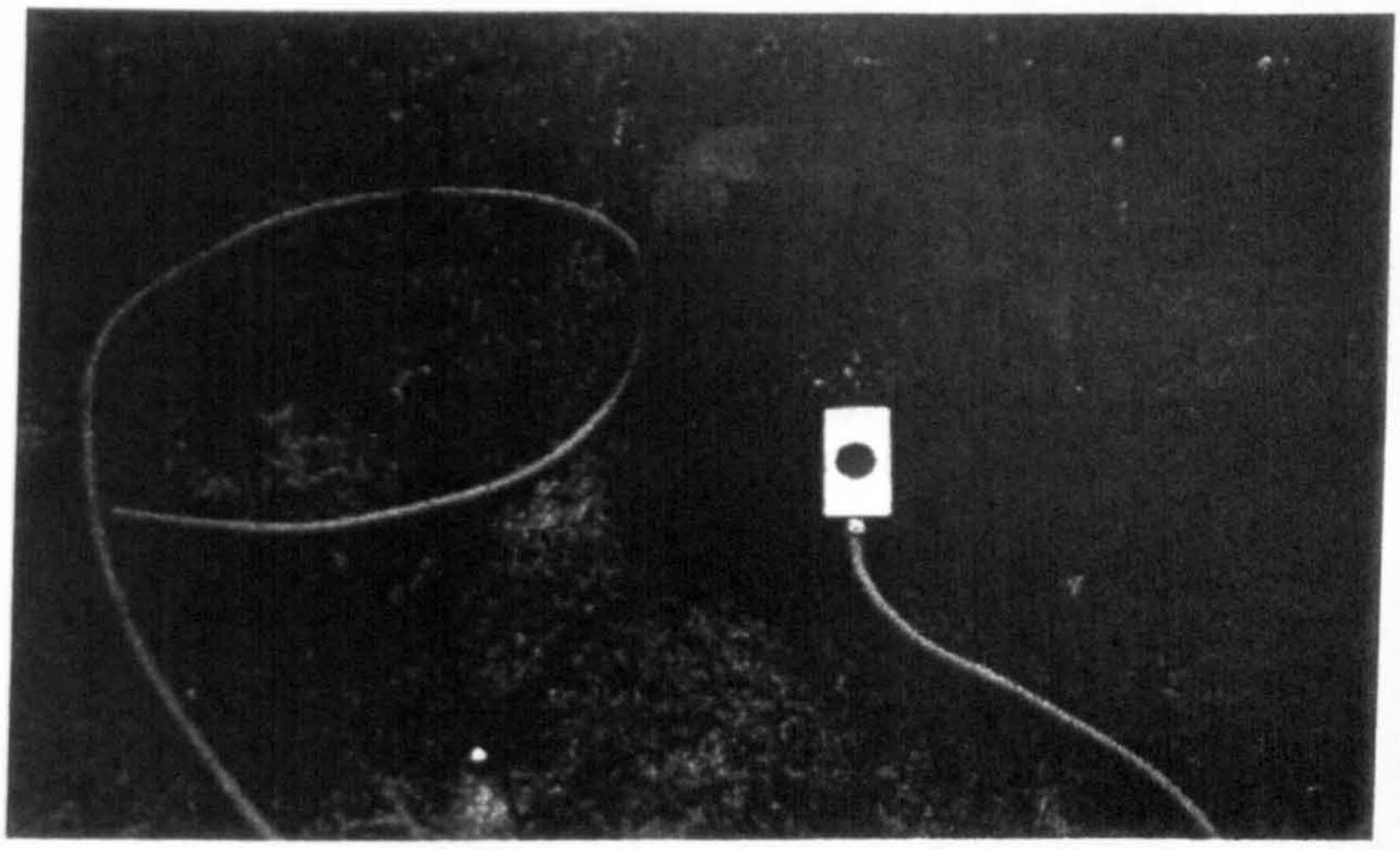

Figure 8-14: Square tube antenna 320 x 320 mm for the orifice

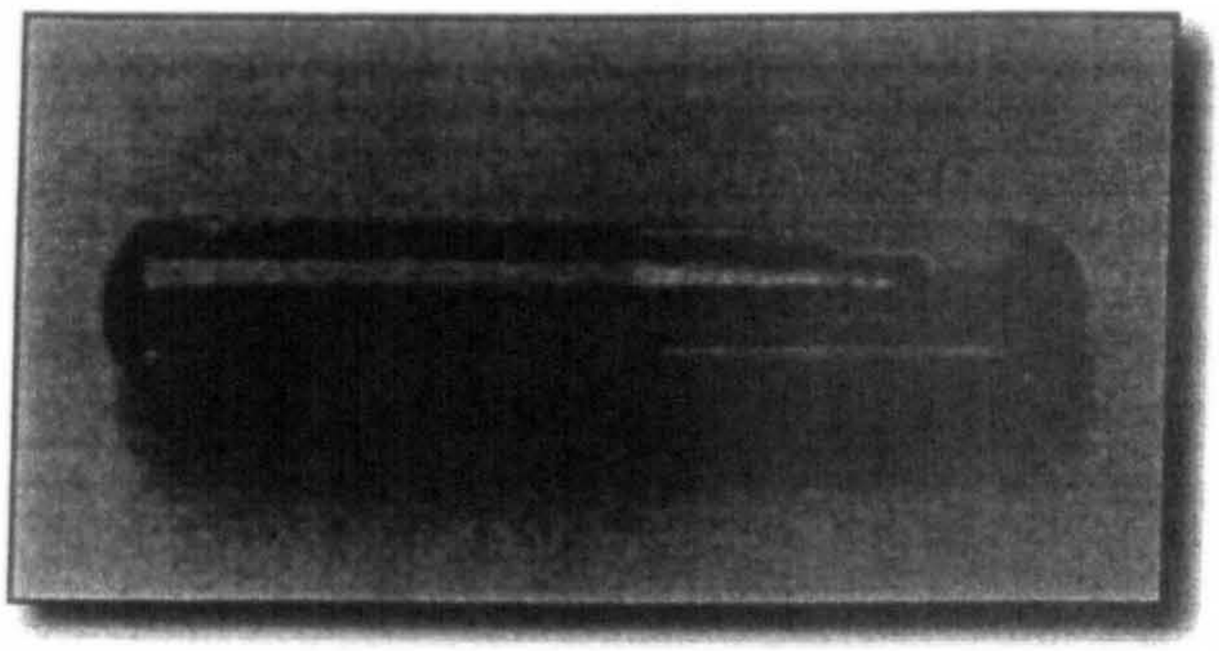

Figure 8- 15: Glass Transponder (12mm(L) x 2.12mm(D))

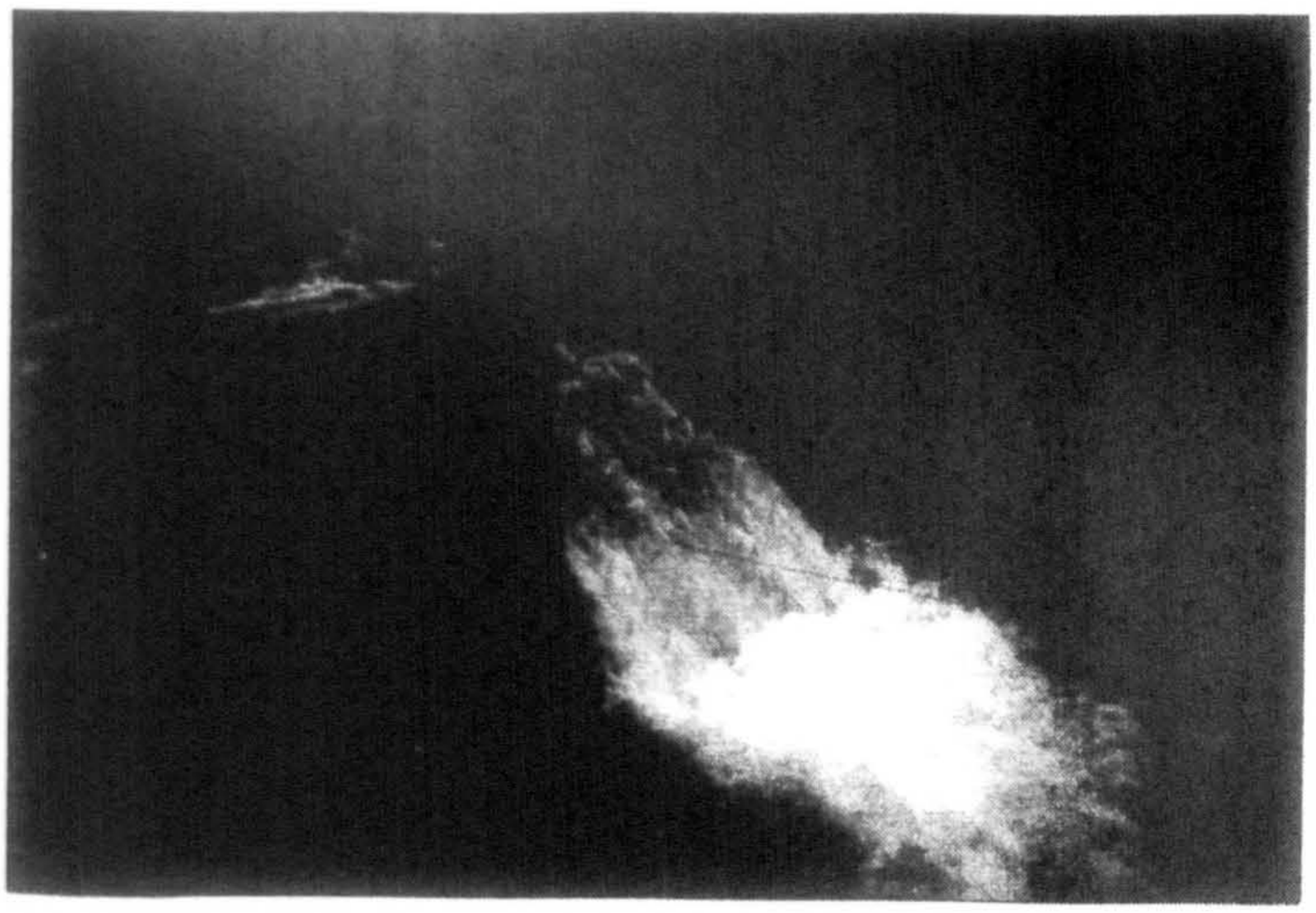

Figure 8-16: Trap

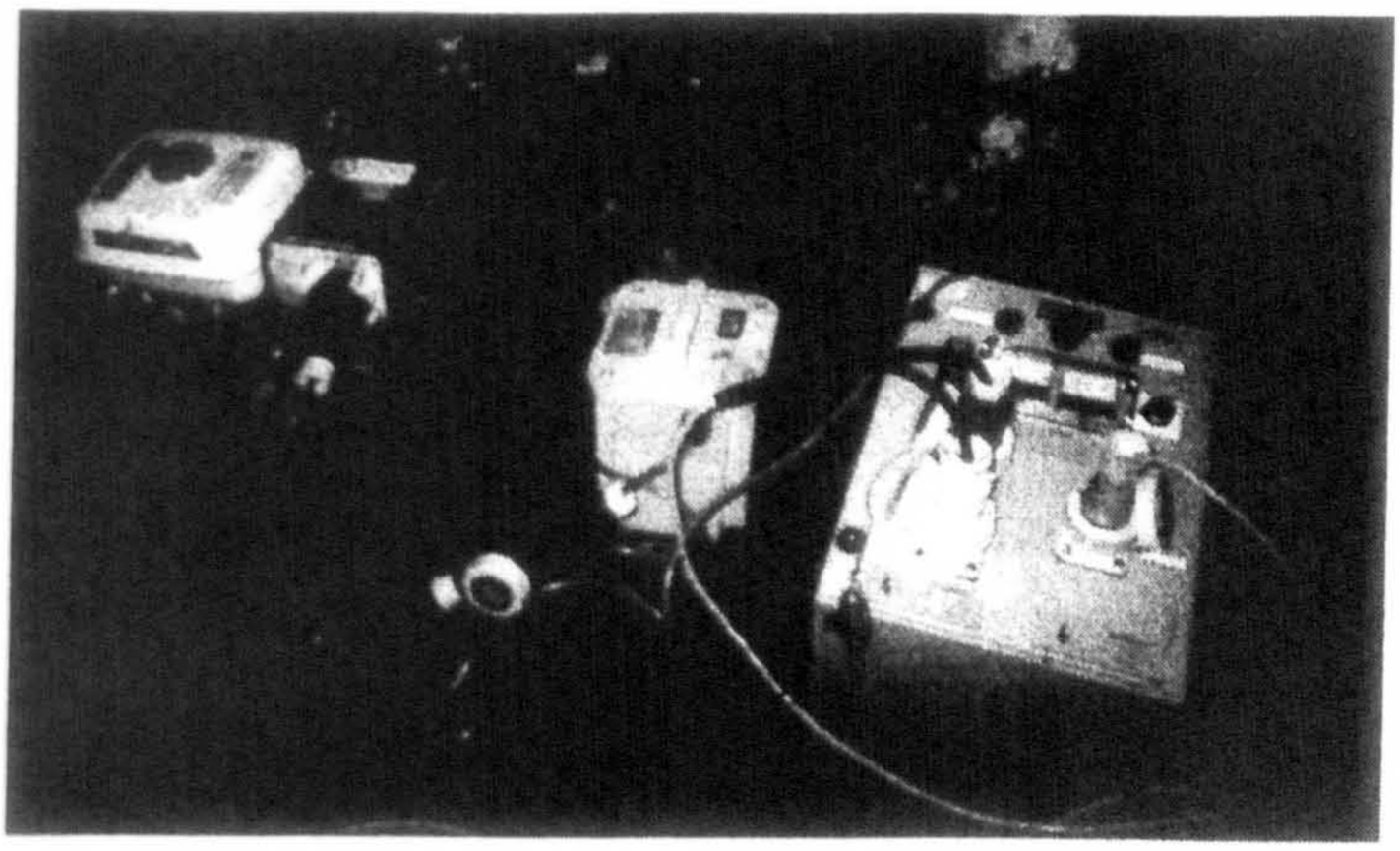

Figure 8-17: Electric fishing equipment (generator, control box and transformer).

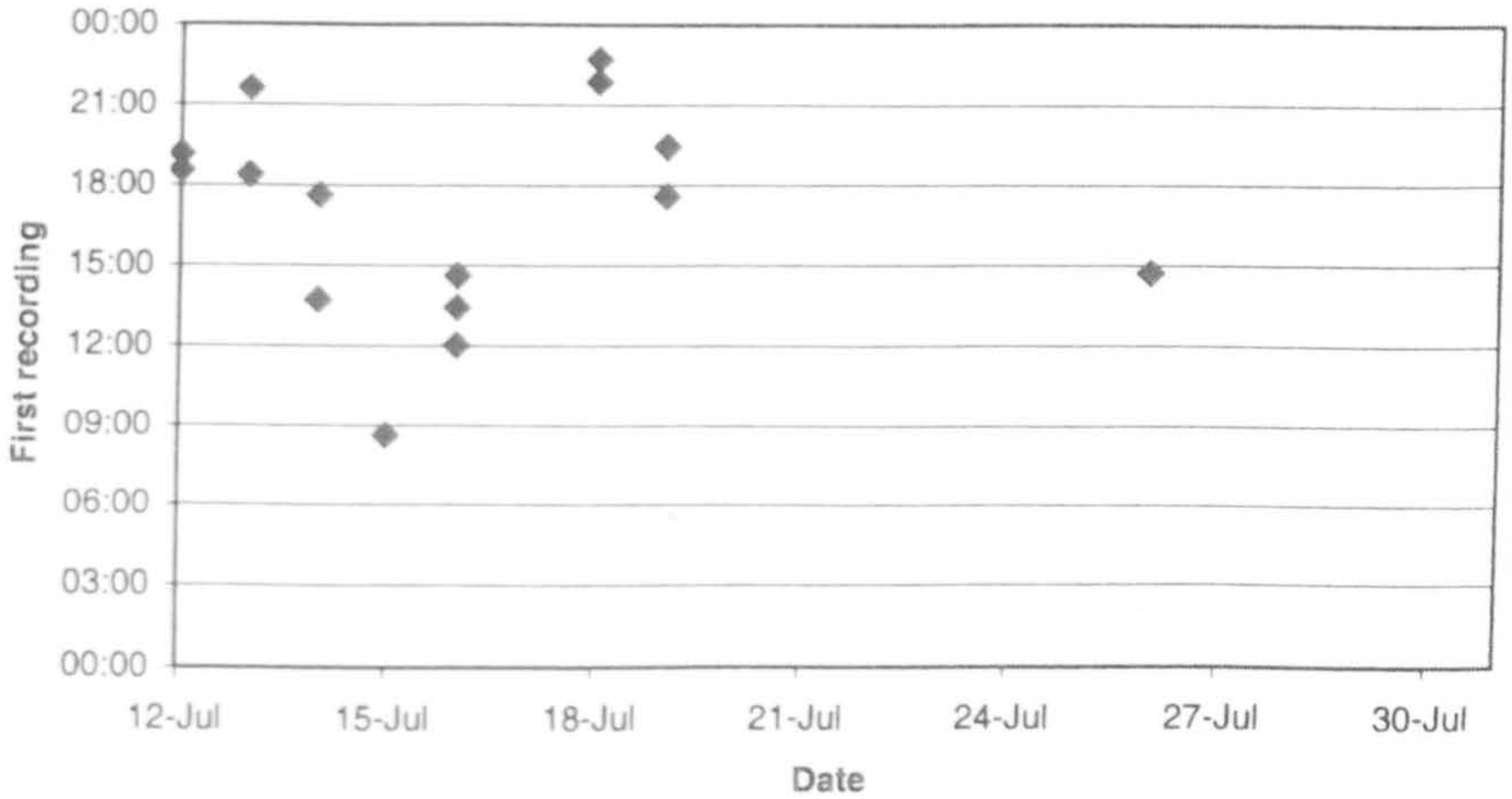

Figure 8-18: Time during the day of first recording at one of the antennae